

THE JOURNAL OF PHYSICAL CHEMISTRY

(Registered in U. S. Patent Office)

CONTENTS

Herman F. Cordes: The Thermal Decomposition of 1,1-Dimethylhydrazine	1473	Bojan Hamlin Jennings and Suzanne N. Townsend: The Sonochemical Reactions of Carbon Tetrachloride and Chloroform in Aqueous Suspension in an Inert Atmosphere	1574
H. F. Walton, D. E. Jordan, S. R. Samedy and W. N. McKay: Cation Exchange Equilibria with Divalent Ions	1477	Mitsugi Senda and Paul Delahay: Electrode Processes with Specific or Non-Specific Adsorption: Faradaic Impedance and Rectification	1580
A. M. Shams El Din, S. E. Khalafalla and Y. A. El Tantawy: Studies on the Anodic and Cathodic Polarization of Amalgams. Part IV. Passivation of Cadmium and Cadmium-Zinc Amalgams in Alkaline Solutions	1484	O. K. Rice: Effects of Quantization and of Anharmonicity on the Rates of Dissociation and Association of Complex Molecules	1588
Bruce B. Benson and Peter D. M. Parker: Relations Among the Solubilities of Nitrogen, Argon and Oxygen in Distilled Water and Sea Water	1489	Allen L. Bowman: The Variation of Lattice Parameter with Carbon Content of Tantalum Carbide	1596
Gus A. Ropp and W. A. Guillory: Isotopic Studies Involving Formic Acid and its Derivatives. VII. Oxygen-18 Isotope Effect in the Photochemical Reaction of Formic Acid with Chlorine	1496	O. D. Bonner and J. R. Overton: The Effect of Temperature on Ion-Exchange Equilibria. IV. The Comparison of Enthalpy Changes Calculated from Equilibrium Measurements and Calorimetrically Measured Values	1599
Kōzo Shinoda and Kōji Itō: Selective Adsorption Studies by Radio Tracer Technique: The Selective Adsorption between Calcium and Sodium Ions at the Ionized Interface	1499	O. D. Bonner and William C. Rampey: The Activity and Osmotic Coefficients of Some <i>p</i> -Toluenesulfonates at 40°, 60°, and 80°	1602
E. Hayon: Effect of Solute Concentration on the Recombination of H and OH in γ -Irradiated Aqueous Solutions	1502	R. B. Ingalls: Hydrogen Formation in the Radiolysis of Toluene	1605
Charles M. Cook, Jr., and Wendell E. Dunn, Jr.: The Reaction of Ferric Chloride with Sodium and Potassium Chlorides	1505	Edward P. Egan, Jr., Zachary T. Wakefield and Basil B. Luff: Thermodynamic Properties of Potassium and Ammonium Taranakites	1609
L. E. Topol, S. J. Yosim and R. A. Osteryoung: E.M.F. Measurements in Molten Bismuth-Bismuth Trichloride Solutions	1511	A. W. Taylor and E. L. Gurney: Solubilities of Potassium and Ammonium Taranakites	1613
Wesley W. Wendlandt and John L. Bear: The Thermal Deaquation of Some Aquopentamminecobalt(III) Complexes	1516	P. Ausloos: Intramolecular Rearrangements. II. Photolysis and Radiolysis of 4-Methyl-2-hexanone	1616
P. Ausloos and E. Murad: The Fluorescence and Phosphorescence of Trifluoroacetone Vapor	1519	Sonja Krause: Light Scattering of Copolymers. I. The Composition Distribution of a Styrene-Methyl Methacrylate Block Copolymer	1618
E. J. Meehan and Willard H. Beattie: Kinetics of Formation and Growth of Silver Bromide Particles	1522	NOTES	
Tad A. Beckman and Kenneth S. Pitzer: The Infrared Spectra of Marginally Metallic Systems: Sodium-Ammonia Solutions	1527	A. D. Osborne, J. N. Pitts, Jr., and Sandra L. Fowler: Investigation of the Photooxidation of Acetone at 3130 Å. Using Infrared Analysis	1622
C. P. Fenimore and G. W. Jones: Formation of Carbon Monoxide in Methane Flames by Reaction of Oxygen Atoms with Methyl Radicals	1532	E. U. Monse, T. I. Taylor and W. Spindel: A Preparation of Highly Concentrated Nitrogen-15 by Exchange of NO and N ₂ O ₂	1625
George Scatchard and N. J. Anderson: The Determination of the Equilibrium Water Content of Ion Exchange Resins	1536	F. R. Duke and H. M. Garfinkel: Complex Ions in Fused Salts. Cadmium and Lead Bromides	1627
G. S. Reddy and J. H. Goldstein: Proton Magnetic Resonance Spectra of Furan and Methylfurans	1539	H. M. Garfinkel and F. R. Duke: Complex Ions in Fused Salts. Effect of Solvent Cation	1629
Charles E. Lang and Adolf F. Voigt: Recoil Reactions of Carbon-11 in n -Hexane and Cyclohexane	1542	Karol J. Mysels and Emanuel Gonick: An Approach to Gas Membrane Osmometry	1631
A. F. Gabrysh, H. Eyring and T. A. Ree: Formation of Color Centers in Sapphire by Solar Radiation	1547	Joshua Jortner and Uriel Sokolov: Absorption Spectra of Oxygen and Nitric Oxide in Solution	1633
John C. Angus and Edward E. Hucke: The Electrolysis of Sodium Amalgams	1549	Mirko Mirnik: Potential Determining Ions and the Coagulation Value	1635
R. E. Glick: On The Diamagnetic Susceptibility of Gases	1552	James S. Hyde and Eli S. Freeman: E.P.R. Observations of NH ₃ ⁺ Formed by X-Ray Irradiation of Ammonium Perchlorate Crystals	1636
George J. Nolan and Edward S. Amis: The Rates of the Alkaline Hydrolyses of Ethyl α -Haloacetates in Pure and Mixed Solvents	1556	Fred H. Brock: Kinetics of the 2,4-Tolylene Diisocyanate-Alcohol Reaction	1638
Louis J. Stief and P. Ausloos: Vapor Phase γ -Radiolysis of Acetone	1560	E. V. Ballou, R. T. Barth and R. A. Flinn: The Effect of Fluorination on the Surface Acidity of Catalytic Alumina and the Loss in Acidity due to Water Vapor Adsorption	1639
R. R. Bernecker and F. A. Long: Heats of Formation of Some Organic Positive Ions and their Parent Radicals and Molecules	1565	Walter W. Harvey: Hole Injection during Reduction of Ferricyanide at a Germanium Electrode	1641
Edmond R. Tucci, Brother Edward Dcody and Norman C. Li: Acid Dissociation Constants and Complex Formation Constants of Several Pyrimidine Derivatives	1570	Efthimios Chinopoulos and Nicholas Papathanasopoulos: The Structure of Tartar Emetic and Evidence of the Existence of Pentavalent Antimony as [Sb(OH)] ⁺	1643
		S. G. Tandon: The Ionization Constants of 2-Thiophene- <i>trans</i> -aldoxime and 2-Furan- <i>trans</i> -aldoxime	1644

THE JOURNAL OF PHYSICAL CHEMISTRY

(Registered in U. S. Patent Office)

W. ALBERT NOYES, JR., EDITOR

ALLEN D. BLISS

ASSISTANT EDITORS

A. B. F. DUNCAN

EDITORIAL BOARD

A. O. ALLEN
C. E. H. BAWN
J. BIGEISEN
D. D. ELEY

D. H. EVERETT
S. C. LIND
F. A. LONG
K. J. MYSELS

J. E. RICCI
R. E. RUNDLE
W. H. STOCKMAYER
A. R. UBBELOHDE

E. R. VAN ARTSDALEN
M. B. WALLENSTEIN
W. WEST
EDGAR F. WESTRUM, JR.

Published monthly by the American Chemical Society at 20th and Northampton Sts., Easton, Pa.

Second-class mail privileges authorized at Easton, Pa. This publication is authorized to be mailed at the special rates of postage prescribed by Section 131.122.

The *Journal of Physical Chemistry* is devoted to the publication of selected symposia in the broad field of physical chemistry and to other contributed papers.

Manuscripts originating in the British Isles, Europe and Africa should be sent to F. C. Tompkins, The Faraday Society, 6 Gray's Inn Square, London W. C. 1, England.

Manuscripts originating elsewhere should be sent to W. Albert Noyes, Jr., Department of Chemistry, University of Rochester, Rochester 20, N. Y.

Correspondence regarding accepted copy, proofs and reprints should be directed to Assistant Editor, Allen D. Bliss, Department of Chemistry, Simmons College, 300 The Fenway, Boston 15, Mass.

Business Office: Alden H. Emery, Executive Secretary, American Chemical Society, 1155 Sixteenth St., N. W., Washington 6, D. C.

Advertising Office: Reinhold Publishing Corporation, 430 Park Avenue, New York 22, N. Y.

Articles must be submitted in duplicate, typed and double spaced. They should have at the beginning a brief Abstract, in no case exceeding 300 words. Original drawings should accompany the manuscript. Lettering at the sides of graphs (black on white or blue) may be pencilled in and will be typeset. Figures and tables should be held to a minimum consistent with adequate presentation of information. Photographs will not be printed on glossy paper except by special arrangement. All footnotes and references to the literature should be numbered consecutively and placed in the manuscript at the proper places. Initials of authors referred to in citations should be given. Nomenclature should conform to that used in *Chemical Abstracts*, mathematical characters be marked for italic, Greek letters carefully made or annotated, and subscripts and superscripts clearly shown. Articles should be written as briefly as possible consistent with clarity and should avoid historical background unnecessary for specialists.

Notes describe fragmentary or incomplete studies but do not otherwise differ fundamentally from articles and are sub-

jected to the same editorial appraisal as are articles. In their preparation particular attention should be paid to brevity and conciseness. Material included in Notes must be definitive and may not be republished subsequently.

Remittances and orders for subscriptions and for single copies, notices of changes of address and new professional connections, and claims for missing numbers should be sent to the American Chemical Society, 1155 Sixteenth St., N. W., Washington 6, D. C. Changes of address for the *Journal of Physical Chemistry* must be received on or before the 30th of the preceding month.

Claims for missing numbers will not be allowed (1) if received more than sixty days from date of issue (because of delivery hazards, no claims can be honored from subscribers in Central Europe, Asia, or Pacific Islands other than Hawaii), (2) if loss was due to failure of notice of change of address to be received before the date specified in the preceding paragraph, or (3) if the reason for the claim is "missing from files."

Subscription rates (1961): members of American Chemical Society, \$12.00 for 1 year; to non-members, \$24.00 for 1 year. Postage to countries in the Pan-American Union \$0.80; Canada, \$0.40; all other countries, \$1.20. Single copies, current volume, \$2.50; foreign postage, \$0.15; Canadian postage, \$0.10; Pan-American Union, \$0.10. Back volumes (Vol. 56-64) \$30.00 per volume; foreign postage, per volume \$1.20, Canadian, \$0.40; Pan-American Union, \$0.80. Single copies: back issues, \$3.00; for current year, \$2.50; postage, single copies: foreign, \$0.15; Canadian, \$0.10; Pan-American Union, \$0.10.

The American Chemical Society and the Editors of the *Journal of Physical Chemistry* assume no responsibility for the statements and opinions advanced by contributors to THIS JOURNAL.

The American Chemical Society also publishes *Journal of the American Chemical Society*, *Chemical Abstracts*, *Industrial and Engineering Chemistry*, International Edition of *Industrial and Engineering Chemistry*, *Chemical and Engineering News*, *Analytical Chemistry*, *Journal of Agricultural and Food Chemistry*, *Journal of Organic Chemistry*, *Journal of Chemical and Engineering Data*, *Chemical Reviews*, *Chemical Titles* and *Journal of Chemical Documentation*. Rates on request.

Yoneho Tabata, Hiroshi Sobue and Eisuke Oda: Radiation Induced Ionic Polymerization of Butadiene.....	1645	ture Difference Method.....	1655
Y. Marcus: Extraction of Tracer Quantities of Uranium(VI) From Nitric Acid by Tri- <i>n</i> -butyl Phosphate.....	1647	Gerasimos J. Karabatso, John D. Graham and Floie Vane: Spin-Spin Coupling Constants between Nonbonded C ¹³ and Proton. II. Dependence of J _{C-H} on Hybridization of C ¹³	1657
David A. Anderson and Eli S. Freeman: The Kinetic Order of the Reaction between Sodium Nitrite and Oxygen.....	1648	R. W. Green and Gwenda M. Parkins: Complexes of Iron with <i>d</i> -Tartaric and <i>meso</i> -Tartaric Acids.....	1658
Irving Shain and Daniel S. Polcyn: Electrolysis with Constant Potential: Effect of Diffusion Coefficients on Reversible Reactions at a Spherical Electrode.....	1649	J. O. Konecny: The Racemization of the Dimethyl Ester of <i>l</i> -Bromosuccinic Acid by Lithium Bromide in Acetone.....	1660
Louis Watts Clark: Kinetic Studies on the Decarboxylation of Oxamic Acid in Dimethyl Sulfoxide and in Triethyl Phosphate.....	1651	Jack F. Tate and Mark M. Jones: Foreign Cation Effects on Measured Stability Constants.....	1661
A. G. Turnbull: Thermochemistry of Zirconium Halides.....	1652	Eli S. Freeman and D. A. Anderson: Observations on the Decomposition of X-Ray Irradiated Ammonium Perchlorate.....	1662
S. D. Hamann and D. R. Teplitzky: The Influence of Pressure on the Cationic Polymerization of Isoamyl Vinyl Ether.....	1654		
G. F. Reynolds and H. J. Guggenheim: Crystallization on a Seed from Fused Salt Solutions by the Tempera-		COMMUNICATION TO THE EDITOR	
		Sydney Ross and James P. Olivier: Evidence for Electronic Interaction between Iodine and a Solid Surface.....	1664

THE JOURNAL OF PHYSICAL CHEMISTRY

(Registered in U. S. Patent Office) (© Copyright, 1961, by the American Chemical Society)

VOLUME 65

SEPTEMBER 27, 1961

NUMBER 9

THE THERMAL DECOMPOSITION OF 1,1-DIMETHYLHYDRAZINE

BY HERMAN F. CORDES

Chemistry Division, U. S. Naval Ordnance Test Station, China Lake, California

Received August 22, 1960

The thermal decomposition of 1,1-dimethylhydrazine has been studied in the gas phase in a flow reactor near 400°. The decomposition is first order in reactant and independent of the surface-to-volume ratio of the reactor. The data, when fitted to an Arrhenius equation, give an activation energy of 28.7 kcal./mole and a pre-exponential factor of $10^{7.8}$ sec.⁻¹. A mechanism has been proposed for the decomposition. This mechanism explains the major products of the decomposition and the abnormally low pre-exponential factor.

Introduction

The hydrazine system of compounds has been of interest for some years as a source of high energy fuels. Knowledge concerning the decomposition of these substances is valuable in predicting storability and possible precombustion reactions. The decomposition of hydrazine, itself, has been extensively studied¹⁻³; however, little or no information is available concerning the thermal stability of the alkyl substituted hydrazines. The purpose of this study was to investigate the thermal decomposition of one of the more important members of this series—1,1-dimethylhydrazine.

Experimental

Apparatus.—The decompositions were carried out in a heated "Pyrex" flow reactor.

Helium gas, free of oxygen, was passed at constant flow rate through two parallel-connected, calibrated flow meters. The flow meters were designed so that there was about a ten-to-one ratio in their flow rates at any given pressure head. The helium stream passing through the smaller flow meter then was passed through a saturator containing the 1,1-dimethylhydrazine. This saturator was immersed in a constant temperature bath to ensure a constant rate of evaporation at any one flow rate through the saturator. There was also a by-pass around the saturator so that helium could stream through the system until a steady state temperature distribution could be reached. The concentration of 1,1-dimethylhydrazine entering the reactor was controlled by varying the temperature of the bath around the saturator. After leaving the saturator the gas stream passed through a warm tube and into a mixing chamber. The warm tube was maintained at about 50° to prevent recondensation of the 1,1-dimethylhydrazine when the saturator was above room temperature.

The mixing chamber served to unite the gas containing the 1,1-dimethylhydrazine with the helium stream from the larger flow meter. This large stream had been preheated by passing down a spiral glass coil wrapped between the heating coils of the reaction furnace. The outlet from the mixing chamber led directly to the reaction chamber.

The mixed stream passed down the reactor and out into a trapping system. This system consisted of a tower of a 1 N H₂SO₄ solution; the exit gases from the reactor were forced into this solution through a fritted glass disc and allowed to bubble up through the tower. The efficiency of this tower was tested by passing a known amount of 1,1-dimethylhydrazine through the system at room temperature and then titrating the amount recovered in the tower. Even at the highest flow rates possible with the system, all of the 1,1-dimethylhydrazine was recovered. This tower was replaced by cold traps when products were collected for identification.

The temperature of the reactor was controlled manually by a pair of heater coils wrapped around two concentric aluminum tubes. The helium preheat line passed between these tubes and the reactor was inside the center tube. A Pt-Pt, 10% Rh thermocouple was inserted in a tube down the axis of the cylindrical reactor. The output of the thermocouple was amplified on a Leeds and Northrup D. C. microvolt amplifier and then sent to a recorder. In a test with N₂ flowing through the system, the temperature in the thermocouple well was compared with the gas temperature as measured by inserting a second thermocouple down the exit tube. The temperatures so measured were found to be within $\pm 1/2^\circ$ of one another except near the end of the reaction chamber where the gas temperature was higher than temperature in the well. After a steady state had been attained, the temperature at any given point along the axis of the reactor remained constant to $\pm 1/2^\circ$ during the time of an experiment.

The temperature profile in the gas stream was determined. From this profile the point, along the axis, of average temperature was determined and all subsequent temperatures were measured with the thermocouple inserted to this depth in the well. Rates, in general, are strong functions of temperature and over a range of temperatures the average rate will not correspond to the rate at the average temperature. However, for the small change in temperature along

(1) P. J. Askey, *J. Am. Chem. Soc.*, **52**, 970 (1930).

(2) T. J. Hanrathy, J. N. Pattison, J. W. Clegg and A. W. Lemmon, *Ind. Eng. Chem.*, **43**, 1113 (1951).

(3) M. Szwarc, *J. Chem. Phys.*, **17**, 505 (1949).

the axis, about 5°, and for the observed activation energy of this reaction, the difference in these two "average" rates is much less than the experimental error.

After sufficient data had been gathered in the unpacked reactor the reactor was removed from the heating jacket, cut open and filled with a number of "Pyrex" rods. The area and volume of these rods was measured accurately. The packed reactor was sealed and placed in the heating jacket. A series of experiments then was made with this new reactor.

Procedure during a Run.—With the saturator by-passed, helium gas was passed through the system at a nearly constant ($\pm 2\%$) flow rate for about half an hour. After this time the reactor had reached a steady temperature. In some cases it was necessary to apply a negative pressure head on the sulfuric acid solution in order to allow the gases to pass through the fritted disc. The pressure in the system, relative to the atmosphere, was measured and the barometric pressure was recorded. After the steady state had been established, the by-pass stream around the saturator was allowed to flow through the saturator and simultaneously a stopwatch was started. The system was allowed to run for 15–60 minutes, while recording the temperature. At the end of this period the saturator was again by-passed and the stopwatch was stopped.

The saturator was weighed before and after each experiment to determine the total amount of reactant entering the system. The amount of reactant leaving the system was determined by diluting the sulfuric acid solution to a standard volume and then titrating an aliquot with $1/60$ molar KIO_3 to a starch-iodide end-point.⁴ The equivalent weight of 1,1-dimethylhydrazine in this titration is 30.05.

The flow rate in liters per minute passing through the reactor was determined from the flow meter calibration and the reactor temperature assuming constant pressure. A correction was applied for the increase in flow rate due to the 1,1-dimethylhydrazine evaporated. The moles of reactant entering the reactor per unit time were computed from the total amount of reactant used and the total time of the experiment. The residence time in the reactor was found by dividing the internal volume of the reactor by the flow rate. The negative logarithm of the fraction of unreacted material was divided by the residence time to give an empirical first-order rate constant.

The purity of the 1,1-dimethylhydrazine was determined under the same conditions as existed when the unreacted material was determined. Sample sizes were arranged to use about the same volume of reagents, thereby eliminating any need for end-point corrections. The known products of the reaction were found to have no effect on the position of the end-point although the color of the solution was somewhat yellowish and fading was more pronounced than for the pure samples.

Products of the Reaction.—For the purpose of product analysis the sulfuric acid trap in the decomposition train was replaced by two Pyrex traps connected in series. The trap closest to the furnace was maintained at -78° and the second trap was maintained at -196° . The material that collected during a run in the -196° trap was warmed to -78° and an infrared spectrum was taken on the gases evolved. Strong absorption was noticed in the 3.3μ region and appeared to be due to C-H vibrations. A mass spectral analysis of the same sample showed the presence of methane, ethane and propane in the ratios of 1:0.14:0.002.

The material that had collected at -78° was allowed to warm up to room temperature and the first gases evolved were subjected to infrared spectral study. The characteristic absorption of ammonia in the 11μ region was observed. The spectra also gave indications of the presence of dimethylamine and possibly the presence of monomethylamine. The spectrum of 1,1-dimethylhydrazine obscured most of the region covered by the instrument. Due to difficulty in obtaining a consistent mass spectrum for the 1,1-dimethylhydrazine no additional evidence could be obtained from a mass spectral analysis of this sample.

The presence of dimethylamine was positively determined by preparation of the benzenesulfonamide. This derivative melted at $45-47^\circ$ and a mixed melting point with a

known sample (m.p. $46-47^\circ$) also melted at $45-47^\circ$. No positive information could be found as to the presence of moromethylamine. It is felt that this species should be present at least in small quantities as dimethylamine pyrolysis gives monomethylamine at these temperatures.

A viscous liquid was observed to collect in the outlet line from the reactor. This liquid was found to have an infrared spectrum identical with the spectrum of the trimer of methylene methylamine (1,3,5-trimethyl-1,3,5-triazacyclohexane).

A test was made for cyanide by treating a portion of the -78° fraction with $FeSO_4$ and $NaOH$. The mixture was heated and $FeCl_3$ was added. No blue color was observed and HCN is presumed not to be among the products.

A series of decompositions was made at 250° using sealed Pyrex vessels. Known pressures of 1,1-dimethylhydrazine and helium were placed in these vessels. The presence of the helium served to furnish a concentration standard for a mass spectral analysis of gases volatile at -198° . The length of time of heating of the vessels at 250° varied between 10 and 50 minutes. The products volatile at -198° were methane and nitrogen with small amounts of hydrogen. The data are summarized in Table II.

The Rate Data. Unpacked Reactor.—The decomposition was measured at three temperatures: 623.2, 674.7 and $726.0^\circ K$. The empirical first-order rate constants showed no dependence on the residence time at any of these temperatures. No reasonable constancy of rate constants could be found for fits of the data to zero order, $1/2$ order, $3/2$ order or second-order rate equations. At the highest temperature the empirical first-order rate constant was found to vary with the initial concentration of reactant. This effect was not noticed at the lower two temperatures. At the highest temperature an increase of recorded temperature was noted immediately after the 1,1-dimethylhydrazine was allowed to enter the reactor. This increase was about $1-2^\circ$ and the temperature remained high until the saturator was by-passed, when the reactor temperature returned to the steady state value. The rates of decomposition were quite high at this temperature and the apparent increase of rate with reactant concentration could be due to self heating and the temperature might not be properly indicated by the thermocouple. Since this variation of rate constant with concentration was roughly linear, a least squares fit of the data was made to the equation

$$k = k_0 + a[UDMH]$$

k_0 was taken as the true rate constant at $726.0^\circ K$.

The data for the three temperatures are summarized in Table I. The values of k listed in this Table are nominal ones for the indicated temperature. The actual values were obtained at slightly different temperatures ($\pm 2^\circ$). These temperature deviations were corrected for by using the raw data to obtain a rough temperature coefficient for the rate constant. The extremely high scatter at the lowest temperature was due primarily to the inaccuracy of measuring the small percentage of decomposition.

Packed Reactor.—The reactor used in the first series of experiments was cut open and filled with Pyrex rods of a known volume and area. This packed reactor had a surface-to-volume ratio of 3.76 times that of the unpacked reactor and an area of 2.78 times that of the unpacked reactor.

Data were gathered at 623.2 and at $674.7^\circ K$ using the packed reactor. The data were treated

(4) W. R. McBride and H. W. Kruse, "Analytical Procedures for 1,1-Dimethylhydrazine," NAVORD Report 5263, NOTS TP 1475, Naval Ordnance Test Station, China Lake, California, 23 May, 1956 (unclassified).

TABLE I
 SUMMARY OF RATE DATA

<i>T</i> , °K.	<i>k</i> _{obs} , sec. ⁻¹
623.2	(6.14 ± 3.84) × 10 ^{-3a}
623.2	(7.41 ± 3.45) × 10 ^{-3b}
674.7	(3.47 ± 0.18) × 10 ^{-2a}
674.7	(4.26 ± 0.81) × 10 ^{-2b}
726.0	(1.56 ± 0.05) × 10 ^{-1a,c}

^a Unpacked reactor *S/V* = 1.43 cm.⁻¹. ^b Packed reactor *S/V* = 5.37 cm.⁻¹. ^c *k* = (1.56 ± 0.05) × 10⁻¹ + (0.111 ± 0.011) × 10⁻⁴ [UDMH]. Concentration is in moles per liter.

in the same manner as for the unpacked reactor. These data are also summarized in Table I.

Within experimental error there was no difference in the rate constants obtained using the data from the different reactors, although the rates were very slightly higher in the packed reactor. These results indicate that the reaction is not primarily controlled by surface catalysis. In both the packed and unpacked reactors, rates were often noticeably higher after the reactor had been unused and open to the atmosphere for a few days. After the first run of a new series the rates returned to the lower values. Data taken when the surface of the reactor had not been well seasoned were discarded.

TABLE II

ANALYSES OF PRODUCTS FROM 522°K. DECOMPOSITIONS^{a,b}

Run no.	Time, sec.	(CH ₄)/(DMH) ₀ × 10 ⁴	(H ₂)/(DMH) ₀ × 10 ⁴	(CH ₄)/(DMH) ₀ × 1/ <i>t</i> sec. ⁻¹ × 10 ⁶	[N ₂][CH ₄]
1	600	5.9	1.8	0.98	0.450*
2	1200	9.7	2.2	.81	.599
3	2400	19.4	1.8	.81	.582
4	1800	16.1	3.0	.88	.671
5	3000	26.3	1.9	.88	.621
6	3000	21.4	2.1	.71	.606
				0.85	0.59 ± 0.07 or 0.62 ± 0.03 omitting *

^a (DMH) = 40.8 mm. at 273.2° K. ^b *k*_{obsd.} extrapolated to 522°K. = 6.4 × 10⁻¹ sec.⁻¹.

Temperature Dependence.—The calculated first-order rate constant has the standard Arrhenius dependence on the temperature. A weighted least squares fit of the data from the unpacked reactor to the equation

$$\ln k = \ln A - \frac{\Delta E}{RT}$$

was made. The results were

$$A = 10^{7.83 \pm 0.21} \text{ sec.}^{-1}$$

$$\Delta E = 28.68 \pm 0.68 \text{ kcal./mole}^\circ\text{K.}$$

The limits of error shown are one standard deviation. The data from the packed reactor yield the results

$$A = 10^{7.46 \pm 2.6} \text{ sec.}^{-1}$$

$$\Delta E = 28.4 \pm 8.1 \text{ kcal./mole}^\circ\text{K.}$$

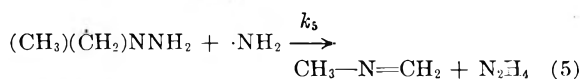
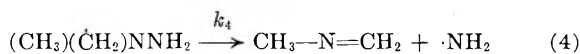
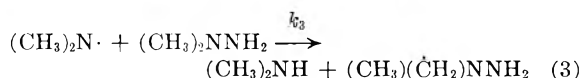
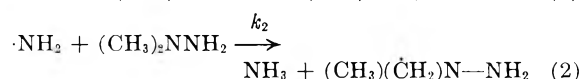
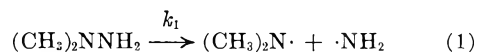
In this case the errors listed are the combined contributions of the standard deviations at the individual temperatures.

Interpretation of Results

The variety and character of the products, the abnormally low pre-exponential factor and the low activation energy associated with the empirical first-order rate constant all point to a complex mechanism for the decomposition of 1,1-dimethylhydrazine. The weakest bond in the molecule is the N-N bond with a strength near to 60 kcal.³ The C-N bond is about 80 kcal.⁵ The C-H and N-H bonds are about 101 and 104 kcal., respectively.^{5,6} All of these values are so much higher than the observed activation energy of 28 kcal. that it is certain that the observed first-order rate constant does not directly measure a dissociation process. In addition, the observed pre-exponential factor is four orders of magnitude less than the minimum value of 10¹² sec.⁻¹ expected for a unimolecular decomposition. Were the reaction heterogeneous, then both the low activation energy and the low pre-exponential factor could be explained in terms of a surface complex. The data in the packed and unpacked reactors are, however, identical within experimental error and no major heterogeneous reaction is indicated. The presence of methane, ethane and propane in those runs in which major amounts of decomposition occurred, strongly suggests the presence of methyl radicals. The relative amounts of these species are also consistent with this view. In the very low temperature runs, where the rate of decomposition was slower, and where presumably the methyl radicals would be in lower concentration only methane was found.

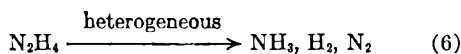
The formation of methane and nitrogen in the 250° runs in sealed bulbs showed a linear increase with time (see Table II). The empirical rate for the over-all decomposition was extrapolated to 250°. The calculated amount of decomposition was found to be about 75 times the amount of methane formed at these temperatures indicating that methane is not a major product of the decomposition. The hydrogen produced was constant and independent of the time. This may indicate a small amount of impurity or a rapidly inhibited surface reaction.

A mechanism can be written which leads to first-order kinetics and also explains the general features of the decomposition, although considerably more data need to be gathered to place any high degree of confidence in this mechanism.



(5) M. Szwarc, *Proc. Roy. Soc. (London)*, **A198**, 285 (1949).

(6) F. D. Rossini, "Selected Values of Chemical Thermodynamic Properties," Circular of the National Bureau of Standards 500, U. S. Government Printing Office, 1952.



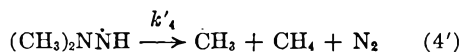
The heterogeneous step (6) is first order and yields a variety of products depending upon the temperature. At 300° the stoichiometry is nearly $\text{N}_2\text{H}_4 \rightarrow \frac{4}{3} \text{NH}_3 + \frac{1}{3} \text{N}_2$, only a small amount of hydrogen being formed.^{2,5} This mechanism is one of the general type considered by Rice and Herzfeld.⁷ The steady state rate assuming a long chain length is

$$-\frac{d[\text{UDMH}]}{dt} = \sqrt{\frac{k_1 k_4 k_2}{k_5}} [\text{UDMH}]$$

In terms of this mechanism then the empirical first-order constant k_{obs} is interpreted as the coefficient of $[\text{UDMH}]$. The intermediate radical $(\text{CH}_3)(\text{CH}_2)\text{NNH}_2$ has been taken as the "normal" product of a hydrogen abstraction from the parent molecule although there is no direct indication that hydrogens are removed more easily from carbon than from nitrogen. The general indications for those few reactions studied show that hydrogen abstractions from a nitrogen have about the same order of magnitude pre-exponential factors and similar activation energies as for hydrogen abstractions from carbon.⁸

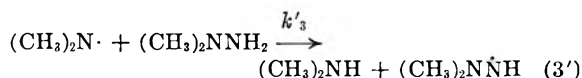
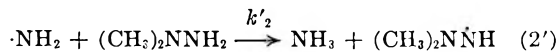
This radical has been chosen since it leads by a reasonable path to one of the known products $\text{CH}_3\text{-N}=\text{CH}_2$. The methylene-methylamine could also be formed from disproportionation of the dimethylamino radicals.

The alternate radical, obtained by abstraction of a hydrogen from the nitrogen of the parent molecule, can be considered for a possible explanation of the methane production. Since the amount of



hydrogen found among the products is constant and unrelated to the amount of methane produced, an alternative mode of decomposition to give $2\text{CH}_3 + \text{N}_2 + \text{H}$ is ruled out.

The radical decomposition by step (4') is assumed to be formed to a slight extent by



followed by (4') and



The amount of reaction by this mode will be assumed to be small enough not to affect the steady state concentrations derived above. Step (7) will be considered as the only abstraction reaction, the analogous step to produce $(\text{CH}_3)_2\text{NNH}_2$ will be assumed negligible. Assuming a steady state for these reactive intermediates the rate of production of methane can be derived to be

$$\frac{d[\text{CH}_4]}{dt} = \frac{2k'_2}{k_2} k_{\text{obs}} [\text{UDMH}]$$

For small amounts of decomposition, as in the runs made at 250°, $[\text{UDMH}]$ is a constant in time and the methane should increase linearly in time as is observed. The ratio k'_2/k_2 can be obtained from

$$\frac{[\text{CH}_4]}{[\text{UDMH}] \cdot t} = \frac{2k'_2}{k_2} k_{\text{obs}}$$

The data in Table II then lead to

$$\frac{k'_2}{k_2} = 6.6 \times 10^{-3}$$

Now if the pre-exponential factors associated with k'_2 and k_2 differ only by the number of available hydrogens for each mode of reaction, then the activation energy difference for the two abstractions can be calculated.

$$\frac{k'_2}{k_2} = \frac{2}{6} e^{-(\Delta E)/RT} = 6.6 \times 10^{-3}$$

whence

$$\Delta E = E'_2 - E_2 = 4.1 \text{ kcal.}$$

This is just about the difference in bond strengths for the two bonds N-H and C-H.^{5,6}

In addition, one more check can be made on the data gathered at 250°. From the mechanism one can derive

$$\frac{[\text{N}_2]}{[\text{CH}_4]} > 0.50$$

The observed ratio (neglecting the first datum point which deviates from the rest and is also less than 0.5) is 0.62 ± 0.03 .

The abnormally low pre-exponential factor and low activation energy for k_{obs} can now be discussed. If the rate constants are written in the Arrhenius form

$$k = A e^{-E/RT}$$

then

$$A_{\text{obs}} = \sqrt{\frac{A_1 A_4 A_2}{A_5}}$$

$$E_{\text{obs}} = \frac{E_1 + E_4 + E_2 - E_5}{2}$$

Now, k_2 and k_5 are bimolecular rate constants and their pre-exponential factors should not differ by more than three orders of magnitude. k_1 is a unimolecular rate constant and its pre-exponential factor should lie between 10^{12} and $10^{15} \text{ sec.}^{-1}$.

$$10^{-2} < A_4 < 10^7$$

This is a very low value of a pre-exponential factor, however, the value of 10^7 to 10^8 sec.^{-1} or less is observed for the rate constant for decomposition of "hot" molecules—either the excited species of unimolecular decompositions⁹ or species formed by reactions with radicals.¹⁰ To check the possibility that step (4) is exothermic requires a knowledge of the enthalpies of formation of NH_2 , $\text{CH}_3\text{-N}=\text{CH}$ and $(\text{CH}_3)(\dot{\text{C}}\text{H}_2)\text{N-NH}_2$. The enthalpy of formation is known for NH_2 to be +41 kcal.³ An estimation of the enthalpies of formation of $\text{CH}_3\text{-N}=\text{CH}_3$ and $(\text{CH}_3)(\dot{\text{C}}\text{H}_2)\text{-NH}_2$ was made by use of the table of bond energies given by Cottrell.¹¹

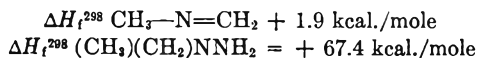
(9) H. S. Johnston, *J. Am. Chem. Soc.*, **73**, 4542 (1951).

(7) F. O. Rice and K. F. Herzfeld, *J. Am. Chem. Soc.*, **56**, 284 (1934).

(8) E. W. R. Steacie, "Atomic and Free Radical Reactions," Vol. II, Chapter 9, Reinhold Publ. Corp., New York, N. Y., 1954.

(10) B. S. Rabinovitch and R. W. Diesen, *J. Chem. Phys.*, **30**, 735 (1959).

(11) T. L. Cottrell, "The Strength of Chemical Bonds," Butterworth Scientific Publications, London, 1958.



These enthalpies of formation lead to a value for the enthalpy of reaction 4 of -24 kcal. The uncertainty of enthalpies of formation that are calculated in this fashion are usually no more than 2-3 kcal., although they might be somewhat higher in the case of a radical. It is doubtful that the errors could be so great that the true enthalpy of reaction for step (4) is positive. It seems quite proper to assume step (4) to be exothermic and spontaneous.

A further consequence of the spontaneity of step (4) is that $E_4 = 0$. Then

$$\Delta E_{\text{obs}} = \frac{E_1 + E_2 - E_5}{2}$$

Since E_1 is expected to be near 60 kcal., E_2 and E_5 must have nearly the same numerical value.

It is possible then to account for the low empirical pre-exponential factor by assuming the preceding mechanism with

$$A_1 \cong 10^{13} \text{ sec.}^{-1}; A_4 \cong 10^6 \text{ sec.}^{-1}; \text{ and } \frac{A_2}{A_5} \cong 10^{-3}$$

The preceding discussion suggests several additional experiments. The rate of methane production should be measured over a range of temperatures so that A_2'/A_2 and $E_2' - E_2$ can be directly determined (with k_{obs} known). As of this date there are no data which allow a direct comparison of the relative ease of hydrogen abstraction from carbon and nitrogen. By use of gas chromatography the products ammonia and dimethylamine might be separable from the reaction mixture. The rate of production of ammonia should yield k_{obs} so that this quantity can be determined directly at lower temperatures and, it is hoped, with higher precision. The rate of production of dimethylamine should yield a direct value of k_1 . If all of the hydrazine produced in step (5) is destroyed on the walls, then a careful determination of the excess nitrogen over that accompanying the methane production should yield the ratio k_5/k_4 .

CATION EXCHANGE EQUILIBRIA WITH DIVALENT IONS

BY H. F. WALTON, D. E. JORDAN, S. R. SAMEDY AND W. N. MCKAY

University of Colorado, Boulder, Colorado

Received September 23, 1960

Equilibrium distributions have been measured for exchanges of hydrogen ions in sulfonated polystyrene resins with perchlorates of Ba^{++} , Cd^{++} , Pb^{++} and UO_2^{++} . Three degrees of resin crosslinking were used, and each exchange was studied at two or more temperatures. Values of ΔF^0 and ΔH were evaluated. Activity coefficient ratios for the pairs of ions $\text{Cd}^{++}\text{-H}^+$ and $\text{Pb}^{++}\text{-H}^+$ in perchlorate solutions were found from e.m.f. measurements, and water and salt uptakes of the resins were measured. The binding of metal ions by the resins increased with crosslinking, solution concentration, temperature (except for Ba^{++}), and proportion of metal ion in the resin. Evidence is presented for formation of ion pairs.

The thermodynamics of ion exchange have been studied by a number of workers.¹⁻³ Most studies have been restricted to univalent ions with measurements at a single temperature. However, Bonner and co-workers have recently measured cation exchange equilibria with divalent ions⁴ and have begun a systematic study of temperature effects.^{5,6} Cruickshank and Meares⁷ have measured heats of ion exchange calorimetrically and made a careful thermodynamic study of certain cation exchanges.³ Kraus and Raridon⁸ have studied cation exchange equilibria from 2 to 200° using tracer quantities of one of the exchanging ions; they worked primarily with ions of the alkali and alkaline earth metals. Kraus, Raridon and Holcomb⁹ have studied temperature effects in anion exchange.

(1) F. Helfferich, "Ionenaustauscher," Verlag Chemie, Berlin, 1959, Chap. V.

(2) G. E. Myers and G. E. Boyd, *J. Phys. Chem.*, **60**, 521 (1956).

(3) E. H. Cruickshank and P. Meares, *Trans. Faraday Soc.*, **54**, 174 (1958).

(4) O. D. Bonner and F. L. Livingston, *J. Phys. Chem.*, **60**, 530 (1956).

(5) O. D. Bonner and L. L. Smith, *ibid.*, **61**, 1614 (1957).

(6) O. D. Bonner and R. R. Pruett, *ibid.*, **63**, 1417, 1420 (1959).

(7) E. H. Cruickshank and P. Meares, *Trans. Faraday Soc.*, **53**, 1289, 1299 (1957).

(8) K. A. Kraus and R. J. Raridon, *J. Phys. Chem.*, **63**, 1901 (1957).

(9) K. A. Kraus, R. J. Raridon and D. L. Holcomb, *J. Chromatography*, **3**, 178 (1960).

We have measured exchange equilibria for the divalent ions, Ba^{++} , Cd^{++} , Pb^{++} and UO_2^{++} , exchanging with hydrogen ion in sulfonated polystyrene resins. These ions were chosen because each reacts with sulfate ions in a specific way, forming precipitates or complex ion, and specific or anomalous reactions with a sulfonic acid resin might be expected. The hydrogen ion was chosen as one of the exchanging ions in every case to avoid difficulties from hydrolysis, and perchlorate salts were used to avoid complex ion formation in solution. Resins of three different degrees of crosslinking were used, and the effect of temperature was studied in every exchange. Measurements were made over a wide range of cation ratios in the resin.

To aid in the interpretation of the equilibrium data we measured the water uptake and salt uptake of individual resins. We also measured the activity coefficient ratios, $\gamma_{\text{H}^+}^2/\gamma_{\text{M}^{++}}$, for cadmium and lead ions by electromotive force. Activity coefficients in the resin phase and standard free energies of exchange were calculated from the data by an approximation to the method of Gaines and Thomas.¹⁰

Experimental

(a) Materials.—The sulfonated polystyrene cation ex-

(10) G. L. Gaines, Jr., and H. C. Thomas, *J. Chem. Phys.*, **21**, 714 (1953).

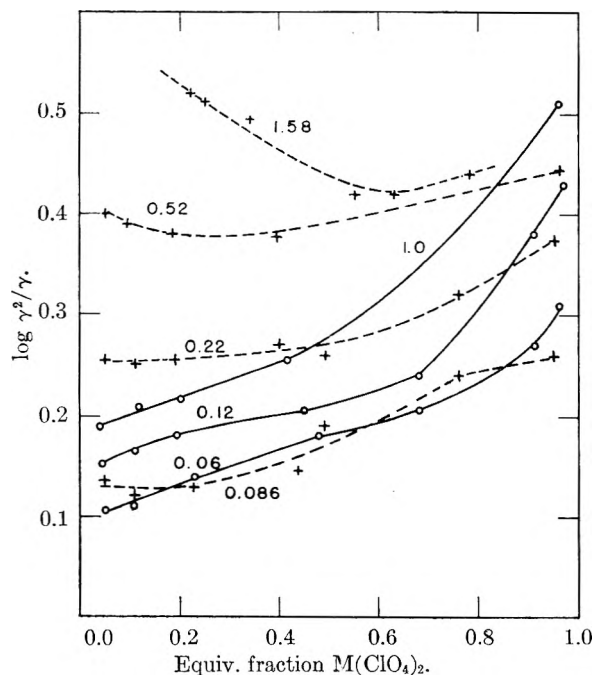


Fig. 1.—Activity coefficient ratios at constant ionic strength: dashed lines, Pb-H mixtures; solid lines, Cd-H mixtures. Numbers on curves indicate the ionic strength.

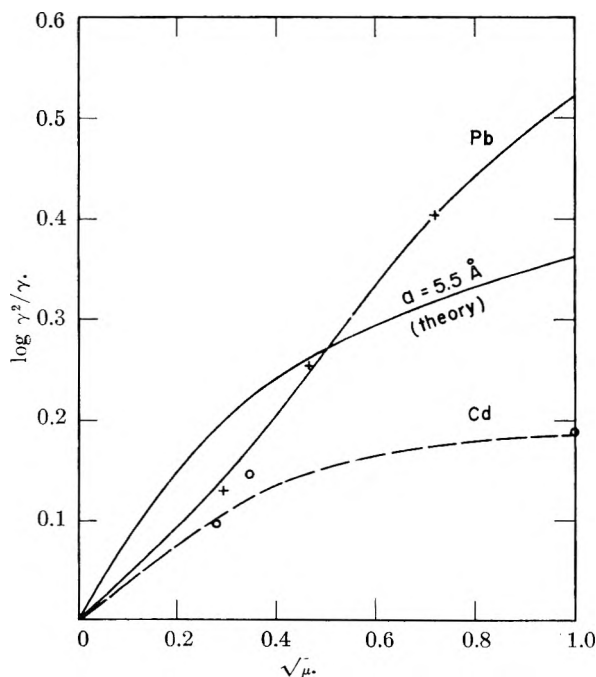


Fig. 2.—Activity coefficient ratios for low metal ions: hydrogen ion ratios, as a function of ionic strength. Evaluation of the "theory" curve is discussed in the text.

change resins were supplied by the Dow Chemical Company. Most experiments were made with the grades Dowex 50W \times 4 and Dowex 50W \times 8, "white" resins with 4 and 8% nominal divinylbenzene crosslinking. These were found to be remarkably homogeneous materials, containing only a very small proportion of more weakly crosslinked or more highly sulfonated beads.¹¹ Some tests were also made with a dark colored 16% crosslinked resin. All resins were 50–100 mesh and were washed thoroughly with dilute hydrochloric acid, methanol and water, then stored in the

air-dried condition with about 30% moisture. Moisture content and exchange capacity were determined in the usual way. For certain experiments the resins were nearly saturated with the metal ion before use, retaining 2–3% of hydrogen ion to avoid hydrolysis.

Barium and lead perchlorates were obtained from the G. Frederick Smith Chemical Co. The perchlorates of cadmium and uranium(VI) were made from cadmium metal and uranyl nitrate, respectively, and were recrystallized before use. Stock solutions of the perchlorates were prepared and analyzed as described below. All except barium perchlorate contained perchloric acid to prevent hydrolysis.

(b) Analytical Methods.—Lead and cadmium were determined by EDTA titration. Barium was determined in the solution from the equilibration tests by pipetting a known volume into a weighed platinum crucible, adding sulfuric acid, evaporating and heating briefly to redness, then weighing the crucible with its barium sulfate.

Uranium was determined both gravimetrically and photometrically. When the amount in the sample exceeded 5–10 mg. precipitation with 8-hydroxyquinoline was used.¹² There is a question in the literature about the composition of this precipitate.¹³ By igniting several samples of precipitate to U_3O_8 we found the uranium content 33.86%, in agreement with the formula UO_2Q_2HQ .¹⁴ Small amounts of uranium were measured by the dibenzoylmethane method^{15,16}; the yellow color was developed in solutions containing 55–60% ethanol by volume and at apparent pH 6.5–7.2, and was measured at 400 $m\mu$, usually with a Cary recording spectrophotometer.

Free perchloric acid in solutions of lead and cadmium perchlorates was titrated potentiometrically after adding sodium chloride to complex the metal ion and inhibit hydrolysis. No satisfactory potentiometric method was found to titrate free acid in presence of uranyl ion. Addition of thiocyanate to complex the uranyl ions gave reasonably good inflections, but the accuracy was poor. A better way was to titrate the free acid conductometrically with standard sodium hydroxide.

To analyze resins for metal ion the best way was through wet ashing with perchloric and sulfuric acids,¹⁷ though the metal ion could also be eluted. The exchangeable hydrogen ion in the resins was determined by direct potentiometric titration in a solution of sodium chloride (this applied in presence of Cd, Pb and Ba) or by elution in a column with barium chloride solution, followed by conductometric titration with standard base (this was necessary if UO_2^{++} was present).

(c) Equilibration.—For the equilibrium measurements which were the main purpose of this research, weighed amounts of air-dried resins were placed in flasks with known volumes of solutions and stirred or shaken, with temperature constant to $\pm 1^\circ$, until no further change in solution composition was noted. In most series of tests, variable amounts of hydrogen resin and constant volumes of metal perchlorate solution were used; that is, series of experiments were run at constant total normality.

Exchanges are slower with divalent ions than with univalent ions on account of their smaller diffusion rates.¹⁸ It is better to start with hydrogen ion in the resin than with metal ion, because the exchange rate is governed primarily by the diffusion of the ion which is initially in the resin.^{19,20} Starting with hydrogen resin we found six hours to be more than enough to reach a steady concentration unless the residual metal ion concentration in solution was very low, when times up to 2 days were required.

The proper criterion of equilibrium is the attainment

(12) A. Claassen and J. Visser, *Rec. trav. chim.*, **65**, 211 (1946).

(13) C. Duval, "Inorganic Thermogravimetric Analysis," Elsevier, 1953, p. 510.

(14) E. P. Bullwinkle and P. Noble, *J. Am. Chem. Soc.*, **80**, 2955 (1958).

(15) J. H. Yoe, F. Will and R. A. Black, *Anal. Chem.*, **25**, 1200 (1953).

(16) J. A. S. Adams and W. J. Maack, *ibid.*, **26**, 1635 (1954).

(17) H. Diehl and G. F. Smith, *Talanta*, **2**, 209 (1959).

(18) G. E. Boyd and B. A. Soldano, *J. Am. Chem. Soc.*, **75**, 6091 (1953).

(19) M. S. Plesset, F. Helfferich and J. N. Franklin, *J. Chem. Phys.*, **29**, 1064 (1958).

(20) F. Helfferich and M. S. Plesset, *ibid.*, **28**, 418 (1958).

(11) M. G. Suryaraman and H. F. Walton, *Science*, **131**, 829 (1960).

of the same final distribution from two directions. Where the distribution shifted with temperature this test could be made very simply by measuring the solution composition at one temperature, changing the temperature and measuring the new distribution, then returning to the original temperature and analyzing the solution again. Such tests were made in several cases, and particularly with the $\text{UO}_2\text{-H}^+$ exchange in 16% crosslinked resin where the approach to equilibrium is relatively slow. Very good checks were obtained, proving that equilibrium was reached. Adequate checks were obtained by shaking cadmium-saturated resins with perchloric acid and comparing the final distributions with those reached from hydrogen-saturated resins and cadmium perchlorate (Fig. 4).

To withdraw samples of solution for analysis a pipet was used with a plug of glass wool over the tip to filter out resin particles. If necessary the solutions were centrifuged. In recovering the resins for analysis after equilibration it was important to separate resin and solution as completely as possible before rinsing the resin, since dilution shifts the equilibrium. The resin analysis served as a check on the solution analysis and was particularly important when the proportion of hydrogen ion in the resin was low.

(d) **Water Uptake.**—The amount of water taken up by the swollen resin beads was determined for the hydrogen resins and for the resins saturated with each of the metal ions used. (The uranyl resin retained about 5% hydrogen ion to avoid hydrolysis.) The water uptake of two mixed hydrogen-barium resins was also measured.

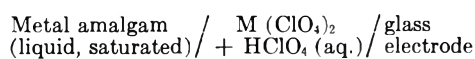
Two methods were used. In one, a weighed amount of air-dried resin (about 0.5 g.) was wetted with water, allowed to stand at least an hour, then blotted dry on filter paper and quickly transferred to a bottle which was stoppered and weighed. This procedure was repeated until weights constant to 10 mg. were obtained. This technique has been used by other workers.²¹ However, it is empirical and liable to yield values which are too high.

The second method was an isopiestic vapor uptake method. Weighed 0.3-g. samples of air-dried resins were placed in weighing bottles which were supported, without their stoppers, in a small aluminum desiccator by means of rubber rings. This desiccator, which had holes drilled in its sides, was placed inside a glass vacuum desiccator, the bottom of which contained 1.25 *M* sodium sulfate solution. The bottoms of the weighing bottles just touched the surface of this solution. The glass desiccator was closed and evacuated by means of an aspirator, then shaken gently at $25 \pm 1^\circ$ until the resins had come into equilibrium with the water vapor. This took 24–36 hours.

The relative humidity above 1.25 *M* Na_2SO_4 is 95.7% at 25° . According to the vapor pressure curves of Boyd and Soldano²² an 8% crosslinked H-resin has about 91% of its maximum water content at this humidity. Though this fraction is not the same for all cationic forms of the resin, the water uptakes measured at 95.7% humidity will be comparable for the different resins and will indicate a lower limit to the maximum water uptake.

(e) **Salt Uptake.**—To measure the uptake of neutral salt or of co-ions, weighed 5-g. quantities of resins saturated with different metal ions were placed in small flasks with measured volumes (15–20 ml.) of standardized solutions of salts of the same metal that was in the resin. The flasks were shaken for an hour and the solutions then analyzed. The water uptake measured by the blotting method was used to compute the molal co-ion concentration, and hence the salt invasion, in the resin beads. This was compared with the co-ion concentration expected from the Donnan equilibrium, assuming complete ionization in the resin and ideal solution laws.

(f) **Activity Coefficient Ratios.**—To measure the ratios $\gamma_{\text{H}^{+2}}/\gamma_{\text{Cd}^{+2}}$ and $\gamma_{\text{H}^{+2}}/\gamma_{\text{Ba}^{+2}}$ this cell was used



The e.m.f. of this cell is

$$E = E^0 + \frac{RT}{2F} \ln \frac{M_{\text{H}^{+2}}}{M_{\text{M}^{+2}}} + \frac{RT}{2F} \ln \frac{\gamma_{\text{H}^{+2}}}{\gamma_{\text{M}^{+2}}} - (1)$$

E^0 was evaluated by several series of experiments with suc-

(21) O. D. Bonner, W. J. Argersinger and A. W. Davidson, *J. Am. Chem. Soc.*, **74**, 1044 (1952).

(22) G. E. Boyd and B. A. Soldano, *Z. Elektrochem.*, **57**, 162 (1953).

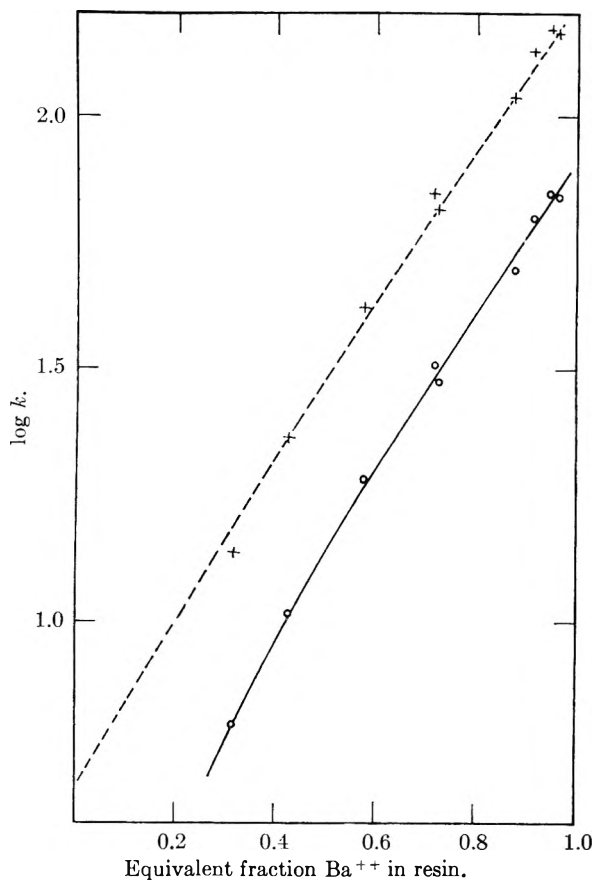


Fig. 3.—Barium-hydrogen exchange, 8% crosslinked resin, 25° . So lid line, concentration quotient; dashed line, activity quotient. The data for 50° are so close to those for 25° that they are not plotted.

cessive dilutions of the cell liquid, keeping the ratio of metal ion to hydrogen ion concentration constant. The quantity $(E - RT/2F \ln M_{\text{H}^{+2}}/M_{\text{M}^{+2}})$ was plotted against the square root of the ionic strength and extrapolated to zero ionic strength. After E^0 had been determined, further series of experiments were made in which the ratio of metal ion to hydrogen ion concentration was varied while the ionic strength was kept constant.

Exclusion of air was essential, and the cell was designed so that known volumes of solutions could be added and removed without admitting air. The solutions were purged with purified nitrogen. The amalgam was supported in a cup, and its surface could be renewed at any time. The temperature was $25 \pm 0.01^\circ$, the e.m.f. was measured with a Leeds and Northrup Type K potentiometer and thermionic amplifier.

Results

(a) **Water Uptake.**—These data are shown in Table I. The blotting method gives results which appear to be slightly high, if we assume that the water uptake at 100% humidity is about 10% more than that at 95.7% humidity. Our results for the 8% crosslinked resins agree satisfactorily with those of Bonner and Smith.²³

There is no obvious correlation between water uptake and affinity of ions for the resin. The non-linear dependence of water uptake on resin composition for mixed barium-hydrogen resins is unexplained, and does not seem to influence the ion exchange equilibrium.

The water uptakes were used to calculate the co-ion concentrations in the resins, which appear

(23) O. D. Bonner and L. L. Smith, *J. Phys. Chem.*, **61**, 326 (1957).

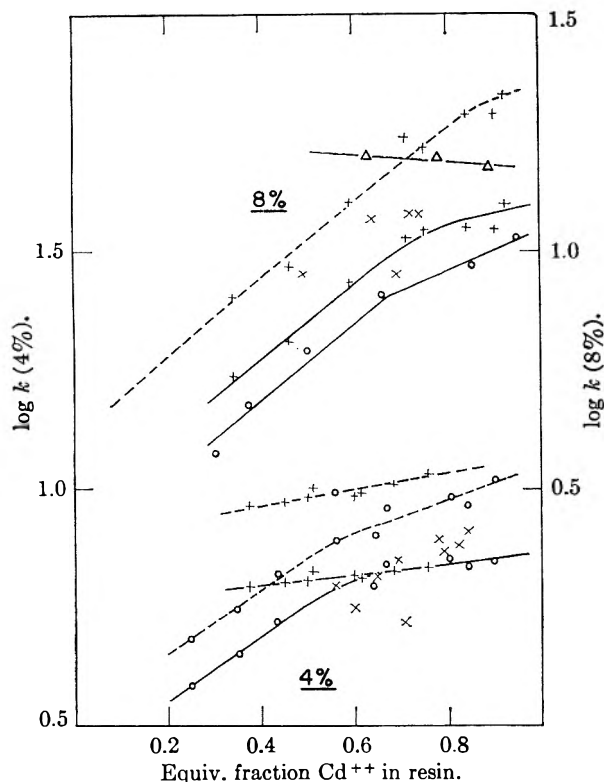


Fig. 4.—Cadmium-hydrogen exchange, 8% and 4% crosslinked resins. Solid lines, concentration quotients; dashed lines, activity quotients. For 8% crosslinking: + 0.146 *N*, 25°; o, 0.146 *N*, 0°; x, Cd resin plus HClO₄, 0.12 *N*, 25°. For 4% crosslinking: +, 0.210 *N*, 25°; o, 0.05 *N*, 25°; x, Cd resin plus HClO₄, 0.18 *N*, 25°. Triangles refer to 16% crosslinked resin, 0.20 *N*, 25°.

in Table II. They were also used to make a small correction to the volume of the solution in the ion exchange equilibrium experiments.

(b) **Salt Uptake.**—The salt uptake by a resin placed in an aqueous solution is a rough indication of ion pairing within the resins or other departure from the behavior of an ideal strong electrolyte. The last column of Table II gives the co-ion uptake expected according to the Donnan equilibrium if the resin phase behaves as an electrolyte solution having the same activity coefficients as the external solution. The measured co-ion uptake was never less than this ideal value, except in one case where there was obviously a small experimental error. Among the divalent metal ions, the uranyl ion showed the least association or departure from ideality; cadmium and barium showed more departure, and lead showed the most. This is roughly, but not exactly, the order of increasing affinity for the resin.

The metal ions may associate with the perchlorate ions, or with the sulfonate ions of the resin, or both. Association with the sulfonate ions seems more likely. If ion pairing occurs the activity of the metal ion in the resin will be reduced, and the activity and concentration of the perchlorate ion correspondingly increased to preserve the Donnan equilibrium. Ion pairing, therefore, could account for the observed co-ion uptake.

(c) **Activity Coefficient Ratios in Solution.**—Figure 1 shows a series of curves for the activity

TABLE I
WATER UPTAKE BY RESINS

Resin cross-linking, %	Cation	Water uptake, g./meq. resin	
		Blotting method	Isopiestic, 96% humidity
4	H ⁺	0.44	...
	Cd ⁺⁺	.35	...
	Pb ⁺⁺	.34	...
	UO ₂ ⁺⁺	.45	...
8	H ⁺	.25	0.192
	70% H ⁺ , 30% Ba ⁺⁺	.21	.134
	40% H ⁺ , 60% Ba ⁺⁺	.13	.099
	Ba ⁺⁺	.13	.102
	Cd ⁺⁺	.19	.159
	Pb ⁺⁺	.145	.120
	UO ₂ ⁺⁺	.18	.143

TABLE II
CO-ION UPTAKE BY RESINS

Resin cross-linking, %	Cation (counter-ion)	Co-ion	Co-ion concn., equiv./kg. water		
			In soln.	In resin	In resin (ideal Donnan)
4	Pb ⁺⁺	ClO ₄ ⁻	0.152	0.123	0.033
	UO ₂ ⁺⁺	ClO ₄ ⁻	.380	.110	.110
	UO ₂ ⁺⁺	ClO ₄ ⁻	.040	.003	.0012
8	H ⁺	ClO ₄ ⁻	.211	.032	.009
	Ba ⁺⁺	ClO ₄ ⁻	.210	.092	.034
	Cd ⁺⁺	ClO ₄ ⁻	.179	.072	.031
	Pb ⁺⁺	ClO ₄ ⁻	.149	.103	.025
	UO ₂ ⁺⁺	ClO ₄ ⁻	.19	(.005)	.0075
	UO ₂ ⁺⁺	Cl ⁻	.090	.011	.011

coefficient ratio, $\gamma_{H^+}/\gamma_{M^{++}}$, as a function of solution composition at constant total ionic strength. In Fig. 2 the activity coefficient ratio for low metal ion:hydrogen ion ratios is plotted against the square root of the ionic strength. Here the experimental curves for lead and cadmium are compared with a curve calculated from the Debye-Hückel equation

$$\log \gamma_{\pm} = - \frac{Az_+z_-\sqrt{\mu}}{1 + Ba\sqrt{\mu}} \quad (2)$$

where μ is the ionic strength, z_+ , z_- are the charges on the ions, a is the mean distance of closest approach (taken as 5.5 Å.), and A , B are equal to 0.509 and 0.330, respectively, for aqueous solutions at 25°. The desired activity coefficient ratio is, of course, $\gamma_{\pm(HClO_4)}/\gamma_{\pm[M(ClO_4)_2]}$. It is assumed that there are no specific ionic interactions.

Neither lead perchlorate-perchlorate mixtures nor cadmium perchlorate-perchloric acid mixtures obey equation 2 exactly. For uranyl perchlorate-perchloric acid mixtures, however, the activity coefficient ratio had to be estimated by using equation 2, since it could not be measured experimentally. For barium perchlorate-perchloric acid mixtures the activity coefficient ratios were calculated by means of Harned's rule, taking the activity coefficients for the individual perchlorates from the compilation of Robinson and Stokes²⁴ and using the interaction coefficients found for barium chloride-hydrochloric acid mixtures.²⁵

(24) R. Robinson and R. H. Stokes, "Electrolytic Solutions," Butterworth's Scientific Publications, London, 1955.

(25) H. S. Harned and R. Gary, *J. Am. Chem. Soc.*, **76**, 5924 (1954).

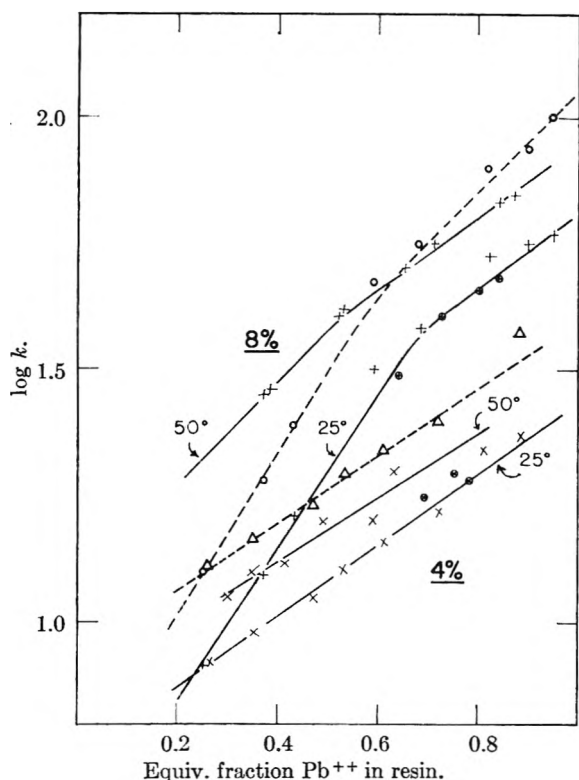


Fig. 5.—Lead-hydrogen exchange, 8% and 4% crosslinked resins. Solid lines, concentration quotients; dashed lines, activity quotients (25° only). +, values for 8% crosslinking; x, values for 4% crosslinking. Circled crosses show k for Pb resin plus 0.126 N $HClO_4$, 25°. Other solution normalities were 0.139 (25°) and 0.146 (50°).

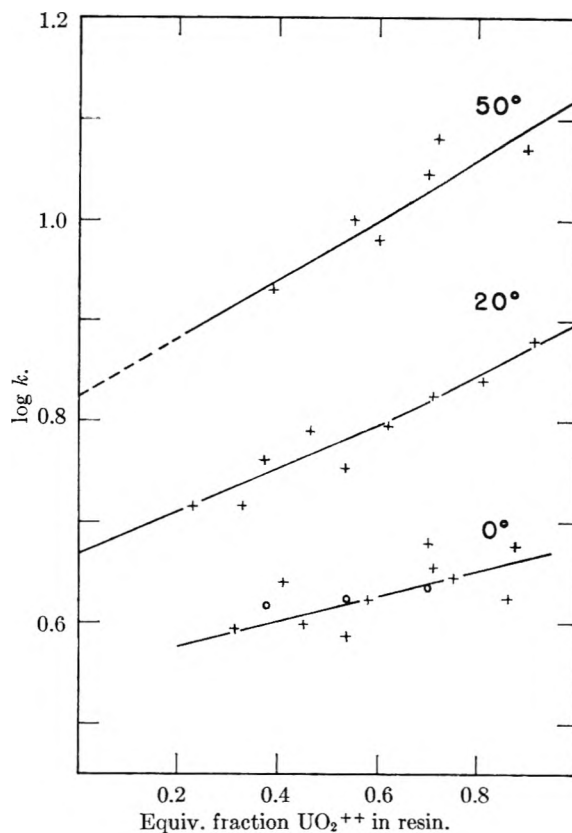


Fig. 7.—Uranyl-hydrogen exchange, 8% crosslinked resin. Concentration quotients only. Crosses, 0.04 N ; circles, 0.09 N .

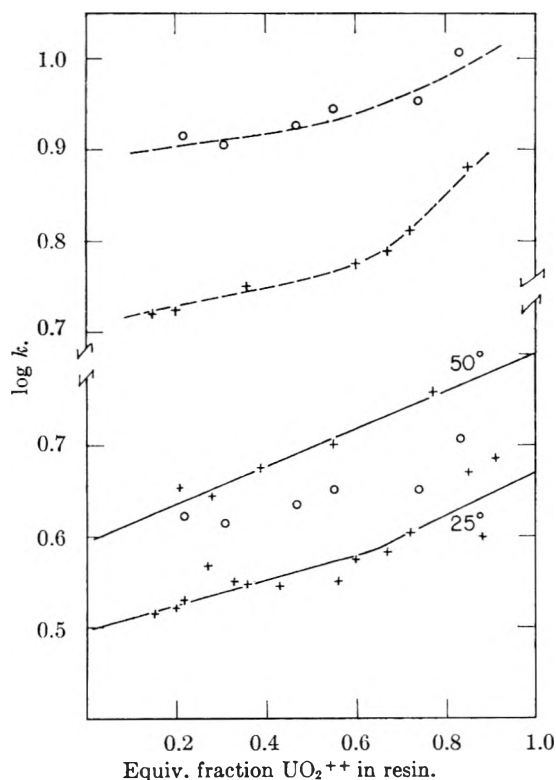


Fig. 6.—Uranyl-hydrogen exchange, 4% crosslinked resin. Solid lines, concentration quotients; dashed lines, activity quotients at 25°: +, 0.09 N ; o, 0.34 N , 25°.

Fortunately, uncertainties in activity coefficient ratios affect the shape of the ion exchange distribution curves only slightly. In most of our equilibrations the final concentration of metal ion in solution was very low, and exceeded the concentration of hydrogen ion only for the very highest metal ion loadings of the resin. Thus the correction of distribution quotients for solution activities did not change the shape of the curves significantly except at the highest values of $N_{M^{++}}$, the equivalent fraction of metal ion in the resin.

(d) **Ion Exchange Distributions.**—In Figs. 3 to 8, distribution quotients are plotted against equivalent fraction of metal in the resin for sets of experiments at constant total normality. The distribution quotient is defined by

$$k = \frac{N_{M^{++}}}{N_{H^+}^2} \times \frac{C_{H^+}^2}{C_{M^{++}}} \quad (3)$$

where the N 's are equivalent fractions of ions in the resin, that is, the number of gram-equivalents per gram-equivalent of resin anions, and the C 's are concentrations in solution in gram-equivalents per liter.

Correcting for solution activities the quotients $k_a = k\gamma_{H^+}^2/\gamma_{M^{++}}$ are obtained. These are plotted as dashed lines in Figs. 3 to 8.

To evaluate activity coefficients for the cation-resin combinations one must choose standard reference states. Then one can define a standard free energy for the ion exchange process. Gaines and Thomas¹⁰ choose as standard states the "pure" res-

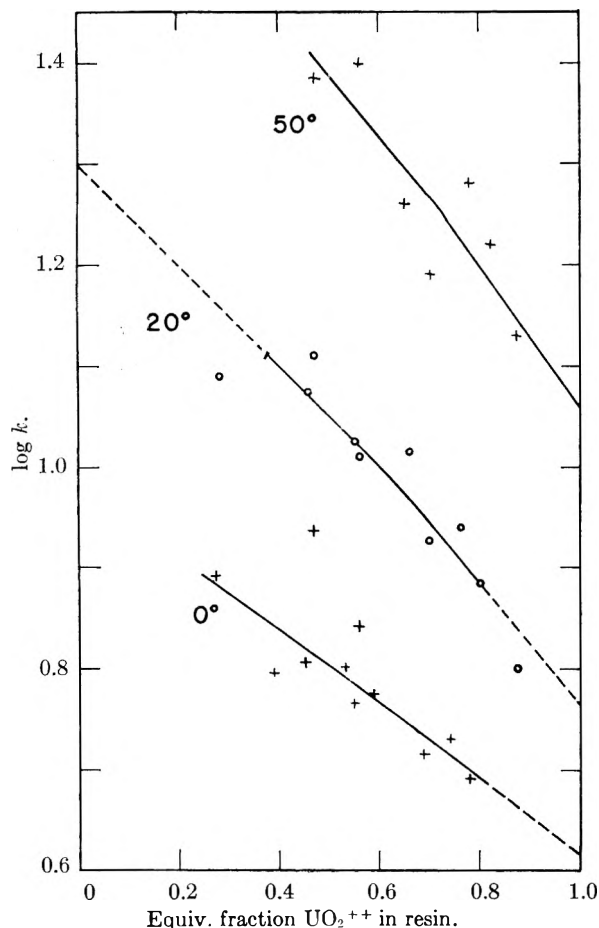
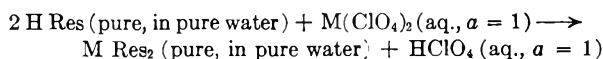


Fig. 8.—Uranyl-hydrogen exchange, 16% crosslinked resin. Concentration quotients only; solutions all 0.04 *N*.

ins, containing one kind of counterion only, in equilibrium with pure water. For the reaction



they show that the equilibrium constant, K , and the standard free energy, ΔF^0 , are given by the equation (here written for divalent ions displacing univalent ions from the resin)

$$\ln K = -\frac{\Delta F^0}{RT} = -1 + \int_0^1 \ln K_a dN_H + \ln \frac{f_M(a)}{f_H^2(b)} - 2 \int_a^b n_a d \ln a_s \quad (4)$$

K_a is expressed in equivalent fractions in the resin and molar concentrations in solution; it equals $2k_a$. The quantities $f_m(a)$ and $f_H(b)$ are the activity coefficients of the pure metal and hydrogen resins in salt and acid solutions of the concentrations used in measuring K_a ; n_a is the number of moles of water per equivalent of exchange sites, and a_s its activity.

The last two terms in equation 4 relate to the water uptake of the resin and its degree of swelling. They were shown by Cruickshank and Meares to contribute not more than 3 cal. to ΔF^0 for the hydrogen-sodium exchange in 0.1 *N* solution.⁷ In the exchanges we studied their contribution is certainly larger. Furthermore, the co-ion uptake, neglected in deriving equation 4, is appreciable.

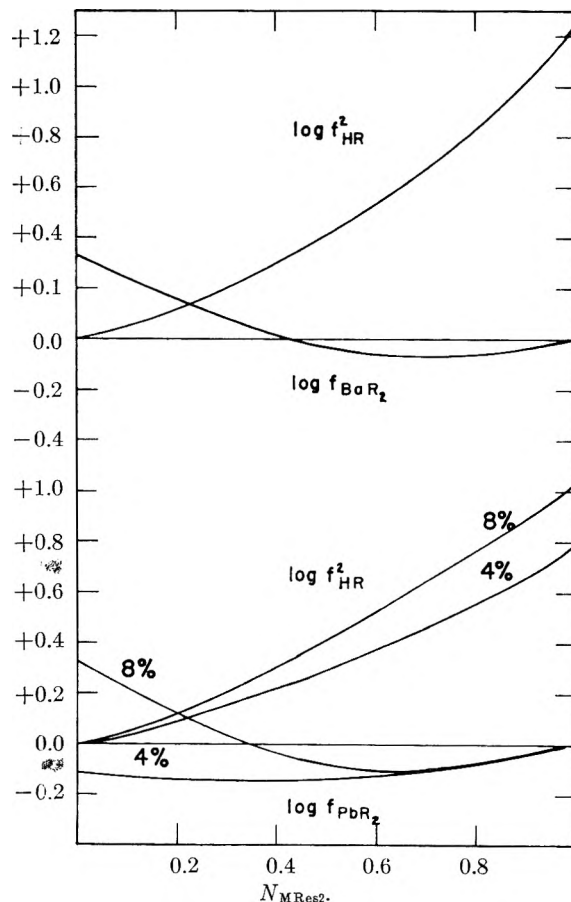


Fig. 9.—Resin activity coefficients, barium-hydrogen and lead-hydrogen exchanges at 25°.

We do not yet have the experimental data to evaluate these effects, and therefore have ignored them in our calculations.

Putting $f_M(a)$, $f_H(b)$ and a_s equal to unity, the activity coefficients of the resins in a mixed resin of composition N_H , N_M are given by¹⁰

$$\ln f_M = -N_H - N_H \ln K_a + \int_0^{N_H} \ln K_a dN_H \quad (5)$$

$$\ln f_H^2 = N_M + N_M \ln K_a - \int_{N_H}^1 \ln K_a dN_H \quad (6)$$

The equilibrium constant then equals

$$K = K_a f_M / f_H^2 \quad (7)$$

Activity coefficients calculated by equations 5 and 6 are shown in Figs. 9 and 10.

Figure 11 shows the temperature dependence of $\log k$ for the $\text{UO}_2^{++}\text{-H}^+$ exchange. The enthalpies of replacement of two moles of hydrogen ion in the resin by one mole of metal ion in this and the other exchanges are given in Table III. For various reasons no great accuracy is claimed for these values.

TABLE III

Cation	ENTHALPY OF EXCHANGE					
	Ba	Cd	Pb		UO ₂	
Resin cross-linking	8	8	4	8	4	8 16
ΔH , cal./mole M^{++}	-50	1600	2000	4400	2600	3000 4600

Discussion of Exchange Equilibria

The most striking feature of the data shown in Figs. 3 to 7 is the increase of distribution quotients with increasing proportion of metal ions. Figure 8, for 16% crosslinked resin, shows a decrease in k with increasing metal ion loading; in all other cases the affinity of the resin for metal ions seems to rise as the proportion of these ions increases.

In part this tendency reflects the choice of equivalent fractions, rather than mole fractions, to describe the concentrations of the metal resinate. A change to mole fraction units would divide k by 2 for $N_M = 0$, by 4 for $N_M = 1$; that is, the rise in k would be diminished by a factor of 2. This would reverse the slope of the graphs in a few cases (mainly for 4% crosslinked resins), but not, for example, in the barium-hydrogen exchange, where k_a increases by a factor of more than 30 as barium replaces hydrogen in the resin.

One might also choose to express metal resinate concentrations with respect to the water content of the resin, that is, as molal concentrations, yet a glance at Table I shows that the change in water content as barium ions replace hydrogen ions, for example, is not nearly enough to explain the change of k with N on a concentration basis alone. There seems no doubt that the affinity of the resin for metal ions increases with increasing loading. The same trend has been found for the $\text{Sr}^{++}\text{-H}^+$ exchange,³ the $\text{Hg}^{++}\text{-H}^+$ exchange,²⁶ and, at high metal ion loadings, for the $\text{Cu}^{++}\text{-H}^+$ and $\text{Zn}^{++}\text{-H}^+$ exchanges. It is observed with certain univalent exchanges too, such as $\text{Cs}^+\text{-K}^+$ and $\text{Ag}^+\text{-H}^+$.²⁸

The selectivity of ion exchange resins is increased by increasing the crosslinking. This is a general trend which many people have observed. Now, the substitution of divalent ions for hydrogen ions has a similar effect to an increase in crosslinking; it shrinks the resin and reduces its water uptake. Another influence that shrinks the resin is an increase in external solution concentration; this particularly affects weakly crosslinked resins. Figures 4 and 6 show that an increase in solution concentration favors the binding of Cd^{++} and UO_2^{++} by 4% cross-linked resin. The increase in k_a is even more than the increase in k . It is more noticeable at lower metal: hydrogen ratios, that is, when the resin swelling is greater.

Thus it seems that any factor which shrinks the resin favors the binding of these divalent ions. An important influence (except, perhaps, with UO_2^{++}) is probably the formation of ion pairs. Ion pairing depends on charges and ionic radii, and should increase greatly as the resin loses water and its internal dielectric constant falls. Evidence for ion association comes from the salt uptake data of Table II. It is also worth noting that in the $\text{Ag}^+\text{-H}^+$ exchange study by Bonner, *et al.*,²⁸ the salt uptake rose sharply with N_{Ag} , paralleling the equilibrium quotient.

(26) H. F. Walton and J. M. Martinez, *J. Phys. Chem.*, **63**, 1318 (1959).

(27) N. J. Meyer, W. J. Argersinger and A. W. Davidson, *J. Am. Chem. Soc.*, **79**, 1024 (1957).

(28) O. D. Bonner, W. J. Argersinger and A. W. Davidson, *ibid.*, **74**, 1044 (1952).

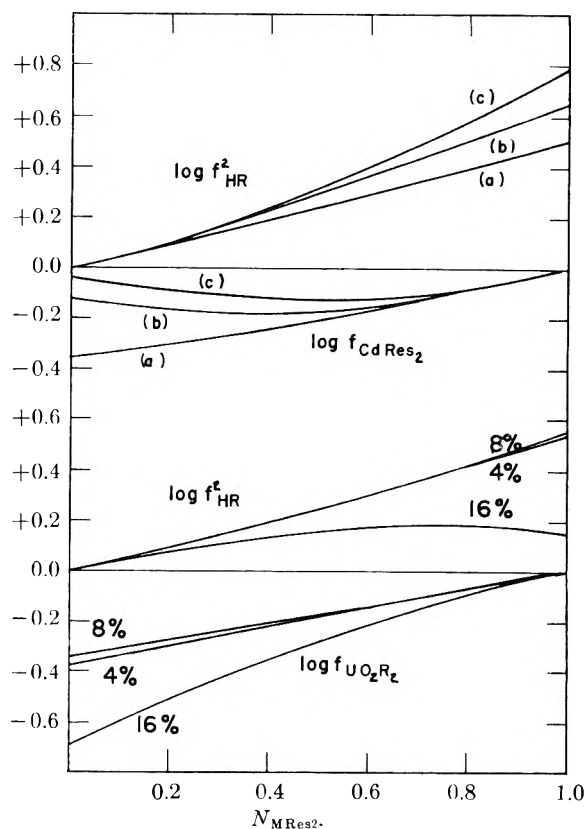


Fig. 10.—Resin activity coefficients, cadmium-hydrogen and uranyl-hydrogen exchanges at 25°. Cadmium-hydrogen: curves (a) and (b), 4% crosslinking, 0.210 and 0.059 N solutions, respectively; curve (c), 8% crosslinking, 0.146 N . Uranyl-hydrogen: 4% crosslinking, 0.09 N solutions; 8 and 16% crosslinking, 0.04 N solutions. Constant activity coefficient ratios are assumed in the uranyl-hydrogen exchanges.

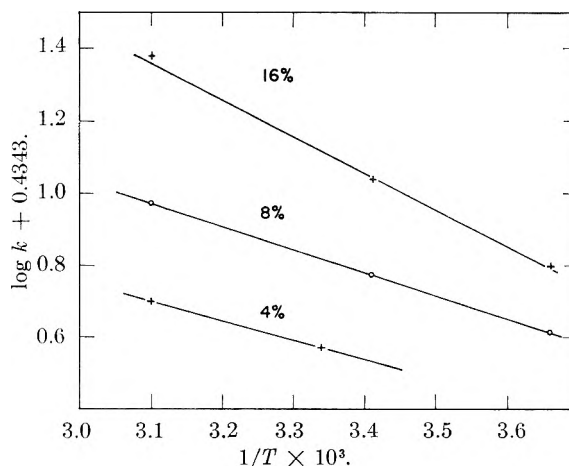


Fig. 11.—Equilibrium constants and temperature, uranyl-hydrogen exchanges.

With high resin crosslinking the steric effect may hinder the uptake of the larger metal ions. The data for the $\text{UO}_2^{++}\text{-H}^+$ exchange in 16% crosslinked resin can be explained in this way (Fig. 8).

In discussing the $\text{UO}_2^{++}\text{-H}^+$ exchange the question arises whether our results might be complicated by hydrolysis of the uranyl ion. We do not think this is likely, because the perchloric acid concen-

tration in solution was almost always more than 0.02 *M*, and Ahrlund²⁹ found the hydrolysis of uranyl perchlorate to be negligible below *pH* 2.5. We made two experiments at *pH* 3-4 and found that hydrolysis products of UO_2^{++} are actually hindered from entering the resin.

The enthalpies of exchange (Table III) are of the same order as those reported by other workers. Direct comparison with the values of Kraus and Raridon⁸ is not possible, as these workers used a resin with 12% crosslinking and loaded it with metal ions to less than 1% of its capacity. For the Ba^{++} - H^+ exchange their data yield a mean

(29) S. Ahrlund, *Acta Chem. Scand.*, **3**, 374 (1949).

ΔH between 25 and 50° of -980 cal./equiv. or -1960 cal./mole, where we found only -50 cal./mole. For the Cd^{++} - H^+ exchange they quote a value of +2800 cal./mole; we found 1600 cal./mole with an 8% crosslinked resin.

Further discussion of the thermodynamics of heavy metal ion exchanges must await more complete and more accurate data, particularly concerning electrolyte uptake and water uptake.

Acknowledgment.—This work was supported by the U. S. Atomic Energy Commission under Contract No. AT (11-1)-499. We wish to express our appreciation, not only for financial support, but for helpful discussions.

STUDIES ON THE ANODIC AND CATHODIC POLARIZATION OF AMALGAMS. PART IV. PASSIVATION OF CADMIUM AND CADMIUM-ZINC AMALGAMS IN ALKALINE SOLUTIONS

BY A. M. SHAMS EL DIN,¹ S. E. KHALAFALLA AND Y. A. EL TANTAWY

Chemistry Department, Faculty of Science, Cairo University, Egypt, U.A.R.

Received November 12, 1960

The passivation of cadmium amalgams of different concentrations was studied in 0.1 *N* NaOH solutions at 25°. The polarization curves obtained under constant currents exhibited one step corresponding to the formation of $\text{Cd}(\text{OH})_2$. The potential of this process depends on the mole fraction of cadmium in the amalgam. The process of passivation is coulombic in nature. The anodic oxidation of cadmium-zinc amalgams gives one oxidation step for high and two oxidation steps for low zinc concentrations. The effect of cadmium on the oxidation step of zinc and that of zinc on the oxidation step of cad-

mium is explained. For the reaction $\text{Zn} + \text{Cd}(\text{OH})_2 \xrightleftharpoons[k_b]{k_f} \text{Zn}(\text{OH})_2 + \text{Cd}$ k_f and k_b are calculated to be 2.33×10^{-21} and 3.53×10^{-46} cm. min.⁻¹, respectively.

The study of the anodic behavior of metallic amalgams offers some advantages over that of solid electrodes of which three deserve mentioning. First, it allows a new variable, *viz.*, the metal atom concentration to be examined. This helps in gaining a deeper insight into the mechanism of passivation of metals. Second, amalgams can be easily prepared in a high state of purity and thus the effect of other metallic impurities is excluded. As will be seen from the results of the present investigation, such traces of impurities can alter the electrodic behavior of the metal under study to a greater or lesser extent depending on their relative concentrations. Finally, due to the liquid nature of the amalgam, both the geometrical and the true surface area of the electrode are the same.

In continuation of previous work on the electrodic behavior of metallic amalgams in solutions where passivity can readily set in, this paper deals with the behavior of simple cadmium amalgams and cadmium-zinc amalgams. No previous reports on amalgams from this standpoint have been published.

The behavior of cadmium amalgams has been studied by some authors in acid and neutral media. Thus, Heyrovsky and Kalousek,² Lingane,³ and

Stakelberg and Freyhold⁴ found that the dropping cadmium electrode (by analogy to the dropping mercury electrode) gave anodic (oxidation) waves in neutral or acid supporting electrolytes due to the dissolution of the cadmium from the amalgam. The limiting currents thus obtained were proportional to the cadmium concentration in the amalgam. Hickling and co-workers^{5,6} invented the inverse polarography where the metal (or metals) present in solution is deposited cathodically on a stationary mercury electrode and then anodically stripped by reducing in steps the cell voltage. Potter and Cooke⁷ applied the same technique but in stripping the metal a continuously changing potential was used. The resulting curves exhibited a peak whose height was proportional to the metal ion concentration in the original solution. Kemula and co-workers⁸ used the hanging mercury drop. Delahay and co-workers^{9,10} applied the potential

(4) M. von Stakelberg and H. V. Freyhold, *Z. physik. Chem.*, **46**, 120 (1940).

(5) A. Hickling and J. Maxwell, *Trans. Faraday Soc.*, **51**, 44 (1955).

(6) A. Hickling, J. Maxwell and J. V. Shenan, *Anal. Chim. Acta*, **14**, 287 (1956).

(7) J. T. Potter and W. D. Cooke, *J. Am. Chem. Soc.*, **77**, 1481 (1955).

(8) W. Kemula, E. Rakowska and Z. Kublik, *J. Electroanal. Chem.*, **1**, 205 (1960).

(9) P. Delahay and C. C. Mattax, *J. Am. Chem. Soc.*, **76**, 874 (1954).

(10) G. Mamantov, P. Papoff and P. Delahay, *ibid.*, **79**, 4034 (1957).

(1) Laboratory of Electrochemistry and Corrosion, National Research Center, Dokki, Cairo.

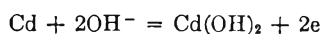
(2) J. Heyrovsky and N. Kalousek, *Coll. Czech. Chem. Commun.*, **11**, 464 (1939).

(3) J. J. Lingane, *J. Am. Chem. Soc.*, **61**, 976 (1939).

step and the current step techniques for the study of traces of metals in solution.

Early work on massive cadmium electrodes was mainly in conjunction with their use in batteries.^{11,12} The last two years have shown, however, an intensified interest in studying the mechanism of cadmium passivation. Lake and Casey's experiments¹³ were conducted under conditions of constant current. The product $i t_p$ (where t_p was the time after which the potential changed to oxygen evolution values—usually hours) was not constant. This value was found to depend on the experimental conditions such as the electrolyte composition and concentration, temperature and current density. As a primary passivating species, CdO was proposed which would later convert to the hydroxide or carbonate—depending on the electrolyte composition—through a soluble intermediate.

Croft,¹⁴ on the other hand, studied the reaction



as a function of over-potential, time and alkali concentration. The results thus obtained showed that the product $i t^{1/2}$ was a constant. In some experiments, however, a continuous transition from $i t = \text{const.}$ to $i t^{1/2} = \text{const.}$ was observed.

Sanghi and co-workers¹⁵ studied the anodic behavior of cadmium in alkaline solutions both galvanostatically and potentiostatically. Polarization curves obtained under constant currents showed one or two arrests depending on the concentration of the alkali and on the current density. Stirring was found to shorten the arrest in dilute solutions and to prolong it in concentrated ones. $i t^{1/2}$ terms were not constant denoting that diffusion was not the rate-determining step in the passivation process.

Lorenz¹⁶ examined galvanostatically the process of passivation of cadmium in sulfate and chloride solutions free from and containing different additions of the corresponding normal cadmium salts. In all the cases studied, the $i \sqrt{t}$ law was found to be obeyed. Nucleation (Keimbildung) of the salt on the surface of the anode was considered to be the rate-determining step in the process of passivation.

Experimental

The electrical circuit used in obtaining anodic and cathodic potential-time curves under conditions of constant current was described in Part I.¹⁷ The electrolytic cell has the same features as described before¹⁷ with the modifications mentioned in Part III.¹⁸ The area of the amalgam electrode amounts to 1.806 cm.². The cadmium amalgam was prepared electrolytically *in situ* from a cadmium sulfate bath containing 0.1620 g. Cd/ml. The exact strength of the plating solution was determined—after its accurate hundred-

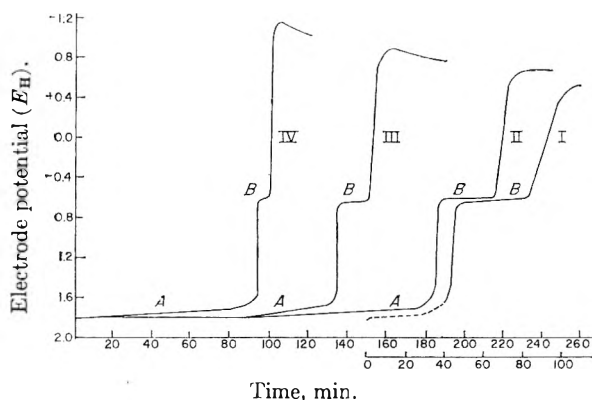


Fig. 1.—Anodic polarization of 1% cadmium amalgam in 0.1 *N* sodium hydroxide solution: I, 15; II, 20; III, 35; and IV, 50 $\mu\text{a.}/\text{electrode}$. Dotted part 300 $\mu\text{a.}/\text{electrode}$.

fold dilution—by titration against an exact 0.01 *M* complexone solution using eriochrome black T as indicator.¹⁹ The complete deposition of the cadmium was ascertained by a spot test using a solution of 8-hydroxyquinoline (0.5 g./100 ml. methyl alcohol).²⁰ The non-appearance of the usual bright golden yellow spot in ultraviolet light indicated the absence of cadmium.

The mixed cadmium-zinc amalgams also were prepared electrolytically. The zinc plating bath was 2 *M* in zinc sulfate and 1 *N* in sulfuric acid. The complete deposition of both metals was ascertained by applying spot tests utilizing 8-hydroxyquinoline²⁰ for zinc and 8-hydroxyquinoline for cadmium. Binary amalgams of the composition (1% Zn + 1% Cd), (0.1% Zn + 1% Cd), (0.1% Zn + 5% Cd) and ($7.25 \times 10^{-4}\%$ Zn + 5% Cd) were prepared by proper dilution. The amalgam was then washed several times with conductivity water and the water was drained off by a special pipet and then by small strips of filter paper. Each experiment was carried out on a new electrode and a fresh solution.

The experiments here described were performed mainly in 0.1 *N* sodium hydroxide solution. The experimental procedure for obtaining the anodic and cathodic polarization curves, as well as the anodic decay curves, was described before.^{17,18} All measurements were carried out at $25 \pm 0.2^\circ$.

Results and Discussion

The Behavior of the Cadmium Amalgam.—The variation of the amalgam-anode potential with time is shown in Fig. 1 for a 1% cadmium amalgam at currents lying between 15–50 $\mu\text{a.}/\text{electrode}$. Amalgams of other cadmium concentrations gave also the same type of curves. As is seen from these curves, two steps A and B are to be distinguished. Part A is ascribed by analogy to the case of pure mercury¹⁷ and the zinc amalgam¹⁸ to the discharging of the sodium amalgam formed during the pre-cathodization period. The quantities of electricity consumed in this process are reproducible to $\pm 5\%$ and depend primarily on the concentration of the cadmium in the amalgam. Average values for this quantity are 330, 254 and 128 mcoulomb. for the three amalgams 5, 1 and 0.1%, respectively. The quantity of electricity used in building up of the sodium amalgam amounts to 3600 mcoulomb. This shows that the presence of the cadmium impurities in the mercury decreases the efficiency of formation of the sodium amalgam. This has been attributed in the case of the zinc amalgam¹⁸ to the ease of evolution of hydrogen on the metal

(19) W. Biedermann and G. Schwarzenbach, *Chimia*, **2**, 56 (1958).

(20) I. I. M. El Beih and M. A. Abou El Naga, *Anal. Chim. Acta*, **17**, 397 (1957).

(11) G. Grube and E. Doetsch, *Z. Elektrochem.*, **42**, 247 (1936).

(12) V. S. Lyzlov and co-workers, *Russ. Pat.*, 53,522 and 53,523, 1939, cited in *C. A.*, **35**, 2800 (1941).

(13) P. E. Lake and E. J. Casey, *J. Electrochem. Soc.*, **105**, 52 (1958).

(14) G. T. Croft, *ibid.*, **106**, 278 (1959).

(15) I. Sanghi, S. Viswanathan and S. Anathanarayanan, *Electrochim. Acta*, **3**, 65 (1960).

(16) W. Lorenz, *Z. physik. Chem. N.F.*, **20**, 95 (1959).

(17) A. M. Shams El Din, S. E. Khalafalla and Y. A. El Tantawy, *J. Phys. Chem.*, **62**, 1307 (1958).

(18) S. E. Khalafalla, A. M. Shams El Din and Y. A. El Tantawy, *ibid.*, **63**, 1252 (1959).

possessing the lower hydrogen overvoltage (zinc and cadmium, respectively). The cathodic current will distribute itself, therefore, between the deposition of sodium on mercury and the evolution of hydrogen on cadmium. The potential of this process will approximate that taking place at the high overpotential metal but the reaction will mostly occur at the low overpotential one. The increase in the sodium deposition efficiency with increasing cadmium content of the amalgam is not, however, fully understood. It might be that cadmium belongs to those metals, *e.g.*, Pb, As, Sn, Sb and Hg, which easily form an alkali metal alloy.²¹

After the completion of the dissolution process of the sodium amalgam, there follows a rapid build up of potential ascribed to the charging of the double layer.^{22,23} The potential range over which this process occurs amounts to approximately 0.9 v. When this process comes to an end, the potential of the electrode remains practically constant (Step B) over a range of time which depends on both the polarizing current and the cadmium content of the amalgam.

The different authors seem not to be in agreement regarding the primary passivation products of cadmium in alkaline solutions. Huber²⁴ from electron diffraction photographs concluded that the primary oxidation product of cadmium in alkaline solutions (NaOH and Na₂CO₃) was the oxide, which was later converted to the hydroxide and carbonate, respectively. The same opinion seems to be accepted by Lake and Casey¹³ and by Sanghi.¹⁵ On the other hand, Croft¹⁴ from X-ray diffraction patterns established that the passivation product of cadmium was the hydroxide and no evidence for the oxide was observed.

According to Huber,²⁴ the conversion of CdO to Cd(OH)₂ is in accordance with the fact that the solubility product of the hydroxide is about one tenth that of the oxide. However, since the reaction between cadmium (atom or ion) and discharging OH⁻ ions is not subject to any overvoltage effect, and as the concentration of the oxygen ions O⁼ is vanishingly small, one is bound to exclude the idea that the rate of crystallization of CdO is higher than that of Cd(OH)₂, thus permitting CdO to deposit first.

The results of the present investigation seem to support the conclusion of Croft¹⁴ rather than that of Huber.²⁴ Table I gives a comparison between the potentials of the systems Cd-Cd(OH)₂ and Cd-CdO and those of Step B observed in the polarization curves at corresponding pH values. The values in columns 3 and 4 are calculated from known thermal data²⁵ and by applying the equation

$$E = E^0 + 0.059 \text{ pOH} - 0.029 \log X_{\text{Cd}} \quad (1)$$

where X_{Cd} is the mole fraction of the cadmium in the alloy. The agreement between the measured

(21) G. Bredig and F. Haber, *Ber.*, **31**, 2741 (1898); F. Haber, *Trans. Electrochem. Soc.*, **2**, 190, 1904.

(22) A. Hickling, *Trans. Faraday Soc.*, **41**, 353 (1945).

(23) S. E. S. El Wakkad and T. M. Salem, *J. Chem. Soc.*, 1389 (1955).

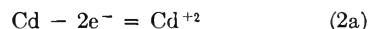
(24) K. Huber, *J. Electrochem. Soc.*, **100**, 37 (1953).

(25) W. M. Latimer, "Oxidation Potentials," Prentice-Hall, New York, N. Y., 1953, pp. 39, 173.

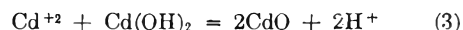
TABLE I

% Cd in amalgam	Starting potent. of Step B	Equil. potent. of Cd-Cd(OH) ₂	Equil. potent. of Cd-CdO
0.1	-0.66	-0.664	-0.621
1.0	- .70	- .692	- .649
5.0	- .72	- .741	- .698

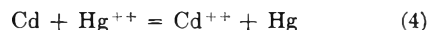
potentials and those of the system Cd-Cd(OH)₂ suggests, therefore, that Cd(OH)₂ is the primary reaction product of cadmium and the discharging OH⁻ ions. This conclusion finds its support in the recent work of Ohse²⁶ in which the anodic behavior of cadmium in alkaline solutions was studied by the intermittent galvanostatic technique. The oscillograms thus obtained showed two potential arrests corresponding to



and then



Similar to the results obtained with the zinc amalgam¹⁸ no step in the polarization curves was observed for the oxidation of mercury. The reason for this appears to be the instantaneous reduction by cadmium (or zinc) of any mercuric ions that may form. Consideration of the standard free energy of the reaction



which has a $\Delta F = -57.96$ kcal. indicates that this reaction is spontaneous. Thus, the mercury has no chance to show its oxidation step.

From the number of coulombs that passed during Step B, one can calculate the number of oxygen atoms that discharged. And by assuming that the number of cadmium atoms on the surface of the electrode is that of the bulk concentration, one can easily calculate the thickness of the hydroxide formed. By so doing, values ranging between 250-1000 molecules were obtained. The oxide thickness decreases, however, as the cadmium concentration in the amalgam is increased. Trials to extend the present study to higher cadmium concentrations and preserving in the meantime the liquid nature of the electrode were unsuccessful.

The plot of the logarithm of the polarizing current i as a function of that of the time of passivation τ yielded almost parallel straight lines for the three amalgams studied. The slopes of these were -0.99, -1.01 and -1.01 for the 5, 1 and 0.1% Cd amalgam, respectively. The average slope could, therefore, be safely taken as -1. This result suggests that the relation between the two variables is $i\tau = \text{const.}$, denoting that the passivation of cadmium amalgams in alkaline solutions is coulombic in nature. In this respect cadmium amalgam differs from both pure mercury^{17,27} and zinc amalgams¹⁸ where diffusion controlled processes were proved to be operative. The behavior of the cadmium amalgam resembles, however, that of the noble metals platinum,²⁸ palladium²⁹ and gold.³⁰

(26) R. W. Ohse, *Z. Elektrochem.*, **64**, 1171 (1960).

(27) A. M. Shams El Din, S. E. Khalafalla and Y. A. El Tantawy, *J. Phys. Chem.*, **63**, 1224 (1959).

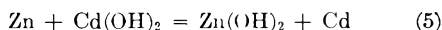
Cathodic polarization curves were obtained when the electrode was at oxygen evolution potentials by reversing the polarizing current so as to make the working electrode the cathode. The behavior of the three amalgams studied is almost the same. The curves showed the reduction of the cadmium hydroxide layer at more or less its reversible potential before the electrode changed to potentials characteristic for the deposition of hydrogen (and sodium).

Anodic decay experiments showed the potential of the electrode to drop directly to the value of the system Cd-Cd(OH)₂ at the corresponding pH value and the particular cadmium metal concentration. Thus this system functions as a proper metal-metal oxide electrode.

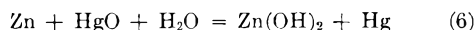
The Behavior of Cadmium-Zinc Amalgams.—

The anodic behavior of copper-tin (speculum)³¹ and zinc-tin³² alloys was studied in this Laboratory. Two general conclusions were reached from these researches. First, each of the alloyed metals oxidizes separately at its particular reversible potential independent of the other metal. Thus, the behavior of the alloy on anodic polarization was the combined behavior of its constituents. Second, the quantities of electricity consumed in the passivation of the alloys were considerably less than those for the pure metals under the same experimental conditions. This revealed the noble character of the alloy. It was of interest to determine whether these conclusions apply also to the case of amalgams.

In Fig. 2 time-potential curves for the mixed amalgam (5% Cd + 0.01% Zn) obtained with constant currents are shown. The currents used varied between 250–500 μ a./electrode. The curves of Fig. 2 show that after the dissolution of the sodium amalgam, there occurs only one step before the electrode changed to the potential of oxygen evolution. The potential of this step corresponds to the building of Zn(OH)₂ at the pH value of the medium and at that particular zinc metal concentration. Neither cadmium nor mercury was oxidized although their concentrations were 500 and 10,000 times that of the zinc. The reason for the disappearance of the cadmium and mercury steps can be easily understood if one takes into consideration the free energy change of the reactions



and



which amount to -19.96 and -61.92 kcal., respectively.³³ The large decrease in the free energy of the above reactions makes the reduction of Cd(OH)₂ and HgO instantaneous so that these two

(28) S. E. S. El Wakkad and S. H. Emara, *J. Chem. Soc.*, 461 (1952).

(29) S. E. S. El Wakkad and A. M. Shams El Din, *ibid.*, 3094 (1954).

(30) S. E. S. El Wakkad and A. M. Shams El Din, *ibid.*, 3098 (1954).

(31) S. E. S. El Wakkad, T. M. Salem, A. M. Shams El Din and Z. Hanafi, *ibid.*, 2857 (1956).

(32) S. E. S. El Wakkad, A. M. Shams El Din and H. Kotb, *J. Electrochem. Soc.*, **105**, 47 (1958).

(33) Ref. 25, pp. 169, 173, 175.

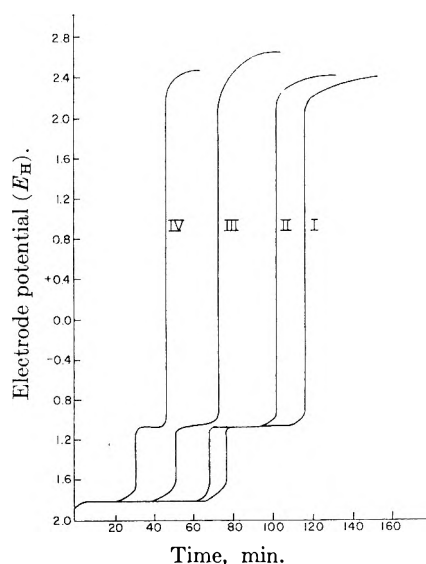


Fig. 2.—Anodic polarization of 5% Cd + 0.01% Zn amalgam in 0.1 *N* sodium hydroxide solution: I, 250; II, 300; III, 400; and IV, 500 μ a./electrode.

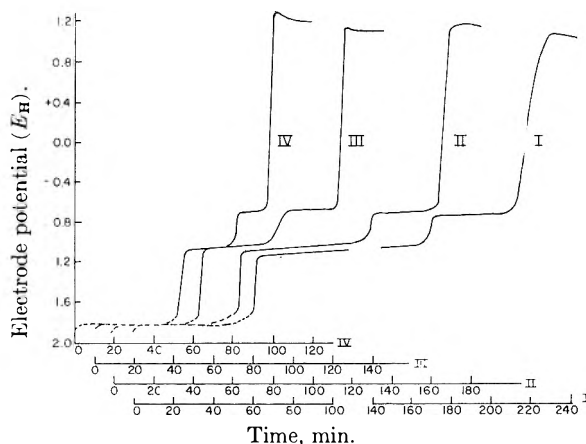


Fig. 3.—Anodic polarization of 5% Cd + 7.25×10^{-4} % Zn amalgam in 0.1 *N* sodium hydroxide solution: I, 35; II, 50; III, 75; and IV, 100 μ a./electrode.

oxidation steps will not appear in the polarization experiment.

It was felt that if one decreases the concentration of zinc in the amalgam to a very low value and increases that of the cadmium to a comparatively high one, one can vary the free energy change of reaction 5 in the direction of zero or possibly positive values. This would give the cadmium in the amalgam a chance to oxidize in its normal way. Several amalgams having high Cd/Zn concentration ratio were experimented with and the amalgam having the composition of (5% Cd + 7.25×10^{-4} % Zn) gave the expected result. In Fig. 3 the anodic oxidation of this amalgam under different polarizing currents is shown. The dotted parts of the curves show the discharge of the sodium amalgam at a current of 300 μ a./electrode to enhance its dissolution. The rest of the curves were run at the currents given in the legend. The starting potential of the zinc oxidation step is -1.06 v. and that of the cadmium is -0.70 v. Calculated values are, respectively, -1.05 and -0.72 v. The agreement between the two sets of potentials is convincing

that both metals are oxidized. Under these conditions of metal concentration (or with still lower Zn/Cd ratio) the behavior of the mixed amalgams resembles that of metallic alloys.

Of extreme interest is the influence of the cadmium on the oxidation process of zinc. Thus, it has been shown that the oxidation of zinc amalgams is a diffusion controlled process.¹⁸ A plot of the logarithm of the passivation time τ against that of the passivating current gave parallel straight lines whose slope amounted to -2 . Similar plots for the (5% Cd + 0.01% Zn) amalgam (in which the oxidation step of cadmium does not appear) gave a straight line of slope equal to -1.56 . The (5% Cd + 7.25×10^{-4} % Zn) amalgam, on the other hand, (in which the oxidation step of cadmium appears) gave a slope of -1.27 .

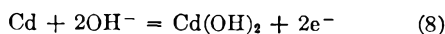
Thermodynamically it is improbable for $\text{Cd}(\text{OH})_2$ to form in the presence of metallic zinc. However, from the kinetic point of view, it is equally probable that a discharging OH^- ion can react with a cadmium or a zinc atom on the surface of the electrode. This probability increases as the concentration of the cadmium in the amalgam increases or that of zinc decreases. Once cadmium hydroxide is formed, it is reduced to the metallic state by zinc. This state of affairs could be treated in a more quantitative manner as follows.

The oxidation of the zinc in the amalgam—being a diffusion controlled process—is expected to follow the relation

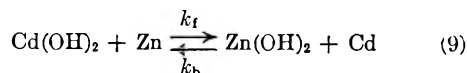
$$i\tau^{1/2} = \frac{nFC\pi^{1/2}D^{1/2}}{2} \quad (7)$$

where D is the diffusion coefficient and C the concentration of the diffusing species. For pure zinc amalgams the product $i\tau^{1/2}$ is constant and independent of the polarizing current i .¹⁸ For the mixed zinc-cadmium amalgams, on the other hand, this is not the case. The plot of $i\tau^{1/2}_{\text{Zn}}$ against the polarization current i gave a perfect straight line which could be expressed in the form $i\tau^{1/2}_{\text{Zn}} = 285 + 2.77_8 i$. This shows that the process occurring at this potential is not completely diffusion controlled.

Evidently such deviation from expectation is due to the reaction



followed by the kinetic reaction



The result of the occurrence of reaction 9 is that the zinc step should increase at the expense of the cadmium present. Expressed in other words, the step in the anodic polarization curves occurring at the Zn-Zn(OH)₂ potential is in fact composed of two parts. The first one is that which should occur if the amalgam contained only zinc. Its duration is determined by a diffusion process and could be represented by τ_d . The second part is that due to the generation of newly formed zinc hydroxide by some of the cadmium which struggles to form a hydroxide but is reduced by the zinc metal of the amalgam. This added duration to the

zinc step is kinetic in nature and could be symbolized by τ_k .

For a pure zinc amalgam (not containing cadmium) of a concentration of 7.25×10^{-4} % Zn, the product $i\tau^{1/2}$ is practically constant and amounts to $285 \mu\text{a. min}^{1/2}/\text{electrode}$.³⁴ The difference between the measured $i\tau^{1/2}_{\text{Zn}}$ values at the different currents and $i\tau^{1/2}_d$ will give the corresponding values of $i\tau^{1/2}_k$.

For an anodic electrochemical reaction preceded by a chemical reaction, $i\tau^{1/2}_k$ is related to the polarizing current i and to the reaction constants by the equation³⁵

$$i\tau^{1/2}_k = i\tau^{1/2}_d - \frac{\pi^{1/2}}{2K(k_f + k_b)^{1/2}} \times i \quad (10)$$

where K is the equilibrium constant for the first-order chemical reaction preceding the electrochemical one, k_f and k_b are the forward and backward rate constants for the chemical reaction. This shows that the plot of $i\tau^{1/2}_{\text{Zn}}$ vs. i possesses a slope of

$$\frac{\pi^{1/2}}{2K(k_f + k_b)^{1/2}}$$

The equilibrium constant K of reaction 9 could be calculated from thermodynamical data. Thus, at 25°

$$\Delta F = -RT \ln K = -20.14 \text{ kcal.}^{36}$$

Hence

$$K = \frac{k_f}{k_b} = 6.61 \times 10^{14}$$

On the assumption that reaction 9 occurs in one step and with the help of the slope of the $i\tau^{1/2}_{\text{Zn}}$ vs. i plot (2.77₈) and the value of K one calculates

$$k_f = 2.33 \times 10^{-31} \text{ cm. min.}^{-1}$$

and

$$k_b = 3.53 \times 10^{-46} \text{ cm. min.}^{-1}$$

The presence of zinc in the amalgam also affects the process of oxidation of cadmium but, however, in a different manner. Although the process of oxidation remains coulombic in nature, yet the quantities of electricity consumed in the cadmium hydroxide step are larger in the presence of zinc than in its absence. For the pure 5% Cd amalgam (not containing zinc) the average quantity of electricity consumed in building up of the cadmium hydroxide layer amounts to $42700 \mu\text{coulomb}$. The corresponding figure for the same amalgam but containing 7.25×10^{-4} % Zn is $103100 \mu\text{coulomb}$. This increase in the quantity of electricity is due to both a further oxidation of the zinc along this step and to the reoxidation of the cadmium reduced by the zinc metal.

Another fact to be mentioned in connection with the presence of zinc on the polarization characteristic of the amalgam concerns the potential of oxygen evolution on the mixed amalgam electrode. Thus, the presence of traces of zinc in the amalgam increases the overpotential of oxygen evolution from that characteristic for cadmium to that on

(34) Y. A. El Tantawy, M.Sc. Thesis, Cairo University, 1959.

(35) P. Delahay, "New Instrumental Methods in Electrochemistry," Interscience Publishers Inc., New York, N. Y., 1954, p. 199.

(36) Ref. 25, pp. 168 and 173.

zinc and zinc amalgams. The same behavior was also observed on solid alloys of zinc and tin.³¹

Cathodic polarization curves for the mixed amalgams are rather simple. These curves show only one step corresponding to the reduction of the zinc hydroxide film at its reversible potential. No step for the reduction of $\text{Cd}(\text{OH})_2$ is observed. Most probably the process of reduction of the oxides starts at the interface metal-oxide. The generated zinc atoms will reduce the cadmium hydroxide layer chemically before it has a chance to be reduced electrochemically. The same type of curves also is observed with amalgams not showing the $\text{Cd}(\text{OH})_2$ oxidation step.

Anodic decay curves on the other hand reveal that the cadmium hydroxide is stable once it is separated from the metallic electrode by a layer of zinc hydroxide. Amalgams not showing the oxidation step of cadmium give anodic decay curves characteristic of zinc.

In conclusion, it is here suggested that the product $i\tau^{1/2}$, obtained under conditions of constant

currents, be termed the "Passivation Index" since it gives a clear understanding of the process of passivation. Thus, when this index is constant and independent of the polarizing current, then the process of oxide formation is governed by diffusion. The variation of the experimental conditions will enable the establishment of the diffusing species.

On the other hand, when the index $i\tau^{1/2}$ increases parabolically with the polarizing current, *i.e.*, $i\tau = At^{1/2}$ or $i\tau = \text{const.}$, then the formation of the oxide film is coulombic.

Finally, when the product $i\tau^{1/2}$ increases linearly with the polarizing current, then the metal (or alloy) contains a second constituent—perhaps in traces—which is nobler than the metal whose oxide is being formed. The duration of the oxide formation is thus partly due to a kinetic process. The noble metal might or might not be oxidized depending on its relative concentration and on the difference between the formal electrode potentials of the two metals.

RELATIONS AMONG THE SOLUBILITIES OF NITROGEN, ARGON AND OXYGEN IN DISTILLED WATER AND SEA WATER¹

BY BRUCE B. BENSON AND PETER D. M. PARKER²

Department of Physics, Amherst College, Amherst, Massachusetts, and Woods Hole Oceanographic Institution, Woods Hole, Massachusetts

Received December 12, 1960

Experiments have been carried out with a mass spectrometer to determine the ratio of the solubilities of nitrogen and argon in distilled water and sea water as a function of temperature. The literature on the solubilities of nitrogen, oxygen and argon has been examined critically in an attempt to clarify a generally confusing situation. The nitrogen/argon ratios, together with the results from somewhat less precise nitrogen/oxygen solubility ratio measurements reported here, have been used to intercompare the solubility determinations on the three gases as made by various workers. For distilled water seven independent lines of evidence are internally consistent, and it is suggested that the most reliable results are oxygen solubility coefficients from Elmore and Hayes, "atmospheric nitrogen" solubility coefficients from Hamberg, and the ratios of the solubility coefficients for nitrogen and argon from this research. From these, all the solubility coefficients for distilled water can be calculated. For sea water the situation is less clear cut, but it is suggested that the best data available are oxygen solubilities from Fox, Rakestraw and Emmel nitrogen solubilities corrected to dry air, and nitrogen to argon solubility ratios from this research. A combination of the last two provides the first information available on the solubility of pure argon in sea water.

Introduction

During the course of experiments by Benson and Parker,³ and Richards and Benson,⁴ on gaseous nitrogen and argon dissolved in sea water, it became desirable to know with an accuracy approaching 0.1%, the ratio of the saturated solubilities of the two gases in sea water equilibrated with atmospheric air.

Values for the solubility of nitrogen in sea water have been given by Fox⁵ and Rakestraw

and Emmel.⁶ Their results disagreed markedly with one another. For example, at 0° Rakestraw and Emmel reported values approximately 1.2% higher than Fox (after correction for argon), while at 25° their values were lower than those of Fox by 7.5%. The only available data for argon were those of Rakestraw and Emmel,⁶ which they have stated⁷ to be "probably no more accurate than to about 5% . . ." Furthermore, the "argon" to which they referred was the total residual gas after removal of carbon dioxide, oxygen and nitrogen.

Because the uncertainties in the nitrogen and argon solubilities were considerably greater than the accuracy required for our work, new experiments employing a mass spectrometer were undertaken to determine the ratio of the two solubilities

(1) Contribution No. 1154 from the Woods Hole Oceanographic Institution. This research was supported in part by National Science Foundation grant G4650 to Amherst College. A major part of the preparation of the material for the manuscript was carried out during 1959, when B.B.B. was the recipient of a John Simon Guggenheim Memorial Fellowship.

(2) Now National Science Foundation Fellow and Danforth Fellow, Department of Physics, California Institute of Technology, Pasadena, California.

(3) B. B. Benson and P. D. M. Parker, *Deep-Sea Res.*, **7**, 237 (1961).

(4) F. A. Richards and B. B. Benson *ibid.*, **7**, 254 (1961).

(5) C. J. J. Fox, *Trans. Faraday Soc.*, **5**, 68 (1909).

(6) N. W. Rakestraw and V. M. Emmel, *J. Phys. Chem.*, **42**, 1211 (1938).

(7) N. W. Rakestraw and V. M. Emmel, *J. Marine Res.*, **1**, 207 (1938).

in sea water as a function of temperature and salinity, and in distilled water as a function of temperature.

In addition an attempt was made to obtain the individual solubilities of nitrogen and argon. The procedure involved gasometric determinations of the total nitrogen, oxygen and argon extracted from water equilibrated with air, together with measurements of the ratio of nitrogen to oxygen and the ratio of nitrogen to argon. Unfortunately, the volumetric results were not reliable and they are not reported here, but it was realized that the two kinds of ratio measurements, alone, provided a means for at least a partial clarification of the generally confusing situation with respect to gas solubilities. Recently, for example, the solubility of oxygen has been a subject of particular controversy.⁸⁻¹¹

In general, it probably is correct to state that although the precision of solubility measurements—gauged by the gross amplitude of scatter of repeated measurements—has ranged approximately from 1 to 0.5%, the results from various workers have differed by as much as 3%, even for a gas as extensively studied as oxygen. Stated in another way: gas solubility measurements have been subject to small random errors but large systematic errors.

In the absence of demonstrable sources of systematic error, the only basis for choosing one set of results as probably the most reliable for a particular gas has been substantiation by several workers on that single gas. For example, the fact that the values for oxygen in distilled water found by Elmore and Hayes,¹¹ Morris,¹⁰ Fox,⁵ and Winkler¹² are in essential agreement (0 to 1%, depending upon temperature), justifies the conclusion that some average of these values *probably* is more accurate than the values of Truesdale, *et al.*⁸ (The fact that Elmore and Hayes carried out more experiments than anyone else, and found excellent "consistency," indicates only that their precision was very good, not that they had a smaller systematic error than, for example, Fox.) Nevertheless, the odds of 4 to 1 against Truesdale, *et al.*, are not overwhelming, and it is of interest to obtain further evidence on the question. With respect to nitrogen and argon, and to oxygen in sea water, the situation is still cloudier, because fewer measurements have been made and, as indicated earlier, the differences among workers are larger.

Direct measurements of the ratios of solubilities are of particular interest, because they permit *intercomparisons* of measurements of various workers on *different* gases, in addition to comparisons of determinations on a single gas. The procedure is an extension of the idea above—an attempt is made to find internally consistent sets of solubility and solubility ratio results for two or

more gases. Alternatively, if the solubilities of one gas have been established accurately, ratio measurements can yield the solubilities of other gases. In either case, it is customary to make the tacit assumption that the solubility of a gas under normal atmospheric conditions is independent of the other gases present. In the absence of evidence to the contrary, we shall in this paper take this assumption to be valid.

Ratio measurements with a mass spectrometer have certain inherent advantages for attacking the question of systematic errors in gas solubility determinations. Lack of achievement of "true" equilibrium, variation of atmospheric pressure, incomplete extraction of the dissolved gases, uncertainties in relative humidity, and gas impurities, cause either no effect or, at worst, second-order effects due to differences in rates of solution. The only serious source of systematic error in the measurement of solubility ratios is in the preparation of standards for calibrating the mass spectrometer.

The results reported here should be considered preliminary, and some of the conclusions tentative. Nevertheless, we believe that certain of the values are more reliable than those previously available, and that partial clarification of the issue regarding gas solubilities has been achieved. Further experiments are now in progress for very accurate determinations of both solubilities and solubility ratios.

Experimental Procedures

For purposes of discussion, the procedures employed can be divided into three parts: (A) water-air equilibration; (B) extraction of the dissolved gases; and (C) mass spectrometric analyses of the gases.

A. The procedure for equilibration was suggested by the work of Rakestraw and Emmel.⁶ Four flasks, open to the atmosphere, were almost completely immersed in a constant temperature bath. One of the flasks contained distilled water and the other three contained natural, untreated sea water with salinities of approximately 32, 34 and 36‰, respectively. The 32 and 34‰ waters were made by diluting the 36‰ water with distilled water. The partially submerged flasks were suspended in such a way that they were subject to a constant but gentle agitation from the motion of the water in the bath. The bath was maintained at a given temperature to within $\pm 0.05^\circ$. At the time the measurements were made no standard thermometer was available. Since then, however, the thermometer which was used has been checked and found to be sufficiently accurate (maximum error 0.15°) for these preliminary solubility ratio determinations.

After equilibrating a set of samples for at least sixty hours, each sample was transferred to a glass sample bulb, which had been brought to the temperature of the bath by partial immersion. A six millimeter T-bore, pressure type, precision grade stopcock attached to the bulb permitted a thistle tube to be inserted through it to the bottom of the bulb. In this way the air in the bulb could be displaced gently without trapping air bubbles. After flowing the water up through the stopcock, the stopcock was closed, thereby isolating the water sample which completely filled the bulb. The bulbs had volumes of approximately 200 cc. Samples of water from each flask also were put in small bottles, sealed, and sent to the Woods Hole Oceanographic Institution where the salinity of each was determined.

B. For extraction of the dissolved gases, a water sample bulb was attached by means of a standard taper joint to a vacuum system consisting of a one liter "extraction bulb," a Dry-Ice-acetone trap for water vapor, a liquid air trap for other condensable vapors, particularly carbon dioxide, and a mercury Toepler pump and gasometric system.

(8) G. A. Truesdale, A. L. Downing and G. F. Lowden, *J. Appl. Chem.*, **5**, 53 (1955).

(9) H. Steen, *Limnology and Oceanography*, **3**, 423 (1958).

(10) J. C. Morris, Final Report, Contract No. SAPH 69705, Department of Health, Education and Welfare with Harvard University, 5/1/58 to 1/31/59.

(11) H. L. Elmore and T. W. Hayes, *Proc. ASCE*, **86**, 2556 (1960).

(12) L. W. Winkler, *Ber. Deutsch. Chem. Ges.*, **22**, 1764 (1889); Winkler, *ibid.*, **24**, 3602 (1891).

After pumping down the system (including the T-bore stopcock on the water sample bulb) to approximately one micron, the sample was admitted to the system and the dissolved gases Toepler-pumped off. To ensure complete extraction of the dissolved gases the procedure of Cook and Hanson¹³ was followed. They reported complete extraction when 10 to 20% of the solvent was boiled off over a period of one to two hours. In our case between 40 and 90% (on the average approximately 70%) of the water in the extraction bulb was evaporated, and retrapped in the Dry Ice-acetone trap, over a period of one hour. With the condensable vapors removed, gas was transferred to a gas sample tube for analysis on the mass spectrometer. (Procedures carried out for the attempt at solubility determinations have not been included in this description.)

C. With the exception of the electronic circuitry, the mass spectrometer is like the 60° magnetic sector, single-focusing machine described by Nier.¹⁴ In addition the instrument is equipped with a dual sample system [McKinney, *et al.*¹⁵] for precision isotope ratio analysis.

Employing "single collection" techniques with the mass spectrometer, the relative sizes of the beams for $m/q = 28, 32$ and 40 (molecular nitrogen, oxygen and argon, respectively) were determined for each extracted gas sample and for carbon dioxide-free air used as a standard gas to calibrate the spectrometer. From these measurements the ratio of nitrogen to oxygen, and a tentative value for the ratio of nitrogen to argon, could be calculated with accuracies of approximately 1%.

"Standard air" samples were taken outdoors by opening an evacuated and outgassed sample tube while holding it at arm's length and approximately five feet above the ground. Within the precision of our measurements, no differences in the nitrogen/oxygen/argon ratios were apparent between winter and summer. Carbon dioxide (and water vapor) were removed by immersing the tube in liquid air and transferring the uncondensed gases to another evacuated tube. The percentages of the gases in air were taken to be nitrogen 78.08%, oxygen 20.94%, argon 0.93%, carbon dioxide 0.032%, and traces of the rarer gases. The figure for oxygen is the mean of the values from P. F. Scholander as quoted by Richards,¹⁶ and the figure for nitrogen was chosen to be consistent with the oxygen value. The percentage for argon is from Paneth.¹⁷

For more accurate analysis of the ratio of nitrogen to argon, another portion of the extracted gas was processed to remove the oxygen by cycling the gas through a manifold consisting of a "Vycor" furnace filled with copper turnings at 700°, in series with a liquid air trap. This procedure is necessary for precise analyses of nitrogen, because when oxygen is present in a gas sample, the high temperature conditions in the mass spectrometer ion source cause a small part of the oxygen to combine with carbon impurities to form carbon monoxide. Since carbon monoxide also has a molecular weight of 28 for the most abundant isotopes, the 28/40 ion beam ratio will not be a measure of the true nitrogen to argon ratio. With a "clean" mass spectrometer the effect is small enough so that when both the sample and the standard gases contain oxygen, and when appropriate corrections are made, an accuracy of 1% is possible for the nitrogen/argon ratio, but higher accuracy requires removal of the oxygen in both samples. It is evident that analyses of nitrogen should not be carried out on a mass spectrometer used for analyses of organic materials. Tests have shown that when a pure nitrogen and argon mixture is processed in the "Vycor" furnace, the ratio of nitrogen to argon is unaffected.

After processing, the samples were reanalyzed on the spectrometer. In these measurements the amplifier system was made more sensitive by inserting a "bucking" potential so that the recorded signal was the difference between the beam signal and the bucking potential. In addition the effect of spectrometer drift was reduced by a magnetic

field switching arrangement which permitted rapid switching from one beam to the other. The gross scatter of these measurements of the nitrogen to argon ratio was approximately $\pm 0.3\%$ ($\pm 0.15\%$ each, for the sample and standard).

In order to avoid any possible dependence of mass spectrometer ion source "discrimination" upon the nitrogen to argon ratio (this was a significant question because the ratio in the dissolved gases is approximately 39 to 1, whereas in air it is 84 to 1), standard samples were made up from tank nitrogen and tank argon with ratios comparable to those for the dissolved gases. Appropriate corrections were made for impurities in the tank gases.

As a check an air standard, with the oxygen removed, also was analyzed. The spectrometer correction factor (*i.e.*, the number by which the 28/40 beam ratio was multiplied to give the nitrogen to argon ratio) obtained was somewhat smaller than with the artificial standards. Unfortunately, the experiments had to be terminated before it could be established definitely that this result was caused by a difference in discrimination and was not the result of a systematic error in the volumetric preparation of the standards. For this reason we must assign a possible systematic error of $-0, +1.5\%$ to the absolute values for the nitrogen/argon ratios. The ratios given are based on the artificial standards. This possible systematic error would not apply, however, to the results on gases dissolved in the oceans reported in (3) and (4), because the same spectrometer correction factor was used in that work as in these solubility measurements.

Experimental Results and Discussion

As used throughout this paper, the solubility of a particular gas is defined to be the number of cc. of gas, measured at standard temperature and pressure, dissolved in one liter of water in equilibrium with a normal, free, dry atmosphere with total pressure 760 mm. of mercury. As stated earlier, a "normal" atmosphere was assumed to have a composition by volume of 78.08% nitrogen, 20.94% oxygen, 0.93% argon, 0.032% carbon dioxide, and traces of rarer gases. By "dry" is meant that the total partial pressure of the atmospheric gases, excluding water vapor, is 760 mm. of mercury. The symbols N_2' , O_2' and A' denote the respective solubilities.

The solubility coefficient α for a particular gas is the number of cc. of gas, measured at standard temperature and pressure, dissolved in one liter of water in equilibrium with the gas when its partial pressure is 760 mm. of mercury. We shall use solubility coefficients when discussing pure water, and solubilities when referring to sea water.

Following Fox,⁵ "atmospheric nitrogen"¹⁸ is defined in this paper to be a mixture of nitrogen and argon, although, of course, as measured by him and others it is truly a mixture of nitrogen, argon, helium and the other inert gases, and perhaps nitrous oxide, etc. (depending upon the techniques used to prepare the gas). A moment's reflection reveals that neglecting the gases other than nitrogen and argon introduces a negligible error in the calculations of both nitrogen and argon, when the "true" nitrogen/argon ratio is combined with the "atmospheric nitrogen" solubility.

Table I gives the experimental data for the ratios

(13) M. W. Cook and D. N. Hanson, *Rev. Sci. Instr.*, **28**, 370 (1957).

(14) A. O. Nier, *Rev. Sci. Instr.*, **18**, 398 (1947).

(15) C. R. McKinney, J. M. McCrea, S. Epstein, H. A. Allen and H. C. Urey, *ibid.*, **21**, 724 (1950).

(16) F. A. Richards, "Some Current Aspects of Chemical Oceanography," in "Physics and Chemistry of the Earth," Vol. 2, page 103, Pergamon Press, New York, N. Y., 1957.

(17) F. A. Paneth, *Quart. J. Roy. Meteorol. Soc.*, **63**, 433 (1937).

(18) With the availability of various modern analytical techniques, we suggest that in the future this use of the phrase "atmospheric nitrogen" be dropped. It would seem to make more sense to have it mean literally "nitrogen in or from the atmosphere," so that, for instance, one could distinguish clearly and easily between dissolved nitrogen whose source was the atmosphere and dissolved nitrogen from other sources such as biochemical activity.⁴

N_2'/A' and N_2'/O_2' at various temperatures and salinities. It may be noted that the measured salinities for the sea water measurements at 30° are slightly higher than for the lower temperatures. This presumably resulted from partial net evaporation of water from the samples in the open flasks. The standard deviation of the N_2'/A' mass spectrometric determinations was approximately 0.2%. As indicated above, less care was taken with the N_2'/O_2' measurements, and the analytical precision was approximately $\pm 1\%$. The fourth figure, therefore, is not significant.

TABLE I

EXPERIMENTAL DATA FOR N_2'/A' AND N_2'/O_2' AS FUNCTIONS OF TEMPERATURE AND SALINITY

Salinity, ‰	Temp., °C.	N_2'/A'	N_2'/O_2'
0.066	0.0	37.92	1.836
.066	5.0	38.29	1.825
.48	10.0	38.42	1.826
.066	15.0	38.66	1.859
.084	20.0	39.03	1.887
.11	25.0	39.43	1.941
.102	30.0	39.71	1.987
32.59	0.0	37.78	1.833
32.565	5.0	37.78	1.803
32.60	10.0	38.00	1.830
32.65	15.0	37.51 ^a	1.821 ^a
32.58	20.0	38.47	1.907
32.65	25.0	38.78	1.934
32.97	30.0	39.25	1.954
34.70	0.0	37.52	1.845
34.70	5.0	37.64	1.816
34.71	10.0	38.05	1.828
34.67	15.0	37.96	1.833
34.695	20.0	38.28	1.858
34.65	25.0	38.89	1.947
35.11	30.0	39.23	1.926
36.12	0.0	37.74	1.860
36.14	5.0	37.72	1.821
36.17	10.0	37.80	1.803
36.16	15.0	37.96	1.830
36.17	20.0	38.45	1.870
36.23	25.0	38.73	1.914
36.61	30.0	39.24	1.918

^a These two values were rejected.

A. Distilled Water.—A plot of the values for N_2'/A' vs. temperature in distilled water yields a straight line within the analytical precision of $\pm 0.2\%$. The least squares fit for the data is

$$N_2'/A' = 37.90 + 0.0590t$$

with a standard deviation of 0.076 or approximately 0.2% of the mean N_2'/A' . Values calculated from this equation are tabulated in Table II. As stated previously, they may be systematically high by approximately 1.5%.

In Table III the ratios of the solubility coefficients have been calculated from the expression

$$\frac{\alpha_{N_2}}{\alpha_A} = \frac{0.93N_2'}{78.08A'}$$

using our values for N_2'/A' . The values for $\alpha_{N_2Atm.}$ from the work of Hamberg,¹⁹ Winkler¹²

and Fox⁵ have been taken from Coste,^{20,21} who included corrections (first suggested by Fox) to the Winkler and Fox results, required because of the effect of differences in the solubilities of nitrogen and argon in the closed system absorptometric type of experiment. Since $\alpha_{N_2Atm.} = 0.98823\alpha_{N_2} + 0.01177\alpha_A$, it can be shown that

$$\alpha_{N_2} = \frac{\alpha_{N_2Atm.}}{0.98823 + \frac{0.01177}{(\alpha_{N_2}/\alpha_A)}}$$

$$\alpha_A = \alpha_{N_2}/(\alpha_{N_2}/\alpha_A)$$

Using our values for α_{N_2}/α_A and the values of $\alpha_{N_2Atm.}$ from Hamberg, Winkler, and Fox, respectively, these equations have been used to calculate the values for α_{N_2} and α_A shown in Table III.

The values for α_{N_2} differ slightly from the values calculated by Coste, who apparently used values for α_A from Estreicher, which we believe to be less reliable than our α_{N_2}/α_A values. This implies, further, that the corrected values given by Coste for $\alpha_{N_2Atm.}$ also are slightly in error, but the error probably is not large enough to warrant a complete recalculation of all the original data.

The final three rows in Table III show values for α_A obtained by Estreicher,²² Winkler,²³ and Lannung,²⁴ as given by Lannung, and by Åkerlöf.²⁵ Åkerlöf found $\alpha_A = 33.2$ at 25°. A comparison of the six sets of values for α_A is fruitful. The Hamberg plus B. P. values agree very well with the Fox plus B.P. results at the higher temperatures, but at lower temperatures the difference is 2.5%. The Winkler plus B.P. value for 25° is lower than the previous two by 4%, but in essential agreement with the Fox plus B.P. value at 0°. The agreement between the Hamberg plus B.P. results and those of Lannung is particularly evident. It is unfortunate that Lannung did not extend his measurements to lower temperatures. Nevertheless, the results at 10° suggest that Lannung and Hamberg plus B.P. agree better at lower temperatures than do Lannung and Fox plus B.P. The values for α_A from Estreicher and Winkler, especially the former, are distinctly higher than the others and not in agreement with each other.

From the above discussion and the fact that our α_{N_2}/α_A values are high, if anything, we form the tentative conclusion that the results of Hamberg, Fox, Lannung, and Benson and Parker are probably the most reliable, with the Hamberg, Lannung, and Benson and Parker results in best agreement for the solubility coefficients of argon, and therefore for nitrogen as well. Coste reached the conclusion in 1927 that the Hamberg and Fox "atmospheric nitrogen" results were the most reliable. It is surprising to note that the Winkler values still persist in the "Handbook of Chemistry and Physics." In essence, the inclusion of our results and those of Lannung doubles the probability

(20) J. H. Coste, *J. Phys. Chem.*, **31**, 81 (1927).

(21) In this discussion, and in the discussions to follow, we have not attempted to include values from all the sources quoted by Coste or others, but only those which seem to be customarily considered as among the most reliable.

(22) T. Estreicher, *Z. physik. Chem.*, **31**, 176 (1899).

(23) L. W. Winkler, *ibid.*, **55**, 344 (1906).

(24) A. Lannung, *J. Am. Chem. Soc.*, **52**, 68 (1930).

(25) G. Åkerlöf, *ibid.*, **57**, 1196 (1935).

(19) Hamberg, *J. prakt. Chem.*, **33**, 433 (1886).

TABLE II

ADOPTED VALUES FOR N_2'/A' vs. TEMPERATURE IN DISTILLED WATER, CALCULATED FROM THE LEAST SQUARES EQUATION
$$N_2'/A' = 37.90 + 0.0590t$$

°C.	0	1	2	3	4	5	6	7	8	9
0	37.90	37.96	38.02	38.08	38.14	38.20	38.25	38.31	38.37	38.43
10	38.49	38.55	38.61	38.67	38.73	38.78	38.84	38.90	38.96	39.02
20	39.08	39.14	39.20	39.26	39.32	39.38	39.43	39.49	39.55	39.61
30	39.67									

TABLE III

Results of combining the ratios of nitrogen and argon solubility coefficients from this research, with the solubility coefficients for "atmospheric nitrogen" found by Hamberg, Winkler and Fox, to obtain the individual solubility coefficients for nitrogen and argon. For comparison, values for the solubility coefficients for argon from Estreicher, Winkler and Lannung are included.

	Temp., °C.	0	5	10	15	20	25	30
Benson and Parker	N_2'/A'	37.90	38.20	38.49	38.78	39.08	39.38	39.67
	α_{N_2}/α_A	0.4514	0.4550	0.4584	0.4619	0.4655	0.4690	0.4725
Hamberg	$\alpha_{N_2 \text{ atm.}}$	24.21	21.42	19.15	17.37	15.98	14.94	...
Winkler	$\alpha_{N_2 \text{ atm.}}$	23.54	20.86	18.61	16.85	15.45	14.34	13.42
Fox	$\alpha_{N_2 \text{ atm.}}$	23.59	21.03	18.95	17.31	15.98	14.89	...
Hamberg + B. and P.	α_{N_2}	23.87	21.12	18.89	17.14	15.77	14.74	...
Winkler + B. and P.	α_{N_2}	23.21	20.57	18.35	16.62	15.24	14.15	13.25
Fox + B. and P.	α_{N_2}	23.26	20.74	18.69	17.08	15.77	14.69	...
Hamberg + B. and P.	α_A	52.88	46.42	41.21	37.11	33.88	31.43	...
Winkler + B. and P.	α_A	51.42	45.21	40.03	35.98	32.74	30.17	28.04
Fox + B. and P.	α_A	51.53	45.58	40.77	36.98	33.88	31.32	...
Estreicher	α_A	45.2	...	37.9	...	32.5
Winkler	α_A	42.0	...	35.0	32.6	30.0
Lannung	α_A	41.1	37.1	33.6	31.4	28.9

that Coste's conclusion was correct, and suggests that the Hamberg plus B.P. values for α_{N_2} and α_A (or those of Lannung for α_A) are to be preferred over those obtained from Fox's data. This will be discussed further below.

A graph of the data for N_2'/O_2' vs. temperature in distilled water suggests the possibility that the temperature gradient of the ratio may increase with an increase in temperature. This, however, may be an artifact of the measurements, since no attempt was made to prevent B.O.D. (biochemical oxygen demand), as our original interest was not in oxygen. The water samples were not stored very long before gas extraction, but it is possible that B.O.D. has made the N_2'/O_2' results systematically high and subject to greater random fluctuations. In view of the uncertainties it was decided that the most objective manner of treating the data was to obtain a linear least squares fit, as was done with N_2'/A' . The result is

$$N_2'/O_2' = 1.800 + 0.00533t$$

with the standard deviation of the experimental points from the least squares fit equal to 0.025 or approximately 1.3% of the mean N_2'/O_2' .

Values for N_2'/O_2' calculated from the least squares solution are shown in Table IV. The values for $\alpha_{N_2}/\alpha_{O_2}$ were calculated from the equation

$$\frac{\alpha_{N_2}}{\alpha_{O_2}} = \frac{20.94N_2'}{78.08O_2'}$$

The next four rows list the results for α_{O_2} from Winkler,¹² Fox,⁵ Truesdale, Downing and Lowden,⁸ and Elmore and Hayes.¹¹ The Winkler values actually were taken from the "Handbook of Chemistry and Physics," 33rd Edition, 1951-1952,

and the Truesdale, *et al.*, and Elmore and Hayes numbers were obtained by converting their solubility values, in parts per million from a "wet" atmosphere, to solubility coefficients.

The values for α_{N_2} shown in the next four rows were calculated by multiplying each of the oxygen solubility coefficients from the four sources by our solubility coefficient ratios. The last three rows consist of α_{N_2} values obtained in Table III from independent evidence.

There is striking agreement among the values for α_{N_2} from the Elmore and Hayes plus B.P. results for α_{O_2} and $\alpha_{N_2}/\alpha_{O_2}$, the Winkler plus B.P. results for α_{O_2} and $\alpha_{N_2}/\alpha_{O_2}$, the Fox plus B.P. results for α_{O_2} and $\alpha_{N_2}/\alpha_{O_2}$, and the Hamberg plus B.P. results for $\alpha_{N_2 \text{ atm.}}$ and α_{N_2}/α_A . The first and last show the best agreement, differing by less than 0.5% except at 25° where the difference is still only 0.7%. Recall, also, the excellent correspondence between the Lannung α_A and the Hamberg plus B.P. values from $\alpha_{N_2 \text{ atm.}}$ and α_{N_2}/α_A .

It is possible that the consistency of the whole scheme is fortuitous. Indeed, we might expect it to be, in view of the fact that there are possible systematic errors of 1.5% in each of our measurements alone, not to mention unknown systematic errors in all the other determinations. Nevertheless, one cannot remain unimpressed when seven independent sets of measurements (Winkler, Fox, and Elmore and Hayes oxygen solubilities, Benson and Parker N_2'/A' and N_2'/O_2' solubility ratios, Hamberg "atmospheric nitrogen" solubilities, and Lannung argon solubilities) by different workers, on three gases, using a wide variety of methods, all lead to an internally consistent scheme to within approximately 1%. Still further support for this

TABLE IV

Results of combining the ratios of nitrogen and oxygen solubility coefficients from this research, with solubility coefficients for oxygen found by Winkler, Fox, Truesdale, Downing and Lowden, and Elmore and Hayes, to obtain the individual solubility coefficients for nitrogen. For comparison, the independently determined values for α_{N_2} from Table III are included.

	Temp., °C.	0	5	10	15	20	25	30	
Benson and Parker	N_2'/O_2'	1.800	1.827	1.853	1.880	1.907	1.933	1.960	
	$\alpha_{N_2}/\alpha_{O_2}$	0.4827	0.4900	0.4970	0.5042	0.5114	0.5184	0.5257	
Winkler	α_{O_2}	48.89	42.87	38.02	34.15	31.02	28.31	26.08	
Fox	α_{O_2}	49.24	43.21	38.37	34.55	31.44	28.90	26.65	
Truesdale, D. and L.	α_{O_2}	47.65	41.74	36.98	33.20	30.27	28.00	26.28	
Elmore and Hayes	α_{O_2}	49.30	43.16	38.16	34.13	30.88	28.25	25.97	
Winkler + B. and P.	α_{N_2}	23.60	21.01	18.90	17.22	15.86	14.68	13.71	
Fox + B. and P.	α_{N_2}	23.77	21.17	19.07	17.42	16.08	14.98	14.01	
T., D. and L. + B. and P.	α_{N_2}	23.00	20.45	18.38	16.74	15.48	14.52	13.82	
E. and H. + B. and P.	α_{N_2}	23.80	21.15	18.97	17.21	15.79	14.64	13.65	
From Table III	Hamberg + B. and P.	α_{N_2}	23.87	21.12	18.89	17.14	15.77	14.74	...
	Winkler + B. and P.	α_{N_2}	23.21	20.57	18.35	16.62	15.24	14.15	13.25
	Fox + B. and P.	α_{N_2}	23.26	20.74	18.69	17.08	15.77	14.69	...

impression is provided by still incomplete and unpublished determinations of the solubility coefficients for pure nitrogen by Klots and Benson. These new results are higher than those of Hamberg plus B.P. by only 0.2% at 5° and 0.7% at 15°, and lower by 0.5% at 25°.

The agreement between Truesdale, Downing and Lowden plus B.P. results and the Fox ($\alpha_{N_2 \text{ Atm.}}$) plus B.P. values, is good, though not as satisfactory as the above, but they do not have the support of several other lines of investigation.

Incidentally, there was a potential source of systematic error in the measurements of Truesdale, *et al.*, which they apparently did not correct for, and which no one else seems to have recognized. In order to maintain gas flow in their apparatus a negative pressure gradient was required in the direction of gas flow. Consequently, the actual pressure inside the vessel must have been greater than, rather than equal to, barometric pressure. With a small flow tube, which their drawing suggests, the error might be considerable. Unfortunately, this does not explain why their values are lower than those of other workers, because a correction for the effect would lower their results still further.

To summarize our conclusions for distilled water, we suggest on the basis of present evidence that the most reliable results are the Elmore and Hayes oxygen solubility coefficients, the Hamberg "atmospheric nitrogen" solubility coefficients, and the Benson and Parker nitrogen to argon solubility coefficient ratios, from which all the solubility coefficients, solubilities and solubility ratios for the three gases can be calculated as illustrated above.

B. Sea Water.—When the N_2'/A' data are plotted against the temperature, it is evident that the random errors in the data preclude the possibility of deducing the dependence of the solubility ratio upon salinity for the range of salinities studied. (There is a small variation of N_2'/A' with salinity, however, as can be seen from a comparison of Table II and Table V.) Furthermore, such a graph indicates a possible small non-linear dependence of the ratio upon temperature. These fluctuations and the apparent non-linearity may

have been the result of experimental difficulties, but perhaps for a different reason. The gasometric measurements, although unreliable, indicated a smaller amount of total gas extracted from the samples at 0° and 5° than would have been expected from the measurements at the higher temperatures. This could have resulted from a greater B.O.D., or from incomplete equilibrations. The former would not have influenced the N_2'/A' ratios, but the latter could have caused an error in them. For reasons implied in the introduction, this error would have been small, but at the sensitivity of these measurements it might show up.

On the basis of the above it was deemed preferable to consider all the data applying to an average salinity of 34.5‰, and to obtain a linear least squares fit as in the previous cases. The resulting dependence of the ratio upon temperature is given by

$$N_2'/A' = 37.48 + 0.0522t$$

for a salinity of 34.5‰, with a standard deviation of 0.175 or approximately 0.46‰—over twice as large as the estimated error due to the spectrometer measurements alone. The adopted values for N_2'/A' , calculated from the least squares equation, are shown in Table V. The possible error in the mass spectrometer calibration could have made these solubility ratios systematically too high by approximately 1.5%.

In Table VI the values for $N_2'_{\text{Atm.}}$ were calculated from Fox's equation. The Fox plus B.P. values for N_2' and A' were obtained by combining N_2'/A' with the relation $N_2'_{\text{Atm.}} = N_2' + A'$. The Rakestraw and Emmel $N_2'^*$ and A'^* results were taken from their paper.⁶ (The reason for the asterisks will appear below.) The numbers in parentheses were found by extrapolation. Table VI includes values for only one salinity because these are sufficient for the purpose of this discussion.

On the basis of the fact that Rakestraw and Emmel had found sea water from nearly all sources to be unsaturated relative to Fox's solubilities, they "suspected that his [Fox] systems might have been supersaturated." Another interpretation is

from the least squares fit was 0.028 or approximately 1.5% of the mean ratio.

Table VII shows values for N_2'/O_2' obtained from the equation above, together with values of O_2' calculated from Fox's equation and the O_2' results of Truesdale, Downing and Lowden corrected to dry solubilities. The last section of the table gives the results for N_2' calculated from the N_2'/O_2' values and the respective oxygen solubilities. The final two lines show the N_2' results from Table VI, which were derived from independent measurements.

The recalculated "dry" N_2' Rakestraw and Emmel values at each temperature are very nearly equal to the mean of the Fox plus B.P. oxygen-derived values and the Truesdale, *et al.*, plus B.P. values. The Fox plus B.P. nitrogen-derived results show the poorest agreement with a distinctly different slope from the other three. This could not have resulted from a possible error in our N_2'/A' measurements due to incomplete equilibrium at low temperatures, because the ratio determinations influence the calculated N_2' values very little.

Choosing among the other three sets of results is more difficult. If it is assumed that incomplete equilibration was a negligible source of error in the N_2'/O_2' measurements, we would be inclined to prefer the Fox oxygen results in sea water for two reasons: (1) The Truesdale, *et al.*, sea water results might be expected to be too low—especially at low temperatures—on the basis of their oxygen results in distilled water. (This is not a very convincing argument since the Fox nitrogen solubilities are taken to be in error even though his oxygen results will be considered the best. It has some validity, however, on the basis that Fox and Truesdale, *et al.*, are each internally consistent with respect to oxygen in distilled water and sea water.) (2) Any possible B.O.D. effects on our N_2'/O_2' determinations would tend to make the ratios and, consequently, the two oxygen derived sets for N_2' , too high. Correction for this would improve the

agreement between the Fox plus B.P. results and the Rakestraw and Emmel N_2' results and have the opposite effect on the Truesdale, *et al.*, plus B.P. results. If incomplete equilibration was a source of error in our measurements, the nature of the non-linear dependence of both N_2'/A' and N_2'/O_2' on temperature would indicate that either our nitrogen concentrations were too high at low temperatures or oxygen and argon too low. Correction for this would again favor the Fox values over Truesdale, *et al.*

In summarizing the situation for sea water, it is suggested—although with much less confidence than indicated earlier for distilled water—that possibly the most reliable data are the Fox oxygen solubilities, the Rakestraw and Emmel corrected nitrogen solubilities, and the N_2'/A' ratios from this research. The argon solubilities obtained from a combination of the latter two sets of results are the first information available on the solubility of pure argon in sea water. Although we have chosen to consider dry solubilities in this paper, it is suggested that for comparisons with oceanographic measurements wet solubilities probably are preferable. Finally, it is clear that much further work needs to be done on the solubilities of all the gases in sea water.

Acknowledgments.—We wish to express our appreciation to Mr. Nathaniel Corwin for obtaining the sea water, to Mr. Dean Bumpus for the salinity determinations, to Dr. Eva Kuhn Hilfer, Mr. Robert A. R. Parker and Mr. Noel S. Bartlett, who carried out part of the gas sample processing and mass spectrometer measurements, and to Dr. Mary Sears for her patience and help in preparing the manuscript for publication. Thanks are due Professor Arnold B. Arons and Dr. Cornelius E. Klots for critical reading of the manuscript. Conversations with Dr. Klots, Dr. James H. Carpenter, Professor Francis A. Richards and Dr. Leslie H. N. Cooper have been very helpful.

ISOTOPIC STUDIES INVOLVING FORMIC ACID AND ITS DERIVATIVES.¹ VII. OXYGEN-18 ISOTOPE EFFECT IN THE PHOTOCHEMICAL REACTION OF FORMIC ACID WITH CHLORINE

By GUS A. ROPP² AND W. A. GUILLORY

Chemistry Division, Oak Ridge National Laboratory, Operated by Union Carbide Nuclear Company for the U. S. Atomic Energy Commission, Oak Ridge, Tenn.

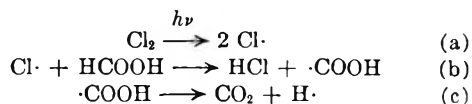
Received December 16, 1960

The oxygen-18 isotope effect on the rate of the photochemical reaction of formic acid with chlorine in the vapor phase was found to have a net value of $k_{16}/k_{18} = 1.002$ at 20°. It was concluded that abstraction of the hydroxyl hydrogen from formic acid by chlorine atoms makes no large contribution to the reaction mechanism.

Introduction

The vapor phase photochemical reaction of formic acid with chlorine is interesting in that it

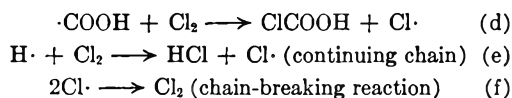
has been reported to proceed by a mechanism³ similar to that of the hydrogen-chlorine reaction



(1) Previous papers in the Series: (I) *J. Am. Chem. Soc.*, **73**, 5573 (1951); (II) **79**, 4944 (1957); (III) **80**, 3509 (1958); (IV) **80**, 5573 (1958); (V) **82**, 842 (1960); (VI) **82**, 4252 (1960).

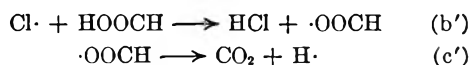
(2) Parma Research Center, Union Carbide Consumer Products Co., Parma, Cleveland, Ohio.

(3) H. West and G. K. Rollefson, *ibid.*, **58**, 2140 (1936).



Reaction (d), which has no counterpart in the hydrogen-chlorine reaction, was proposed by West and Rollefson³ on the basis of kinetic evidence. However, mass spectrometric tests⁴ have revealed no trace of chloroformic acid during the reaction.

Since the radicals, $\cdot\text{COOH}$ and $\text{H}\cdot$, would be expected to be very short-lived, acceptance of the mechanism of West and Rollefson leads to the conclusion that step (b) should play a significant role in controlling the reaction rate and that kinetic isotope effects should be observed in experiments using formic- C^{13} acid and formic- d (DCOOH) acid. The expected carbon-13⁽¹¹⁾ and deuterium⁵ isotope effects have in fact been observed and measured. The measured value⁵ of the deuterium isotope effect, $k_{\text{H}}/k_{\text{D}} = 2$, indicates that a large proportion of the reaction has as its rate-limiting step the cleavage of the carbon-hydrogen bond in the formic acid molecule. It does not, however, rule out the possibility of a dual mechanism with an appreciable part of the reaction having as its rate step abstraction of the hydroxyl hydrogen as indicated in step (b')



Steps (a), (e) and (f) would be common to both parts of the dual mechanism.

It might be supposed that a study of the kinetic isotope effect using formic acid- d (HCOOD) would reveal whether oxygen-hydrogen cleavage (b') contributes to the rate-limiting step just as the study⁵ of the kinetic isotope effect with formic- d acid served as a test for carbon-hydrogen cleavage (b) in the rate-limiting step. Unfortunately the deuterium in formic acid- d , unlike that in formic- d acid, exchanges very rapidly with compounds such as HCl that contain active hydrogen atoms. Consequently any attempt to measure a kinetic isotope effect using formic acid- d probably would fail completely or lead to a doubtful conclusion. A test for the occurrence of oxygen-hydrogen cleavage in the rate-limiting step can, however, be made by studying the oxygen-18 kinetic isotope effect, and such a study is described in the present paper. Oxygen-18 substitution in reactions in which the substituted oxygen atom is kinetically significant can lower the specific reaction rate constant as much as 7%.^{6,7} Since the ratio mass spectrometer can be used to detect kinetic isotope effects of 0.1% or smaller, a test for the oxygen-18 isotope effect in the reaction of formic acid with chlorine should be amply sensitive to reveal whether abstraction of hydroxyl hydrogen makes any ap-

preciable contribution to the rate-limiting step of that reaction.

Method

Normal formic acid having the natural abundance of oxygen-18 and carbon-13 was permitted to react in a vacuum line with chlorine in visible light.¹⁽¹¹⁾ Samples of carbon dioxide formed were treated with quinoline to remove hydrogen chloride and excess formic acid or excess chlorine, whichever was present. The carbon dioxide samples were passed through a trap cooled by Dry Ice to condense quinoline vapor and were collected in evacuated bulbs prior to analysis with a ratio mass spectrometer. The mass spectrometer analyses of the carbon dioxide were used to calculate both the oxygen-18 and the carbon-13 isotope effects. The fact that the calculated carbon-13 kinetic isotope effect checked well with the previously measured value⁽¹¹⁾ for the carbon-13 isotope effect indicated that the method was satisfactory.

Six runs were made using different aliquots of the same batch of formic acid. The first two runs were made using excess chlorine and yielded carbon dioxide whose isotopic abundance represented the initial isotopic abundance of the formic acid since conversion to carbon dioxide was complete. The δ values, calculated by the equations below, for these two carbon dioxide samples agreed to within 1 part per ten thousand, which is about the limit of sensitivity of the mass spectrometer

$$\begin{aligned} \delta \text{C}^{13} &= 1000 \left[\frac{\left(\frac{\text{C}^{13}}{\text{C}^{12}}\right) - \left(\frac{\text{C}^{13}}{\text{C}^{12}}\right) \text{Standard}}{\left(\frac{\text{C}^{13}}{\text{C}^{12}}\right) \text{Standard}} \right] \\ \delta \text{O}^{18} &= 1000 \left[\frac{\left(\frac{\text{O}^{18}}{\text{O}^{16}}\right) - \left(\frac{\text{O}^{18}}{\text{O}^{16}}\right) \text{Standard}}{\left(\frac{\text{O}^{18}}{\text{O}^{16}}\right) \text{Standard}} \right] \end{aligned}$$

The necessary corrections of the ratios due to O^{17} and C^{13} were made before calculation of the δ values.

The third and fourth runs were each made with sufficient chlorine to effect 20% conversion of the formic acid to carbon dioxide. The fifth and sixth runs were made with enough chlorine to effect, respectively, 85 and 89% conversion of the formic acid. The residual formic acid was recovered and converted by excess chlorine to carbon dioxide which represented the final 15 and 11%, respectively, of the reaction in runs 5 and 6. These final carbon dioxide samples were used in the isotopic analyses for these runs.

Carbon dioxide collected in run 1 was used as the standard for comparison in the ratio mass spectrometric analyses of the carbon dioxide produced in runs 3, 4, 5 and 6. Over-all experimental values of the oxygen-18 and carbon-13 isotope effects in runs 3 and 4 were calculated using the equation on which Fig. 1 of ref. 1 (V) was based. For runs 5 and 6 calculations were made using the equation on which Fig. 2 of ref. 1 (V) was based. Table I reports δ values obtained by mass spectrometric analysis of carbon dioxide samples.

TABLE I

RESULTS OF MASS SPECTROMETRIC ANALYSES		
Run	δ Carbon-13	δ Oxygen-18
2	0.00	0.00
3	-11.84	-13.75
4	-6.27	-4.45
5	+19.30	+13.47
6	+17.47	+13.21

The signs of the δ values indicate that the isotope effects are in the normal direction. The initially-formed product is enriched in the light isotopes in each case and the residual reactant is enriched in the heavy isotopes. Accordingly the light species react more rapidly than the corresponding heavy species. The values of the rate constant ratios are presented in Table II. The symbols r and r' are used as defined in ref. 1 (V).

Run 3 is out of line with Runs 4, 5 and 6. Run 3 has been ignored and an average value of the isotope effects measured

(4) G. A. Ropp, C. E. Melton and P. S. Rudolph, *J. Chem. Phys.*, **34**, 688 (1961).

(5) G. A. Ropp, "Evaluation of Deuterium Isotope Effects in Photochemical Reactions of Formic- d Acid by Use of Carbon-14," Paper RICC/171 presented at the "Conference on the Use of Radioisotopes in the Physical Sciences and Industry," Copenhagen, Denmark, September, 1960, sponsored by the International Atomic Energy Agency, Vienna, Austria.

(6) A. E. Cahill and H. Taube, *J. Am. Chem. Soc.*, **74**, 2312 (1952).

(7) G. A. Ropp, *Nucleonics*, **10**, 22 (1952).

TABLE II
CALCULATED ISOTOPE EFFECT RATIOS

Run	Carbon-13			Oxygen-18		
	r	r'	k_{12}/k_{13}	r	r'	k_{16}/k_{18}
3	0.98816		1.0132	0.98625		1.0152
4	0.99373		1.0070	0.99555		1.0060
5		1.01930	1.0100		1.01347	1.0070
6		1.01747	1.0081		1.01321	1.0060
	Mean of runs 4, 5 and 6		1.0084			1.0063

in runs 4, 5 and 6 has been taken as the best value. The best value of the carbon-13 isotope effect so calculated, $k_{12}/k_{13} = 1.0084$, is in reasonable agreement with the value of the carbon-13 isotope effect measured earlier.¹⁽¹¹⁾ The mean value of the carbon-13 isotope effect reported¹⁽¹¹⁾ earlier was 1.008. This agreement was considered to be sufficient justification for ignoring the results of Run 3. However, even if Run 3 had been considered in calculation of the average value of k_{12}/k_{13} , the average value reported in Table II would not have been altered greatly.

The best value of the oxygen-18 isotope effect, $k_{16}/k_{18} = 1.0063$, reported in Table II must be corrected for the fact that it includes a purely physical effect, the effect of molecular weight on the collision frequency of formic acid with chlorine atoms. This correction was applied earlier to the carbon-13 isotope effect.¹⁽¹¹⁾ The calculation of the collision frequency isotope effect is shown in Table III. Formic acid vapor consists of about two thirds dimer and one third monomer under the conditions of reaction. The corrected

TABLE III
CALCULATION OF THE OXYGEN-18 COLLISION FREQUENCY ISOTOPE EFFECT IN THE REACTION OF FORMIC ACID WITH CHLORINE ATOMS

Mono- mer	HCOOCH vs. HCOO ¹⁸ H	$\sqrt{\frac{46 + 35.5}{48 + 35.5}} = 1.0092$
Dimer	(HCOOH) ₂ vs. (HCOOH.HCOO ¹⁸ H)	$\sqrt{\frac{92 + 35.5}{94 + 35.5}} = 1.0029$

Mean weighted for:

- (a) $\frac{2}{3}$ dimer and $\frac{1}{3}$ monomer 1.00518
 (b) relative collision rate of monomer to dimer = 1.13

isotope effect, $k_{16}/k_{18} = 1.0011$, is obtained by dividing the experimentally determined ratio, 1.0063, by the collision frequency isotope effect, 1.00518. Finally, on a statistical basis, only half of the oxygen-18 atoms can be expected to be attached to hydrogen in formic acid molecules, the other half of the oxygen-18 atoms being bound only to carbon. Accordingly one half of the oxygen-18 atoms could never exert a primary isotope effect on the rate of reaction even if oxygen-hydrogen cleavage were entirely rate-determining. Therefore a second correction factor needs to be applied to

the experimentally measured isotope effect: it should be multiplied by 2. When this correction has been made the net oxygen-18 isotope effect ratio is

$$k_{16}/k_{18} = 1.002.$$

Discussion of Results

Cahill and Taube⁶ have pointed out that the theoretical value of the oxygen-18 isotope effect for simple cleavage of an oxygen-hydrogen bond should be small because the percentage shift in vibrational frequency upon substitution of oxygen-18 for oxygen-16 is small. However, the high frequency of the O-H stretching partly offsets the fact that the oxygen is attached to an atom of small mass.⁸ Using the value of Wilmhurst⁹ for the frequency of the O-H stretching, 3567 cm.⁻¹, the frequency shift upon oxygen-18 substitution is calculated to be 11 cm.⁻¹ which is equivalent to 16 cal./mole. Assuming that this oxygen-hydrogen frequency is completely lost in proceeding to the transition state in a chemical reaction, the theoretical value of the oxygen-18 isotope effect at 20° is estimated to be

$$k_{16}/k_{18} = 1.028$$

This calculation is admittedly crude, but it nevertheless indicates that for a reaction having oxygen-hydrogen cleavage as its rate-determining step an oxygen-18 isotope effect of about 3% can be expected at room temperature. The method of calculation of the theoretical value of k_{16}/k_{18} was similar to that described by Daniels.¹⁰

Since the net oxygen-18 isotope effect observed for the photochemical reaction of formic acid with chlorine amounted to about 0.2%, it follows that not more than 5 to 10% of the reaction proceeds *via* a process in which oxygen-hydrogen cleavage is rate determining. Therefore it appears that steps (b') and (c') make no large contribution to the reaction mechanism.

Acknowledgment.—The authors express their appreciation to Dr. T. C. Hoering, Geophysical Laboratory, Carnegie Institution of Washington, Washington 8, D. C., for performing the mass spectrometric analyses.

(8) G. A. Ropp and E. M. Hodnett, *J. Chem. Phys.*, **25**, 587 (1956) as indicated in this reference, a similar situation occurs in the calculation of the carbon-14 isotope effect to be expected in cleavage of a carbon-hydrogen bond.

(9) J. K. Wilmhurst, *ibid.*, **25**, 478 (1956).

(10) F. Daniels, "Chemical Kinetics," Cornell University Press, Ithaca, New York, N. Y., 1938, Chapter X.

SELECTIVE ADSORPTION STUDIES BY RADIO TRACER TECHNIQUE: THE SELECTIVE ADSORPTION BETWEEN CALCIUM AND SODIUM IONS AT THE IONIZED INTERFACE

By KŌZŌ SHINODA AND KŌJI ITŌ

Department of Chemistry, Faculty of Engineering, Yokohama National University, Minamiku, Yokohama, Japan

Received January 17, 1961

A comparison of the adsorption of calcium and sodium ions at air-solution interface from aqueous solutions of dodecyl sulfate or di-octyl sulfosuccinate indicates a strong selective adsorption of calcium ions by the negatively ionized monolayer. For example, the adsorption of calcium ion from a solution containing 6×10^{-3} mole/l. of sodium dodecyl sulfate and 2×10^{-6} mole/l. of calcium was 200 times greater than that of sodium ion. The experiments were carried out below the critical micelle concentration, and the results were interpreted semi-quantitatively in terms of the electrical potential of the ionized monolayer. Like the electrical potential, the selective adsorption was of course affected by the concentration and valency of the gegenions. Our values for selective adsorption are much larger than those previously reported which were obtained with solutions above the c.m.c. The adsorption of calcium at the air-solution interface from aqueous solutions of a non-ionic agent, octyl-glucoside, was also determined. There is some adsorption of calcium ions at the monolayer of the non-ionic agent, but much less, about 10^{-4} , as compared with that at the ionized layer. As the relative adsorption was determined from a ratio of radio-counts, errors in the absolute determination of radioactivity do not affect the results.

Introduction

In the solution of a surface active agent, such as sodium dodecyl sulfate, containing two kinds of gegenions, for example calcium and sodium ions, the former are preferentially adsorbed at the interface, the adsorption sites being the adsorbed dodecyl sulfate ions.

Judson, *et al.*,^{1,2} have studied the competition between chloride and sulfate anions at the air solution interfaces of Aerosol SE (stearamido-propyldimethyl-2-hydroxyethylammonium sulfate) and cetylpyridinium chloride solutions; they determined the surface count due to sulfate ion adsorption at various sodium sulfate concentrations and constant Aerosol SE chloride concentration, and at constant sodium sulfate concentration and various Aerosol SE concentrations. Walling, *et al.*,³ found that multivalent ions are preferentially adsorbed from a solution of sodium palmitoyl methyltaurine; the adsorption of Ca^{++} or Mg^{++} was 9-49 times that of Na^+ . As the concentrations of the solutions studied in these papers were above the c.m.c., a quantitative interpretation of the results was complicated by the competitive adsorption of multivalent ions by micelles.

The present investigation was undertaken to determine the selective adsorptivity of calcium with respect to univalent cations at the ionized monolayer of sodium dodecyl sulfate or Aerosol OT as a function of the concentration of gegenions. The adsorption of calcium at the adsorbed layer of octyl glucoside was also determined for comparison.

Experimental

Materials.—Radioactive calcium, $^{45}\text{Ca}^{++}$ in HCl solution, was obtained from the Oak Ridge National Laboratory through the kindness of Daiichi Pure Chemicals Co. Ltd. Sodium dodecyl sulfate⁴ and β -D-octyl glucoside⁵ were the

(1) C. M. Judson, A. A. Lerew, J. K. Dixon and D. J. Salley, *J. Phys. Chem.*, **57**, 916 (1953).

(2) H. Sobotke, "Monomolecular Layers," *Am. Assoc. Adv. Sci.*, p. 63 (1954).

(3) C. Walling, E. E. Ruff and J. L. Thornton, Jr., *J. Phys. Chem.*, **61**, 486 (1957).

(4) K. Shinoda and K. Mashio, *ibid.*, **64**, 54 (1960).

(5) K. Shinoda, T. Yamanaka and K. Kinoshita, *ibid.*, **63**, 648 (1959).

same materials described in earlier experiments. Aerosol OT, 100% surface active sodium dioctylsulfosuccinate manufactured by the American Cyanamid Company, was used without further purification. As the foam stability of Aerosol OT solution was not good, a short draining tube about 30 cm. in length was used.

Procedures.—The apparatus used was similar to that shown in Fig. 1 of the previous paper.⁴ As the concentration of calcium ions was very low and the selective adsorptivity was large, the radioactivity of the solution decreased rapidly in the course of bubble generation. As we found that the radioactivity of the collapsed foams shows some delay and diffuse distribution, the total radioactivity of adsorbed gegenions in the collapsed foams was calculated from the total decrease of counts, ΔR , of the solution. The volume, ΔV , and the concentration, C_f , of the collapsed foams were determined. The count per unit volume of collapsed foam is $\Delta R/\Delta V$. The count from a definite amount of agent in the adsorbed state is given by

$$\frac{\Delta R \cdot v}{\Delta V} \frac{C_b}{C_f - C_b} = R_{\text{ads}} \quad (1)$$

where C_b denotes the concentration of the solution and v the volume of the micropipet used for the sampling of the solution.

The local decrease in calcium concentration in the course of the bubble generation due to inefficient circulation was a source of serious error in a preliminary experiment. Therefore, the nearly horizontal tubing⁴ was filled with solution because the movement of bubbles promoted circulation of the solution. We also used a thicker and shorter length of tubing than in the previous experiment to improve the circulation.

Results

The adsorption of calcium ions at the air-solution interface of an aqueous solution of sodium dodecyl sulfate containing a small amount of calcium ions was measured, and the results are reported in Table I. The concentration of the agent was maintained at an almost constant level below the c.m.c. throughout the experiment. An aliquot of the solution was dried and its radioactivity determined, R_{bulk} (see column 1, Table I); the radioactivity from the same amount of dried agent in the adsorbed layer, R_{ads} , was calculated from equation 1. The fraction of calcium ions in the solution, $X_{\text{bulk}} = 2C_{\text{Ca}}/(C_{\text{Na}} + 2C_{\text{Ca}})$, is given in the 2nd column, where C_{Ca} and C_{Na} are the mole concentrations of calcium and sodium ions, respectively. The concentration of the agent was 0.007 mole/l. for lines 1~7 and 0.006 mole/l. for

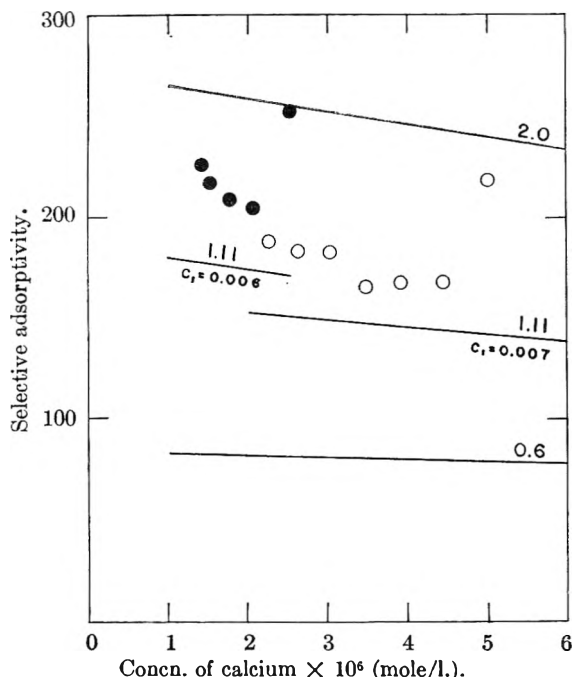


Fig. 1.—Selective adsorption of calcium against sodium ions at the air-solution interface of sodium dodecyl sulfate at 25°.

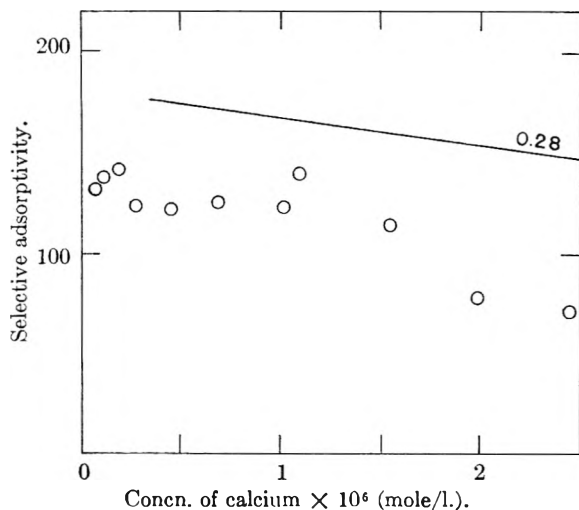


Fig. 2.—Selective adsorption of calcium against sodium ions at the air-solution interface of Aerosol OT at 18°.

lines 8~12. The ratio of the concentration of the agent in collapsed foam to that of the solution was about 2.72.

The fraction of the adsorbed cations due to calcium ions, X_{ads} , was obtained from

$$X_{\text{ads}} = \frac{R_{\text{ads}}}{R_{\text{bulk}}} X_{\text{bulk}} \quad (2)$$

The selective adsorptivity of calcium to univalent cations was calculated from

$$S = \frac{X_{\text{ads}}}{1 - X_{\text{ads}}} \bigg/ \frac{X_{\text{bulk}}}{1 - X_{\text{bulk}}} \quad (3)$$

X_{ads} is the fraction of the adsorbed gegenions due to calcium ions, where the adsorbed gegenions are not just the ions directly fixed on the adsorption sites, but the total amount of gegenions necessary

TABLE I
SELECTIVE ADSORPTION OF CALCIUM AGAINST SODIUM IONS AT AIR-SOLUTION INTERFACE IN AQUEOUS SOLUTION OF SODIUM DODECYL SULFATE CONTAINING A SMALL AMOUNT OF CALCIUM IONS $^{45}\text{Ca}^{++}$ AT 25°

	Count (bulk) R_{bulk}	Fraction of Ca^{++} (bulk) X_{bulk}	Counts (ads. layer) R_{ads}	Fraction of Ca^{++} (ads. layer) X_{ads}	Selective adsorptivity S
1	780	0.00141	129600	0.234	217
2	692	.00125	95500	.173	167
3	613	.00111	86400	.156	167
4	541	.00098	76700	.139	165
5	474	.000856	74500	.135	182
6	411	.000744	65900	.119	182
7	355	.000643	59100	.107	187
8	95 ^a	.000846	19800	.176	252
9	78 ^a	.000694	13900	.124	204
10	66 ^a	.000592	12300	.110	208
11	57 ^a	.000508	11080	.099	216
12	48 ^a	.000482	9760	.098	226

^a Radioactivity of calcium ions is different for different series of experiments.

for electrical neutrality. The selective adsorption of bivalent to univalent gegenions directly fixed on the ionized layer may be much larger. The specific activity of calcium was different in the different experiments.

The relation between the selective adsorptivity and the concentration of calcium ions is shown in Fig. 1.

Similar experiments were carried out with a solution of dioctyl sodium sulfosuccinate containing a small amount of calcium. The concentration of the agent in solution was 0.00150~0.00144 mole/l. throughout the experiments. The average concentration of the agent in the collapsed foams was 0.00423 mole/l. The results are summarized in Table II.

TABLE II
SELECTION ADSORPTION OF CALCIUM AGAINST SODIUM IONS AT AIR-SOLUTION INTERFACE OF AQUEOUS SOLUTION OF DI-OCTYL SODIUM SULFOSUCCINATE CONTAINING A SMALL AMOUNT OF CALCIUM IONS $^{45}\text{Ca}^{++}$ AT 18°

	Count (bulk) R_{bulk}	Fraction of Ca^{++} (bulk) X_{bulk}	Count (ads. layer) R_{ads}	Fraction of Ca^{++} (ads. layer) X_{ads}	Selective adsorptivity, S
1	114	0.00322	6682	0.189	72
2	93	.00263	6659	.188	79
3	71	.00218	6474	.199	114
4	51	.00147	6470	.186	139
5	200	.00138	20885	.144	122
6	135	.000934	15113	.105	125
7	88	.000608	9937	.0686	121
8	60	.000362	7063	.0426	123
9	37	.000256	5063	.0350	141
10	23	.000159	3076	.0213	137
11	15	.000107	1952	.0139	131

The relation between the selective adsorptivity and the concentration of calcium ions is shown in Fig. 2.

The adsorption of calcium ions at the air-solution interface from aqueous solutions of octyl glucoside has been measured. As the foam stability decreased markedly with increasing calcium

chloride concentration, experiments were carried out at a calcium chloride concentration below 0.015 mole/l. The concentration of octyl glucoside was 0.025 mole/l. The results are summarized in Table III.

TABLE III
ADSORPTION OF CALCIUM IONS $^{45}\text{Ca}^{++}$ AT
AIR-SOLUTION INTERFACE OF AQUEOUS SOLUTION
OF OCTYL GLUCOSIDE AT 25°

	1	2	3	4
Count (bulk)	1625	1639	1550	1550
Concn. of soln. (wt. %)	0.00753	0.00802	0.00974	0.00974
Concn. of calcium, mole/ l. (bulk)	0.00155	0.005	0.0155	0.0155
Ratio of the concn. of Ca^{++} to octyl glucoside	1/18	1/5	1/1.6	1/1.6
Count (foams)	2896	2628	1925	1907
Concn. of foams (wt. %)	0.0148	0.0160	0.0130	0.0133
Ratio of adsorbed Ca^{++} to octyl glucoside	1/25	1/8	1/2.7	1/3.0

Discussion

Several features of these experiments should be noted. 1. Since the selective adsorptivity is based on the ratio of radiocounts, it is not affected by errors in the absolute values for radioactivity. 2. The results can be analyzed quantitatively because the charge density of the ionized interface is known for a given surface active agent. 3. We are dealing with a condition of electrical neutrality, as the amounts of adsorbed agent and of calcium ions were determined from the concentration and radioactivity of collapsed foam. The fraction of calcium ions occupying the adsorption sites, which are the adsorbed surface active ions, was calculated. In regard to the measurement of surface radioactivity, we can measure the radioactivity due to multi-layer adsorption, but are unable to determine the fraction due to ions directly fixed to the adsorption sites. The concentrations of the solutions examined were close to, or slightly less than, the c.m.c. of the respective surface active agent containing a small amount of bivalent cation.^{5,7} Accordingly, the ratio of the cations in the singly dispersed state is equal to the ratio of the stoichiometric concentrations. With solutions above the c.m.c., the ratio changes markedly due to the preferential adsorption of multivalent ions on the surface of the micelle.

A surface hydrolysis of sodium *n*-octylsulfosuccinate and stearamidopropyl-2-hydroxyethylammonium sulfate has been reported⁸ on the basis of the surface counts at the air-solution interface. Since the apparent surface hydrolysis occurred only at high dilution (about 80% of sodium ions was adsorbed at the c.m.c.),⁹ and was detected as a deficiency of sodium or sulfate ions in the surface by radioactive counting, we feel that the apparent decrease of radioactivity was not due to surface hydrolysis. If surface hydrolysis occurs to a considerable extent, the c.m.c. values of octylsulfosuccinic acid or stearamidopropyl-2-hydroxy-

ethylammonium sulfuric acid would be very much smaller than the c.m.c. values of their sodium salts; however, alkyl sulfonic acids and sulfuric acids are fairly strong acids which have c.m.c. values that are comparable to those of their salts. Walling, *et al.*,³ found that the adsorption of hydrogen ions at the air-solution interface of *n*-palmitoyl methyltaurine is almost equal to that of sodium ions, a result which supports our view.

The electrical potential, ϕ_0 , of an ionized monolayer is given as a function of the concentration and valency of the gegenions by eq. (4)^{7,10,11}

$$\frac{2000\pi\sigma^2}{DNkT} = C_1 \exp\left(\frac{e\phi_0}{kT}\right) + C_2 \exp\left(\frac{2e\phi_0}{kT}\right) \quad (4)$$

where σ is the surface charge density, D the dielectric constant of the medium, e the elementary charge, C_1 the concentration of i-valent gegenions in mole/l. in the bulk of the solution, k the Boltzmann constant and T the absolute temperature.

If the electrical potential at the ionized monolayer is ϕ_0 , the average electrical energy decrease due to the transfer of a univalent gegenion from the bulk to the ionized surface is $\lambda e\phi_0$ and that due to a bivalent gegenion is $2\lambda e\phi_0$, where λ is a constant smaller than one. We would expect the selective adsorptivity of bivalent against univalent gegenions to be about $\exp(\lambda e\phi_0/kT)$. The substitution of σ , D , T , C_1 , C_2 in equation 4 gives a reasonable value for selective adsorptivity, provided $\lambda = 0.5 \sim 0.6$.

Instead of substituting the respective values of σ , D and T , we can estimate experimentally the value of the left-hand side of equation 4 from the c.m.c. values of $\text{R}_{12}\text{SO}_4\text{Na}$ and $\text{R}_{12}\text{SO}_4^{1/2}\text{Ca}$.⁶ Namely, the c.m.c. is expressed as a function of the concentration of gegenions as⁷

$$\ln \text{CMC}_1 = K_{g1} \ln \frac{2000\pi\sigma^2}{DNkTC_1} + \text{Const.}_1 \quad (5)$$

$$\ln \text{CMC}_2 = \frac{K_{g2}}{2} \ln \frac{2000\pi\sigma^2}{DNkTC_2} + \text{Const.}_2 \quad (6)$$

where K_{g1} and K_{g2} are the experimental constants obtained from the CMC_i vs. C_i relation. We may assume that the constants in equations 5 and 6 are equal, for the gegenions differ only in the number of the charge. Then introducing $\text{CMC}_1 = 0.0066$, $\text{CMC}_2 = 0.0029$, $K_{g1} = 0.52$ and $K_{g2} = 0.56$ in equations 5 and 6, we obtain

$$\frac{2000\pi\sigma^2}{DNkT} = 1.19 \text{ at } 70^\circ, \text{ or } \frac{2000\pi\sigma^2}{DNkT} = 1.11 \text{ at } 25^\circ$$

Introducing $2000\pi\sigma^2/DNkT = 1.11$ in equation 4, we can calculate the selective adsorptivity of calcium to sodium ions in aqueous solution of dodecyl sulfate as a function of C_1 and C_2 . With $2000\pi\sigma^2/DNkT = 2.0$, 1.11 or 0.6, the selective adsorptivities were calculated and the results are given by solid lines in Fig. 1. In the case of Aerosol OT solution, the charge density of the adsorbed monolayer would be about one-half of the dodecyl sulfate value. Accordingly, we obtain $2000\pi\sigma^2/DNkT = 0.28$ for Aerosol OT solution at 18~25°. Introducing this value into equation 4, we can cal-

(6) H. Lange, *Kolloid-Z.*, **121**, 66 (1951).

(7) K. Shinoda, *Bull. Chem. Soc. Japan*, **28**, 340 (1955).

(8) C. M. Judson, A. A. Lerew, J. K. Dixon and D. J. Salley, *J. Chem. Phys.*, **20**, 519 (1952).

(9) Ref. 2, p. 78, Fig. 3.

(10) A. B. D. Cassie and R. C. Palmer, *Trans. Faraday Soc.*, **37**, 156 (1941).

(11) E. J. W. Verwey and J. Th. G. Overbeek, "Theory of the Stability of Lyophobic Colloids," Elsevier Publishing Co., Inc., New York, N. Y., 1948.

culate the selective adsorptivity of calcium to sodium ions at the air-solution interface of Aerosol OT as a function of $C_1 = 0.0015$ mole/l. and C_2 . The values are shown by the solid line in Fig. 2. The agreement between the experimental and calculated values is quite satisfactory, and in both cases the selective adsorptivity tends to decrease with increasing calcium ion concentration. The electrical potential of the ionized monolayer, $\phi_0 = (kT/\lambda e) \ln S$, was estimated as about 200~250 mv. for our solutions.

We might presume that the monolayer of a non-ionic agent at an air-solution interface would not adsorb small ions. However, Judson, *et al.*,¹ found that sulfate was adsorbed at the interface from aqueous solutions of a non-ionic agent, Aerosol NL-10. The amount adsorbed was proportional to the concentration of sulfate ions in the solution. To obtain further evidence for the adsorption of inorganic ions at an air-solution interface of a non-ionized layer, we have determined the ratio of calcium ions to adsorbed octyl glucoside. From these results we can conclude that there is some adsorption of calcium ions at the adsorbed layer of octyl glucoside, and that for a given octyl

glucoside concentration the ratio of calcium ions to adsorbed octyl glucoside increases roughly with the bulk concentration of calcium ions. The relative adsorptivity of calcium ions is, however, far less at a non-ionized layer than at an ionized layer. In a solution of dodecyl sulfate (1×10^{-2} mole/l.) containing 1×10^{-6} mole/l. of calcium chloride the ratio of calcium ions to surface active ions in the adsorbed layer was about 0.1, whereas in solution of octyl glucoside (2.5×10^{-2} mole/l.) containing 1×10^{-2} mole/l. of calcium chloride the ratio of calcium to surface active molecules at the surface was about 0.1. The ability of the adsorbed layer of these two solutions to adsorb calcium differs by a factor of about 10^4 . The ratio of calcium ions to dodecyl sulfate ions at the surface was about 100 times greater than the corresponding ratio in the bulk of the solution, whereas the ratio of calcium ions to octyl glucoside at the surface was about half of that in the solution.

Acknowledgment.—We wish to thank the Ministry of Education and the Asahi Chemical Industry Foundation for supporting this work. We also wish to thank Mrs. L. H. Weissberger for assistance in preparing the manuscript.

EFFECT OF SOLUTE CONCENTRATION ON THE RECOMBINATION OF H AND OH IN γ -IRRADIATED AQUEOUS SOLUTIONS¹

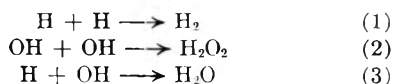
BY E. HAYON²

Chemistry Department, Brookhaven National Laboratory, Upton, Long Island, New York

Received January 30, 1961

It is shown that on addition of high concentrations of inorganic solutes reactive to H atoms and OH radicals the recombination of H and OH to form water in γ -irradiated aqueous solutions is reduced. The presence of 0.43 M Ce^{4+} , 0.1 M Tl^+ in 0.8 N H_2SO_4 solution increases G_{-H_2O} from 4.50 to 5.24. The yields of molecular hydrogen from air-free solutions of Ce^{4+} - Tl^+ , Tl^+ , Ce^{3+} , Br^- and arsenite have been measured. $G_{H_2} \approx 0.4$ in 0.8 N H_2SO_4 or HCl solutions as compared to ~ 0.45 for neutral Br^- and arsenite solutes. A mechanism is suggested which could explain the decrease in the molecular yield of hydrogen in acid solutions.

Water is decomposed on irradiation to give H, OH, H_2 and H_2O_2 . The H_2 and H_2O_2 are thought to result from combination of like radicals in regions ("spurs"), where the concentration of radicals is high, and reaction (3) has been assumed



to occur by analogy with (1) and (2). The H atom and OH radicals are the reactive intermediates formed in the radiation chemistry of dilute aqueous solutions. Their yields are now fairly well accepted.³ It was found, however, on irradiation of aqueous systems containing relatively high con-

centrations of organic⁴ solutes that the yields of radiation-induced products are dependent upon the concentration of the solute, and cannot be accounted for on the basis of the accepted radical yields.³ It was suggested^{4b} that at high concentration the solute was reducing the extent of recombination of H and OH in water (reaction 3). Though in certain cases this did seem likely, one could provide an alternative interpretation, *e.g.*, the observed increase in yields with increase in solute concentration could be explained by electronic excitation of the solute molecules by sub-excitation electrons⁵ produced by the radiation, or by direct absorption of energy by the solute resulting in dissociation of the organic molecule. It seemed therefore of interest to investigate the effect of concentration of inorganic solutes since the increase in yields cannot in this case be due to dissociation of the solute, and any contribution due to direct absorption of energy at high concentrations of inorganic solutes could be calculated and corrected for.

(1) Research performed under the auspices of the U. S. Atomic Energy Commission.

(2) Department of Physical Chemistry, Cambridge University, Cambridge, England.

(3) (a) N. F. Barr and R. H. Schuler, *J. Phys. Chem.*, **63**, 808 (1959); (b) T. J. Sworski, *J. Am. Chem. Soc.*, **76**, 4687 (1954).

(4) (a) H. Fricke, E. J. Hart, H. P. Smith, *J. Chem. Phys.*, **6**, 229 (1938); C. R. Maxwell, D. C. Peterson, N. E. Sharpless, *Radiation Res.*, **1**, 530 (1954); (b) G. R. A. Johnson, G. Scholes and J. Weiss, *Nature*, **177**, 883 (1956); D. M. Donaldson, N. Miller, *Radiation Res.*, **9**, 487 (1958); J. T. Allan, E. Hayon and J. Weiss, *J. Chem. Soc.*, 3913 (1959).

(5) J. Weiss, *J. chim. phys.*, **52**, 539 (1955); R. L. Platzman, *Radiation Res.*, **2**, 1 (1955).

Experimental

Ceric sulfate, $\text{Ce}(\text{HSO}_4)_4$, supplied by G. Frederick Smith Chemical Co., and thallium sulfate, Tl_2SO_4 , by A. D. Mackay, Inc., were used without further treatment. A stock solution of ceric sulfate (0.5 M) in 0.8 N H_2SO_4 was prepared and allowed to stand in the dark for two weeks previous to irradiation. Water was triply distilled from acid dichromate, alkaline permanganate, and a final distillation.⁶

A 1100 curie cylindrical Co^{60} γ -source was used,^{7a} with a dose rate of 4.22×10^{20} e.v./l.-min. based on the Fricke dosimeter (10^{-3} M FeSO_4 , 10^{-3} M NaCl , 0.8 N H_2SO_4) taking $G(\text{Fe}^{3+}) = 15.5$. Irradiations of air-saturated solutions were carried out in 1.2 cm. diam., 18 cm. long Pyrex glass tubes, which were preirradiated to a dark brown color. Air-free solutions for H_2 gas determination were prepared as described by Schwarz, Losee and Allen.^{7b} Ceric ion concentrations before and after irradiation were determined by absorption spectrophotometry at 320 m μ using an extinction coefficient of 5580 in 0.8 N H_2SO_4 solutions.⁸ Dilution of concentrated ceric solutions was carried out with 0.8 N H_2SO_4 containing 10 μM Ce^{4+} .

Direct interaction of the radiation with Ce^{4+} and Tl^+ becomes appreciable at the relatively high solute concentrations used. The dose absorbed in these solutions was corrected for using the equation

$$D_s = D_{\text{Fricke}} \left(\frac{\epsilon_s}{\epsilon_D} + \alpha \frac{\epsilon_s}{\epsilon_D} + \tau \right)$$

where D_s is the corrected dose, D_{Fricke} the dose as measured by the Fricke dosimeter, ϵ_s and ϵ_D the electron density of the irradiated solutions and dosimeter, respectively, τ the correction for the photoelectric effect, α the correction for the absorption of low-energy scattered radiation inside the Co^{60} source by materials of high atomic number.¹⁰ τ was calculated using the mass absorption coefficient⁹ for γ -rays at wave length 0.01 Å. for Pb and Sn, these having about the same atomic numbers as Tl and Ce, respectively. In order to calculate the electron density the specific gravities of the solutions were determined, and the results and the calculated corrections are shown in Table I. The corrected doses are good to $\pm 2\%$. The implied assumption made here is that the "extra" energy absorbed by the Ce^{4+} and Tl^+ is transferred to the solvent (water), but that no energy is transferred from the water to the solutes.

Arsenite solutions were prepared by dissolving 5×10^{-3} M arsenious oxide in 0.1 N NaOH and rapidly neutralizing the solution with sulfuric acid.

Hydrogen was measured by combustion with oxygen on a platinum filament.

Results

The ceric-thallosulfate system developed by Sworski⁸ was chosen for this study because both constituents have a relatively high solubility in water. On irradiation of air-saturated 10^{-3} M Ce^{4+} , 10^{-3} M Tl_2SO_4 in 0.8 N H_2SO_4 solution, $G(\text{Ce}^{3+})$ was found to be 7.80 which is slightly lower than Sworski's value of 7.92.⁸ Sworski's results that addition of up to 10^{-1} M Tl_2SO_4 to 10^{-4} – 10^{-3} M $\text{Ce}(\text{HSO}_4)_4$ in 0.8 N H_2SO_4 does not affect $G(\text{Ce}^{3+})$ were also confirmed. It was found, however, on increasing the concentration of Ce^{4+} ions that $G(\text{Ce}^{3+})$ increased over and above the contribution from the decrease in the yield of molecular hydrogen.^{11,12} Table II gives values of

$G(\text{Ce}^{3+})$ corrected for direct absorption of the radiation by the thallosulfate and ceric ions present in solution in relatively high concentrations. The error in determining the slopes of the yield-dose plot is at the highest $[\text{Ce}^{4+}]$, $\pm 3\%$. Figure 1 shows the yields of $G(\text{Ce}^{3+})$ corrected for absorption of radiation, as a function of $\text{Ce}(\text{HSO}_4)_4$ concentration. It can be seen that increasing the concentration of Ce^{4+} ions at constant $[\text{Tl}^+]$ results in an increase in $G(\text{Ce}^{3+})$.

TABLE I
DOSIMETRIC CORRECTION ON IRRADIATION OF Ce^{4+} IN 0.1 M Tl_2SO_4 IN 0.8 N H_2SO_4

Ce^{4+} concn., M	Density, g./ml.	ϵ_s/ϵ_D	$\tau \times 10^3$	$\alpha \times 10^3$	Cor- rection, %
0.06	1.086	1.041	7.6	20	6.8
.10	1.104	1.048	7.9	21	7.8
.16	1.122	1.056	8.4	22	8.8
.25	1.145	1.065	8.8	24	10.0
.43	1.208	1.090	10	28	13.0
.15 ^a	1.081	1.04	4	6.7	5

^a Containing 2×10^{-2} M Tl_2SO_4 .

Table II gives the corrected yields of molecular hydrogen as measured in air-free 0.8 N H_2SO_4 solutions of ceric sulfate in 10^{-1} M Tl_2SO_4 . The presence of thallosulfate ions does not affect $G(\text{H}_2)$, as seen from the irradiation of a 0.11 M Ce^{4+} solution in the absence of Tl^+ . The value of $G(\text{H}_2)$ extrapolated to infinite dilution from the plot of $G(\text{H}_2)$ vs. $\sqrt{[\text{Ce}^{4+}]}$ is 0.395.

TABLE II
 $G(\text{Ce}^{3+})$ AND $G(\text{H}_2)$ YIELDS FROM γ -IRRADIATED 0.8 N H_2SO_4 CERIC SOLUTIONS IN 10^{-1} M Tl_2SO_4

$[\text{Ce}^{4+}]$, M	$G(\text{Ce}^{3+})_{\text{cor.}}^a$	$[\text{Ce}^{4+}]$, M	$G(\text{H}_2)_{\text{cor.}}^b$
0.062	8.15	2×10^{-4}	0.364
.095	8.56	5.26×10^{-4}	.355
.165	9.19	7.77×10^{-3}	.313
.257	9.40	8.2×10^{-2}	.236
.431	9.70	3.74×10^{-1}	.187
.150 ^b	8.98	1.1×10^{-1c}	.23

^a Yields corrected for direct interaction of the radiation with the solutions (see Experimental section). ^b Containing 2×10^{-2} M Tl_2SO_4 . ^c No thallosulfate ion added.

The value of 0.395 for the molecular yield of H_2 is lower than that recently obtained by Mahlman and Boyle¹³ from 0.8 N H_2SO_4 solutions of bromide and by Schwarz and Hritz¹⁴ from ferrous chloride solutions in 0.4 M HCl, $G_{\text{H}_2} = 0.45$. The yield in neutral solution, $G_{\text{H}_2} = 0.45$, seems to be generally agreed on. It seemed worthwhile to check this discrepancy. The yield of H_2 from air-free H_2SO_4 solutions of KBr, Tl^+ , Ce^{3+} and arsenite, and of KBr and arsenite in neutral solutions are shown in Table III. The values of $G(\text{H}_2)$ measured in every run are included. As can be seen, in all cases the yields of H_2 are slightly lower in acid than in neutral solution. Figure 2 gives a plot of $G(\text{H}_2)$ from air-free bromide solutions vs. pH. The yield of H_2 in 0.8 N HCl in the presence or absence of 10^{-3} M KBr also gives a value near 0.4.

(13) H. A. Mahlman and J. W. Boyle, *J. Am. Chem. Soc.*, **80**, 773 (1958).

(14) H. A. Schwarz and J. M. Hritz, *ibid.*, **80**, 5636 (1958).

(6) E. R. Johnson and A. O. Allen, *J. Am. Chem. Soc.*, **74**, 4147 (1952).

(7) (a) H. A. Schwarz and A. O. Allen, *Nucleonics*, **12**, #2, 58 (1954); (b) H. A. Schwarz, J. P. Losee and A. O. Allen, *J. Am. Chem. Soc.*, **76**, 4693 (1954).

(8) T. J. Sworski, *Radiation Res.*, **4**, 483 (1956).

(9) "Handbook of Chemistry and Physics," 39th ed., p. 2459.

(10) W. Bernstein and R. H. Schuler, *Nucleonics*, **13**, #11, 110 (1955).

(11) J. A. Ghormley and C. J. Hochanadel, *Radiation Res.*, **3**, 227 (1955).

(12) J. T. Harlan and E. J. Hart, *Nucleonics*, **17**, #8, 102 (1959).

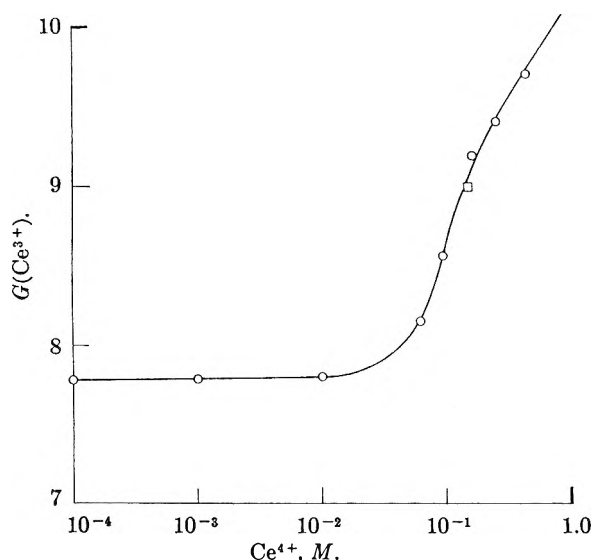


Fig. 1.— $G(\text{Ce}^{3+})$ plotted as a function of $[\text{Ce}^{4+}]$ obtained from irradiation of air-saturated $0.1 M \text{Ti}_2\text{SO}_4$, $0.8 N \text{H}_2\text{SO}_4$, except for one run (\square) in $0.02 M \text{Ti}_2\text{SO}_4$.

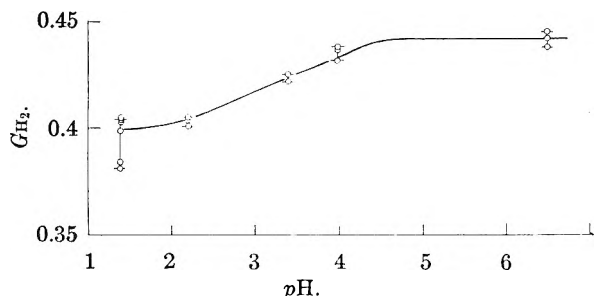


Fig. 2.—Yields of $G(\text{H}_2)$ vs. pH obtained from Co^{60} γ -irradiation of air-free KBr solutions. All runs are included on the graph.

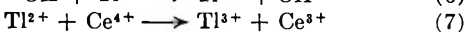
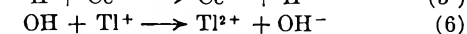
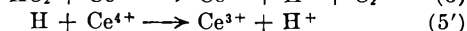
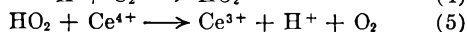
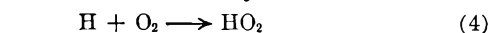
TABLE III
HYDROGEN YIELDS FROM γ -IRRADIATED AIR-FREE AQUEOUS SOLUTIONS

Solute	pH	$G(\text{H}_2)$
$10^{-3} M \text{KBr}$	5.5	0.438; 0.445; 0.442
$10^{-3} M \text{KBr}$	3.0	.432; .437; .438
$10^{-3} M \text{KBr}$	2.4	.422; .425
$10^{-3} M \text{KBr}$	1.2	.405; .401; .404
$10^{-3} M \text{KBr}$	0.4 ^a	.384; .404; .403; 0.381; .404; .399
$10^{-3} M \text{Ti}_2\text{SO}_4$	0.4 ^a	.409; .422; .425
$10^{-1} M \text{Ti}_2\text{SO}_4$	0.4 ^a	.409
$10^{-3} M \text{Ce}_2(\text{SO}_4)_3$	0.4 ^a	.399; .404
$10^{-3} M \text{arsenite}$	0.4 ^a	.377; .372; .376
$10^{-3} M \text{arsenite}$	2.2	.422; .425
$10^{-3} M \text{arsenite}$	6.0	.434; .447
$0.8 N \text{HCl}$	0.4	.413; .414; .411
$10^{-3} M \text{KBr}, 0.8 N \text{HCl}$	0.4	.404; .399; .400

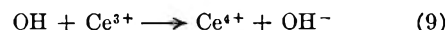
^a $0.8 N \text{H}_2\text{SO}_4$ solutions.

Discussion

The following reactions explain the radiation-induced reduction of ceric by thallos ions⁸



This mechanism holds up to nearly complete consumption of the ceric ions present in solution as long as the concentration of thallos ions is greater than that of cerous ions formed, since $k_4/k_5 = 38$.⁸ $G(\text{Ce}^{3+})$ is therefore equal to $2G_{\text{H}_2\text{O}_2} + G_{\text{H}} +$



G_{OH} . Increasing the thallos concentration decreases $G_{\text{H}_2\text{O}_2}$ by reaction of Ti^{2+} with OH radicals in the spurs before they recombine to form H_2O_2 . But the sequence of reactions 6 and 7 is equivalent to (8) so that $G(\text{Ce}^{3+})$ remains unchanged.⁸ Increasing the ceric ion concentration in the absence of thallos ions has been shown^{11,12} to reduce the yields of molecular hydrogen appreciably, as a result of reaction 5' occurring in the spurs, leading to an increase in $G(\text{Ce}^{3+})$.

From the mechanism proposed by Sworski

$$\begin{aligned} G(\text{Ce}^{3+}) &= 2G_{\text{H}_2\text{O}_2} + G_{\text{H}} + G_{\text{OH}} \\ &= 2G_{-\text{H}_2\text{O}} - 2G_{\text{H}_2} \end{aligned}$$

since from the stoichiometric balance $G_{-\text{H}_2\text{O}} = 2G_{\text{H}_2\text{O}_2} + G_{\text{OH}} = 2G_{\text{H}_2} + G_{\text{H}}$, or

$$\Delta G_{-\text{H}_2\text{O}} = \frac{1}{2}\Delta G(\text{Ce}^{3+}) + \Delta G_{\text{H}_2} \quad (10)$$

where ΔG_{H_2} is negative since the yield of H_2 has decreased. On a statistical basis one would expect that the increase in $G_{-\text{H}_2\text{O}}$ (reaction 3) with increase in concentration of the inorganic solutes would reach an optimum value equal to $2G_{\text{H}_2}$ or $2G_{\text{H}_2\text{O}_2}$. But since G_{H_2} and $G_{\text{H}_2\text{O}_2}$ are not equal,³ the maximum increase in $G_{-\text{H}_2\text{O}}$ would to a first approximation be equal to $G_{\text{H}_2} + G_{\text{H}_2\text{O}_2}$, or 1.20 in $0.8 N \text{H}_2\text{SO}_4$. Ignoring the difference in the molecular yield of hydrogen in air-saturated solution compared to air-free solution, due to scavenging of H atoms by O_2 , one can to a first approximation calculate $\Delta G_{-\text{H}_2\text{O}} = 0.18$ for air-free and $G(\text{Ce}^{3+}) = 9.70$ for air-saturated $0.43 M \text{Ce}^{4+}$ in $10^{-1} M \text{Ti}_2\text{SO}_4$, $0.8 N \text{H}_2\text{SO}_4$ solutions, giving a value for $\Delta G_{-\text{H}_2\text{O}} = 0.735$ according to equation 10.

$G(\text{Ce}^{3+})$ seems to be independent of $[\text{Ti}^{2+}]$ (Fig. 1) in concentrated ceric ion solutions. One must, therefore, assume that the reaction of H atoms with Ti^{2+} must be as fast as the reaction of H atoms with OH radicals, but that in the presence of Ce^{4+} the H atoms react with it instead of with OH or Ti^{2+} .

The yield of molecular hydrogen in air-free $0.8 N \text{H}_2\text{SO}_4$ solutions has been in some controversy, values of $G(\text{H}_2) = 0.45$ ^{13,14} and 0.40 ^{7b} have been obtained. The values of $G(\text{H}_2)$ measured in a number of different systems (Table III, Fig. 2) seem to indicate that the yields of H_2 are slightly lower in acid than in neutral solution. It seems, therefore, that in the radiation chemistry of water with Co^{60} γ -rays, the yield of molecular hydrogen does not increase with increase in the hydrogen ion concentration, whereas the yields of H, OH, H_2O_2 and $G_{-\text{H}_2\text{O}}$ ^{3,15} do. This difference of G_{H_2} with pH raises an interesting argument in connection with the mode of formation of H_2 in the track of the radiation, and gives support to a recent suggestion¹⁶ that in neutral solution molecular

(15) A. O. Allen and H. A. Schwarz, *Proc. 2nd International Conf., Geneva*, 29, 30 (1958).

(16) E. Hayon and J. Weiss, *ibid.*, 29, 80 (1958).

hydrogen is formed from recombination of two hydrated electrons in the water (*cf.* reaction 1)



In acid solution the hydrated electrons can, in the absence of other solutes with which it can react directly as an H_2O^- ,^{16,17} be converted to H atoms



which would then have to recombine to give molecular hydrogen (reaction 1). Ce^{4+} ions present in solution could be expected to compete with the hydrogen ions for reaction with the hydrated electrons. In order to explain the decrease of G_{H_2} with increase in the $[\text{H}^+]$ it is possible that either the H atoms recombine (reaction (1)) more slowly than hydrated electrons (reaction (11)), or

(17) E. Hayon and J. Weiss, *J. Chem. Soc.*, 5091 (1960).

that the rates of reactions (1) and (11) are of the same order of magnitude but that as a result of reaction (12) the dimensions of the spurs are increased¹⁸ and the probability of like-species recombination reduced.

NOTE ADDED.—The results by Mahlman (*J. Am. Chem. Soc.*, **81**, 3203 (1959)) on the determination of $G(\text{H}_2)$ from air-free Ce^{4+} solutions were brought to the attention of the author, after submission of this paper. It does not seem possible to account for the disagreement in our values for $G(\text{H}_2)$.

Acknowledgment.—The author wishes to thank Drs. A. O. Allen and H. A. Schwarz for many discussions and valuable suggestions in connection with this work.

(18) H. A. Schwarz, J. M. Caffrey, Jr., and G. Scholes, *J. Am. Chem. Soc.*, **81**, 1801 (1959).

THE REACTION OF FERRIC CHLORIDE WITH SODIUM AND POTASSIUM CHLORIDES

BY CHARLES M. COOK, JR., AND WENDELL E. DUNN, JR.

Pigments Department, E. I. du Pont de Nemours & Co., Inc., Wilmington, Delaware

Received February 9, 1961

The equimolar complexes of FeCl_3 with NaCl and KCl have been studied by phase behavior, X-ray diffraction, thermochemical and vapor pressure methods. The phase diagrams show double eutectics, the FeCl_3 - NaCl system at $X_{\text{NaCl}} = 0.48$ and 0.51, and FeCl_3 - KCl at $X_{\text{KCl}} = 0.45$ and 0.52. The standard heat of the reaction $\text{NaCl} + \text{FeCl}_3 = \text{NaCl} \cdot \text{FeCl}_3$ at 25° is -0.8 kcal./mole; that to form $\text{KCl} \cdot \text{FeCl}_3$ is -7.2 kcal./mole. The temperature and composition dependence of ferric chloride pressure above its mixtures with NaCl and KCl indicate the 1:1 complexes to be stable in the melt and to be as $\text{M}^+ \text{FeCl}_4^-$. Evidence is presented for the existence of $\text{NaCl} \cdot \text{FeCl}_3$ and $\text{KCl} \cdot \text{FeCl}_3$ in the vapor phase.

Introduction

Ferric chloride is known to form 1:1 addition compounds with molecules capable of supplying a chloride ion, *e.g.*, with Et_4NCl ,¹ NH_4Cl ,² TiCl_4 ,³ NOCl ,⁴ CNCl ,⁵ POCl_3 ,⁶ PCl_5 .⁷ These compounds are regarded as containing the $[\text{FeCl}_4]^-$ ion; their solutions in non-aqueous solvents are electrically conducting, and electrolysis of FeCl_3 in CNCl transports Fe to the anode.⁵

Two previous studies of the FeCl_3 - NaCl phase diagram have indicated a single eutectic, without evidence of compound formation.^{8,9} Although the vapor pressure of ferric chloride is strongly reduced in the presence of sodium chloride, Johnstone, *et al.*,⁸ who determined the ferric chloride pressure above melts containing up to 46 mole % NaCl , explained this reduction as the normal effect of the solute in lowering vapor pressure and found no evidence for the existence of a compound. This explanation, however, is not compatible with the ob-

servation by Dunn¹⁰ that, below 400°, the ferric chloride pressure drops rapidly to nearly zero at 50 mole % NaCl .

In the chemically similar system NaCl - AlCl_3 both the vapor pressure¹¹ and phase diagram¹² data are consistent in indicating the NaAlCl_4 compound.

Experimental

Sample Preparation.—Two alternate procedures for preparation of FeCl_3 - NaCl melts were employed. Those FeCl_3 - NaCl mixtures having less than 50 mole % NaCl that were used in measurement of the ferric chloride vapor pressures were prepared by mixing FeCl_3 (B & A Code 1733 Sublimed Technical) and NaCl (B & A, C.P.). The resulting mixture was treated with COCl_2 for several days to remove traces of ferric oxide before vapor pressure measurements were carried out. Melt compositions were determined at the beginning and end of each vapor pressure run by sampling and analysis.

The ferric chloride-alkali chloride melts used for the remaining vapor pressure, the phase diagram, and the calorimetric studies were prepared in the following manner. Alkali chloride was added to the bulb which was to contain the salt mixture. Air was removed by evacuation and back filling with Cl_2 , and the salt was warmed to 300°. Iron wire, contained in a side tube attached to this bulb, was burnt in a stream of chlorine, and the ferric chloride sublimed into the salt. The traces of iron and alkali chloride carried by the chlorine from the pot during sample preparation were trapped in a Pyrex wool plug located before the exit bubbler and were determined by analysis. The melt

(1) V. Gutmann and F. Mairinger, *Z. anorg. allgem. Chem.*, **289**, 279 (1957).

(2) K. Hachmeister, *Z. anorg. Chem.*, **109**, 145 (1919).

(3) G. Scarpa, *Atti Acad. Lincei*, [5] **21**, 720 (1912).

(4) J. Lewis and D. B. Sowerly, *J. Chem. Soc.*, 1617 (1957).

(5) A. A. Woolf, *ibid.*, 252 (1954).

(6) V. V. Dadape and M. R. A. Rao, *J. Am. Chem. Soc.*, **77**, 6192 (1955).

(7) Ya. A. Fialkov and Ya. B. Burzanov, *Doklady Akad. Nauk S.S.S.R.*, **92**, 585 (1953).

(8) H. F. Johnstone, H. C. Weingartner and W. E. Winsche, *J. Am. Chem. Soc.*, **64**, 241 (1942).

(9) I. S. Morozov and D. Ya. Toptygin, *Zhur. Neorg. Khim.*, **2**, 2129 (1957).

(10) W. E. Dunn, Jr., presented at A.C.S. Delaware Valley Regional Meeting, Feb. 16, 1956.

(11) E. W. Dewing, *J. Am. Chem. Soc.*, **77**, 2639 (1955).

(12) U. J. Shvarteman, *Zhur. Fiz. Khim.*, **14**, 254 (1940).

compositions were determined from the weights of salt and iron put into the mixture.

The sodium chloride and potassium chloride were purified by fusion in HCl and were crushed and stored under a dry atmosphere. The iron wire was Baker Analyzed reagent grade; the chlorine was Matheson "oxygen-free."

In subsequent discussion where melt compositions are expressed as mole fraction of alkali chloride, MCl, this is an input or nominal mole fraction; $X_{MCl} = N$ input MCl/ N input MCl + N input FeCl₃. The mole fractions of MFeCl₄, on the other hand, are believed to represent the actual concentrations of MFeCl₄ in the melt and are calculated presuming reaction 2 to be quantitative. In MCl-rich melts $X_{MFeCl_4} = N$ input FeCl₃/ N input MCl.

Phase Diagrams.—The salt mixtures used in the phase studies were prepared in 30 mm. d. by 4" Vycor bulbs and were sealed off under a Cl₂ pressure of 90 mm. The bulbs were then placed inside a cavity, formed of "TIPERSUL" insulation, inside a 7" length of 2.5" d. heavy wall steel pipe located within a well-insulated tube furnace. Agitation of the molten mixture was provided by rocking the tube furnace.

The transition temperatures of the salt mixtures were determined from their cooling curves. Salt temperatures were measured by a Chromel-Alumel thermocouple, which had been standardized previously against the melting point of bismuth, located in a well along the axis of the bulb. The phase transitions were located by following the temperature differential between sample and surrounding pipe, measured by two pairs of Chromel-Alumel thermocouples, on a Minneapolis-Honeywell Brown recorder. Changes in cooling rate appeared as sharp discontinuities in the slope of the differential temperature vs. time plot. Transformation temperatures measured by this method were reproducible to $\pm 1^\circ$ below 250° and to $\pm 2^\circ$ for higher temperatures.

X-Ray Powder Patterns.—Mixtures of NaCl-FeCl₃ and KCl-FeCl₃ were taken from the sample bulbs after cooling curves were run, ground in a dry box and loaded into 0.5 mm. Lindemann glass capillaries and exposed to iron filtered 35 Kv. cobalt radiation for four hours in a powder camera.

The D spacings were read from the Debye-Scherrer photographs with a Mies scale, and the intensities of the lines were estimated visually.

Calorimetric Measurements.—The solution calorimeter was a one-liter Dewar flask closed with a cork through which were brought a Beckmann thermometer, a stirrer, and tube for introducing samples. The calorimeter contained 800 cc. of HCl + NaCl + KCl solution in which the ferric chloride-containing salts were readily soluble. The water equivalent of the calorimeter plus the solution was measured by observing the temperature rise per watt minute passed through a resistor inside the calorimeter.

Approximately 10-g. samples of NaCl, KCl, FeCl₃, NaFeCl₄ and KFeCl₄ were loaded in a dry box into glass bottles which were then paraffined and stored in a desiccator until use. The FeCl₃ had been purified by sublimation in Cl₂; the NaFeCl₄ and KFeCl₄ had been prepared and used in the phase studies. These salts were stored in sealed bulbs until this use.

A sample bottle was weighed, the calorimeter entry tube unstoppered, the sample quickly uncapped and dumped through the tube into the HCl solution, the calorimeter closed and the emptied bottle reweighed. In this process the salts were exposed to the atmosphere for less than three seconds. Heats of solution were determined from the temperature change. The calorimeter was operated near room temperature; thus corrections for the sensible heat introduced with the salt were small.

Measured heats of solution were

in 4.92 N HCl

NaCl = -2.2 kcal./mole
KCl = -4.0 kcal./mole
FeCl₃ = 20.8 kcal./mole
NaFeCl₄ = 18.1 kcal./mole
KFeCl₄ = 9.6 kcal./mole

in 6.14 N HCl, 0.125 N NaCl, 0.125 N KCl

NaCl = -2.3 kcal./mole
KCl = -3.9 kcal./mole
FeCl₃ = 18.8 kcal./mole
NaFeCl₄ = 15.6 kcal./mole
KFeCl₄ = 6.8 kcal./mole

Heats of fusion and heat capacities were determined in a drop calorimeter constructed in the same fashion as the solution calorimeter except that the entry port was replaced by a Pyrex test-tube and the calorimeter contained H₂O rather than HCl solution. The test-tube, extending into the water, was padded on the bottom with a plug of Pyrex wool and contained 10 cc. of silicone oil to facilitate heat transfer.

The sample was sealed into a Pyrex ampoule and this was suspended by a fine copper wire inside a tube furnace. The sample temperature was measured with a Chromel-Alumel thermocouple placed in a thermocouple well extending about three-quarters of the way into the ampoule. The tube furnace was constructed of an electrically heated, asbestos-jacketed, 3/4" by 11" l. copper pipe. The top of the furnace was sealed with an asbestos plug through which passed the sample thermocouple and the copper wire suspending the ampoule. In the region of the sample the furnace wall temperature was uniform to $\pm 2^\circ$.

When the sample had come to constant temperature, the tube furnace was swung into position over the calorimeter, an aluminum radiation shield removed, and the sample dropped into the test-tube by cutting the copper wire. The furnace then was removed and the test-tube corked. Because of the short time of exposure and the relatively low temperatures employed, radiative heat transfer from the furnace to the calorimeter during the release of the sample was not significant.

The heat content of the Pyrex in the ampoule was calculated assuming that for Pyrex $C_p = 0.20$ cal./g.

For calibration, the heat contents of a sample of bismuth were determined at two temperatures using the drop calorimeter with the above procedure.

Temp., °K.	Obsd. $H_T - H_{300}$ cal./mole	Actual $H_T - H_{300}$, ¹³ cal./mole
518	1470	1460 \pm 30
584	4550	4560 \pm 80

Vapor Pressure.—The pressures of FeCl₃ and MFeCl₄ above ferric chloride-alkali chloride mixtures were measured by a transpiration method. The molten salts were contained in a long-necked Vycor flask immersed in molten solder. The carrier gas, Cl₂ at 40-120 cc./min., was brought into the melt by a side arm sealed to the flask. For melt temperatures in excess of 600° the Cl₂ was preheated with a Nichrome winding around the side arm before it passed through the solder bath into the Vycor flask. After bubbling through the melt the Cl₂ passed through a condenser and was exhausted through a bubbler. Cl₂ flow was measured by capillary flowmeters or by titration of I₂ liberated from KI solutions.

The condenser was a Vycor tube sealed at the one end to a standard taper grind and formed at the other end into a cup to trap any liquid running down the inside surface. The condenser was inerted through the neck of the Vycor flask, the grind sealing to a corresponding grind on the neck of the flask, the cup extending down into the heated zone. A plug of Refrasil wool in the condenser opening at the cup end prevented splattered melt from being carried by the Cl₂ into the condenser.

In a typical run the condenser was flushed with Cl₂ and inserted into the flask. A constant flow rate of Cl₂ was then bubbled through the melt for a known time, after which the condenser was removed and the deposited chlorides washed out and analyzed for Fe (by Volhard procedure) and Na (with zinc uranyl acetate) or K (with NaBPh₄). An argon purge, entering through a side arm in the neck of the flask, blanketed the melt during changing of condensers.

The observed data, the moles of Fe(III) and M(I) transported per mole Cl₂, were converted to vapor pressures on the assumption that the gas phase species were FeCl₃(g), Fe₂Cl₆(g) and MFeCl₄(g). Duplicate runs at different Cl₂ flow rates indicated the vapor pressures to be independent of Cl₂ flow.

The vapor pressure data are presented as P_{FeCl_3} , the combined vapor pressures of ferric chloride monomer and dimer, and as P_{MFeCl_4} , the vapor pressure of the presumed monomeric complex.

(13) O. Kubaschewski and E. Evans, "Metallurgical Thermochemistry," 2nd Ed., John Wiley and Sons, New York, N. Y., 1956.

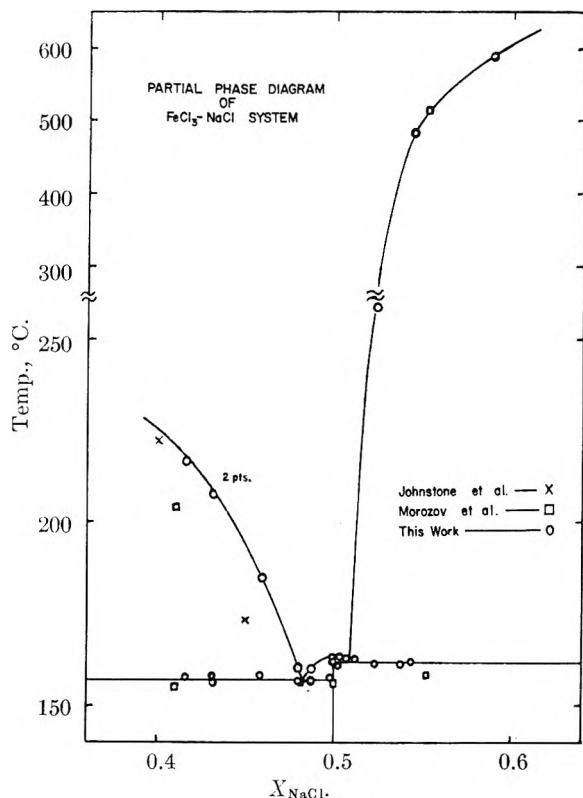


Fig. 1.—Partial solid-liquid phase diagram of the system $\text{FeCl}_3\text{-NaCl}$. Eutectics at $X_{\text{NaCl}} = 0.48, 157^\circ$; $X_{\text{NaCl}} = 0.51, 162^\circ$. Congruent m.p. = 163° .

Discussion

Phase Data.—Figures 1 and 2 show the phase diagrams of $\text{FeCl}_3\text{-NaCl}$ and $\text{FeCl}_3\text{-KCl}$ in the regions between 40 and 60 mole % FeCl_3 . Both of these diagrams are seen to be consistent with the formation of a congruently melting 1:1 compound. The low melting point of NaFeCl_4 causes the $\text{FeCl}_3\text{-NaCl}$ phase diagram to resemble that of a simple eutectic; the existence of the compound is apparent, however, in the consistent 4.5° difference in eutectic temperatures above and below $X_{\text{NaCl}} = 0.50$. The higher melting KFeCl_4 shows clearly as a congruently melting compound in the $\text{FeCl}_3\text{-KCl}$ system.

A poorly-defined solid state phase transformation occurs at $\sim 156^\circ$ in the $\text{FeCl}_3\text{-KCl}$ system.

The existence of the compounds NaFeCl_4 and KFeCl_4 was confirmed by X-ray patterns of the powdered salt mixtures. A complex pattern of lines was observed, with the most intense occurring at 3.18, 3.02, 2.91, 2.82, 2.43, 2.26, 2.24, 2.07, 1.76, 1.72 and 1.55 Å. for NaFeCl_4 and at 3.86, 3.70, 2.75, 2.66, 2.48, 2.36 and 1.74 Å., for KFeCl_4 . In addition to the MFeCl_4 patterns, in mixtures containing more than 50 mole % alkali chloride NaCl or KCl lines appeared strongly. For mixtures with less than 50 mole % alkali chloride the pattern of ferric chloride was present and alkali chloride lines appeared only weakly if at all.

Calorimetric Data.—The difference between the heats of solution in aqueous HCl of $\text{MFeCl}_4(\text{c})$ and of $\text{MCl}(\text{c})$ plus $\text{FeCl}_3(\text{c})$ is $\Delta H^0_{(1,\text{M})}$, the enthalpy change at 25° of the reaction

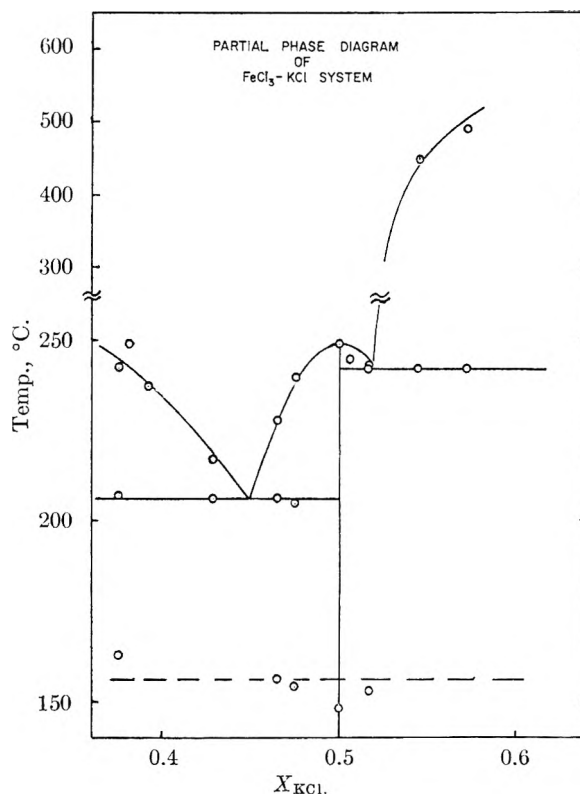
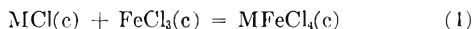


Fig. 2.—Partial solid-liquid phase diagram of the system $\text{FeCl}_3\text{-KCl}$. Eutectics at $X_{\text{KCl}} = 0.45, 206^\circ$; $X_{\text{KCl}} = 0.52, 242^\circ$. Congruent m.p. = 249° .

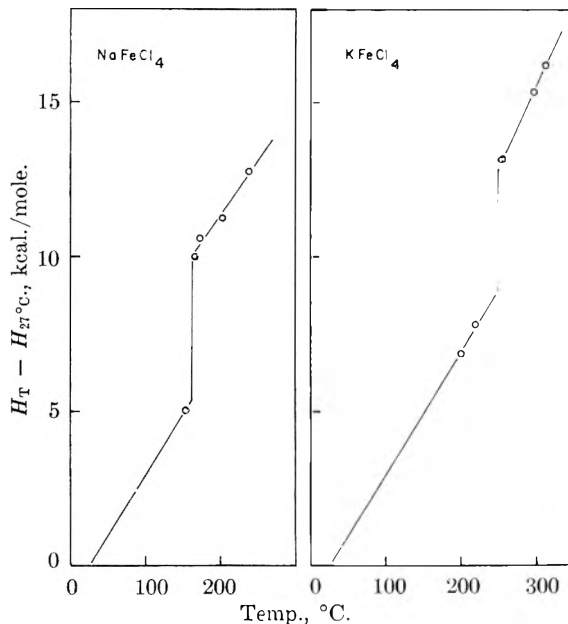


Fig. 3.—Relative enthalpies of NaFeCl_4 and KFeCl_4 .

Reaction 1 is exothermic for $\text{NaFeCl}_4(\text{c})$ and $\text{KFeCl}_4(\text{c})$, although for the former the heat effect is slight.

$$\Delta H^0_{(1,\text{Na})} = -0.8 \pm 0.6 \text{ kcal./mole}$$

$$\Delta H^0_{(1,\text{K})} = -7.2 \pm 1 \text{ kcal./mole}$$

The difference in exothermicity between K and Na salts is in part due to the smaller lattice energy¹⁴ of $\text{KCl}(\text{c})$ ($-169.9 \text{ kcal./mole}$).

(14) D. Cubicciotti, *J. Chem. Phys.*, **33**, 1579 (1960).

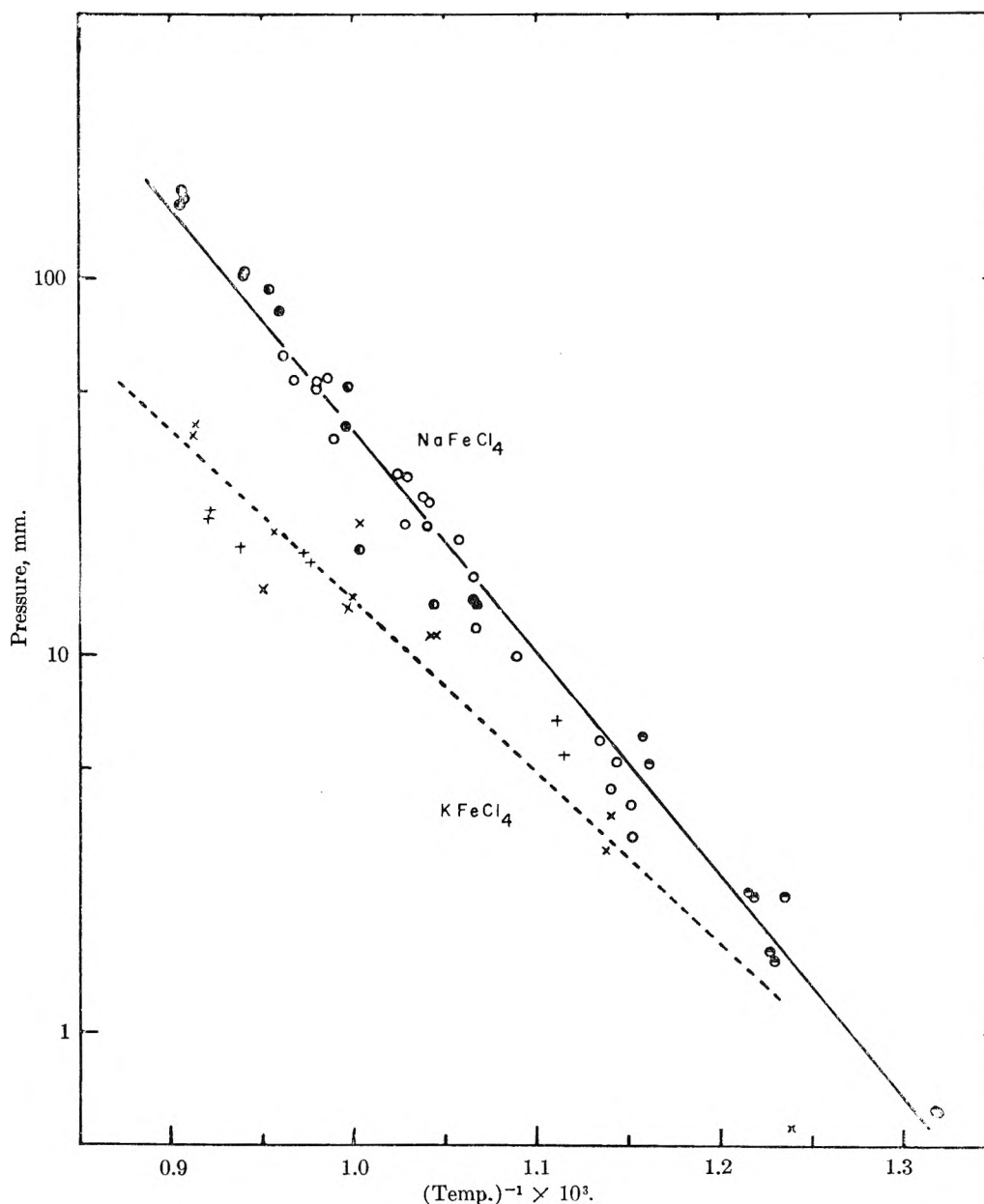
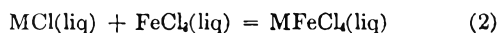


Fig. 4.—Vapor pressures of NaFeCl_4 and KFeCl_4 : \odot , $X_{\text{NaCl}} = 0.514$; \circ , $X_{\text{NaCl}} = 0.540$; \bullet , $X_{\text{NaCl}} = 0.575$; \odot , $X_{\text{NaCl}} = 0.650$; \times , $X_{\text{KCl}} = 0.525$; $+$, $X_{\text{KCl}} = 0.575$.

Figure 3 shows the variation with temperature of molar heat content of NaFeCl_4 and KFeCl_4 measured with the drop calorimeter. The values of heat capacities and heats of fusion, determined from the slopes of the lines and from the step heights in this figure, respectively, are in Table I.

Compd.	C_p solid, cal./mole C.	C_p liquid, cal./mole C.	ΔH Fusion, kcal./mole	ΔS Fusion, e.u./mole
NaFeCl_4	39.5	42.1	4.30	9.86
KFeCl_4	40.0	53.0	3.85	7.36

The above thermodynamic values indicate that the tetrachloroferrate complex should form exothermically, not only in the solid state, but also in the melt. Thus, at temperature $T^\circ\text{K}$., the reaction



will have enthalpy change

$$\Delta H_{(2,M)} = \Delta H^0_{(1,M)} + [\Delta H_{F(\text{MFeCl}_4)} - \Delta H_{F(\text{FeCl}_3)} - \Delta H_{F(\text{MCl})}]_{(298)} + \int_{298}^T [\Delta C_{p(\text{liq})} - \Delta C_{p(\text{e})}] dT \quad (3)$$

Substitution of the heat of fusion^{15,16} and heat capacity¹⁷ values for MCl , FeCl_3 and MFeCl_4 into (3) yields

$$\Delta H_{(2,\text{Na})} = -7600 - 5.35T \text{ cal./mole, } 300^\circ\text{K.} < T < 600^\circ\text{K.}$$

$$\Delta H_{(2,\text{K})} = -19900 + 5.81T \text{ cal./mole, } 300^\circ\text{K.} < T < 600^\circ\text{K.}$$

(15) N.B.S. Circular 500, "Selected Values of Chemical Thermodynamic Properties," 1952.

(16) The values $\Delta H_{(580.7)}(\text{FeCl}_3 \text{ Fusion}) = 9 \pm 0.4$ kcal./mole FeCl_3 and $\Delta H_{(580.7)}(\text{FeCl}_3 \text{ Vap.}) = 14.9 \pm 0.8$ kcal./mole FeCl_3 are used herein. C. M. Cook, Jr., unpublished work.

(17) C_p values are from K. K. Kelley, "Contributions to The Data on Theoretical Metallurgy. XIII," Bulletin 584, U. S. Bureau of Mines (1960).

for the liquid state reaction of the sodium and potassium salts, respectively.

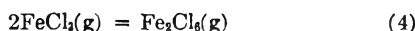
Vapor Pressure. $MFeCl_4$.—Chlorine passing through a ferric chloride-alkali chloride melt transports, in addition to ferric chloride, appreciable quantities of sodium or potassium salts. Since pure NaCl or KCl is not significantly volatile within the experimental temperature range, and since the Fe(III)/M(I) ratio transported is never less than unity, it appears reasonable that the vapor above the melt contains a complex species, probably $MFeCl_4$. Dewing¹¹ has reported volatilization of $NaAlCl_4$ from $AlCl_3$ -NaCl melts and Porter and Zeller¹⁸ find $LiAlF_4(g)$ above molten AlF_3 -LiF.

For melts at constant composition the logarithms of the vapor pressures of $NaFeCl_4$ and $KFeCl_4$ vary linearly with reciprocal temperature as is shown in Fig. 4. The plotted points are the observed vapor pressures divided by the X_{MFeCl_4} in the melt. The solid line represents the least squares fit of the P_{NaFeCl_4} data, the dotted line of the P_{KFeCl_4} data. The partial pressures of $MFeCl_4$ over liquids of nominal composition $MFeCl_4$ are calculated to be

$$\log P_{NaFeCl_4} \text{ (mm.)} = 7.496 - 5904T^{-1} \\ 750^\circ\text{K.} \leq T \leq 1100^\circ\text{K.}$$

$$\log P_{KFeCl_4} \text{ (mm.)} = 5.657 - 4517T^{-1} \\ 850^\circ\text{K.} \leq T \leq 1100^\circ\text{K.}$$

Ferric Chloride.—Ferric chloride vapor below 400° exists primarily as the dimer, $Fe_2Cl_6(g)$, and above 600° as the monomer, $FeCl_3(g)$. The equilibrium is



with¹³

$$\Delta H^\circ = -32.55 \text{ kcal.}, \Delta S^\circ = -31.65 \text{ e.u.}; \\ 778^\circ\text{K.} \leq T \leq 998^\circ\text{K.}$$

Within the experimental temperature range, 250 – 750° , ferric chloride vapor will be present both as monomer and dimer. For convenience in presentation the ferric chloride pressures in equilibrium with the $FeCl_3$ -MCl melts are expressed in Fig. 5 and 6 as a combined pressure of monomer and dimer *i.e.*

$$P_{FeCl_3}^t = P_{FeCl_3} + 2P_{Fe_2Cl_6} \quad (5)$$

Addition of NaCl to ferric chloride brings about a steep, titration-like decrease in vapor pressure to almost zero at 50 mole % NaCl. As shown in Fig. 5, at 352° the vapor pressure drops by 2.5 orders of magnitude as the melt composition changes from 45 to 50 mole % NaCl. This behavior is consistent with the existence in the melt of a 1:1 compound between $FeCl_3$ and NaCl.

The solid and the dashed curves in Fig. 5 represent the $P_{FeCl_3}^t$ composition dependence anticipated if the unreacted ferric chloride is dissolved in the ionized $NaFeCl_4$ melt as Fe_2Cl_6 or as $FeCl_3$, respectively, and if Raoult's law is obeyed.¹⁹

The dependence upon temperature of ferric chloride pressure above $FeCl_3$ -MCl melts is shown in

(18) R. F. Porter and E. E. Zeller, *J. Chem. Phys.*, **33**, 858 (1960).

(19) The $FeCl_3$ -NaCl liquidus temperatures of Johnstone, *et al.*, are ca. 10° higher than the freezing points calculated from $d \ln X_{Fe_2Cl_6} / dT^{-1} = -\Delta H_F / R$ presuming $\Delta H_F = 18$ kcal./mole Fe_2Cl_6 and the f.p. of $Fe_2Cl_6 = 307.5^\circ$. This temperature difference indicates $\gamma_{Fe_2Cl_6} \sim 1.5$ at 290° .

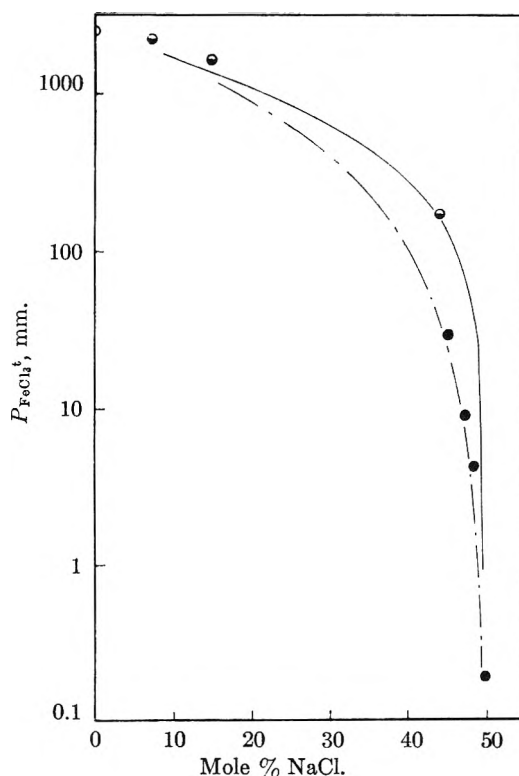
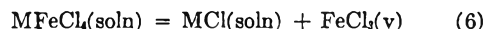


Fig. 5.—Vapor pressure of ferric chloride above $FeCl_3$ + NaCl mixture at 352° : \circ , Stirneman; \ominus , Johnstone, *et al.*; \bullet , this work.

Fig. 6. The straight lines, which are least squares averages of the $P_{FeCl_3}^t$ vs. T^{-1} data at constant composition, show, for melt compositions below 50 mole % NaCl, slopes approximately parallel to the slope of the $FeCl_3$ liquid vapor pressure curve given by Stirneman²⁰; above 50 mole % NaCl the slopes steepen. The KCl-containing melts exhibit lower ferric chloride vapor pressures and steeper $d \log P_{FeCl_3}^t / dT^{-1}$ slopes than similar NaCl melts.

In Table II concentration equilibrium constants for the reaction



are presented for $FeCl_3$ -MCl mixtures containing excess alkali chloride. The approximate constancy of the K_{eq} values is consistent with the formation of the $MFeCl_4$ species.

TABLE II
EQUILIBRIA AT 1000°K. ACCORDING TO REACTION 6

Mole %	MCl	X_{MFeCl_4}	P_{FeCl_3} , mm.	$K_{eq} = \frac{X_{MCl}}{X_{MFeCl_4}} \frac{P_{FeCl_3}}{P_{MFeCl_4}}$
54.0	NaCl	0.855	73.3	12.0
57.5	NaCl	.739	37.2	13.0
65.0	NaCl	.539	18.8	16.0
52.5	KCl	.905	24.3	2.6
57.5	KCl	.739	7.46	2.6

As a check of agreement between calorimetric and vapor pressure data it is instructive to compare enthalpies of solution of ferric chloride in $MFeCl_4$ derived from the slopes of the curves in Fig. 6 with the enthalpies of reaction 2. From the $d \log$

(20) E. Stirneman, *Neues Jahrb. Min. Geol. Paleontology*, **A62**, 334, 353 (1925).

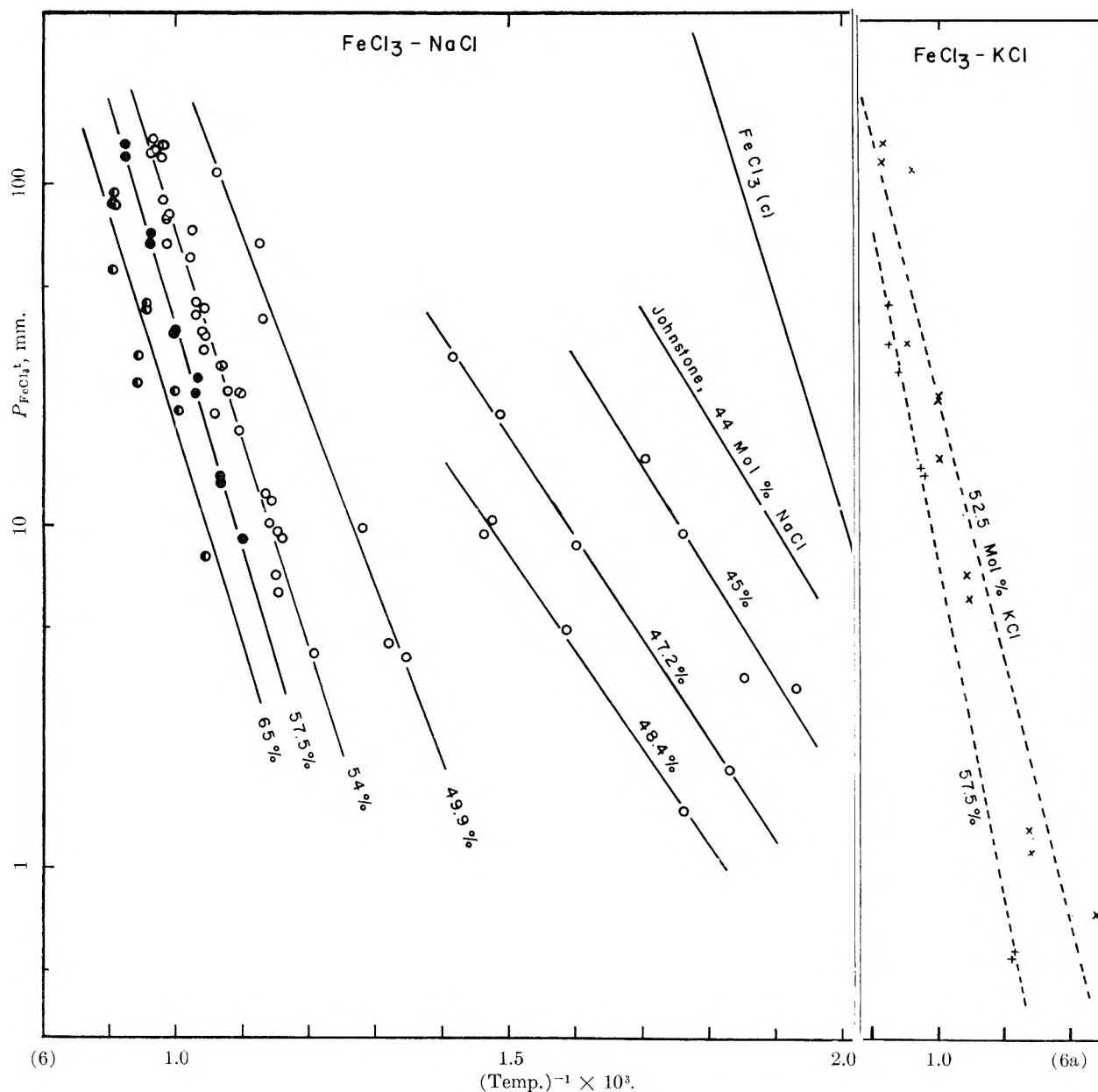
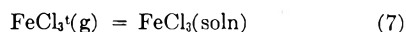


Fig. 6.—Temperature dependence of ferric chloride vapor pressure above $\text{FeCl}_3 + \text{NaCl}$ and $\text{FeCl}_3 + \text{KCl}$ mixtures.

$P_{\text{FeCl}_3}/dT^{-1}$ values of Fig. 6 the enthalpy changes, $\Delta H_{(7)}$'s, of the reaction

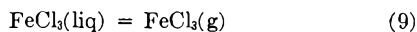


can be obtained at the several melt compositions. Assuming $\Delta C_{p(8)} = -15 \text{ cal./mole } ^\circ$, the enthalpy of vaporization



$$\Delta H_{(8)} = 16160 - 15T \text{ cal./mole}$$

combined with the enthalpy of reaction 4 at 888°K . yields for



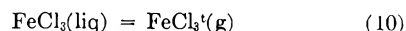
$$\Delta H_{(9)} = 19 \text{ kcal./mole}$$

An average enthalpy of vaporization, $\Delta H_{(10)}$, can be computed for a series of P_{FeCl_3} data points at constant composition by combining $\Delta H_{(8)}$ and $\Delta H_{(9)}$ in proportion to the average fraction of the FeCl_3 present as Fe_2Cl_6 and FeCl_3 , respectively.

TABLE III

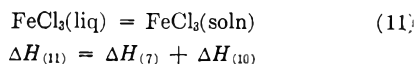
ESTIMATION OF THE HEAT OF SOLUTION OF $\text{FeCl}_3(\text{liq})$ IN MOLTEN $\text{MFeCl}_4 + \text{MCl}$ MIXTURES FROM $d \log P_{\text{FeCl}_3}/dT^{-1}$ (i.e., $\Delta H_{(11)}$); AND FROM CALORIMETRIC DATA (i.e., $\Delta H_{(2,M)}$)

X_{NaCl}	Av. temp., $^\circ\text{K}$.	$\Delta H_{(11)}$, kcal.	$\Delta H_{(2,\text{Na})}$, kcal.
0.472	630	+1	0
.484	640	+1	0
.499	830	-8	0
.514	810	-10	-12
.540	950	-10	-13
.575	980	-12	-13
.650	1050	-10	-13
X_{KCl}	Av. temp.	$\Delta H_{(11)}$	$\Delta H_{(2,\text{K})}$
0.525	970	-16	-14
0.575	1000	-25	-14



$$\Delta H_{(10)} = 2\Delta H_{(8)} [P_{\text{Fe}_2\text{Cl}_6}/(P_{\text{Fe}_2\text{Cl}_6} + P_{\text{FeCl}_3})]_{\text{avg.}} + \Delta H_{(9)} [P_{\text{FeCl}_3}/(P_{\text{Fe}_2\text{Cl}_6} + P_{\text{FeCl}_3})]_{\text{avg.}}$$

Adding equations 7 and 10



yields $\Delta H_{(11)}$, the apparent heat of solution of liquid FeCl_3 in the melt as derived from the slope of the vapor pressure curves.

Now if indeed it is true that ferric chloride reacts with sodium chloride according to reaction 2, then for initial FeCl_3/MCl mole ratios greater than unity $\Delta H_{(11)}$ should be approximately zero, and for FeCl_3/MCl ratios less than unity $\Delta H_{(11)}$ should

approximate $\Delta H_{(2,M)}$. In Table III the values of $\Delta H_{(11)}$ calculated from the $\log(\text{vapor pressure})-\text{temp.}^{-1}$ slopes are compared with the values of $\Delta H_{(2,M)}$ calculated from the calorimetric data and equation 3. In view of the uncertainties introduced with measurements of slope and with the 400° extrapolation of reaction 2 the agreement between $\Delta H_{(11)}$ and $\Delta H_{(2,M)}$ is satisfactory. The apparent disagreement in the last KCl series is possibly the result of analytical error in the pair of points at $T^{-1} = 1.11$; if these are omitted the $\Delta H_{(11)}$ derived from the least squares slope of the remaining points is -18 kcal., in better agreement with $\Delta H_{(2,K)}$.

E.M.F. MEASUREMENTS IN MOLTEN BISMUTH-BISMUTH TRICHLORIDE SOLUTIONS¹

By L. E. TOPOL, S. J. YOSIM AND R. A. OSTERYOUNG

Atomics International, A Division of North American Aviation, Inc., Canoga Park, California

Received February 27, 1961

E.m.f. studies on cells of the type $\text{C, Bi}(N_1), \text{BiCl}_3(1 - N_1) \parallel \text{BiCl}_3(1 - N_2), \text{Bi}(N_2), \text{C}$ where N denotes mole fraction, were made at 238, 270, 300, 325 and 350° ; also, the effects of varying acidity were observed by examining a cell containing a 70 mole % BiCl_3 -30 mole % KCl melt at 325° , and another with a 75% BiCl_3 -25% AlCl_3 melt at 270° . The Bi concentration N_1 in the reference half-cell was held constant, and the Bi concentration N_2 in the other half-cell was varied from 0 to about 0.06 by coulometric addition. A cell containing higher concentrations, *i.e.*, $N_2 = 0.07$ to 0.25, was studied in a similar manner. Plots of the e.m.f. vs. \log Bi concentration yielded initially straight lines which changed slope at low metal concentrations, *i.e.*, $N_2 < 0.01$; the metal concentration at which this departure from linearity occurred increased with temperature and with the acidity of the system. For the low concentration region a slope corresponding to a Nernst n of 2.05 ± 0.10 , consistent with the species Bi^+ , was found at all temperatures. The data for the higher Bi concentrations, *i.e.*, $N_2 > 0.01$, are interpreted in terms of the species Bi_2Cl_4 . The equilibrium constant, K_N , for the reaction $4\text{BiCl} = \text{Bi}_2\text{Cl}_4$ can be expressed as $\log K_N = [(4.49 \pm 0.54) \times 10^3]/T^\circ\text{K} - 1.930 \pm 0.945$ for $N_{\text{Bi}} < 0.09$ and the temperature range 238 to 350° .

Introduction

Although the phase diagram^{2,3} and properties⁴⁻⁷ of the bismuth-bismuth trichloride system have been investigated, the mode of solution of the metal in its molten salt is still uncertain. The solid subhalide BiCl has been isolated,⁸ and a cryoscopic study^{9a} yielded results which were consistent with the species Bi_2Cl_4 ^{9a,b} in solution. In a recent polarographic study¹⁰ it was found that in BiCl_3 melts containing low concentrations of bismuth (less than 0.002 mole fraction) the species resulting from solution of the metal could be oxidized, and this reaction appeared to be reversible at an inert electrode. In addition, an analysis of the polarograms yielded apparent Nernst n 's of 1.5-1.8. These results, although inconclusive, suggest Bi^+

(for which $n = 2.0$) as the most probable entity at low bismuth concentrations.

In conjunction with the polarographic work above, an e.m.f. study was performed on this system. The potentiometric method has been utilized with apparent success in the $\text{Cd}-\text{CdCl}_2-\text{KCl}$,¹¹ $\text{Li}-\text{LiCl}$,¹² $\text{Pb}-\text{PbCl}_2$,¹³ $\text{Ce}-\text{CeCl}_3$ ¹⁴ and $\text{Sb}-\text{SbI}_3$ ¹⁵ systems, and appropriate concentration cells should yield more conclusive information as to species in $\text{Bi}-\text{BiCl}_3$ solutions at low bismuth concentrations. In addition, the effect of changes in acidity was investigated by the addition of AlCl_3 , in one case, and KCl , in another, to the system.

Experimental

Materials.—The purification of most of the materials used has been described elsewhere.^{3,10} Reagent grade KCl was dried by heating at 600° under vacuum. Anhydrous AlCl_3 was prepared by repeated sublimation of the reagent grade salt *in vacuo*.

Apparatus and Procedure.—The cells and procedure employed in the bulk of this work were similar to those used in a polarographic study.¹⁰ However, the e.m.f. cells differed from these in that they usually incorporated several reference half-cells; the reference half-cells contained weighed amounts of Bi and BiCl_3 to give metal mole fractions of 0.0025, 0.005

(1) This work was carried out under the auspices of the Research Division of the Atomic Energy Commission.

(2) M. A. Sokolova, G. G. Urazov and V. G. Kuznetsov, *Akad. Nauk, S.S.S.R., Inst. Gen. Inorg. Chem.*, **1**, 102 (1954).

(3) S. J. Yosim, A. J. Darnell, W. G. Gehman and S. W. Mayer, *J. Phys. Chem.*, **63**, 230 (1959).

(4) D. Cubicciotti, F. J. Keneshea, Jr., and G. M. Kelley, *ibid.*, **62**, 463 (1958).

(5) F. J. Keneshea, Jr., and D. Cubicciotti, *ibid.*, **62**, 843 (1958).

(6) M. A. Bredig, H. A. Levy, F. J. Keneshea and D. Cubicciotti, *ibid.*, **64**, 191 (1960).

(7) A. J. Darnell and S. J. Yosim, *ibid.*, **63**, 1813 (1959).

(8) J. D. Corbett, *J. Am. Chem. Soc.*, **80**, 4757 (1958).

(9a) S. W. Mayer, S. J. Yosim and L. E. Topol, *J. Phys. Chem.*, **64**, 238 (1960).

(9b) M. A. Bredig, *ibid.*, **63**, 978 (1959).

(10) L. E. Topol and R. A. Osteryoung, *J. Electrochem. Soc.*, **108**, 573 (1961).

(11) S. Karpachev and A. Stromberg, *Zhur. Fiz. Khim.*, **13**, 397 (1939).

(12) S. Karpachev and E. Jordan, *ibid.*, **14**, 1495 (1940).

(13) S. Karpachev, A. Stromberg and E. Jordan, *ibid.*, **18**, 43 (1944).

(14) S. Senderoff and G. W. Mellors, *J. Electrochem. Soc.*, **105**, 224 (1958); *cf.*, however, H. R. Bronstein, A. S. Dworkin and M. A. Bredig, *J. Phys. Chem.*, **64**, 1344 (1960).

(15) J. Corbett and F. C. Albers, *J. Am. Chem. Soc.*, **82**, 533 (1960).

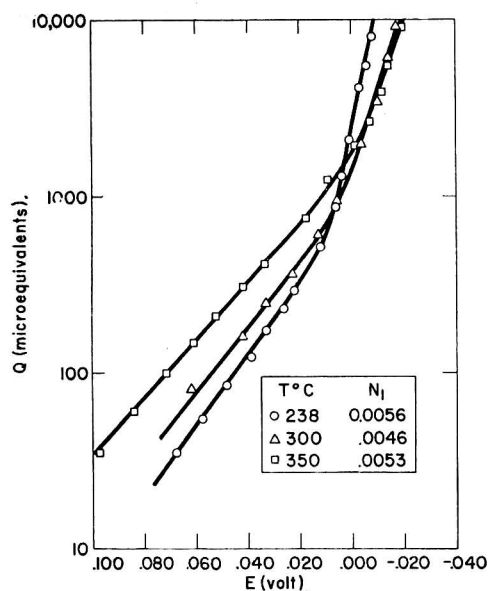


Fig. 1.—Log Q vs. E results for cells of the type: $\text{Bi}(N_1)$, $\text{BiCl}_3 \parallel \text{BiCl}_3, \text{Bi}(Q)$.

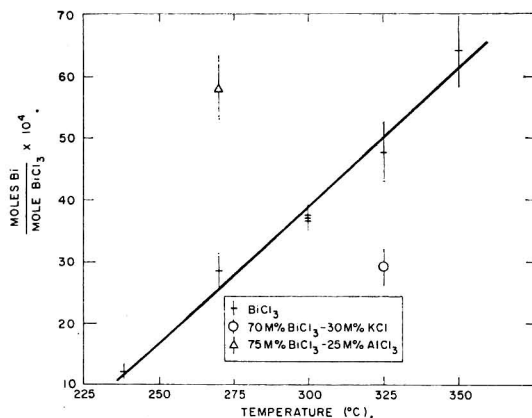


Fig. 2.—Effect of temperature on concentration of Bi where departure from Henry's law occurs.

and/or 0.010. The graphite electrode in the center compartment of these cells served not only to measure the potential of the half-cell but also as the cathode in the constant-current electrolysis which introduced bismuth coulometrically into the compartment.

In experiments carried out to check the coulometric procedure, especially where high concentrations of Bi were studied, cells containing weighed amounts of Bi and BiCl_3 were used. These cells consisted of several compartments, each joined to a center one by means of an asbestos fiber.

Although the cell and procedure for the 70 mole % BiCl_3 -30 mole % KCl mixture were similar to those above, some changes were made with the 75% BiCl_3 -25% AlCl_3 cell. Due to the volatility of AlCl_3 , an evacuated, sealed, cell which could be completely immersed in the bath was employed. To prevent pressure differentials in the cell which would result in mass flow, the upper legs of the compartments were connected and a platinum anode was substituted for the tungsten. (Chlorine is not evolved at platinum anodes at these temperatures.) All electrode lead wires were insulated from the metal bath by means of glass tubes.

A Sargent Coulometric Source was used to increase the concentration of the Bi metal species by the electrolytic reduction of BiCl_3 . (The product of this reduction is unimportant in the analysis of the data, provided that the passage of one faraday of electricity is equivalent to the addition of $1/3$ mole of bismuth metal to the center compartment.) After each electrolysis or temperature change, the potentials between the reference half-cells and the center compartment were read at various time intervals with a

Rubicon B potentiometer. It was found that equilibrium was attained quite rapidly (within 15 minutes) with melts dilute in bismuth and at the higher temperatures. However, as the concentration of metal increased, or as the temperature decreased, as well as with KCl-BiCl_3 , longer periods of time (as much as two hours) were required before the e.m.f.'s became constant. Once a steady e.m.f. had been attained, the cells were quite stable as indicated by the potentials which were constant to ± 1 millivolt and remained constant for periods of several days.

Results

Cells of the type



where N denotes mole fraction, were run at 238, 270, 300, 325 and 350°. In addition, a cell containing a 75 mole % BiCl_3 -25% AlCl_3 melt was studied at 270°, and another containing a 70% BiCl_3 -30% KCl melt was run at 325°.

The e.m.f. vs. $\log Q$ (equivalents of electricity passed) results of some typical experiments, corrected for initial Bi concentration (see below), are shown in Fig. 1. These cells, run at 238, 300 and 350°, contained 35.32, 33.25 and 37.21 g. of BiCl_3 , respectively, in the center compartments. The plots for each temperature are very similar and depict initially straight lines which undergo a large change in slope at fairly low metal concentrations. These concentrations of Bi metal, where the initial slopes change, *i.e.*, where departure from Henry's law occurs, increased with temperature and with the acidity of the system as shown in Fig. 2. The initial slopes of the plots at all temperatures yielded an apparent Nernst n (see below) of about 2; lines drawn through the higher concentration points yielded slopes that gave an apparent n of approximately 6 at all temperatures except 238° where an n of about 8 was found. (However, as will be shown below both apparent n 's are consistent with the same species.)

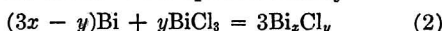
It was noticed in virtually every case that the first points, *i.e.*, those at very low bismuth additions, fell below the line of $n = 2$ slope. These results, which suggest that the true concentration of Bi is greater than that added coulometrically, are attributed to the presence of lower-valent bismuth species in the original BiCl_3 as was reported in the polarographic study.¹⁰ The original concentrations of lower-valent bismuth species were determined for each cell by measuring the polarographic limiting current as a function of the concentration of Bi metal and extrapolating to zero current.¹⁰ The extrapolations yielded Q 's of 20-30 microequivalents/35 g. BiCl_3 , corresponding to about 8×10^{-5} mole fraction of Bi. These corrections for the original metal concentration not only increased the concentration range where linearity of the initial ($n = 2$) plots occurred, but they also changed the slopes of these lines (Fig. 3) so that the original average apparent Nernst n (derived from the slopes) of 2.28 ± 0.12 was decreased to 2.05 ± 0.10 . In several experiments the electrode in the center compartment was made the anode at first to oxidize the dissolved metal present to Bi^{+3} . In these cases, depending on the extent of electrolysis, the limiting currents (and thus the corrections, were found to decrease or become negligible.

The validity of the coulometric procedure of in-

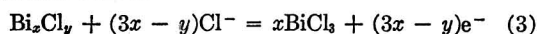
roducing bismuth was checked in two ways. First, the concentration of bismuth generated in the center compartment was compared with that of the reference compartment of known composition when the potential between the two compartments was zero; for most cases these compositions checked within a few per cent. of each other. Second, the e.m.f.'s of half-cells, containing accurately weighed amounts of Bi and BiCl₃, were measured at various temperatures, and the apparent Nernst *n*'s computed. These *n* values for the appropriate concentration ranges were identical with those found by the coulometric procedure. These results as well as the linearity of the polarographic limiting current *vs.* Bi concentration plots¹⁰ served to confirm the validity of the procedure.

Discussion

An interpretation of these results may be made by consideration of the reactions (a) the solution of Bi in BiCl₃ to form the species Bi_{*x*}Cl_{*y*}



where *x* and *y* are integers and *y* may also equal zero, and (b) the electrode reaction in which Bi_{*x*}^{+*y*} is oxidized to Bi⁺³



For a reversible half-cell the e.m.f. is given by the Nernst equation

$$E = E^0 - \frac{RT}{nF} \ln \frac{a_{BiCl_3}^x}{a_{Bi_xCl_y} \cdot a_{Cl^-}^{(3x-y)}} \quad (4a)$$

Since the chloride ion activity is unity and the Nernst *n* = 3*x* - *y*

$$E = E^0 - \frac{RT}{(3x - y)F} \ln \frac{N_{BiCl_3}^x \gamma_{BiCl_3}^x}{N_{Bi_xCl_y} \gamma_{Bi_xCl_y}} \quad (4b)$$

For any number of Bi metal species Bi_{*x_i*}Cl_{*y_i*} the mole fraction *N_i* of the *i*th species can be calculated from the number of coulombs of electricity passed. For low concentrations of Bi

$$N_i = \frac{Q_i / (3x_i - y_i)}{[BiCl_3]_0} \quad (5)$$

where *Q_i* is the number of equivalents used to generate species *i*, [BiCl₃]₀ denotes the initial number of moles of BiCl₃ and the other symbols have the same meaning as before.

Assuming *N_{BiCl₃}* and the activity coefficients are essentially unity or constant and substituting (5) into (4), one obtains for reaction 3

$$E = E^0_i + \frac{RT}{(3x_i - y_i)F} \ln \frac{Q_i / (3x_i - y_i)}{[BiCl_3]_0} \quad (6)$$

In the concentration range where one Bi_{*x_i*}Cl_{*y_i*} predominates, *i.e.*, where *Q_i* = *Q*(total)

$$E = \frac{RT}{(3x_i - y_i)F} \ln Q + \text{constant} \quad (7)$$

and a plot of *E* (measured against a reference half-cell) *vs.* ln *Q* at constant temperature should yield a line, the slope of which is determined by the species present, *i.e.*, by (3*x_i* - *y_i*).

Thus, if the cells studied are reversible and if liquid junction and activity effects, *i.e.*, departure from Henry's law, are negligible, the Nernst *n* = 2, observed initially, indicates the species Bi_{*x*}^{+(3*x* - 2)} is present. In view of phase diagram results^{2,3} Bi⁺ (*x* = 1) appears to be the most reasonable

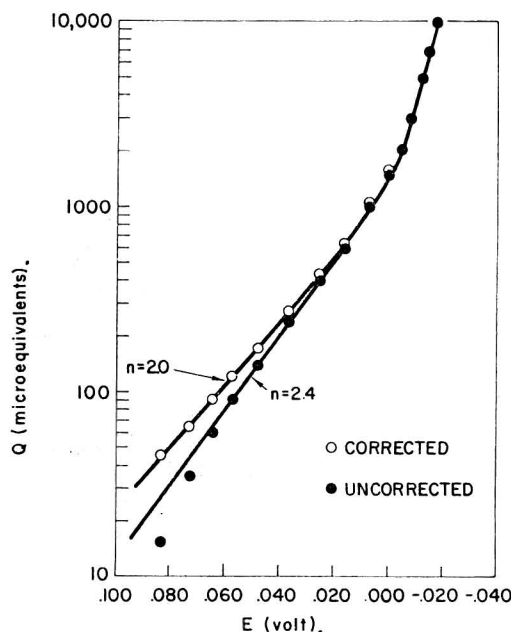


Fig. 3.—Log *Q vs.* *E* results corrected for initial Bi impurity (325°).

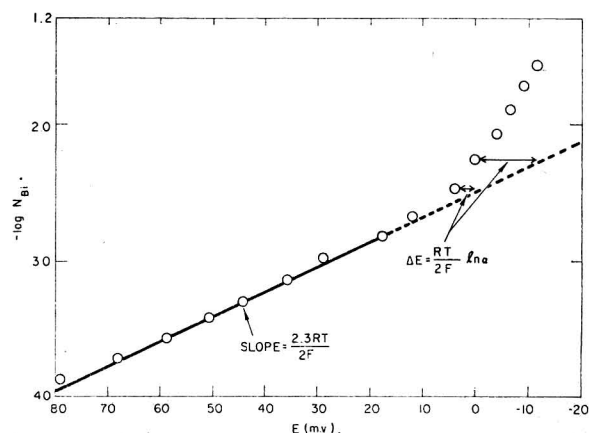


Fig. 4.—Deviation of e.m.f. data from Henry's law at 270°.

species and is assumed to be the one present. In the dilute solutions, where BiCl predominates, the conditions for reversibility, etc., appear to be met; this conclusion is substantiated both by the polarographic results¹⁰ which indicate that the electrode reactions are reversible in dilute melts and by conductivity data¹⁶ which do not indicate any electronic conductivity over the concentration range examined in this study.

The large change in slope in the e.m.f. *vs.* log *Q* plots (Fig. 1) may be ascribed to a departure of the system from Henry's law behavior, and the deviations α are represented by

$$\alpha = \text{antilog} \frac{E_{\text{ideal}} - E_{\text{exptl.}}}{2.3RT/2F} \quad (8)$$

where

$$E_{\text{ideal}} = E_{\text{ref.}} - \frac{2.3RT}{2F} \log N_{Bi^+} \quad (9)$$

$$= E_{\text{ref.}} - \frac{2.3RT}{2F} \log \frac{3}{2} N_{Bi} \quad (\text{from equation 2}) \quad (9a)$$

(16) A. H. W. Aten, *Z. physik. Chem.*, **68**, 641 (1909).

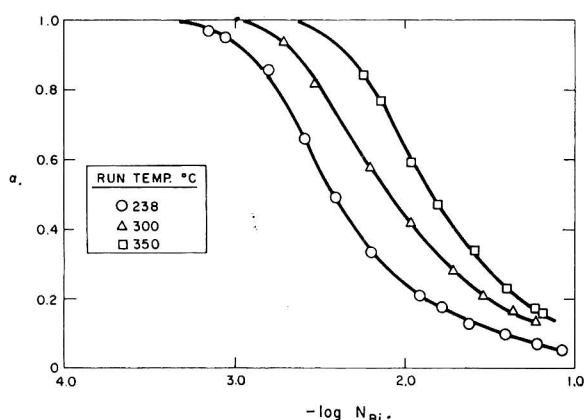


Fig. 5.—Variation of fraction, α , of BiCl monomer with concentration of Bi.

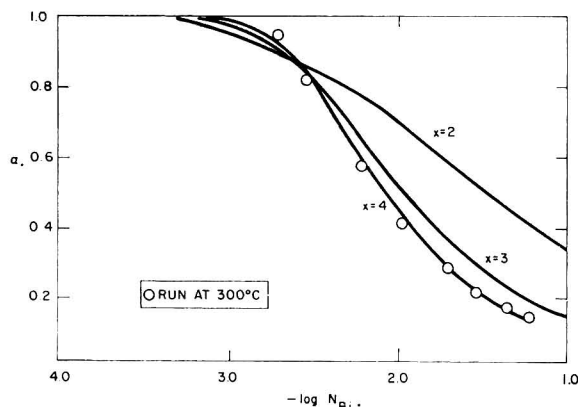


Fig. 6.—Comparison of experimental data with theoretical for variation of monomer fraction, α , for the reaction $x\text{BiCl} = \text{Bi}_x\text{Cl}_x$.

and

$$E_{\text{exptl.}} = E_{\text{ref.}} - \frac{2.3RT}{2F} \log \frac{3}{2} N_{\text{Bi}} \alpha \quad (9b)$$

These α 's can be calculated as shown in Fig. 4 and correspond to activity coefficients based on the infinitely dilute solution of Bi^+ as the reference state.

An interpretation of this non-ideal behavior is that another low-valent Bi species exists, *e.g.*, Bi_2 , Bi_3Cl_3 , Bi_4Cl_6 , etc., which correspond to an n of 6 or Bi_3^+ , Bi_4Cl_4 , Bi_5Cl_7 , etc., which correspond to an n of 8, and this species becomes predominant as the bismuth metal concentration increases. Other evidence supporting this view has been reported in a spectroscopic¹⁷ study. Boston and Smith¹⁷ found that spectra in the visible range of molten BiCl_3 , containing up to 6 mole % Bi, indicated two Bi species resulted from solution of the metal. Furthermore, from their plot of the integrated absorbancy *vs.* formal Bi concentration, the concentrations of metal, where departure from Beer's law occurs, can be estimated. These concentrations at 260 and 350° are approximately 0.0012 and 0.0032 mole fraction, respectively, in qualitative agreement with the concentrations where the E *vs.* $\log Q$ plots change their initial slope (Fig. 2).

(17) C. R. Boston and G. P. Smith, Annual Progress Report, Metallurgy Division, Oak Ridge National Laboratory, ORNL-2988, p. 9-16 (July, 1960).

In order to determine what species other than BiCl may be present in Bi-BiCl_3 solutions, one can examine the variation of α , the deviation from Henry's law, with concentration of metal. If these deviations are now attributed to another equilibrium species and activity coefficients of unity hold, then it is seen from equations 9b and 13a,b below that α may be considered the fraction of Bi metal that reacts with BiCl_3 to form BiCl and $(1 - \alpha)$ the fraction forming other species. If it is also assumed that only one additional species is present and that this species is a polymer Bi_xCl_x , then the shape of an α *vs.* $\log N_{\text{Bi}}$ plot for dilute solutions should depend only on the species involved, *i.e.*, on the reaction



(It can be shown that for dilute solutions the slope of the α *vs.* $\log N$ curve is independent of N_{Bi} and K , and a change in K merely displaces the curve along the $\log N_{\text{Bi}}$ axis.) Typical plots of α *vs.* $\log N_{\text{Bi}}$ for cells at 238, 300 and 350° are shown in Fig. 5. A comparison between the experimental and theoretical curves for reaction 10 with $x = 2, 3$ and 4 (Fig. 6) suggests that tetramer formation occurs in all the cells studied. (The theoretical curves were formulated by assuming values of K and a series of concentrations of one of the components for reaction 10; the concentration of the other entity then was calculated and from these concentrations and relation 2, the α 's were determined.) Unfortunately, the theoretical plot for pentamer formation, which is not included in Fig. 6, is difficult to distinguish from that for the tetramer. However, as will be seen below, the data appear to be more consistent with tetramer species than with pentamers. The apparent $n = 6$ slopes for the E *vs.* $\log Q$ data that were found (instead of $n = 8$) are thought to be due to the concentration range of Bi not being large enough to give true limiting slopes, *i.e.*, these higher concentration points actually yield curves and not straight lines. Measurements of cells with higher concentrations of metal, 0.07 to 0.25 mole fraction, in an attempt to approach the limiting slope will be discussed later.

If one assumes that BiCl and Bi_4Cl_4 are the predominant species present when bismuth dissolves in its chloride, and ideal behavior exists, then the equilibrium constant, K , for reaction 10 where $x = 4$ can be calculated. From the reactions



and



one finds

$$n_{\text{BiCl}} = 3\alpha a/2 \quad (13a)$$

$$n_{\text{Bi}_4\text{Cl}_4} = 3(1 - \alpha)a/8 \quad (13b)$$

and

$$n_{\text{BiCl}_3} = b - a/2 \quad (13c)$$

where n denotes moles, a ($= Q/3$) and b are the initial number of moles of Bi and BiCl_3 , respectively, and α is the fraction of Bi metal that forms BiCl . The equilibrium constant K in terms of mole fraction is given by

$$K_N = \frac{N_{\text{Bi}_4\text{Cl}_4}}{N_{\text{BiCl}_3}^4} = \frac{3(1-\alpha)a/8}{b - a(1-9\alpha)/8} \quad (14)$$

$$= \frac{3(1-\alpha)(8-9N_{\text{Bi}} + 9\alpha N_{\text{Bi}})^3}{(12)^4 \alpha^4 N_{\text{Bi}}^3} \quad (15)$$

where

$$N_{\text{Bi}} = \frac{a}{a+b}$$

The self-consistency in K_N for a tetramer as well as a trimer and pentamer model, calculated in a similar manner, is shown in Table I for a cell at 325°. The results, *i.e.*, the standard deviation in K_N being smallest for the tetramer and largest for the trimer, are typical of virtually all the cells studied and may be indicative that the tetramer

TABLE I

TYPICAL VARIATION OF K_N WITH COMPOSITION FOR THE REACTION $x\text{BiCl}_3 = \text{Bi}_x\text{Cl}_x$

$N_{\text{Bi}} \times 10^2$	K_N at 325°		
	$x = 3$	$x = 4$	$x = 5$
0.308	2.98×10^3	5.54×10^3	$(10.97) \times 10^7$
.471	3.47	4.80	7.08
.716	4.69	5.28	6.35
1.03	5.11	4.83	4.86
1.35	5.89	5.05	4.62
1.88	7.23	5.64	4.69
2.53	8.69	6.29	4.86
3.40	9.74	6.45	4.54
4.37	10.70	6.58	4.30
5.90	9.67	5.09	2.85
7.63	11.58	5.79	3.07
Av. K_N :	$(7.25 \pm 3.02) \times 10^3$	$(5.57 \pm 0.64) \times 10^3$	$(5.29 \pm 1.41) \times 10^7$

species is the most probable. Furthermore, the small, non-systematic variation in K with concentration for each tetramer run suggests that deviations from ideality are negligible or that the activity coefficient ratio $\gamma_{\text{Bi}_4\text{Cl}_4}/\gamma_{\text{BiCl}_3}^4$ is approximately constant over the composition range studied. The effect of temperature on the equilibrium constants for tetramer formation is depicted in Fig. 7, and the relation for solutions of Bi in BiCl_3 can be expressed by

$$\log K_N = \frac{(4.49 \pm 0.54) \times 10^3}{T^\circ\text{K}} - 1.930 \pm 0.945 \quad (16)$$

If K_N approximates the true equilibrium constant, *i.e.*, if activity effects are negligible, values for ΔH^0 , ΔF^0 and ΔS^0 for the hypothetical pure liquid standard state are -20.5 , -15.5 kcal. and -8.7 e.u., respectively, for the tetramer reaction 10 at 300°. This entropy may be compared with the value, -7.6 e.u., estimated from Latimer's tables.¹⁸ It should be noted that Latimer's tables are for solids at 25°, whereas the value in this study is for the hypothetical pure liquid, and so the agreement in ΔS^0 may not be significant. However, heat of fusion and heat capacity corrections for the liquids at 300° may be small, and in this event the agreement may be due to the system being close to ideal.

In Fig. 7 are also plotted the K_N 's, calculated in the same way as above, for the BiCl_3 -KCl and BiCl_3 -AlCl₃ melts for concentrations of Bi up to

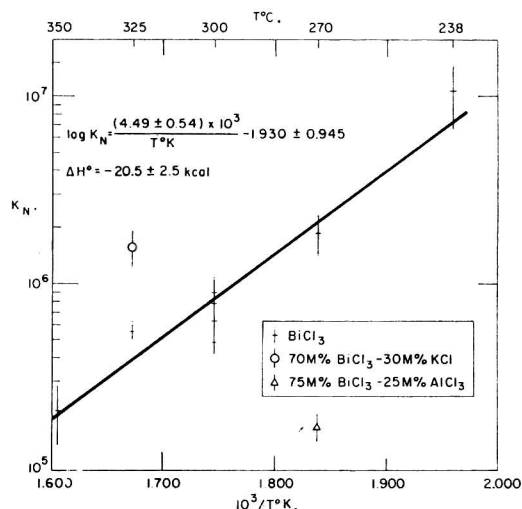


Fig. 7.—Effect of temperature on equilibrium constant for the reaction $4\text{BiCl}_3 = \text{Bi}_4\text{Cl}_4$.

0.050 and 0.017 mole fraction, respectively. If the tetramer reaction 10 also occurs in these systems, the ratio of K_N with the salt mixture to K_N with BiCl_3 alone at the same temperature should give a measure of the activity effects in the acid or base system with respect to that in BiCl_3 . In Table II are listed the average $\gamma_{\text{Bi}_4\text{Cl}_4}/\gamma_{\text{BiCl}_3}^4$ ratios in BiCl_3 -AlCl₃ and BiCl_3 -KCl to those in BiCl_3 alone and also the solubilities of Bi (determined by quenching) in moles of Bi per mole BiCl_3 in these systems. The increased solubility and decreased activity coefficient ratio in the BiCl_3 -AlCl₃ melt indicate that although both the monomer and tetramer subhalides are stabilized in the acid melt, the monomer is stabilized to a much greater extent than the tetramer; the converse holds for the basic KCl- BiCl_3 melt. These results are in accord with acid-base theory as Bi^+ should be the least acid (and therefore stabilized most in acid media), Bi_4^{+4} intermediate, and Bi^{+3} the most acid bismuth species (as deduced from charge to radius ratio) in these systems.

The behavior of concentrated Bi- BiCl_3 solutions was examined with cells similar to those described for the dilute melts except that the center compartment contained an initial known composition of Bi instead of pure BiCl_3 . The results indicated that the apparent Nernst n decreases from a value of about 7 (close to the limiting $n = 8$) in the concentration range 7–10 mole % Bi to a value of approximately 2 in the 22–25% range. These results are in essential agreement with those of other investigators.¹⁹ This apparent decrease in n with increasing Bi may be ascribed to concentration as well as liquid junction and activity effects. If, however, it is assumed that the chloride ion transference number is unity, *i.e.*, no liquid junction potential, the e.m.f. of a cell containing concentrated solutions is given by

$$E = \frac{RT}{2F} \ln \frac{N'_{\text{BiCl}_3} \gamma'_{\text{BiCl}_3}}{N''_{\text{BiCl}_3} \gamma''_{\text{BiCl}_3}} \frac{N''_{\text{Bi}_4\text{Cl}_4} \gamma''_{\text{Bi}_4\text{Cl}_4}}{N'_{\text{Bi}_4\text{Cl}_4} \gamma'_{\text{Bi}_4\text{Cl}_4}} \quad (17)$$

$$= \frac{RT}{2F} \ln \frac{(3/2)N'\alpha'}{(3/2)N''\alpha''} \frac{N''_{\text{BiCl}_3} \Gamma}{N'_{\text{BiCl}_3} \Gamma} \quad (18)$$

(18) W. M. Latimer, "The Oxidation States of the Elements and their Potentials in Aqueous Solutions," Second Edition, Prentice-Hall, Inc., New York, N. Y., 1952.

(19) J. D. Corbett and R. A. Sallach, private communication.

TABLE II

THE EFFECT OF AlCl_3 AND KCl ON THE ACTIVITY COEFFICIENTS AND SOLUBILITY OF Bi IN BiCl_3

Melt composition, mole %	T, °C.	K × 10 ⁻³	$\frac{R_{\text{MCl}_2-\text{BiCl}_3}}{R_{\text{BiCl}_3}}$	Solubility (moles Bi mole BiCl_3)
AlCl_3 (25.0)- BiCl_3 (75.0)	270	0.18	0.09 ^b	1.4
KCl (30.0)- BiCl_3 (70.0)	325	1.8	4.7 ^c	0.07
BiCl_3	270	2.1	1.0	.58
	325	0.38	1.0	.82

^a $R = \gamma_{\text{Bi}_2\text{Cl}_2} / \gamma_{\text{BiCl}}$. ^b Average value for Bi concentrations up to 1.7 mole %. ^c Average value for Bi concentrations up to 5.0 mole %.

where $\Gamma = \gamma'_{\text{BiCl}} \gamma''_{\text{BiCl}_2} / \gamma''_{\text{BiCl}} \gamma'_{\text{BiCl}_2}$ and E is positive when N' (mole fraction of Bi metal) is greater than N'' . Substituting for $\alpha'/\alpha'' = (8-9N')N''/(8-9N'')N'$ from equation 15 assuming $\alpha \ll 1$, one finds

$$E = \frac{RT}{8F} \ln \left(\frac{8-9N'}{8-9N''} \right)^3 \left(\frac{N'}{N''} \right) \left(\frac{1-N''}{1-N'} \right)^4 + \frac{RT}{2F} \ln \Gamma \quad (19)$$

or

$$E_{\text{meas.}} - E_{\text{ideal}} = \frac{RT}{2F} \ln \Gamma \quad (20)$$

Now values for $\gamma''_{\text{BiCl}_2} / \gamma'_{\text{BiCl}_2}$ for these melts can be calculated from vapor pressure data⁴ and thus the ratio $\gamma'_{\text{BiCl}} / \gamma''_{\text{BiCl}}$ can be obtained. The results for some of the melts measured at 300° are

TABLE III

ACTIVITY COEFFICIENT RATIOS FOR BiCl IN CONCENTRATED SOLUTIONS AT 300°

N'_{Bi}	N''_{Bi}	$E_{\text{meas.}}$	E_{ideal}	$(\gamma''/\gamma')_{\text{BiCl}_2}$ ^a	$(\gamma'/\gamma'')_{\text{BiCl}}$
0.0935	0.1300	0.0051	0.0022	1.025	1.10
.0935	.1587	.0081	.0035	1.046	1.17
.0935	.2000	.0136	.0051	1.072	1.32
.0935	.2540	.0195	.0068	1.097	1.54

given in Table III and show reasonable values for activity coefficient ratios.

Additional information as to species in this system has been reported from the results of a vapor pressure,⁴ a cryoscopy,⁹ and an X-ray²⁰ study. Corbett,²¹ using the vapor pressures of Cubicciotti, *et al.*,⁴ has shown that the data at 301 and 356° are consistent with the species Bi_4Cl_4 up to a Bi mole fraction of 0.25. Although these results agree with those of this investigation, the results of the cryoscopy and X-ray studies do not. X-Ray diffraction patterns of solid and molten bismuth(I) chloroaluminate have been interpreted to indicate the trimer Bi_3 ⁺³ exists in this system. The cryoscopic data suggested that the species Bi_2Cl_2 could account for the freezing point depression of BiCl_3 by Bi over the entire liquidus, *i.e.*, to approximately 30 mole % Bi. However, no measurements were made on melt compositions below 0.1 mole % Bi, where BiCl is indicated to predominate in the present investigation and, furthermore, it is doubtful whether the cryoscopic approach is accurate enough to enable one to distinguish between BiCl and Bi_2Cl_2 in such a dilute range. Calculations of freezing point depressions for given concentrations of Bi on the basis of BiCl and Bi_4Cl_4 mixtures, *i.e.*, with equations 15 and 16 and the Raoult-van't Hoff relation, resulted in ΔT values which were lower than the experimentally measured ones, this difference increasing from 0.4 to 2.3° at Bi mole fractions of 0.04 and 0.08, respectively. Although the e.m.f. data of this study are consistent with the species BiCl and Bi_4Cl_4 , undoubtedly some dimers and trimers as well as Bi atoms also exist; in addition the possibility of solvates should not be excluded. If the concentrations of these species could be calculated, better agreement between the results of the two methods would be obtained.

(20) H. A. Levy, M. A. Bredig, M. D. Danford and P. A. Agron, *J. Phys. Chem.*, **64**, 1959 (1960).

(21) J. D. Corbett, *ibid.*, **62**, 1149 (1958).

THE THERMAL DEAQUATION OF SOME AQUOPENTAMMINECOBALT(III) COMPLEXES¹

BY WESLEY W. WENDLANDT AND JOHN L. BEAR

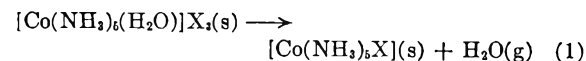
Department of Chemistry, Texas Technological College, Lubbock, Texas

Received February 27, 1961

The thermal deaquation of $[\text{Co}(\text{NH}_3)_5\text{H}_2\text{O}]\text{X}_3$ type complexes, where X is Cl^- , Br^- , I^- and NO_3^- , was studied by the techniques of DTA, TGA and other methods. The kinetics of the deaquation reaction was found to obey a first-order rate law, with E^* values ranging from 19 ± 2 to 31 ± 3 kcal. The heats of deaquation, as determined by quantitative DTA, were 6.1 and 7.8 kcal. mole⁻¹ for the chloride and bromide complexes, respectively. Dissociation pressure measurements of the deaquation reaction showed it to be irreversible in the solid state.

Introduction

The aquopentamminecobalt(III) complexes, $[\text{Co}(\text{NH}_3)_5(\text{H}_2\text{O})]\text{X}_3$, are unstable with respect to the deaquation reaction



both in the solid state and in solution.²⁻⁶ In the solid state, the reaction takes place slowly at room temperature but proceeds very rapidly at about 100°.

(2) W. Gibbs and F. A. Genth, *Am. J. Sci.*, [2] **23**, 234 (1857).

(3) S. M. Jorgensen, *Z. anorg. allgem. Chem.*, **17**, 453 (1898).

(4) A. Werner, *Ber.*, **44**, 877 (1911).

(5) A. B. Lamb and J. W. Marden, *J. Am. Chem. Soc.*, **33**, 1873 (1911).

(6) R. Pers, *Compt. rend.*, **153**, 673 (1911).

(1) Taken in part from the Ph.D. thesis of John L. Bear, Texas Technological College, August, 1960.

Mori and co-workers have recently determined the thermodynamic functions of the thermal deauration reaction for $[\text{Co}(\text{NH}_3)_5\text{H}_2\text{O}]\text{Cl}_3$,⁷ $[\text{Co}(\text{NH}_3)_5\text{H}_2\text{O}]\text{Br}_3$ ⁸ and $[\text{Co}(\text{NH}_3)_5\text{H}_2\text{O}](\text{NO}_3)_3$.⁸ Lobanov, *et al.*,⁹ studied the differential thermal analysis (DTA) of the $[\text{Co}(\text{NH}_3)_5(\text{H}_2\text{O})](\text{NO}_3)_3$ and $[\text{Co}(\text{NH}_3)_5\text{H}_2\text{O}]\text{SO}_4\text{Br}$ complexes. A well-defined endothermic peak at 118–120° was found for the deauration reaction of the former complex while a similar peak was found at 210° for the latter complex. The enhanced thermal stability of the sulfate-bromide complex is rather surprising since $[\text{Co}(\text{NH}_3)_5\text{H}_2\text{O}]\text{Br}_3$ is completely converted to $[\text{Co}(\text{NH}_3)_5\text{Br}]\text{Br}_2$ on heating at 100°.¹⁰ Apparently, the sulfate ion exhibits a pronounced anion effect.

Because the above studies were incomplete, as far as a series of different anions is concerned, the aquopentamminecobalt(III) chloride, bromide, iodide and nitrate complexes were studied by the methods of thermogravimetric analysis (TGA) and DTA. Also, the kinetics of the solid state thermal deauration reaction was determined.

Experimental

Reagents.—All of the chemicals used were of C.P. quality except the $\text{CoCl}_2 \cdot 6\text{H}_2\text{O}$, which was Reagent Grade.

Thermobalance.—The automatic recording thermobalance and its modification have been described previously.^{11,12}

Sample sizes ranged in weight from 50 to 100 mg. and were run in duplicate or triplicate. The heating rate of the furnace was approximately linear with time at about 5° min.⁻¹. An air atmosphere was maintained in the furnace during the pyrolysis of the sample.

DTA Apparatus.—The DTA apparatus consisted of a furnace and sample holder similar to that previously described,^{13,14} and a strip-chart microvolt recorder.¹⁵ The differential temperatures were detected by Chromel–Alumel thermocouples, placed in the center of the ceramic sample chambers, which were 0.25 inch in diameter by 0.75 inch in length. Sample sizes ranged in weight from 100 to 150 mg. The reference material used was ignited α -alumina. A furnace heating rate of about 6° per min. was employed with an air atmosphere in contact with the sample during the pyrolysis.

Heat of Deauration.—The DTA apparatus employed was similar to the above apparatus except that the differential thermocouple output was amplified by a Beckman, Model 14, breaker-type d.c. amplifier and recorded on the vertical axis of a Moseley, Model 5S, X-Y recorder. The furnace temperature, as detected by the reference chamber thermocouple, was recorded on the horizontal axis.

A "sandwich" type of sample packing was employed which consisted of the following layers: 100 mg. of α -alumina; 100 mg. of sample; and then 300 mg. of α -alumina. Each layer was uniformly tamped into place with a glass rod as the sample chamber was filled. The reference chamber contained 500 mg. of α -alumina. A furnace heating rate of 10° per min. was employed with an air atmosphere in contact with the sample during the pyrolysis.

The apparatus was calibrated by use of the metal salt hydrates: $\text{CuSO}_4 \cdot 5\text{H}_2\text{O}$, $\text{CaSO}_4 \cdot 2\text{H}_2\text{O}$ and $\text{BaCl}_2 \cdot 2\text{H}_2\text{O}$, using the procedure as previously described.¹⁶ The curve

peaks were integrated by tracing the curves onto good quality tracing paper, cutting out the peaks, and weighing them on a semi-micro analytical balance. The calibration factor was 8.250 cal. per 0.1 g. of paper. The areas of the curves could be reproduced to within $\pm 2\%$.

Kinetic Studies.—The rates of deauration of the $[\text{Co}(\text{NH}_3)_5\text{H}_2\text{O}]\text{X}_3$ type complexes were determined by means of a modified Smith–Menzies isoteniscope apparatus.¹⁷ The isoteniscope was placed in an oil-bath, the temperature of which was controlled to $\pm 0.1^\circ$. Sample sizes ranged in weight from 25 to 50 mg., with a range in sample particle sizes between 200 and 400 mesh. The pressure of the system was measured either with a 0.1–10 mm. McLeod gauge or a mercury manometer, depending on the pressure range.

Dissociation Pressure Apparatus.—The dissociation pressures of the $[\text{Co}(\text{NH}_3)_5\text{H}_2\text{O}]\text{X}_3$ type complexes were determined by means of the apparatus previously described by Mori and Tsuchiya.¹⁸ The temperature of the sample was controlled to $\pm 0.1^\circ$ with a thermostated stirred oil-bath. Sample sizes ranged in weight from 50 to 100 mg. The dissociation pressures were measured with a mercury manometer and a cathetometer.

Preparation of Complexes.—The aquopentamminecobalt(III) complexes were prepared as previously described.^{19–22}

The complexes were studied by the various techniques immediately after preparation and analysis since they are unstable with respect to deauration even at room temperature. The complexes were analyzed for anion content (except the nitrate complex) by a argentimetric titration; water content by weight-loss at 100–110°; and cobalt content by the complexometric titration method of Schlaefler and Kling.²² Results of the analyses were: $[\text{Co}(\text{NH}_3)_5\text{H}_2\text{O}]\text{Cl}_3$: Found: Co, 20.97; H_2O , 6.92; Cl, 38.50. Theor.: Co, 21.95; H_2O , 6.71; Cl, 39.20. $[\text{Co}(\text{NH}_3)_5\text{H}_2\text{O}]\text{Br}_3$: Found: Co, 14.19; H_2O , 4.49; Br, 59.10. Theor.: Co, 14.68; H_2O , 4.48; Br, 59.66. $[\text{Co}(\text{NH}_3)_5\text{H}_2\text{O}]\text{I}_3$: Found: Co, 10.21; H_2O not determined because of total decomposition of the complex when heated; I, 68.20. Theor. Co, 10.85; I, 70.14. $[\text{Co}(\text{NH}_3)_5\text{H}_2\text{O}](\text{NO}_3)_3$: Found: Co, 13.16; H_2O , 4.96. Theor. Co, 16.92; H_2O , 5.17.

Experimental Results

TGA and DTA Studies.—The DTA curves for the complexes are given in Figs. 1 and 2.

The weight-loss curves (TGA) showed that the minimum deauration temperatures for the complexes varied somewhat with the anion. These temperatures were 40, 50, 70 and 80, for the chloride, nitrate, iodide and bromide complexes, respectively. Horizontal weight levels, or breaks in the curves, were found in the 100 to 150° temperature range which corresponded to a curve composition for the monoanionic substituted complexes, $[\text{Co}(\text{NH}_3)_5\text{X}]\text{X}_2$. However, the bromo- and iodo-pentamminecobalt complexes appeared to be less stable than the other two complexes as evidenced by the lack of a horizontal weight-level in this temperature region. In the case of the former, the halopentammine cobalt complex began to decompose immediately after the deauration reaction.

(7) M. Mori, R. Tsuchiya and Y. Okano, *Bull. Chem. Soc. Japan*, **32**, 1029 (1959).

(8) M. Mori and R. Tsuchiya, *ibid.*, **33**, 841 (1960).

(9) N. I. Lobanov, I. S. Rassonskaya and A. V. Ablov, *Zhur. Neorg. Khim.*, **3**, 1355 (1958).

(10) S. M. Jorgensen, *J. prakt. Chem.*, [2] **31**, 50 (1885).

(11) W. W. Wendlandt, *Anal. Chem.*, **30**, 56 (1958).

(12) W. W. Wendlandt, *ibid.*, **32**, 848 (1960).

(13) W. Lodding and L. Hammel, *Rev. Sci. Instr.*, **30**, 885 (1959).

(14) W. Lodding and L. Hammel, *Anal. Chem.*, **32**, 657 (1960).

(15) W. W. Wendlandt, *J. Chem. Educ.*, **37**, 94 (1960).

(16) W. W. Wendlandt and T. D. George, *J. Inorg. Nucl. Chem.*, in press.

(17) G. W. Thompson, "Physical Methods of Organic Chemistry," Vol. I, A. Weissberger, Ed., Interscience Publishers, Inc., New York, N. Y., 1949, p. 175.

(18) Mori and Tsuchiya, ref. 8.

(19) A. King, "Inorganic Preparations," D. Van Nostrand Co., New York, N. Y., 1936, pp. 103 and 106.

(20) H. Diehl, H. Clark and H. H. Willard, "Inorganic Syntheses," Vol. I, H. S. Booth, Ed., McGraw-Hill Book Co., New York, N. Y., 1939, p. 186.

(21) F. Basol and R. K. Murmann, "Inorganic Syntheses," Vol. IV, J. C. Bailar, Ed., McGraw-Hill Book Co., New York, N. Y., 1953, p. 174.

(22) H. L. Schlaefler and O. Kling, *Z. anorg. allgem. chem.*, **302**, 1 (1959).

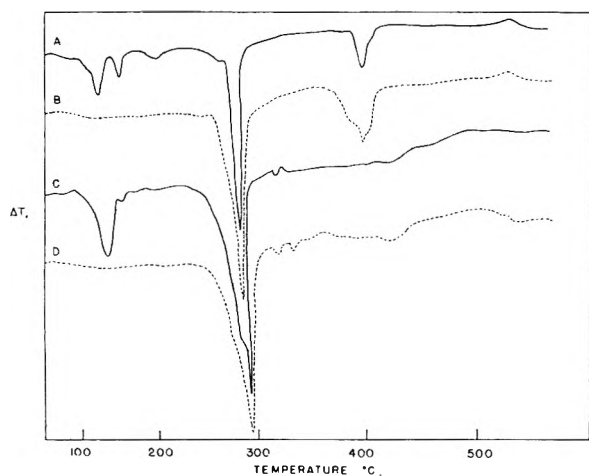


Fig. 1.—Differential thermal analysis curves of the aquopentamine- and halopentamminecobalt(III) complexes: Curve A, $[\text{Co}(\text{NH}_3)_5\text{H}_2\text{O}]\text{Cl}_3$; B, $[\text{Co}(\text{NH}_3)_5\text{Cl}]\text{Cl}_2$; C, $[\text{Co}(\text{NH}_3)_5\text{H}_2\text{O}]\text{Br}_3$; and D, $[\text{Co}(\text{NH}_3)_5\text{Br}]\text{Br}_2$.

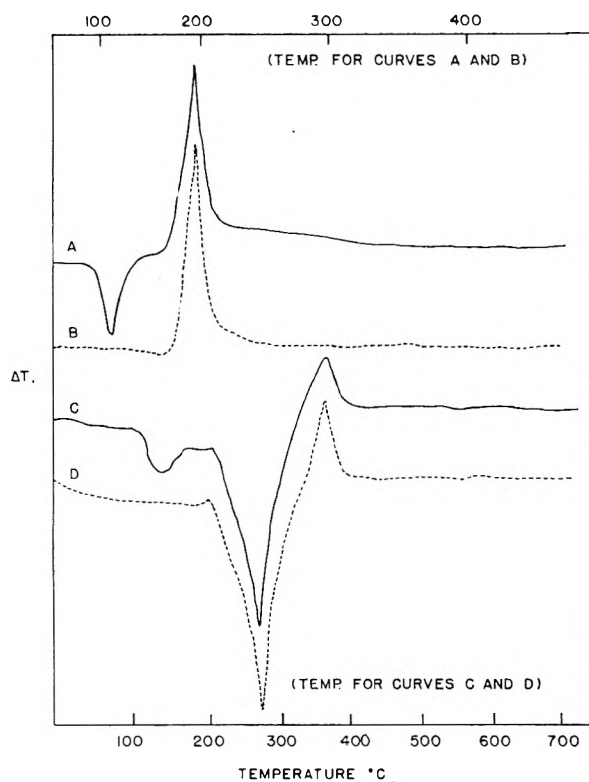


Fig. 2.—Differential thermal analysis curves of the aquopentamine- and anionpentamminecobalt(III) complexes. Curve A, $[\text{Co}(\text{NH}_3)_5\text{H}_2\text{O}](\text{NO}_3)_3$; B, $[\text{Co}(\text{NH}_3)_5\text{NO}_3](\text{NO}_3)_2$; C, $[\text{Co}(\text{NH}_3)_5\text{H}_2\text{O}]\text{I}_3$; and D, $[\text{Co}(\text{NH}_3)_5\text{I}]\text{I}_2$.

On further heating, the monoanionic substituted complexes decomposed with the evolution of ammonia, nitrogen and ammonium halide, along with a subsequent oxidation reaction, to give the Co_3O_4 oxide levels in the 190 to 690° temperature region. The curve for $[\text{Co}(\text{NH}_3)_5\text{H}_2\text{O}]\text{Cl}_3$ had a break at 350° which corresponded closely to the composition for CoCl_2 . As was expected,²³ $[\text{Co}(\text{NH}_3)_5\text{H}_2\text{O}](\text{NO}_3)_3$ exploded at about 280–290°, leaving a residue of Co_3O_4 which was less than cal-

culated, perhaps due to the explosive violence of the reaction. The monoanionic substituted complexes were also studied by TGA and their curves were similar to those found for aquopentamminecobalt complexes, after the deaquation reaction.

The DTA curves for the aquopentamminecobalt complexes, in general, gave an endothermic peak (or peaks) in the 100 to 125° temperature region which was due to the deaquation reaction. This was followed by additional endothermic peaks (except for the nitrate complex) in the 175 to 250° temperature range, which were caused by the decomposition of the monoanionic substituted complexes. Additional endothermic and exothermic peaks were also observed which corresponded to further decomposition and oxidation reactions.

Only one of the complexes, $[\text{Co}(\text{NH}_3)_5\text{H}_2\text{O}]\text{Cl}_3$, gave two endothermic peaks for the deaquation reaction. It is tempting to postulate a two-step reaction for the water loss; however, there is no evidence for this from the TGA curve. From the $[\text{Co}(\text{NH}_3)_5\text{H}_2\text{O}]\text{I}_3$ curve, it can be seen that the complex began to decompose before the deaquation reaction was completed.

Fair agreement was observed between this work and that previously reported⁹ for $[\text{Co}(\text{NH}_3)_5\text{H}_2\text{O}](\text{NO}_3)_3$. The curve shows an endothermic peak, centered at 110°, followed by a large exothermic peak at 195°; previously reported values were 118 and 215°, respectively. The vigorous exothermic nature of the decomposition reaction can be seen from the DTA curve.

Kinetic Studies of the Deaquation Reaction.—

The kinetics of the deaquation reaction, as shown in equation 1, were evaluated by following the pressure increase in the system, due to the liberation of gaseous water, by means of an isoteniscope. It was assumed that the number of moles of gaseous water produced upon the completion of the reaction is equal to the number of moles of reactant initially present. Therefore, the final pressure, a , represented the number of moles of complex at the beginning of the reaction, and x , the pressure after time t , represented the number of moles of water produced up to time t . A plot of $\log a/(a - x)$ versus t was made for each complex at three different temperatures. A straight line was obtained for each temperature indicating that all of the deaquation reactions followed a first-order rate law. From the first-order rate constants obtained at various temperatures, the activation energies were calculated using the Arrhenius equation.

The first-order rate constants and the activation energies for the complexes are given in Table I. It was not possible to study the deaquation of $[\text{Co}(\text{NH}_3)_5\text{H}_2\text{O}]\text{I}_3$ because of the secondary decomposition of $[\text{Co}(\text{NH}_3)_5\text{I}]\text{I}_2$. The activation energy obtained for $[\text{Co}(\text{NH}_3)_5\text{H}_2\text{O}]\text{Cl}_3$ was in fair agreement with the 21.47 kcal. value previously reported by Mori, *et al.*⁷ The results reported here indicated a slight anion effect in that E^* increased in the order: chloride < bromide < nitrate. However, the effect of particle size on the rate of deaquation was not studied. Reproducible results were obtained on different preparations having roughly the same particle size range.

(23) M. Figlarz, *Compt. rend.*, **249**, 2780 (1959).

TABLE I
FIRST-ORDER RATE CONSTANTS AND ACTIVATION ENERGIES
FOR THE AQUOPENTAMMINECOBALT(III) COMPLEXES

Compound	Temp., °C.	$-\log k$	Order	E^* , kcal.
[Co(NH ₃) ₅ H ₂ O]Cl ₃	86	3.37	1	19 ± 2
	90	3.24		
	95	3.10		
[Co(NH ₃) ₅ H ₂ O]Br ₃	85	3.32	1	25 ± 2
	90	3.12		
	93.7	2.94		
[Co(NH ₃) ₅ H ₂ O](NO ₃) ₃	82	3.77	1	31 ± 3
	85	3.60		
	88	3.45		

Dissociation Pressure Measurements.—Although Lamb and Marden⁵ concluded that the transformation illustrated in equation 1 was non-reversible in the solid state, Mori, *et al.*,⁷ assumed that they obtained equilibrium dissociation pressures for the chloride complex in the 21 to 48° temperature range. They reported a dissociation pressure of 2.15 mm. at 25° and 6.93 mm. at 48°. Previous rough measurements⁵ yielded values of approximately 5, 4 and 4 mm. for the chloride, bromide and nitrate complexes, respectively, at 25°.

In this investigation, an attempt was made to confirm the results of Mori, *et al.*,⁷ and establish the reversibility of the reaction. For the [Co(NH₃)₅H₂O]Cl₃ complex, after 100 hr. at 28.0°, a dissociation pressure of 28.0 mm. was obtained. The temperature then was lowered to 25.0° and after 500 hr. the pressure did not change from its initial value. Similar results were obtained for the bromide and nitrate complexes. Mori²⁴ stated that the system reached an equilibrium dissociation pressure after about 12 hr. at any specific temperature. However, it is apparent from the above results that the system is not reversible.

(24) M. Mori, private communication.

Heat of Deaquation by DTA.—The ΔH of the deaquation reaction was determined by the method of quantitative DTA. This method is based upon the premise that under certain experimental conditions, the heat of reaction can be evaluated by integration of the differential curve peak of peaks. From the various theories on quantitative DTA,²⁶⁻²⁷ that of Speil, *et al.*,²⁵ states that the peak area is

$$\text{peak area} = \int_{t_1}^{t_2} \theta dt = \frac{\Delta HM}{g\lambda}$$

where t_1 and t_2 are the time limits of the peak, θ is the differential temperature, ΔH is the heat of reaction involved in the chemical change, M is the mass of reactive sample present, λ is the thermal conductivity of the sample, and g is a constant dependent on the furnace and sample holder geometry. To determine the above constants, the apparatus was calibrated by studying reactions of known thermal effects.

The heats of deaquation, at 108°, obtained by use of the above method were 6.1 and 7.8 kcal. mole⁻¹ for [Co(NH₃)₅H₂O]Cl₃ and [Co(NH₃)₅H₂O]Br₃, respectively. Because of the many variable factors involved, no great accuracy is claimed for the above results. However, the values obtained are probably indicative of the true heats of deaquation.

Acknowledgments.—The assistance of T. D. George, W. Robinson and P. Kuhn is gratefully acknowledged. This work was supported in part by the U. S. Air Force, Office of Research and Development, through Contract No. AF-49(638)-787.

(25) S. Speil, L. H. Berkelhamer, J. A. Pask and B. Davis, U. S. Bureau of Mines, Tech. Paper 664 (1945).

(26) M. J. Vold, *Anal. Chem.*, **21**, 683 (1949).

(27) S. L. Boersma, *J. Am. Ceram. Soc.*, **38**, 281 (1955).

THE FLUORESCENCE AND PHOSPHORESCENCE OF TRIFLUOROACETONE VAPOR¹

BY P. AUSLOOS AND E. MURAD²

National Bureau of Standards, Washington, D. C.

Received February 28, 1961

The fluorescence and phosphorescence of trifluoroacetone has been investigated at 2652, 2804, 3025, 3130 and 3341 Å. The effect of concentration and temperature on the yields of triplet and single-state emissions are comparable to those observed for acetone. The emissions from 2-butanone and 2-pentanone have been investigated briefly. Both compounds phosphoresce very weakly and their fluorescence yields are nearly identical with those observed for acetone and trifluoroacetone.

Introduction

Recent studies^{3,4} on the fluorescence of hexafluoroacetone have clearly shown that the emis-

(1) This research was supported in part by a grant from the U. S. Public Health Service, Department of Health, Education, and Welfare.

(2) National Academy of Sciences—National Research Council Postdoctoral Research Associate 1959–1960.

(3) H. Okabe and E. W. R. Steacie, *Can. J. Chem.*, **36**, 137 (1958).

(4) G. Giacometti, H. Okabe and E. W. R. Steacie, *Proc. Roy. Soc. (London)*, **A250**, 287 (1959).

sion from this compound differs considerably from that reported for acetone.^{5,6} For instance, in the case of hexafluoroacetone, emission was observed from the upper singlet-state, and the yield was strongly dependent on temperature and pressure. In contrast with this behavior, the phosphorescence of acetone may be quite strong, depending on

(5) For a review see: W. A. Noyes, Jr., G. B. Porter and J. E. Jolley, *Chem. Revs.*, **56**, 49 (1956).

(6) J. Heicklen, *J. Am. Chem. Soc.*, **81**, 3863 (1959).

temperature and pressure, whereas the fluorescence is independent of pressure and temperature.

Although the photochemistry of trifluoroacetone has been investigated,^{7,8} no information is available in the literature on the emission of the excited state of this compound.

Experimental

Trifluoroacetone was obtained from Merck and Company and was purified by g.l.c. techniques. Acetone (Spectrograde), 2-butanone and 2-pentanone were obtained from Eastman Kodak Company and were purified by distilling on a spinning band column. No biacetyl could be detected in the fractions used in this work. All compounds were thoroughly degassed and stored at -80° .

The cell was made of quartz and was T-shaped. It was 56 mm. in length and 28 mm. in diameter. The light source was a Hanovia SH-type mercury lamp. A Bausch and Lomb grating monochromator with a focal length of 250 mm. was used. The widths of the exit and entrance slits were 0.5 mm. The emitted light passed through a Corning No. 3850 filter to a 1P28 photomultiplier tube. The phototube used to measure the transmitted light was calibrated against a thermopile at the NBS. The relative fluorescence yields were obtained from an equation identical with the one used in the study³ of CF_3COCF_3 . No correction has been applied to readings made at large absorbed intensities.

Results

The absorption of trifluoroacetone follows Beer's law over the concentration range reported in this work. The molar extinction coefficients, k (l. mole⁻¹ cm.⁻¹) measured at several wave lengths are given in Table I. For comparison, the extinction coefficients of acetone and hexafluoroacetone³ are included in the same table. It can be seen that the maxima of absorption for trifluoroacetone lie between the maxima for acetone and hexafluoroacetone.

TABLE I

MOLAR EXTINCTION COEFFICIENTS AT 25°

Wave length, Å.	CH_3COCH_3	CH_3COCF_3	CH_2COCF_2
2537	7.7	3.2	1.4
2652	11.2	5.58	2.8
2804	12.4	8.15	5.6
2894	10.3	8.35	...
3025	6.32	6.55	8.1
3130	2.86	3.95	7.0
3341	< 0.1	0.61	2.6

In this paper the emission which is not inhibited by oxygen is designated as fluorescence. The phosphorescence is thus the total emission minus the fluorescence.

The numbers given in Tables II, III and IV represent relative emission yields. The absolute emission yields are approximately 1/100 as large. The values obtained at 3341 Å. may be slightly in error by a constant factor, because of the inaccuracy of the low extinction coefficient measured at this wave length.

Although no detailed analysis has been made of the fluorescence and phosphorescence spectra of trifluoroacetone, it may be pointed out that they are both displaced to longer wave lengths as compared to the emission spectra obtained for acetone under identical conditions. The displacement is

TABLE II

EFFECT OF CONCENTRATION ON THE RELATIVE PHOSPHORESCENCE YIELD OF CF_3COCH_3 AT 30°^a

Concn., mole/l. $\times 10^3$	2652 Å.	2804 Å.	3025 Å.	3130 Å.	3341 Å.
9.78	1.61 (0.52)	1.83	1.80	1.58 (1.59)	1.38
7.05	1.36 (.324)	1.83	1.96	1.67	1.47
5.05	1.05 (.185)	1.64	2.06	1.79 (1.67)	1.60
3.62	0.755 (.09)	1.385	2.06	1.88	1.62
2.59	.503 (.042)	0.77	1.98	1.92 (1.71)	1.70
1.85	.295	.545	1.85	1.95	1.71
1.325	.184	.318	1.70	1.92 (1.73)	1.72
0.95		.221	1.54	1.92	
.68			1.23	1.88 (1.66)	
.485			1.11	1.82	
.348			0.96	1.71 (1.59)	
.249			.81	1.66	
.178			.605	1.60 (1.47)	
.091				1.40	

^a The values given in parentheses are the phosphorescence yields of acetone.

TABLE III

EFFECT OF TEMPERATURE ON THE RELATIVE PHOSPHORESCENCE YIELDS OF CF_3COCH_3 ^a

Temp., °C.	2652 Å.	2804 Å.	3025 Å.	3130 Å.	3341 Å.
23	1.93	2.12	2.00	1.74	1.54
64	1.17	1.36	1.28	1.28	1.24
94	0.66	0.75	0.765	0.75	0.74
126	...	0.188	0.203	0.23	.22

^a Concn. 9.8×10^{-3} mole/l.

TABLE IV

T, 30°

Compound	Phosphorescence	Fluorescence
CH_3COCF_3	1.92	0.217
CH_3COCH_3	1.73	0.215
$\text{CH}_3\text{COC}_2\text{H}_5$	0.12	0.230
$\text{CH}_3\text{COC}_3\text{H}_7$	<0.02	0.215

comparable in magnitude to the shift between the extinction curves of both compounds.

Fluorescence.—The fluorescence yield of trifluoroacetone (data not given) is, within experimental error, independent of pressure (10 to 200 mm.), temperature (25 to 150°), and wave lengths (2652 to 3130 Å.). Also, the data given in Table IV indicate that the fluorescence yields are surprisingly similar for the compounds listed.

Phosphorescence. 1. The Effect of Concentration.—The results given in Table II show that at 3341, 3130 and 3025 Å. there is a slight increase in the yield of phosphorescence with decrease in concentration. At the low concentrations, however, there is a definite decrease in the yield with decrease in concentration, the latter effect being more pronounced at the shorter wave lengths. The values given in parentheses, which correspond to the phosphorescence of acetone, indicate that at 3130 Å. the effect of pressure on the phosphorescence of acetone follows the same general trend. At 2652 Å. a decrease in concentration causes the yield of phosphorescence to drop considerably faster in the case of acetone as compared to trifluoroacetone.

The phosphorescence yields measured under identical conditions observed for 2-butanone and 2-pentanone (Table IV) are considerably lower than those of acetone and trifluoroacetone.

(7) R. A. Sieger and J. G. Calvert, *ibid.*, **76**, 5197 (1954).

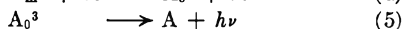
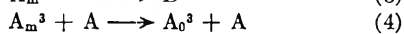
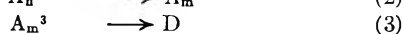
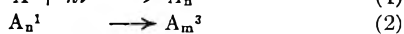
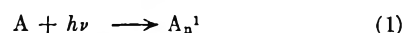
(8) R. M. Smith and J. G. Calvert, *ibid.*, **78**, 2345 (1956).

2. Effect of Temperature.—The phosphorescence yields decrease with increase in temperature at all wave lengths. This effect seems to be of comparable magnitude at the different wave lengths. Plots of $\ln Q$ as a function of $1/T$ are strongly curved, so that a constant activation energy cannot be deduced. The higher temperature points correspond roughly to a temperature coefficient of 11–12 kcal.

Discussion

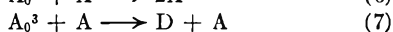
The results clearly indicate that the triplet and singlet-state emission of acetone and trifluoroacetone at 3130 Å. are nearly identical.⁹

The phosphorescence results thus can be tentatively explained by a scheme similar to the one proposed for acetone⁵



(A_n^1 = trifluoroacetone molecule in upper vibrational level of excited singlet state, A_m^3 = trifluoroacetone molecule in upper vibrational level of triplet state, A_0^3 = trifluoroacetone molecule in the lowest vibration level of the triplet state, D = dissociation products.)

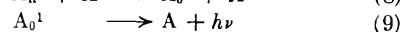
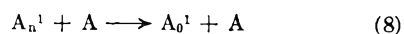
Competition between steps 3 and 4 explains the pressure effects at low concentrations and at short wave lengths (Table II). In order to account for the quenching of the phosphorescence with increase in pressure at the longer wave lengths, step 6 and/or 7 must be included



An internal conversion step may have to be considered as well, although no definite evidence is available for such a process.

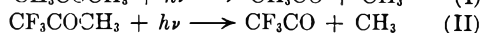
The independence of the fluorescence yield as a function of concentration and temperature is more difficult to visualize. A sequence of processes such as (8) and (9)

(9) A singlet and triplet-state of trifluoroacetone lying below those for acetone would explain the difference in magnitude of the concentration effect at 2652 Å. for both compounds. The shift of the extinction curves as well as of fluorescence and phosphorescence spectra substantiates this view.



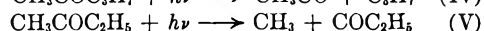
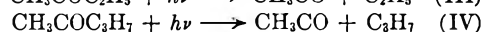
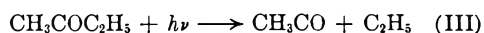
would lead to an effect of pressure on the fluorescence in view of the competition between steps 2 and 8. A resonance fluorescence might explain the observed pressure independence.

Correlation between the Phosphorescence and the Photolysis.—A correlation is rather difficult because of the limited amount of data available on the low-temperature photolysis of trifluoroacetone. In view of the comparable phosphorescence and fluorescence yields for acetone and trifluoroacetone, we may, however, expect that they undergo similar photochemical processes.



The photochemical data do not reveal any evidence for the formation of the acetyl radical in the primary process,⁶ which would lead to the conclusion that initially the same bond is broken in both compounds. In view of the instability of the CF_3CO radical, the low CO yield observed by Sieger and Calvert⁷ at temperatures below 100° does indicate that, as in the case of acetone, the quantum yield of decomposition is lower than unity.

The much lower phosphorescence yields, in the case of 2-butanone and 2-pentanone, may be due to a shorter dissociative lifetime of the triplet state A_m^3 which in turn may be related to the cleavage of a weaker bond in the primary process



Strong evidence in favor of III as compared to the alternative mode of decomposition V has been obtained in several recent investigations.^{10,11,12} It should be pointed out, however, that a greater probability of an internal conversion of the triplet state to the singlet-ground state in 2-butanone and 2-pentanone as compared to acetone should explain the trends equally well.

(10) F. E. Blacet and J. N. Pitts, *J. Am. Chem. Soc.*, **72**, 2810 (1950).

(11) G. R. Martin and H. C. Sutton, *Trans. Faraday Soc.*, **48**, 823 (1952).

(12) P. Ausloos and E. W. R. Steacie, *Can. J. Chem.*, **33**, 1062 (1955)

KINETICS OF FORMATION AND GROWTH OF SILVER BROMIDE PARTICLES¹

BY E. J. MEEHAN AND WILLARD H. BEATTIE

School of Chemistry of the University of Minnesota, Minneapolis, Minn.

Received March 8, 1961

The kinetics of formation of aqueous sols of silver bromide has been investigated, using light scattering methods for the determination of particle size as a function of time. At sol concentrations in the range 5×10^{-3} to $5 \times 10^{-4} M$, the sol particles grow rapidly for about a minute, then continue to grow at a much smaller rate for 20 to 30 hours. The dependence of growth rate on conditions of formation and variation of concentration was investigated. The particle size measured immediately after mixing (30 seconds from start of addition) has only a slight dependence on temperature, amounting to 3.5% (by volume) per degree. On the other hand, the rate of the subsequent slow growth has a considerable dependence on temperature, the heat of activation for slow growth being 24 kcal. mole⁻¹. The results are interpreted in terms of fast flocculation and slow Ostwald ripening.

Introduction

This work was carried out to investigate the mechanism of formation of aqueous silver bromide sols. In particular it was desired to learn the relative importance of the processes of fast flocculation and Ostwald ripening, and the way in which these processes depend upon concentration of reactants and variables of the mixing process. Light scattering methods were used to measure particle diameters. These methods are particularly advantageous for the present purpose in that they permit continuous and non-destructive measurements of size. Suitable scattering methods have been shown to yield reliable results for silver bromide sols, and are discussed in detail elsewhere.²

Experimental

Preparation of Sols.—Stock solutions of potassium bromide and silver nitrate were prepared from reagent grade chemicals dried 2 hours at 105°, dissolved in dust-free doubly distilled water in polyethylene containers and stored in the dark. The silver nitrate solution was standardized by titration with the potassium bromide solution. The standard preparation of sols was as follows. Under subdued light 25 ml. of $1.100 \times 10^{-2} M$ potassium bromide (25°) in a 250-ml. polyethylene beaker was stirred at 900 r.p.m. using a centrally placed Pyrex rod with a one-inch right angle arm placed within $\frac{1}{4}$ inch of the bottom of the beaker. An equal volume of $1.000 \times 10^{-2} M$ silver nitrate (25°) was added by a pipet held almost vertical in a fixture so that the tip was the height of the beaker lip and the stream entered one inch from the center of the beaker. The addition took 32 seconds and stirring was continued 40 to 50 seconds after delivery. Sols were stored in blackened bottles at 25°. The resulting suspension was $5 \times 10^{-3} M$ in silver bromide, $5 \times 10^{-3} M$ in potassium nitrate and $5 \times 10^{-4} M$ in potassium bromide. Average particle diameters in sols prepared in this way were reproducible within 4%. The effects of variations from the standard procedure are reported in "Results."

Light Scattering Measurements.—An Aminco light scattering photometer was used to measure the intensity of the vertically polarized component scattered at angles from 60 to 25°. Most measurements were made at 546 m μ , but for the most dilute sols 436 m μ was used. Sols containing particles of diameter less than ca. 0.05 μ exhibit Rayleigh scattering, so measurement at a single angle (usually 40°) was sufficient to determine the particle diameter. For sols containing larger particles the angular scattering was extrapolated to 0°. Transmission measurements were made in a Beckman DU spectrophotometer with restricted angle of view, using path lengths from 0.1 to 50 cm., depending upon transmission. The details of measurements and calculations of size have been described already.²

Conductance measurements were made at 25.0° using an Industrial Instrument Co. conductivity cell with a Brown recorder. The accuracy was about 1%. The measurements were started within one minute after formation of the sols.

Potentiometric measurements were used to determine bromide ion concentration in the sols. A silver electrode was coated with silver bromide by dipping it in concentrated nitric acid containing a little hydrobromic acid, followed by thorough washing. Potentials with different electrodes were reproducible to 0.5 mv. Potentials were measured against a saturated calomel electrode connected to the sol through an agar bridge containing 0.01 M potassium nitrate. (Use of the conventional concentrated salt bridge causes partial flocculation in some sols.) The concentration of bromide was obtained by comparing the potential with that observed with solutions containing known concentrations of potassium bromide in 0.005 M potassium nitrate, saturated with silver bromide. A plot of e.m.f. vs. log[Br⁻] had a slope of 0.059 ± 0.003 . A slow potential drift during measurement (due to unstable salt bridge potential) was reduced to less than 1 mv. by letting the electrode stand before measurement in a solution with bromide concentration similar to that to be measured. The accuracy of the determination of concentration was estimated at about 5%.

In a few instances bromide concentration in sols was determined by titration with 0.002 M silver nitrate to the clear point.

Dye adsorption measurements were made using wool violet 5BN, the adsorption of which has been used as a measure of relative specific surface in silver bromide sols.^{3,4} Upon the addition of 5 ml. of solution containing 121 mg. dye per liter to an equal volume of sol, particle growth ceased. After 20 minutes of shaking to attain adsorption equilibrium one ml. of 0.33 M calcium nitrate was added to flocculate the sol, the mixture was centrifuged for 10 minutes, and the concentration of unadsorbed dye was determined spectrophotometrically at 550 m μ .

Results

The conductivity of sols prepared in the standard manner was practically constant one minute after mixing. A slight increase in conductivity, not much larger than the 1% accuracy of measurement, occurred during the next 30 minutes. The final conductivity corresponded to the potassium nitrate and bromide in the sol.

Potentiometric measurements of bromide concentration in a standard sol gave the results (equilibrium value, $5.0 \times 10^{-4} M$)

time after mixing	1.5 min.	15 min.	38 hours
[Br ⁻] $\times 10^4$	4.1	4.4	4.7

Similar results were found when the silver nitrate was added in 2 seconds instead of over 32 seconds. Within the accuracy of the conductivity meas-

(1) Taken from the Ph.D. Thesis of Willard H. Beattie, October 1958.

(2) E. J. Meehan and W. H. Beattie, *J. Phys. Chem.*, **64**, 1006 (1960).

(3) I. M. Kolthoff and A. S. O'Brien, *J. Am. Chem. Soc.*, **61**, 3409 (1939).

(4) I. M. Kolthoff and R. C. Bowers, *ibid.*, **76**, 1503 (1954).

urements, the increase in conductivity agreed with the increase in bromide concentration. (A decrease in bromide concentration below the equilibrium value has been noted previously,⁵ but the optical data were unsuitable for determination of particle size.) Upon titration of bromide with silver nitrate, practically the theoretical value was found both in few-minute and one-day old sols.

Particle Diameters. Effect of Concentration of Sols.—Variation of diameter with time in the standard sol is shown by curve 1 in Fig. 1A and 1B. There was a rapid initial increase in diameter, subsequently a prolonged period of much slower growth. Even after 24 hours the diameter was increasing slowly, but the growth rate became practically zero after about 36 hours (not shown in Fig. 1B). Several sols were made with identical conditions of mixing, but with concentrations of silver bromide equal to $5 \times 10^{-4} M$, $5 \times 10^{-5} M$ and $5 \times 10^{-6} M$, each being $5 \times 10^{-4} M$ in potassium bromide. Results are shown in Fig. 1A and 1B (curves 2, 3 and 4). The limiting particle size was a minimum at a sol concentration around $5 \times 10^{-4} M$.

Effect of Mixing Variables.—The particle diameter was unaffected by variation of stirring speed during mixing in the range 600–1000 r.p.m. Reduction of speed to 300 r.p.m. caused an increase of 20% in the initial diameter, but the diameter-time curve was parallel to that observed at higher speeds. Continued stirring (1100 r.p.m.) after addition of silver nitrate caused an increase in diameter of only 0.7, 1 or 2% after 1, 4 or 7.5 hours of stirring, respectively, compared to an unstirred sol. Violent shaking (900 two-inch strikes per min.) for 2 or 4 hours caused an increase of diameter of 7 or 16%. After 16 hours of shaking the sol had flocculated. The particle diameter was unaffected when the time of addition of silver nitrate was varied from 24 to 65 seconds; slower or faster addition gave larger particles. Increase in concentration of silver nitrate solution (same total amount added) caused an increase in initial particle size, but did not otherwise affect the diameter-time curve. A few experiments in which potassium bromide was added to silver nitrate showed that much larger particles were produced than in the standard method; however, the effect practically disappeared when the bromide was added rapidly (within 2 seconds).

Surface Area.—Figure 2, curve 1, shows the variation with time up to 200 min. of specific surface of a standard sol, expressed as cm^2 per ml. sol, calculated from light scattering diameters, assuming a monodisperse distribution. Curve 2 gives the relative specific surface derived from the adsorption of wool violet. The right-hand ordinate gives the experimental value of mg. dye per g. silver bromide. The adsorption area for wool violet was obtained by comparing the dye adsorption with the light scattering diameter of a 42-hour sol, assuming that particles of this age are smooth spheres of uniform size. On this basis the

(5) G. H. Jonker, H. R. Kruyt and L. S. Ornstein, *Proc. Acad. Sci., Amsterdam*, **42**, 454 (1939).

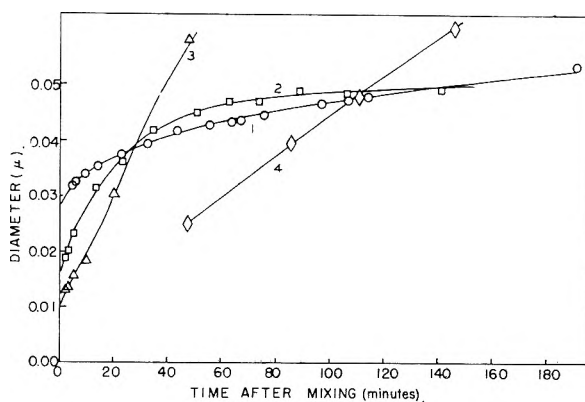


Fig. 1A.—Particle diameter vs. time in $5 \times 10^{-4} M$ KBr with silver bromide concentrations equal to: curve 1, $5 \times 10^{-3} M$; curve 2, $5 \times 10^{-4} M$; curve 3, $5 \times 10^{-5} M$; curve 4, $5 \times 10^{-6} M$.

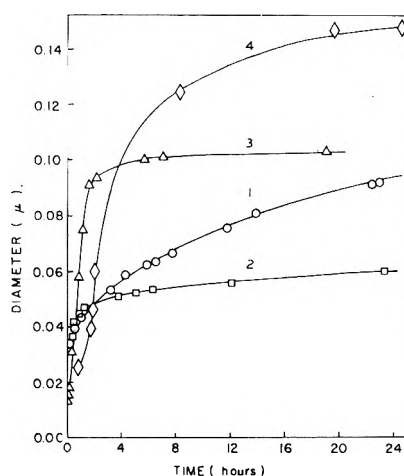


Fig. 1B.—Same as Fig. 1A for longer period of time.

adsorption area per wool violet molecule is 74 \AA^2 . A somewhat better estimate, allowing for the distribution of particle sizes, which can be derived by turbidity measurements at two wave lengths,² yields an adsorption area of 90 \AA^2 per molecule. The relatively larger specific surface from dye adsorption at short times (Fig. 2) undoubtedly is due to roughness of surface of the fresh particles.

Dilution Effects. (a) Stable Dialyzed Sol.—Portions of a dialyzed sol similar to one previously described,² with an average particle diameter of 0.17μ , were diluted 500-fold with water and with $10^{-3} M$ potassium bromide. No detectable change in scattering at 40° , $546 m\mu$, occurred in three hours in either portion. The specific turbidity ($546 m\mu$) of the dialyzed sol upon dilution with water was measured in cells of the appropriate length with the results given in Table I. The specific turbidity is independent of concentration in the range studied, showing that dialyzed sol may be diluted without measurable effect on particle size and that extrapolation to infinite dilution is unnecessary for silver bromide sols for concentrations less than $5 \times 10^{-3} M$ and diameter less than *ca.* 0.2μ .

(b).—A two-day old standard (undialyzed) sol was diluted 250-fold with water or potassium bromide solutions. The bromide concentrations after

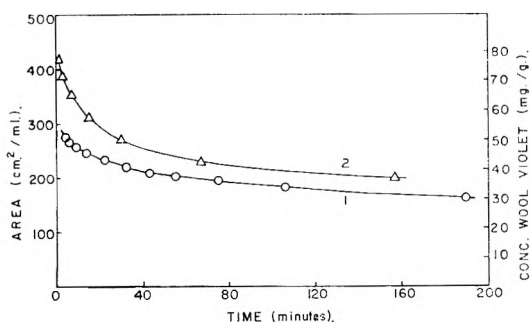


Fig. 2.—Area per ml. of sol, derived from light scattering (curve 1) and from adsorption of wool violet (curve 2).

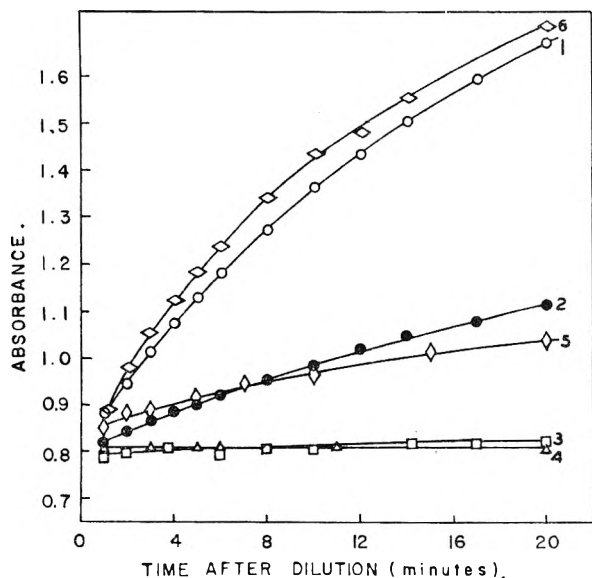


Fig. 3.—Absorbance (50 cm. cell, 450 $m\mu$) after dilution of a two day-old sol. Concentration in diluted sol: curve 1, $2 \times 10^{-6} M$ KBr; curve 2, $1.2 \times 10^{-6} M$ KBr; curve 3, $10^{-4} M$ KBr; curve 4, $10^{-3} M$ KBr; curve 5, $0.017 M$ KBr; curve 6, $2 \times 10^{-6} M$ KBr and $10^{-3} M$ KNO_3 .

TABLE I

SPECIFIC TURBIDITY OF STABLE DIALYZED SOL

τ = turbidity; c = concn. in g./ml.; for details see ref. 2.
($\tau/c \times 10^{-4}$)

Cell thickness, cm	0.1	1	10
Undiluted	1.29 ± 0.02		
6-fold dilution	1.26 ± 0.03	1.26 ± 0.01	
60-fold dilution		1.24 ± 0.02	1.27 ± 0.01

dilution are given in the legend of Fig. 3. The effect of change in refractive index ratio was negligible. The turbidity was measured (450 $m\mu$, 50 cm. path length) for 20 min. after dilution. A relatively rapid increase in turbidity, corresponding to particle growth, occurred upon dilution with water. Practically no change occurred upon dilution with 0.001 M potassium bromide. This is in accordance with previous observations on the rate of increase in turbidity of silver bromide sols.^{6,7} Apparently growth rate was slightly increased by dilution with 0.001 M potassium nitrate (curve 6) as compared to water (curve 1). Upon dilution with water containing gelatine, the growth rate was nearly zero at 0.04 and 0.004%

(6) K. Jablczyński, *Bull. soc. chim. France*, **33**, 1392 (1923).

(7) M. Schneller, *Kolloid Z.*, **71**, 180 (1935).

gelatine. With 0.0004% gelatine, the growth rate was about that of curve 3, Fig. 3. Remarkably, however, the turbidity immediately after dilution was 20 to 40% greater than the initial value after dilutions made without gelatine.

(c) Dilution of a 10-Minute Old Sol.—In these experiments the diameters were obtained both from dissymmetry and specific forward scattering, which gave results in good agreement. The diameters observed during 800 min. after dilution are shown in Fig. 4. As with the aged sol, the slowest growth occurred in *ca.* 0.001 M potassium bromide, but in none of the solutions tested was the growth rate equal to zero. Curve 6 corresponds to an undiluted sol (*cf.* Fig. 1A, curve 1). Apparently an abrupt increase in size occurred upon dilution (*vide infra*). No concentration of gelatine was found that would stabilize a 10-minute old sol.

The abrupt increase of size referred to above was investigated in detail for dilution with 0.001 M potassium bromide. Sols of various ages were diluted by various amounts and the angular scattering was measured immediately before and after dilution. Diameters before and after were calculated by extrapolation of the forward scattering to the time of dilution. Table II gives the % increase in diameter.⁸

TABLE II

% INCREASE IN DIAMETER UPON DILUTION WITH 0.001 M POTASSIUM BROMIDE

Dilution	Age of sol:	% Increase					
		10 min.	79 min.	2 hr.	6.2 hr.	30 hr.	42 hr.
10-fold		7	10	..	1.5
25-fold		13	..	5.5	..	0	0
50-fold		1	..
100-fold		17	1.5	..
250-fold		0.5
500-fold		23

Effect of Other Electrolytes.—Various electrolytes were added either to the potassium bromide solution before addition of silver nitrate or to the silver bromide sol. Results are shown in Fig. 5. Only the initial diameter was affected by the electrolyte; the diameter *vs.* time curves were eventually about parallel.

Temperature.—(a) Sols were made by the standard procedure except that the temperature of the solutions upon mixing ranged from 7 to 48°. The scattering (546 $m\mu$) at angle of 40° was measured for several minutes and extrapolated to 32 seconds, the time at which mixing was complete. Over this temperature range the 32-second diameter (d in μ) is related to temperature (T°) by the equation: $d = 0.020 + 3.0 \times 10^{-4} T$.

(b) A standard sol 37 minutes old was divided into portions which were placed in thermostats

(8) The increase in specific turbidity or specific scattering upon dilution could easily be misinterpreted as due to increase in coherent scattering. According to D. Sinclair, "Handbook of Aerosols," U. S. Atomic Energy Commission, Wash., D. C., 1950, Chapt. 7, independent scattering occurs when the particle separation is 10 to 100 times the particle radius. In standard sols, this distance is 30 times the particle radius, independent of radius and therefore of age of sol. Hence, non-independent scattering is inconsistent with the results of Table I, and the effect is a real increase in size upon dilution, most pronounced in fresh sols.

at temperatures from 20 to 53°. The turbidity derived from absorbance (1 cm. cell, 546 m μ), is shown in Fig. 6. The particle sizes were small enough so that Rayleigh scattering occurred, hence the absorbance A , equal to $\tau/2.3$, was proportional to weight average particle volume. The heat of activation for growth, calculated from the slope of $\log dA/dt$ vs. T^{-1} (t = time, T = absolute temperature) is 24 kcal. mole $^{-1}$.

Discussion

The principal results may be summarized as follows. No supersaturation exists in the standard sol one minute after mixing. The particles grow rapidly for 1 to 2 minutes up to a diameter of about 0.03 μ , then continue to grow at a much lower rate. The initial (1–2 minute) size is increased by (a) decrease in stirring speed during addition, (b) either relatively very rapid or slow addition of silver nitrate, (c) increased concentration in the solution of silver nitrate added (same total amount added), (d) presence of small amounts of Al(III) or Ba(II) during mixing and (e) increase of temperature at which mixing occurs. The growth rate after 2 minutes is not affected by any of the variables (a) to (e), but it is increased by (f) increase of temperature during growth period, and (g) prolonged stirring (relatively small effect) or violent shaking.

Growth Mechanisms.—Two mechanisms exist for increase in particle size. In one, particles grow by ionic or molecular accretion from supersaturated solution. This may occur also when the solution is supersaturated and unsaturated with respect to large and small particles, respectively, giving rise to Ostwald ripening. In the other mechanism, particles grow by coalescence, which in turn may be fast (every collision results in coalescence) or slow. According to von Smoluchowski's theory of fast flocculation,⁹ the temperature dependence of the rate in aqueous suspensions should increase about 2.5% per degree, due to the change in viscosity. Fast flocculation ceases when the potential energy barrier at the particle surface exceeds kT . Verwey and Overbeek¹⁰ calculated that the energy barrier depends on size and charge of particle, and the surrounding electrolyte. Jonker and Kruyt¹¹ calculated that the barrier is roughly proportional to the radius. For this reason fast flocculation ceases when the particles reach a critical size.

Ostwald ripening amounts to transfer of material from smaller to larger particles by way of the solution. Since the dissolution process involves ion hydration, the activation energy for Ostwald ripening is equal to or larger than the heat of solution for large particles.

If the initial deficiency of bromide ion (*cf.* potentiometric measurements) is due to occlusion of potassium bromide, subsequently released during recrystallization (Ostwald ripening), an approxi-

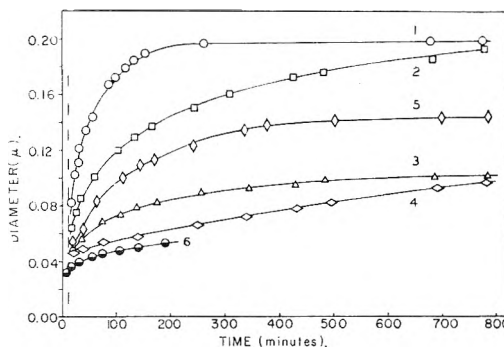


Fig. 4.—Diameter after dilution at 10 minutes; concentration of diluted sol: curve 1, 10 $^{-6}$ M KBr; curve 2, 10 $^{-5}$ M KBr; curve 3, 10 $^{-4}$ M KBr; curve 4, 10 $^{-3}$ M KBr; curve 5, 0.01 M KBr; curve 6 represents an undiluted sol.

mate rate of release of bromide to the solution can be calculated as follows. Assume n_1 particles each of volume v_1 are present initially, and these recrystallize into n_2 particles each of volume v_2 . This is equivalent to the complete dissolution of $(n_1 - n_2)$ particles, and to the transfer by recrystallization of the total volume $n_2(v_2 - v_1)$. The conductivity data showed that no measurable supersaturation existed one minute after mixing. Hence $n_1v_1 = n_2v_2$, and the fraction of the total volume which recrystallized is $(1 - v_1/v_2)$. On the other hand, if the deficiency of bromide is due to adsorption on the surface, the increase of bromide concentration with time can be calculated directly from the change in diameter (Fig. 1A). The results agree with the assumption that the bromide deficiency is due mainly to adsorption, and this is substantiated by the results of direct titration of bromide.

Assuming the Ag $^{+}$ -Br $^{-}$ distance on the surface is 2.89 Å., as it is in the cubic crystal, the maximum adsorption of bromide ions is 6.0×10^{14} ions-cm. $^{-2}$. In a standard sol at 1.5 minutes, the light scattering diameter corresponds to a specific surface of 294 cm. 2 per ml. of sol, and the observed bromide deficiency (0.9×10^{-4}) corresponds to 1.8×10^{14} ions per cm. 2 , or 31% of the available sites. Using the specific surface at 1.5 minutes from dye adsorption (Fig. 2), the adsorption corresponds to 22% of the available sites. Because of the probable roughness of the surface of fresh particles already referred to, the dye adsorption may give a more reliable estimate of % occupancy than the value calculated from diameter. Also, it is possible that the occupancy may be somewhat less than 22%, if the bulky dye molecule does not fill all small cavities.

The value in a fresh sol is much larger than in aged sols. Davies and Holliday¹² measured the immobile part of the surface charge in well aged silver bromide sols by electrophoresis. Their data in 5×10^{-4} M potassium bromide corresponded to adsorption at only 0.7% of the available sites, in agreement with calculations by Grimley¹³ based on conductivity measurements in

(9) See H. R. Kruyt, "Colloid Science," Elsevier Press, New York, N. Y., 1952, Vol. 1, Chap. 7.

(10) E. J. W. Verwey and J. Th. Overbeek, "Theory of Stability of Lyophobic Colloids," Elsevier Press, New York, N. Y., 1948, Chap. 12.

(11) G. H. Jonker and H. R. Kruyt, *Disc. Faraday Soc.*, **18**, 170 (1954).

(12) K. N. Davies and A. K. Holliday, *Trans. Faraday Soc.*, **48**, 1061, 1066 (1957).

(13) T. B. Grimley, *Proc. Roy. Soc. (London)*, **A201**, 40 (1950); "Fundamental Mechanisms of Photographic Sensitivity," edited by J. W. Mitchell, Butterworths, London, 1951, p. 46.

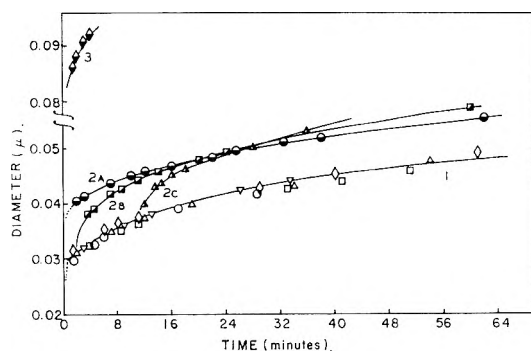


Fig. 5.—Effect of electrolytes on particle diameter. Concentration of added electrolyte: curve 1, none added (O), 0.01 M KNO_3 (\square), 0.01 M HNO_3 (∇), $9 \times 10^{-6} M$ $Ba(NO_3)_2$ (Δ), or $7 \times 10^{-6} M$ $Al(NO_3)_3$ (\diamond); curves 2A, B, C, $4.8 \times 10^{-4} M$ $Ba(NO_3)_2$ added at different times; curve 3, $1.8 \times 10^{-5} M$ $Al(NO_3)_3$.

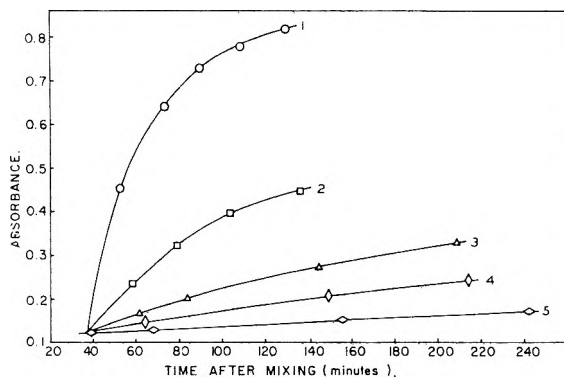


Fig. 6.—Change of absorbance at various temperatures of sol prepared and kept at 25° for 37 minutes: curve 1, 53° ; curve 2, 40° ; curve 3, 30° ; curve 4, 25° ; curve 5, 20° .

the solid. Also Basinski¹⁴ calculated the amount of adsorbed bromide in dialyzed sols from the difference between concentration of hydrogen ion and bromide ion. Particle size was estimated ultramicroscopically. In the presence of $1.2 \times 10^{-5} M$ bromide, the adsorption corresponded to 0.5% of the available sites. Apparently, fresh sols adsorb about 50 times as much bromide per unit surface as do aged sols.

Considering next the process during the period of slow growth, the observed activation energy of *ca.* 24 kcal. mole⁻¹ is somewhat larger than the heat of solution for large particles, 20.1 kcal. mole⁻¹.¹⁵ This is consistent with Ostwald ripening, but is far too large for a flocculation process. Also, this interpretation agrees with the effects of solvents and non-solvents on growth rate¹⁶ and with the present observation that the rate of slow growth is hardly affected by continued stirring.

The effect of $[Br^-]$ on the rate of slow growth (Fig. 3) undoubtedly involves at least two factors. The minimum rate at about $10^{-3} M$ Br^- corresponds roughly to the minimum solubility of silver bromide. Upon increase from 10^{-3} to $10^{-2} M$ Br^- , the growth rate increases about 10-fold, which is presumably explicable as due to increased solu-

bility ($AgBr_2^-$). Below $10^{-3} M$ Br^- the growth rate is obviously not proportional to the solubility, but apparently depends upon the Ag^+-Br^- ratio. This is consistent with observations of Davies and Jones¹⁷ on growth of silver chloride.

Fast Growth.—The mechanism of fast growth in silver bromide sols is largely a process of coalescence. The temperature dependence of the size at 32 seconds corresponds to about 3.5% (in volume) per degree, which is in fair agreement with the theoretical value of about 2.5%.

Variables Affecting Growth.—A qualitative explanation of the effect of mixing variables is as follows. Consider a stream of silver nitrate entering a solution of potassium bromide. At the interface where the solutions meet, the ion product is 10^7 to 10^8 times the solubility product. Rapid nucleation must occur at this interface. A short distance into the solution, some mixing will have occurred. Going across the boundary of the stream, bromide ion concentration goes from $10^{-2} M$ to 0, and silver ion concentration from 0 to $10^{-2} M$. Near the center of the boundary is a position where silver and bromide ion concentrations are equivalent and most of the silver bromide must be formed at this position where neither ion is deficient.

As mentioned previously, particles will coalesce until the potential is high enough that particles repel each other.^{10,11} The minimum radius necessary for stability is usually of the order 10^{-6} cm. If the particles have low charge, the size attained before repulsion dominates is increased. During mixing the surface charge depends upon the relative concentrations of silver and bromide. Particles located near the region corresponding to the isoelectric point will continue to coalesce until they are moved away from that location. Since most of the silver bromide is formed where the concentrations of silver and bromide ions are equivalent, and this is near the isoelectric point, the amount of coalescence is markedly dependent upon the time a particle spends in the neighborhood where it was formed. This means rapid stirring decreases the extent of coalescence, because it moves the particles to an area of excess either of bromide or of silver, before they have much time to grow. As stirring speed is increased fewer large particles are formed. If particles are moved into a region with excess of bromide faster than they can coalesce, further increase in speed has no effect. This kind of dependence of size upon stirring was found.

When a sol is made by adding a small volume of concentrated silver nitrate to a large volume of dilute potassium bromide, the particles are expected to be larger than those in sols made by mixing equal volumes, because the isoelectric point and equivalence point are located physically closer together than when mixing solutions of equivalent concentrations. This effect also was observed.

When silver bromide sols are made with the order of addition reversed (*i.e.*, potassium bromide added to silver nitrate) the entire sol must pass through the isoelectric point. This would be expected to result in the formation of a sol with ex-

(14) A. Basinski, *Rec. trav. chim.*, **69**, 331 (1940).

(15) B. B. Owen and S. R. Brinkley, Jr., *J. Am. Chem. Soc.*, **60**, 2233 (1938).

(16) S. E. Sheppard and R. H. Lambert, *Colloid Symposium Monograph*, **4**, 281 (1926).

(17) C. W. Davies and A. L. Jones, *Disc. Faraday Soc.*, **5**, 103 (1949).

tremely large particles, as found. However, when addition is completed in 1-2 seconds, the order of addition has only a small effect upon particle size. This must mean that the rate of addition was comparable to the rate of coalescence.

When flocculating electrolytes such as barium nitrate or aluminum nitrate are added to the potassium bromide solution before the addition of silver nitrate, coalescence would be expected to continue until the particles formed were larger than those formed in absence of flocculating electrolyte, as observed. When the identical concentration of flocculating electrolyte was added after the sol was made (Fig. 5), particles quickly grew to a size which was larger, the older the sol at the time of addition. This could be caused by the desorption of bromide, allowing greater coalescence because the potential energy barrier was lowered.

The abrupt increase in particle size upon dilution of a sol has not been reported previously. The fact that it depends markedly upon age indicates that it may be related to the degree of perfection of the particle. The electrical double layer around fresh particles easily may be disturbed by a change in surrounding electrolyte, so as to reduce the repulsion between particles, and allow coalescence during the time of the disturbance. This would lead to greater coalescence, the greater the dilution, as observed. Dilution with gelatin solution leads to a greater increase in particle size than dilution without gelatin. Gelatin possibly creates a greater disturbance of the electrical double layer than electrolytes.

The rate of particle growth depends upon the concentration of the sol (Figs. 1A and 1B). The growth of particles in a $5 \times 10^{-6} M$ sol was most rapid about 2 hours after mixing. The particles grew to a relatively large maximum size. In a $5 \times 10^{-5} M$ sol the period of fastest growth was about 40 minutes after mixing. In a $5 \times 10^{-4} M$ sol, the particles grew most rapidly 1 to 2 minutes after mixing. The final size was a minimum at this sol concentration. In the standard $5 \times 10^{-3} M$ sol, the large increase in turbidity during the last

quarter of the mixing process shows that the growth was most rapid during the mixing process.

Thus, in the range 5×10^{-3} to $5 \times 10^{-6} M$, the period of fastest growth comes at a later time, the more dilute the suspension. The final size decreases with increasing concentration, then increases again. The total growth pattern may be interpreted as a competition between the coalescence and Ostwald ripening. Ostwald ripening continues during both the fast and slow growth processes. During the fast growth period, fast flocculation also occurs. The rate of fast flocculation is proportional to the concentration of silver bromide. Therefore, in dilute sols, a fair amount of aging may occur before coalescence occurs. Particles have time to desorb some bromide, which increases the probability of coalescence by slow flocculation. As a result, coalescence continues for a longer time, the more dilute the sol, and the particles formed are larger due to formation from larger primary particles, the more dilute the sol. The rate of Ostwald ripening after coalescence has ended is slower, the more dilute the sol.

Finally, from all the above it is evident that precipitation reactions can be expected to yield reproducible particle size generally in two cases: (a) the rate of mixing is much greater than the rate of nucleation, resulting in a quasi-"homogeneous" precipitation, or (b) the rate of nucleation is much greater than the rate of addition of reagent, resulting in nucleation in the neighborhood of intermixing. If either rate of addition or mixing is comparable to rate of nucleation, small experimental variations may be expected to have a large effect on particle size. This appears to be the usual situation in precipitations of analytical interest. The lower the solubility, the easier it should be to approach case (b). Even though the rate of nucleation may not be relatively very great, it is still possible to attain reproducible results with well-controlled mixing methods, as attested by the fact that the standard procedure of this paper gives diameters reproducible within 4%.

THE INFRARED SPECTRA OF MARGINALLY METALLIC SYSTEMS: SODIUM-AMMONIA SOLUTIONS

BY TAD A. BECKMAN AND KENNETH S. PITZER

Department of Chemistry and Lawrence Radiation Laboratory, University of California, Berkeley, California

Received March 6, 1961

The sodium-ammonia solution system permits investigation of an array of compositions spanning the transition from non-metallic to metallic bonding. Reflection spectra in the range 1-20 μ were measured for solutions of mole ratio 5.5 to 168 NH_3 per Na. The dilute solutions show peaks characteristic of the vibrations of ammonia and a strong peak near 1.5 μ which is assigned to the solvated Na_2 species. Concentrated solutions show high reflectivity over broad wave length ranges. The results for nearly saturated solutions are fitted reasonably by the free electron model, but in the range of mole ratio 10-15 a complex array of energy absorption processes of finite frequencies are required to fit the spectra.

Introduction

While the nature of the transition from ionic to covalent bonding is now well understood, much less is known concerning the transition from metallic bonding to either sort of non-metallic bonding.

There are not too many series of compounds or solution systems where the non-metallic to metallic transition can be observed, but several are now known. Solutions of metals in liquid ammonia constitute one of the most familiar and

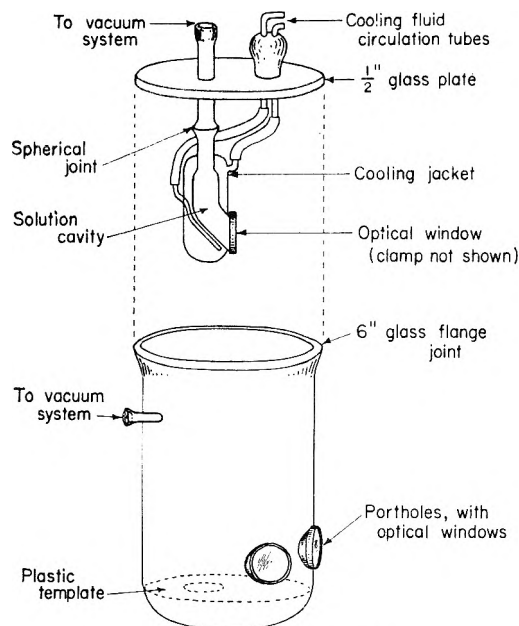


Fig. 1.—Reflection cell.

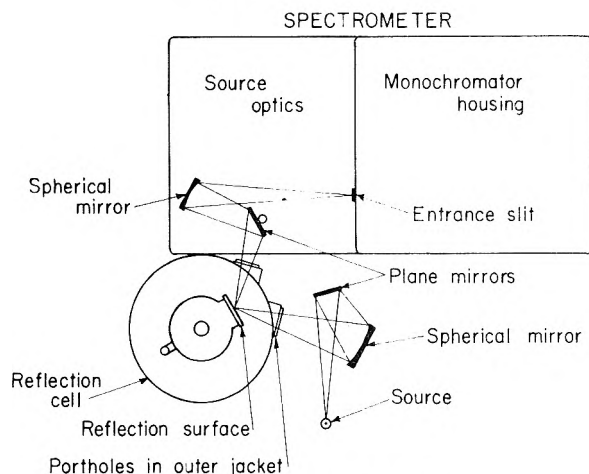


Fig. 2.—Optical arrangement.

convenient systems for such a study. In this paper we report reflection spectra for sodium solutions in liquid ammonia at concentrations spanning the transition from metal to non-metal, and discuss these and other data with respect to the nature of the electronic binding. Solutions of sodium metal in liquid ammonia offer a continuously variable composition from the very dilute to the saturated state above the critical temperature -41° . Phase separation occurs below this temperature. The conductance measurements of Kraus¹ demonstrate very well that these solutions range in their properties from those of a rather strong electrolyte (very dilute solutions) to those of a liquid metal (concentrated solutions).

Experimental Method and Procedure

Transmission measurements have been performed on the very dilute solutions of sodium in ammonia. However, the infrared extinction coefficients of these solutions are so large that transmission spectroscopy becomes totally impractic-

able at concentrations above about $0.1 M$. Thus, in order to study these solutions over a wide range of concentrations it was necessary to employ a reflection technique, the light reflected from a suitable optical surface being analyzed spectroscopically. These measurements are related to the energy absorption processes by a somewhat less direct path, but they provide the only means of investigation in the case of a highly absorbing material.

Reflection might be measured from either the interface between ammonia gas and the top surface of a solution or the interface between a suitable optical window of transparent material and a solution. The former of these involves the problem of light absorption by the ammonia vapor as well as the problem of surface disturbances such as bubbling. The latter involves the complications that very few materials are both transparent in the desired spectral region and insoluble in ammonia and, further, that many of the usable materials are susceptible to thermal shock breakage when being cooled to a low temperature. Both methods were tried, but the solution-window interface proved to be the more satisfactory optical surface for study.

Apparatus.—The reflection cell is illustrated in Fig. 1 and the optical arrangement used with the cell is illustrated in Fig. 2. The spectrophotometer used in this research was a Perkin-Elmer 12c equipped with an amplifier of laboratory design. Lithium fluoride, sodium chloride and potassium bromide prisms were used with this instrument.

The cell is constructed from two glass tubes. At its top the inner tube is connected to the vacuum system through a spherical joint; at its bottom this tube is bent outward and sealed through the second glass tube and is ground flat so that a window can be sealed tightly and held by a steel template and clamp. The outer tube is sealed at its top in a ring-seal around the inner tube, while at its base it is closed to a hemispherical end. The inner tube serves as the solution cavity while the outer tube serves as a cooling jacket. Coolant enters this jacket through a glass tube in back of the window area so that the window is kept as cold as possible. The outer vessel shown in Fig. 1 maintains a protective vacuum around the cell and contains the necessary windows, etc.

In the optical arrangement, light from a Glowbar source was focused by an extra set of standard Perkin-Elmer source optics at the interface between the window and the solution with an angle of incidence of approximately 40° . The reflected light entered the spectrometer through the usual optical system on the Perkin-Elmer instrument.

Acetone was the cooling fluid used in these experiments. The acetone was pumped from a cold reservoir through the cell by a centrifugal pump. The reservoir was cooled by a copper coil through which acetone in thermal contact with a Dry Ice-bath was pumped. A knife blade heater was also inserted in the reservoir which was regulated to $\pm 0.5^\circ$. This system was capable of maintaining a constant temperature of -40° for over 20 hours.

The windows which were used with this reflection cell were quartz, lithium fluoride, barium fluoride and polyethylene supported by cesium iodide. The first three, at least, are fairly common infrared materials, of limited transparency. However, no common window material was available for use in contact with liquid ammonia for the spectral region beyond 12μ . For this region a special window was prepared by sealing a thin polyethylene sheet to a cesium iodide window. Since this seal must endure through a rather large temperature drop, it could not be rigid. Consequently, Kel-F grease was used, and the sheet of plastic was rolled onto the window until most of the grease was squeezed out. This seal held under vacuum and did not crack as the temperature was reduced.

Experimental Procedure.—The solutions of sodium in liquid ammonia were prepared in an atmosphere of ammonia gas at -40° . The ammonia was first dried by distillation into a bulb containing waste sodium at a temperature of -70° . A small amount of hydrogen was pumped off. The dry ammonia was distilled into the cold reflection cell by allowing this bulb to warm gradually to room temperature. Sodium pellets were added to the ammonia in the reflection cell through a glass addition tube sealed into the vacuum system just above the top plate of the outer vessel. The pellets were stored *in vacuo* in side arms of this addition tube so that when the tube was rotated these arms could be tilted downwards toward the cell,

(1) C. A. Kraus, *J. Am. Chem. Soc.*, **43**, 749 (1921) and C. A. Kraus and W. W. Lucasse, *ibid.*, **43**, 2529 (1921); **44**, 1941 (1922).

allowing the desired number of pellets to pass into the ammonia.

Sodium pellets were prepared by cutting a solid block of sodium into many small cubes, rejecting those cubes which had been at or near the surface of the original block; this operation, and all subsequent handling of the sodium, was performed under thiophene-free benzene. The cubes were weighed individually under benzene and were placed in the arms of the addition tube in known order. Once the tube was connected to the system, the benzene was distilled away and the reflection apparatus was evacuated overnight. Since the initial volume of ammonia in the cell could be read from calibration marks and since the total weight of sodium in the solution could be derived from the number of pellets and their weights, the concentration of a given solution was known. This concentration was recorded as dilution V , the number of liters of ammonia per gram atom of sodium, but it is also indicated in terms of the mole ratio. The error should not exceed 5%.

Analysis of Results

Theory of Reflection Spectra.²—A wave equation for light in a transparent and isotropic medium of dielectric constant D can be derived readily from Maxwell's equations. In this relation, it is found that the transverse solution wave travels through the medium with a velocity equal to c (the velocity of light *in vacuo*) divided by $\sqrt{D\mu}$ where μ is the magnetic permeability and is usually unity. Since it is this ratio of the velocities which defines the refractive index of the material, we see that the optical constants may be related to the electrical constants in this way. The refractive index, n , of this simple material is equal to the square root of D .

If the material absorbs light but is still isotropic, the dielectric constant is a complex number given by $D' = D - 4\pi\sigma i/\omega$ where σ is the electrical conductance. Hence, the refractive index of the absorbing medium is also a complex number, $(n - ik)^2 = D'$. Here, n is the real refractive index while k is the absorption coefficient.

Application of the Helmholtz boundary conditions to the incidence of a plane wave of light upon a planar surface of this material gives the following expression for the reflectivity amplitude (normal incidence)

$$r = \frac{n - ik - n_0}{n - ik + n_0} \quad (1)$$

where n_0 is the refractive index of the material in which the light is incident and the reflectivity gives the ratio of reflected to incident amplitude. The measurable quantity is the luminous reflectivity R which is equal to the value of $|r|^2$. Thus

$$R = \frac{(n - n_0)^2 + k^2}{(n + n_0)^2 + k^2} \quad (2)$$

the observation of reflection is indirectly related to an observation of absorption; reflection of light must always accompany the absorption process, being especially strong when the absorption is great.

Drude's theory of dispersion, in turn, relates the microscopic absorption processes to the macroscopically observed optical constants. Drude assumed that a dielectric material could be pictured as an array of oscillators bound to equilibrium positions and having frequencies ω_i . The dis-

placement of a given oscillator under the influence of an applied periodic field, such as a light wave, is given by the equation of motion

$$m(d^2x/dt^2) + m\gamma(dx/dt) + m\omega_0^2x = -eE \exp(i\omega t) \quad (3)$$

where m is the oscillator mass, x is the displacement, γ is the damping constant, ω_0 is the frequency of the oscillator, e is the charge and $Ee^{i\omega t}$ represents the electric field of the light wave. Since the displacement is related to the dielectric constant of the material, expressions for the optical constants may be obtained.

$$n^2 - k^2 = 1 + 4\pi \sum_i \frac{(N_i e_i^2/m_i)(\omega_i^2 - \omega^2)}{(\omega_i^2 - \omega^2)^2 + \gamma_i^2 \omega^2}$$

and

$$nk = 2\pi \sum_i \frac{(N_i e_i^2/m_i) \gamma_i \omega}{(\omega_i^2 - \omega^2)^2 + \gamma_i^2 \omega^2} \quad (4)$$

where N_i is the density of each sort of oscillator with properties ω_i , γ_i , m_i , e_i .

Drude's formulas may be used even in consideration of the free electrons of metals. Since these electrons are unbound, according to classical notions, they represent oscillators of zero frequency. The formulas which result from this substitution predict the optical constants with good accuracy.

A variety of absorption processes in the liquid ammonia-sodium system will cause reflection of light. For instance, both bound and free electrons must exist in these solutions. The bound electrons will produce reflection peaks associated with the absorption frequencies, while the free electrons will yield a general reflection in the infrared with varying intensity. The vibrational motions of ammonia molecules will also give some contribution although, because of the larger masses, we expect these to be small in magnitude.

Observed Spectra.—In measuring the reflection spectrum of any material one must observe both the reflected and incident intensities or the spectrum under identical conditions of some reflection standard whose optical constants are known throughout the region of study. In this research liquid mercury was used as a standard reflector for several reasons. It could be placed inside the cell where its reflection spectrum could be taken under conditions identical with those at which the solutions were studied. Also, liquid mercury obeys the Drude formulas for a metallic reflector so that the solutions were compared directly to a classical metal. No attempt was made in this research to obtain the optical constants of these solutions from the observed spectra. Either one would have to make observations at several different angles of incidence (which is clearly impractical with the reflection cell illustrated) or one would have to apply the Robinson and Price method³ of calculating the phase angle as a function of wave length (which would clearly not be accurate in a case where absorption spreads over a large region of the spectrum). Instead, the reflection was indicated as a percentage ρ obtained by dividing the solution spectra by the corresponding mercury spectra.

(2) J. R. Partington, "An Advanced Treatise on Physical Chemistry," Vol. IV, Physico-Chemical Optics, Longmans, Green and Company, New York, N. Y. 1953.

(3) T. S. Robinson and W. C. Price, "Molecular Spectroscopy, Rept. Cong., Inst. Petroleum, London," 1954, 211 (Pub. 1955).

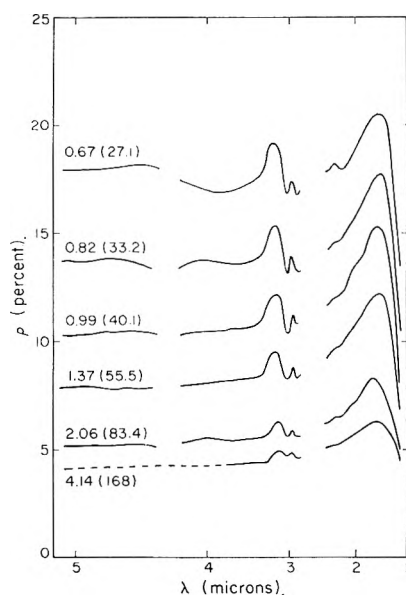


Fig. 3.—Reflection spectra for dilute solutions in the LiF region. The concentration is given in liters of NH_3 per mole Na and (mole ratio NH_3 to Na).

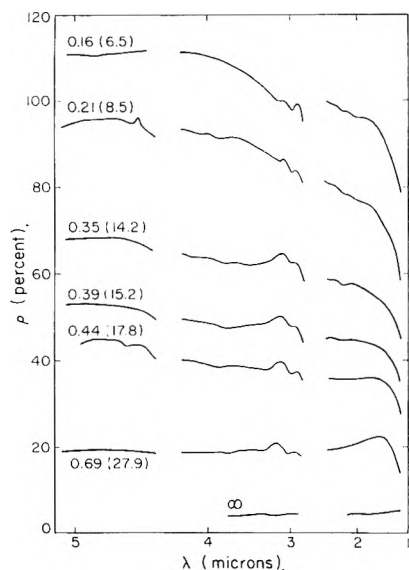


Fig. 4.—Reflection spectra of more concentrated solutions. Concentrations given as in Fig. 3.

Figures 3 and 4 show the spectra taken with the LiF window. The spectra taken with the quartz window yield no additional information.⁴ Regions of intense atmospheric absorption are omitted. The spectra taken with BaF_2 and polyethylene-CsI windows contain only relatively narrow regions of good observation between regions of absorption by atmospheric constituents or the window materials. The Kel-F grease which sealed the thin polyethylene to the CsI plate apparently flowed enough to vary in thickness and hence results are unreliable even in regions where it absorbed only moderately. The resulting reflectivities⁴ (relative to mercury) in each region of good observation were interpolated to even concentrations and are

(4) Figures showing all of the spectra are included in the Ph.D. Dissertation of Tad Alan Beckman, University of California, 1960 (Lawrence Radiation Laboratory Report UCRL-9330).

shown in Fig. 5. The small peaks near 3μ are omitted in Fig. 5.

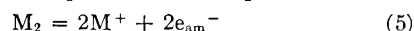
Assignment of Reflection Bands.—Review of the spectra of the dilute solutions indicates that several reflection bands, or maxima, exist; these are to be found at 6200, 3370, 3190 and 1030 to 1050 cm^{-1} . The three low frequency peaks can all be associated with fundamental vibrations of the ammonia molecule. For instance, the 3190 cm^{-1} reflection seems best assigned to the ν_1 vibration of ammonia which is observed by transmission to lie at 3223 cm^{-1} in the crystal.⁵ The 3370 cm^{-1} band can be assigned to ν_3 which absorbs at 3378 cm^{-1} in the crystal. And 1030 to 1050 cm^{-1} is easily assigned to ν_2 which is 1060 cm^{-1} in the crystal. The reflection peak at 6200 cm^{-1} is, however, a property of the sodium-ammonia system as a whole. The concentrated solutions show high reflectivity over wide regions with little or no fine structure.

Discussion

Our interpretation of the spectra will be divided into two parts. In dilute solutions the principal solute species can be inferred by the concentration dependence of various phenomena. Also many other investigations have yielded various types of data for dilute solutions. Our spectra are consistent with this knowledge from other sources. The concentrated solutions and the two phase region offer a more difficult problem and only some preliminary conclusions will be given here. Other experiments will be needed before a very detailed understanding of the concentrated solutions is possible.

In view of the recent and complete reviews by Jolly⁶ and by Symons⁷ an extensive bibliography is unnecessary and only the most pertinent evidence will be cited.

Dilute Solutions.—Most of the properties of dilute alkali metal solutions in ammonia can be attributed to the species in the equilibrium



Here M^+ is just the familiar solvated ion and e_{am}^- is an electron solvated by oriented ammonia molecules with presumably a cavity at the center.⁸ The species M_2 was first suggested by Huster.⁹ The nature of the species M_2 is not established in detail but it contributes to neither the electrical conductance nor the paramagnetic spin resonance. Presumably the Na^+ ions are solvated by ammonia and two such ions are bound together by two electrons of antiparallel spin. Additional species, such as solvated electron pairs or solvated metal atoms, have been proposed but the evidence indicates that they are at most minor species in Na-NH_3 solutions at -40° .

Yost and Russell¹⁰ discuss the evidence for M_2 and Becker, Lindquist and Alder¹¹ calculate

(5) F. P. Reding and D. F. Horning, *J. Chem. Phys.*, **22**, 1926 (1954).

(6) W. L. Jolly, *Progr. Inorg. Chem.*, **1**, 235 (1959).

(7) M. C. R. Symons, *Quart. Revs.*, **13**, 99 (1959).

(8) J. Jortner, *J. Chem. Phys.*, **30**, 839 (1959).

(9) E. Huster, *Ann. Physik*, **33**, 477 (1938).

(10) D. M. Yost and H. Russell, Jr., "Systematic Inorganic Chemistry," Prentice-Hall, Inc., Englewood Cliffs, N. J., 1943, pp. 144-145.

(11) E. Becker, R. H. Lindquist and B. J. Alder, *J. Chem. Phys.*, **25**, 971 (1956).

the equilibrium constants for reaction 5 for potassium solutions at 298, 274 and 240°K. The magnetic data¹² show that the equilibrium constant for sodium is indistinguishable from that for potassium at 240°K. and that its change with temperature is a little more rapid for sodium than for potassium. Only a short extrapolation is required to 233°K., the temperature of our experiments, where we find $K = 3.5 \times 10^{-8}$ if concentrations are in moles per liter. Even in our most dilute solution, $V = 4.14$ or $0.24 M$, this K predicts only 4% dissociation of Na_2 . Consequently, the reflection spectra for relatively dilute solutions in the range 0.24 to 1 M must be dominated by features arising from Na_2 as well as NH_3 , of course. At still lower concentration, however, where absorption spectra are measured, the dissociated ions Na^+ and e_{am}^- become major species. Thus the fraction dissociated is roughly 50% at 0.01 M while at 0.001 M it is greater than 95% at the temperature of spectral measurement.

The reflection spectra of the dilute solutions, Fig. 3, show just one distinct feature attributable to the metal solute—the peak near 1.5 μ . While the equilibrium constant for dilute solutions indicates little dissociation of Na_2 in the concentration range of Fig. 3 ($V = 0.67$ to $V = 4.14$), we have little independent evidence concerning the concentration of larger clusters Na_n with $n > 2$. Our spectra show just a gradual increase in intensity as the concentration increases to $V = 1.0$, but at higher concentration the reflectivity at wave lengths longer than 4 μ increases more rapidly than that at the 1.5 μ peak. This additional reflectivity at longer wave length presumably indicates the appearance of some larger clusters. The 1.5 μ peak may be assigned primarily to the Na_2 species although e_{am}^- contributes in addition. Calculation indicates a corresponding absorption wave length of approximately 2 μ . The nature of the reflection process is such that the reflection peak is observed at shorter wave length than the absorption peak.

Unfortunately the concentration range for good reflection measurement does not overlap with that for absorption measurement, hence a direct comparison is impractical. The absorption spectra¹³ show a peak in this same region with a maximum at 1.4 μ for very low concentration of either Na or K. This band is assigned to e_{am}^- . As the concentration increases above 0.001 M the maximum shifts slowly to longer wave length (about 1.5 μ at 0.004 to 0.01 M) and small differences are noted between sodium and potassium solutions. This shift is in the direction expected as the amount of Na_2 (or K_2) increases. In the case of both the reflection and absorption spectra the intensity corresponds to that of an allowed transition by most if not all of the solute present. Thus the 1.5 μ reflection peak is too intense to be explained by the e_{am}^- species alone. The near equality of frequency for e_{am}^- and for solvated Na_2 may be either accidental or of fundamental significance; we shall hope to learn which in the near future.

(12) C. A. Hutchison and R. C. Pastor, *J. Chem. Phys.*, **21**, 1959 (1953).

(13) R. C. Douthett and J. L. Dye, *J. Am. Chem. Soc.*, **82**, 4472 (1960).

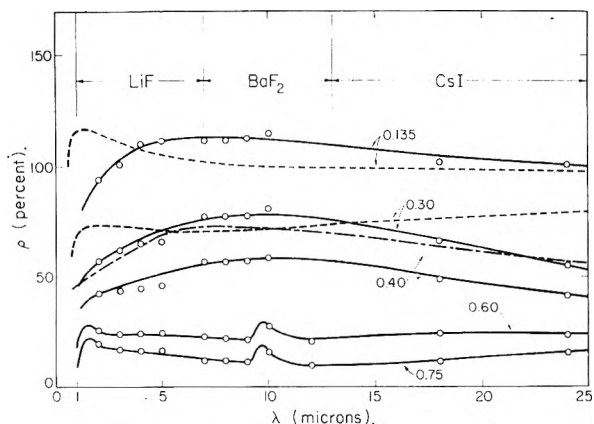


Fig. 5.—Reflectivity (relative to Hg) for Na-NH₃ solutions of the dilution in liters of NH₃ per mole of Na indicated. Dotted curves are calculated for free metallic electrons; the dot-dash curve for $V = 0.30$ is calculated for a more complex model given in the text.

Concentrated Solutions.—The fully metallic nature of very concentrated metal-ammonia solutions was recognized in the early work. The equivalent conductance of a saturated solution of sodium is 6 times that of mercury. Presumably the metal ions are solvated as in the species M_2 but now the electrons have metallic orbitals which pervade the entire solution. One of us¹⁴ has pointed out the analogy between the phase separation below -41.6° in these solutions and the vapor-liquid phase separation in pure sodium. In the solutions the ammonia solvates the solute species but is otherwise a dielectric medium within which a condensation phenomenon can occur. The metallic solutions are those in the liquid-like range, *i.e.*, more concentrated than the critical composition of 4.15 atom % Na.

Exploratory calculations were made of the reflectivity on the free electron model. Equation 4 was used with $\omega_i = 0$ and N_i taken from the known concentration. The observed electrical conductance σ yields γ_i from the relationship

$$\gamma_i = N_i e_i^2 / \sigma m_i \quad (6)$$

where e_i and m_i are the electronic mass and charge, respectively. Figure 5 shows as dashed lines the calculated curves for the concentrations $V = 0.135$ and $V = 0.3$. In the nearly saturated solution where the mole ratio is 5.5 NH₃ to one Na the calculated reflectivity curve resembles the experimental curve rather closely. The agreement is good except that the drop in ρ in the region 3 to 0.5 μ is actually more gradual than that calculated. Doubtless some refinement of the model would remedy this discrepancy. We shall not attempt such modifications at present but rather emphasize the general success of the simple free electron model for the nearly saturated solutions.

At $V = 0.3$, however, the agreement with the free electron model is much poorer. The difficulty near 1 μ remains and in addition the trend with wave length in the 15–25 μ region is wrong. Several more complex models were tested in an effort to fit the observed curve for $V = 0.3$. The curve shown as a dot-dash line on Fig. 5 was cal-

(14) K. S. Pitzer, *ibid.*, **80**, 5046 (1958).

culated for a model with three different absorption processes of finite frequency in addition to a small population of free electrons with a damping constant fitted to the electrical conductance. The following parameters were used

$$\begin{aligned} N_1 &= 4 \times 10^{19}, \gamma_1 = 1.2 \times 10^{13}, \omega_1 = 0 \\ N_2 &= 2.5 \times 10^{20}, \gamma_2 = \omega_2 = 1.5 \times 10^{14} \\ N_3 &= 5 \times 10^{20}, \gamma_3 = \omega_3 = 3 \times 10^{14} \\ N_4 &= 5 \times 10^{20}, \gamma_4 = \omega_4 = 1 \times 10^{16} \end{aligned}$$

The values of γ_i were taken equal to ω_i for each non-zero frequency since relatively broad bands would be expected and there was no justification for independent adjustment of the various γ_i . While the fit of this calculated curve is by no means perfect, it is good enough to confirm this general type of model.

The model for the dot-dash curve may be interpreted as representing a small concentration N_1 of conduction electrons, a rather high concentration N_4 of dimeric, solvated Na_2 , and high concentration $N_2 + N_3$ of a distribution of larger clusters Na_n ($n > 2$) which have primary electronic frequencies distributed over the range indicated by ω_2 and ω_3 . Such larger clusters were suggested by Schmidt¹⁵ on the basis of X-ray data. No

significance should be attached to the exact values given for $N_2, N_3, \omega_2, \omega_3$, etc. This interpretation is plausible on the basis of our knowledge of the more dilute sodium-ammonia solutions and of critical and condensation phenomena in general.

These results indicate that solutions significantly more concentrated than the critical composition, such as $V = 0.3$, do not constitute the sort of simple free-electron metal which is represented by the saturated solution or the pure liquid or solid alkali metal. The clustering of the solute, however, need not be primarily to spherical clusters. It seems likely that much more irregular shapes are involved including thread-like regions sometimes interconnected throughout the solution.

Research is being continued on these systems which will include further experimental measurements as well as discussion of the results in terms of quantum theory of the valence electrons.

Acknowledgments.—We thank Dr. Marvin Ross for certain exploratory calculations and Professor W. L. Jolly for comments and suggestions. This research was carried out under the auspices of the U. S. Atomic Energy Commission.

(15) P. W. Schmidt, *J. Chem. Phys.*, **27**, 23 (1957).

FORMATION OF CARBON MONOXIDE IN METHANE FLAMES BY REACTION OF OXYGEN ATOMS WITH METHYL RADICALS

BY C. P. FENIMORE AND G. W. JONES

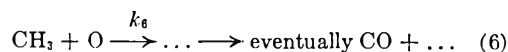
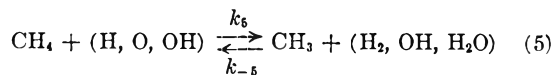
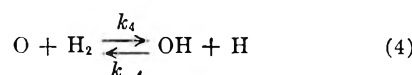
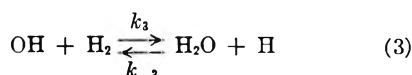
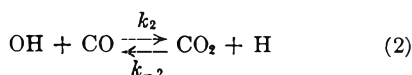
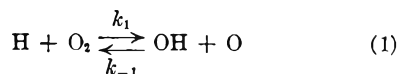
General Electric Research Laboratory, Schenectady, N. Y.

Received March 7, 1961

The carbon monoxide formed in $\text{CH}_4\text{-O}_2$ flames containing H_2O^{18} and O^{18}H does not derive its oxygen from H_2O or OH , and earlier work shows that it does not derive much of its oxygen from O_2 either. It is suggested, therefore, that carbon monoxide is eventually formed when a free O atom reacts with a CH_3 radical; and the suggestion is tested. $[\text{O}]$ is estimated by modifying a method used previously in flames; $[\text{CH}_3]$ is deduced from the rate of formation of C_2 hydrocarbons, or more accurately from $\text{CH}_3 + \text{NO} \rightarrow \text{CH}_3\text{NO} \rightarrow \dots \rightarrow \text{HCN} + \dots$; and then the rate of formation of carbon monoxide is found to equal $k[\text{O}][\text{CH}_3]$ with $k = 1.9 \times 10^{10}$ l. mole⁻¹ sec.⁻¹. A formation of carbon monoxide by $\text{CH}_3 + \text{O}_2 \rightarrow \dots \rightarrow \text{CO} + \dots$ could not compete unless its rate constant were larger than the literature values for the reaction of CH_3 radicals with O_2 . It is probable that methane burns mostly by the known reactions of $\text{H}_2\text{-CO-O}_2$ combustion, plus some means of forming CH_3 radicals, and plus $\text{O} + \text{CH}_3 \rightarrow \dots \rightarrow$ eventually $\text{CO} + \dots$.

Introduction

In this paper we propose, and partly test, the idea that methane burns by the fast reactions of $\text{H}_2\text{-CO-O}_2$ combustion, reactions 1 through 4 below, plus some *ad hoc* device for forming methyl radicals such as reaction 5, and plus the incompletely specified (6).



It has been shown already that oxygen molecules are mostly consumed by reaction 1 in methane flames,¹ and (2), (3), and (4) are included because the flames contain hydrogen molecules and carbon monoxide. It is generally accepted that carbon dioxide is formed mostly in reaction 2. The only novel suggestion is that carbon monoxide is formed eventually when an O atom reacts with a CH_3 radical; and before we test this proposal, it is worth showing why we think it should be the chief means of forming carbon monoxide.

A considerable source of oxygen in some form is

(1) C. P. Fenimore and G. W. Jones, *J. Phys. Chem.*, **63**, 1834 (1959).

needed to make carbon monoxide. If the source is not molecular oxygen, as oxygen molecules are mostly consumed in (1), it might be water, OH radicals, or free O atoms; but water and OH can be ruled out in the following way. Figure 1 shows traverses through a flat, low pressure flame of $\text{CH}_4\text{-O}_2\text{-H}_2\text{O}$ (H_2O containing H_2O^{18}) and the graphs at the bottom of the figure indicate that the carbon monoxide formed had much less O^{18} in its O than did the carbon dioxide. If carbon monoxide derived its oxygen from OH radicals or water, it should have had at least as much O^{18} in its O as the carbon dioxide; for carbon dioxide was formed in reaction 2 from $\text{CO} + \text{OH}$, and the H_2O^{18} in the water was larger than the O^{18} in the O of carbon dioxide. Hence, carbon monoxide did not derive its oxygen from OH or water; and if not from molecular oxygen either, then it probably derived oxygen from O atoms.²

In the formation of carbon monoxide, the reaction partner for the O atom is probably not methane itself; for $\text{O} + \text{CH}_4$ should only react in the sense of (5). The most reasonable guess is that methyl radicals are formed in some way such as (5), and that carbon monoxide is formed in (6). In referring k_6 to the initial interaction of $\text{O} + \text{CH}_3$, we imply that the C-O bond once made is never broken. We have no evidence, however, about what intermediates might occur.

Since the total rate of formation of carbon monoxide is the sum of observed $d[\text{CO}]/dt$ and $d[\text{CO}_2]/dt$, the partial mechanism claims that

$$(d[\text{CO}]/dt + d[\text{CO}_2]/dt) = k_6[\text{O}][\text{CH}_3]$$

By measuring all other quantities, we can obtain k_6 . Though no numerical estimate of this constant is available, it should be very large.³ We will obtain $k_6 = 1.9 \times 10^{10} \text{ l. mole}^{-1} \text{ sec.}^{-1}$ over three-to-eight fold variations in $[\text{O}]$ and $[\text{CH}_3]$, so the mechanism passes this test.

Estimates of Radical Concentrations.— $[\text{O}]$ is estimated in reaction zones from an extension of an equation used before in $\text{H}_2\text{-O}_2\text{-N}_2\text{O}$ flames

$$[\text{O}] = \frac{-d[\text{O}_2]/dt - (d[\text{CO}]/dt + d[\text{CO}_2]/dt)}{k_4[\text{H}_2]}$$

$$k_4 = 2.5 \times 10^9 e^{-7.17/RT} \text{ l. mole}^{-1} \text{ sec.}^{-1.4}$$

The assumptions in this equation are of two kinds. First, there are approximations which can be justified in the same way as before⁴: that $d[\text{O}]/dt = \text{zero}$ in the region where we use the expression, that the reverse of (4) can be neglected compared to (4) itself, and that recombination such as $\text{O} + \text{H} + \text{M} \rightarrow \text{OH} + \text{M}$ can be neglected. Then there are also assumptions about methane burning; that the consumption of O atoms can be neglected in hypothetical reaction (5) or in the unspecified

(2) Figure 1 refers to a fuel-lean, low temperature flame. We should add that in fuel-rich flames containing H_2O^{18} , the CO^{18} content of the carbon monoxide, though starting small just as in Fig. 1, increases in the samples collected farther downstream. CO^{18} is expected to increase in fuel-rich flames, because these require higher temperatures to burn than fuel-lean ones and CO^{18} , OCO^{18} and H_2O^{18} should equilibrate more rapidly via reactions 2, 3, and their reverses at the higher temperatures.

(3) E. W. R. Steacie, "Atomic and Free Radical Reactions," Second Edition, Vol. II, Reinhold Publ. Corp., New York, N. Y., 1954, p. 601.

(4) C. P. Fenimore and G. W. Jones, *J. Phys. Chem.*, **65**, 993 (1961).

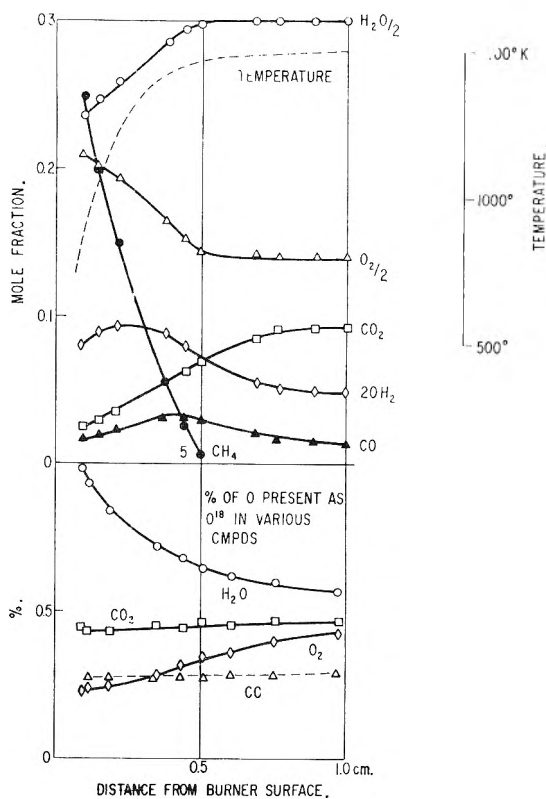
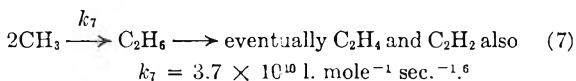


Fig. 1.—Traverses through a flame of $\text{CH}_4 + 5.1 \text{ O}_2 + 3.6 \text{ H}_2\text{O}$ (containing 1.45% H_2O^{18}) burnt at 6 cm. P with a mass flow of $1.26 \times 10^{-3} \text{ g. cm.}^{-2} \text{ sec.}^{-1}$.

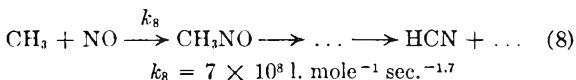
parts of (6). These additional assumptions cannot be proved, though they seem reasonable if the flame contains much molecular hydrogen. In the runs with mixed $\text{H}_2\text{-CH}_4$ fuel, the $[\text{O}]$ deduced does not depend very strongly on the assumptions about methane burning.

The value quoted for k_4 is smaller, in our temperature range, by a factor of two to three than values extrapolated from Clyne and Thrush's results at 409 to 733°K.⁵ We use the quoted value because it was obtained at the temperatures of present use by a method very similar to our present application.

$[\text{CH}_3]$ can be approximated if it is assumed that the C_2 hydrocarbons in methane flames derive from CH_3 radicals



The assumption is reasonable because the fraction of C_2H_6 in the C_2 hydrocarbons is largest in the samples collected farthest upstream. $[\text{CH}_3]$ can also be estimated in the presence of nitric oxide



and this should be equivalent to the determination from C_2 hydrocarbons because k_8 was estimated relative to k_7 . The assumption that an equimolar

(5) M. A. A. Clyne and B. A. Thrush, *Nature*, **189**, 135 (1961).

(6) G. B. Kistiakowsky and E. K. Roberts, *J. Chem. Phys.*, **21**, 1637 (1953).

(7) M. I. Christie, *Proc. Roy. Soc. (London)* **A248**, 1 (1959).

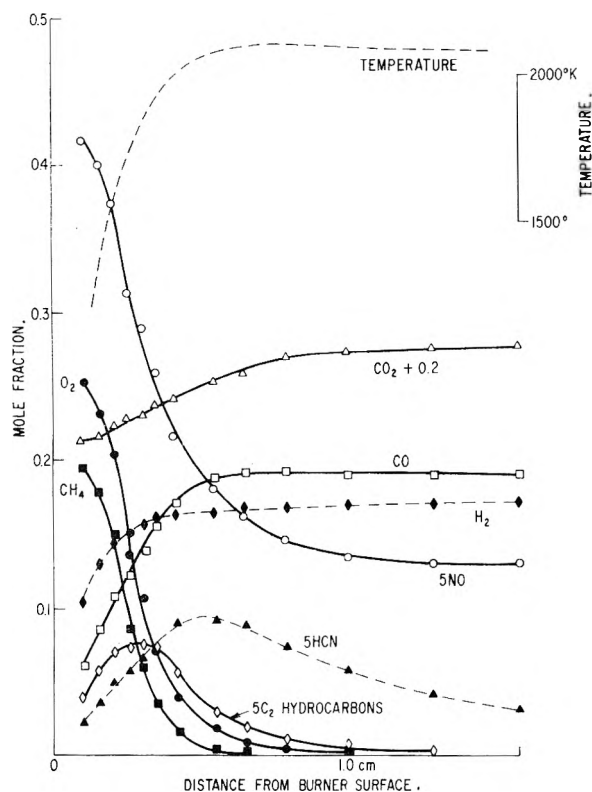


Fig. 2.— $\text{CH}_4 + 1.11 \text{O}_2 + 0.30 \text{NO} + 0.37 \text{A}$ burnt at 4 cm. P with a mass flow of 2.1×10^{-3} g. cm. $^{-2}$ sec. $^{-1}$.

reaction occurs between CH_3 radicals and nitric oxide would be incorrect if the destruction of HCN consumed or re-formed nitric oxide; but no large error could be introduced if, as in all of the H_2 - CH_4 flames, HCN decayed only slowly.

The quoted values of k_7 and k_8 are correct only if the pressure was high enough for the recombinations to be second-order processes. The pressures used, 4 to 16 cm. of Hg, were perhaps marginal and therefore the estimates of $[\text{CH}_3]$ might have been too small; but we do not believe that the error introduced could be larger than the uncertainty in k_8 itself.⁷ For we found evidence that the equilibrium, $\text{H} + \text{CH}_4 = \text{CH}_3 + \text{H}_2$, was satisfied in sufficiently fuel-rich flames; and the equilibrium $[\text{CH}_3]$ agreed with that measured from nitric oxide within the uncertainty in k_8 .

Experimental

The same apparatus and procedures were used as before.^{1,4} A water-cooled, porous burner in a bell jar let us burn flat, low pressure flames which could be scanned with a fine quartz coated thermocouple, and sampled at various positions through a fine quartz probe. In the mass spectrometric analysis, HCN was determined in the presence of C_2 hydrocarbons by collecting two samples at each point, one of them being passed over Ascarite to remove HCN but not C_2H_4 or C_2H_6 which were the interfering species at $m/e = 27$.

The greatest error in the calculated reaction rates probably derives from the necessary diffusion corrections. We applied simplified corrections as before, and assumed that the diffusion coefficients for different species varied inversely with the square root of molecular weight. The diffusion coefficient is reported for the cases illustrated, and similar coefficients were used in other runs.

Results

Results are given for all but two of the flames

studied. The two omitted were CH_4 - O_2 and H_2 - CH_4 - O_2 mixtures which did not have nitric oxide added in the reactants; and though they were consistent with the others, we did not include them in our final estimate of k_6 because $[\text{CH}_3]$ was obtained only approximately. For the other runs, Table I lists $[\text{O}]$, $[\text{CH}_3]$ and $k_6[\text{CH}_3]$. $k_6[\text{CH}_3]$ was obtained from

$$k_6[\text{CH}_3][\text{O}] = (d[\text{CO}]/dt + d[\text{CO}_2]/dt)$$

except in one run where the observed $(d[\text{CO}]/dt + d[\text{CO}_2]/dt)$ could not be equated to $k_6[\text{CH}_3][\text{O}]$ without a large correction.

TABLE I

RESULTS FROM WHICH k_6 CAN BE ESTIMATED

Fig.	Reactants		P , cm.	T , °K.	$[\text{O}]$	$k_6[\text{CH}_3]$	$[\text{CH}_3]$	
	$\text{H}_2/$ CH_4	$\text{O}_2/$ CH_4			$\times 10^7$, mole l.^{-1}	$\times 10^{-4}$, sec. $^{-1}$	mole (1)	$\times 10^7$, l.^{-1} ^a (2)
2	0	1.11	4	1900	15	2.2	~6	9
..	2.5	1.87	4	1510	20	4.5	~15	24
..	9.8	4.23	4	1210	48	0.44	..	2.8
3	5.8	3.11	8	1370	34	1.5	..	8.9
..	2.6	2.04	8	1560	32	2.3	..	11.0

^a The two estimates of $[\text{CH}_3]$ are: (1) from rate of formation of C_2 hydrocarbons; (2) from reaction with nitric oxide.

Figure 2 illustrates the run requiring correction. The profiles through this CH_4 - O_2 - NO -A flame were reduced to reaction rates by use of an assumed diffusion coefficient for oxygen of $D_{\text{O}_2} = 3.3 \times 10^{-4} T^{1.67}$ cm. 2 sec. $^{-1}$. We evaluated $[\text{CH}_3]$, etc., only at the point where $d[\text{C}_2 \text{ hydrocarbon}]/dt = \text{zero}$. Here $[\text{CH}_3] = -d[\text{NO}]/k_8[\text{NO}]dt = 9 \times 10^{-7}$ mole l.^{-1} and $d[\text{HCN}]/k_8[\text{NO}]dt = 5 \times 10^{-7}$; perhaps the difference was due to the destruction of part of the HCN as it was formed. $[\text{CH}_3]$ could also be approximated from the C_2 hydrocarbons as follows: from 0.45 cm. on downstream, the observed $-d[\text{C}_2 \text{ hydrocarbons}]/dt = 3.7 \times 10^3$ $[\text{C}_2 \text{ hydrocarbons}]$ could not have been accompanied by any large simultaneous formation of C_2 hydrocarbons; and if the same destruction occurred farther upstream where the net observed rate was zero, C_2 hydrocarbons would have been formed and destroyed at equal rates of $k_7[\text{CH}_3]^2 = 3.7 \times 10^3$ $[\text{C}_2 \text{ hydrocarbons}]$. Inserting the maximum $[\text{C}_2 \text{ hydrocarbons}]$ gives $[\text{CH}_3] \sim 6 \times 10^{-7}$.

Thus $[\text{CH}_3]$ was estimated approximately, and $[\text{O}]$ was also obtained as described above with fair confidence. It would be wrong to equate $k_6[\text{CH}_3][\text{O}]$ with $(d[\text{CO}]/dt + d[\text{CO}_2]/dt)$ in this flame, however, because the destruction of C_2 hydrocarbons must have contributed to the formation of carbon oxides. If $[\text{CH}_3] = 6$ to 9×10^{-7} , $k_7[\text{CH}_3]^2$ was 22 to 50% of the rate of formation of carbon oxides. The $k_6[\text{CH}_3]$ listed in Table I, for this flame only, was obtained on the assumption that $(d[\text{CO}]/dt + d[\text{CO}_2]/dt)$ was due half to reaction 6 and half to the destruction of C_2 hydrocarbons.

The correction just described is large and very rough. In other runs we used mixed fuels of CH_4 - H_2 in order to obtain smaller transient yields of C_2 hydrocarbons, and to avoid corrections for them. It now became difficult to estimate $[\text{CH}_3]$ from C_2 hydrocarbons, and we depended on the determina-

tion by the decay of added nitric oxide. Figure 3 shows one such run. The reaction rates at the bottom of the figure were obtained with $D_{O_2} = 1.35 \times 10^{-4} T^{1.67} \text{ cm.}^2 \text{ sec.}^{-1}$. $[O]$ reached its maximum value at 0.175 to 0.250 cm. from the burner surface and the concentration of C_2 hydrocarbons in this region was always less than $1/10$ of $[CH_4]$. The values of $[O] k_6[CH_3]$ and $[CH_3]$ for this flame in Table I are averages at 0.175 to 0.250 cm. Separate values of k_6 at 0.025 cm. intervals in this region were 2.0, 1.7, 1.3, $1.8 \times 10^{10} \text{ l. mole}^{-1} \text{ sec.}^{-1}$.

The other flames studied resembled Fig. 3 and average values obtained as for Fig. 3 are tabulated without comment.

It is probable that in most of these flames, the equilibrium



was satisfied in the regions studied. K_0 has been estimated⁸ to be about 10, although no real accuracy was claimed. If we solved for K_0 , taking $[CH_3]$ from the nitric oxide determination and $[H]$ from

$$-d[O_2]/dt = k_1[H][O_2]$$

$$k_1 = 6 \times 10^{11} e^{-18/RT} \text{ l. mole}^{-1} \text{ sec.}^{-1.9}$$

as is legitimate because the reverse of (1) is small compared to (1) itself in the regions studied, we found $K_0 = 5 \pm 1.5$ in all runs except one. The one exception to a constant K_0 was the third run in Table I, $K_0 \sim 1.4$; and this flame contained the largest $[O]/[H_2]$, and was therefore the one least likely to be equilibrated.

Though we made no use of the idea that CH_3 was equilibrated, we could have assumed so and then found about the same $[CH_3]$ as that found from nitric oxide in all runs but one.

If each $k_6[CH_3]$ in Table I is divided by $[CH_3]$ from nitric oxide

$$k_6 = 1.9 \pm 0.3 \times 10^{10} \text{ l. mole}^{-1} \text{ sec.}^{-1}$$

with no marked temperature dependence. This very reasonable value for k_6 must be considered only approximate because k_4 might have a systematic error of about a factor of two, as discussed earlier, and because Christie considered that her estimate of k_8 might be uncertain by a factor of three.⁷

Discussion

The proposal that reaction 6 is the chief path by which carbon monoxide is formed was shown to be reasonable in the introduction; and since it also accounts for $(d[CO]/dt + d[CO_2]/dt)$ over three-to-eight fold variations in $[O]$ and $[CH_3]$, the partial mechanism seems very probable.

A reaction between methyl radicals and oxygen molecules is thought to be important in slow oxidations at lower temperatures, and one might wonder that our mechanism does not include it. A sufficient reason for omitting it is that reaction 1 alone accounts for $-d[O_2]/dt$ when $[H]$ is varied widely in different CH_4-O_2 flames.¹ But also, there is no very good reason to believe that a reaction of methyl radicals with oxygen molecules should be important in flames.

(8) A. F. Trotman-Dickenson, *J. Chem. Phys.*, **21**, 211 (1953).

(9) C. P. Fenimore and G. W. Jones, *J. Phys. Chem.*, **63**, 1154 (1959).

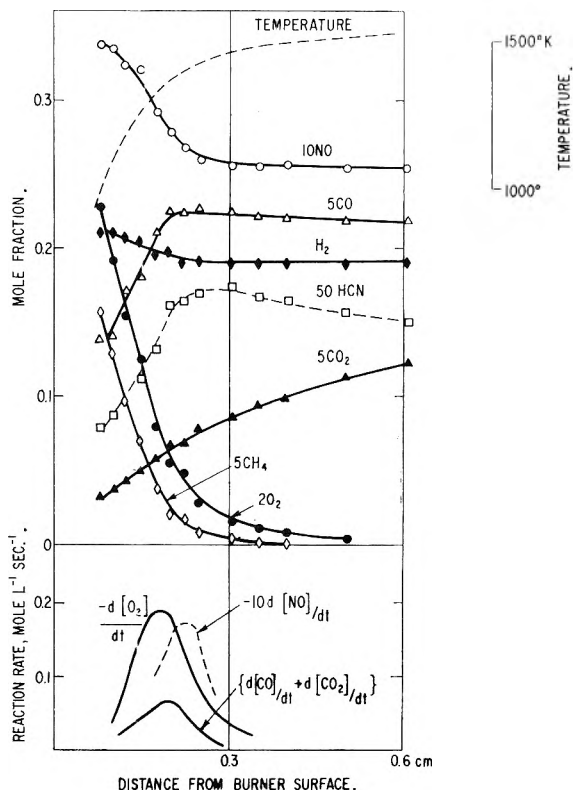


Fig. 3.— $H_2 + 0.17 CH_4 + 0.54 O_2 + 0.105 NO + 1.05 A$ burnt at 8 cm. P with a mass flow of $3.7 \times 10^{-3} \text{ g. cm.}^{-2} \text{ sec.}^{-1}$.

At far lower than flame temperatures, the reaction of methyl radicals with nitric oxide is second order and relatively fast⁷ under conditions where the reaction with oxygen molecules is third order and slower.¹⁰ The reaction with nitric oxide does not depend on temperature up to $1200^\circ K$.¹¹; and although that with oxygen is much less certain at high temperatures, it has the same rate at $470^\circ K$ as at $390^\circ K$.¹² and at least approximately the same rate at $1370^\circ K$.¹³ as at the lower temperatures. Thus as far as the literature goes, it suggests that methyl radicals would react faster with nitric oxide than with oxygen molecules even in flames. If so, this rules out any significant reaction of methyl radicals with molecular oxygen in the flame described by Fig. 2; for when $[NO] = [O_2]$, the rate of reaction of methyl radicals with nitric oxide is only $1/3$ of $-d[O_2]/dt$ and only about $1/4$ of the $(d[CO]/dt + d[CO_2]/dt)$ corrected for C_2 hydrocarbons.

A similar argument can be made for the other fuel-rich flames, that the rate constant for the reaction of methyl radicals with oxygen molecules must be several times the rate constant for the reaction with nitric oxide in order for the former process to be important. But there is no reason to believe this requirement is satisfied.

Even in a fuel-lean flame, there is little reason to think that a reaction of CH_3 radicals with molecular

(10) D. E. Hoare and A. D. Walsh, *Trans. Faraday Soc.*, **53**, 1102 (1957).

(11) W. A. Bryce and K. U. Ingold, *J. Chem. Phys.*, **23** 1968 (1955).

(12) F. B. Marcotte and W. A. Noyes, Jr., *Disc. Faraday Soc.*, **10**, 236 (1951).

(13) K. U. Ingold and W. A. Bryce, *J. Chem. Phys.*, **24**, 360 (1956).

oxygen should compete with reaction 6. In Fig. 1, $[O]$ can be estimated from the rate of formation of OO^{13} to be 1%¹⁴ of $[O_2]$ in the post-flame gas 0.6 to 0.9 cm. from the burner surface. In the reaction zone itself, $[O]$ doubtless is larger; and therefore a reaction of CH_3 with molecular oxygen might need a rate constant of a few per cent. of k_6 in order to compete with (6). But the literature does not suggest that the rate constant for CH_3 radicals and O_2 molecules is as large as about 10^9 l. mole⁻¹ sec.⁻¹.

Oxygen molecules are mostly consumed by reaction 1 in flames of other hydrocarbon fuels,¹ and traverses through a flame fed with H_2O^{13} have been reported¹⁴ from which one could conclude, by the argument in the introduction, that the carbon monoxide in at least one acetylene flame derived its oxygen mostly from free O atoms. Therefore the reaction of O atoms with other hydrocarbon species than methyl radicals is probably important in flames of other fuels.

NOTE ADDED IN PROOF.—Westenberg and Fristrom¹⁵ showed recently that in very fuel-lean

(14) C. P. Fenimore and G. W. Jones, 8th Combustion Symposium at Pasadena, Calif., Sept. 1960.

(15) A. A. Westenberg and R. M. Fristrom, *J. Phys. Chem.*, **65**, 591 (1961).

methane flames reaction 5 probably should be specified $OH + CH_4 \rightarrow CH_3 + H_2O$. They also proposed that methyl radicals disappear by $CH_3 + O_2 \rightarrow H_2CO + OH$ because, "No other plausible mechanism of H_2CO formation is apparent to us." It is plausible, however, that the initial step of (6) is $O + CH_3 \rightarrow H + H_2CO$.

Their paper really supports our assertion that the probable rate constant, $\sim 10^8$ l. mole⁻¹ sec.⁻¹ according to them, is too small for the reaction of O_2 with CH_3 to be important. (6) will outrun it if $[O] > \sim 10^8 [O_2]/k_6 = 0.5\%$ of $[O_2]$. But, even in their finally equilibrated products, they calculate $[O]$ of this order; and since $[O]$ must have been much larger in their reaction zone, (6) predominated.

(1) will outrun their proposed reaction if $[H] > \sim 10^8 [CH_3]/k_1 = 3\%$ of $[CH_3]$ at 1750°K. Since $[CH_3]$ in their very lean flames could not have been nearly the $[CH_3]$ in the rich flames of this paper, so that $[CH_3] \ll 10^{-8}$ mole l.⁻¹; and since $[H]$ was at least as large as that calculated in their equilibrated products; $[H] \gg 3\%$ of $[CH_3]$, and (1) predominated. Therefore, reactions (1) and (6) outran their proposed reaction in consuming O_2 and CH_3 respectively.

THE DETERMINATION OF THE EQUILIBRIUM WATER CONTENT OF ION EXCHANGE RESINS

BY GEORGE SCATCHARD AND N. J. ANDERSON

Department of Chemistry and the Laboratory for Nuclear Science, Massachusetts Institute of Technology, Cambridge, Mass.

Received March 10, 1961

The weights of two types of ion-exchanger beads, Dowex 1-X8 and Dowex 50W-X8 are linear functions of the weights of glass beads centrifuged at the same time from 425 to 3000 *g*. The slopes are the same for solutions of HCl and NaCl as for water. The weights of the resin beads without retention of external water are obtained by extrapolation to the weight of dry glass beads. The volumes of water retained by unit volume of beads at any centrifugal force are in the ratios: glass 1, Dowex 1 (Cl) 0.88, Dowex 50 W (Na) 0.84, and Dowex 50 W (H) 0.74. The differences appear to be attributable to differences in the number of contacts per bead.

The precise study of ion exchange requires a knowledge of the relative quantities in the resin of water, fixed ions, gegen-ions and co-ions. It is helpful to study these first in systems with only one species of each class in an ion-exchange resin in equilibrium with an aqueous solution of a single electrolyte. The most fundamental of these quantities is the water content of the resin, which is inversely proportional to the molality of the fixed ions.

The volume of a resin particle is difficult to determine, or even to define. The boundary of a resin particle is not a true surface, but has a thickness of 10–1000 Å., or even more for low cross-linking. If we define the volume as that volume which makes the concentration of the fixed ions zero outside the resin and contains the same amount of water inside as if the fixed-ion concentration were uniform up to the surface, there is still the operational difficulty that we have no independent method of determining what this concentration should be. This definition would also lead to a small positive

or negative surface concentration for any other solute component. Any uncertainty due to this cause will usually be small, however, relative to the error in separating the resin quantitatively from the external phase. This latter difficulty increases as the resin particles become smaller and the surface to volume ratio therefore increases.

For large pieces of resin such as membranes, and perhaps for very large beads, the excess aqueous phase may be removed with blotting paper,^{1,2} but with ordinary sized beads the amount of water removed varies so much with the procedure that it is not certain that any procedure gives an acceptable answer.

The dye dilution³ method appears simple and direct. A solution of a dye with molecules too large to penetrate the resin and with the same

(1) W. C. Bauman and J. Eichhorn, *J. Am. Chem. Soc.*, **69**, 2830 (1947).

(2) H. P. Gregor, K. M. Held and J. Bellin, *Anal. Chem.*, **23**, 620 (1951).

(3) K. W. Pepper, D. Reichenberg and D. K. Hale, *J. Chem. Soc.*, **8**, 3129 (1952).

sign charge as the fixed ions is added to a mixture of the resin and a small amount of aqueous phase. The change in dye concentration measures the amount of water not in the resin. We were unable to obtain satisfactory results by this method, perhaps because of surface adsorption in spite of the charge on the dye ion.

The water contents of resin in equilibrium with water vapor at some definite pressures may be determined and the contents extrapolated to the vapor pressure of water from the aqueous phase.^{2,4} At this vapor pressure all the interbead volume should be filled with solution, and even at much smaller pressures there is adsorption near the contact points. Therefore the extrapolation must be carried out over a large pressure range. We did not obtain acceptable results by this method.

The aqueous phase may be removed more or less efficiently by centrifuging.²⁻⁴ Gregor and co-workers² assumed that centrifugation at "3000 r.p.m." removed all the external water. Pepper and co-workers³ assumed that the external water retained at 285-530 *g* (*g* is standard gravity) is the same for a sulfonated polystyrene resin as for the same volume of beads sulfonated only on the surface. This they found to be independent of the size of the beads from 100 to 400 μ radii, and 4% of the weight of the fully sulfonated beads. Kraus and Moore⁴ assumed that the external water retained at about 300 *g* is the same for a trimethylaminopolystyrene anion exchanger (Dowex 1-X) as for the same volume of glass beads. Preston and co-workers^{5,6} found that the weight of water retained by fibers is a linear function of the reciprocal of the centrifugal force.

We have studied the centrifugation of beads of glass, of a sulfonated polystyrene cation exchanger and of a trimethylaminopolystyrene anion exchanger in order to extrapolate to no retention of external solution.

Experimental Procedure

The centrifugations were carried out simultaneously on duplicate samples of Dowex 1-X8 (about 8 g.) in the chloride form, Dowex 50W-X8 (about 9.5 g.) in the hydrogen form or in the sodium form, and glass beads (about 17 g.), all of 20-50 mesh.⁷ The six samples had approximately equal volumes. The beads were contained in glass filtering crucibles of 25 mm. diameter with "medium porosity" fritted glass bottoms. During centrifugation each crucible rested on three sheets of filter paper on two perforated rubber stoppers. It was centered by a cork ring and protected with a perforated plastic cover. The centrifuge cup contained a small amount of distilled water. They were centrifuged for 20 minutes at about 10°, at about 425, 750, 1500 and 3000 *g*, and usually in that order. Blanks were run on the empty crucibles for water, and the weight of beads plus adhering liquid at each rate of centrifugation was taken as the weight of the crucible plus beads and liquid minus the weight of the crucible plus water centrifuged at the same rate.

Before use the resins were conditioned by washing with the following series of liquids: 1 *M* NaOH, water, ethanol, water, 1 *M* HCl, water (several times). Immediately before each centrifugation they were washed six times with

gentle suction. If the solution was changed from that of the preceding run the washing was more thorough, particularly if the solute was changed. The runs were done in the order: water, 1 *M* HCl, 0.5 *M* HCl, 0.25 *M* HCl, water, 1.0 NaCl, 0.5 *M* NaCl, 0.25 *M* NaCl, water, 2 *M* NaCl, 4 *M* NaCl, 5 *M* NaCl, 2 *M* HCl, 4 *M* HCl.

The dry weights of the glass beads were determined before the centrifuging. The dry weights of the resin beads were determined on separate samples of the same resin lots by drying at 70° *in vacuo*. The wet beads of Dowex 1-X8 without external water contained 39.0% water and those of Dowex 50W-X8 contained 47.8% water. The capacities were 3.307 meq. per gram dry resin for the Dowex 1 and 5.033 meq. per gram dry resin for the Dowex 50 W. These values correspond to 5.16 *m* for Dowex-1 and 5.49 *m* for Dowex 50 W. The densities of the beads at 25° without retained water were 2.507 for the glass beads, 1.095 for Dowex 1-X8 in the chloride form, 1.209 for the hydrogen form and 1.315 for the sodium form of Dowex 50 W-X8. We are very grateful to Dr. U. Schödel and Mr. C. V. McDaniel for the determination of the capacities, dry weights and densities of the resins.

Results and Discussion

The average weight of water retained by unit weight of glass beads is 0.0070 at 3000 *g*, 0.0118 at 1500 *g*, 0.0161 at 750 *g* and 0.0174 at 425 *g*. The product of the weight of retained solution and the centrifugal force, which is a constant for fibers, decreases regularly from 21 at 3000 *g* to 4.7 at 425 *g*. It is approximately equal to 28/(1 + 1000/*G*) if *G* is the centrifugal force in *g*.

The weight of ion exchanger beads equilibrated with water or a solution of HCl or NaCl is a linear function of the weight of glass beads equilibrated with the same solution and centrifuged at the same time. Moreover, the slope of the lines is constant for each resin as long as it remains in the same form. Normalized to the weights without external water, the slopes are 2.015 for Dowex-1, 1.541 for the hydrogen form of Dowex-50W, and 1.60 for the sodium form. When the abscissa is the weight of the dry glass beads, the ordinate is the weight of ion-exchanger beads with no external water.

Figure 1 illustrates these results by exhibiting the weights of Dowex-1 beads *vs.* those of glass beads in water and in sodium chloride solutions. The weights given are the sums of the weights of the beads in two crucibles.

Figure 1 also illustrates a disturbance which we cannot explain. The first two runs with water agree excellently, as do the three runs with dilute HCl made between them. The third water run, made after those with dilute NaCl, agrees well with the others at the smaller values of the centrifugal force, but there is a small discrepancy at 1500 *g* and a much larger one at 3000 *g*. The fact that the displacement is horizontal shows that the disturbance arises from too large a weight of the glass beads. Examination of the curves for the solutions shows that the disturbance began in the 1 *M* solution and started to decrease in the next solution for 1500 *g* but remained about the same in the 0.5 and 0.25 *M* solutions for 3000 *g* and then decreased through all the succeeding runs. There was a similar though much smaller effect with the Dowex-50W. This was the more troublesome because the form of this resin was changed with the 1 *M* NaCl run.

The weight of the sodium form of Dowex

(4) K. A. Kraus and G. E. Moore, *J. Am. Chem. Soc.*, **75**, 1457 (1953).

(5) J. M. Preston, *J. Textile Inst.*, **40**, 764 (1949).

(6) J. M. Preston, M. V. Numkar and S. P. Gundara, *ibid.*, **42T**, 79 (1951).

(7) We are grateful to Mr. Robert M. Wheaton of the Dow Chemical Company for the gift of these and other resins.

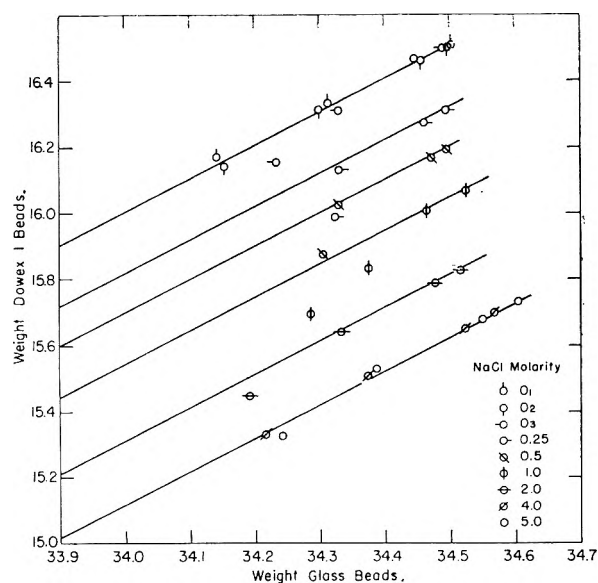


Fig. 1.—Corresponding weights of Dowex 1-X8 beads and glass beads centrifuged at same time. The weight of dry glass beads is 33.907.

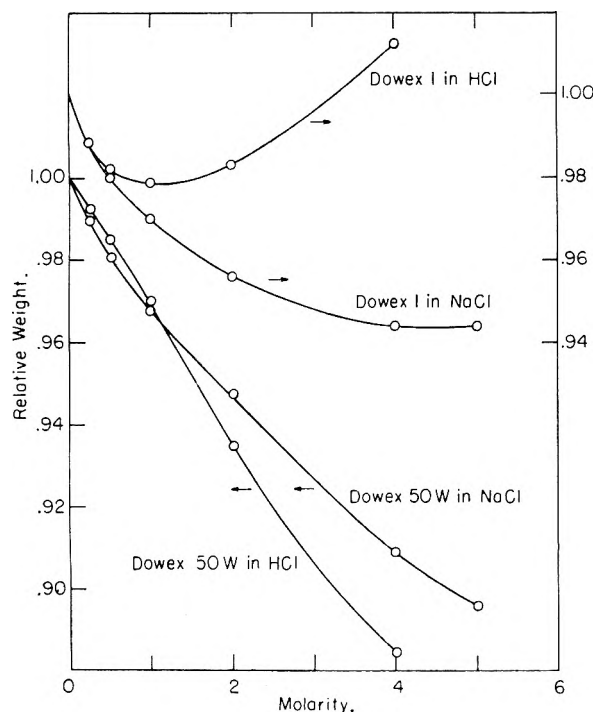


Fig. 2.—Relative weights of Dowex 1-X8 and of Dowex 50W-X8 beads in electrolyte solutions.

50W-X8 without external water is 1.8% less than that of the hydrogen form in spite of the 3.8% increase due to the change of cation. The loss of water is therefore about 5.6% of the weight of the wet resin or about 11% of the weight of the water in the hydrogen form.

The weights of the wet resins in equilibrium with the solutions relative to the weights when in equilibrium with water are shown in Fig. 2. All weights are for beads without external solution. The relative weight of the hydrogen form of Dowex 50W decreases approximately linearly in HCl to a value of 0.885 at 4 *M*. The sodium form in NaCl

starts to decrease more rapidly but soon changes more slowly to 0.896 at 5 *M*. The chloride form of Dowex 1 starts to lose weight in both HCl and NaCl at the same rate as Dowex 50W in NaCl but soon changes much less rapidly. In NaCl it reaches a minimum weight between 4 and 5 *M*, and in HCl it reaches a minimum at about 1 *M* and the weight at 4 *M* is greater than that in water. A minimum in the volume of Dowex 1 in HCl has been observed by Freeman in this Laboratory by photomicroscopy⁷ and by Nelson at the Oak Ridge National Laboratory by visual microscopy.⁸

The fluid imbibed from electrolyte solutions is not pure water. The resins in equilibrium with concentrated solutions contain large amounts of electrolyte. From the measurement of Bauman and Eichhorn,¹ we calculate for Dowex 50 in equilibrium with 4 *M* HCl that the imbibed fluid is 6% HCl. Dowex 50W should be about the same. The electrolyte concentration is even higher in Dowex 1. From the measurements of Nelson and Kraus⁹ with Dowex 1-X10, we calculate that the imbibed fluid is about 16% HCl when in equilibrium with 4 *M* HCl, and about 13% NaCl when in equilibrium with 5 *M* NaCl. We should expect the values for 8% cross linking to be somewhat smaller in HCl and somewhat larger in NaCl solutions, but not greatly different from the results for 10% cross linking.

The comparison of the slopes for beads of different materials should be made with slopes normalized to equal volumes. These values relative to glass are 0.88₀ for the chloride form of Dowex 1, 0.74₃ for the hydrogen form and 0.84₀ for the sodium form of Dowex 50W. These slopes are equal to the relative amounts of water held by unit volume of beads at any centrifugal force.

All the beads are wet by water. They are probably not appreciably compressed in the centrifuge. The amount of water retained should then be independent of the material of the beads and depend only on the geometry of the bed. The important factors in this geometry are the sizes of the beads and the number of contacts per bead, which is 6(12/2) for closest packing of spheres of equal size, but is decreased by any variation in sizes of beads in the bed and by accidents of packing. Since 20–50 mesh is 840–300 μ , there may well be sufficient difference in size or in size distribution to account for the measured slope ratios.

The approximate analytical expression given above may be written $V_W/V_B = ax/(1+bx)$, in which V_W/V_B is the volume of external water retained by unit volume of beads, x is 1000/*G*, and a and b are parameters characteristic of the beads. Since the force acting to remove the liquid is proportional to *G* and to the density, ρ , and the force acting to retain it is proportional to the surface tension, γ , and to the reciprocal of the radius of the beads, r , both a and b are proportional to the ratio $\gamma/\rho r$; a is also proportional to the num-

(7) D. H. Freeman, Nuclear Science Laboratory, Massachusetts Institute of Technology, Progress Report, October 31, 1959.

(8) Frederick Nelson, private communication.

(9) F. Nelson and K. A. Kraus, *J. Am. Chem. Soc.*, **80**, 4154 (1958).

ber of contacts, but b should be nearly independent of them. It follows that

$$(V_W/V_B)_R = a_R(V_W/V_B)_G/[a_G + (b_R - b_G)(V_W/V_B)_G]$$

if the subscript R refers to the resin and G refers to glass. The fact that the lines are straight shows that there must be little difference in b_R and b_G , and indicates that there is little difference between r_R and r_G , but that the differences in a are largely due to difference in the number of contacts per bead.

When water is replaced by a solution, all the parameters are changed in the same ratio by the changes in γ and ρ . Although we should expect a change in slope for Dowex 50W as the volume of the beads changes with changing electrolyte concentration, no such change is apparent.

The fact that Pepper, Reichenberg and Hale³ found no trend in external water for sulfonated

polystyrene beads at 285 to 530 g when the radii varied from 100 to 400 μ probably is due largely to the fact that the retained water was near the maximum in all their measurements. In terms of our approximate expression, bx was so much greater than unity that multiplying both a and b by four made little change in the external water compared to their estimated precision of 0.4% of the resin weight. Moreover the relative size distribution is probably larger for the smaller beads and this would reduce the effect of changing size.

We believe that our method gives the weight of resin without retained external water within 0.2%, and usually within 0.1%. The reproducibility of the centrifuging is sufficient so that a single centrifugation without glass beads is sufficient to determine the weight of a resin sample of a type we have studied.

PROTON MAGNETIC RESONANCE SPECTRA OF FURAN AND METHYLFURANS

BY G. S. REDDY AND J. H. GOLDSTEIN

Department of Chemistry, Emory University, Atlanta 22, Georgia

Received March 10, 1961

Well resolved n.m.r. spectra of furan, 2-methylfuran and 2,5-dimethylfuran taken at 40 Mc./sec. in tetramethylsilane have provided values of all chemical shifts and coupling constants, except the couplings between the almost magnetically equivalent protons, H_3 and H_4 . These results have been used to assess the effect of methyl substitution at the 2-position on the remaining n.m.r. parameters, including CH_3 -H couplings and the transannular H-H coupling.

Introduction

Simple heterocyclic compounds and their methyl substituted derivatives have been extensively studied by a variety of physical techniques, including nuclear magnetic resonance (n.m.r.) spectroscopy. This latter method is relatively easy to apply in the case of furan and its methyl derivatives because the spectra are strictly first order which means that all the theoretical parameters are easily and directly obtainable from well-resolved spectra. This communication reports the results obtained for furan, 2-methylfuran and 2,5-dimethylfuran all studied under comparable conditions in the highly inert solvent, tetramethylsilane. In addition to values for the chemical shifts and coupling constants for furan, it has been possible to determine in some detail the over-all effects of methyl substitution on the spectral parameters. The substituent effect on the shifts is at least qualitatively understandable, but the detailed behavior of the coupling constants apparently requires further study and comparison with results for other heterocyclic compounds.

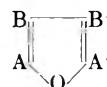
Experimental

All of the furans studied were the commercially available compounds and required no further purification. The spectra were obtained at 21° using a Varian Model 4300B High Resolution Spectrometer operating at 40 Mc./sec. and equipped with a Flux Stabilizer. Purified tetramethylsilane (TMS) was used as solvent and internal reference for all the compounds except furan, in which case acetone was also used to obtain maximum resolution, with 10% TMS added to serve as an internal reference. Calibrations were obtained by the usual side-band technique. The

estimated maximum deviation in the calibrated frequency of any peak is 0.1 c.p.s. However, the separation of any two closely spaced peaks is believed to be accurate to 0.05 c.p.s., which reduces the uncertainty in the coupling constants to about 0.05 c.p.s. All the spectra were measured in solutions containing about 10% solute by volume in order to minimize uncertainties in the chemical shifts due to concentration effects.

Results

1. **Furan.**—The spectrum of furan in TMS, shown in Fig. 1, is similar to the spectra previously reported by Corey, *et al.*,¹ and Abraham and Bernstein.² The observed pattern of two triplets about 40 c.p.s. apart, and each with relative intensities of 1:2:1, led previous investigators to infer equality of the AB and AB' coupling constants



However, the spectrum of furan dissolved in acetone, shown in Fig. 2, consists of two quartets with all peaks of approximately equal intensity. Since the pattern is essentially first order, it is clear that J_{AB} and $J_{AB'}$ must be slightly different, contrary to the previous results.

The calibrated spectrum is given in Table I. The spacings between peaks 1 and 2 and between 1 and 3 can be taken as the two coupling constants since the spectrum is first order. The values so

(1) E. J. Corey, G. Slomp, Sukh Dev, S. Tobinaga and E. R. Glazier, *J. Am. Chem. Soc.*, **80**, 1204 (1958).

(2) R. J. Abraham and H. J. Bernstein, *Can. J. Chem.*, **37**, 1056 (1959).

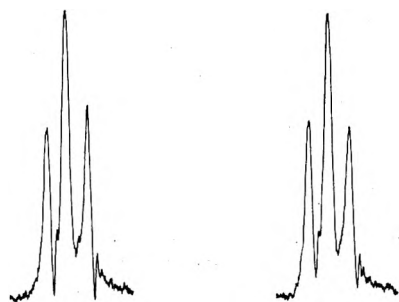


Fig. 1.—Nuclear magnetic resonance spectrum of furan in TMS taken at 40 Mc./sec.

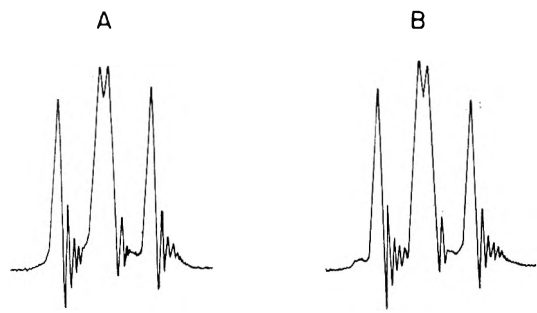


Fig. 2.—Nuclear magnetic resonance spectrum of furan in acetone taken at 40 Mc./sec.: A, protons A and A'; B, protons B and B'.

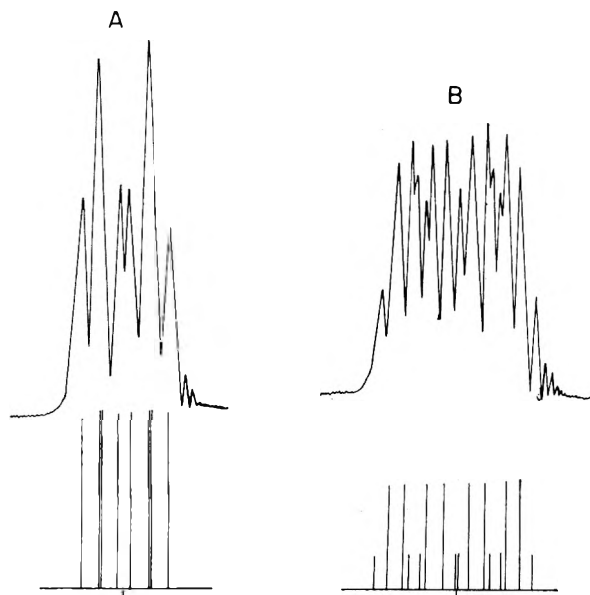


Fig. 3.—Nuclear magnetic resonance spectrum of 2-methylfuran taken at 40 Mc./sec.: A, methyl protons; B, proton C.

obtained are 1.2 and 1.4 c.p.s., respectively. The spectrum is independent of the assignment of these couplings, but it appears preferable to designate the smaller value as the longer-range, or transannular coupling, $J_{AB'}$. The low-field quartet is reasonably assigned to the protons nearer to the oxygen atom, and this is verified by the spectra of the methylfurans. On this basis we obtain $\omega_A = -298.7$ c.p.s. and $\omega_B = -254.5$ c.p.s. in acetone relative to the internal TMS reference. For purposes of comparison, however, the chemical

shifts for furan given in Table IV were obtained using TMS as solvent and internal reference.

TABLE I

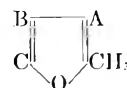
OBSERVED N.M.R. SPECTRUM OF FURAN IN ACETONE

Peak	Frequency in c.p.s. from TMS ^a	Peak	Frequency in c.p.s. from TMS ^a
1	-300.0	5	-255.8
2	-298.8	6	-254.6
3	-298.6	7	-253.4
4	-297.4	8	-253.2

^a About 10% TMS was added to the acetone solution to serve as internal reference. In this and the succeeding tables, the spectra were taken at 40 Mc./sec.

NOTE ADDED IN PROOF:—We recently have succeeded in obtaining and analyzing the C^{13} -H spectrum of furan, in natural isotopic abundance. This spectrum has provided these unambiguous values for all the coupling constants: $J_{AA} = 1.4$ c.p.s., $J_{BB} = 3.29$ c.p.s., $J_{AB} = 1.75$ c.p.s., and $J_{AB'} = 0.85$ c.p.s., all within 0.1 c.p.s. These results will be submitted for publication in the near future.

2. 2-Methylfuran.—The spectrum of 2-methylfuran, shown in Figs. 3 and 4, is a first-order $ABCX_3$ pattern. Thus all the shifts and coupling constants are obtainable from the calibrated spectrum given in Table II.



The chemical shifts can be assigned on the basis of the observed coupling of the methyl group with the three ring protons, and from other considerations. From the methyl group spectrum (Fig. 3) coupling constants of 1.1, 0.4 and 0.4 c.p.s. are ob-

TABLE II

OBSERVED SPECTRUM OF 2-METHYLFURAN^a

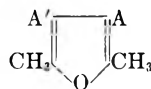
Peak	Frequency from TMS	Peak no.	Frequency from TMS
1	-287.1	21	-245.8
2	-286.8	22	-245.4
3	-286.5	23	-245.1
4	-286.3	24	-244.7
5	-286.1	25	
6	-285.9	26	-244.4
7	-285.5	27	-244.0
8	-285.1	28	-243.6
9		29	-242.8
10	-284.8	30	-242.4
11	-284.5	31	-242.0
12	-284.3	32	-241.6
13	-284.1	33	-236.4
14	-283.9	34	-235.5
15	-283.6	35	
16	-283.3	36	-234.5
17	-247.7	37	
18	-247.3	38	
19	-246.9	39	-233.5
20	-246.6	40	
41		48	-229.4
42	-232.4	49	-87.9
43		50	-87.5
44	-231.4	51	-87.1
45		52	-86.7
46	-230.4	53	-86.3
47		54	-85.9

^a Entries opposite braces designate overlapping lines.

tained directly. However, on occasion it has been possible to further resolve peaks 2 and 5 of the methyl group pattern into doublets separated by about 0.1 c.p.s. (These are not shown in Fig. 3.) It has, consequently, seemed advisable to adjust the two smaller coupling values to 0.45 and 0.35 c.p.s.

Since the methyl group is expected to couple most strongly with proton A, and since the high-field region of the ring proton spectrum (in Fig. 4) exhibits a coupling of 1.1 c.p.s., this region is assigned to proton A. Since it is unlikely that substitution of a methyl group will raise the chemical shift of proton C above that of B, the low-field and middle regions are to be assigned to protons C and B, respectively. It should be remarked that couplings of about 0.4 c.p.s., presumably with the methyl group, are observed in both these regions of the spectrum.

3. 2,5-Dimethylfuran.—The spectrum of 2,5-dimethylfuran, shown in Fig. 5, exhibits the degree of resolution obtained in this study. The middle portion of the methyl pattern is a doublet with a separation of about 0.1 c.p.s., which indicates that J_{AX} and $J_{A'X}$ differ by about 0.1 c.p.s., as was the case in 2-methylfuran. The observed



coupling constants between the methyl group and the ring protons are 0.4 and 0.3 c.p.s., the smaller value being, perhaps, more reasonably assigned to the longer-range coupling.

The low-field region of the spectrum, belonging to protons A and A', is a barely resolved quartet, which is reasonable since J_{AX} and $J_{A'X}$ are small and nearly equal, and the width of the peaks is sufficient to conceal the additional structure originating in the two slightly unequal coupling constants.

Discussion

To facilitate comparison of the results, all the parameters obtained in this study are given in Table IV, with TMS as the solvent and internal reference for all three molecules.

TABLE III

OBSERVED SPECTRUM OF 2,5-DIMETHYLFURAN ^a			
Peak	Frequency from TMS	Peak	Frequency from TMS
1	-228.3	7	-227.1
2		8	
3	-227.9	9	-85.8
4		10	-85.4
5	-227.5	11	-85.4
6		12	-85.1

^a Entries opposite braces designate overlapping lines.

The spectrum of furan, shown in Fig. 2, clearly indicates that the coupling constants J_{AB} and $J_{AB'}$ are slightly but unmistakably different, and that accordingly, the A and B protons do not constitute magnetically equivalent sets of nuclei. However, the difference in J_{AB} and $J_{AB'}$, ~ 0.2 c.p.s., is so small that effects due to the coupling constants

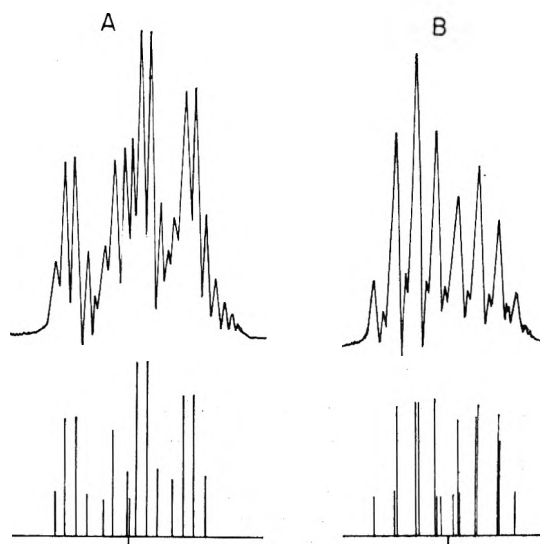


Fig. 4.—Nuclear magnetic resonance spectrum of 2-methylfuran taken at 40 Mc./sec.: A, proton B; B, proton C.

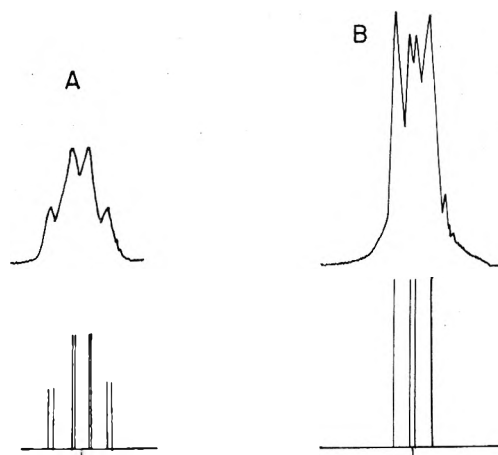


Fig. 5.—Nuclear magnetic resonance spectrum of 2,5-dimethylfuran taken at 40 Mc./sec.: A, ring proton; B, methyl protons.

$J_{AA'}$ and $J_{BB'}$ are for all practical purposes not observable. Similarly, in 2,5-dimethylfuran the difference in J_{AX} and $J_{A'X}$ is too small to render the effect of $J_{AA'}$ observable. On the other hand, in the analogous heterocyclic compound, thiophene, J_{AB} and $J_{AB'}$ differ sufficiently to permit a determination of $J_{AA'}$ and $J_{AB'}$.³

In 2-methylfuran the two H-H coupling constants differ significantly, J_{AB} being 1.9 c.p.s. while $J_{AB'}$ is only 1.0 c.p.s. This relatively large change with methyl substitution suggests that transfer of coupling constants in a series of substituted heterocyclic compounds³ may not be entirely reliable. In furan the effect of methyl substitution is to increase the H-H coupling across the double bond and to decrease the long-range H-H coupling. Accordingly the value of $J_{AA'}$ obtained for 2-methylfuran cannot be assumed to hold also for the unsubstituted furan.

The short-range H-CH₃ coupling is almost equal to the short-range H-H coupling in furan, despite

(3) S. Gronowitz and R. A. Hoffman, *Arkiv. Kemi*, **13**, 279 (1958).

TABLE IV
CHEMICAL SHIFTS AND COUPLING CONSTANTS IN FURAN AND METHYLFURANS

	ω_1	ω_2	ω_4	ω_5	J_{23}	J_{24}	J_{25}	J_{34}	J_{35}	J_{45}
	-291.9	-250.0	-250.0	-291.9	1.4	1.2	1.2	1.4
	-86.9	-233.0	-244.8	-285.9	1.1	0.4	0.35	3.4	1.0	1.9
	-85.45	-227.7	-227.7	-85.45	0.4	0.3	0.3	0.4

the fact that the former coupling involves an additional intervening bond. However, in 2,5-dimethylfuran the short-range H-CH₃ coupling is reduced from 1.1 to 0.4 c.p.s., approximately the same as the longer-range coupling.

Substitution of a methyl group at the 2-position increases the chemical shift of the adjacent proton by about 16 c.p.s., which is about equal to the effect observed in ethylene.⁴ The other two proton shifts are each increased by about 7 c.p.s. A second methyl group at the 5-position produces corresponding additional increases in the chemical shifts approximately equal to the above values. Substitution of a second methyl group also increases the methyl shift by about 1.4 c.p.s.

(4) G. S. Reddy and J. H. Goldstein, *J. Am. Chem. Soc.*, **83**, in press (1961).

In general it appears that the effect of methyl substitution on the chemical shifts in the furans is in accord with expectations based on the electron-releasing properties of the methyl group. These effects are principally conditioned by the attachment of methyl to an sp²-hybridized carbon atom, but with modifications in detail arising from delocalization within the ring. The corresponding effects on the coupling constants are, however, not as easily explained, but the accumulation of more relevant data for other heterocyclic systems should facilitate understanding of these effects.

Acknowledgments.—The authors wish to thank Mr. J. C. Randall for his assistance with the calibrations. They are indebted to The National Institutes of Health for a Research Grant, A2397 (C3), in partial support of this work.

RECOIL REACTIONS OF CARBON-11 IN *n*-HEXANE AND CYCLOHEXANE¹

BY CHARLES E. LANG AND ADOLF F. VOIGT

Contribution No. 1004 from The Institute for Atomic Research and Department of Chemistry, Iowa State University, Ames, Iowa

Received March 11, 1961

Cyclohexane and *n*-hexane have been irradiated with X-rays from a 47 Mev. electron synchrotron to produce the reaction C¹²(γ ,n)C¹¹. The distribution of the recoil C¹¹ in hydrocarbons of low molecular weight has been studied using gas chromatographic separation with a scintillation counter monitoring the exit gas stream. Cyclohexane was irradiated at 30, 0 and -78° and *n*-hexane at 30°. The total C¹¹ produced was determined by irradiating carbon under comparable conditions, burning it to CO₂ and measuring its activity in the same manner. Under most conditions acetylene-C¹¹ was the most abundant radioactive product with up to 15% of the total C¹¹ appearing in this form. Methane-C¹¹ and ethylene-C¹¹ were produced in 2 to 7% yield depending on conditions. Radioactive ethane, propane and propylene were separated; 4-carbon compounds were observed as a group. Since the yield of C¹¹ was small, no attempts were made to analyze for it in the parent compound or others of similar size. The results are discussed in terms of various mechanisms for recoil reactions. It appears that they can be explained on the basis of random fragmentation of the irradiated material by the very energetic C¹¹ atoms and subsequent reactions of C¹¹H_x radicals with these fragments.

Introduction

To a large extent investigations of the Szilard-Chalmers effect in organic systems have been concerned with the recoil effects of halogens in organic halides. Although these studies have elucidated several important concepts including phase, scavenger, and isotope effects,² and have led to the formulation of various models^{2,3} the nature of the Szilard-Chalmers effects in organic systems is as yet imperfectly understood.

(1) Work was performed in the Ames Laboratory of the U. S. Atomic Energy Commission.

(2) J. E. Willard, *Ann. Rev. Nuclear Sci.*, **3**, 193 (1953).

(3) (a) W. F. Libby, *J. Am. Chem. Soc.*, **69**, 2523 (1947); (b) L. Friedman and W. F. Libby, *J. Chem. Phys.*, **17**, 647 (1949); (c) G. Harbottle and N. Sutin, *J. Phys. Chem.*, **62**, 1244 (1958).

Because of the difficulties in working with the carbon isotopes, the study of carbon recoils, which would be of particular relevance, has received much less attention. However, within the last several years a growing interest in the use of carbon-14 recoils for synthesis of labeled compounds has been evident.⁴ Wolf and co-workers have studied recoil reactions of carbon-14 produced by the N¹⁴(n,p)C¹⁴ reaction in a variety of organic substrates. For example, after the irradiation of a mixture of benzene and 2-methylpyrazine⁵ C¹⁴

(4) A. P. Wolf, "Use of Recoiling Carbon-14 as a New Technique in Labeling Organic Compounds," *Radioisotopes Sci. Research Proc. Intern. Conf., Paris, Sept., 1957, Vol. 2, pp. 114-135 (Pub. 1958)*, also *Angew. Chem.*, **71**, 237 (1959).

(5) A. P. Wolf, et al., *J. Am. Chem. Soc.*, **78**, 2657 (1956).

was found in benzene and toluene to the extent of 1.9 and 1.0% of the total produced. Following hydrolysis of irradiated acetamide,⁶ C¹⁴-labeled acetic and propionic acids were isolated; their combined activity represented about 13% of the total. A study by Mackay and Libby⁷ of the effects of C¹⁴ recoils in *n*-pentane and isopentane, using aniline or aliphatic amines as the nitrogen source of the C¹⁴, revealed the production of a variety of labeled 5-membered and larger hydrocarbons. Hydrocarbons of less than 5-members were not resolved but as a group represented 7% of the activity in *n*-pentane and about 5% in isopentane.

Only a few investigations have been made involving carbon-11 recoils and these have mainly been in inorganic systems.⁸ The short half-life of carbon-11, 20 minutes, was a considerable deterrent to its use until the development of gas chromatography made possible the rapid separation of tracer amounts of volatile compounds. Recently Suryanarayana and Wolf⁹ in a study of the chemical effects of carbon-11 produced by the C¹²(*n*,2*n*)C¹¹ reaction in benzene found that about 4.5% of the total activity produced was accounted for in benzene and 2.2% in toluene.

In the present study the recoil products examined are the low molecular weight compounds containing C¹¹ produced by the irradiation of *n*-hexane and cyclohexane. The reaction C¹²(γ ,*n*)C¹¹ was induced with X-rays from the Iowa State University synchrotron. The cross section for the photo-nuclear process is not large and the beam intensity was only moderate. Hence, the activity produced was not sufficient for a determination of all of the products and the more volatile, low molecular weight products were the only ones studied. It was considered that the comparison of a straight chain and a cyclic hydrocarbon would give a better insight into the mechanism of the recoil chemical reaction.

Experimental

Materials.—Eastman Kodak Company Spectro Grade cyclohexane and Phillips Petroleum Co. Research Grade *n*-hexane (99.96 mole % purity) were used after drying over sodium wire. The various gases used to establish elution sequences and positions were C.P. Grade from the Matheson Co. Helium used as a carrier gas was obtained from the U. S. Bureau of Mines with a purity in excess of 99.99%. Carbon Pearls obtained from Cabot Co. were freed of absorbed oxygen, nitrogen and water by flushing with helium at 800° for 12 hours. The carbon was stored under a helium atmosphere.

Chromatographic Columns.—It was necessary to employ a variety of columns because no single column could effectively resolve all of the products. A ten foot silica gel (14–20 mesh) column was used to separate methane, ethane and ethylene. After its preparation, the silica gel column was heated to about 150° and flushed for several hours with helium gas in order to remove any adsorbed material. It was always flushed for at least two hours before use in a particular analysis. In some of the early runs a 12 foot ethyl acetoacetate column was used (67 g. of ethyl aceto-

acetate to 100 g. of Celite). This column separated methane, ethane–ethylene, propane, propylene–propyne, and acetylene–isobutane, but was of limited usefulness due to its failure to separate propylene from propyne and acetylene from isobutane. A more useful separation was provided by a mixed column with a six foot length of diisodicyl phthalate and 16 foot length of dimethylsulfolane. This "DMS-DIDP" column, prepared with 40 g. of organic liquid to 100 g. of 28–35 mesh Celite, separated methane, ethane–ethylene, propylene, propane, isobutane and *n*-butane. Propyne and the other four carbon materials had retention times greater than that of *n*-butane. It was observed for the DMS-DIDP column that the isobutane peak preceded the acetylene peak, which is contrary to the elution sequence reported by Fredericks and Brooks.¹⁰ A 12-foot dioctyl phthalate column (43 g. of dioctyl phthalate to 100 g. of 48–65 mesh Celite) provided a good separation of compounds of intermediate molecular weight such as *n*-hexane and cyclohexane. All columns with the exception of the silica gel column were prepared by addition of the organic liquids in suitable solvents to Johns–Mansville Celite-22 firebrick which had been previously cleaned, fired and sieved.

Bombardments.—Approximately 1-g. air-free samples contained in sealed Pyrex ampoules were irradiated in the X-ray beam at the Iowa State University electron synchrotron operated at 47 Mev. for a constant time period of 1 hour. The cross section of the C¹²(γ ,*n*)C¹¹ reaction integrated from threshold to 47 Mev. is ~60 Mev.-mb.¹¹ and in an average run a total activity of the order of 0.3 mc./ml. was produced. The only emitter observed in these experiments was carbon-11.

Low temperature bombardments at 0 and –78° were made in a tube designed so that the appropriate coolant surrounded the ampoule during the irradiation.

A 5 mm. thick Synthane plug positioned in front of the ampoule was irradiated in every run and the C¹¹ activity produced in the plug served as a monitor for the beam. The activity of the Synthane monitor was determined by counting the C¹¹ annihilation photo peak with a NaI(Tl) scintillation crystal and a Nuclear Chicago γ -ray spectrometer, Model 1820.

Product Analysis.—The Szilard–Chalmers products were analyzed and counted according to a procedure suggested by Evans and Willard.¹² In the present investigation the products of interest were the gaseous hydrocarbons from methane through the butanes. As produced by the irradiation these materials were dissolved in the irradiated liquids; solid samples were melted before analysis. The products were removed from solution by placing the sample in a cell provided with a fritted disc through which helium was passed to "flush" the volatile material from solution on to the column of a Consolidated Electrodynamic Corporation gas phase chromatograph, X26-201. In this process the volatile substances were completely removed from the solution and a small amount of less volatile material was picked up by the helium carrier. This was removed from the gas stream by adsorption on the chromatographic column and did not interfere with the subsequent analysis of the radioactivity.

After separation, the counting rates of the products as flowing gases were determined by passing the gas stream through a via. which was placed in the well of a NaI(Tl) well-type scintillation crystal. The crystal, 1.5 inches in diameter by 1 inch thick with a 0.75 inch hole, had reasonably good efficiency for the detected radiation which was the 0.51 Mev. annihilation γ -ray from the positron emitted by C¹¹. The crystal was mounted on an RCA 5819 photomultiplier tube, and the pulses were sent through a cathode follower to a Nuclear Chicago Model 162 scaling unit which provided a combination linear amplifier and discriminator and reduced the background to permit the detection of low counting levels.

The output from a Nuclear Chicago Model 1620 Rate-meter and from the thermal conductivity cell were displayed

(6) A. P. Wolf, *et al.*, *J. Am. Chem. Soc.*, **79**, 3717 (1957).

(7) C. S. Mackay and W. F. Libby, "Carbon-14 Hot Atom Chemistry of *n*-Pentane and Isopentane," *Radioisotopes Sci. Research Proc. Intern. Conf.*, Paris, Sept., 1957, Vol. 2, pp. 136–145 (Pub. 1958).

(8) (a) F. S. Rowland and W. F. Libby, *J. Chem. Phys.*, **21**, 1493 (1953); (b) L. J. Sharman and K. J. McCallum, *J. Am. Chem. Soc.*, **77**, 2989 (1955).

(9) B. Suryanarayana and A. P. Wolf, *J. Phys. Chem.*, **62**, 1369 (1958).

(10) E. M. Fredericks and F. R. Brooks, *Anal. Chem.*, **28**, 297 (1956).

(11) W. C. Barber, W. D. George and D. D. Reagan, *Phys. Rev.*, **98**, 73 (1955).

(12) J. B. Evans and J. E. Willard, *J. Am. Chem. Soc.*, **78**, 2909 (1956).

on a dual pen Brown recording potentiometer. Flow rates were determined using a soap-film flow meter suggested by Keulemans.¹³ The Szilard-Chalmers products were identified by comparing their elution times to those of known samples. Liquid products were analyzed by the same procedure except that a 0.1-ml. liquid sample was introduced directly onto the column by injection with a hypodermic syringe.

The production of unlabeled decomposition products was not detected by the thermal conductivity cell. However, it can be estimated from the dosage received by the sample that the amount of such products formed approached the detection limit of the cell which is in the range of 10^{-6} mole. Typically, the dosage rate was ~ 500 rad./min. or 3×10^4 rad. during the 60 minute irradiation. This is equivalent to 1.9×10^{18} e.v. in γ -ray energy dissipated in the 1-g. sample. If a *G*-value (molecules of product per 100 e.v. absorbed) of 5 is assumed as an upper limit for any one product, $\sim 10^{-7}$ mole of this product would be present. The C^{11} activity produced was ~ 0.3 mc. corresponding to a production rate of 7.5×10^8 /min. or a total of 4.5×10^{10} atoms of C^{11} produced. If the average recoil energy is 0.5 Mev., an additional 2.2×10^{16} e.v. would be introduced into the system from this source contributing $\sim 10^{-9}$ mole of products. Only a small fraction of the kinetic energy of the neutrons would be dissipated in the small sample since the mean free path for neutrons of this energy is ~ 10 cm. However, since the kinetic energy of the neutrons is eleven times that of the carbon recoils, this source of decomposition energy could approach that from the recoils themselves, but would add $< 10^{-9}$ mole to the total amount of decomposition products.

Total Activity.—Eight samples of air-free Carbon Pearls were bombarded under a helium atmosphere in the same geometry as the hydrocarbon samples. From these runs, 25 approximately 50-mg. portions of carbon were ignited in a stream of oxygen and the volatile oxides were counted as flowing gases according to the procedure previously described. All transfers of the carbon samples before ignition were made in a dry box. The standard deviation of the 25 activity determinations was about 10%.

Activity Calculations.—For each component, the area under the curve of count rate vs. time was measured with a planimeter and corrected to the time at which the synchrotron beam was shut off, using a value of 20.4 minutes for the half-life of C^{11} . The result, the counts recorded, was also standardized to a constant synchrotron flux and 1-g. sample. No correction was necessary for decay during the interval between the beginning and end of an activity peak since this time period was small compared to the C^{11} half-life. The corrected area was multiplied by the flow rate at which the particular component was eluted to obtain a value for the activity of the component.¹⁴ The ratio of this value on a molar basis to the analogous value obtained from the carbon bombardments yielded the per cent. of total activity associated with the particular component.

Results

In Table I, results are summarized for the irradiation of liquid *n*-hexane and cyclohexane at 30° and of solid cyclohexane at 0 and -78° . The values listed are averages of the number of determinations which is given in parentheses before the value. The standard deviations in the relative yields range from 10 to 20% with an average of about 14%. Since the standard deviation in the determination of the total yield was about 10%, the over-all error in the yields was estimated as approximately 17%.

Cyclohexane.—The irradiation of liquid cyclohexane yielded a number of carbon-11 labeled hydrocarbons. Acetylene was the major product, followed by methane, ethylene and 4-carbon

TABLE I
ORGANIC YIELDS OF THE LOW MOLECULAR WEIGHT HYDROCARBONS FROM THE $C^{12}(\gamma,n)C^{11}$ PROCESS IN CYCLOHEXANE AND *n*-HEXANE

Product	Yields from cyclohexane, %			Yields from <i>n</i> -hexane, %
	30°	0°	-78°	
Methane	(10) ^a 6.7 ^b	(6) ^a 5.3 ^b	(4) ^a 5.7 ^b	(11) ^a 5.6 ^b
Ethane	(4) 0.64	(1) 0.28	(4) 1.0
	(4) 4.2 ^c			(6) 7.4 ^c
Ethylene	(6) 2.7	(5) 2.1	(3) 1.7	(4) 6.3
Acetylene	(6) 14	(6) 11	(4) 4.2	(8) 15
Propane	(2) 0.52
Propylene	(6) 0.89	(6) 0.99	(4) 0.85	(8) 3.1
4-Carbon	(4) 1.8	(6) 2.3	(1) 1.3	(7) 3.2

^a Number of determinations. ^b Average value of yield.

^c Ethane and ethylene were not resolved in these runs and the values represent the sum of the two products.

compounds. Ethane and propylene, the products of lowest yield among those detected, were produced in about equal amounts. No attempt was made to resolve the 4-carbon material which may be any combination of 4-carbon hydrocarbons other than isobutane. The production of carbon-11 labeled propane or isobutane was not observed and no attempt was made to analyze for propyne.

The phase studies showed that methane, acetylene, ethane and ethylene all decreased in amount with a change from the liquid to solid phase. For methane, the decrease was noticeable but not large compared to the standard deviations which were ~ 1 in the yield value for the experiments at 30 and 0°. In the case of ethane, no activity was observed in the runs at -78° and its identification at zero degrees is doubtful since it was observed in only one run. The yield of acetylene also decreased with a decrease in temperature in the solid state, while the ethylene yield decreased to a lesser extent and the methane yield remained essentially constant. The amount of propylene produced was apparently constant with respect to both phase and temperature. The change in the amount of 4-carbon compounds with temperature and phase probably is not much outside the experimental error, so that the apparent high value at zero degrees cannot be considered to be real.

A few qualitative experiments were run on the nature of the liquid products in the irradiations of cyclohexane at 30°. Labeled cyclohexane and at least three other compounds of slightly lower molecular weight were observed.

***n*-Hexane.**—The nature and amounts of labeled materials produced in hexane at 30° show strong similarities to those in liquid cyclohexane. However, propane was also observed and for almost every compound the relative amount produced is greater for *n*-hexane. Only in the case of methane was less produced in *n*-hexane than in cyclohexane and in this case the difference is of the same magnitude as the experimental error. The major product was acetylene which was accompanied by ethylene, methane, 4-carbon compounds, propylene, ethane and propane. The 4-carbon and propylene amounts were about the same. The experiments to determine liquid products at 30° showed the formation of labeled hexane together with at least two other non-volatile compounds.

No studies of the effect of phase were made on

(13) A. I. M. Keulemans, "Gas Chromatography," 2nd ed., Reinhold Publ. Corp., New York, N. Y., 1959, pp. 58-60.

(14) For a flowing gas the activity is defined by $A = Nf/v$ in which N is the number of counts observed, in this case the corrected area, f is the flow rate of the gas, and v is the volume of the counting cell.

n-hexane because the low temperature at which it freezes, -94° , could not be maintained for the period of the irradiation under the conditions used in these experiments.

Discussion

Liquid *n*-Hexane and Cyclohexane.—The energy of recoil for an atom resulting from a γ, n reaction can be calculated from equation (1), in which the momentum imparted to the atom by the impinging γ -ray is neglected. In this equation, E

$$E_r = (E + Q) \frac{m}{m + M} \quad (1)$$

is the γ -ray energy and Q the energy released in the nuclear reaction; M and m are the masses of the recoiling atom and the neutron, respectively. The yield of C^{11} as a function of the energy of the *bremstrahlung* depends both on the cross section *vs.* energy curve for the reaction $C^{12}(\gamma, n)C^{11}$ and the energy spectrum of the beam. Published yield curves¹¹ indicate that the highest yield occurs with *bremstrahlung* between 20 and 30 Mev., with the peak in the production curve at 23 Mev. Since Q for the reaction is -18.7 Mev., most of the values of E_r will lie between 0.1 and 1 Mev., with an average value of about 0.4 Mev.

If the recoiling atom does not sever all of its bonds in the recoil process, a portion of the energy appears as internal energy of the complex. The internal energy is given by¹⁵

$$E_i = E_r \frac{M'}{M + M'} \quad (2)$$

in which M is the mass of the recoiling atom and M' is the mass of the substituents attached to it. Even in the most extreme case in which M' is one, the internal energy of the carbon-11 recoil complex would be about 30,000 e.v., which is greatly in excess of the 4 e.v. carbon-hydrogen bond energy. Consequently rupture of all bonds to the carbon-11 is assured.

The unbonded carbon-11 recoil atom is undoubtedly ionized as a result of its high kinetic energy. The energy of an electron having the same velocity as the recoiling atom is given by

$$E_e = \frac{M_e}{M} E_r \quad (3)$$

in which M_e is the mass of the electron. If E_e is above the binding energy of an electron E_B , there will be a finite probability that the moving atom will lose the electron. This probability falls off for $E_e > E_B$.¹⁶ Taking the first, second and third ionization potentials of carbon as 11.3, 24.4 and 47.9 e.v.,¹⁷ the minimum values of the recoil energy necessary to cause a loss of 1, 2 and 3 electrons are 0.23, 0.49 and 0.98 Mev. On this basis a charge of $+1$ is quite likely, a charge of $+2$ will occur frequently, and charges of greater than $+2$ are less likely.

Consequently it would be expected that carbon-11

(15) H. Suess, *Z. physik. Chem.*, **B45**, 312 (1940).

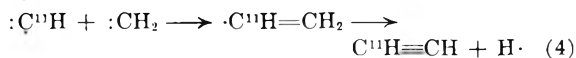
(16) F. Seitz and J. S. Koehler, "Displacement of Atoms During Irradiation" in "Solid State Physics," Vol. 2, Academic Press, Inc., New York, N. Y., 1956, pp. 338-343.

(17) C. E. Moore, "Atomic Energy Levels," National Bureau of Standards Circular No. 467, 1949, Vol. 1, pp. 21-26.

recoil atoms would be produced with initial energies of about 0.1 to 1 Mev. and charges of $+1$ or $+2$. These recoil atoms slow down, dissipating their energy by a combination of ionization and excitation processes and collisions in which bonds are broken and radicals produced. When the energy of the recoiling atom drops below about 48 e.v., carbon-hydrogen radicals such as $C^{11}H$, $C^{11}H_2$ and $C^{11}H_3$ will form. The corresponding singly charged species are also possible. However, only for $C^{11}H_3$ in cyclohexane and *n*-hexane and possibly for $C^{11}H$ in cyclohexane are the ionization potentials for the formation of singly charged ions less than those for the organic solvents.¹⁸ Hence in most cases the tagged fragment probably would be uncharged by the time it entered into reactions.

If it is assumed that the carbon-11 recoil atoms are incorporated into various hydrogen complexes when they reach the end of their path, a mechanism can be constructed by which the observed Szilard-Chalmers chemistry of liquid *n*-hexane and liquid cyclohexane is explained using the Willard "random fragmentation" model.² That is, products are formed, either in hot or thermal regions, as a result of reactions of $C^{11}H$, $C^{11}H_2$ and $C^{11}H_3$ with free radicals which the carbon-11 produces in slowing down. In the absence of scavenger experiments the relative contributions of hot and thermal reactions cannot be assessed; it is assumed that both occur.

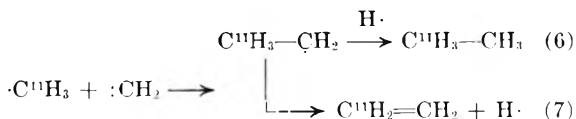
It is difficult to explain the formation of acetylene in terms of any radical mechanism except one which involves $C^{11}H$ radicals. The production of CH_2 radicals is likely in both irradiated compounds as recoil atoms are slowed down. The amount of decomposition by γ -radiation and slowing down of recoil atoms was not enough to give observable peaks in the thermal conductivity cell (see above). However, the concentration of CH_2 and other fragments in the path of the recoiling atom and, hence, in its neighborhood when it recombines will be much higher than the average concentration of these radicals. Interaction of $C^{11}H$ with CH_2 by means of the reaction



is, thus, suggested as a synthesis path for acetylene. The CH_2 radical could also react with $C^{11}H_2$ and $C^{11}H_3$ by means of the reactions



and

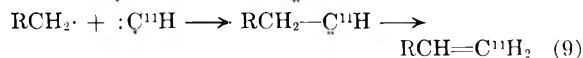
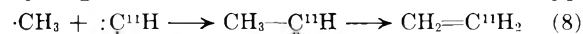


On the basis of the smaller yields of ethane and ethylene compared to that of acetylene it seems likely that both $C^{11}H_2$ and $C^{11}H_3$ are present in much lower concentrations than $C^{11}H$.

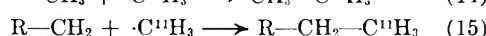
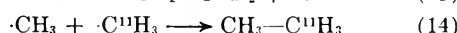
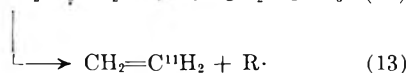
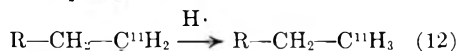
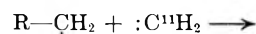
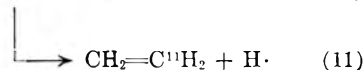
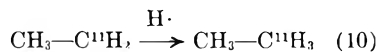
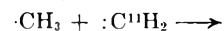
A number of reactions are possible between the $C^{11}H$, $C^{11}H_2$ and $C^{11}H_3$ and the methyl, ethyl and propyl radicals. These are present in the *n*-

(18) F. H. Field and J. L. Franklin, "Electron Impact Phenomena," Academic Press, Inc., New York, N. Y., 1957, pp. 247-270.

hexane system, as they are in electron radiolysis of hexane,¹⁹ and can be produced from cyclohexane by multiple bond rupture together with subsequent hydrogen abstraction. Reactions of the types



are certainly possible with hot C^{11}H radicals and likely with cold radicals as well. Of the reactions



those which lead to the saturated materials can proceed in the thermal region while those which lead to ethylene are known to occur in hot processes.²⁰ Since C^{11}H is taken to be the most abundant carbon-11 hydrogen complex, the unsaturated compounds with three or more carbons, reaction 9, are favored over the corresponding saturated materials, reactions 12 and 15. This is in agreement with the relative yields of propane and propylene in both *n*-hexane and cyclohexane. Ethylene is favored by a number of reaction paths, reactions 5, 7, 8, 11 and 13; consequently, the rather large yields of ethylene from both compounds are expected. Presumably methane is produced by means of hydrogen abstraction in either thermal or hot processes.

It is of interest to compare these results with those of Dewhurst^{19,21} obtained by electron bombardment of both *n*-hexane and cyclohexane. The principal difference is in the yield of acetylene. Little, if any acetylene was observed in the electron bombardment of these compounds but the

(19) H. A. Dewhurst, *J. Phys. Chem.*, **62**, 15 (1958).

(20) E. E. Royals, "Advanced Organic Chemistry," Prentice-Hall, Inc., Englewood Cliffs, N. J., 1954, pp. 46-53, 124-138, 312-317.

(21) H. A. Dewhurst, *J. Phys. Chem.*, **61**, 1466 (1957); **63**, 813 (1959).

yield of ethylene was high, roughly 8 to 10 times the yields of methane and ethane. One explanation could be that in the recoil experiments the fragment which is ultimately observed due to its label reacts with other carbon-containing fragments while it is still in the form of C^{11}H before it picks up additional hydrogen atoms. In the electron bombardment experiments, CH_2 would be the principal form for the C_1 radicals and very few CH radicals would be formed. Thus, reaction 4 is probably the most important mechanism for the formation of C_2 hydrocarbons in the recoil experiments.

Compounds of higher molecular weight are also produced. Some of these were detected, *e.g.*, C^{11} -labeled hexanes from *n*-hexane and compounds with 4 to 6 carbons from both *n*-hexane and cyclohexane. Since the activity produced was insufficient for specific identification, little can be said other than conjecture. Products of reactions of various radicals, such as butyl, pentyl and hexyl with the C^{11} -bearing complex would be expected, and the C^{11}H_2 radical would react with the original substrate to form labeled heptanes. The fact that most of the gaseous products are found in lower yields from cyclohexane than from *n*-hexane probably is due to the production of relatively fewer methyl, ethyl and propyl radicals in the former.

Phase and Temperature Effects.—The study of the effect of temperature on the yields from cyclohexane indicates that for the volatile compounds detected there is a definite reduction in yield with reduction in temperature. This is particularly true for acetylene but to a lesser extent for the other compounds. The effect may be due in part to change in phase but the differences in the yields of acetylene in the solid state irradiations at 0 and -78° are very pronounced. There is much less effect for methane and the yields of propylene are largely insensitive to temperature or phase changes. These results are insufficient as yet to serve as a basis for discussing the mechanism, but it seems likely that thermal reactions play a fairly important role in the observed processes. Scavenger experiments will enable relative assessment of the thermal and hot reactions.

Acknowledgment.—The assistance of Dr. A. J. Bureau and the synchrotron crew in providing the irradiations is gratefully acknowledged. Mr. D. B. DeVries assisted in a number of the experiments.

FORMATION OF COLOR CENTERS IN SAPPHIRE BY SOLAR RADIATION

BY A. F. GABRYSH, H. EYRING AND TAIKYNE A. REE

Institute for the Study of Rate Processes, University of Utah, Salt Lake City, Utah

Received March 14, 1961

An appreciable increase in light absorption along the "C" axis in Corundum ($\alpha\text{-Al}_2\text{O}_3$), after its exposure to an oxygen atmosphere followed by exposure to solar energy, is found over the range from 230 to 290 $m\mu$. Color centers are induced by heating in oxygen and an absorption peak at 260 $m\mu$ is further enhanced after exposure to solar energy. Assuming an oscillator strength of unity for the absorbing center, the optical density is estimated to be increased by about 4.3×10^{16} centers per cc. after exposure to solar energy. The absorption curves show that a color center concentration at the 236 $m\mu$ energy level is shifted to a higher energy level, 233 $m\mu$, by the solarization.

A number of authors have reported data for the transmission of sapphire in the ultraviolet, visible and infrared regions.¹⁻⁵ Measurements have also been made in the Shuman region of the ultraviolet.⁶ Rieke and Daniels have studied⁷ light-induced thermoluminescence of various crystal phases of aluminum oxide. Wood⁸ and Rindone⁹ have reported on the "antagonistic behavior" of short and long wave lengths, and solar energy, in forming color centers in glass. No data concerning the optical properties of synthetic sapphire, after its "oxygenation" and "solarization," have been found in the literature. The terms "oxygenation" and "hydrogenation" are used in this paper to describe the effect of heating crystals at high temperatures in these atmospheres. The term "solarization" relates to the net effect of the ultraviolet, visible and infrared components of solar radiation in producing changes in the light transmission of oxygenated sapphire.

Measurements of the transmission of synthetic single-crystal sapphire spheres¹⁰ have been made after exposures to (a) oxygen atmosphere, at high temperatures (1525°) and then (b) to solar radiation. These absorption data are compared with non-oxygenated, non-solarized disc used as a control. While the conclusions drawn from these data are regarded as tentative, they are considered of sufficient interest, from the stand point of sapphire

as a precision lens element, to warrant reporting at the present time.

The C and A axes in the single-crystal spheres were determined by the back-reflection method.¹¹ The Geringer chart and Wulff net were used to orient the axes of the spheres to within 3° of coincidence with the X-ray beam line and the axis of a specially designed holder. The spheres were ground so that two parallel, optically polished, facets were formed perpendicular (within 3°) to the axes. Facets were also ground at 45° to these axes and at right angles to both C and A axes. The crystal thickness along the "C" axis was 8.8 mm. Reflection loss for normal incidence at the surface was approximately 0.076.

The absorption spectra were measured with the aid of a Beckman DU Quartz spectrophotometer located in a temperature controlled (25°) room, over the wave length range of 220 $m\mu$ (5.78 e.v.) to 1,200 $m\mu$ (1.035 e.v.). Beginning at 1,200 $m\mu$ the data were taken at intervals of 50 down to 700 $m\mu$; from 700 to 500 at intervals of 20 $m\mu$; from 500 to 300 at 10 $m\mu$ intervals and from 300 to 220 $m\mu$ at intervals of 5 $m\mu$. The sensitivity of the phototube did not permit reliable measurements above 1,200 $m\mu$.

In Figs. 1 and 2 are shown the optical density with energy for light passing along the C axis in the spheres. Measurements were also made along the norms to all other pairs of parallel facets and are recorded elsewhere.¹² None of these showed the "solarization" effect observed along the C axis.¹³

Figure 1a shows the method of heating the specimens in continuously flowing gas. The system was sealed by a sintered alumina plug containing a gas inlet and outlet. Gas entering the system was passed through a drying column containing calcium chloride, Ascarite, magnesium perchlorate and activated alumina. The escaping hot gas passed through a water-bath. The tubings and sample-holding "boat" were obtained from Morganite and were specified as fabricated from material showing a chemical analysis of 99.7% Al_2O_3 . Specimens were rested, out of contact with the alumina boats, on sections of single-crystal polished rod. The temperature was measured with an optical pyrometer. The maximum

(1) G. Calingaert, S. D. Heron and R. Stair, *Soc. Automotive Eng. J.*, **39**, 448 (1936).

(2) R. A. Hunt and R. H. Schuler, *Phys. Rev.*, **89**, 664 (1953).

(3) P. W. Levy and G. J. Dienes, "Report of the Conference of Defects on Crystalline Solids," H. H. Wills Physical Laboratory, University of Bristol, July 1954. Also, *Phys. Rev.*, **94**, 1409(A) (1954).

(4) National Bureau Standards, NBS Test, 451d-14/47.

(5) R. W. Kebler, "Optical Properties of Synthetic Sapphire," F-8727, Linde Air Products Company, Indianapolis, Ind.

(6) R. Bauple, A. Gilles, J. Ramand and B. Vodar, *J. Opt. Soc.*, **40**, 788 (1950).

(7) J. K. Rieke and F. Daniels, *J. Phys. Chem.*, **61**, 629 (1957).

(8) A. R. Wood and M. N. Leathwood, *Nature*, **124**, 441 (1929).

(9) G. E. Rindone, Report; Reprinted from the *Travaux du IV Congress International du Verre*, Paris, 1956.

(10) The optically polished spherical specimens were obtained from the Linde Company, Crystal Products Division. The samples were fabricated from alumina powder which showed the following spectroscopic analysis:

CaO	0.0030%	Mn ₂ O ₃	0.0001
Cr ₂ O ₂	.0008	NiO	.0020
CuO	.0003	SiO ₂	.0010
Ga ₂ O ₃	.0020	Na ₂ O	.0010
Fe ₂ O ₃	.0025	Ag ₂ O	.0001
PbO	.0040	SnO ₂	.0002
MgO	.0001		

(11) B. P. Cullity, "Elements of X-Ray Diffraction," Addison-Wesley Publishing Co., Boston, Mass., 1956, Chapter 8.

(12) A. F. Gabrysh (unpublished); Institute for the Study of Rate Processes, University of Utah.

(13) It has been found in other samples that the absorption was decreased somewhat if the oxygenated Al_2O_3 sample was heated in a hydrogen atmosphere (hydrogenated) at around 1500°.

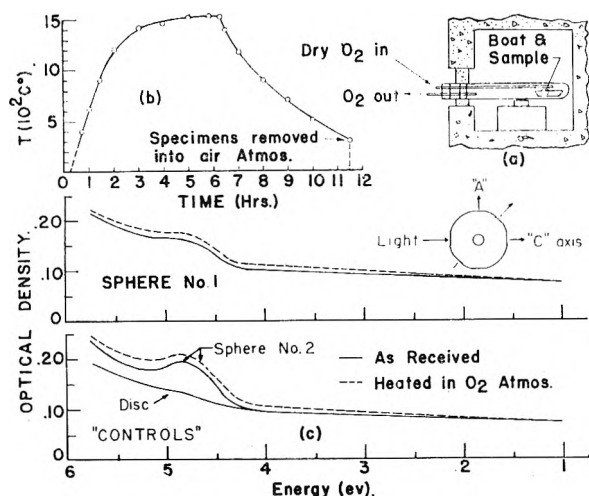


Fig. 1.—(a) Method of exposing samples to oxygen atmosphere; (b) heating history; (c) control curves represent three readings on sphere 2 and two readings on a disc ("as received," solid curve; after heating in O_2 atmosphere, broken curve). The readings were taken in parallel with readings on sphere 1 each time the oxygenated sample was exposed to solar energy.

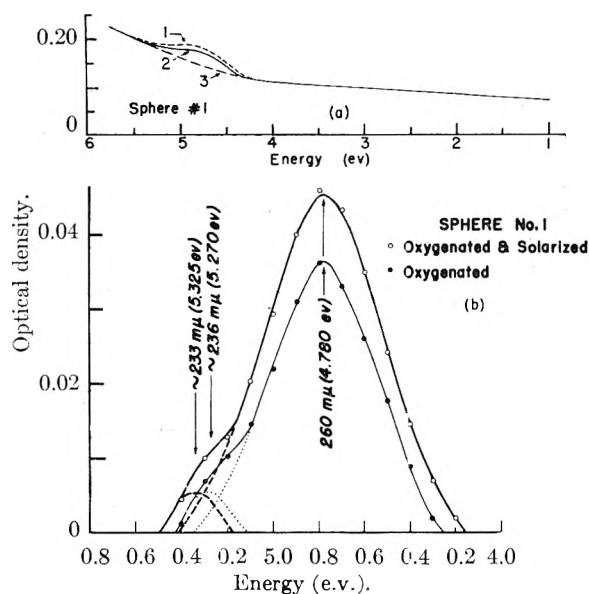


Fig. 2.—(a) Curve 1 shows increase in light absorption in the 230–290 $m\mu$ range after the oxygenated sample (curve 2) was solarized. (b) Amplified plot of optical density ($-\log I/I_0$) versus energy: The light results when the "Background" optical density is subtracted from the optical density after oxygenation (curve 2 minus curve 3 in Fig. 2a). The heavy curve is the result of subtracting the background optical density from the optical density found in the crystal after its exposure to oxygen atmosphere followed by the exposure to solar energy (curve 1 minus curve 3 in Fig. 2a).

temperature was 1525° for a period of 1 hour, Fig. 1b.

The solid line curves, Fig. 1c, show the optical density versus energy for the specimens "as received" from the manufacturer (and after the crystals were X-rayed, facets ground and polished). All readings were referenced to 100% transmission, for each wave length, in an open (free air) path. The broken lines show the increased absorption after the samples were exposed to a dry oxygen atmosphere in the manner given in 1a and 1b.

Curve 1 in Fig. 2a shows the final optical density curve of sphere #1 after its direct exposure to the rays of the sun for a total of 24 hours in three periods of 8 hours each. The average temperature of the crystals was about 30° . The temperature was recorded on a mercury thermometer placed near the crystals.

After the first exposure of sphere #1 to the solar energy, readings showed some divergence in the 290–230 $m\mu$ range but remained the same (within 0.2%) for the other wave lengths as those observed after oxygenation. Readings from the control (non-solarized) sphere were taken in parallel with sphere #1 and were within 0.2% of previous (oxygenated) readings. Because of the non-availability of another sphere, a disc, non-oxygenated and non-solarized, was added as a further control. Parallel readings were taken on all three specimens after the second and third exposures of sphere #1 to the sun's rays. The data for the controls, sphere #2 and the disc remained within 0.2% of previous readings.

Curve 3 of Fig. 2a is the "background," 2 is the curve resulting after the sphere had been exposed to the oxygen atmosphere, and 1 shows the data after oxygenated sphere #1 was exposed for the third time to solar energy. From this controlled experiment one can conclude that the increase in absorption is not due to a time effect, but is influenced by solar energy.

Figure 2b is an amplified plot of optical density vs. energy for the 290–230 $m\mu$ region. The compound curves show that both processes, oxygenation and solarization, influence a common absorption peak at 260 $m\mu$ (4.78 e.v.); however, a 236 $m\mu$ peak is merely shifted, after solarization, to a higher energy absorption, 233 $m\mu$. At 260 $m\mu$ the absorption coefficient, after oxygenation, is approximately 0.301 cm.^{-1} while after solarization it is approximately 0.327 cm.^{-1} . The absorption coefficients for the 236 $m\mu$ peak (before solarization) and the 233 $m\mu$ peak (after solarization) are approximately 0.352 cm.^{-1} . Using the formulas¹⁴ of Smakula, as corrected by Hilsch and Pohl, and assuming an oscillator strength of unity for the absorbing center, the color center concentration at 260 $m\mu$ in the oxygenated sphere, before solarization, is 2.98×10^{17} per cc., and 3.41×10^{17} per cc. after solarization. The color center concentration of 1.24×10^{17} per cc., appearing before solarization at 236 $m\mu$, remains the same as the absorbing center shifts to 233 $m\mu$ after solarization.

This study reveals that (1) both oxygenation and solarization influence a common absorption peak (260 $m\mu$), (2) the absorption curve in reality is compound in nature and (3) the color-center with lesser density is not influenced in magnitude by solar radiation but is shifted to a higher energy level. It is thought that the absorption at 260 $m\mu$

(14) $N_0 f = 1.31 \times 10^{17} n^2 / (n^2 + 2)^2 \alpha_m W$, where N_0 is the density of absorbing centers, f is the oscillator strength of the transition, n^2 is the index of refraction, α_m is the absorption coefficient in cm.^{-1} at the maximum and W is the width of the absorption curve in electron volts, at half maxima. The cylindrical volume in the crystal traversed by the light was about $4.4 \times 10^{-3} \text{ cm.}^3$. (For a complete discussion see, F. Seitz, "The Modern Theory of Solids," 1st ed., p. 664, McGraw Hill Book, Co., New York, N. Y., 1940.)

results (as suggested in other studies)¹⁵ from a photosensitive couple of oxygen and the Al_2O_3 crystal lattice inhomogeneities such as aluminum vacancies and dislocations. The shift of the lesser peak to a higher energy could, perhaps, be traced to the direct involvement of trace impurities, after the crystal is exposed to solar energy, and lattice strains.

All these samples used above were subsequently treated differently. For a more detailed analysis, data will be obtained from a solarized, non-oxygenated sample; also, data with respect to the decay with time of the color-centers induced by solar energy will be of great importance to the analysis.

A microscope examination of the sphere specimens which were used in the above experiment showed

a small amount of cavitation appearing in the crystals exposed to oxygenation and solarization. Cavitation also was produced in straight-rod samples which were merely flame polished. A better controlled study should show to what extent each treatment is responsible for the cavitation and it should help in the understanding of the role that cavitation has in influencing the formation of color centers.

Acknowledgment.—We thank the National Science Foundation for supporting this work, Mrs. B. Staker for assistance in calculations and Miss Nola McKee for assistance with the calculations, preparation of drawings and the manuscript.

(15) (a) F. P. Clarke, *Phil. Mag.*, **2**, 607 (1957); (b) R. Chang, Report NAA-SR-3339, Atomics International, a Division of North American Aviation, Inc., Nov. 13, 1958.

THE ELECTROLYSIS OF SODIUM AMALGAMS¹

BY JOHN C. ANGUS² AND EDWARD E. HUCKE

Department of Chemical and Metallurgical Engineering, University of Michigan, Ann Arbor, Michigan

Received March 15, 1961

The electrolysis of 0.097 and 0.485 weight % sodium amalgams was studied at temperatures up to 344°. Below approximately 290° the sodium is transported to the anode; above 290° the direction of transport reverses and the sodium migrates to the cathode. This effect, which has heretofore never been observed, is postulated as caused by the thermal decomposition of "compounds" or associations which persist in the liquid amalgam.

Introduction

Kremann³ showed that when Na amalgams were electrolyzed, the direction of transport of the Na and Hg depended on the concentration of the amalgam. That is, at 240° for Na concentrations greater than about 2.0 weight % Na, the Na migrates to the cathode; when the Na concentration is below 2.0 weight %, the Na migrates to the anode. This curious effect has been observed in the K-Hg,⁴ Ba-Hg⁴ and Na-K⁵ systems. In each case the concentration of the reversal occurs at, or very close to, a composition where compounds are present in the solid phase. Moreover, in each case the component in stoichiometric excess of the compound composition migrates to the cathode. It has been pointed out⁶ that in 38 of 40 binary and ternary alloy systems, the component with the smallest atomic mass moves to the cathode upon electrolysis. On the basis of this empirical correlation the authors postulated that the reversal was caused by "compounds," or associations, existing in the liquid metal. In the Na-Hg

system, for example, if an undissociated species Na_nHg_m exists in the liquid state, one would expect to find predominantly Na_nHg_m and Na on the high Na side of the "compound" composition and Na_nHg_m and Hg on the high Hg side. The correlation then suggests that in these cases a reversal should occur in the direction that is, in fact, observed. If this interpretation is correct, one might expect the reversal to vanish at sufficiently high temperatures if the associations are broken down by thermal agitation.

In the present work two amalgams (0.485 and 0.097 weight % Na) that show transport of the Na to the anode at 240° were electrolyzed at temperatures approaching the normal boiling point of the amalgams.

Experimental

Materials.—Mallinckrodt analytical reagent grade Na with a reported purity of 99.9% and Merck and Mallinckrodt A.C.S. Reagent grade mercury was used without further purification.

Preparation of Amalgams.—Amalgams of known composition were prepared in a glove box under dry nitrogen. Sodium metal was added to previously weighed polyethylene bottles which were then tightly stoppered, taken out of the dry box, and reweighed. The Na and enough Hg to make the desired amalgam composition were then brought back into the dry box where the amalgamation was performed in a Pyrex beaker. At room temperature the amalgams could be handled in air for short periods of time with negligible scum formation.

Equipment and Procedure.—The electrolyses were carried out in thin walled Pyrex tubes approximately 15 cm. long and with an inside diameter of 0.075 cm. The tubes were closed at one end and open at the other. A 0.008 inch diameter tungsten electrode wire was sealed into the closed end. The electrolysis tube was situated within a cell consisting of a vertical, 60 mm. diameter Pyrex tube which was sealed at the bottom. The necessary vacuum and elec-

(1) Taken from a portion of the dissertation submitted by John C. Angus to the Rackham Graduate School, University of Michigan, Ann Arbor, Michigan, in partial fulfillment of the requirements of the Ph.D. degree.

(2) Minnesota Mining and Manufacturing Co., St. Paul, Minnesota.

(3) R. Kremann, A. Vogrin and H. Scheibel, *Monatsh. Chem.*, **57**, 323 (1931).

(4) For a review of these experiments see K. Schwarz, "Elektrolytische Wanderung in flüssigen und festen Metallen," J. A. Barth, Leipzig, 1940.

(5) S. I. Drakin and A. K. Maltsev, *Zhur. Fiz. Khim.*, **31**, 2036 (1957).

(6) J. C. Angus, J. D. Verhoeven and E. E. Huckle, Paper presented to the International Symposium on the Physical Chemistry of Process Metallurgy, AIME, Pittsburgh, 1959.

trical connections were made through a brass fitting attached to the top of the large tube. A large, approximately 2000 g., reservoir of amalgam was placed in the bottom of the large tube. The apparatus was designed so that the electrolysis tube could be moved vertically without affecting the vacuum within the cell.

To make a run the electrolysis tube was raised above the reservoir while the amalgam was stirred to ensure uniformity and thoroughly degassed. The cell was evacuated to a pressure of approximately 5×10^{-4} mm. and the capillary lowered below the surface of the amalgam. (The amalgams used in this work are completely liquid at room temperature.) Helium was bled into the cell until the absolute pressure reached from 25 to 45 p.s.i. The helium pressure served two purposes. First, it forced the amalgam into the capillary tube where it made contact with the electrode at the far end. (The other current electrode was immersed in the amalgam reservoir.) Secondly, positive pressure reduced the tendency of small bubbles to nucleate in the electrolysis tube. These bubbles would grow in size and would eventually form an open circuit.

The temperature was raised to the desired level by means of a resistance furnace and the direct current turned on. After the current was passed through the capillary for the desired length of time, it was turned off and the tube immediately raised from the reservoir. Several extra tubes through which no current was passed were attached to each electrolysis tube. These tubes were for the purpose of collecting blank samples of the reservoir of amalgam. All of the tubes were chemically analyzed to determine the direction and the extent of electrolysis.

The direct current was supplied by UdyLite and Nobatron rectifiers. The drift during the course of the run and the ripple were less than 1%. Approximately 1 ampere of the total furnace heater current (from 3 to 5 amperes) was controlled by an off-on type controller for temperature regulation. The total temperature variation throughout the course of the runs was normally about $\pm 3^\circ$. To minimize convection the top of the liquid metal reservoir was maintained hotter than the bottom. The gradient was approximately $0.8^\circ/\text{cm}$.

Three capillary shapes were used: (1) straight tubes, (2) hairpin shaped tubes (one 180° bend), and (3) tubes with two 180° bends. All three shapes were used in a vertical position.

During the preliminary experiments the apparatus was modified so that three electrolysis tubes could be run simultaneously. The tubes were electrically in parallel. It was helpful to run several capillaries at once, since at the high temperatures the capillaries often became open circuited because of the formation of bubbles mentioned earlier.

Analytical Procedure.—The Na was determined flame photometrically at 589 m μ with a Beckman Model DU spectrophotometer. The Na was dissolved from the amalgams with 1% by volume HNO_3 . The emission in a hydrogen-oxygen flame was compared with the emission of previously prepared standard solutions. The analyses of the reservoir metal in all cases were within 3% of the weighed in values. The analyses invariably were lower than the weighed in values. This probably was caused by the slight scum that formed on the amalgam during its formation and subsequent handling in air. The standard deviation of an individual analysis from a set of blank capillaries was normally less than 1% of the average value.

Discussion of the Experimental Procedure.—Properly designed experiments can be used to determine the magnitude of the electrical mobility of the solute atoms as well as simply the direction of transport. When the electric field is applied to the liquid alloy, the solute atoms reach a steady state drift velocity. Solute will cross the reservoir-capillary boundary. The flux of solute across this boundary plane per cm^2 per sec. is given by the definition of the mobility

$$J = ucE \quad (1)$$

where u is the mobility of the solute in $\text{cm}^2/\text{sec. volt}$, c the concentration of the solute, and E the electric field strength. By applying the principle of the conservation of mass to the electrolysis tube equation 1 may be rewritten

$$u = \frac{\Delta m}{cIt\rho} \quad (2)$$

where Δm is the change in mass of solute in the capillary,

I the direct current, ρ the resistivity, and t time. Notice that the cross sectional area of the mouth of the capillary does not appear in equation 2. The experimental method used here is similar to the one described by Mangelsdorf.⁷ His method is not readily applicable at high temperatures, however.

Equation 2 will give correct mobilities as long as the concentration at the mouth of the capillary remains constant and as long as the only solute flux across the boundary plane is caused by the electrolysis. The first condition is easily met by using a sufficiently large reservoir. The second is met by ensuring that the concentration change in the capillary does not proceed to the point where a concentration gradient is formed at the reservoir-capillary boundary. When this happens, solute is transported across the reservoir-capillary boundary by ordinary diffusion. This diffusion flux will always oppose the solute flux caused by the electric field, causing the mobility calculated from equation 2 to be too low. The concentration in the capillary first changes at the closed end of the capillary. There will therefore be an initial period when the average concentration in the capillary will change linearly with time. If the electrolysis is stopped during this period, equation 2 will give the true mobility. One can test whether back diffusion takes place by performing experiments with different capillary lengths and for different periods of time. Any experiment with too short a tube or run for too long a time will give a mobility lower than the others.⁸

Results

Test of the Experimental Technique.—The method was tested by electrolyzing the amalgams at room temperature. Schwarz⁴ has previously measured the mobility of Na in dilute amalgams at room temperature by two independent methods. His value was $1.19 \times 10^{-4} \text{ cm}^2/\text{sec. volt}$. In the present work the average of four runs on 0.485 weight % Na and two runs on 0.0976 weight % Na amalgams was $1.23 \times 10^{-4} \text{ cm}^2/\text{sec. volt}$. The standard deviation of a single determination was 0.20×10^{-4} . In view of the rather large standard deviation the excellent agreement with Schwarz's value is certainly fortuitous. Clearly, however, the method gives values that are essentially correct. The scatter in the data arises from the fact that in order to calculate the mobility, the analysis of the reservoir must be subtracted from the analysis of the capillary. Since the total change in composition was normally less than 10%, any analytical uncertainties were considerably magnified. The capillary shape had no apparent effect on the results, nor was there any noticeable difference in the results at the two different concentrations. Sixty cycle alternating current was passed through three capillaries. No statistically significant changes were observed.

Results at High Temperatures.—The data are shown in Table I. The sixth and seventh columns give the original and final compositions of the capillary tube. The original composition is taken as the average of the blank tube analyses. The last column gives the per cent. confidence of the observed change in alloy composition. It was taken as $100 - P$ where P is the per cent. chance that a blank tube from that particular run could have given an analysis as far from the mean of the blank analyses as the capillary in question. Student's " t " distribution for $n - 1$ degrees of freedom was used, where n is the number of blank tubes. For

(7) P. Mangelsdorf, Jr., *J. Chem. Phys.*, **30**, 1170 (1959).

(8) For a more complete discussion of the experimental method see the Ph.D. dissertation of J. C. Angus, University of Michigan, 1960, available from University Microfilms, Ann Arbor, Michigan.

TABLE I
ELECTROLYSIS DATA

Capillary	Temp., °C.	D.c., ^a amp.	Time, hr.	Wt. of capillary metal, g.	Original wt. % Na	Final wt. % Na	Confidence level of change
1	232	+4.0	27.0	0.9335	0.486	0.506	99.0
2	245	+3.4	59.0	.9814	.474	.495	94.0
3	286	+2.48	49.75	.8338	.488	.480	56.0
4	342	+3.75	19.0	.9398	.480	.439	99.9
5	344	-3.09	52.0	.8643	.484	.538	99.9
6	343	-3.40	31.0	.8803	.484	.532	99.9
7	344	-2.53	52.0	1.2730	.484	.512	99.9
8	338	-2.42	48.8	.8731	.482	.514	99.6
9	338	-2.80	48.8	.8783	.482	.521	99.7
10	334	+2.44	30.5	.8269	.0968	.0897	99.5
11	334	+3.22	30.5	.9398	.0968	.0934	98.0
12	334	+2.95	30.5	1.0332	.0968	.0929	98.5

^a The sign (+ or -) indicates the polarity of the electrode at the end of the capillary.

the capillary run at 286° the confidence level is the per cent. chance that the composition of any one blank tube lies as far from the mean as the capillary through which direct current was passed.

From these data one can see that the predicted reversal of transference direction was indeed observed. The room temperature data and the mobilities calculated from capillaries 1, 2, 3, 4 and 6 in Table I are plotted *vs.* temperature in Fig. 1. At 286°, where no significant change was observed, the bar indicates the estimated sensitivity of the measurements. A positive mobility means the Na migrates to the anode; negative, to the cathode. In order to calculate the mobility from equation 2 it is necessary to know the resistivity of the reservoir amalgam and the concentration of Na in the reservoir in g./cm.³. The mass fractions of Na were converted to concentrations by multiplying by the density of pure Hg at the temperature in question. The error introduced by not using the densities of the amalgams is negligible compared to the scatter of the data. The resistivities were taken from Müller.⁹ The capillaries not used in Fig. 1 had significant back diffusion which made a quantitative estimation of the mobility impossible.⁸

Discussion

There is support from other types of measurements for the idea that "compounds" do exist in liquid alkali metal amalgams. Kubaschewski and Catterall¹⁰ come to the conclusion that there are "fairly strong ionic bonds" in the liquid K-Hg system on the basis of the entropy of mixing of K and Hg. Müller^{9,11} concluded from his resistivity measurements that the NaHg₂ species may persist in the liquid state.

The compounds NaHg₃ and NaHg₂ are formed at 2.8 and 5.4 weight % Na.¹² The former melts incongruently and the latter congruently. Consequently, one might expect NaHg₂ to be the species present in the liquid metal; however, the re-

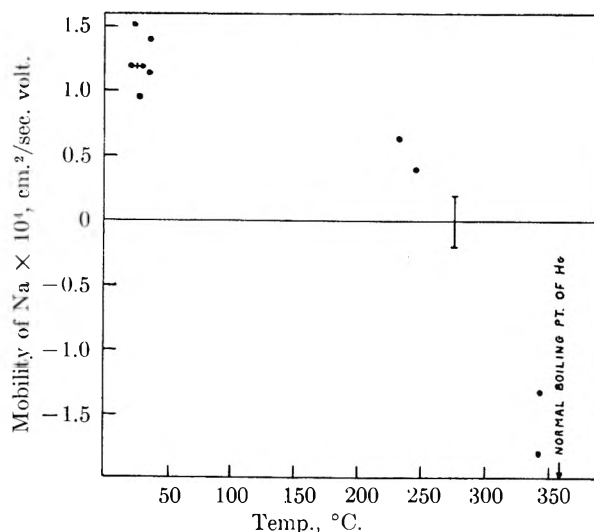


Fig. 1.—Mobility of Na *versus* temperature: +, Schwarz's value; ●, this work.

versal of transport direction with concentration takes place at approximately 2.0 weight % Na. The associations or "compounds" that persist in the liquid state may not correspond exactly to the compositions of compounds in the solid. One would expect, however, that the composition of any association in the liquid metal to be in the general region where strong compound forming tendencies are found in the solid.

It has been predicted^{13,14} that in dilute alloys the solute should concentrate at the anode if it decreases the conductivity of the alloy compared with the pure metal, and *vice versa*. At 240° the Na-Hg system obeys this rule. At 340°, however, the Na goes to the cathode, even though the conductivity decreases with increasing Na concentration at this temperature.⁹

Acknowledgments.—The authors gratefully acknowledge the financial assistance of the U.S. Atomic Energy Commission under contract AT-(11-1)-771 and the invaluable assistance of Mr. John Verhoeven in the experimental work.

(9) P. Müller, "Die elektrische Leitfähigkeit der Metallegierungen im flüssigen Zustande," Doctor's dissertation, Royal Technical High School at Aachen, 1911.

(10) O. Kubaschewski and J. A. Catterall, "Thermochemical Data of Alloys," Pergamon Press, London, 1956, p. 22.

(11) K. Bornemann and P. Müller, *Metallurgie*, **7**, 396 (1910).

(12) M. Hansen, "Constitution of Binary Alloys," McGraw-Hill Book Co., New York, N. Y., 1958.

(13) P. Mangelsdorf, Jr., paper presented to the International Symposium on the Physical Chemistry of Process Metallurgy, AIME, Pittsburgh, 1959.

(14) F. Skaupy, *Z. physik. Chem.*, **58**, 560 (1907). For a review of all of Skaupy's works see ref. 4.

ON THE DIAMAGNETIC SUSCEPTIBILITY OF GASES¹

BY R. E. GLICK

*Department of Chemistry, The Florida State University, Tallahassee, Florida**Received March 15, 1961*

The diamagnetic susceptibility of He (χ_{He}) has been calculated using 14, 18 and 20 term Hylleraas wave functions. Employing certain assumptions, these values are plotted against the corresponding energies. χ_{He} , corresponding to that which would be obtained using a wave function with an infinite number of terms, is $(-1.8914 \pm 0.0002) \times 10^{-6}$. This value is recommended as a standard in the experimental determination of the diamagnetic susceptibility of gases. An analysis of experimental data is performed, most probable values of diamagnetic susceptibilities of gaseous elements are obtained, and this analysis is used to obtain most probable susceptibilities for gaseous hydrocarbons.

Interest in theoretical and experimental aspects of molecular magnetism has reappeared, based seemingly on details connecting molecular magnetism and nuclear magnetic resonance spectroscopy, and catalyzed by the rich variety of applications to molecular theory and analysis issuing from nuclear resonance studies.² The basis for this relationship centers on electronic effects observed when a molecular system is perturbed by a magnetic field. Molecular diamagnetism is related to magneto-electronic effects as seen by an observer external to the molecular system, while nuclear resonance spectral shifts arise from magneto-electronic effects as seen by an observer residing at a particular site within the molecule. In discussing elements relating these two experiments, some difficulties, characterized by lack of precise experimental data, exist. As for example, theoretical calculations of the diamagnetic susceptibility for the lower hydrocarbon gases such as methane, ethylene and acetylene have recently appeared^{3,4} and seem to be capable of high precision; the need for reliable experimental values is obvious. Not until very recently, however, have experimental values for these quantities⁵ been obtained, and, to a certain extent, the values so determined need more adequate referencing. In this connection, there is a need for a suitable standard in experiments designed to investigate the diamagnetic susceptibility of gases. This difficulty appears to be related to the nature of present experimental methods.

In the several experimental methods⁶⁻¹⁰ that have been employed for determining the diamagnetic susceptibility of gases, the standard reference value has been the paramagnetic susceptibility of oxygen, χ_{O_2} . In general such methods are ratio methods with responses that are directly proportional to the values measured. Since the mag-

nitude of the susceptibility of a diamagnetic gas will be 0.01th or less than oxygen's, sensitivity is severely taxed. Although experimental determinations of χ_{O_2} do not agree,¹¹ as will be discussed later in this paper, no serious difficulty arises since a reasonable choice, based upon theory and experiment, can be made. It is the purpose of this paper to introduce the value for the diamagnetic susceptibility of helium, χ_{He} , determined by calculation rather than experiment, as the primary reference.

Presently available quantum solutions are such that only for helium can high precision (one part in a thousand or less) diamagnetic susceptibility calculations be made. Exact ground state wave functions are available for helium¹² and such wave functions axiomatically reflect those properties of the dilute gas that can be obtained from them. That only ground state wave functions are required in this calculation can be seen from an examination of the theoretical expression for magnetic susceptibility.

The value for the magnetic susceptibility of any chemical species (χ_m , molar) can be obtained from a three term expression¹³; a temperature dependent term and two temperature independent terms

$$\chi_m = \frac{Nn^2}{3kt} + \frac{2}{3} N \sum_{n' \neq n} \frac{(n | m^0 | n')^2}{E_{n'} - E_n} - \frac{Ne^2}{6mc} \sum_i \bar{r}_i^2 \quad (1)$$

The first term, the leading term for paramagnetic substances, depends strongly on the number of unpaired electrons in the atom or molecule. The last two terms, important for substances with paired electrons, are the so-called paramagnetic or high frequency contribution to molecular diamagnetism and the classical diamagnetic or Larmor term, respectively. For substances with paired electrons the first term is zero.¹³ For atoms with paired electrons the second term is also zero.¹³ It is necessary, therefore, to evaluate $(\psi | \sum_i \bar{r}_i^2 | \psi)$

in order to determine the diamagnetic susceptibility of a substance such as a noble gas. The constants¹⁴ for the third term in (1) are; Avogadro's number (N), the electric charge (e), electron mass (m), and velocity of light (c). Also,

(11) Ref. 6, p. 245 f.

(12) C. L. Pekeris, *Phys. Rev.*, **112**, 1649 (1958), describes a function determined by the variation method which yields a non-relativistic energy accurate to 0.01 cm.⁻¹. See also J. C. Slater, "Quantum Theory of Atomic Structure," McGraw-Hill Book Co., Inc., New York, N. Y., 1960, Vol. II, p. 36 f.

(13) J. H. Van Vleck, "The Theory of Electric and Magnetic Susceptibilities," Oxford University Press, London, 1932, Chapter 10.

(14) Values are those due to Bearden and Thomson taken from C. D. Hodgman, Editor-in-Chief, "Handbook of Chemistry and Physics," Chemical Rubber Publishing Company, 40th Ed., p. 3332.

(1) Support by a grant from the Petroleum Research Fund, American Chemical Society, is gratefully acknowledged.

(2) See for example, Chapters 2, 3, 5 and 7 in J. A. Pople, W. G. Schneider and H. J. Bernstein, "High Resolution Nuclear Magnetic Resonance," McGraw-Hill Book Co., Inc., New York, N. Y., 1959.

(3) In particular see J. Guy and J. Tillieu, *Compt. rend.*, **242**, 1279 (1956); *J. Chem. Phys.*, **24**, 1117 (1956); R. E. Glick and D. F. Kates, *ibid.*, **33**, 308 (1960).(4) W. Wenter, *ibid.*, **28**, 477 (1958).(5) C. Barter, R. G. Meisenheimer and D. P. Stevenson, *J. Phys. Chem.*, **64**, 1312 (1960).

(6) For general reference to experimental methods see: P. W. Selwood, "Magnetochemistry," Interscience Publishers, Inc., New York, N. Y., 1956, 2nd Ed., Chapters 1-4.

(7) G. G. Havens, *Phys. Rev.*, **43**, 992 (1933).(8) K. E. Mann, *Z. Physik*, **98**, 548 (1926).(9) A. P. Wills and I. G. Hector, *Phys. Rev.*, **23**, 209 (1924).(10) T. Soné, *Phil. Mag.*, **29**, 305 (1920).

TABLE I
WAVE FUNCTION COEFFICIENTS

Terms Term	14	14	18	20
<i>l</i>	+1	+1	+1	+1
<i>u</i>	+1.03474 × 10 ⁻¹	+1.05602 × 10 ⁻¹	+1.37507 × 10 ⁻¹	+1.07770 × 10 ⁻¹
<i>l</i> ²	+1.19705 × 10 ⁻²	+1.24325 × 10 ⁻²	+1.43009 × 10 ⁻²	+1.39125 × 10 ⁻²
<i>s</i>	+3.08547 × 10 ⁻³	-1.09544 × 10 ⁻²	+7.53535 × 10 ⁻³	-1.35267 × 10 ⁻³
<i>s</i> ²	+1.37733 × 10 ⁻³	+1.77158 × 10 ⁻³	+3.40002 × 10 ⁻⁴	+3.27772 × 10 ⁻³
<i>u</i> ²	-8.09208 × 10 ⁻³	-8.04649 × 10 ⁻³	-1.90588 × 10 ⁻²	-1.04978 × 10 ⁻²
<i>su</i>	+5.21399 × 10 ⁻³	+3.84558 × 10 ⁻³	+5.33987 × 10 ⁻³	+5.49697 × 10 ⁻³
<i>l</i> ² <i>u</i>	-1.48873 × 10 ⁻³	-1.41782 × 10 ⁻³	-2.20582 × 10 ⁻⁴	-2.17180 × 10 ⁻³
<i>u</i> ³	+3.94007 × 10 ⁻⁴	+4.16680 × 10 ⁻⁴	+7.96309 × 10 ⁻⁴	+8.22586 × 10 ⁻⁴
<i>l</i> ² <i>u</i> ²	+6.61307 × 10 ⁻⁵	+6.54696 × 10 ⁻⁵	+1.98073 × 10 ⁻⁴	+1.81478 × 10 ⁻⁴
<i>sl</i> ²	+7.51844 × 10 ⁻⁴	+5.71026 × 10 ⁻⁴	+4.94663 × 10 ⁻⁴	+5.50529 × 10 ⁻⁴
<i>s</i> ³	+2.14655 × 10 ⁻⁵	-2.38855 × 10 ⁻⁵	+1.25093 × 10 ⁻⁴	-1.63861 × 10 ⁻⁴
<i>l</i> ² <i>u</i> ⁴	-3.08377 × 10 ⁻⁸	-3.69166 × 10 ⁻⁸	+1.54382 × 10 ⁻⁷	+1.52497 × 10 ⁻⁷
<i>u</i> ⁴	-9.38369 × 10 ⁻⁶	-1.02680 × 10 ⁻⁵	-4.52176 × 10 ⁻⁵	-4.11474 × 10 ⁻⁴
<i>u</i> ⁵			+1.10026 × 10 ⁻⁶	+8.13960 × 10 ⁻⁷
<i>l</i> ² <i>u</i> ³			-8.89790 × 10 ⁻⁶	-8.35347 × 10 ⁻⁶
<i>s</i> ² <i>l</i> ²			+1.39964 × 10 ⁻⁵	+1.02691 × 10 ⁻⁵
<i>s</i> ⁴			-3.66743 × 10 ⁻⁷	+6.09189 × 10 ⁻⁶
<i>sl</i> ² <i>u</i>				+7.15755 × 10 ⁻⁶
<i>l</i> ⁴				+3.38258 × 10 ⁻⁶
<i>η</i>	1.3617172	1.3633714	1.3504631	1.36686946

r_i is the radius of the *i*th electron, and the sum is carried over for all electrons.

The wave functions employed for the purpose of determining $\sum_i r_i^2$ are of the Hylleraas¹⁵ type as given by

$$\psi = \eta e^{-ks/2} \sum c_{lmn} k^{l(m+n)} s^l t^m u^n \quad (2)$$

For equation 2, *s*, *t* and *u* are functions of *r₁*, *r₂* and *r₁₂* the coordinates of the two electrons and their distances from one another and are given by

$$s = r_1 + r_2, t = r_2 - r_1, u = r_{12}$$

Hylleraas wave functions as determined by Chandrasekhar and Herzberg and co-workers¹⁶⁻¹⁸ have been employed in this study. Those used contain 14, 18 and 20 terms. The combinations of *s*, *t* and *u* for these wave functions are given in the first column of Table I. Rather than determining *c_{lmn}*, these workers tabulated *c_{lmn}* · *k^{l(m+n)}*.

For our purposes, *c_{lmn}* is more useful. These are also shown in Table I. The electron radii (atomic units) in terms of the Hylleraas variables are given

(15) J. H. Bartlett, J. J. Gibbons and C. G. Dunn, *Phys. Rev.*, **47**, 679 (1935), have shown that Hylleraas wave functions cannot be "formal" solutions to the Schrödinger equation since recurrence relations for the Schrödinger equation in this case require that *c_{lmn}* = 0 for all *l, m, n*. T. Kinoshita, *Phys. Rev.*, **106**, 1490 (1957), in examining this question, derived a set of functions, *s* = *s*, *p* = *u/s*, and *q* = *l/s* and constructed a new wave function

$$\psi = \eta e^{-s/2} c_{lmn} s^l p^m q^n = \eta e^{-s/2} \sum c_{lmn}^{-1} s^{l-m} u^{m-n} l^n$$

which is a formal solution to the Schrödinger equation. This set, containing the Hylleraas function as a subset and, in addition, negative powers of the variables, satisfies the formal solution requirements for the Schrödinger equation. These requirements have been given by T. Kato, *Trans. Am. Math. Soc.*, **70**, 195, 212 (1951). Such requirements do not preclude the use of Hylleraas functions as sufficient solutions for our purposes, as these functions appear to converge, if energy is to be the criterion, with sufficient rapidity. This conclusion could not be dismissed by Kinoshita.

(16) S. Chandrasekhar, D. Elbert and G. Herzberg, *Phys. Rev.*, **91**, 1172 (1953).

(17) S. Chandrasekhar and G. Herzberg, *ibid.*, **98**, 1050 (1955).

(18) J. F. Hart and G. Herzberg, *ibid.*, **106**, 79 (1957).

by

$$\sum_{i=1}^2 r_i^2 = \frac{1}{2} (s^2 + t^2) \quad (3)$$

In the calculation of $\langle \psi | \sum_i r_i^2 | \psi \rangle$ all of the integrals are easily evaluated and are of the form

$$\int_0^\infty e^{-as} s^a ds \int_0^s b^b db \int_0^t w^c dw = \frac{(a+b+c+2)!}{(b+1)(b+c+2)}$$

The values for the diamagnetic susceptibility of helium (χ_{He}) obtained by employing the 14, 18 and 20 term wave functions are given in the second column of Table II.

TABLE II

THE DIAMAGNETIC SUSCEPTIBILITY AND ENERGY OF He AS OBTAINED FROM VARIOUS HYLLERAAS WAVE FUNCTIONS

Terms	χ_{He}^{in} (× 10 ⁶)	χ_{He}^{out} (× 10 ⁶)	<i>E</i> (a. u.)	<i>k_{in}</i>	<i>k_{out}</i>
14	-1.8888		-2.9037006 ^a	3.85 ^a	3.8499301 ^a
14	-1.8895	-1.889	-2.9037009 ^a	3.75 ^a	3.7500555 ^a
18	-1.8896	-1.890	-2.9037063 ^a	3.85 ^a	3.8499613 ^a
20	-1.8912	-1.8912	-2.9037179 ^b	3.87 ^b	3.8699977 ^b
∞			-1.8914	-2.9037237 ^c	

^a Ref. 17. ^b Ref. 18. ^c T. Kinoshita, *Phys. Rev.*, **105**, 1490 (1957).

Before discussing these solutions, the quality of the wave function must be considered. A measure of quality would be as follows¹⁷: the coefficients for these wave functions are obtained by the variation method except for the exponential constant, *k*. In principle, the best value for the energy that may be obtained for a given number and selection of terms will be found when the *k* used in the trial function equals that obtained by relations defining *k* as a function of the coefficients.¹⁹ Thus *k* is not an independent variable, and the best solution must be determined by an iterative process. As this process required extensive computational effort, even with high-speed

(19) Not only are *k* and *E* functions of the coefficients, but in the general solution $k = 2\sqrt{-E}$. See ref. 12.

TABLE III
DIAMAGNETIC SUSCEPTIBILITIES OF SOME GASEOUS ELEMENTS ($\times 10^6$)

	He	Ne	Ar	Kr	Xe	H ₂	N ₂
Mann ^a		-6.70	-19.4	-27.8	-42.23		
Havens ^b	-1.95	-7.85	-19.7			-4.11	-12.24
Hector ^c	-2.04 ^e	-7.21 ^e	-19.7 ^k			-4.27 ^d	-12.8 ^e
Roth ^e			-19.7				
Abonnenc ^f			-19.7	-29.9	-45.2		
Soné ^g						-4.10	
BMS ^h	-2.05	-7.08	-19.6 ^k	-29.5	-45.9		
Average ⁱ	-2.01	-7.21	-19.6	-29.7 ⁿ	-45.5 ⁿ	-4.16	-12.5
Most probable ^m	-1.89	-7.10	-19.5	-29.6	-45.4	-4.04	-12.4

^a K. E. Mann, *Z. Physik*, **98**, 548 (1936). ^b G. G. Havens, *Phys. Rev.*, **43**, 992 (1933). ^c L. G. Hector, *ibid.*, **24**, 418 (1924). ^d A. P. Wills and L. G. Hector, *ibid.*, **23**, 209 (1924). ^e W. Gerlach and A. Roth, *Z. Physik*, **85**, 544 (1933). ^f L. Abonnenc, *Compt. rend.*, **208**, 986 (1939). ^g T. Soné, *Phil. Mag.*, **39**, 305 (1920). ^h C. Barter, R. G. Meisenheimer and D. P. Stevenson, *J. Phys. Chem.*, **64**, 1312 (1960). ^k This is the standard value used in BMS and Hector studies and is the average of χ_{Ar} from other studies. ⁱ Arithmetic mean. ^m Average minus -0.12×10^{-6} . ⁿ Mann's values not included.

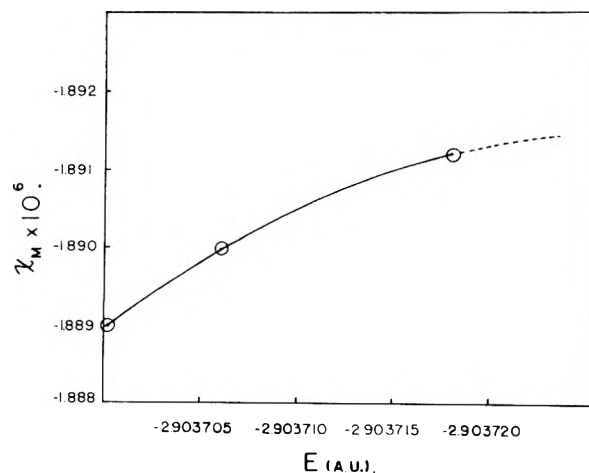


Fig. 1.—The molar magnetic susceptibility of helium using “best quality” 14, 18 and 20 term Hylleraas wave functions (left to right) versus the total electronic energy as obtained from these functions. The dotted extrapolation terminates at the non-relativistic limit expected from this type of wave function.

computers, reasonable choices in k are usually made. The best quality wave function for a given set of variables, therefore, will be obtained when k_{in} equals k_{out} as well as when the energy has been minimized. In this connection, reference may be made to the appropriate columns in Table II for the 14 term wave function. For this case, the best wave function will be bracketed such that k_{in} will lie between 3.85 and 3.75. This is based upon the relationship between k_{in} and k_{out} such that for the higher choice k_{in} is less than k_{out} and the converse is true for the lower choice. The best quality wave function, however, will yield an energy that is lower than that in either case.

In treating the magnetic susceptibility data of Table II, we make the following assumptions: (1) the best quality wave function will yield a magnetic susceptibility, Table II, column 3, which varies continuously and monotonically with energy; (2) this value will yield upon extrapolation to infinity, where infinity refers to the number of terms in the expression, the best value for the χ_{He} . For this extrapolation the energy value for an infinite series of terms is that of Kinoshita obtained by employing a similar extrapolation. These values are given in Table II, as ∞ entry.

A plot of the diamagnetic susceptibility versus the energy is presented in Fig. 1. To the extent that this extrapolation is valid, the limiting molar diamagnetic susceptibility for helium is $-1.8914 \times 10^{-6} \pm 0.0002$ (chemical scale). There is no *a priori* reason to expect that a function derived from a wave function determined by the variation method will yield an observable varying in the same way as does the energy. Nevertheless, on examining Fig. 1, it appears, even with the limited data, that this relationship exists.

Although many calculations²⁰ of χ_{He} have been performed, none have taken advantage of the complete wave functions that have been employed in this study. The value herein obtained should be accurate to the indicated error $\sim \pm 0.01\%$, with the error most probably associated with the knowledge of the physical constants used in the evaluation of the last term in (1) rather than uncertainties in the wave function.

Although experimental values for χ_{He} might be interpreted as consistent with the calculated value, a closer examination reveals some decided inconsistencies. The values that have been obtained experimentally are: Havens,⁷ -1.91×10^{-6} ; Hector,²¹ -1.88×10^{-6} ; and most recently, Barter, Meisenheimer and Stevenson,⁵ (BMS), -2.02×10^{-6} . The precision in the latter study is $\pm 4\%$, and less than 1% for the other two. In order to make a direct comparison between these various values, however, it is necessary to adjust them to a common basis. This is presented in Table III.

In Table III, all of the determinations of the diamagnetic susceptibility for gaseous substances have been collected, and have been adjusted by three self-consistent ways. (1) In the studies of Mann,⁸ Havens⁷ and Soné,¹⁰ χ_O , has been used as a standard. The values entered in Table III have been normed to the best theoretical²² and experimental²³ value for the magnetic susceptibility of oxygen, $+3.42 \times 10^{-3}$ (20°). (2) Abonnenc used the susceptibility of hydrogen as his standard, and his values are normed to χ_{H_2} as found in Table

(20) For a compilation of these see ref. 6, p. 72, using reasonable wave functions, susceptibilities in the range $(-1.6$ to $-2.0) \times 10^{-6}$ are obtained.

(21) L. G. Hector, *Phys. Rev.*, **24**, 418 (1924).

(22) M. Tinkham and M. W. P. Strandberg, *ibid.*, **97**, 937 (1955).

(23) Ref. 13, p. 266 f.

III. (3) The values obtained by Barter, Meisenheimer and Stevenson (BMS) and Hector are normed to χ_{Ar} as adjusted above. The value of χ_{Ar} due to Gerlach and Roth²⁴ was obtained by an absolute method and has not been adjusted. The average values are simply the mean.

As is seen from Table III, the average experimental value for χ_{He} is -2.01×10^{-6} . This is considerably different from the value herein calculated. As the calculated value is most probably correct, within the indicated limits of error, the average experimental value must be incorrect. Probable values are listed in Table III, as the final entry, and are obtained by applying a correction based on the assumption that the response, under the various experimental conditions employed, would be the poorest for the lighter and least diamagnetic elements. This is consistent with error, for example, in the study of Barter, Meisenheimer and Stevenson and as pointed out by Gerlach and Roth²⁴ for Havens' experiment. Both of these studies used essentially the same experimental method. This adjustment is made by assuming an absolute error of -0.12×10^{-6} , and subtracting this quantity from all values. In this way, χ_{He} is adjusted to the value calculated in the study.

χ_{H_2} as corrected is found to agree with that obtained by a direct calculation using the 11 term James and Coolidge wave function for the radial part of the susceptibility, $(\chi_{H_2})_r$, the last term of equation 1; the value²⁵ is -4.15×10^{-6} . To this is added the value for the second term²⁶ of (1), $+0.0846 \times 10^{-6}$ as determined from molecular beam experiments.²⁷ Thus, χ_{H_2} theoretical, equals -4.07×10^{-6} , while the experimental value is -4.04×10^{-6} .

In addition, it is of importance to re-examine the values obtained by BMS for other gaseous substances. The correction is simple multiplication of the various χ 's by 19.6/19.3, the ratios of the scale values, χ_{Ar} , used in this study as compared to that of BMS. These values are recorded in Table IV. In addition, ΔCH_2 , the increment in magnetic susceptibility for CH_2 's in homologous series, is adjusted to -11.6×10^{-6} , and compares favorably with that of Angus,²⁸ -11.68×10^{-6} , in an analysis of the susceptibility of liquids.

(24) W. Gerlach and A. Roth, *Z. Physik*, **85**, 544 (1933).

(25) E. E. Wittmer, *Phys. Rev.*, **51**, 383 (1937).

(26) I. Espe, *ibid.*, **103**, 1254 (1956); see also N. F. Ramsey, "Molecular Beams," Oxford University Press, New York, N. Y., 1956.

(27) For a discussion of other calculations see W. Weltner, *J. Chem. Phys.*, **28**, 477 (1958).

TABLE IV

DIAMAGNETIC SUSCEPTIBILITIES OF SOME GASEOUS MOLECULES

Hydrocarbon	Gas ^a	Liq.
Methane	-17.6	
Ethane	-27.1	
Propane	-39.1	
n-Butane	-51.0	-50.0 ^a
n-Pentane	-62.4	-63.3 ^a -63.05 ^b
Isobutane	-51.2	-51.7 ^c
Isopentane	-63.9	-64.40 ^b
Neopentane	-63.9	-63.1 ^c
Cyclopropane	-39.7	
Cyclobutane	-40.5	
Cyclopentane	-57.0	59.2 ^b
Acetylene	-21.0	
Ethylene	-19.0	
Allene	-25.6	
Propylene	-31.1	-31.5 ^b
1,2-Butadiene	-36.1	
1,3-Butadiene	-32.5	
1-Butene	-41.6	
Isobutylene	-41.3	-44.4 ^b
ΔCH_2	-11.6	

^a Ref. 5. ^b S. Broersma, *J. Chem. Phys.*, **17**, 873 (1949).
^c J. R. Lacher, J. W. Pollock, W. E. Johnson and J. D. Park, *J. Am. Chem. Soc.*, **73**, 2838 (1951).

Furthermore, the values obtained for a given substance in the liquid phase as compared to the vapor phase agree more closely. This correspondence, that the diamagnetic susceptibility is independent of phase, seems to be general for non-polar substances. Susceptibility measurements on benzene, for example, quite closely exhibit this phase independence. Benzene might be expected to show extreme behavior, based on the decided magnetic anisotropy found in this system.²⁹

In summary, this re-examination of the diamagnetic susceptibility of gases is based, provisionally, on three theoretical χ 's: those of oxygen, hydrogen and helium. It is felt that if more sensitive equipment were to be employed in the determination of diamagnetic susceptibilities, the absolute standard, χ_{He} , could be employed. This would require an apparatus approximately two orders of magnitude more sensitive than existing equipment. Such equipment would not be suitable for measurement of χ_{O_2} , but certainly sufficient for all diamagnetic gases.

(28) W. R. Angus, G. I. W. Llewelyn and G. Stott, *Trans. Faraday Soc.*, **55**, 887 (1959); W. R. Angus, F. B. Hollows, G. Stott, D. D. Khanolkar and G. I. W. Llewelyn, *ibid.*, **55**, 890 (1959).

(29) J. Hoarau, N. Lumbroso and A. Pacault, *Compt. rend.*, **242**, 1702 (1956).

THE RATES OF THE ALKALINE HYDROLYSES OF ETHYL α -HALOACETATES IN PURE AND MIXED SOLVENTS¹

BY GEORGE J. NOLAN AND EDWARD S. AMIS

Chemistry Department of the University of Arkansas, Fayetteville, Arkansas

Received March 16, 1961

The rates of the basic hydrolyses of several ethyl α -haloacetates were measured at temperatures 15.00, 25.00 and 30.00° in water and in 49.75 and 91.77 weight % ethanol-in-water. The effects of halogen substitution and of solvent on the rates of hydrolyses were determined, and partial explanations of these effects are considered. Energies and entropies of activation and Arrhenius frequency factors were calculated from the rate data and are used in conjunction with the discussion of the rates. The order of the rates of hydrolyses of the ethyl α -multihalogen-substituted esters was explained on the basis of inductive effects, while the order of the rates of hydrolyses of the ethyl α -monohaloesters was explained on the basis of inductive effects in conjunction with other effects. The dielectric constant dependence of the rates was accounted for by an equation formerly proposed by Amis and based on electrostatics.

Introduction

This investigation was undertaken to study the effects on the rates of alkaline hydrolyses of halogen substitution in esters of the type $R \cdot CO_2C_2H_5$ where R is $-CH_2X_1$, $-CHX_2$ and $-CX_3$. In these formulas X represents F , Cl or Br . The effect of solvent on the rates was of interest as were the temperature coefficients of the rates.

Experimental

The esters were purified by fractional distillation and their purity checked by saponification equivalent measurements using a standard sodium hydroxide solution of $1.259 \times 10^{-3}M$. In addition their boiling points and refractive indexes were measured and checked against values recorded in the literature.²

The values of boiling points and refractive indexes, measured and from the literature, together with the percentage purities from saponification numbers are listed in Table I.

The ethanol was purified by the method of Smith.³ The water used in preparing the aqueous solutions of ethanol and of sodium hydroxide was always freshly boiled, deionized water. The water was deionized by passing it through a column prepared from Amberlite C-211 cation-exchange resin and Amberlite A-244 anion exchange resin. The freshly boiled water was allowed to cool in an atmosphere of carbon dioxide-free air.

TABLE I

THE MEASURED AND LITERATURE VALUES OF BOILING POINTS AND REFRACTIVE INDEXES AND THE CALCULATED PURITIES OF THE ESTERS

Ester	Observed		Lit.		% purity from NaOH equiv.
	B.p., °C.	n_D	B.p., °C.	n_D	
EtFAc	119.5	...	120	...	98
EtClAc	142-144	1.4268	144.2	1.42274	97
EtBrAc	158	1.4554	157-159	1.5420	97
EtBr ₂ Ac	189-190	1.5014	194	1.5017	99
EtCl ₂ Ac	156-157	1.4372	158.2	1.43860	99
EtCl ₃ Ac	165-166	1.4507	168	1.4507	99

Sodium carbonate-free sodium hydroxide was prepared in the usual manner and diluted with carbonate-free water or alcohol as the need arose. The solution was standardized with potassium acid phthalate by titrating to pH of 8.260 in aqueous solution and to a pH of 8.560 in alcohol-water solutions. These pH values were determined from titration curves. A Beckman Model GS pH meter which gave pH readings over the range 1.000 to 14.000 with a precision of ± 0.002 pH unit, was used to determine the pH . From this standard solution a $3.778 \times 10^{-3}M$ solution of sodium hydroxide was prepared by appropriate dilution.

(1) The authors wish to thank the United States Atomic Energy Commission for the financial support which made this research possible.

(2) S. Beilstein, "Handbuch der Organische Chemie," 4th Edition, Vol. II, Berlin, 1920, pp. 193, 214, 197, 203, 219, 209.

(3) E. L. Smith, *J. Chem. Soc.*, 1288 (1927).

The glass electrode used was made of special glass which gave negligible sodium-ion error in the pH range employed in the experiments and was used in conjunction with a saturated calomel electrode. The potentiometer was calibrated against a NBS buffer solution of pH 10.00 ± 0.02 before each run.

Volumetric glassware was calibrated using weighing techniques. The temperature of the bath was controlled to $\pm 0.01^\circ$, and the temperature was read on a Beckmann thermometer which had been calibrated against a NBS thermometer.

The rates of the hydrolyses were studied at 15.00, 25.00 and 30.00° in pure water and in ethanol-water mixtures containing 49.75 and 91.77 weight % ethanol. Each run was repeated two or three times and the velocity constant for the run was taken as the average of the individual constants. The ionic strength was constant at 1.259×10^{-3} in each run.

The run was prepared and its rate of change followed as described below. The 250-ml. reaction flask was flushed out with carbon dioxide-free air. Into this flask was pipetted the required amounts of carbonate-free sodium hydroxide and carbonate-free water or water-ethanol solution. The flask was placed in the constant temperature bath. The materials in the flask were protected at all times from CO_2 of the air by passing carbon dioxide-free air, saturated with vapor of the same composition as the reaction medium, over the sample during the entire time required for temperature equilibration and measurements. An amount of ester sufficient to give $1.259 \times 10^{-3}M$ was weighed accurately in a glass bulb. The bulb was sealed and the bulb together with the electrodes of the pH meter were placed in the reaction sample and the entire sample was allowed to come to temperature equilibrium. This required 20 to 30 minutes as indicated by equilibrium of the pH meter reading. The bulb containing the ester was broken by means of a glass rod, and the rod and escaping air from the bulb were used to mix the solution well.

The first pH reading and all subsequent ones were timed accurately using a stopwatch from the time of breaking the bulb. The time of making the first reading was, when the rate was sufficiently slow, 10 to 20 seconds and subsequent readings were taken at 10 to 15 second intervals until usually nine readings were taken. This number of readings was the limit for most of the rapid hydrolyses and corresponded to 70% completion for the slower rates. In fact, the fastest rates studied were 75% complete within 5 to 6 seconds, and the slowest runs required 110-120 minutes for 70% completion. Most runs required 120-140 seconds for 70 to 80% completion.

The change of the hydroxyl ion concentration corresponding to the pH change was calculated as follows. Let X_a and X_t be the molar concentration of the hydroxide ion corresponding to the initial pH of the solution and the pH at time t . Also let x be the decrease in concentration of hydroxyl ion at time t and a be the initial stoichiometric concentration of hydroxyl ion. Then

$$x = \frac{X_a - X_t}{X_a} a$$

Plots of $1/(a - x)$ values versus time were made for the different runs and gave straight lines up to 70-80% completion. The slopes of these lines gave the second-order k

TABLE II

THE BASIC HYDROLYSIS VELOCITY CONSTANTS IN L. MOLE⁻¹ SEC.⁻¹ OF ETHYL α -HALOACETATES IN WATER AND WATER-ETHANOL SOLVENTS

t , °C.	% EtOH	D	$\mu = 1.259 \times 10^{-3}$; NaOH = ester = $1.259 \times 10^{-3} M$				precision values are in %			
			fluoroacetate	chloroacetate	ethyl salts: bromoacetate	k	dibromoacetate	dichloroacetate	trichloroacetate	
15.00	0	81.8	6.40 \pm 5	14.7 \pm 4	20.1 \pm 2	
15.00	49.75	51.8	3.25 \pm 1	5.46 \pm 1	6.72 \pm 1	20.5 \pm 3	90 \pm 10	
15.00	91.77	29.1	0.36 \pm 3	1.02 \pm 2	0.93 \pm 3	2.44 \pm 1	9.46 \pm 2	16.6 \pm 33	
25.00	0	78.2	12.1 \pm 0.4	25.8 \pm 2	32.1 \pm 4	
25.00	49.75	49.2	6.79 \pm 2	11.3 \pm 4	13.5 \pm 3	31.4 \pm 4	240 \pm 23	370 \pm 20	
25.00	91.77	27.5	1.16 \pm 0.1	1.95 \pm 0.2	1.52 \pm 0.7	6.11 \pm 3	19.3 \pm 4	32.7 \pm 2	
30.00	0	76.8	18.5 \pm 3	33.2 \pm 2	43.7 \pm 2	
30.00	49.75	47.9	10.9 \pm 4	18.4 \pm 4	19.6 \pm 3	
30.00	91.77	26.7	1.59 \pm 1	3.24 \pm 4	2.44 \pm 1	9.28 \pm 4	28.6 \pm 3	46.5	

values since the concentrations ($1.259 \times 10^{-3} M$) of the sodium hydroxide and ester were the same in all cases.

Tests were made by adding $AgNO_3$ to samples of several of the runs for the production of halide ions by hydrolysis, but in no run was such a reaction observable.

This method of measuring the reaction rates was checked using ethyl acetate. Duplicate runs were made and the constants obtained were 0.101 and 0.105 l. mole⁻¹ sec.⁻¹ compared to the value recorded in the literature⁴ of 0.108 l. mole⁻¹ sec.⁻¹ at 25°.

Data

In Fig. 1 are plotted representative data of a run at 25.00° between sodium hydroxide and ethyl bromoacetate each at a concentration of $1.259 \times 10^{-3} M$. The slope of the plot of the $1/(a-x)$ vs. t in seconds gave a value of the specific velocity constant k of 31.25 l. mole⁻¹ sec.⁻¹. Four runs were made under these conditions and the additional three values of k were 30.30, 34.48 and 32.52 l. mole⁻¹ sec.⁻¹. The average value of k was $32.1 \pm 4\%$. The range of precision was usually 2 to 3% which is good considering the extreme velocity of these reactions. Our care in weighing, timing, measuring pH, etc., was such that we feel our accuracy is as good as our precision.

The specific velocity constants for the hydrolyses of the various esters at various temperatures and at various solvent compositions and dielectric constants are given in Table II. The precision values in terms of per cent. are tabulated for the constants. For three very fast runs the precision is seen to be only 10–23%. Two values are without precision numbers. In these cases only one run was made.

Table III presents energies of activation, ΔE , and the logarithm of the Arrhenius frequency factor, $\log Z$, calculated by use of the equations

$$\log \frac{k_2}{k_1} = \frac{\Delta E(T_2 - T_1)}{2.303RT_1T_2} \quad (1)$$

and

$$\log k = \log Z - \frac{\Delta E}{2.303RT} \quad (2)$$

Entropies of activation, ΔS , calculated from the equation

$$\log Z = \log \frac{kT}{h} + \frac{\Delta S}{2.303R} \quad (3)$$

are also included in Table III.

Discussion of Data

Plots of $\log k$ vs. the reciprocal of the dielectric constant were in most cases somewhat curved as is

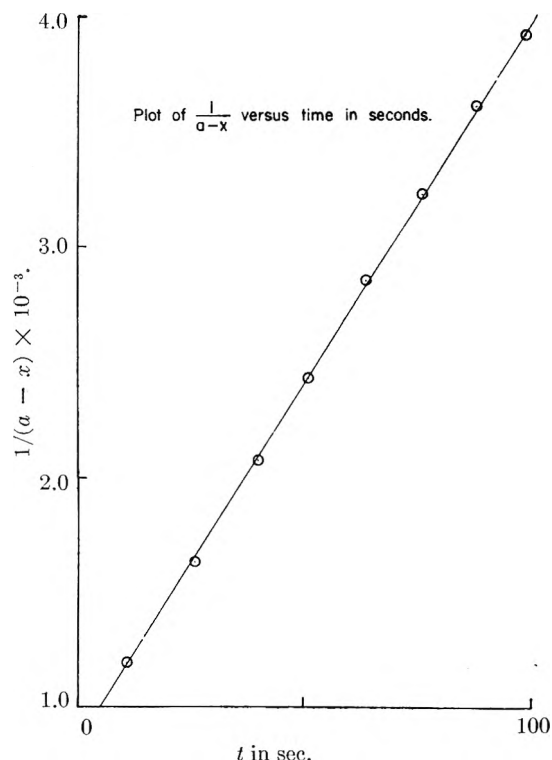


Fig. 1.—Plot of $1/(a-x)$ vs. time in sec.

shown in Fig. 2. The signs and magnitudes of the slope were those predicted by the equation

$$\log k_{D=D} = \log k_{D=\infty} + \frac{Z\epsilon\mu}{DkTr^2} \quad (4)$$

for the rate dependence of a dipolar molecule with a negative ion.⁵ If the average slopes were taken reasonable values of the r parameter were obtained as shown in Table IV. The terms in equation 4 have the following meanings: $k_{D=D}$ and $k_{D=\infty}$ are the specific velocity constants at dielectric constant D and infinity, respectively, $Z\epsilon$ is the charge on the ion, μ the dipole moment of the molecule, k the Boltzmann gas constant, T the absolute temperature, and r the distance of approach for reaction between the ion and dipolar molecule. The values of r recorded in Table IV are of the right order of magnitude for a molecular radius. These data cover the range of dielectric constant of 82.0 for water at 15° to 26.7 for 91.77

(4) S. Arrhenius, *Z. physik. Chem.*, **1**, 110 (1887).

(5) E. S. Amis, *Anal. Chem.*, **27**, 1672 (1955).

TABLE III
ENERGIES OF ACTIVATION, ARRHENIUS FREQUENCY FACTORS AND ENTROPIES OF ACTIVATION

$\mu = 1.259 \times 10^{-3}$, NaOH = ethyl α -haloacetate = $1.259 \times 10^{-3}M$

Reagent	ΔE , cal. mole ⁻¹		log <i>Z</i> (15°) corresponding to the two values of ΔE		ΔS , cal. mole ⁻¹ deg. ⁻¹ (15°) corresponding to the two values of ΔE	
	15.00-25.00°	15.00-30.00°				
Pure water						
Ethyl fluoroacetate	10,900	12,300	9.8	10.1	-13.5	-12.1
Ethyl chloroacetate	9,600	9,300	8.4	8.3	-19.9	-20.6
Ethyl bromoacetate	8,000	9,000	7.4	9.1	-24.8	-26.8
49.75 wt. % ethanol						
Ethyl fluoroacetate	12,600	14,000	10.1	11.2	-12.5	-7.5
Ethyl chloroacetate	12,400	14,100	10.2	11.4	-11.9	-6.2
Ethyl bromoacetate	11,800	12,400	9.8	10.2	-13.6	-11.7
Ethyl dibromoacetate	12,200	...	10.4	..	-11.4	...
91.77 wt. % ethanol						
Ethyl fluoroacetate	20,000	17,200	14.7	12.6	+ 8.8	- 0.85
Ethyl chloroacetate	11,100	13,400	8.4	10.2	-20.0	-12.0
Ethyl bromoacetate	8,400	11,200	6.3	8.4	-29.5	-19.9
Ethyl dibromoacetate	15,700	15,400	12.3	12.1	- 2.32	- 3.06
Ethyl dichloroacetate	12,100	12,500	10.2	10.5	-11.8	-10.4
Ethyl trichloroacetate	11,500	11,100	9.0	8.7	-17.4	-18.9

TABLE IV
VALUES OF $r(\text{\AA})$ AND CALCULATED AND OBSERVED VALUES OF ΔE_c (CAL./MOLE) IN ISODIELECTRIC MEDIA

Reagent	Dipole moment (Debyes)	$r(\text{\AA})$	ΔE_c cal./mole calcd.		ΔE_c cal./mole obsd.				ΔE_c (obsd.)/ ΔE_c (calcd.)			
			Temp. range →		15-25°		15-30°		15-25°		15-30°	
			81.8-52.8	81.8-29.1	81.8-51.8	81.8-29.1	81.8-51.8	81.8-29.1	81.8-51.8	81.8-29.1	81.8-51.8	81.8-29.1
Ethyl fluoroacetate	2.09	1.29	610	1930	2400	13,000	2200	8800	3.93	6.74	3.61	4.56
Ethyl chloroacetate	2.64	1.35	710	2210	3900	4,000	5700	7700	5.49	1.81	8.03	3.48
Ethyl bromoacetate	2.64	1.30	760	2390	5600	4,800	4900	6800	7.37	2.01	6.45	2.85

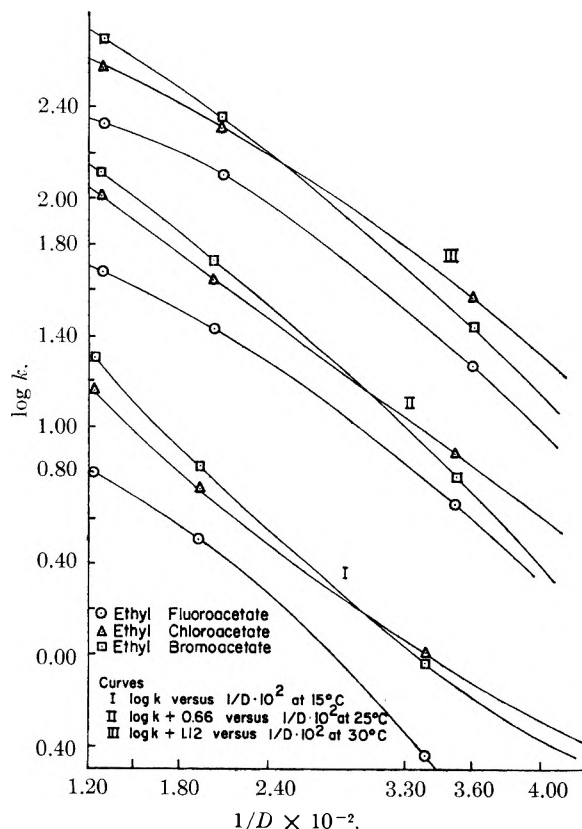
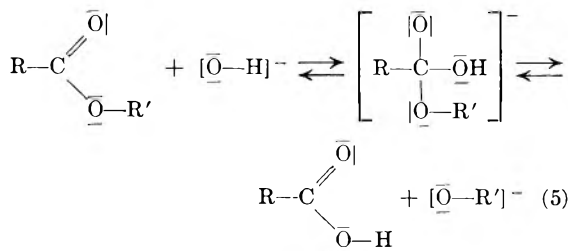


Fig. 2.—Relationships between the velocity constants of the ethyl α -monohaloacetates and the dielectric constant of the reaction medium,

weight % ethanol in water at 30°. This is a wide range for such data to approximate theory. Calculations were made only for the monohalogen compounds at 25°. Other calculations were not made since sufficient dielectric constant data were available only in these cases. The values for the dipole moments for ethyl fluoroacetate and ethyl bromoacetate which are listed in Table IV were estimated from the ratio of the dipole moments of *p*-fluoroanisole, *p*-chloroanisole and *p*-bromoanisole which were available in the literature⁶ and the dipole moment listed in the literature for ethyl chloroacetate.⁷

The obedience of the data to the requirements of equation 4 indicates that the rate-controlling step of the process is between a negatively charged ion and a dipolar molecule. This is in harmony with the mechanism proposed by Hammett⁸ which is



Since this is an ion-dipolar molecule mechanism,

(6) N. W. Sidgwick, *Trans. Faraday Soc.*, **30**, Appendix (1934).

(7) R. J. W. La Ferte and H. Vine, *J. Chem. Soc.*, 1795 (1938).

(8) L. P. Hammett, "Physical Organic Chemistry," McGraw-Hill Book Co., Inc., New York, N. Y., 1940, p. 355.

the coulombic energy of activation, ΔE_c , can be calculated using the equation⁹

$$\Delta E_c = \frac{Z\epsilon\mu}{D_1 D_2 r^2} \Delta D \quad (6)$$

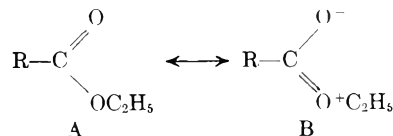
In this equation, $Z\epsilon$, μ and r have the same meaning as in equation 4 and ΔD is the difference between dielectric constants D_2 and D_1 . The results using this equation are recorded in Table IV, where a comparison of calculated and observed coulombic energy values are given for isodielectric solvents. Isodielectric data for the velocity constants, and hence for energies of activation, were obtained by reading from Fig. 2 values of $\log k$ for all monohalogen esters and all temperatures at the same dielectric constant. Three such dielectric constants were chosen, namely, 81.8, 51.8 and 29.1. Again calculations were made only for those substances for which sufficient dielectric constant data were available and the dipole moments of which could be found in the literature or estimated in a reasonable manner from data in the literature. The calculated values of ΔE_c are those corresponding to the dielectric constant range used in making the activation energy calculations. Agreement between calculated and observed values of coulombic energies have been observed down to a dielectric constant of about 40.^{9,10} Variations between calculated and observed values of ΔE_c have been attributed to enhancement of the moment of the molecule by the solvent medium.¹¹ From equation 6 if the moment μ of the dipolar molecule is enhanced, the coulombic energy would be greater than the coulombic energy calculated using the normal moment of the dipolar molecule. The ratios between calculated and observed values in the present case have different trends depending on the range of the dielectric constant and, hence, apparently the comparatively large values of observed coulombic energy are not due entirely to enhancement by the solvent medium of the dipole moment of the ester.

From comparison of the rate constant values recorded in Table II for the hydrolyses of the halogenated ethyl acetates with the values from the literature⁴ for the unhalogenated ester, it can be seen at like temperatures in like solvents (pure water, for example) that the monofluoroester hydrolyzes about 120 times as fast as the unhalogenated ester. The monochloro- and monobromoesters hydrolyze about 260 and 320 times as fast, respectively, as the unhalogenated ester. The polyhalogenated esters react much faster in proportion. This is attributed to an inductive effect whereby the halogens attract electrons to themselves and leave the carbonyl carbon more electropositive, thus increasing its attraction for the negative hydroxyl ion and making the collisions of the hydroxyl ion with the reaction center more energetic, and thus increasing the rate of hydrolysis. The lower estimated dipole moment of the fluoroester as compared to the chloro- and bromoesters might indicate the smallest inductive effect for the fluoroester and, therefore, the slowest

rates of hydrolyses of this compound as was observed in the different media. However, from the standpoint of electronegativity only, if the induction were the whole story the order of increase should be in the order bromo, chloro, fluoro for the monosubstituted compounds. The reverse is true for this series in all but the lowest dielectric constant solvent containing 91.77% EtOH. However, the inductive effect does predict correctly the order of increase in the case of the polysubstituted halogen esters—the rates increasing in the order dibromo-, dichloro-, trichloroacetate (see Table II).

There is a noticeable regularity in the ratios of the observed to the calculated coulombic energies. If from Table IV the ratio of the observed to calculated coulombic energies of the monosubstituted halogen compounds is inspected for the higher dielectric constant range (*i.e.*, the 81.8–51.8 range), it will be seen that the value of the ratio increases, with one exception, from the fluoro- through the chloro- to the bromohalogenated compound which is just the order of the relative increase of rates from Table II. Thus there is a second influence which governs the relative increase of rates though all are enhanced by induction. This second effect has an enhancement in the same direction as the enhancement of coulombic energy by halogen substitution, and in the opposite direction to the values of the ionization constants, K_a , of the halogenated acids which are in dilute aqueous solution 2.1×10^{-3} , 1.52×10^{-3} , 1.35×10^{-3} for the fluoroacetic, chloroacetic and bromoacetic acids, respectively. There is a larger difference in the hydrolysis rates in going from fluoro- to chloroester than in going from chloro- to bromoester. In the solvent of lowest dielectric constant (91.77 weight % ethanol) there is an increase in the rate of hydrolysis in going from fluoro- to chloroester and then a decrease in going from chloro- to bromoacetate. The differences in the ratios of coulombic energies for the esters in this solvent range with one exception decrease in going from fluoro- to chloro- to bromoester. This directional trend in the ratios of observed to calculated coulombic energies is just the opposite to that in the range of solvent having higher dielectric constants, that is, in water and in 49.75 weight % ethanol.

Consider the resonance forms of carboxylic acid esters



where R is CH_3 -, FCH_2 -, ClCH_2 -, BrCH_2 -. Suppose, as influenced by the inductive effect at higher dielectric constants of the solvent, resonance form B with its double bond between the carbon and the ethoxide group is favored more by fluoro-substitution than by chloro-substitution. Suppose also under these conditions that the form B is favored more by chloro- than by bromo-substitution. As a consequence, the hydrolysis would increase in going from fluoro- to chloro- to bromoester, since the double bond character of the bond between carbon and the ethoxide group would make this

(9) E. S. Amis, *J. Am. Chem. Soc.*, **63**, 1606 (1941).

(10) E. S. Amis and F. C. Holmes, *ibid.*, **63**, 2231 (1941).

(11) J. E. Potts, Jr., and E. S. Amis, *ibid.*, **71**, 2112 (1949).

bond more stable than would be the single bond between carbon and ethoxide in resonance form A. This is reflected in the trend toward larger energy of activation in the higher dielectric constant range for the fluoro- as compared to the chloroester hydrolysis and for the chloro- as compared to the bromoester hydrolysis. The coulombic energy of activation is the opposite of this, perhaps due to the electrostatics of the approach of the hydroxyl ion to the two resonance forms. This whole effect, it must be remembered, is a secondary effect imposed on a large inductive effect.

In the 91.77 weight % ethanol solvent apparently the relatively large proportion of resonance form B is still present in the fluoroester, but not in the chloroester as compared to the bromoester. This possibly arises from some specific solvation effect. Thus fluorine with its strong hydrogen bonding characteristics might cause the fluoroester to cling more tenaciously to the last traces of water than would the chloro- or bromoesters. When this low dielectric constant solvent is included in the coulombic energy calculations, the trends in ΔE_c and the trends of the ratios between observed and calculated values are reversed from those obtained using the higher dielectric constants. The total energies are not far different in their trend in this solvent from that of the solvents of higher dielectric constants.

In the di- and trisubstituted esters, this secondary effect is not observed, and the increase in the rate of hydrolysis in going from dibromo- to di-

chloro- to trichloroester is that expected from inductive effects. The total energy of activation reflects this trend since it decreases in going from the dibromo- to the dichloro- to the trichloroester. Sufficient dielectric constant data were not available to make possible the calculation of coulombic energies.

The large negative entropies in most all cases perhaps indicate a more rigid intermediate than initial reactant state. The trends of the entropies and Arrhenius frequency factors are similar to that of the energy of activation.

There is a possibility that hydrogen bonding with solvent might influence these relative rates. Fluorine is a strong hydrogen bond forming element, chlorine less so and bromine maybe slightly so. Hydrogen bonding might be expected to enhance inductive effect. If, however, hydrogen bonding hindered inductive effect, fluorine would be most influenced, chlorine next most, and bromine least influenced, especially in water or water-rich solvents where hydrogen bonding is prominent. Thus the reversal of relative rates as expected from inductive effects and as observed in this investigation for monohalogen esters in water-rich solvents might occur. Also in the lowest dielectric constant solvent, the fluoroester, due to the strong hydrogen bonding characteristics of fluorine, might cling more tenaciously to water than would the chloro- or bromoester. Thus in 91.77 weight % alcohol, the fluoroester would continue to show a relatively less inductive effect.

VAPOR PHASE γ -RADIOLYSIS OF ACETONE¹

BY LOUIS J. STIEF² AND P. AUSLOOS

Division of Physical Chemistry, National Bureau of Standards, Washington, D. C.

Received March 17, 1961

The effect of scavengers, pressure, temperature and added xenon on the vapor-phase radiolysis of acetone- d_6 and acetone-acetone- d_6 mixtures has been investigated. Most of the results can be explained on the basis of free radical reactions similar to those occurring in the photolysis of acetone- d_6 . Values for the ratio of rate constants $k_1/k_2^{1/2}$ for the reactions $CD_3 + CD_3COCD_3 \rightarrow CD_4 + CD_2COCD_3$ (1) and $CD_3 + CD_3 \rightarrow C_2D_6$ (2) determined from the radiolysis data are in excellent agreement with values based on photolysis experiments, indicating that methane and ethane are formed by the reactions of thermalized methyl radicals. Methane and hydrogen formed in the presence of scavengers are mainly attributed to the occurrence of molecular elimination processes.

Introduction

The vapor-phase radiolysis of acetone³ is known to yield carbon monoxide, methane, ethane, ethylene and hydrogen. Certain minor products, such as acetylene and propylene were also reported. The effect of temperature⁴ on $CD_4/(C_2D_6)^{1/2}[CD_3COCD_3]$ values suggests the possibility of certain similarities between radiolysis results and photochemical data⁵ for acetone- d_6 . The present investigation was undertaken to establish the extent

of the similarity and to provide more extensive data in an attempt to corroborate the results obtained in the radiolysis of azomethane.⁶ The deuterated compound was chosen because it enables us to distinguish between abstraction from acetone by methyl (yielding CD_4) and abstraction from water⁴ on the wall of the reaction vessel (yielding CD_3H). Since this effect is more pronounced in the radiolysis system,⁴ we must be able to make such a distinction in order to get a better comparison between the photolysis and radiolysis results. In addition, abstraction reactions are favored over radical-radical reactions due to the small steady state concentration of radicals arising from the low intensity of absorbed γ -rays in vapor-phase experiments. This limits the temperature range in

(1) This research was supported by a grant from the U. S. Atomic Energy Commission. (Presented in part at the 138th Meeting of the American Chemical Society, New York, N. Y., Sept. 1960.)

(2) National Academy of Sciences-National Research Council, Postdoctoral Research Associate, 1960-1961.

(3) P. Ausloos and J. Paulson, *J. Am. Chem. Soc.*, **80**, 5117 (1958).

(4) P. Ausloos and J. Paulson, *J. Phys. Chem.*, **62**, 501 (1958).

(5) E. Whittle and E. W. R. Steacie, *J. Chem. Phys.*, **21**, 993 (1953).

(6) L. J. Stief and P. Ausloos, *J. Phys. Chem.*, **65**, 877 (1961).

which measurable amounts of ethane may be obtained. The somewhat higher activation energy for abstraction for the deuterated compound should enable us to extend the temperature range over which the radiolysis is investigated.

Experimental

Materials.—Acetone- d_6 was obtained from Merck and Company, purified by vacuum distillation and stored in contact with Drierite at -80° . Mass spectrometric analysis showed that the acetone was 99.5% deuterated. Assayed reagent grade oxygen and xenon were obtained from the Air Reduction Company, Inc., and used without further purification. Phillips research grade ethylene and Eastman Kodak "Spectrograde" CH_3COCH_3 were purified by vacuum distillation. Nitric oxide, obtained from the Matheson Company, Inc., was purified by distilling a sample from a trap at -160° to a trap at -195° and then degassing at -210° .

Irradiations.—The 2,000-Curie cobalt-60 γ source at the National Bureau of Standards was used in this investigation. The procedure has been described previously.⁶ The Pyrex cells were thoroughly flamed out on the vacuum line before introducing the acetone in order to minimize as much as possible the effect of water absorbed on the walls. Conversions were between 0.003 and 0.05%; the majority of the experiments were done at less than 0.01% conversion.

Analysis.—The analytical procedure was essentially the same as that described previously.⁶ Hydrogen, methane and carbon monoxide were removed at -196° (or -210° for experiments with C_2H_4 , NO or Xe present), and ethane and ethylene at -170° . All fractions were analyzed in a Consolidated 21-101 mass spectrometer. The distribution of the isotopic methanes was calculated from cracking patterns reported in the literature.⁷ The C_3 fraction in these experiments was usually less than 1% of the CO yield.

Dosimetry.—The G -value for any of the products from the vapor-phase radiolysis of acetone- d_6 may be obtained by multiplying the rate per mole (cc. (NTP)/min.-mole) by the factor 135. This is based on the measured hydrogen production in the radiolysis of ethylene, assuming the value $G_{\text{H}_2} = 1.3$ molecules/100 e.v.⁸

Results

The principal gaseous products of the γ -radiolysis of acetone- d_6 are CO, CD_4 , C_2D_6 and D_2 . C_2D_4 was also detected in yields up to 10% of the CO. There were no evident trends in C_2D_4 production with pressure. Under conditions where C_2D_4 could be measured with sufficient accuracy (C_2D_4 greater than 10% of the C_2D_6), there was no effect of scavengers or temperature on the C_2D_4 production. H_2 is also produced in varying amounts and is particularly significant at low pressures and high temperatures.⁹

The results obtained in the radiolysis of acetone- d_6 are shown in Tables I, III and IV; those obtained in the radiolysis of acetone-acetone- d_6 mixtures are shown in Tables II and V. All results have been expressed in rates (cc. (NTP)/min.) per mole of acetone present. This has been done in order to make comparisons between experiments performed at different pressures of acetone, since increased pressure leads to increased absorption of energy. The effect of conversion (dose), scavengers, pressure, temperature and xenon on the principal products can be summarized as follows.

Conversion.—A fivefold increase in dose has no

(7) F. L. Mohler, V. H. Dibeler and E. Quinn, *J. Research Natl. Bur. Standards*, **61** 171 (1958).

(8) M. C. Sauer Jr., and L. M. Dorfman, Abstracts 137th Meeting American Chemical Society, April, 1960

(9) While the formation of HD is essentially completely inhibited by scavengers, H_2 is relatively unaffected. This indicates that H_2 is formed molecularly, possibly from water absorbed on the wall.

effect, within experimental error, on the yields of any of the products at 50.5 mm. and 16° (Table III).

TABLE I

RADIOLYSIS OF ACETONE- d_6 : EFFECT OF SCAVENGERS
 CD_3COCD_3 , 50.0 mm. at 25° ; reaction temp., 16° ; n. d., not determined

	No scavenger	O_2 (0.4%) Cc. (NTP)/min.-mole $\times 10^2$	NO (1%) (1%) Cc. (NTP)/min.-mole $\times 10^2$	C_2H_4 (3%)
CO	2.67	4.23 ^a	2.38	2.54
CD_4	0.653	0.093	0.029	0.365
CD_3H	0.133	< .01	< .01	0.280
C_2D_6	2.30	.053	.098	n.d.
D_2	1.15	.697	.658	0.700
HD	0.096	< .01	< .01	< 0.01

^a CO is a product of the oxidation reaction.

TABLE II

RADIOLYSIS OF ACETONE-ACETONE- d_6 : EFFECT OF SCAVENGERS
 CH_3COCH_3 , 50.0 mm. at 25° ; CD_3COCD_3 , 50.0 mm. at 25° ; reaction temp., 16°

	No scavenger	O_2 ^b (0.2%) Cc. (NTP)/min.-mole $\times 10^2$	NO (1%)
CO	2.59	2.93 ^a	2.64
CD_4	0.185	0.029	0.028
CD_3H	.522	.011	.015
CH_3D	.118	< .01	< .01
CH_4	.577	.039	.039
D_2	.282	.245	.254
HD	.902	.116	.131
H_2	1.14	.393	.355

^a CO is a product of the oxidation reaction. ^b Average of two experiments.

Scavengers.—In the radiolysis of CD_3COCD_3 the CO production is not altered by the presence of nitric oxide or ethylene (Table I). The effect of oxygen is masked by the production of CO in the oxidation reaction. Oxygen and nitric oxide reduce CD_4 and C_2D_6 by about 95%. D_2 is reduced by 40% in the presence of ethylene, oxygen or nitric oxide. The formation of both CD_3H and HD is essentially inhibited by scavengers.¹⁰ For the system CH_3COCH_3 - CD_3COCD_3 (Table II), CD_4 and CH_4 are the principal methanes formed in the presence of scavengers while CD_3H and CH_4 are the most important methanes formed in the absence of scavengers. The yield of HD is more strongly reduced than that of either H_2 or D_2 .

Pressure.—The rates of production of CO and D_2 per mole of acetone present (relative G) are independent of pressure from 2.0 to 130.5 mm. of acetone (Table III). The yield of CD_3H is more significant below 10 mm. than it is at higher pressures. Above 10 mm. it varies between 5 and 10% of the CO, independent of pressure of acetone. The yield of HD is also more significant at low pressures.

Temperature.—The effect of temperature on the acetone- d_6 radiolysis is shown in Table IV. At all but one temperature, experiments were done in

(10) This means that these products probably are formed by the abstraction of an H atom from a H_2O molecule adsorbed on the wall. The amount of CD_3H and HD is too large to be accounted for by incomplete deuteration of acetone

TABLE III
 RADIOLYSIS OF ACETONE-*d*₆: EFFECT OF PRESSURE

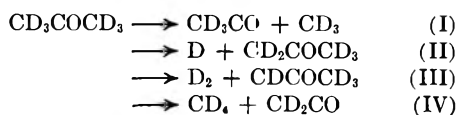
Pressure (mm. at 25°)	Reaction temp., 16°; n.d., not determined								
	2.0	5.0	10.0	25.0	50.5	50.5	80.0	100.0	130.5
Reaction time (min.)	2990	963	1130	303	191	930	162	367	157
	Cc. (NTP)/min.-mole × 10 ²								
CO	3.11	3.08	2.91	2.90	2.43	2.78	2.95	2.63	2.70
CD ₄	0.266	0.465	0.392	0.709	0.769	0.654	0.669	0.718	0.750
CD ₃ H	1.58	0.835	0.150	0.167	0.154	0.207	0.286	0.161	0.221
C ₂ D ₆	n.d.	2.09	2.67	2.85	2.53	2.70	2.37	2.25	2.28
D ₂	1.13	0.991	1.01	1.06	1.28	1.20	1.08	1.15	0.744
HD	0.621	0.063	0.179	0.161	0.118	0.106	0.116	0.093	0.032
C ₂ D ₆ + 1/2(CD ₄ + CD ₃ H)	...	0.89	1.01	1.13	1.23	1.13	0.97	1.02	1.02
CO									

the absence and in the presence of a scavenger. Although there is some scatter in the results, the rate of production of CO shows no obvious trend and may be considered independent of temperature, at least up to 154°. The methane and ethane formed in the presence of scavengers are approximately the same at all temperatures up to 195°; above this temperature, the scavenging effect of oxygen is doubtful.

Xenon.—The effect of xenon on the radiolysis of acetone-acetone-*d*₆ mixtures is shown in Table V. The yields of CO, D₂, HD and H₂ are approximately proportional to the pressure of xenon. The yield of the methanes is relatively unaffected. Assuming that (a) ionization or excitation is proportional to the total number of electrons in the system, and (b) the CO yield is proportional to the *G*-value for decomposition, it may be calculated that, for 100 mm. of acetone and 200 mm. xenon at 16°, the efficiency of transfer of energy from xenon to acetone corresponds to 0.69. A value of 0.71 was obtained under similar conditions for the system xenon-azomethane.⁶ The last columns of Tables II and V show the effect of xenon on the methanes and hydrogens formed in the presence of scavengers. All increased upon addition of xenon.

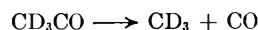
Discussion

Primary Events.—The experimental results are consistent with the occurrence of the following initial chemical conversion



The fact that the CO production is independent of temperature from 16 to 154° suggests that the acetyl radical, formed in the primary dissociation process I, is "hot" and undergoes immediate decomposition. Also, the formation of thermal acetyl radicals should lead to values of C₂D₆ + 1/2(CD₄ + CD₃H)/CO (see discussion of secondary reaction for basis of this ratio) considerably less than unity. Finally, the fact that biacetyl has not been detected¹¹ in the radiolysis of acetone is evidence against the presence of thermal acetyl radicals. Assuming that the acetyl radical which

may initially be formed in process I decomposes according to



two methyl radicals are produced for every CO molecule.

In the radiolysis of acetone-*d*₆, the reduction of the D₂ yield in the presence of scavengers is consistent with the occurrence of process II, followed by the abstraction reaction



The formation of HD in the radiolysis of acetone-acetone-*d*₆ mixtures, as will be shown later, is also evidence for the removal of an H and D atom from CH₃COCH₃ and CD₃COCD₃, respectively. The acetyl radical produced in process II may decompose as a result of excess energy carried over in the process



Acetic acid, which would result from the reaction of ketene with water, has been shown to be an important product in the vapor-phase radiolysis of acetone.¹¹ Also, the fact that C₂D₆ + 1/2(CD₄ + CD₃H)/CO is sometimes larger than unity indicates that there may be another source of methyl radicals in addition to process I.

In the radiolysis of acetone-acetone-*d*₆ mixtures in the presence of scavengers, HD is reduced to about 10% of its value in the absence of scavengers. Thus the contribution of hot hydrogen atom or ion-molecule processes to the hydrogen production is small. Consequently, the production of D₂ in the presence of scavengers may best be accounted for by the molecular elimination process III. Results obtained in the radiolysis of CH₃COOCD₃¹² clearly demonstrate that D₂ may be split off from one carbon.

The yield of CD₄ is two to three times that of the CD₃H in the radiolysis of acetone-acetone-*d*₆ mixtures in the presence of scavengers. If the methane formed in the presence of scavengers were the product of hot radical or ion-molecule processes, CD₄ would at most equal CD₃H. Most of the CD₄ formed in the presence of scavengers may thus be explained by an intramolecular process such as IV. Molecular elimination of hydrogen or methane has not been observed in the long wave length photolysis of acetone. It would, however, be in-

(11) J. F. Paulson, Doctoral Dissertation, University of Rochester, 1958.

(12) P. Ausloos and C. N. Trumbore, *J. Am. Chem. Soc.*, **81**, 2866 (1959).

TABLE IV
RADIOLYSIS OF ACETONE- d_6 : EFFECT OF TEMPERATURE
CD₃COCD₃, 80.0 mm. at 25°

Temp., °C. Scavenger Reaction time (min.)	16		95		147		154		195		234	
	No	Yes	No	Yes	No	Yes	No	Yes	No	Yes	No	Yes
CO	3.27	3.11	3.29	4.03 ^a	2.60	9.23 ^a	3.11	3.91	3.84	8.78 ^a	3.84	19.89 ^a
CD ₄	0.729	0.073	1.24	0.091	2.93	0.172	3.86	6.60	7.68	0.136	7.68	0.770
CD ₃ H	0.142	0.13	0.211	0.18	0.368	0.051	0.468	1.25	0.476	0.034	0.476	0.066
C ₂ D ₆	3.06	0.114	2.76	0.121	0.802	0.10	0.978	0.692	0.0869	0.10	0.0869	0.0308
D ₂	1.08	0.622	1.08	0.593	1.44	0.986	1.66	2.25	1.64	1.09	1.64	1.56
HD	0.092	0.083	<0.01	<.01	0.166	0.070	0.257	<0.20	0.071	<0.10	0.071	0.084
C ₂ D ₆ + 1/2(CD ₄ + CD ₃ H)	1.07	...	1.06	...	0.94	...	1.01	1.18	1.09	...	1.09	...
$\frac{R_{CD_4}}{R^{1/2}_{C_2D_6}[A]} \times 10^{14}$	2.234	[2.045]	4.005	[3.795]	17.54	[17.66]	20.93	42.54	44.19	[45.02]	44.19	[156.5]

^a CO is a product of the oxidation reaction.

TABLE V

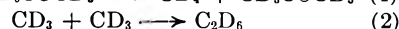
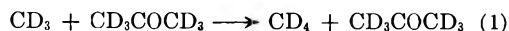
RADIOLYSIS OF ACETONE-ACETONE- d_6 : EFFECT OF XENON
CH₃COCH₃, 50.0 mm. at 25°; CD₃COCD₃, 50.0 mm. at 25°,
reaction temp. 16°

Pressure of Xe (mm. at 25°)	Cc. (NTP)/min.-mole $\times 10^2$			
	0	100	200	200 ^a
CO	2.59	5.30	8.61	8.85
CD ₄	0.185	0.201	0.221	0.057
CD ₃ H	.522	.473	.527	0.025
CH ₃ D	.118	.180	.211	<0.02
CH ₄	.577	.470	.590	0.091
D ₂	.282	.693	1.02	1.03
HD	.902	1.99	2.66	0.597
H ₂	1.14	2.07	2.78	1.54
HD/CO	0.35	0.37	0.31	

^a 1 mm. NO added.

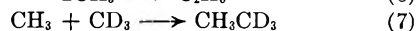
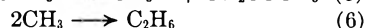
interesting to look for this in the short wave length photolysis since such processes have been observed to be very important in the direct photolysis of ethane¹³ at short wave lengths. The production of ethane in the presence of scavengers may be attributed to hot-radical reactions, ion-molecule processes, or intramolecular reactions.¹⁴ As yet no evidence has been obtained for intramolecular formation of ethane in photochemical studies.

Secondary Reactions.—Since 95% of the methane and ethane are removed by radical scavengers at low temperatures, these products result mainly from the secondary reactions of methyl radicals produced in process I. Since the carbon monoxide



yield was not reduced by the presence of scavengers, we can exclude such effects as the scavenger deactivating an excited molecule or acting as a trap for electrons in explaining the reduction in methane and ethane.

The isotopic methanes and ethanes formed in the radiolysis of acetone-acetone- d_6 mixtures may be accounted for by (1) and (2), plus the reactions



The yields of the three isotopic ethanes formed in the radiolysis of acetone-acetone- d_6 mixtures are: C₂D₆, 0.656; CH₃CD₃, 1.58; and C₂H₆, 0.877 cc. (NTP)/min.-mole $\times 10^2$. The ratio CH₃CD₃/ $\sqrt{C_2D_6} \sqrt{C_2H_6}$ calculated from these results is 2.07. If the ethanes are formed mainly by reactions 2, 6 and 7, the distribution of the ethanes should correspond to a statistical one; that is, the ratio CH₃CD₃/ $\sqrt{C_2D_6} \sqrt{C_2H_6}$ should equal 2.00. This statistical distribution is consistent with the occurrence of reaction 2, 6 and 7. Assuming a steady state concen-

(13) H. Okabe and J. R. McNesby, *J. Chem. Phys.*, **34**, 668 (1961).

(14) A knowledge of the distribution of the isotopic ethanes formed in the radiolysis of acetone-acetone- d_6 mixtures in the presence of scavengers would be useful. However, the amount of non-scavengable ethane is quite small and the interpretation of the mass spectrometer cracking pattern for this C₂ fraction is complicated by the presence of isotopic ethylenes in amounts comparable to the ethane.

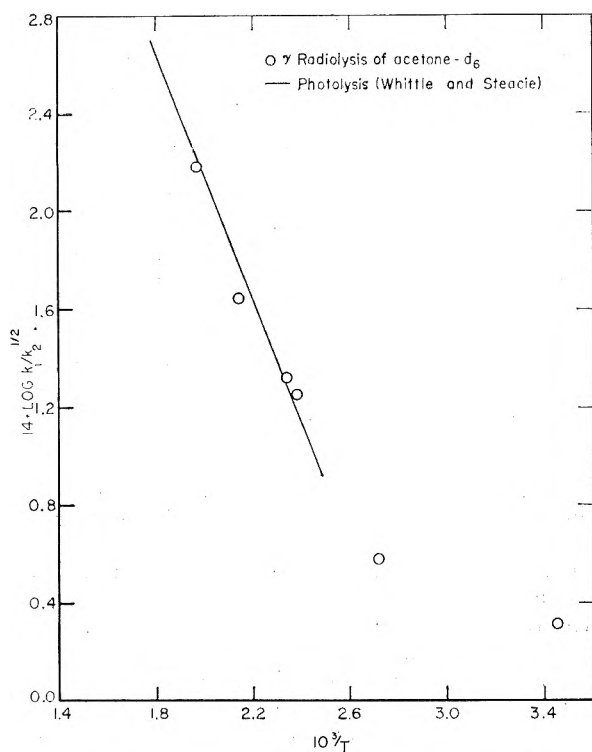


Fig. 1.

tration of methyl radicals, it may be shown that, as has been well established in photochemical studies

$$\frac{R_{CD_4}}{R^{1/2}_{C_2D_6} (CD_3COCD_3)} = \frac{k_1}{k_2^{1/2}}$$

where R is the rate of formation of the substance indicated. The ratio $R_{CD_4}/R^{1/2}_{C_2D_6}(CD_3COCD_3)$ at various temperatures has been calculated (Table IV) according to this equation using the values for the rate¹⁵ of methane and ethane production, per mole of acetone. This ratio has also been calculated at each temperature (except 154°) using values of methane and ethane corrected for the fraction not removed by scavengers. These values are shown in brackets in Table IV. It may be seen that only at 234° is the correction significant. It may be noted that the methane formed in the presence of scavengers is approximately independent of temperature at least up to 195°. This is consistent with the identification of most of the non-scavengable methane as the product of an intramolecular process. In Fig. 1, a plot of $\log k_1/k_2^{1/2}$ as a function of $1/T$ is shown on the same graph with the Arrhenius plot obtained by Whittle and Steacie⁵ in the photolysis of acetone- d_6 . The excellent agreement obtained makes it evident that the rate of the reaction of the methyl radicals is the same in the radiolysis and the photolysis systems. That is, methane and ethane are mostly formed by the reactions of thermal methyl radicals. The curvature obtained in the Arrhenius plot at lower temperatures has been observed also in the

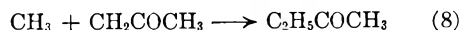
(15) In terms of rate per mole of acetone, the equation becomes

$$\frac{k_1}{k_2^{1/2}} \left(\frac{\text{cc.}^{1/2}}{\text{molec.}^{1/2} \text{ sec.}^{1/2}} \right) = \frac{R'_{CD_4} \times 1.11 \times 10^{-15}}{R'^{1/2}_{C_2D_6} (CD_3COCD_3)^{1/2}}$$

where R' is the rate/mole in the units cc. (NTP)/min.-mole and (CD_3COCD_3) indicates concentration of acetone- d_6 in moles/cc.

photolysis of CH_3COCH_3 and has been attributed¹⁶ to the reaction of methyl radicals adsorbed on the walls of the reaction vessel. A similar effect is to be expected for CD_3COCD_3 . Obviously, other effects may contribute to this curvature. It is interesting to note that such a pronounced curvature was not observed for azomethane.⁶

The acetyl radical formed in the abstraction reaction 3 may disappear by reaction with a methyl radical to form methyl ethyl ketone



or by combination with another acetyl to form acetylacetone (biacetyl)



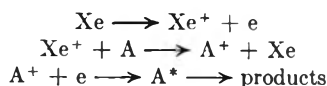
Paulson¹¹ found acetylacetone to be a major heavy product in the radiolysis of acetone.

If two methyls are produced for every CO molecule (process I) and if the important secondary reactions of the methyl radical are abstractions from acetone- d_6 (yielding CD_4), abstraction from water adsorbed on the wall (yielding CD_3H) and combination with another methyl to yield ethane, then the ratio $[C_2D_6 + 1/2(CD_4 + CD_3H)]/CO$ should equal unity. Additional sources of methyl radicals, such as the decomposition of the acetyl radical formed in process II, will raise the value and the occurrence of reaction 8 will lower this value.

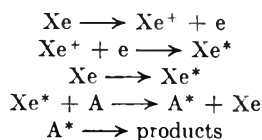
Xenon Sensitized Decomposition.—The increase of CO upon addition of xenon to the acetone-acetone- d_6 system indicates that process I is enhanced by xenon. The fact that the ratio HD/CO is constant with added xenon shows that the hydrogen or deuterium atom removal process increases to the same extent as process I. D_2 or H_2 formed in the presence of scavengers is a measure of the molecular hydrogen elimination process III. Since the ratios D_2/CO and H_2/CO , in the presence of NO, are the same ($\pm 10\%$) in the absence of xenon and with 200 mm. of xenon present, we concluded that the relative importance of the hydrogen molecule elimination process as compared to the radical producing steps is preserved in the xenon sensitized decomposition. The ratios CD_4/CO and CH_4/CO , in the presence of NO, decrease upon addition of 200 mm. of xenon, indicating that the molecular methane elimination process may be less important in the presence of xenon.

The fact that methanes formed in the absence of scavengers do not increase with added xenon is consistent with the formation of methane by hydrogen atom abstraction reactions. Addition of xenon increases the dose rate and leads to a higher steady state concentration of methyl radicals, which favors radical-radical reactions such as (2), (6), and (7). Since the relative importance of processes I, II and III (which account for more than 90% of the over-all decomposition process) was preserved in the presence of xenon, it may be argued that the acetone which decomposes is similar in both the direct decomposition and in the xenon sensitized decomposition. The excited acetone molecule may be formed in the xenon system either by a charge transfer process

(16) P. Ausloos and E. W. R. Steacie, *Can. J. Chem.*, **33**, 47 (1955).



or by an excited atom process



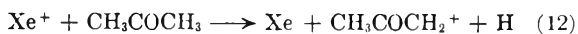
However, Melton¹⁷ has shown that for the argon-methane system in the mass spectrometer, the reaction



is more probable by a factor of five than the simple charge transfer process



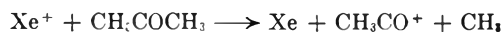
The reaction analogous to (10) in the xenon-acetone system would be



The occurrence of (12) would, however, lead to an enhanced production of hydrogen atoms in the xenon experiments. This would be evidenced by an increase in the HD/CO ratio upon the addition of xenon to the acetone-acetone-*d*₆ system. Since this effect was not observed in these experi-

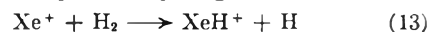
(17) C. E. Melton, *J. Chem. Phys.*, **31**, 647 (1960).

ments, it may be concluded that reaction 12 does not occur in this system. An additional reaction in the xenon-acetone system analogous to reaction 10 would be

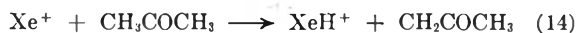


However, it would be difficult on this basis to account for the fact that the relative importance of the radical producing steps and the molecular hydrogen elimination process is preserved in the xenon sensitized decomposition.

In addition, the hydrogen abstraction reaction proposed by Lampe¹⁸ for hydrogen



does not occur with acetone



since this would eventually lead to an enhanced production of hydrogen atoms, which, as shown above, is inconsistent with the experimental results obtained in this investigation.

Acknowledgment.—The authors here wish to express their thanks to Professor W. Albert Noyes, Jr., for critically examining the manuscript prior to submission for publication. They are also indebted to one of the referees for pointing out an error in the dosimetry calculation. The factor quoted in this paper should also be applied to the results obtained in the radiolysis of azomethane.⁵

(18) F. W. Lampe, *J. Am. Chem. Soc.*, **82**, 1551 (1960).

HEATS OF FORMATION OF SOME ORGANIC POSITIVE IONS AND THEIR PARENT RADICALS AND MOLECULES

BY R. R. BERNECKER¹ AND F. A. LONG

Department of Chemistry, Cornell University, Ithaca, N. Y.

Received April 1, 1961

Heats of formation are tabulated for the gaseous molecules, radicals and positive ions which are formed from C, H and O, the list being restricted, however, to compounds with no more than four carbon atoms. The data for the ionization potentials come from spectroscopic, photoionization and electron impact studies. The tabulation includes new electron impact data for esters, ethers and acids and experimental details are given.

In the interpretation of the mass spectra of complex molecules and especially in the application of reaction rate theories to the data,²⁻⁴ information on the energetics of the ionization process and the decomposition steps are invaluable. As Franklin and Field have emphasized,⁵ a particularly convenient way to tabulate such data is to list heats of formation of the species concerned and the compilation by these authors of some heats of formation (Table 45 of ref. 5) has been most useful. However, for at least two reasons, this is an appropriate time for a new tabulation. A number of

new sets of data have appeared in the last few years, the extensive set of photoionization potentials of Watanabe, Nakayama and Mottl⁶ being perhaps the most important. Furthermore the need has been increasing for the heats of formation not only of the ions of organic radicals but of the uncharged radicals themselves. As an example to illustrate this need, the common decomposition reaction of a positive organic ion is of the type



from which it is evident that ΔH for the reaction involves ΔH_f for a molecule ion (obtainable from conventional ionization potential studies) and also the ΔH_f values for a neutral radical and a radical ion.

Table III lists ΔH_f values for a set of molecules and radicals and their positive ions. It includes

(6) K. Watanabe, T. Nakayama and J. Mottl, "Final Report on Ionization of Molecules by a Photoionization Method," University of Hawaii, December, 1959.

(1) Holder of NSF Coöperative Fellowship in 1959-1960 and of Standard Oil of New Jersey Fellowship in Chemistry in 1960-1961.

(2) H. M. Rosenstock, M. B. Wallenstein, A. L. Wahrhaftig and H. Eyring, *Proc. Natl. Acad. Sci., U. S. A.*, **38**, 667 (1952).

(3) H. M. Rosenstock, A. L. Wahrhaftig and H. Eyring, *J. Chem. Phys.*, **23**, 2200 (1955).

(4) E. Friedman, F. A. Long and M. Wolfsberg, *ibid.*, **27**, 613 (1957).

(5) F. H. Field and J. L. Franklin, "Electron Impact Phenomena," Academic Press, New York, N. Y., 1957.

the available data for compounds of C, H and O which contain four carbon atoms or less. The species are listed by structural formulas since in most cases these are well established. It will be evident, however, that in several instances the structures are distinctly uncertain. The ΔH_f values are for 298°K.⁷ and are given in electron volts (1 e.v. = 23.06 kcal./mole = 8067 cm.⁻¹). The symbols in the Quality column represent *personal* estimates of the precision of the data. The meanings of the symbols are: S, spectroscopic data; 1, data of good precision, not usually from electron impact studies; 2, good quality electron impact and related data; 3, less precise electron impact data or from estimates. The probable limits of error for the ΔH values range from ± 0.01 e.v. or less for the best spectroscopic data to perhaps ± 0.3 e.v. for the poorer electron impact data.

Two further points should be made. One concerns the choice between values of ionization potentials determined by photoionization and by spectroscopy. The studies of Watanabe and co-workers serve to establish photoionization as a highly reliable procedure which can give ionization potentials of only slightly lower accuracy than the best spectroscopic data. They also indicate that the chief danger in spectroscopic studies of complex molecules is that of misinterpretation of the data. Given these two points, our procedure has been to accept the spectroscopic ionization potential for simple molecules and to do the same for complex molecules when the agreement with the photoionization data is good. But when there is a significant discrepancy we have chosen the photoionization result.

The problem of ionization potentials from electron impact is a rather different one. It is well known that values from this method (even when done by approved techniques) tend to be somewhat higher than those from either spectroscopy or photoionization. Our survey of the recent data supports this conclusion but also suggests that the discrepancy is not so serious as to call for rejection of electron impact data. Specifically, a comparison between electron impact and photoionization for seventeen randomly chosen polyatomic molecules indicates that ionization potentials by the impact method are about 0.15 e.v. higher than those from photoionization. Since the quoted error for potentials from electron impact is commonly in the order of ± 0.2 e.v. the implication is that within this rather large error limit the electron impact method gives useful data.

Interpretation of appearance potentials of fragment ions from a compound involves further difficulties. These ions result from decomposition reactions such as (1) above and it is always possible that there is an energy of activation involved. Products may be formed either in excited

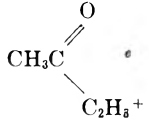
states or with excess kinetic energy. The evidence suggests that neither of these ordinarily amounts to more than 0.1 e.v. at least for primary decomposition reactions. Since this value is within the limit of error of electron impact measurements we have ignored it in the calculations which are involved in Table III. But it must be borne in mind that later study may reveal specific instances where activation or excitation energy is large enough to lead to an unacceptable error for heats of formation of a radical or its ion.⁸

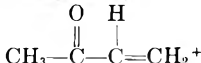
Several of the data of Table III result from appearance measurements made in this Laboratory. The section which follows gives details of these studies and also includes comparison of electron impact data with data from other methods.

TABLE I
COMPARISON OF OBSERVED APPEARANCE POTENTIALS WITH
IONIZATION POTENTIALS

Compound	Appearance potential	I.P. (lit.)	Ref.
Krypton	14.0 ₆	13.996 (spectro)	11
Carbon dioxide	13.7 ₈	13.79 (spectro)	12
Neon	21.5 ₇	21.559 (spectro)	11
Methane	13.1 ₁	12.98	6
Nitrogen	15.6 ₀	15.55 ₇ (spectro)	13
Dimethyl ether	10.0 ₆	10.00	6
Ethylene	10.5 ₈	10.51	6
Formic acid	11.4 ₀	11.33 (spectro)	14
		11.05	6
Methyl vinyl ether	9.1 ₅	8.93	6
Ethyl acetate	10.1 ₂	10.11	6

TABLE II
APPEARANCE POTENTIALS OF SELECTED IONS

Ion	Parent compound	Obsd. A.P.	ΔH_f of ion
DCOOH ⁺	DCOOH	11.5 ₇	+7.6 ^a
DCOO ⁺	DCOOC ₂ H ₅	12.1 ₅	+7.2
CH ₃ O ⁺	CH ₃ OCH ₃	12.5 ₁	+9.2
CH ₂ OCH ₃ ⁺	CH ₃ OCH ₃	11.4 ₆	+7.3
C ₂ H ₃ ⁺	C ₂ H ₅ COOH	12.9 ₀	... ^b
COOH ⁺	C ₂ H ₅ COOH	12.8 ₄	+7.0
C ₂ H ₅ CO ⁺	C ₂ H ₅ COOH	12.2 ₀	+7.0
C ₂ H ₄ COOH ⁺ c	C ₂ H ₅ COOH	11.7 ₀	+4.7
C ₂ H ₄ CO ⁺ d	C ₂ H ₅ COOH	11.5 ₇	+9.3
C ₂ H ₃ O ⁺	CH ₃ OC ₂ H ₃	11.4 ₄	+8.8
CH ₃ COOH ₂ ⁺	CH ₃ COOC ₂ H ₅	10.7 ₅	+3.4
	CH ₃ COOC ₂ H ₅	10.4 ₃	+8.4
C ₃ H ₇ O ⁺	DCOOC ₃ H ₇	11.2 ₂	+7.1
H ₃ O ⁺	HCOOC ₂ H ₅	14.5 ₀	+9.0

^a Assuming for DCOOH that $\Delta H_f = -3.96$ e.v. ($\text{HCOOH} = -3.92$ e.v.¹⁵). ^b Leads to $\Delta H_f = -1.7$ for —COOH radical. ^c Most probable structure is $\text{CH}_3\text{—CH—COOH}^+$. ^d Most probable structure is $\text{CH}_3\text{—CH=C=O}^+$. ^e The structure seems definitely to be  since the analogous ion from CD₃COOC₂H₅ has $m/e = 73$.

(7) Electron impact studies are usually made with an ionization chamber which is heated to around 500°K. However, there is considerable uncertainty as to whether the entering gas is equilibrated to this temperature. Since experimentally there is little evidence of a temperature coefficient for mass spectrometric appearance potentials, we have ignored this temperature problem and have simply listed the observed data.

(8) A specific instance of somewhat special behavior is the recently reported dependence of appearance potentials of certain fragment ions from hydrocarbons on the magnitude of the repeller voltage (L. Friedman, F. A. Long and M. Wolfsberg, *J. Chem. Phys.*, **31**, 755 (1959)). This effect seems, however, to be restricted to fragments formed by loss of hydrogen atoms, a type of process which is not of much importance in the calculations which have led to Table III.

TABLE III
 $\Delta H_f(g)$ VALUES AT 298°K. FOR NEUTRAL SPECIES AND THEIR POSITIVE IONS

Species	Un-ionized			Ionized		
	ΔH_f , e.v.	Qual.	Ref.	ΔH_f , e.v.	Qual.	Ref.
H	+2.259	1	16	+15.854	1	11
H ₂	0.000	+15.422	S	13
O	+2.557	S	17	+16.171	1	11
OH	+0.387	S	18, 68	+13.57 ^a	2	19
H ₂ O	-2.506	1	16	+10.11	S	20
H ₃ O				+9.0	3	21
O ₂	0.000	+12.075	1	6
HO ₂	+0.2	3	22	+11.8	3	22
H ₂ O ₂	-1.410	1	69	+9.8 ₆	2	23
CH	+6.16	1	16	+17.29	S	24
CH ₂	+2.5 ^b	3	25, 26	+14.4 ^b	3	25
CH ₃	+1.39	1	16	+11.23	S	27
CH ₄	-0.7758	1	16	+12.20	1	6
CO	-1.146	1	16	+12.85	S	13
HC=O	~0	3	28, 29, 30	+9.6	3	42
H ₂ C=O	-1.20	1	16	+9.68	S	31
CH ₃ O	-0.0 ₂	2	32	+9.2	3	21
CH ₂ OH	-0.4	3	33	+7.8 ^c	3	4
CH ₃ OH	-2.085	1	16	+8.76	1	6
CO ₂	-4.079	1	16	+9.71	S	12
HC(=O)O	-1.84(?)	3	9	+7.2	3	21
-C(=O)OH	-1.7	3	21	+7.0	3	21
HCOOH	-3.919 ^c	1	15	+7.13	1	6
HCOOH ₂				+5.0 ^f	3	9
HC≡C	+5.0	3	74	+17.9	3	34
C ₂ H ₂	+2.350	1	16	+13.75	S	35
C ₂ H ₃	+2.8 ₃	2	36	+12.2 ₂	2	36
C ₂ H ₄	+0.5419	1	16	+11.05	S	37
C ₂ H ₅	+1.1 ₀	2	38	+9.8 ₈	2	39
C ₂ H ₆	-0.8775	1	16	+10.77	1	6
CH ₂ =C=O	-0.633	1	16	+8.97	S	40
CH ₃ C=O	-0.47	2	41	+7.4 ₁	2	42
CH ₂ =CH-O				+8.8	3	21, 42
CH ₂ -CH=O						
CH ₃ CHO	-1.724	1	16	+8.51	S	43
$\overline{\text{CH}_2\text{CH}_2\text{-O}}$	-0.5286	1	16	+10.04	1	6
C ₂ H ₅ O	-0.3 ₇	2	32	+8.8	3	9
C ₂ H ₄ OH	-0.7	3	33	+6.3 ^g	3	4
CH ₂ OCH ₃				+7.3	3	21
CH ₃ OCH ₃	-1.92	1	16	+8.08	1	6
C ₂ H ₅ OH	-2.439	1	16	+8.04	1	6
CH ₃ C(=O)O	-1.9 ₅	2	44			
-C(=O)OCH ₃				+6.7 ^h	3	9
HCOOCH ₃	-3.63	1	16	+7.19	1	6
CH ₃ COOH	-4.57	1	16, 45	+5.80	1	6
CH ₃ COOH ₂				+3.4 ^k	3	21
HOCH ₂ CH ₂ OH	-4.0 ₂ ^l	2	16			
CH ₃ C≡C				+11.5 ^m	3	34
CH ₂ =C=CH				+11.3 ⁿ	3	46
CH ₂ -C≡CH						
CH ₃ C≡CH	+1.922	1	48	+12.28	1	6
CH ₂ =C=CH ₂	+1.991	1	48	+12.18	S	49
CH ₂ -CH=CH ₂	+1.3 ₀	2	38	+9.4 ₆	2	50
CH ₃ CH=CH						
CH ₃ -C=CH ₂						
C ₃ H ₆	+0.2116	1	48	+9.94	1	6
$\overline{\text{H}_2\text{CCH}_2\text{CH}_2}$	+0.42	1	51	+10.48	1	6
CH ₃ CHCH ₃	+0.7 ₃	2	52	+8.6 ₅	2	39
CH ₃ CH ₂ CH ₂	+0.9 ₆	2	53	+9.6 ₅	2	54
C ₃ H ₈	-1.076	1	48	+9.99	1	6
CH ₂ =CHCHO	-1.0 ^l	3	51	+9.10	S	55
HC≡CC ₂ H ₄ OH	+0.44	1	51			

TABLE III (Continued)

Species	Un-ionized			Ionized		
	ΔH_f , e.v.	Qual.	Ref.	ΔH_f , e.v.	Qual.	Ref.
$C_2H_4-C=O$				+ 9.3	3	21
$CH_3CH_2C=O$				+ 6.6	3	42
$CH_3C(=O)CH_3$	-2.25	1	56	+ 7.44	1	6
$CH_2=CHCH_2OH$	-1.4 ^t	3	51	+ 8.2 ₇	1	6
$CH_3CH_2CH=O$	-2.11	1	51	+ 7.87	1	6
CH_3CHCH_2-O	-0.955	1	70	+ 9.27	1	6
$CH_3OCH=CH_2$	-1.2	3	57	+ 7.7 ₃	1	6
C_3H_6OH				+ 6.3	3	4
$CH_3CH_2CH_2O$	-0.5 ₆	2	32	+ 7.5	3	21
$(CH_3)_2CHO-$	-0.7 ₈	2	32			
<i>n</i> -C ₃ H ₇ OH	-2.70	1	71	+ 7.50	1	6
<i>i</i> -C ₃ H ₇ OH	-2.843	1	72, 73	+ 7.32	1	6
$CH_3OC_2H_5$	-2.26	1	51			
$CH_2=CHCOOH$	-3.4 ^t	3	51	+ 7.5	3	58
C_2H_4COOH				+ 4.7	3	21
$C_2H_5C(=O)O$	-2.3 ₄	2	44			
C_2H_6COOH	-4.7 ₅ ^t	2	59	+ 5.49	1	6
$HCOOC_2H_5$	-3.85	1	51	+ 6.76	1	6
CH_3COOCH_3	-3.88	1	51	+ 6.39	1	6
$CH_2(OCH_3)_2$	-3.7 ^t	3	51	+ 6.3 ₆	1	6
$CH_3C\equiv CCH_2$	+2.8	3	74	+11.5	3	34
$CH_2=CHCH=CH_2$	+1.142	1	48	+10.205	8	60
$CH_2=C=CH_2CH_3$	+1.681	1	48	+11.2 ₅	2	46
$C_2H_5C\equiv CH$	+1.712	1	48	+11.89	1	6
$CH_3C\equiv CCH_3$	+1.516	1	48	+11.3 ₇	2	61
C_4H_7	+0.8 to 1.1 ["]	3	62, 63	+ 8.8	3	62
$CH_2=CHC_2H_5$	-0.0013	1	48	+ 9.58	1	6
$CH_2=C(CH_3)_2$	-0.175	1	48	+ 9.06	1	6
$CH_3CH=CHCH_3$ (<i>cis</i>)	-0.0724	1	48	+ 9.06	1	6
$CH_3CH=CHCH_3$ (<i>trans</i>)	-0.116	1	48	+ 9.01	1	6
<i>n</i> -C ₄ H ₉	+0.8	3	53	+ 9.4 ₁	2	54
<i>i</i> -C ₄ H ₉	X (unk)			+ 8.35 + X	2	54
<i>s</i> -C ₄ H ₉	Y (unk)			+ 7.93 + Y	2	54
<i>t</i> -C ₄ H ₉	+0.2	3	53	+ 7.6 ₂	2	54
<i>n</i> -C ₄ H ₁₀	-1.307	1	48	+ 9.32	1	6
<i>i</i> -C ₄ H ₁₀	-1.394	1	48	+ 9.18	1	6
$CH_3CH=CHCHO$	-1.3 ^t	3	51	+ 8.4 ₂	1	6
$CH_3OCH_2C\equiv CH$	+0.85	1	51			
$(CH_2=CH)_2O$	-0.14	2	64			
$CH_3C(=O)C_2H_5$				+ 8.4	3	21
$C_2H_5CH_2CHO$	-2.2 ^t	3	65	+ 7.6 ₆	1	6
$(CH_3)_2CHCHO$	-2.29	1	51	+ 7.4 ₅	1	6
$CH_3OCH_2CH=CH_2$	-1.11	1	51			
$CH_3C(=O)-C_2H_5$	-2.5 ₂ ^t	2	73	+ 7.01	1	6
$C_2H_5OCH=CH_2$	-1.4 ₆	2	64			
<i>n</i> -C ₄ H ₉ O	-0.7 ₄	2	32			
$(CH_3)_2CHCH_2O$	-0.7 ₃	2	32			
$C_2H_5CH(CH_3)O$	-0.8 ₇	2	32			
$(CH_3)_3C-O$	-1.1	2	32			
<i>n</i> -C ₄ H ₉ OH	-2.87	1	77	7.17	1	6
<i>i</i> -C ₄ H ₉ OH	-2.94	1	77	+ 7.2	3	66
<i>t</i> -C ₄ H ₉ OH	-3.25	1	77	+ 6.7	3	66
$(C_2H_5)_2O$	-2.618	1	75	+ 6.91	1	6
$HCOOCH_2CH=CH_2$	-2.40	1	51			
$CH_3C(=O)C(=O)CH_3$	-3.39	1	76	+ 5.84	1	6
$CH_3COOCH=CH_2$	-3.2 ^t	3	51	+ 5.9 ₆	1	6
$C_3H_7C(=O)O$	-2.6 ₀	2	44			
<i>n</i> -C ₃ H ₇ COOH	-4.9 ₂ ^t	2	51	+ 5.2 ₁	1	6
<i>i</i> -C ₃ H ₇ COOH	-5.1 ₄ ^t	2	51	+ 4.88	1	6
$CH_3COOC_2H_5$	-4.56	1	51	+ 5.55	1	6
$C_2H_5COOCH_3$	-4.22	1	51	+ 5.93	1	6
$HCOOCH_2C_2H_5$	-4.0	3	67	+ 6.5 ₄	1	6

^a From I.P. of OH radicals. ^b Used A.P. (CH_2^+) from CH_3 to calculate ΔH_f for CH_2^+ and $\text{I}(\text{CH}_2^+)$ from CH_2 to calculate ΔH_f for CH_2 . ^c Used A.P. *m/e* 31 of CH_3OH . ^d Used A.P. *m/e* 29 of HCOOC_2H_5 . ^e Used ΔH vaporization of ref. 15. ^f Used A.P. *m/e* 47 of HCOOC_2H_5 . ^g Used A.P. *m/e* 45 of $\text{C}_2\text{H}_5\text{OH}$. ^h Used A.P. *m/e* 59 of HCOOCH_3 ; see also R. Renaud and L. C. Leitch, *Canad. J. Chem.*, **34**, 179 (1956). ⁱ Used A.P. *m/e* 61 of $\text{CH}_3\text{COOC}_2\text{H}_5$. ^j Data available only for compound in liquid state; corrected to gaseous state using vapor pressure data. ^k Used A.P. *m/e* 39 of 2-butyne. ^l Used 1,2-butadiene and 1-butyne. ^m The range of values is for different species, e.g., $\text{CH}_2=\text{C}-\text{CH}_2$ vs. $\text{CH}_3\text{CH}=\text{CHCH}_2$.



Experimental

The data were taken on a Consolidated Engineering Corporation mass spectrometer, Model 21-401, which had been modified as described previously.^{9,10} The principal features of the appearance potential measurements are the use of the vanishing current method and use of argon, krypton or neon as a calibrating gas. The techniques have been discussed previously.¹⁰ To check the voltage scale the ionization potential of argon was selected as an "absolute" value and the appearance potentials of ten other gases were determined relative to this. They are listed in Table I. The good agreement with literature values for the ionization potentials indicates the absence of consistent errors. The appearance potentials of fourteen other species, previously undetermined, are listed in Table II along with the resulting calculated heats of formation of the ions. All data appearing in Tables I and II are averages of from 3 to 5 runs for each species.

The methyl vinyl ether, argon, carbon dioxide, methane, nitrogen, dimethyl ether and ethylene were purchased from Matheson in lecture bottles and used without further purification. Neon and krypton were obtained from Matheson in breakseal flasks and were of research grade quality. Formic-d acid (99%) was purchased from Volk Radiochemical Company. The remaining organic compounds were purified and distilled before use and were stored in Dry Ice when not in use.

- (9) A. B. King, Ph.D. Thesis, Cornell University, February, 1957.
- (10) A. B. King and F. A. Long, *J. Chem. Phys.*, **29**, 374 (1958).
- (11) C. E. Moore, Natl. Bur. Standards, Circ. No. 467, 1949.
- (12) W. C. Price and D. M. Simpson, *Proc. Roy. Soc. (London)*, **A169**, 501 (1939).
- (13) G. Herzberg, "Molecular Spectra and Molecular Structure. I. Spectra of Diatomic Molecules," D. Van Nostrand Co., New York, N. Y., 1950.
- (14) W. C. Price and W. M. Evans, *Proc. Roy. Soc. (London)*, **A162**, 110 (1937).
- (15) G. C. Sinke, *J. Phys. Chem.*, **63**, 2063 (1959).
- (16) F. D. Rossini, D. D. Wagman, W. H. Evans, W. H. Levine and I. Jaffe, Natl. Bur. Standards, Circ. No. 500, 1952.
- (17) P. Brix and G. Herzberg, *J. Chem. Phys.*, **21**, 2240 (1953).
- (18) R. F. Barrow, *Arkiv Fysik*, **11**, 281 (1956).
- (19) S. N. Foner and R. L. Hudson, *J. Chem. Phys.*, **25**, 602 (1956).
- (20) W. C. Price, *ibid.*, **4**, 147 (1936).
- (21) This research.
- (22) S. N. Foner and R. L. Hudson, *J. Chem. Phys.*, **23**, 1364 (1955).
- (23) L. P. Lindemann and J. C. Guffy, *ibid.*, **29**, 247 (1958).
- (24) A. E. Douglas and G. Herzberg, *Can. J. Research*, **A20**, 71 (1942).
- (25) A. Langer, J. A. Hipple and D. P. Stevenson, *J. Chem. Phys.*, **22**, 1836 (1954).
- (26) J. D. Waldron, *Trans. Faraday Soc.*, **50**, 102 (1954).
- (27) G. Herzberg and J. Shoosmith, *Can. J. Phys.*, **34**, 523 (1956).
- (28) F. H. Dorman and A. S. Buchanan, *Austral. J. Chem.*, **9**, 25 (1956).
- (29) L. Schoen, 5th Intern. Symposium on Combustion, p. 787, 1955.
- (30) R. I. Reed, *Trans. Faraday Soc.*, **52**, 1195 (1956).
- (31) W. C. Price, *J. Chem. Phys.*, **3**, 256 (1935).
- (32) P. Gray, *Trans. Faraday Soc.*, **52**, 344 (1956).
- (33) Reference 5, p. 137.
- (34) F. H. Coates and R. C. Anderson, *J. Am. Chem. Soc.*, **77**, 895 (1955).
- (35) W. C. Price, *Phys. Rev.*, **47**, 444 (1935).
- (36) A. G. Harrison and F. P. Lossing, *J. Am. Chem. Soc.*, **82**, 519 (1960).
- (37) W. C. Price and W. T. Tuttle, *Proc. Roy. Soc. (London)*, **A174**, 207 (1940).
- (38) M. Szwarc, *Chem. Revs.*, **47**, 75 (1950).
- (39) J. B. Farmer and F. P. Lossing, *Can. J. Chem.*, **33**, 861 (1955).
- (40) W. C. Price, J. P. Teegan and A. D. Walsh, *J. Chem. Soc.*, 920 (1951).
- (41) M. Szwarc and J. Taylor, *J. Chem. Phys.*, **23**, 2310 (1955).
- (42) J. R. Majer, C. R. Patrick and J. C. Robb, *Trans. Faraday Soc.*, **57**, 14 (1961).
- (43) A. D. Walsh, *Proc. Roy. Soc. (London)*, **A185**, 176 (1946).
- (44) L. Jaffe, E. J. Prosen and M. Szwarc, *J. Chem. Phys.*, **27**, 416 (1957).
- (45) J. O. Halford, *ibid.*, **9**, 859 (1941).
- (46) J. Collin and F. P. Lossing, *J. Am. Chem. Soc.*, **79**, 5848 (1957).
- (47) J. B. Farmer and F. P. Lossing, *Can. J. Chem.*, **33**, 861 (1955).
- (48) F. D. Rossini, K. S. Pitzer, R. L. Arnett, R. M. Baum and G. C. Pimentel, "Selected Values of Physical and Thermodynamical Properties of Hydrocarbons and Related Compounds," Carnegie Press, Pittsburgh, 1953.
- (49) L. H. Sutcliffe and A. D. Walsh, *J. Chem. Soc.*, 899 (1952).
- (50) F. P. Lossing, K. Ingold and I. Henderson, *J. Chem. Phys.*, **22**, 621 (1954).
- (51) M. S. Kharasch, *J. Research Natl. Bur. Standards*, **2**, 359 (1929).
- (52) D. P. Stevenson, *Disc. Faraday Soc.*, **10**, 35 (1951).
- (53) M. Szwarc, *ibid.*, **10**, 336 (1957).
- (54) F. P. Lossing and J. B. de Sousa, *J. Am. Chem. Soc.*, **81**, 281 (1959).
- (55) A. D. Walsh, *Trans. Faraday Soc.*, **41**, 498 (1945).
- (56) C. B. Miles and H. J. Hunt, *J. Phys. Chem.*, **45**, 1346 (1941).
- (57) Estimated from heats of formation of dimethyl ether, diethyl ether and ethyl vinyl ether.
- (58) J. D. Morrison and A. J. Nicholson, *J. Chem. Phys.*, **20**, 1021 (1952).
- (59) E. Schjånberg, *Z. physik. Chem.*, **A172**, 197 (1935).
- (60) W. C. Price and A. D. Walsh, *Proc. Roy. Soc. (London)*, **A174**, 220 (1940).
- (61) J. L. Franklin and F. H. Field, *J. Am. Chem. Soc.*, **76**, 1994 (1954).
- (62) Reference 5, p. 262.
- (63) C. A. McDowell, F. P. Lossing, I. H. S. Henderson and J. B. Farmer, *Can. J. Chem.*, **34**, 345 (1956).
- (64) M. A. Dolliver, T. L. Gresham, G. B. Kistiakowsky, E. A. Smith and W. E. Vaughan, *J. Am. Chem. Soc.*, **60**, 440 (1938).
- (65) Estimated from other aldehyde data.
- (66) I. Omura, K. Higasi and H. Baba, *Bull. Chem. Soc., Japan*, **29**, 504 (1956).
- (67) Estimated from studies of heats of formation of acetates and propionates.
- (68) P. Gray, *Trans. Faraday Soc.*, **55**, 408 (1959).
- (69) P. A. Giguère and I. D. Liu, *J. Am. Chem. Soc.*, **77**, 6477 (1955).
- (70) P. Gray and A. Williams, *Trans. Faraday Soc.*, **55**, 760 (1959).
- (71) F. D. Rossini, *J. Research Natl. Bur. Standards*, **13**, 189 (1934).
- (72) G. S. Parks and B. Barton, *J. Am. Chem. Soc.*, **50**, 24 (1928).
- (73) G. S. Parks, J. R. Mosley and P. V. Peterson, Jr., *J. Chem. Phys.*, **18**, 152 (1950).
- (74) Estimated from data of S. H. Bauer (personal communication).
- (75) Private communication from G. Pilcher, Manchester University.
- (76) G. R. Nicholson, M. Szwarc and J. W. Taylor, *J. Chem. Soc.*, 2767 (1954).
- (77) I. A. Skinner and A. Snolson, *Trans. Faraday Soc.*, **56**, 1776 (1960).
- (78) H. A. Skinner and F. W. Evans, *ibid.*, **55**, 260 (1959).
- (79) C. A. McDowell and J. W. Warren, "Mass Spectrometry," Institute of Petroleum, London, 1952, p. 27.

ACID DISSOCIATION CONSTANTS AND COMPLEX FORMATION CONSTANTS OF SEVERAL PYRIMIDINE DERIVATIVES¹

BY EDMOND R. TUCCI, BR. EDWARD DOODY AND NORMAN C. LI

Duquesne University, Pittsburgh, Pa., and Christian Brothers College, Memphis, Tenn.

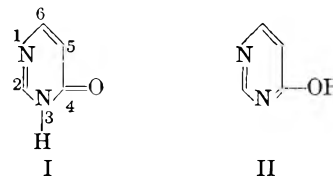
Received April 10, 1961

Acid dissociation constants of uracil-5-carboxylic acid (isoörotic acid), 2-ethylthio-isoörotic acid, uracil-6-carboxylic acid (orotic acid), 5-nitroörotic acid and adenosine-5'-monophosphate have been determined at an ionic strength of 0.1, 25°. The formation constants of the Cu(II), Ni(II), Co(II), Zn(II), Mn(II), Cd(II) complexes of some of these pyrimidine derivatives were determined using pH and ion-exchange methods. The binding sites in uracil-5-carboxylic acid and 2-ethylthio-isoörotic acid toward metal ions are probably the carboxylate anion and the adjacent oxygen atom. The postulated sites in 5-nitroörotic acid toward metal ions and uracil-6-carboxylic acid toward Ni ion are the carboxylate and adjacent ring nitrogen anions. The formation constants of the zinc complexes of uracil-5-carboxylic acid and 5-nitroörotic acid, and of the sodium and manganese complexes of adenosine-5'-zinc monophosphate obtained by the pH method are in agreement with the corresponding values obtained by the ion-exchange method, indicating that these complexes are mononuclear.

Introduction

The pyrimidine derivatives constitute a very important class of compounds because they are components of nucleic acids and various enzymes, because they exert a pronounced physiological action, and because they pose some interesting problems of structure. As part of a general program on studies of metal complexation with compounds of biological interest, this paper presents the results on the acid dissociation constants and formation constants of metal complexes of a number of pyrimidine derivatives: uracil-5-carboxylic acid (isoörotic acid), 2-ethylthio-isoörotic acid, uracil-6-carboxylic acid (orotic acid), 5-nitroörotic acid,² and adenosine-5'-monophosphoric acid.

The outstanding structural problem of the pyrimidines is the tautomerism possible between the ketonic and enolic forms (lactam-lactim). Considerable data on ultraviolet and infrared absorption spectra have been reported^{3,4} and there is general agreement that the preferred structure for the pyrimidines is the ketonic form rather than the enolic form. Thus Lacher, *et al.*,^{3a} found that a strong absorption band at 1.43 μ , corresponding to the first O-H stretching overtone in phenol, was lacking in uracil and its derivatives. Absorption was found in the region corresponding to the first N-H overtone, 1.50 μ , for uracil and 5-chlorouracil, and again at 1.99–2.00 μ indicating a second carbonyl overtone vibration which lies in this region. Brown and Short,^{3b} from ultraviolet and pH data, conclude that in aqueous solution the 4-"hydroxypyrimidine" exists predominantly in the ketonic (lactam) form, I, rather than the enolic (lactim) form, II.

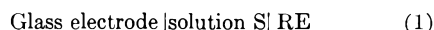


Experimental

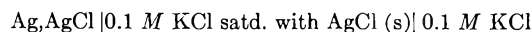
Materials.—The pyrimidine derivatives, gifts of Sigma Chemical Co., St. Louis, Mo., were dried *in vacuo* at room temperature over calcium chloride. Stock solutions of these, always freshly prepared, were analyzed by determination of their neutralization equivalents using potentiometric methods. Solutions of metal salts were prepared and analyzed by conventional means. All chemicals were of C.P. grade.

Carrier-free Mn-54 and Na-22 were obtained from Nuclear Science and Engineering Corp., Pittsburgh, Pa. High activity Zn-65 was obtained from Oak Ridge National Laboratory in the form of zinc chloride in HCl solution. For the cation-exchanger, Dowex-50, 8% cross-linked, 100–200 mesh, was used. The capacity of this type of resin has been found to be independent of pH over a wide pH range.⁵

Apparatus and Procedure.—The hydrogen ion concentration of solution S was determined with the cell



where RE is the reference half-cell



The general design of the cell was that of Forsling, *et al.*, A Beckman Type 40498 glass electrode was used. Ag⁶ AgCl electrodes were prepared by the method described by Biedermann.⁷ The potentials of the cell were read to 0.01 mv. with a Leeds and Northrup Type K potentiometer, using a Cary Model 31 Vibrating Reed Electrometer and a Minneapolis-Honeywell Brown Elektronik strip chart recorder as null point indicator. All measurements were carried out in an oil thermostat controlled to 25 ± 0.02°. The hydrogen ion concentration was obtained from the measured e.m.f. values using the relation

$$E = E' + 59.16 \log h \quad (2)$$

where h , the hydrogen ion concentration, is in mM/l. The determination of the empirical constant E' , which includes corrections for γ_{\pm} , liquid-liquid junction potentials and for deviations of the glass electrode from the Nernst slope, was obtained in the manner described by Tobias.⁸

The titrations were made in the following manner. Exactly 30.00 ml. of a solution with 0.002 M pyrimidine compound, 0.002 M or 0.02 M metal nitrate and sufficient

(1) Abstracted from the Ph.D. thesis of E. R. Tucci at Duquesne University, and supported by National Science Foundation Grant No. NSF G7447 at D.U. and by Atomic Energy Commission Contract No. AT (40-1)-2005 at C.B.C.

(2) In the Sigma Chemical Co. catalog, these compounds carry the names of 5-carboxy-2,4-dihydroxypyrimidine, 5-carboxy-2-ethylmercapto-4-hydroxypyrimidine, 6-carboxy-2,4-dihydroxypyrimidine, and 6-carboxy-5-nitro-2,4-dihydroxypyrimidine, respectively.

(3) (a) J. R. Lacher, D. E. Campion and J. D. Park, *Science*, **110**, 300 (1949); (b) D. J. Brown and L. N. Short, *J. Chem. Soc.*, 331 (1953).

(4) J. R. Loofbourov, M. M. Stimson and M. J. Hart, *J. Am. Chem. Soc.*, **75**, 148 (1953).

(5) W. C. Baumann and J. Eichhorn, *ibid.*, **69**, 2830 (1947).

(6) W. Forsling, S. Hietanen and L. G. Sillen, *Acta Chem. Scand.*, **6**, 901 (1952).

(7) G. Biedermann, *Arkiv Kemi*, **9**, 277 (1956).

(8) R. S. Tobias, *J. Am. Chem. Soc.*, **82**, 1070 (1960).

tetramethylammonium bromide or potassium chloride to keep the total ionic strength 0.1, was pipetted into the titration flask. This solution, designated S in (1), then was titrated with either tetramethylammonium hydroxide or potassium hydroxide. Nitrogen was passed through a 0.1 M tetramethylammonium bromide or potassium chloride solution, and then slowly bubbled through solution S during the titration.

In the ion-exchange method, the Dowex-50 resin was rendered iron-free by percolation with 6 N HCl at room temperature. The ion-exchange technique, except as otherwise noted, has been described previously.⁹ The flasks containing resin and solutions were agitated at $25 \pm 1^\circ$. After a four-hour shaking period, a 4-ml. sample of supernate was removed from each flask for radiochemical analysis using a scintillation well counter.

Results and Discussion

(A) **Acid Dissociation Constants.**—In all the titrations involving the pyrimidine derivatives, sharp breaks in the titration curves were obtained, as indicated in Figs. 1–3. The apparent pK_a values of the pyrimidine derivatives determined at an ionic strength of 0.1, 25° are assembled in Table I. pK_1 refers to proton dissociation from the carboxyl group and pK_2 that from a pyrimidine ring nitrogen. For adenosine-5'-phosphoric acid, pK_1 refers to proton dissociation from the protonated amino group on the pyrimidine ring while pK_2 refers to that from the phosphoric acid group.

It has been shown previously by many workers^{3b,10,11} that the pyrimidines exist predominantly in the ketonic form. Uracil is known to exist in the ketonic form until well above the neutral point, up to pH 9.5. Stimson and Reuter¹² found from ultraviolet absorption spectra that enolization occurs at a somewhat lower pH in isoörotic acid than uracil due to the influence of the carboxyl group. At pH 7.0, they found that the absorption of the uracil band in isoörotic acid is considerably weakened, but the spectra did not indicate an enol shift. In the region of pK_1 , therefore, isoörotic acid may still be regarded as in the ketonic form.

TABLE I
APPARENT DISSOCIATION CONSTANTS OF PYRIMIDINE
DERIVATIVES, $\mu = 0.1$, 25°

Compound	Ionic medium	pK_1	pK_2	pK_2 , lit.
Uracil-6-carboxylic acid (orotic acid)	KCl	2.07	9.45	9.45 ¹³
Uracil-5-carboxylic acid (isoörotic acid)	KCl	4.16	8.89	
2-Ethylthio-isoörotic acid	$(\text{CH}_3)_4\text{NBr}$	6.01	10.52	
5-Nitroörotic acid	$(\text{CH}_3)_4\text{NBr}$	<1.5	4.94	
Adenosine-5'-monophosphate	KCl		6.30	6.32 ¹⁴ (20°) 6.14 ¹⁵

(9) N. C. Li, W. M. Westfall, A. Lindenbaum, J. M. White and J. Schubert, *J. Am. Chem. Soc.*, **79**, 5864 (1957).

(10) L. N. Short and H. Thompson, *J. Chem. Soc.*, 168 (1952).

(11) E. R. Blout and M. Fields, *J. Am. Chem. Soc.*, **72**, 479 (1950).

(12) M. M. Stimson and M. A. Reuter, *ibid.*, **65**, 151 (1943).

(13) D. Shugar and J. J. Fox, *Biochim. et Biophys. Acta*, **9**, 199 (1952).

(14) R. M. Smith and R. A. Alberty, *J. Phys. Chem.*, **60**, 180 (1956).

(15) A. E. Martell and G. Schwarzenbach, *Helv. Chim. Acta*, **39**, 693 (1956).

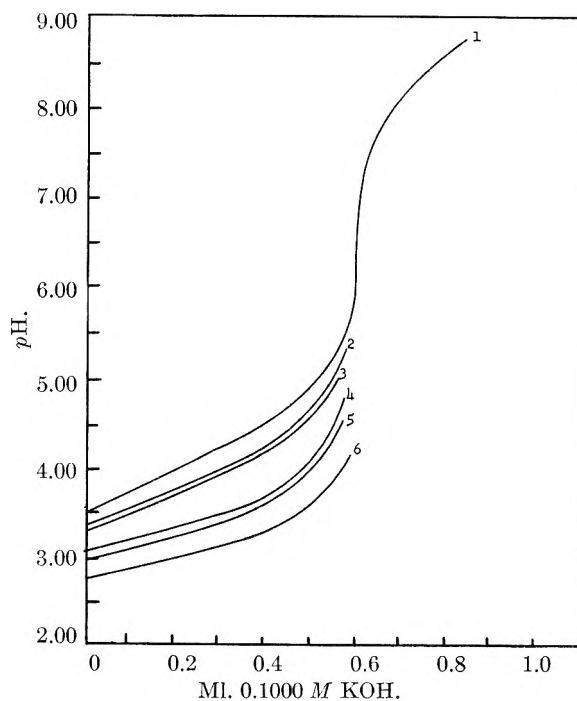
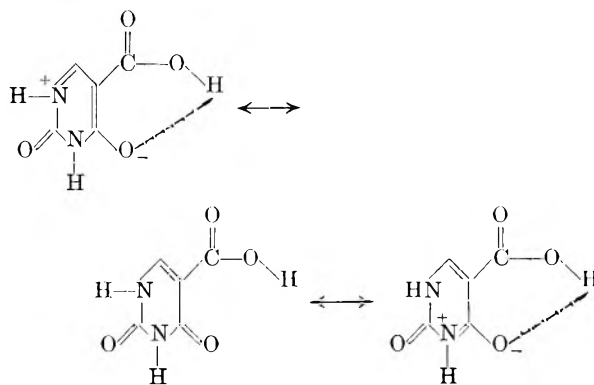


Fig. 1.—Titration of 30.00 ml. of 0.002 M uracil-5-carboxylic acid, 0.02 M divalent metal nitrate, $\mu = 0.1$. Curve 1, no divalent metal; 2, Cd(II); 3, Mn(II); 4, Zn(II); 5, Ni(II); 6, Cu(II).

Isoörotic acid is structurally favorable for intramolecular hydrogen bonding, and resonance enhances the interaction between the carboxyl hydrogen and the adjacent oxygen. The resonance structures are depicted as



and probably account for the higher pK_1 and lower pK_2 values for isoörotic acid as compared to orotic acid. Our value of $pK_2 = 9.45$ for orotic acid is in agreement with that found by Shugar and Fox.¹³ As comparison it is interesting to note that the pK_1 values of uracil, 1-methyluracil and 3-methyluracil are 9.45, 9.99 and 9.71, respectively.¹⁶ The very high values of pK_1 and pK_2 found for 2-ethylthio-isoörotic acid may be ascribed to the positive inductive effect of the ethylthio group.

In 5-nitroörotic acid, because of the negative inductive effect of the adjacent nitro group, one would expect an increase in the acidity of the carboxyl group. This is shown in Table I. The pK_2 of this compound is 4.94, considerably smaller

(16) P. A. Levene, L. W. Bass and H. S. Simms, *J. Biol. Chem.*, **70**, 229 (1926).

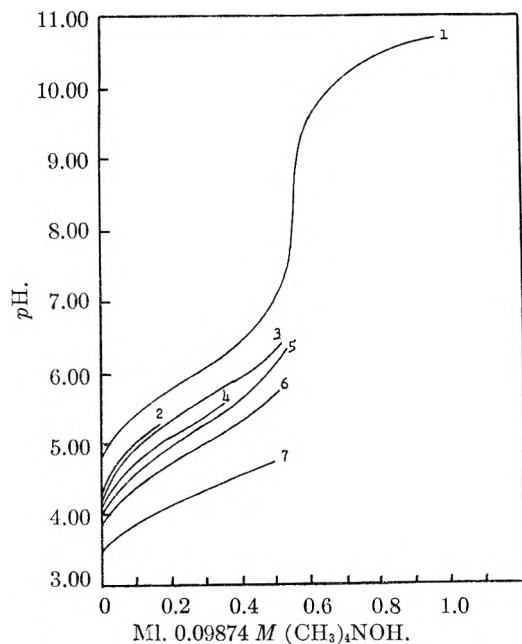


Fig. 2.—Titration of 30.00 ml. of 0.001826 *M* 2-ethylthioisoörotic acid, 0.02 *M* divalent metal nitrate, $\mu = 0.1$: Curve 1, no divalent metal; 2, Cd(II); 3, Mn(II); 4, Zn(II); 5, Co(II); 6, Ni(II); 7, Cu(II).

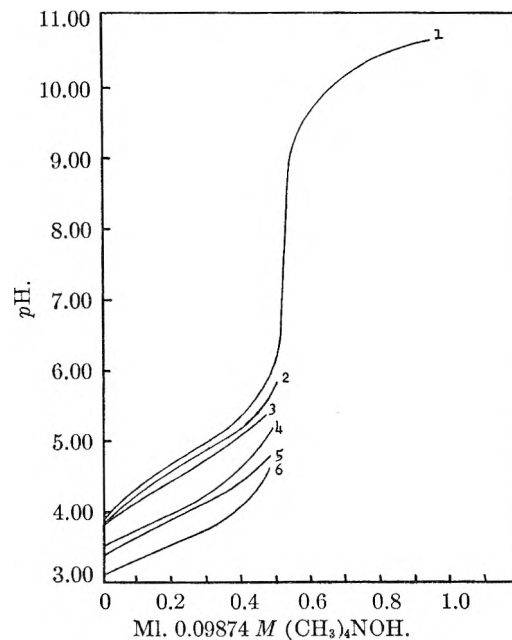
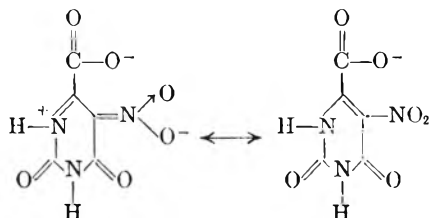


Fig. 3.—Titration of 30.00 ml. of 0.0017 *M* potassium salt of 5-nitroörotic acid, 0.02 *M* divalent metal nitrate, $\mu = 0.1$. Curve 1, no divalent metal; 2, Mn(II); 3, Cd(II); 4, Co(II); 5, Zn(II); 6, Ni(II).

than orotic acid. This can be interpreted in terms of the resonance contribution



Resonance contribution from nitrogen in the 3-position is not significant, so that pK_2 of 5-nitroörotic acid refers predominantly to proton ionization from the nitrogen-1 atom.

The pK_2 values of adenosine-5'-monophosphate, AMP, are in good agreement with those found by Smith and Alberty.¹⁴ The lower value of pK_2 in KCl medium relative to that found in $(\text{CH}_3)_4\text{NBr}$ medium has been ascribed to complexation of AMP by K^+ .¹⁴

(B) Formation Constants of Metal Complexes.

—Table II illustrates the titration data obtained with a mixture of $\text{Zn}(\text{NO}_3)_2$ and 5-nitroörotic acid. A summary of the formation constants of the 1:1 complexes of Cu(II), Ni(II), Co(II), Zn(II), Mn(II), Cd(II) with isoörotic acid, 2-ethylthioisoörotic acid and 5-nitroörotic acid obtained by titration of 1:10 (ligand:metal) molar mixtures is given in Table III.

In the calculation of the formation constants of the isoörotic acid and 2-ethylthioisoörotic acid complexes, the values of pK_1 listed in Table I for these two acids were used. For the formation constant of the 5-nitroörotic acid complex, the value of pK_2 was used. k_1 was calculated by the method described by Li and Chen¹⁷ for titration

(17) N. C. Li and M. C. M. Chen, *J. Am. Chem. Soc.*, **80**, 5678 (1958).

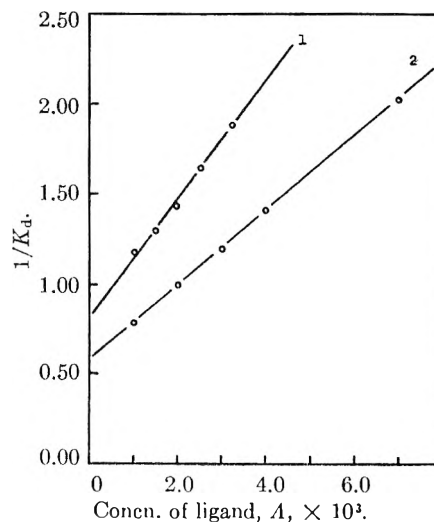


Fig. 4.—Ion-exchange experiments with Zn-65 complexes of: (1) uracil-5-carboxylic acid, pH 4.47; (2) 5-nitroörotic acid, pH 5.15. $\mu = 0.1$, 25°.

TABLE II

30.00 ml. of 0.002 *M* 5-nitroörotic acid, 0.020 *M* $\text{Zn}(\text{NO}_3)_2$, 0.04 *M* $(\text{CH}_3)_4\text{NBr}$, plus *v* ml. of 0.09874 *M* $(\text{CH}_3)_4\text{NOH}$, 25°

<i>v</i> , ml.	pH	log k_1
0.20	3.926	2.52
.25	4.055	2.52
.30	4.192	2.50
.35	4.325	2.50
.40	4.466	2.50
.45	4.632	2.50

Av. 2.51

of 1:10 (ligand:metal ion) molar mixtures. The formation constants of the metal complexes of isoörotic acid were also determined in 1:1 (ligand:metal ion) molar mixtures. The values agree with those listed in Table III to within 0.05 log unit.

TABLE III
FORMATION CONSTANTS OF SEVERAL METAL COMPLEXES OF
PYRIMIDINE DERIVATIVES, $\mu = 0.1, 25^\circ$

	Isoörotic acid	$\log k_1$ 2-Ethylthio- isoörotic acid	5-Nitroörotic acid
Cu(II)	4.12	3.14	
Ni(II)	2.95	2.70	3.04
Co(II)		2.47	2.42
Zn(II)	2.69	2.33	2.51
Mn(II)	2.19	2.07	1.79
Cd(II)	2.02	1.98	1.91

The binding sites in isoörotic acid and 2-ethylthio-isoörotic acid toward the metal ions are probably the carboxylate anion and the adjacent oxygen atom. Because of the positive inductive effect of the ethylthio group, one might expect the metal complexes of 2-ethylthio-isoörotic acid to be more stable than the corresponding isoörotic acid complexes. Table III indicates the reverse to be true. Short and Thompson¹⁰ from infrared data show that in 4-hydroxy-2-methylthio-6-methyl- or 6-amino-4-hydroxy-2-methylthio-pyrimidine, the structure is probably enolic. Therefore if 2-ethylthio-isoörotic acid is enolic whereas isoörotic acid is ketonic, the former complex would be less stable than the latter, since metal binding by oxygen in -OH is probably weaker than by ketonic oxygen. Table III shows that the metal complexes of 2-ethylthio-isoörotic acid are indeed less stable than the corresponding isoörotic acid complexes, for all of the six metal ions investigated.

5-Nitroörotic acid was obtained as the potassium salt, and titration curves of the potassium salt with base are given in Fig. 3. The formation constants listed in Table III for the 5-nitroörotic acid complexes may seem too high, in view of the strong negative inductive effect of the nitro group. However, the binding sites are probably the carboxylate anion and the adjacent ring nitrogen, with the nitrogen having a negative charge because of proton removal. The influence of the nitro group is thus somewhat counterbalanced, and the metal complexes of 5-nitroörotic acid have about the same stability as the isoörotic complexes.

Titration curves of orotic acid in the presence of Ni(II) ion indicate that two protons are released on complexation. In calculating the formation constant of the Ni(II) complex, therefore, both acid dissociation constants, K_1 and K_2 , of orotic acid must be used. The binding sites in orotic acid are probably the carboxylate and the adjacent ring nitrogen anions. The value of $\log k_1$ is calculated to be 6.95 at $\mu = 0.1, 25^\circ$, as compared with $\log k_1 = 5.9$ for the Ni(II) complex of picolinic acid¹⁸ at $\mu \cong 0.02, 25^\circ$. In picolinic acid, the binding sites are taken to be the carboxylate anion and the adjacent ring nitrogen. However, the ring nitrogen is uncharged, so that the picolinic acid complex is not expected to be as stable as the corresponding orotic acid complex.

In order to elucidate the role of the carboxyl group in complexation, the methyl esters of isoörotic acid and of 5-nitroörotic acid were titrated in the absence and presence of metal ions, and only weak

complexation was observed. This indicates the necessity of the carboxylate anion in stabilizing the chelate. A similar drop in metal complexation is observed when glycine ester replaces glycine^{19,20} in the formation of Ni(II) and Cu(II) complexes.

(C) **Ion-exchange Studies.**—Ahrland, *et al.*,²¹ have shown that the complex formation curve is dependent on concentration of metal ion, if polynuclear complexes exist; while if the complex formation curve is independent of metal ion concentration, the complex is mononuclear. In the pH experiments described in section (B), the total metal ion concentration was either 0.02 or 0.002 *M*. In order to obtain a wider range of metal ion concentration for the purpose of deciding whether the complexes are mononuclear or polynuclear, we have carried out several ion-exchange experiments using radioisotopes, where the metal ion concentration is of the order of 10^{-6} *M*.

Figure 4 summarizes the ion-exchange results obtained with Zn-65 complexes of isoörotic acid and 5-nitroörotic acid. K_d is the distribution coefficient defined as

$$K_d = \frac{\% \text{ of tracer metal in resin phase } (M_r)}{\% \text{ of tracer metal in soln. phase } (M_s)} \times \frac{\text{ml. of soln. phase}}{\text{g. of resin}}$$

The formation constants, calculated from the slopes of the lines in the manner described by Li, *et al.*,⁹ were found to be: $\log k_1 = 2.65$ and 2.54 for the isoörotic acid and 5-nitroörotic acid complexes, respectively. These values agree with those listed in Table III for the corresponding complexes to within 0.04 log unit.

Smith and Alberty¹⁴ from pH measurements found that Na^+ complexes with adenosine monophosphate, AMP^{-2} , and that $k_1 = 2.9 \pm 0.4$ at $\mu = 0.2$, on the basis of the assumption that tetrapropylammonium cations do not form complexes. We have carried out ion-exchange experiments at pH 7.0, using tracer Na-22, Dowex-50 resin in the tetramethylammonium form, with the total ionic strength kept constant at 0.25 with tetramethylammonium bromide. In the AMP concentration range of 0.03 to 0.1 *M*, k_1 was calculated to be 2.8 ± 0.1 , in agreement with the pH result of Smith and Alberty.¹⁴

The AMP^{-2} complex with Mn-54 also was studied using the ion-exchange method and Veronal buffer at pH 6.9, $\mu = 0.1, 25^\circ$. The concentration of the sodium diethyl barbiturate in the buffer was 0.009 *M* and it has been shown previously⁹ that at this concentration, correction for any interaction of the Veronal buffer with Mn(II) cation is negligible. The value of $\log k_1$ was calculated to be 2.19, in exact agreement with that obtained by Smith and Alberty²² using the pH method. Phosphoryl oxygen is probably the coordination site in AMP toward Mn(II) ion. This is evidenced

(19) J. M. White, R. A. Manning and N. C. Li, *J. Am. Chem. Soc.*, **78**, 2367 (1956).

(20) I. M. Klotz, I. L. Faller and J. M. Urquhart, *J. Phys. Colloid Chem.*, **54**, 18 (1950).

(21) S. Ahrland, R. Larsson and K. Rosengren, *Acta Chem. Scand.*, **10**, 705 (1956).

(18) F. Holmes and W. R. C. Crimmin, *J. Chem. Soc.*, 1175 (1955).

by the essentially identical value of $\log k_1$ found²³ when Mn-AMP was studied in 99.8% D₂O medium.

The formation constants of the four complexes described in this section, using the ion-exchange method, agree closely with the values obtained

(22) R. M. Smith and R. A. Alberty, *J. Am. Chem. Soc.*, **78**, 2376, (1956).

(23) P. Tang, unpublished results.

using the pH method. Since the difference in the metal ion concentration used in the two methods is clearly very great, the agreement must mean that these complexes are mononuclear.

Acknowledgment.—The authors are indebted to Mr. R. Scrugg and Miss P. Tang for assistance in carrying out the ion-exchange experiments.

THE SONOCHEMICAL REACTIONS OF CARBON TETRACHLORIDE AND CHLOROFORM IN AQUEOUS SUSPENSION IN AN INERT ATMOSPHERE

BY BOJAN HAMLIN JENNINGS AND SUZANNE N. TOWNSEND

Department of Chemistry, Wheaton College, Norton, Massachusetts

Received April 1, 1961

The sonochemical reactions of CCl₄-H₂O mixtures in an argon atmosphere have been investigated and compared with those of HCCl₃-H₂O mixtures. The observed products from the CCl₄ reaction were CO₂, O₂, Cl₂, HCl, C₂Cl₆ and C₂Cl₄. After an initiation period, the rates of formation of certain products were found to be constant: $d(\text{Cl})/dt = 9.6 \mu\text{equiv./min.}$; $d(\text{C}_2\text{Cl}_6)/dt = 4.2 \mu\text{moles/min.}$ (20°); the rate of production of C₂Cl₄ was an order of magnitude slower; the elemental Cl₂ concentration remained essentially constant after the first half hour of reaction. After the initial period, the rate of production of inorganic chlorine was insensitive to a 15° temperature change. The products identified from the HCCl₃ reaction were HCl, C₂Cl₆ and C₂Cl₄: $d(\text{Cl})/dt = 4.1 \mu\text{equiv./min.}$ (20°). Some interrelationships between cavitation and chemical reaction are discussed. A free radical mechanism is proposed to account for the rate data and observed products.

Introduction

In 1927 Richards and Loomis¹ conducted a preliminary experimental survey of the chemical effects of high frequency sound waves. Since that time many chemical reactions have been observed to occur in an ultrasonic field.² Addition, hydration, hydrolysis,³ decomposition,⁴ oxidation,⁵ reduction,⁶ and rearrangements⁷ are among the types of reaction reported to be initiated or accelerated by ultrasound. Polymerization⁸ and depolymerization⁹ reactions also have been investigated under various conditions.

Recently there have been several successful attempts to interpret experimental results on the basis of free radical reaction mechanisms.¹⁰⁻¹³ This

suggests the possible use of ultrasound as a means of generating free radicals at room temperature.

In order to gain further insight into the nature of ultrasonic reactions, we investigated the effects of ultrasonic energy on a relatively simple system, carbon tetrachloride-water in an inert atmosphere. Although mixtures of CCl₄-H₂O, with added KI, were among the first to receive attention in ultrasonic chemistry,^{11,14} the reactions of CCl₄ alone in aqueous suspension have been the object of but little research. It has been recognized¹⁵⁻¹⁶ that oxidation occurs, but mechanistic studies, in the absence of air, have never been made. We have attempted to characterize all the products generated when CCl₄-H₂O mixtures are ultrasonicated and have followed the rate of production of some of the major components. We have compared these results with those obtained from HCCl₃-H₂O under the same reaction conditions. Such analyses should increase our understanding of the nature of the reaction intermediates.

Experimental

Apparatus.—Cylindrical glass vessels, 8'' long and 2'' in diameter, used for all rate experiments, were furnished with essentially sound transparent bottoms made of 50 gauge Saran (Dow Chemical Co.). Each vessel top was provided with a gas outlet tube, an inlet tube and a thermometer; the latter two were raised above the liquid surface during ultrasonic runs to minimize non-reproducible sonic reflections. Glass bottomed vessels were used for runs on which qualitative tests for CO₂ and O₂ were made.

The source of sound energy for most of the experiments

(1) W. T. Richards and A. L. Loomis, *J. Am. Chem. Soc.*, **49**, 3086 (1927).

(2) A comprehensive bibliography of ultrasonic chemical reactions covering the literature through 1949 is given by A. Weissler, *J. Acoust. Soc. Amer.*, **25**, 651 (1953). References to more recent work are found in subsequent footnotes.

(3) D. Thompson, F. C. Vilbrandt and W. C. Gray, *ibid.*, **25**, 485 (1953).

(4) D. L. Currell and L. Zechmeister, *J. Am. Chem. Soc.*, **80**, 205 (1958).

(5) (a) A. I. Virtanen and N. Ellfolk, *Acta Chem. Scand.*, **4**, 93 (1950); (b) P. Renaud, *J. chim. phys.*, **50**, 136 (1953); (c) R. O. Prudhomme, *ibid.*, **54**, 332 (1957).

(6) A. V. Sokol'skaia and I. E. El'piner, *Soviet Phys.: Acoustics*, **3**, #3, 313 (1957).

(7) C. W. Porter and L. Young, *J. Am. Chem. Soc.*, **60**, 1497 (1938).

(8) (a) A. S. Ostroski and R. B. Stambaugh, *J. Appl. Phys.*, **21**, 478 (1950); (b) O. Lindstrom and O. Lamm, *J. Phys. Colloid Chem.*, **55**, 1139 (1951); (c) R. Schulz, G. Renner, A. Henglein and W. Kern, *Makromol. Chem.*, **12**, 20 (1954).

(9) (a) R. O. Prudhomme, *J. chim. phys.*, **47**, 795 (1950); (b) H. H. G. Jellinek, *J. Polymer Sci.*, **22**, 149 (1956); (c) M. A. K. Mostafa, *ibid.*, **33**, 295, 311, 323 (1958); (d) W. Roberts, E. Yeager and F. Hovorka, Tech. Rept. 18, Office of Naval Research Ultrasonics Research Laboratory, Western Reserve University, Cleveland, Ohio, 1957.

(10) A. R. Schulz and A. Henglein, *Z. Naturforsch.*, **8B**, 160 (1953); (b) P. Alexander and M. Fox, *J. Polymer Sci.*, **12**, 533 (1954); (c) see also ref. 5c and 8b.

(11) A. V. M. Parke and D. Taylor, *J. Chem. Soc.*, 4442 (1956).

(12) M. Del Duca, E. Yeager, M. O. Davies and F. Hovorka, *J. Acoust. Soc. Amer.*, **30**, 301 (1958).

(13) A. Weissler, *J. Am. Chem. Soc.*, **81**, 1077 (1959).

(14) A. Weissler, H. W. Cooper and S. Snyder *ibid.*, **72**, 1769 (1950); and literature referred to herein.

(15) (a) A. Kling and R. Kling, *Compt. rend.*, **223**, 1131 (1946); (b) S. Prakash and S. C. Srivastava, *Z. physik. Chem. (Leipzig)*, **208**, 127 (1958); (c) M. R. Levy, *Nature*, **185**, 159 (1960).

(16) S. C. Srivastava, *ibid.*, **182**, 47 (1958).

was a Birtcher Medical Ultrasonic Generator, Megason Model 110, modified to by-pass the timer. This unit operates at a frequency of 1 mc./sec. with a rated electrical output of 15 watts (3 watts/cm.²). The corresponding acoustical power inside the reaction vessel was 6.1 watts as measured by substitution calorimetry.¹⁷ The runs used for CO₂ and O₂ analyses were carried out on a more powerful General Electric Ultrasonic Generator, Model GEI-29578, 300 kc./sec., 75 ma. plate current; acoustical power received by the reacting solution through glass bottomed vessels, 5.0 watts.¹⁷ It was established by experiment that the difference in frequency between the two units did not affect the nature of the products.

Procedure.—Before use, distilled water was boiled for at least an hour and aspirated (~2 cm. Hg) for at least 45 min. 99.99% pure commercial argon (Linde Air Products), further purified by passage through a train containing Fieser's solution,¹⁸ saturated lead acetate solution, and Ascarite, was used to pump the deaerated water through a suitable pipet into the reaction vessel from which air previously had been swept by a stream of argon.

Spectroscopic or analytical grade CCl₄ and HCCl₃ (Matheson, Coleman and Bell) were deaerated by boiling just prior to use, rapidly cooled to 20°, and added by pipet through a capillary adapter to the water in the reaction vessel while a continuous flow of argon saturated the system. Inlet and outlet tubes were closed and the vessel seated directly on the quartz transducer in a thermostated water-bath, a thin layer of water serving as a coupling liquid. Reactions were allowed to proceed for time periods from 15 min. to 3 hr.

Analytical. (A) Trichloroacetic Acid and Chloroform.—The reliability of Fujiwara's colorimetric test¹⁹ for HCCl₃ and hydrolytic precursors thereof was confirmed using a series of known mixtures. Reported sensitivity is 1 p.p.m. HCCl₃ in H₂O. Twelve ml. emulsified reaction mixture was treated with 6 ml. of 10% NaOH and 4 ml. of colorless pyridine.

(B) Oxygen.—The gas above the reacted mixture was displaced by means of deaerated water into a basic pyrogallol solution²⁰ prepared and protected under argon.

(C) Carbon Dioxide.—Gas above the reacted mixture was displaced by means of deaerated water into a Ba(OH)₂ solution protected by an argon atmosphere. The base was also added directly to the ultrasonated mixture.

(D) Hydrogen Peroxide.—Titanium sulfate served as a sensitive reagent for determination of H₂O₂.²¹ 0.3 ml. of titanium solution^{21b} was added, with thorough mixing, to 3 ml. of aqueous reaction mixture and the % T at 410 mμ was read on a Beckman DU spectrophotometer (1 cm. cells) against a blank of untreated reaction mixture. This procedure also served as a check that the water used had been thoroughly freed of air; traces of nitrites formed during ultrasonic reaction²² caused the Ti-H₂O₂ complex to fade rapidly. The precision of this colorimetric method is approximately 0.1% as estimated from standard curve determinations with samples of known H₂O₂ concentration. The results from ultrasonic runs used to obtain the rate constant for peroxide production were reproducible within 3%.

(E) Total Inorganic Chlorine. (1) CCl₄ Reactions.—Ca. 5 ml. of 6 N NH₄OH was introduced directly into the reacted mixture,²² the closed vessel agitated and the fumes allowed to settle before transference to an erlenmeyer flask. Additional NH₄OH was put in to repress hydrolysis of the NH₄Cl, the solution evaporated to a suitably low volume and diluted quantitatively to 100 ml. Aliquots were titrated with standard 0.01 N Hg(NO₃)₂ solution using diphenylcarbazone-brom phenol blue mixed indicator.²³ (2) HCCl₃

Reactions.—After the ultrasonated emulsion had separated, 5-ml. aliquots were withdrawn directly from the aqueous phase and titrated as above.²³ Determination of Cl⁻ with Hg(NO₃)₂ is precise to ca. 0.1%; greater error attended the analyses of ultrasonic runs: values averaged for calculation of rate constants were within 10%.

(F) Elemental Chlorine.—The pale yellow CCl₄ reaction mixture was agitated to redissolve any Cl₂ which may have been ultrasonically expelled from the liquid. The whole then was titrated, after transference to an erlenmeyer containing excess KI, against standard 0.01 N Na₂S₂O₃ using the CCl₄ as the indicator. The titration is precise to at least 0.1%; analyses of ultrasonic runs were within 4%.

(G) Total Acidity.—(H⁺) was determined by titration with standard base. Error in results paralleled the error for chloride determination.

(H) Organic Constituents.—C₂Cl₆ was isolated many times from the organic layer as a pure white solid; m.p. 186.9–187.4° in a sealed tube; mixed m.p. with commercial C₂Cl₆ (Matheson, Coleman and Bell) 186–187.5°. Quantitative gas chromatographic analyses were made with a modified Reco Distillograph Model D-2000 (Research Specialties, Richmond, California) using the organic layers left after thiosulfate titration of the entire mixture. For C₂Cl₆ determinations a Silicone GE-SF96 (Wilkins Instrument and Research, Inc., Walnut Creek, Calif.) column packing was used; 9', 1/4" diam. tubing; column temp. 138–142°; carrier gas (He) flow: 28 ml./min.; 1-decene as internal standard. For C₂Cl₄ determinations, the column packing used was Silicone DC-11 (Research Specialties); 8', 1/4" diam. tubing; temp. 90–94°; carrier gas (He) flow: 28 ml./min.; *m*-xylene as internal standard. Peak heights were measured. The precision of the gas chromatographic method itself, estimated from chromatograms made with known amounts of C₂Cl₄ or C₂Cl₆ and internal standard, is within ca. 3%. Less precision (to within ~5%) accompanied the analyses of ultrasonated material because the organic aliquots were slightly wet, being withdrawn by syringe from an aqueous-organic system. The error in C₂Cl₄ determinations, especially for short runs, was much greater than the error in C₂Cl₆ determinations because of the significantly smaller amounts of C₂Cl₄ and correspondingly lower peak heights.

Results

Results of analyses for products from the ultrasonation of CCl₄-H₂O and HCCl₃-H₂O in an inert atmosphere are summarized in Table I. Table II includes the rate data for formation of certain products from the chlorinated hydrocarbons and for peroxide production from deaerated water under the same conditions.

The absence of CCl₃COOH, or HCCl₃ from among the CCl₄ products is noteworthy. No chlorinated hydrocarbons other than C₂Cl₆ and C₂Cl₄ were detected although the gas chromatograms were carefully searched for their presence.

In contrast to the CCl₄ system, no CO₂, Cl₂, or any other oxidizing agent was ever found among the products from HCCl₃. Trace amounts of O₂ were detected as compared with the relatively large amounts formed from the CCl₄ reaction. Much less C₂Cl₆ was produced from HCCl₃ than from CCl₄; trace amounts of C₂Cl₄ were formed; no other chlorinated hydrocarbons were detected.

Table III shows how variation in amount of reagents affects the yield.

Discussion

Precision and Reproducibility of Results.—Throughout the history of ultrasonic reactions there has been persistent recurrence of difficulties in obtaining quantitatively reproducible results. The present investigation offers no exception. Divergence in results as great as 30% occurred more often than would be expected on a statistical basis. Such deviant data were discarded and the

(17) The acoustical energy measurements were made by Josephine N. McFadden working under National Science Foundation Undergraduate Research Participation Grant No. EO/3/43-1427, summer, 1960.

(18) L. F. Fieser "Experiments in Organic Chemistry," 3rd ed., D. C. Heath and Co., Boston, Mass., 1955, p. 299.

(19) K. Fujiwara, *Sitz. Nat. Ges. Rostock*, **6**, 33 (1916); *C. A.*, **11**, 3201 (1917).

(20) D. D. Williams, C. H. Blachly and R. R. Miller, *Anal. Chem.*, **24**, 1819 (1952).

(21) (a) G. M. Eisenberg, *Ind. Eng. Chem., Anal. Ed.*, **15**, 327 (1943); (b) A. Weissler, *ibid.*, **17**, 695 (1945).

(22) N. H. Furman, ed., "Scott's Standard Methods of Chemical Analysis," 5th ed., D. Van Nostrand Co., Inc., New York, 1939, p. 264.

(23) F. E. Clarke, *Anal. Chem.*, **22**, 553 (1950).

TABLE I

OBSERVED PRODUCTS FROM THE ULTRASONORATION OF AQUEOUS CCl_4 AND HCCl_3 IN AN ARGON ATMOSPHERE

Reactants	CO_2^a	O_2^a	H_2O_2^a	$\text{CCl}_3\text{COOH}^a$	Products HCCl_3^a	Cl_2^b	Cl^-^b	H^+^c	C_2Cl_6^b	C_2Cl_4^b
2 ml. HCCl_3 , 20 ml. H_2O	0	trace	0	0	+	+	trace	+
2 ml. CCl_4 , 20 ml. H_2O	+	+	0	0	0	+	+	+	+	+

^a Qualitative tests on 2 hr. runs, 20°. ^b Quantitative determinations on runs from 15 min. to 3 hr.; see Table II for rates. ^c Quantitative determinations on 2 hr. runs only; in all analyses (H^+) = (Cl^-).

TABLE II

OBSERVED RATES OF APPEARANCE OF PRODUCTS FROM ULTRASONORATION OF CCl_4 , HCCl_3 AND H_2O IN AN ARGON ATMOSPHERE; 6.1 WATTS ACOUSTICAL POWER; 1 MC./SEC. FREQUENCY

Substrate	Temp., °C.	Rate	Standard error	No. of time intervals for which data were obtained	Remarks
2 ml. CCl_4 , 20 ml. H_2O	20	$\frac{d(\text{Cl})}{dt} = 9.6$ μequiv./min.	±0.45	8 (from 15- 180 min.)	Total (Cl) includes (Cl^-) plus converted Cl_2 . Initial non-linear rate faster than steady state linear rate established after ~40 min. at 20° and ~25 min. at 35°. Initial rate slower at 35° than at 20°.
	35	$\frac{d(\text{Cl})}{dt} = 9.6$ μequiv./min.	...	4 (from 15- 180 min.)	(Cl) _{40 min.} ^{20°} = 7.0×10^{-4} eq.; (Cl) _{180 min.} ^{20°} = 20.5×10^{-4} eq. (Cl) _{26 min.} ^{35°} = 3.7×10^{-4} eq.; (Cl) _{180 min.} ^{35°} = 18.6×10^{-4} eq.
2 ml. CCl_4 , 20 ml. H_2O	20	$\frac{d(\text{Cl}_2)}{dt} = 0.5$ μequiv./min	±0.14	16 (from 15-180 min.)	Initial non-linear rate faster than steady state linear rate established after ~30 min. (Cl_2) _{20 min.} = 1.5×10^{-4} eq.; (Cl_2) _{180 min.} = 2.2×10^{-4} eq.
2 ml. CCl_4 , 20 ml. H_2O	20	$\frac{d(\text{C}_2\text{Cl}_6)}{dt} = 4.2$ μmoles/min.	±0.25	9 (from 40- 180 min.)	Initial non-linear rate slower than steady state linear rate established after ~40 min. (C_2Cl_6) _{40 min.} = 0.6×10^{-4} moles; (C_2Cl_6) _{180 min.} = 6.5×10^{-4} moles
2 ml. CCl_4 , 20 ml. H_2O	20	$\frac{d(\text{C}_2\text{Cl}_4)}{dt} = 0.3$ μmoles/min.	...	4 (from 90- 180 min.)	Concn. too low to measure before 90 min. Precision of all data low (see Experimental); actual results (av. moles): 90 min. 0.8×10^{-5} ; 120 min. 1.4×10^{-5} 150 min. 2.1×10^{-5} ; 180 min. 3.1×10^{-5} moles
2 ml. HCCl_3 , 20 ml. H_2O	20	$\frac{d(\text{Cl}^-)}{dt} = 4.1$ μequiv./min.	±0.22	7 (from 15- 120 min.)	Initial non-linear rate faster than steady state linear rate established after ~15 min. (Cl^-) _{16 min.} = 1.1×10^{-4} eq.; (Cl^-) _{120 min.} = 5.4×10^{-4} eq.
20 ml. de-aerated H_2O	20	$\frac{d(\text{H}_2\text{O}_2)}{dt} = 6.6 \times 10^{-2}$ μmoles/min.	...	5 (from 10- 120 min.)	H_2O_2 production started slowly, rose comparatively rapidly and tapered off to steady state linear rate after ~40 min. Early reaction faster at 35° than at 20°.
	35	$\frac{d(\text{H}_2\text{O}_2)}{dt} = 6.6 \times 10^{-2}$ μmoles/min.	...	4 (from 15- 120 min.)	(H_2O_2) _{40 min.} ^{20°} = 4.0 μmoles; (H_2O_2) _{120 min.} ^{20°} = 9.3 μmoles (H_2O_2) _{40 min.} ^{35°} = 5.0 μmoles; (H_2O_2) _{120 min.} ^{35°} = 10.3 μmoles

TABLE III

EFFECTS OF VARIOUS AMOUNTS AND RATIOS OF CCl_4 - H_2O ON YIELD OF TOTAL INORGANIC CHLORINE; 2 HOUR RUNS; 20°

Ml. CCl_4	Yield, equiv. Cl $\times 10^4$	
	20 ml. H_2O	100 ml. H_2O
10.0	...	16.1
5.0	...	17.0
3.0	...	16.0
2.0	14.7	16.1
0.4	14.5	...
0.2	15.2	15.3

precision of the information used for calculation of rates is indicated above (see Experimental).

The causes of these large deviations lie not in the analytical procedures themselves but in some aspect of the ultrasonic procedure. At least three sources of error can be suggested. (1) Unless the coupling of the transducer to the reaction vessel is identical from run to run there will be variations in the intensity of the sound reaching the reacting medium with consequent variations in the yield. The use of Saran-bottomed vessels greatly facilitates, but does not guarantee, reproducibility in coupling. (2) A high frequency generator does not maintain absolutely constant electrical output; the acoustical output varies accordingly. Ideally the reacting system should be monitored constantly by some suitable energy detector and compensation should

be made for fluctuations in sound intensity. (3) The amount of gas dissolved in the reacting liquids at the start of reaction is apparently significant. When care was taken to thermostat the water at 20° during argon saturation just prior to reaction, the analytical results (H₂O₂) were precise within 2-3%, representing the best reproducibility attained in this investigation. When, however, gas saturation was effected at the prevailing room temperature (20-27°) reproducibility was only within 6%.

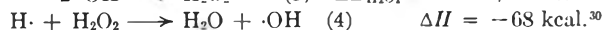
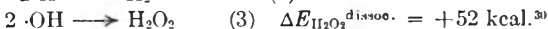
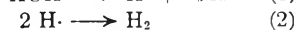
Cavitation and Chemical Reaction.—All chemical reactions occurring in an ultrasonic field are governed by cavitation, which is the formation and collapse of either gaseous or vapor bubbles within the liquid.²⁴ Various theories have been advanced to account for the chemical activation associated with cavitation. At low sound intensities the activation has been attributed to either electrical,²⁵ thermal,²⁶ or pressure²⁷ phenomena which are coincident with bubble collapse. At extremely high intensities there is evidence for the importance of mechanical effects resulting from shearing action in the liquid adjacent to the resonating bubble.^{9d} The initiation or acceleration of chemical reaction is most often achieved in the presence of water, the peculiar efficacy of which must reside in some unique aqueous property, or combination of properties, which allows abnormally high energy release during the cavitation process. For example, the surface tension of water is 72.75 dynes/cm. at 20° compared with approximately 25 dynes/cm. for most organic liquids. This could account for greater energy release on collapse of bubbles formed in water.

In the discussion which follows attention will first be focused on evidence which supports the idea that the cavitation bubbles are indeed the reaction sites. It will then be shown that certain rate results can be understood only by considering how the reacting system itself affects the cavitation process. Finally a mechanism accounting for the observed products will be presented.

When CCl₄ alone was ultrasonicated at an intensity of 6.1 acoustical watts, some cavitation occurred but there was no reaction. When as little as 1 ml. of H₂O was added to 100 ml. of CCl₄, reaction ensued. The total inorganic chlorine yield is not significantly sensitive to large changes in the ratio of CCl₄ to H₂O as can be seen from Table III. These results as well as the zero order²⁸ temperature-independent reaction rates are what would be expected if the rate-determining steps occur in the cavitation bubbles. As long as sufficient reactant is

available the amount which enters the cavitation bubbles per unit of time will be constant and depend on the vapor pressure of the compound. Furthermore, if no chain reactions are involved, and if more molecules are available than energy requisite for reaction, the reaction rate will be determined only by the energy, which is, in turn determined by the amount and intensity of cavitation. The temperature independence of $[d(Cl)/dt]^{CCl_4}$ and $d(H_2O_2)/dt$ implies that the intensity of cavitation is not significantly altered over a 15° ambient temperature rise, also that the rates of primary reactions are indeed determined by the cavitation energy alone: more molecules of reactant would be expected to enter the bubbles at 35° than at 20° (v.p. in mm. Hg: H₂O, 20°, 17.5; 35°, 42.2; CCl₄, 20°, 89.2; 35°, 174). The equality of rates at the two temperatures incidentally emphasizes our poor understanding of the causes of inhibition of cavitation effected by certain volatile materials.^{16,29} The very slight difference in total yield of inorganic chlorine when the amount of water is increased from 20 to 100 ml. (Table III) is consistent with the proposal that the amount and intensity of cavitation determine reaction rates, since the opportunity for effective cavitation is increased only a little, if at all, as the amount of water is increased. Even if the sound energy were sufficient to support more cavitation than occurs in 20 ml., the bubbles themselves place an upper limit on the amount of cavitation which can be produced.²⁹

It is instructive to consider possible reasons for the change in some rates (Cl from CCl₄; Cl⁻ from HCCl₃; and H₂O₂ from H₂O) over the initial period of reaction (see Table II). The causes for these changes cannot be the same in the peroxide case as in the chlorine cases. Consider first the homogenous reacting medium, H₂O. Our data for H₂O₂ production reveal an initial slow rate, lasting a few minutes, followed by a faster rate which is, within 40 min., finally superseded by a slower constant reaction velocity (6.6×10^{-2} μmoles/min.). Parke and Taylor,¹¹ who followed this reaction during its early stages, also noted an initial increase in rate which they attributed to ultrasonic degassing; although some of the evidence concerning this point is conflicting,¹¹ there are indications that the gas content of a liquid can influence the efficiency of cavitation^{15c} (see also Precision of Results). The final constant rate probably results from the eventual establishment of chemical equilibrium involving the decomposition of some of the peroxide formed. Such a reaction has been incorporated in the mechanism proposed for the ultrasonic reactions of water in an inert atmosphere.^{12,13}



(24) (a) A. E. Crawford, "Ultrasonic Engineering," Butterworths Scientific Publications, London, Eng., 1955, Chap. 2; (b) ref. 29, pp. 225-234.

(25) (a) E. N. Harvey, *J. Am. Chem. Soc.*, **61**, 2392 (1939); (b) J. Frenkel, *Acta Physicochim. U.R.S.S.*, **12**, 317 (1940); (c) N. Miller, *Trans. Faraday Soc.*, **46**, 546 (1950).

(26) M. E. Fitzgerald, V. Griffing and J. Sullivan, *J. Chem. Phys.*, **25**, 926 (1956).

(27) M. Kornfeld and L. Suvorov, *J. Appl. Phys.*, **15**, 495 (1944).

(28) It should be pointed out that although the constancy of experimental rates is cited as evidence of the dominating role played by cavitation, the linearity of the total chlorine production from CCl₄ is perhaps fortuitous since, as is suggested in the text, there are evidently several reactions leading to Cl⁻ from CCl₄, some of which are independent of cavitation. As discussed under Mechanism the rates of appearance of Cl₂ and C₂Cl₆ from CCl₄ are each the resultant of a rate of formation and a rate of consumption.

(29) T. F. Hueter and R. H. Bolt, "Sonics," John Wiley and Sons, Inc., New York, N. Y., 1955, Chap. 6.

(30) Bond dissociation energies and the resonance energy of ·CCl₃ are taken from C. Walling, "Free Radicals in Solution," John Wiley and Sons, Inc., New York, N. Y., 1957, pp. 48-50. ΔH values were calculated from appropriate bond dissociation energies.

The decrease in rate of the peroxide production after 40 minutes may be attributed to increased importance of reaction 4 as the H_2O_2 concentration builds up. Del Duca's isotope analyses¹² imply that the reverse of reaction 3 does not occur to any significant extent; furthermore, reaction 4 is energetically the more favorable.

A similar argument cannot be valid for the production of chloride ion from $HCCl_3$ and CCl_4 (total chlorine minus Cl_2), since there is little likelihood that the ion can get into the cavitation bubble to undergo reverse reaction even if such reaction were feasible. In the heterogeneous systems the decrease in reaction rate may be associated with the slow emulsification which occurs during the first 30 to 40 minutes of ultrasonication. It is known that the cavitation threshold and degree of cavitation depend on many characteristics of the supporting liquid.²⁹ The emulsified liquid may not support cavitation, and therefore reaction, as effectively as the simple two-phase system. Added to this effect, in CCl_4 , is the fact that CO_2 is a product and this gas is known to inhibit the progress of many ultrasonic reactions, including the disruption of the CCl_4 molecule.³¹

If cavitation is indeed less effective in the emulsified liquid, a possible explanation is at hand for the fact that the initial rate of total inorganic chlorine production from CCl_4 is not as fast at 35° as at 20°. Emulsification occurs more quickly at the higher temperatures³³ (interfacial tension, CCl_4 - H_2O , 45.05 dynes/cm. at 20°; 43.55 dynes/cm. at 35°).³⁴ The slower constant rate sets in sooner with consequent lower yields of total inorganic chlorine at the higher than the lower temperature.

Reaction Mechanisms.—Cavitation evidently provides the energy which promotes chemical transformations. Whether the nature of this energy is thermal, electrical, or otherwise, there is good evidence that in certain cases it causes homolytic bond scission.¹¹⁻¹³ The resulting free radicals may then react within the cavitation bubble or outside of it. The reactions of CCl_4 and $HCCl_3$ in aqueous suspension in an inert atmosphere can be interpreted on the basis of a free radical mechanism.

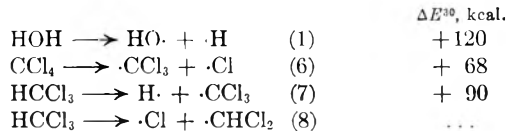
Energy requirements suggest that if H_2O can undergo homolytic dissociation,^{12,13} CCl_4 and $HCCl_3$ molecules, which must also be present in the cavitation bubbles, should likewise experience primary cleavage

(31) V. Griffing, *J. Chem. Phys.*, **18**, 997 (1950).

(32) It has been suggested that the lower yields of total chlorine at the higher temperature are more apparent than real because of the lower solubility of Cl_2 at the higher temperature and consequent losses of Cl_2 into the gas phase. This is considered unlikely for two reasons: (1) in the analytical procedure NH_4OH was introduced directly into the reaction vessel through the inlet tube and the Cl_2 was fixed before the top was removed (see Experimental); (2) the solubility of Cl_2 in water alone is approximately 0.1 g./20 g. H_2O at 35° (interpolated from Handbook values); the amount of Cl_2 produced during an ultrasonic reaction is less than this by more than a power of ten. In addition, CCl_4 , a very good solvent for Cl_2 , is present.

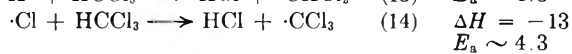
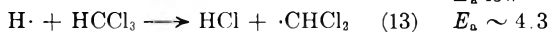
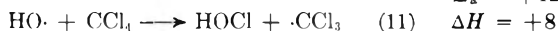
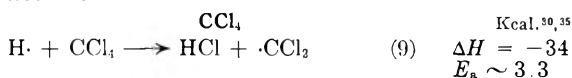
(33) See, however, C. Bondy and K. Sollner, *Trans. Faraday Soc.*, **32**, 556, 616 (1936). These authors state several times that high temperature is disadvantageous to ultrasonic emulsification. No experimental temperatures, frequencies or sound intensities are mentioned in their articles, thus making it difficult to compare their results with those recorded here.

(34) W. D. Harkins and Y. C. Cheng, *J. Am. Chem. Soc.*, **43**, 35 (1921).



Because of the high resonance energy of $\cdot CCl_3$ (12 kcal.³⁰), reaction 7 is expected to occur to some extent, despite the fact that in general C-H bonds are stronger than C-Cl bonds.

Once the radicals are freed their subsequent fate will depend on their concentrations and on energy considerations. Consider these displacement reactions



The concentration of molecules at the reaction site is probably greater than the concentration of primary free radicals, leading to the expectation that radical coupling will compete successfully only when high activation energies are associated with the displacement reactions available to a given radical. Atomic hydrogen could react according to the highly probable reactions 9, in CCl_4 , or 12 and 13, in $HCCl_3$; there is evidence that 12 is preferred over 13.³⁷ The low activation energy of reaction 14 would suggest that any atomic chlorine formed by reaction 8 would be consumed by displacement to the exclusion of chlorine-chlorine coupling, thus accounting for the absence of Cl_2 among the products from the $HCCl_3$ reaction. The less favorable activation energy for a similar reaction between $\cdot Cl$ and CCl_4 , equation 10, would allow the coupling of chlorine atoms to contribute substantially to the production of the observed Cl_2 from CCl_4 . By the same argument, hydroxyl radical coupling could compete successfully with the endothermic displacement by $\cdot OH$ on CCl_4 , reaction 11; but the analogous reaction 15, which is exothermic, would be expected to be more likely than hydroxyl coupling in $HCCl_3$.

This brings us to the conclusion that H_2O_2 could be formed from the CCl_4 system and not to any marked extent from the $HCCl_3$ system. Its presence was observed in neither case; however, the fact that it was not found among the products does not preclude its formation. Any H_2O_2 produced in the CCl_4 - H_2O mixtures would be consumed

(35) Activation energies are taken from E. W. R. Steacie, "Atomic and Free Radical Reactions," 2nd ed., Reinhold Publ. Corp., New York, N. Y., 1954, Ch. X.

(36) E. Cremer, J. Curry and M. Polanyi, *Z. physik. Chem.*, **B23**, 445 (1933).

(37) (a) M. S. Kharasch, E. V. Jensen and W. H. Urry, *J. Am. Chem. Soc.*, **69**, 1100 (1947); (b) M. J. Boeseken and H. Gelissen, *Rec. trav. chim.*, **43**, 869 (1924); (c) A. F. A. Reijhart, *ibid.*, **46**, 72 (1927); (d) D. F. DeTar and D. V. Wells, *J. Am. Chem. Soc.*, **82**, 5839 (1960).

according to reaction 16 which can also account for both the nearly steady concentration of Cl_2 , after the first half hour of reaction, and the appearance of O_2



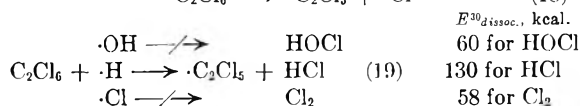
In order to explain the experimental data it is necessary to assume that reaction 16 is fast and that, in the early period of reaction, the Cl_2 is made at a faster rate than is peroxide; as reaction time increases, the two rates become approximately equal, the Cl_2 rate being very slightly faster than the peroxide rate. Traces of O_2 found among the products from HCCl_3 could result from HCl catalyzed³⁸ decomposition of peroxide formed in trace amounts by $\cdot\text{OH}$ coupling.

Coupling of the trichloromethyl radicals leads to C_2Cl_6



This reaction has been postulated many times as a source of C_2Cl_6 in a variety of systems.³⁹ In HCCl_3 , coupling could take place between $\cdot\text{CHCl}_2$, produced by reaction 8 or 13, and $\cdot\text{H}$; further attack by hydrogen atoms on CH_2Cl_2 would lead to the ultimate production of CH_3Cl ⁴⁰ which could not have been detected by our analytical methods.

Tetrachloromethylene can be formed from hexachloroethane *via* the pentachloroethyl radical, which could originate either from reaction 18 or 19.



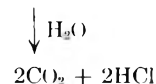
Disproportionation of the $\cdot\text{C}_2\text{Cl}_5$ would lead to C_2Cl_4



If chlorine abstraction occurs and follows the same pattern in both HCCl_3 and CCl_4 , $\cdot\text{H}$ is the correct choice for the abstractor as indicated in equation 19; bond dissociation energies support this alternative.

It has been suggested that intermediate $\cdot\text{C}_2\text{Cl}_5$ can react with O_2 to form CCl_3COCl and COCl_2 in the chlorine-sensitized photooxidation of HC_2Cl_5 ⁴¹ and C_2Cl_4 ⁴² in non-aqueous media. Oxygen-radical interaction may likewise be invoked here to account for the production of CO_2 from the CCl_4 system and its absence from the HCCl_3 system, which is essen-

tially devoid of oxygen



Reaction between $\cdot\text{CCl}_3$ and O_2 could also lead to CO_2 .³⁵ The alternate oxidation of the pentachloroethyl radical to form CCl_3COCl does not occur in the ultrasonic reaction: we demonstrated repeatedly that neither CCl_3COOH nor HCCl_3 , the expected decomposition product thereof, was present among the CCl_4 products. In order to test the possibility that CO_2 arose from intermediate phosgene, ethanol, known to destroy COCl_2 , was added to the CCl_4 (about 1% solution) before ultrasonication. The character of the reaction changed and a semi-solid yellow oil was produced which has not yet been further characterized. Contrary to expectation, CO_2 was still a constituent of the gas above the reacted mixture. It should be noted in this connection that although CO_2 was not an observed product from HCCl_3 , in good accordance with the above scheme, the evidence must be considered in the light of the fact that the HCCl_3 used was stabilized with up to 0.75% alcohol.

If the above proposals approximate the correct mechanism, the rate of appearance of C_2Cl_6 (and possibly also C_2Cl_4 ⁴²) is the resultant of two processes. Consumption as well as production of C_2Cl_6 might well be expected to be zero order, establishing an over-all linear rate once the concentration of C_2Cl_6 reached a sufficiently high value. The low vapor pressure of C_2Cl_6 (m.p. 187° in a sealed tube; b.p. 184°) may restrict the amount of this substance in the bubbles to such a low level that, for reaction 18, available energy is not the sole rate-determining factor.

The experimental results obtained in this study support the hypothesis that the ultrasonic reactions of CCl_4 and HCCl_3 , in aqueous suspension, proceed by primary free radical reactions, followed by the interaction of some of the original products with each other.

Acknowledgments.—The authors gratefully wish to acknowledge financial assistance from the Research Corporation, the Petroleum Research Fund, and the National Science Foundation (Undergraduate Research Participation). The Physics Department of Brown University kindly lent the General Electric Ultrasonic Generator used in some of the experiments. Dr. Maud A. Marshall prepared the standard curve for the hydrogen peroxide analyses and Mr. Harry Landis provided technical assistance in connection with the ultrasonic generators. We are indebted to Dr. Alfred Weissler and Dr. Wesley Nyborg for helpful discussions.

(38) A. Mohammad and H. A. Liebhafsky, *J. Am. Chem. Soc.*, **56**, 1680 (1934).

(39) (a) E. C. Kooyman and E. Farenhorst, *Rec. trav. chim.*, **70**, 867 (1951); (b) Von K. Pfordte, *J. prakt. Chem.*, [4] **5**, 196 (1957); (c) J. W. Schulte, *J. Am. Chem. Soc.*, **79**, 4643 (1957); (d) E. I. Heiba and L. C. Anderson, *ibid.*, **79**, 4940 (1957).

(40) H. Fromherz and H. Schneller, *Z. physik. Chem.*, **B20**, 158 (1933).

(41) H. J. Schumacher and W. Thurauf, *ibid.*, **A189**, 183 (1941).

(42) Ref. 30, p. 448.

ELECTRODE PROCESSES WITH SPECIFIC OR NON-SPECIFIC ADSORPTION: FARADAIC IMPEDANCE AND RECTIFICATION

BY MITSUGI SENDA¹ AND PAUL DELAHAY

Coates Chemical Laboratory, Louisiana State University, Baton Rouge, Louisiana

Received April 11, 1961

Faradaic impedance and faradaic rectification are discussed for processes with specific or non-specific adsorption of reactants and/or reaction products. No explicit form of the rate equation for adsorption kinetics is postulated. Analysis of the faradaic impedance for processes with specific adsorption includes: derivation of a general current-potential characteristic for small amplitudes without the postulating of an explicit form for the rate equation for charge transfer kinetics; an equivalent circuit for electrode processes in which adsorption processes are independent of one another (*e.g.*, as for metal deposition with amalgam formation); variations of the phase angle with frequency and analysis of some existing data in the literature; correction for the double layer capacity. Equivalent circuits for processes with non-specific adsorption of reactants, *i.e.*, with repulsion or attraction of the discharged species, are also derived for the faradaic impedance; and comments are made on a related problem as solved by previous authors (Levich, Matsuda and Delahay). Faradaic rectification is treated for the above cases, and the frequency dependence of the rectification voltage is analyzed in detail. Implications in the determination of kinetic parameters are pointed out.

The characteristics of electrode processes with specific adsorption of reactants and/or products of reaction in relaxation methods have been analyzed by a few authors. Laitinen and Randles² and Llopis and co-workers³ discussed the corresponding faradaic impedance and showed that, under simplifying assumptions, adsorption is accounted for by an additional frequency-independent capacity and resistance in the equivalent circuit. Barker⁴ reached a similar conclusion for absolutely equivalent circuits of the faradaic impedance. Matsuda and Delahay⁵ analyzed the effect of reactant adsorption in the potentiostatic and galvanostatic methods. The adsorption isotherm (Langmuir) is postulated at the onset and the adsorption and desorption rate constants are assumed to be potential-independent in these investigations.⁶ These assumptions render the model for the influence of adsorption quite simple but they are not substantiated by experiment. Specific adsorption of ions does not follow a Langmuir isotherm as was shown by Parsons⁷ and Grahame⁸; and nothing is known about the influence of potential on rate constants for ionic specific adsorption. A more general analysis in which these assumptions are not made *a priori* is discussed for the faradaic impedance and rectification methods. Some comments are also made on electrode processes with non-specific adsorption which had been treated previously in this Laboratory for the conditions prevailing in relaxation methods.⁹

(1) Postdoctoral research associate, January 1960–March 1961; on leave from the Department of Agricultural Chemistry, Kyoto University, Kyoto, Japan.

(2) H. A. Laitinen and J. E. B. Randles, *Trans. Faraday Soc.*, **51**, 54 (1955).

(3) (a) J. Llopis, J. Fernandez-Biarge and M. Perez Fernandez, *Electrochim. Acta*, **1**, 130 (1959); (b) "Transactions of the Symposium on Electrode Processes, Philadelphia," E. Yeager editor, John Wiley and Sons, New York, N. Y., 1959, in course of publication.

(4) G. C. Barker, "Transactions of the Symposium on Electrode Processes, Philadelphia," E. Yeager editor, John Wiley and Sons, New York, N. Y., 1959, in course of publication.

(5) H. Matsuda and P. Delahay, *Coll. Czechoslov. Chem. Commun.*, **25**, 2977 (1960).

(6) With the possible exception of Barker's work for which not enough details are available thus far.

(7) R. Parsons, *Trans. Faraday Soc.*, **51**, 1518 (1955).

(8) D. C. Grahame, *J. Am. Chem. Soc.*, **80**, 4201 (1958).

(9) (a) H. Matsuda and P. Delahay, *J. Phys. Chem.*, **64**, 332 (1960); (b) H. Matsuda, *ibid.*, **64**, 339 (1960).

Faradaic Impedance for Processes with Specific Adsorption

Current-Potential Characteristic for Small Amplitudes.—We consider the over-all reaction $O + ne = R$ for which O and R are soluble in solution and distinguish the sequence of steps in Fig. 1, where arrows correspond to a positive flux of matter¹⁰: mass transfer of O and R, adsorption of O and R as heterogeneous processes, and charge transfer between adsorbed species (to the exclusion of charge transfer involving species O and R in solution). Since the current density I is a function of the potential E and the surface concentrations Γ_O and Γ_R , one has for the first harmonic and for small variations of potential, as prevail in the faradaic impedance and rectification methods¹¹

$$\delta I = (\partial I / \partial E) \delta E + (\partial I / \partial \Gamma_O) \delta \Gamma_O + (\partial I / \partial \Gamma_R) \delta \Gamma_R \quad (1)$$

where the derivatives are taken at equilibrium. Our problem is to evaluate $\delta \Gamma_O$ and $\delta \Gamma_R$ and derive, if possible, the elements of an equivalent circuit. Γ_O and Γ_R in eq. 1 are such that

$$d\Gamma_i/dt = \pm (I/nF) \mp \phi_i^a \quad (2)$$

There i represents O and R; the upper and lower sign correspond to O and R, respectively; the ϕ_i^a 's are the fluxes for the adsorption processes; n is the number of electrons in the charge transfer reaction; and F is the faraday. The flux ϕ_i^a in eq. 2 for species i depends on Γ_O , Γ_R , E , and the concentration C_i^* of species i at the electrode surface. Thus

$$\delta \phi_i^a = (\partial \phi_i^a / \partial \Gamma_O) \delta \Gamma_O + (\partial \phi_i^a / \partial \Gamma_R) \delta \Gamma_R + (\partial \phi_i^a / \partial C_i^*) \delta C_i^* + (\partial \phi_i^a / \partial E) \delta E \quad (3)$$

One further has $\phi_i^* = \mp \phi_i^a$ where ϕ_i^* is the flux for the mass transfer process at the electrode surface for species i . For sinusoidal variations, δC_i^* in eq. 3 is related to ϕ_i^a by

$$\delta C_i^* = \pm (h_{ri} - jh_{xi}) \delta \phi_i^a \quad (4)$$

where j is the operator $(-1)^{1/2}$ and h_{ri} and jh_{xi} are the real and complex parts of a function h_i

(10) This convention is the opposite of the one generally adopted for electrode processes, except in the German literature. "Awkward" signs are avoided with this convention.

(11) (a) The use of eq. 1 as written in terms of volume concentrations is due to D. C. Grahame, *J. Electrochem. Soc.*, **99**, C370 (1952); (b) see summary in P. Delahay, "New Instrumental Methods in Electrochemistry," Interscience Publishers, Inc., New York, N. Y., 1954, pp. 146–178.

whose explicit form, which only depends on mass transfer, will be determined below. One further has

$$d(\delta\Gamma_i)/dt = j\omega\delta\Gamma_i \quad (5)$$

where $\omega = 2\pi f$, f being the frequency. There results by combination of the foregoing equations

$$\delta\Gamma_i = \pm (H_{ri} - jH_{xi})\delta I \pm (G_{ri} - jG_{xi})\delta E \quad (6)$$

where the function H and G can be written (see Appendix) in terms of the function h of eq. 4 and the partial derivatives of eq. 3.

By introducing the $\delta\Gamma_i$'s from eq. 6 in eq. 1, one obtains the I - E characteristic for sinusoidal variations of small amplitude

$$\delta I = [(g_r - jg_x)/(r - jx)]\delta E \quad (7)$$

where the functions g , r and x can be written (see Appendix) in terms of the functions H and G in eq. 6 and the partial derivatives in eq. 1.

Equivalent Circuit.—The analysis of the general eq. 7 in terms of an equivalent circuit would be very involved, and it is useful to consider the case in which the adsorption processes for O and R are independent, *i.e.*, the case in which $\partial\phi_{O^a}/\partial\Gamma_R = 0$ and $\partial\phi_{R^a}/\partial\Gamma_O = 0$. Thus, we assume that the adsorption kinetics for O is independent of the surface concentration of R and *vice versa*. This is the case, for instance, in the deposition of metal with amalgam formation, and the foregoing simplification is not unrealistic. Equations for g , r and x in eq. 7 are then greatly simplified and are given in the Appendix.

One further simplification can be made when the parameter ζ_i defined by

$$\zeta_i = (\partial\Gamma_i/\partial E)_a / (\partial\Gamma_i/\partial E)_c \quad (8)$$

is such that $|\zeta_i| \ll 1$. There, $(\partial\Gamma_i/\partial E)_a$ and $(\partial\Gamma_i/\partial E)_c$ are the values at equilibrium for the adsorption and charge transfer processes, respectively. The condition $|\zeta_i| \ll 1$ implies that the effect of a change of potential on Γ_i is much smaller for the adsorption process than for the charge transfer process. (This implies that the term $(\partial\phi_i^a/\partial E)\delta E$ in eq. 3 can be neglected.) Note that ζ_i can be positive or negative depending on the adsorption process. The current-potential characteristic of eq. 7 becomes for $|\zeta_i| \ll 1$ (see Appendix)

$$\delta I = [1/(r - jx)]\delta E \quad (9)$$

The function h_i for semi-infinite linear diffusion is directly obtained by application of Duhamel's theorem.¹² Thus $h_{ri} = h_{xi} = (2\omega D_i)^{-1/2}$, D_i being the diffusion coefficient of species i . Further, it follows from the Nernst equation that $\partial E/\partial C_i^* = \pm (RT/nF) (1/C_i^0)$, C_i^0 being the bulk concentration of species i . Equations 74 to 79 in the Appendix then reduce to

$$r - jx = r_{ct} + \sum_{i=O,R} \frac{z_{i2}(z_{i1} + z_{i3})}{z_{i1} + z_{i2} + z_{i3}} \quad (10)$$

where r_{ct} is the charge transfer resistance

$$r_{ct} = 1/(\partial I/\partial E) = (RT/nF)(1/I_a^0) \quad (11)$$

I_a^0 being the apparent exchange current density. The first form of r_{ct} is a general one whereas the

(12) H. S. Carslaw and J. C. Jaeger, "Conduction of Heat in Solids," Oxford University Press, London, 1947, p. 57, eq. 9.

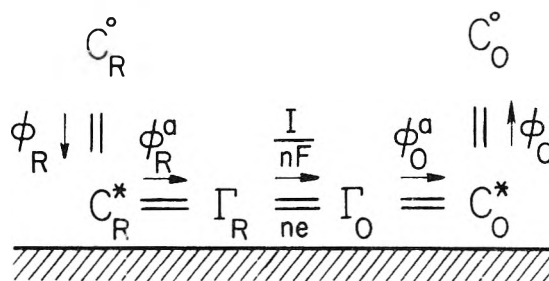


Fig. 1.—Mass transfer, adsorption and charge transfer at the electrode. Arrows correspond to positive flux.

second form applies only when the Butler-*Erdey* Gruz-Volmer equation is valid for charge transfer. One further has

$$z_{11} = r_1^d - jx_1^d \quad (12)$$

$$z_{12} = -jx_1^a \quad (13)$$

$$z_{13} = r_1^a \quad (14)$$

with

$$r_1^d = x_1^d = \frac{RT}{n^2 F^2} \frac{1}{(2\omega D_1)^{1/2}} \frac{1}{C_1^0} \quad (15)$$

$$r_1^a = \frac{RT}{n^2 F^2} \frac{1}{\mp (\partial\phi_1^a/\partial C_1^0)} \frac{1}{C_1^0} \quad (16)$$

$$x_1^a = \frac{1}{\omega} \frac{RT}{n^2 F^2} \frac{1}{(\partial\Gamma_1/\partial C_1^0)} \frac{1}{C_1^0} \quad (17)$$

The equivalent circuit of the faradaic impedance (Fig. 2A) includes, in addition to the charge transfer resistance r_{ct} and the Warburg elements r_1^d and c_1^d ($x_1^d = 1/\omega c_1^d$), the resistance r_1^a and capacity c_1^a ($x_1^a = 1/\omega c_1^a$). It is seen from eq. 16 and 17 that r_1^a and c_1^a are frequency-independent. The resistance r_1^a depends on adsorption kinetics and approaches zero as $(\partial\phi_1^a/\partial C_1^0) \rightarrow \infty$. As one would expect, adsorption increases the resistive part of the faradaic impedance because it constitutes one more barrier in addition to charge and mass transfer. This follows from the model we selected, namely, that charge transfer occurs only between adsorbed species. The capacitance x_1^a depends on adsorption equilibrium, and $x_1^a \rightarrow \infty$ ($c_1^a \rightarrow 0$) where $\partial\Gamma_i/\partial C_i^0 \rightarrow 0$.

The circuit of Fig. 2A is identical to the one proposed by previous authors²⁻⁴ although values of r_1^a and c_1^a previously reported were expressed in a different form. It should be emphasized that the equivalence of that circuit has been proven only for the simplifications made in the general treatment, namely, (a) that the adsorption processes for O and R do not influence each other (*i.e.*, $\partial\phi_{O^a}/\partial\Gamma_R = 0$ and $\partial\phi_{R^a}/\partial\Gamma_O = 0$) and (b) that the effect of a variation of potential on the adsorption process can be neglected in comparison with the effect on the charge transfer reaction (*i.e.*, $|(\partial\Gamma_i/\partial E)_a| \ll |(\partial\Gamma_i/\partial E)_c|$).

Simplified Equivalent Circuits.—Simplified forms of the circuit of Fig. 2A will be derived, and the element r_1^a will be considered first. It follows from eq. 11 and 16 that $r_1^a = r_{ct}$ when $(\partial\phi_1^a/\partial C_1^0)C_1^0 = I_a^0/nF$, *i.e.*, the resistance r_1^a is equal to the charge transfer resistance. If one assumes, for instance, that ϕ_1^a is proportional to C_1^0 , $r_1^a = r_{ct}$ when $\phi_1^a = I_a^0/nF$. The adsorption resistance r_1^a thus can be

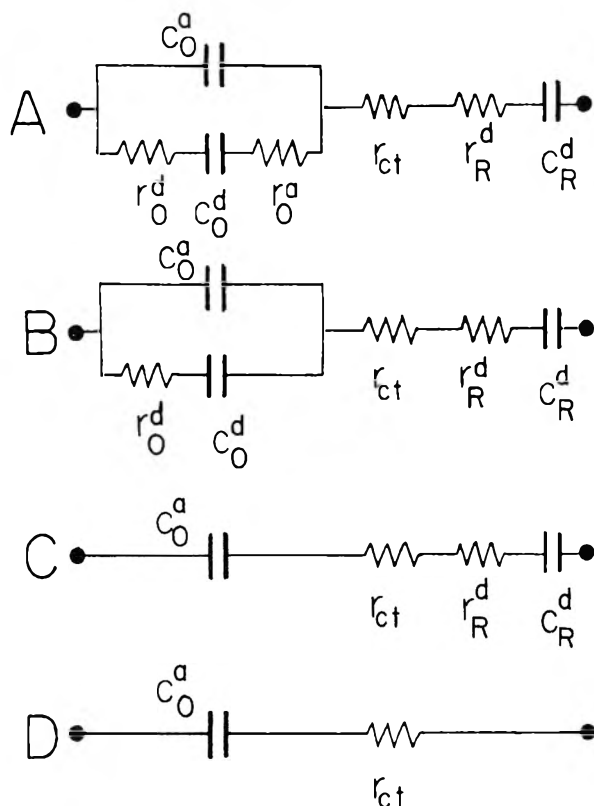


Fig. 2.—Equivalent circuit of faradaic impedance corresponding to eq. 9 for the reaction $O + ne = R$, O being specifically adsorbed: (A) general case; (B) the adsorption exchange rate is large in comparison with charge transfer; (C) case of sufficiently high frequencies satisfying condition 19; (D) same as (C) but for $C_R^0 \gg C_0^0$.

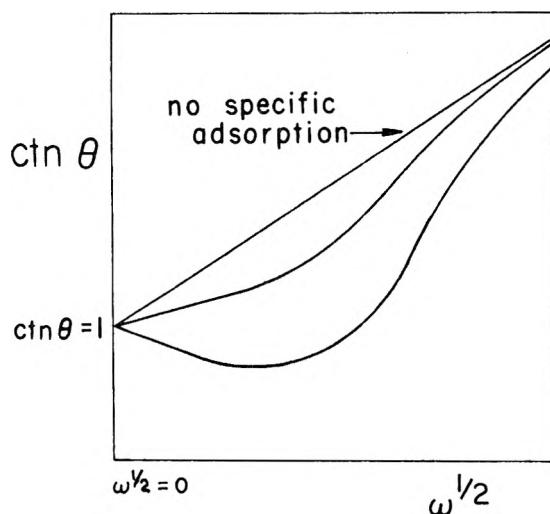


Fig. 3.—Variations of the phase angle θ for the impedance $r - jx$ of eq. 9.

neglected when adsorption kinetics is such that the adsorption exchange rate at equilibrium is much larger than $I^0/nF^{1/2}$ (Fig. 2B).

The adsorption capacitance x_i^a can be neglected when $x_i^d \ll x_i^a$ or, in view of eq. 15 and 17, when

(13) One should compare r_i^a also with r_i^d , but experimental conditions are generally such that r_i^d is not very much smaller than r_{ct} and, in fact, sometimes r_i^d is larger than r_{ct} (processes with large I_a^0).

$$(\omega/2D_i)^{1/2}(\partial\Gamma_i/\partial C_i^0) \ll 1 \quad (18)$$

Since r_i^d and x_i^d depend on $1/\omega^{1/2}$ and x_i^a depends on $1/\omega$, the influence of adsorption increases with frequency. This conclusion is to be expected if one recalls that the amplitude of the reactants concentration variations at the electrode decreases with frequency. The "buffering" action of adsorption thus increases with frequency. For ions with strong adsorption, $\partial\Gamma_i/\partial C_i^0$ can be of the order of 10^{-4} – 10^{-5} cm., and condition 18 is only fulfilled at frequencies somewhat below those normally used in faradaic impedance measurements (e.g., f minimum of 50 to 100 c.p.s.). Conversely, when

$$(\omega/2D_i)^{1/2}(\partial\Gamma_i/\partial C_i^0) \gg 1 \quad (19)$$

the Warburg impedance is much larger than the adsorption capacitance and can be neglected. This is explained, as above, by the "buffering" action of adsorption. Condition 19 is fulfilled for $\omega^{1/2} \gg 50 \text{ sec.}^{-1/2}$ and $\omega^{1/2} \gg 500 \text{ sec.}^{-1/2}$ for $\partial\Gamma_i/\partial C_i^0 = 10^{-4}$ and 10^{-5} cm., respectively, i.e., at relatively high frequencies for a.c. bridge measurements. The equivalent circuit is then very simple (Fig. 2C) and is of interest in the experimental study of adsorption effects. If only one of the species O or R is specifically adsorbed, it is helpful to select a sufficiently high concentration of the other species to render the corresponding Warburg impedance very small at the frequencies being used. Analysis is further simplified (Fig. 2D).

Phase Angle for the Impedance ($r - jx$) of Eq. 9.—The phase angle θ between voltage and current for the equivalent circuit of Fig. 2A is comprised between 0 and $\pi/2$, and the current precedes the voltage. One has $\text{ctn } \theta = r/x$. In the absence of non-specific adsorption, one deduces from eq. 10 to 15: $\theta \rightarrow \pi/4$ and $\text{ctn } \theta \rightarrow 1$ for $\omega \rightarrow 0$; $\theta \rightarrow 0$ and $\text{ctn } \theta \rightarrow \infty$ for $\omega \rightarrow \infty$. Further, $\text{ctn } \theta$ increases linearly with $\omega^{1/2}$ (Fig. 3), namely

$$\text{ctn } \theta = 1 + \frac{r_{ct}}{\frac{1}{2^{1/2}} \frac{RT}{n^2 F^2} \left(\frac{1}{C_0^0 D_0^{1/2}} + \frac{1}{C_R^0 D_R^{1/2}} \right)} \omega^{1/2} \quad (20)$$

or $\text{ctn } \theta = 1 + U\omega^{1/2}$.

The value of $\text{ctn } \theta$ for specific adsorption can be readily written from eq. 10 to 17 but the resulting equation is quite cumbersome. To simplify matters, we shall assume that adsorption is very fast (we neglect r_i^a of eq. 16) and that species R is not adsorbed (e.g., metal deposition on amalgam). If $(\omega/2D_i)^{1/2}(\partial\Gamma_i/\partial C_i^0) < 0.1$, one has

$$\text{ctn } \theta \approx 1 + \left[U - \left(\frac{2}{D_0} \right)^{1/2} \left(\frac{\partial\Gamma_0}{\partial C_0^0} \right) \frac{1}{1 + \exp(-\lambda)} \right] \omega^{1/2} \quad (21)$$

with

$$\lambda = (nF/RT)(E_e - E^0) - \ln [(D_R/D_0)^{1/2}] \quad (22)$$

where E_e and E^0 are the equilibrium and standard potentials, respectively. If the quantity between brackets in eq. 21 is negative, $\text{ctn } \theta$ decreases with $\omega^{1/2}$ and θ exceeds $\pi/4$ (Fig. 3). Further, one must have $\text{ctn } \theta \rightarrow \infty$ for $\omega \rightarrow \infty$ since the faradaic impedance is then purely resistive. A minimum value of $\text{ctn } \theta$ is thus observed when the quantity

between brackets in eq. 21 is negative. One can show (see Appendix) that $\text{ctn } \theta$ is always positive in the present case and that the minimum value of $\text{ctn } \theta$ decreases with $\exp(-\lambda)$ (cf. eq. 21 and 22).

The foregoing analysis seems to account for some of the results recently reported by Bauer, Smith and Elving¹⁴ on the phase angle for Cd^{++} reduction of Cd-amalgam. These authors observed that $\text{ctn } \theta$ either increases or decreases linearly with $\omega^{1/2}$ for values of $\omega^{1/2}$ up to 100 to 150 sec.^{-1/2} according to the nature of the supporting electrolyte, the Cd^{++} concentration and the ratio $C_{\text{Cd}^{++}}/C_{\text{Cd}}$. Frequencies apparently were not high enough in these experiments for observation of the upper branch of the curve $\text{ctn } \theta$ vs. $\omega^{1/2}$ for the case in which a decrease of $\text{ctn } \theta$ with $\omega^{1/2}$ was observed at low frequencies. One infers from the above interpretation of the results of Elving, *et al.*, that specific adsorption of Cd^{++} is much more pronounced in KNO_3 as a supporting electrolyte than in Na_2SO_4 . It should be emphasized, however, that conditions in these experiments may be more complicated than those corresponding to the above analysis. At any rate, correct trends are accounted for. Further support is the experimental evidence for specific adsorption of Cd^{++} on Hg.¹⁵ The results of Randles¹⁶ could possibly be interpreted by the above analysis but not enough details are available yet on this work.

Phase Angle for the Impedance $(r - jx)/(g_r - jg_x)$ of Eq. 7.—We now consider the more general case in which condition 8, namely $|\zeta_i| \ll 1$, is not fulfilled, *i.e.*, we do not assume that the effect of E on Γ_i is necessarily much smaller for adsorption than for mass transfer. If θ' is the phase angle between current and voltage for the impedance $1/(g_r - jg_x)$, the total phase angle between the faradaic current and voltage is $\theta_F = \theta + \theta'$. The value of θ' can be written directly from the form of $g_r - jg_x$. When adsorption processes are independent (*i.e.*, $\partial\phi_0^*/\partial\Gamma_R = 0$ and $\partial\phi_R^*/\partial\Gamma_0 = 0$) eq. 72 and 73 of the Appendix yield

$$g_r - jg_x = 1 - \sum_{i=O,R} \frac{\zeta_i z_{i2}}{z_{i1} + z_{i2} + z_{i3}} \quad (23)$$

where ζ_i is given by eq. 8 and the z 's are given by eq. 12 to 14. Equation 84 of the Appendix is obtained in the case of metal deposition with amalgam formation.

Influence of Double Layer.—Because of specific adsorption of O and R, the double layer impedance, *i.e.*, the *non-faradaic impedance*, may be somewhat different in the absence and presence of species O and R even when there is a large excess of supporting electrolyte. If the latter condition is met, one can assume that the charge density on the electrode is a function of E , Γ_0 and Γ_R only. Hence for sinusoidal variations of the non-faradaic current density one has for the first harmonic

$$\delta I = j\omega \left\{ (\partial q/\partial E)\delta E + (\partial q/\partial\Gamma_0)\delta\Gamma_0 + (\partial q/\partial\Gamma_R)\delta\Gamma_R \right\} \quad (24)$$

When $\omega \rightarrow \infty$, $\delta\Gamma_0 \rightarrow 0$ and $\delta\Gamma_R \rightarrow 0$ because the concentrations no longer can follow the variations of potential, and $\delta I \rightarrow j\omega(\partial q/\partial E)\delta E$ for $\omega \rightarrow \infty$. The variations $\delta\Gamma_i$ are given by eq. 6 which may be written as

$$\delta\Gamma_i = \left(\frac{\partial\Gamma_i}{\partial E} \right)_c \left[\frac{g_r - jg_x}{r - jx} (r_i - jx_i) + (\rho_i - j\xi_i) \right] \delta E \quad (25)$$

with

(14) H. H. Bauer, D. L. Smith and P. J. Elving, *J. Am. Chem. Soc.*, **82**, 2094 (1960).

(15) A. N. Frumkin, "Transactions of the Symposium on Electrode Processes, Philadelphia," E. Yeager ed., John Wiley and Sons, Inc., New York, N. Y., 1959, in course of publication.

(16) J. E. B. Randles, ref. 15, in course of publication.

$$r_i - jx_i = \frac{z_{i2}(z_{i1} + z_{i3})}{z_{i1} + z_{i2} + z_{i3}} \quad (26)$$

$$\rho_i - j\xi_i = \frac{z_{i2}}{z_{i1} + z_{i2} + z_{i3}} \quad (27)$$

The total electrode impedance z_m (non-faradaic and faradaic) is

$$\frac{1}{z_m} = j\omega \left(\frac{\partial q}{\partial E} \right)_{\Gamma_i} + \frac{g_r - jg_x}{r - jx} \left\{ 1 + j\omega \sum_{i=O,R} \left(\frac{\partial q}{\partial\Gamma_i} \right)_E \left(\frac{\partial\Gamma_i}{\partial E} \right)_c \frac{z_{i2}(z_{i1} + z_{i3})}{z_{i1} + z_{i2} + z_{i3}} \right. \\ \left. + j\omega \sum_{i=O,R} \left(\frac{\partial q}{\partial\Gamma_i} \right)_E \left(\frac{\partial\Gamma_i}{\partial E} \right)_c \frac{\zeta_i z_{i2}}{z_{i1} + z_{i2} + z_{i3}} \right\} \quad (28)$$

Analysis from experimental data should prove arduous, and in practice it may be necessary to work under conditions in which the contribution of species i to the double layer capacity is quite negligible. At any rate, the order of magnitude of the change in differential capacity caused by adsorption of species i can be obtained from measurements at potentials at which no electrode reaction occurs for all practical purposes. This method has been applied by Randles.¹⁶

Faradaic Impedance for Processes with Non-specific Adsorption

Correction for the double layer structure in the solving of the mass transfer problem for the faradaic impedance was already considered in a previous paper from this Laboratory^{9b} in the absence of specific adsorption. We shall now expand on this case of *non-specific adsorption*. Equivalent circuits will be obtained for processes with a large excess of supporting electrolyte. It will be assumed that the supporting electrolyte determines the double layer structure.

In view of the definition of the function h_i of eq. 4, one has

$$\delta C_i^* = \pm (h_{r_i} - jh_{x_i}) \frac{\delta I}{nF} \quad (29)$$

with

$$\delta C_i^* = C_i^* - C_i^0 \exp[-(z_i F/RT)\Delta\varphi] \quad (30)$$

There z_i is the ionic valence of species i and $\Delta\varphi$ is the difference of potential across the diffuse double layer. The last term in eq. 30 represents the concentration of species i in the plane of closest approach in the absence of mass transfer polarization. It was shown^{9b} that

$$\delta C_i^* = \{ \pm (\delta I/nF) [1/(j\omega D_i)^{1/2}] G_i \} \exp [(-z_i F/RT)\Delta\varphi] \quad (31)$$

where

$$G_i = \frac{1 + (1/\kappa)(j\omega/D_i)^{1/2} f_i(\pm |z_i/z|)}{1 + (1/\kappa)(j\omega/D_i)^{1/2} f_i(\mp |z_i/z|)} \quad (32)$$

with

$$1/\kappa = (RT\epsilon/8\pi^2 F^2 C_e)^{1/2} \quad (33)$$

$$f(\pm z_i/z) = \frac{\exp \{ [(\pm |z_i/z|) - 1/2] |z| F |\Delta\varphi| / RT \} - 1}{(\pm |z_i/z|) - 1/2} \quad (34)$$

There z is the ionic valence of the supporting electrolyte supposed to be of the z - z type; C_e is the concentration of the supporting electrolyte; ϵ is the dielectric constant in the double layer region (supposed to be constant); and the upper and lower sign in front of $|z_i/z|$ correspond to $z_i\Delta\varphi > 0$ (repulsion) and $z_i\Delta\varphi < 0$ (attraction), respec-

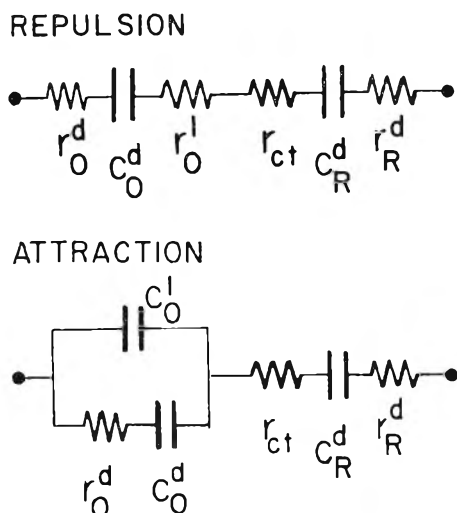


Fig. 4.—Equivalent circuit of faradaic impedance for the reaction $O + ne = R$, only O being non-specifically adsorbed.

tively. Equation 32 for G_i applies only when the conditions are fulfilled (see Note after the Appendix).

$$(1/\kappa)(\omega/D_i)^{1/2} \ll 1$$

$$[(1/\kappa)(j\omega/D_i)^{1/2}]^2 f_i(+|z_i/z|) \ll 1 \quad (35)$$

As shown in the Appendix, two cases can be considered, namely, repulsion or attraction of the discharged species. In the absence of specific adsorption, the part of the faradaic impedance corresponding to transport of species i by semi-infinite linear diffusion and migration is for the repulsion case

$$(z_F)_t = r_i^d - jx_i^d + r_i^i \quad (36)$$

where r_i^d and x_i^d are given by eq. 15 and

$$r_i^i = \frac{RT}{n^2 F^2} \frac{1}{C_i^0} \frac{1}{\kappa D_i} f_i\left(+\left|\frac{z_i}{z}\right|\right) \quad (37)$$

For attraction one has

$$(z_F)_t = \frac{(r_i^d - jx_i^d)(-jx_i^i)}{r_i^d - jx_i^d - jx_i^i} \quad (38)$$

where

$$x_i^i = \frac{1}{\omega} \frac{RT}{n^2 F^2} \frac{1}{C_i^0} \frac{\kappa}{f_i(+|z_i/z|)} \quad (39)$$

It follows from eq. 36 that repulsion results in an additional resistance in series with the Warburg resistance (Fig. 4). One indeed expects $(z_F)_t$ to be larger for repulsion of species i than in the absence of repulsion. Conversely, attraction is accounted for by a capacity ($=\omega x_i^i$; see eq. 39) in parallel with the Warburg impedance. The impedance $(z_F)_t$ is lowered by non-specific adsorption of species i in comparison with $(z_F)_t$ without attraction. It must be emphasized that the apparent exchange current density still must be corrected for the double layer structure (Frumkin correction) beyond the above correction for r_i^i or x_i^i .

It is seen from the equivalent circuits of Fig. 4 that repulsion decreases the phase angle between current and voltage and attraction increases this angle. In particular, the phase angle can exceed $\pi/4$ for an inherently very fast charge transfer process ($r_{ct} \rightarrow 0$). Thus, the phase angle can

exceed $\pi/4$ even in the absence of specific adsorption. (Phase angles larger than $\pi/4$ have been associated exclusively with *specific* adsorption in general.)

The effect of non-specific adsorption was interpreted in a previous paper from this Laboratory^{9b} in terms of a resistance which was positive for repulsion and negative for attraction. The effect of x_i^i (eq. 39) is identical with that of a negative resistance. (See further discussion in section on faradaic rectification.) Conversely, Barker⁴ accounts for non-specific adsorption by a capacity which is positive for attraction and negative for repulsion. Such negative elements are avoided in the equivalent circuits of Fig. 4.

Since r_i^i and ωx_i^i are frequency independent and r_i^d and x_i^d are inversely proportional to $\omega^{1/2}$, the influence of repulsion and attraction becomes more pronounced as the frequency increases. The effect may not be negligible for very fast processes (e.g., Hg_2^{++} discharge¹⁷⁻¹⁹).

Faradaic Rectification

To account for faradaic rectification we include second-order effects in writing eq. 1 and we proceed just as for processes without specific adsorption as in a previous paper from this Laboratory.²⁰ We need the second-order terms for an amplitude V_A of the first harmonic (indicated by the subscript "1") of $\delta_i E$. The mean value of the first harmonic is such that

$$(\delta_i E)_0^2 = V_A^2/2 \quad (40)$$

Likewise (see eq. 25)

$$(\delta_i \Gamma_i \delta_i E)_0 = V_A^2/2 \frac{\partial \Gamma_i}{\partial E} \left[\frac{r_i^i + x_i^i}{r^2 + x^2} + Y_i \right] \quad (41)$$

where

$$Y_i = - \left[\sum_{i=O,R} \zeta_i \rho_i \right] \frac{r_i^i + x_i^i}{r^2 + x^2} + \left[\sum_{i=O,R} \zeta_i \xi_i \right] \frac{r_i^i x - x_i^i r}{r^2 + x^2} + \zeta_i \rho_i \quad (42)$$

Note that Y_i vanishes from eq. 41 when $|\zeta_i| \ll 1$. (See discussion of eq. 8.)

The mean rectification voltage $\Delta \bar{E}_\infty$ after charging of the double layer ($t \rightarrow \infty$) and for control of the mean faradaic current equal to zero ($\bar{I} = 0$) can now be calculated as before.²⁰ If $|\zeta_i| \ll 1$ for O and R and the charge transfer kinetics follows a Butler-Edrey Gruz-Volmer type of equation, one has

$$\Delta \bar{E}_\infty = \frac{nF}{RT} V_A^2 \Psi \quad (43)$$

with

(17) H. Gerischer and M. Krause, *Z. physik. Chem., N.F.*, **14**, 184 (1958).

(18) H. Matsuda, S. Oka and P. Delahay, *J. Am. Chem. Soc.*, **81**, 5077 (1959).

(19) There is hardly any complex formation of ClO_4^- with Hg_2^{++} . Cf. J. Bjerrum, G. Schwarzenbach and L. G. Sillén, "Stability Constants. Part II," The Chemical Society, London, 1958, p. 111.

(20) (a) P. Delahay, M. Senda and C. H. Weis, *J. Am. Chem. Soc.*, **83**, 312 (1961); (b) for a review, see P. Delahay, Ch. 5 in vol. 1 "Advances in Electrochemistry and Electrochemical Engineering," P. Delahay, ed., Interscience Publishers, Inc., New York, N. Y., in course of publication.

$$\psi = \frac{2\alpha - 1}{4} - \frac{\alpha}{2} \frac{r_{\text{O}} + x_{\text{O}}}{r^2 + x^2} + \frac{(1 - \alpha)}{2} \frac{r_{\text{R}} + x_{\text{R}}}{r^2 + x^2} \quad (44)$$

α being the transfer coefficient. Equation 43 is identical with the result previously derived.²⁰ The analysis of the frequency dependence of ψ according to eq. 44 is quite involved, and this equation will be discussed for some particular cases on the assumption that the impedance for R is purely of the Warburg type (e.g., as for metal deposition with amalgam formation).

Simple Warburg Impedance.—This is the simplest possible case which was already analyzed.^{4,20} Results of a different but entirely equivalent form from those previously discussed²⁰ are ($\psi \equiv \psi_{\text{d}}$ here)

$$\psi_{\text{d}} = \frac{2\alpha - 1}{4} + \left[\frac{1 - 2\alpha}{4} + \frac{1}{4} \tanh \frac{\lambda}{2} \right] F_{\text{d}}(P_{\text{d}}) \quad (45)$$

where λ is defined by eq. 22, and

$$P_{\text{d}} = (r_{\text{O}}^{\text{d}} + r_{\text{R}}^{\text{d}})/r_{\text{ct}} \quad (46)$$

$$= \frac{1}{(2\omega)^{1/2}} \frac{I_{\text{A}}^{\text{O}}}{nF} \left(\frac{1}{C_{\text{O}}^{\text{O}} D_{\text{O}}^{1/2}} \right)^{1-\alpha} \left(\frac{1}{C_{\text{R}}^{\text{O}}} \right)^{\alpha} [\exp[-\alpha\lambda] + \exp[(1-\alpha)\lambda]]$$

$$F_{\text{d}}(P_{\text{d}}) = (1 + \text{ctn } \theta)/(1 + \text{ctn}^2 \theta) \quad (47)$$

$$= \frac{P_{\text{d}}[P_{\text{d}} + (1 + P_{\text{d}})]}{P_{\text{d}}^2 + (1 + P_{\text{d}})^2}$$

C_{O}^{O} and C_{R}^{O} being the bulk concentrations of O and R. Since only $F_{\text{d}}(P_{\text{d}})$ is frequency-dependent in eq. 45, $\psi_{\text{d}} = (2\alpha - 1)/4$ is independent of frequency when $\tanh(\lambda/2) = 2\alpha - 1$. Curves representing $\Delta E_{\infty}/V_{\text{A}}^2$ against the equilibrium potential (see eq. 22) thus have a common intersection point for all frequencies (cf. Fig. 9 in ref. 20a).

Impedance for O Composed of the Warburg Impedance in Series with a Frequency-independent Resistance.—This impedance corresponds to electrostatic repulsion of the discharged species. It also corresponds to charge transfer preceded by a chemical reaction provided the frequency is so low that $\omega \ll l$, l being the sum of the rate constants for the forward and backward first-order (or pseudo-first order) chemical reaction.²¹ One has

$$r_{\text{O}} - jx_{\text{O}} = r_{\text{k}} + r_{\text{O}}^{\text{d}} - jx_{\text{O}}^{\text{d}} \quad (48)$$

where r_{k} is frequency-independent. By combination of eq. 44 and 48 one obtains ($\psi \equiv \psi_{\text{k}}$ here)

$$\psi_{\text{k}} = \frac{2\alpha - 1}{4} - \frac{\alpha}{2} \frac{r_{\text{k}}}{r_{\text{ct}} + r_{\text{k}}} F_{\text{k}}(P_{\text{k}}) + \left(\frac{1 - 2\alpha}{4} + \frac{1}{4} \tanh \frac{\lambda}{2} \right) F_{\text{d}}(P_{\text{k}}) \quad (49)$$

where

$$P_{\text{k}} = (r_{\text{O}}^{\text{d}} + r_{\text{R}}^{\text{d}})/(r_{\text{ct}} + r_{\text{k}}) \quad (50)$$

$$F_{\text{k}}(P_{\text{k}}) = \frac{1 + P_{\text{k}}}{P_{\text{k}}^2 + (1 + P_{\text{k}})^2} \quad (51)$$

and $F_{\text{d}}(P_{\text{k}})$ has the form of eq. 47, the argument being now given by eq. 50. As $\omega \rightarrow \infty$, eq. 45 and 49 yield, respectively, $(\psi_{\text{d}})_{\omega \rightarrow \infty} = (2\alpha - 1)/4$ and $(\psi_{\text{k}})_{\omega \rightarrow \infty} = [(2\alpha - 1)/4] - (\alpha/2)[r_{\text{k}}/r_{\text{ct}} + r_{\text{k}}]$. Equation 45, if it is unwittingly applied instead of eq. 49, yields a measured transfer coefficient $\alpha_{\text{m}} = \alpha[r_{\text{ct}}/(r_{\text{ct}} + r_{\text{k}})]$, i.e., $\alpha_{\text{m}} < \alpha$. Serious errors may result when r_{k} is not negligible in comparison with r_{ct} . This conclusion was already pointed out.

Further, ψ_{k} is independent of frequency, i.e.

$$\psi_{\text{k}} = \frac{1}{4} \left[2\alpha \frac{r_{\text{ct}}}{r_{\text{ct}} + r_{\text{k}}} - 1 \right] \quad (52)$$

when

$$2\alpha \frac{r_{\text{ct}}}{r_{\text{ct}} + r_{\text{k}}} - 1 = \tanh \frac{\lambda}{2} \quad (53)$$

The measured transfer coefficient α_{m} one obtains by unwittingly overlooking the effect of r_{k} is then $\alpha_{\text{m}} = \alpha[r_{\text{ct}}/(r_{\text{ct}} + r_{\text{k}})]$. One has $\alpha_{\text{m}} \approx \alpha$ when $r_{\text{ct}} \gg r_{\text{k}}$.

Impedance for O Composed of the Warburg Impedance in Parallel with a Frequency Independent Capacity.—This case corresponds to electrostatic attraction of the discharged species or very fast (reversible) specific adsorption of substance O. This circuit is equivalent to the ($R_{\text{s}} - X_{\text{s}}$) series circuit

$$R_{\text{O}}^{\text{s}} = r_{\text{O}}^{\text{d}} \frac{1}{\left(1 - \frac{x_{\text{O}}^{\text{d}}}{x_{\text{O}}^{\text{s}}}\right)^2 + \left(\frac{r_{\text{O}}^{\text{d}}}{x_{\text{O}}^{\text{s}}}\right)^2} \quad (54)$$

$$X_{\text{O}}^{\text{s}} = x_{\text{O}}^{\text{d}} \frac{1 + \frac{x_{\text{O}}^{\text{d}}}{x_{\text{O}}^{\text{s}}} + \frac{r_{\text{O}}^{\text{d}}}{x_{\text{O}}^{\text{s}}}}{\left(1 + \frac{x_{\text{O}}^{\text{d}}}{x_{\text{O}}^{\text{s}}}\right)^2 + \left(\frac{r_{\text{O}}^{\text{d}}}{x_{\text{O}}^{\text{s}}}\right)^2} \quad (55)$$

When $(x_{\text{O}}^{\text{d}}/x_{\text{O}}^{\text{s}})^2 \ll < 1/2$, eq. 53 reduces to

$$R_{\text{O}}^{\text{s}} \approx r_{\text{O}}^{\text{d}} \frac{1}{1 + 2(x_{\text{O}}^{\text{d}}/x_{\text{O}}^{\text{s}})} \quad (56)$$

$$= r_{\text{O}}^{\text{d}} [1 - 2(x_{\text{O}}^{\text{d}}/x_{\text{O}}^{\text{s}})]$$

$$X_{\text{O}}^{\text{s}} \approx x_{\text{O}}^{\text{d}} \quad (57)$$

Since $r_{\text{O}}^{\text{d}}x_{\text{O}}^{\text{d}}/x_{\text{O}}^{\text{s}}$ is independent of frequency, it follows from eq. 56 and 57 that $R_{\text{O}}^{\text{s}} - jX_{\text{O}}^{\text{s}}$ is composed of the Warburg elements r_{O}^{d} and x_{O}^{d} and a frequency independent resistance. The previous discussion thus can be transposed here. The necessary condition for this simplification ($(x_{\text{O}}^{\text{d}}/x_{\text{O}}^{\text{s}})^2 \ll < 1/2$) is fulfilled only when electrostatic attraction is not too strong (non-specific adsorption) or specific adsorption is relatively weak.

Conclusion

The influence of specific adsorption of reactants and/or reaction products in the faradaic impedance and rectification methods can be analyzed without the use of a particular form of the rate equation for adsorption. Equivalent circuits can be derived and used in the analysis of the influence of frequency in impedance and rectification measurements for specific and non-specific adsorption. Experimental criteria for the detection of adsorption effects can be deduced from the frequency dependence analysis. Implications in the determination of kinetic parameters (exchange current density, transfer coefficient) for electrode processes are immediate, and some unexplained observations in the literature can be accounted for. Adsorption effects should be important in a number of electrode processes, particularly with solid electrodes for which specific adsorption can be quite pronounced.¹⁵ The overlooking of adsorption in the analysis of data and in the correlation of data obtained by different relaxation methods may lead to serious misinterpretation.

Acknowledgment.—This investigation was supported by the Office of Naval Research.

Appendix

Functions H and G of Eq. 6.—One has

(21) (a) H. Gerischer, *Z. physik. Chem.*, **198**, 286 (1951); (b) see ref. 20a for a review.

$$H_{rO} - jH_{xO} = \frac{1}{nF} \frac{\left[1 - \frac{\partial \phi_{O^*}}{\partial C_{O^*}} (h_{rO} - jh_{xO}) \right] B_R - \left[1 + \frac{\partial \phi_{R^*}}{\partial C_{R^*}} (h_{rR} - jh_{xR}) \right] B_O}{A_O B_R - A_R B_O} \quad (58)$$

$$G_{rO} - jG_{xO} = - \frac{B_R \frac{\partial \phi_{O^*}}{\partial E} - B_O \frac{\partial \phi_{R^*}}{\partial E}}{A_O B_R - A_R B_O} \quad (59)$$

$$H_{rR} - jH_{xR} = \frac{1}{nF} \frac{\left[1 - \frac{\partial \phi_{O^*}}{\partial C_{O^*}} (h_{rO} - jh_{xO}) \right] A_R - \left[1 + \frac{\partial \phi_{R^*}}{\partial C_{R^*}} (h_{rR} - jh_{xR}) \right] A_O}{A_O B_R - A_R B_O} \quad (60)$$

$$G_{rR} - jG_{xR} = - \frac{A_R \frac{\partial \phi_{O^*}}{\partial E} - A_O \frac{\partial \phi_{R^*}}{\partial E}}{A_O B_R - A_R B_O} \quad (61)$$

$$A_O = \frac{\partial \phi_{O^*}}{\partial \Gamma_O} + j\omega \left[1 - \frac{\partial \phi_{O^*}}{\partial C_{O^*}} (h_{rO} - jh_{xO}) \right] \quad (62)$$

$$A_R = \partial \phi_{R^*} / \partial \Gamma_O \quad B_O = \partial \phi_{O^*} / \partial \Gamma_R \quad (63)$$

$$B_R = \frac{\partial \phi_{R^*}}{\partial \Gamma_R} - j\omega \left[1 + \frac{\partial \phi_{R^*}}{\partial C_{R^*}} (h_{rR} - jh_{xR}) \right] \quad (64)$$

Functions g, r and x of Eq. 7.—One has

$$r = r_{ct} + r_O + r_R \quad (65)$$

$$x = x_O + x_R \quad (66)$$

$$r_{ct} = 1 / \partial I / \partial E \quad (67)$$

$$r_O = - [(\partial I / \partial \Gamma_O) / (\partial I / \partial E)] H_{rO} \quad (68)$$

$$r_R = [(\partial I / \partial \Gamma_R) / (\partial I / \partial E)] H_{rR} \quad (69)$$

$$x_O = - [(\partial I / \partial \Gamma_O) / (\partial I / \partial E)] H_{xO} \quad (70)$$

$$x_R = [(\partial I / \partial \Gamma_R) / (\partial I / \partial E)] H_{xR} \quad (71)$$

$$g_r = 1 + [(\partial I / \partial \Gamma_O) / (\partial I / \partial E)] G_{rO} - [(\partial I / \partial \Gamma_R) / (\partial I / \partial E)] G_{rR} \quad (72)$$

$$g_x = [(\partial I / \partial \Gamma_O) / (\partial I / \partial E)] G_{xO} - [(\partial I / \partial \Gamma_R) / (\partial I / \partial E)] G_{xR} \quad (73)$$

Values of g, r and x of Eq. 7 for Two Independent Adsorption Processes.—If $\partial \phi_{O^*} / \partial \Gamma_R = 0$ and $\partial \phi_{R^*} / \partial \Gamma_O = 0$, one has

$$r - jx = r_{ct} + \frac{z_{O2}(z_{O1} + z_{O3})}{z_{O1} + z_{O2} + z_{O3}} + \frac{z_{R2}(z_{R1} + z_{R3})}{z_{R1} + z_{R2} + z_{R3}} \quad (74)$$

$$g_r - jg_x = 1 + \frac{(-\zeta_O)z_{O2}}{z_{O1} + z_{O2} + z_{O3}} + \frac{(-\zeta_R)z_{R2}}{z_{R1} + z_{R2} + z_{R3}} \quad (75)$$

where $\zeta_i, r_{ct}, z_{i1}, z_{i2}$ and z_{i3} are defined by eq. 8 and 11 to 14. Further

$$r_i^d = \pm (1/nF)(\partial E / \partial \Gamma_i)_c (\partial \Gamma_i / \partial C_i^*) h_{ri} \quad (76)$$

$$x_i^d = \pm (1/nF)(\partial E / \partial \Gamma_i)_c (\partial \Gamma_i / \partial C_i^*)_a h_{xi} \quad (77)$$

$$r_i^a = \pm (1/nF)(\partial E / \partial \Gamma_i)_c (\partial \Gamma_i / \partial C_i^*)_n / [\mp (\partial \phi_i^* / \partial C_i^*)] \quad (78)$$

$$x_i^a = \pm (1/nF)(1/\omega)(\partial E / \partial \Gamma_i)_c (\partial \Gamma_i / \partial C_i^*)_a (\partial C_i^* / \partial \Gamma_i)_a \quad (79)$$

There the upper and lower signs correspond, respectively, to O and R; and the indices c and a correspond to the derivatives at equilibrium for the charge transfer and adsorption process, respectively.

Minimum of $\text{ctn } \theta$.—One has

$$\text{ctn } \theta_{\text{min}} = \frac{\exp(-\lambda) + Q_{O^*}}{\exp(-\lambda) + Q_{O^*x}} \quad (80)$$

where λ is defined by eq. 22 and Q_{O^*} and Q_{O^*x} are given by

$$Q_{O^*} = \frac{1}{(1+s)^2 + s^2} \quad (81)$$

$$Q_{O^*x} = \frac{1+2s}{(1+s)^2 + s^2} \quad (82)$$

with

$$s = (\omega/2D_O)^{1/2} (\partial \Gamma_O / \partial C_{O^*}) \quad (83)$$

Values of $g_r - jg_x$ for Metal Deposition with Amalgam Formation.—One deduces from eq. 23

$$g_r - jg_x = 1 - \zeta_O \frac{1+s}{(1+s)^2 + s} + j\zeta_O \frac{s}{(1+s)^2 + s} \quad (84)$$

where ζ_O is defined by eq. 8 and s by eq. 83.

Faradaic Impedance for Non-specific Adsorption.—Since

$$\delta C_i^* = \pm (h_{ri} - jh_{xi}) \frac{\delta I}{nF} \quad (85)$$

it follows from eq. 29 to 34 that

$$h_{ri} = jh_{xi} = [1/(\omega D)^{1/2}] [G_i / (j)^{1/2}] \exp[-(z_i F / RT) \Delta \varphi] \quad (86)$$

$$\left(\frac{2}{j}\right)^{1/2} G_i = \left(\frac{2}{j}\right)^{1/2} \frac{1 + j^{1/2} \frac{1}{\kappa} \left(\frac{\omega}{D_i}\right)^{1/2} f_i(\pm |z_i/z|)}{1 + j^{1/2} \frac{1}{\kappa} \left(\frac{\omega}{D_i}\right)^{1/2} f_i(\mp |z_i/z|)} \quad (87)$$

$$= (1-j) \frac{1 + (1+j) \frac{1}{\kappa} \left(\frac{\omega}{2D_i}\right)^{1/2} f_i(\pm |z_i/z|)}{1 + (1+j) \frac{1}{\kappa} \left(\frac{\omega}{2D_i}\right)^{1/2} f_i(\mp |z_i/z|)} \quad (88)$$

Two approximate forms of eq. 88 can be written for repulsion and attraction, respectively. For repulsion

$$\left(\frac{2}{j}\right)^{1/2} G_i = 1 - j + \frac{2}{\kappa} \left(\frac{\omega}{2D_i}\right)^{1/2} f_i(+|z_i/z|) \quad (89)$$

For attraction

$$\left(\frac{2}{j}\right)^{1/2} G_i = \frac{1-j}{1 + (1+j) \frac{1}{\kappa} \left(\frac{\omega}{2D_i}\right)^{1/2} f_i(+|z_i/z|)} \quad (90)$$

$$= \frac{(1-j) \left[-j\kappa \left(\frac{2D_i}{\omega}\right)^{1/2} \frac{1}{f_i(+|z_i/z|)} - 1 \right]}{-j\kappa \left(\frac{2D_i}{\omega}\right)^{1/2} \frac{1}{f_i(+|z_i/z|)} + (1-j)} \quad (91)$$

Since the part of the faradaic impedance $(z_F)_t$ which corresponds to mass transfer is

$$(z_F)_t = \pm \left(\frac{\partial E}{\partial C_i^*}\right) \frac{1}{nF} (h_{ri} - jh_{xi}) \quad (92)$$

one obtains for repulsion and attraction of species the following expressions, respectively: For repulsion:

$$(z_F)_t = \pm \left(\frac{\partial E}{\partial C_i^*}\right) \frac{1}{nF} \frac{1}{(2\omega D_i)^{1/2}} \left(\frac{2}{j}\right)^{1/2} \left[\exp\left(-\frac{z_i F}{RT} \Delta \varphi\right) \right] \left[1 + \frac{1}{\kappa} \left(\frac{2\omega}{D_i}\right)^{1/2} f\left(\pm \frac{|z_i|}{z}\right) - j \right] = r_i^d - jx_i^d + r_i^l \quad (93)$$

where

$$r_i^d = x_i^d = \pm \left(\frac{\partial E}{\partial C_i^*}\right) \frac{1}{nF} \frac{1}{(2\omega D_i)^{1/2}} \exp\left[-\frac{z_i F}{RT} \Delta \varphi\right] \quad (94)$$

$$r_i^l = \pm \left(\frac{\partial E}{\partial C_i^*}\right) \frac{1}{nF} \frac{f(+|z_i/z|)}{\kappa D_i} \exp\left[-\frac{z_i F}{RT} \Delta \varphi\right] \quad (95)$$

For attraction:

$$r_i^d - jx_i^d = \left(\frac{\partial E}{\partial C_i^*} \right) \frac{1}{nF} \frac{1}{(2\omega D_i)^{1/2}} \frac{(1-j) \left[-j\kappa \left(\frac{2D_i}{\omega} \right)^{1/2} \frac{1}{f(+|z_i/z|)} \right]}{(1-j) - j\kappa \left(\frac{2D_i}{\omega} \right)^{1/2} \frac{1}{f(+|z_i/z|)}} \exp \left(- \frac{z_i F}{RT} \Delta\varphi \right) \quad (96)$$

$$= \frac{(r_i^d - jx_i^d)(-jx_i^1)}{r_i^d - jx_i^d - jx_i^1} \quad (97)$$

with

$$x_i^1 = \pm \left(\frac{\partial E}{\partial C_i^*} \right) \frac{1}{nF} \frac{\kappa}{\omega} \frac{1}{f(+|z_i/z|)} \exp \left(- \frac{z_i F}{RT} \Delta\varphi \right) \quad (98)$$

One further has approximately

$$\pm \frac{\partial E}{\partial C_i^*} \exp \left(- \frac{z_i F}{RT} \Delta\varphi \right) \approx \frac{RT}{nF} \frac{1}{C_i^0} \quad (99)$$

if one neglects the term in $\partial\Delta\varphi/\partial E$. Equations 95 and 98 then yield eq. 37 and 39.

Note on the Double Layer Correction for Non-specific Adsorption in Relaxation Methods.—The diffuse double layer is, in general, very much thinner than the diffusion layer, and boundary value problems for mass transfer correction in relaxation methods can be solved without consideration of the double layer structure. The Frumkin correction²² of kinetic parameters for the double layer structure is thus applicable in conjunction with the usual equations for mass transfer polarization.²³ This approach, however, becomes relatively crude for very fast processes. The solution of the boundary value problem for mass transfer with consideration of the double layer structure leads, for relaxation methods and repulsion of the discharged species, to a correction which is essentially the same as the correction for ionic transport in the diffuse double layer in the absence of mass transfer polarization outside the diffuse double layer.⁹ The resulting equation is identical with the one derived by Levich^{24,25} for the double layer correction with ionic transport across the diffuse double layer for repulsion of the discharged species. A discrepancy was noted for attraction in a previous paper^{9a} from this Laboratory but was not examined. This matter is taken up here.

General Treatment.—Consider an electrode process with mass transfer polarization, and assume that the diffusion layer is much thicker than the diffuse double layer thickness (δ_κ). Steady-state for mass transfer can then be assumed in the diffuse double layer, and the concentration C_i of a species involved in the electrode reaction is a solution of (cf. Levich)

$$\frac{d}{dx} \left(\frac{dC_i}{dx} + \frac{z_i F}{RT} C_i \frac{d\varphi}{dx} \right) = 0 \quad (100)$$

where x is the distance from a point in solution to the plane of closest approach, φ is the potential in the diffuse double layer with respect to the bulk of the solution, z_i is the ionic valence of species i with its sign, and R , T and F have their usual significance. Equation 100 will be solved on the assumption that the double layer structure is solely determined by the supporting electrolyte (present in large excess). One has the conditions

$$\begin{aligned} \text{for } x = 0 \quad D_i \left(\frac{dC_i}{dx} + \frac{z_i F}{RT} C_i \frac{d\varphi}{dx} \right) &= \pm \frac{I}{nF} \\ \text{for } x = \delta_\kappa \quad \varphi = d\varphi/dx = 0 \text{ and } C_i &= (C_i)_{\delta_\kappa} \end{aligned}$$

There D_i is the diffusion coefficient of species i , n the number of electrons in the electrode reaction, I the current density, and the \pm sign holds, respectively, for the species being consumed or produced in the electrode reaction. The con-

(22) For reviews see, e.g.: (a) A. N. Frumkin, *Z. Elektrochem.*, **59**, 807 (1955); (b) M. Breiter, M. Kleinerman and P. Delahay, *J. Am. Chem. Soc.*, **80**, 5111 (1958).

(23) See, e.g., G. M. Florjanovich and A. N. Frumkin, *Zhur. fiz. Khim.*, **29**, 1827 (1955).

(24) (a) V. G. Levich, *Dokl. Akad. Nauk S.S.S.R.*, **67**, 309 (1949); (b) **124**, 869 (1959).

(25) For transposition of the Levich treatment to polyvalent discharged ions see: (a) L. Gierst, "Transactions of the Symposium on Electrode Processes, Philadelphia," E. Yeager editor, John Wiley and Sons, New York, N. Y., 1959, in course of publication; (b) H. Matsuda and P. Delahay, *ibid.*, in course of publication; (c) L. Gierst and H. Hurwitz, *Z. Elektrochem.*, **64**, 36 (1960).

centration $(C_i)_{\delta_\kappa}$ at $x = \delta_\kappa$ is a function of t unless steady-state is reached over the whole diffusion thickness. The solution for $x = 0$ is

$$(C_i)_{x=0} = \left[(C_i)_{\delta_\kappa} - \frac{\pm I}{nF D_i} \int_{x=0}^{\delta_\kappa} \exp \left(\frac{z_i F}{RT} \varphi \right) dx \right] \exp \left(- \frac{z_i F}{RT} \varphi_0 \right) \quad (101)$$

where φ_0 is the value of φ for $x = 0$.

The concentration $(C_i)_{\delta_\kappa}$ at $x = \delta_\kappa$ can be derived from usual mass transfer treatments since we assumed that the thickness of the diffusion layer is larger than δ_κ . Thus

$$(C_i)_{\delta_\kappa} = C_i^0 - \frac{\delta_i}{D_i} \left(\pm \frac{I}{nF} \right) \quad (102)$$

where δ_i is the thickness of the diffusion layer for species i . There follows from eq. 101 and 102

$$(C_i)_{x=0} = \left[C_i^0 - \left(\pm \frac{I}{nF} \right) \frac{1}{D_i} \left(\delta_i + \frac{A_i}{\kappa} \right) \right] \exp \left[- \frac{z_i F}{RT} \varphi_0 \right] \quad (103)$$

$$A_i = \kappa \int_0^{\delta_\kappa} \exp \left(\frac{z_i F}{RT} \varphi \right) dx \quad (104)$$

$$\frac{1}{\kappa} = RT \epsilon / 8\pi (|z|)^2 F^2 C_e^{1/2} \quad (105)$$

ϵ being the dielectric constant, z the ionic valence of the supporting electrolyte and C_e the concentration of the supporting electrolyte. The quantity $1/\kappa$ is the Debye thickness of the diffuse layer theory, i.e., $1/\kappa$ is of the order of δ_κ .

Two limiting cases can be considered, namely, for $A_i/\kappa < \delta_i$ and $A_i/\kappa \gg \delta_i$ or the equivalent conditions $A_i \ll \delta_i/\delta_\kappa$ and $A_i \gg \delta_i/\delta_\kappa$. Since $\delta_i/\delta_\kappa \gg 1$ the first condition holds for $A_i \leq 1$ and the Frumkin correction suffices. Conversely, when A_i is so large that $A_i \gg \delta_i/\delta_\kappa$ with $\delta_i/\delta_\kappa \gg 1$, the expression for C_i reduces to the value of C_i in the absence of mass transfer polarization outside the diffuse double layer (cf. Levich²⁴).

When species i is attracted in the diffuse double layer, i.e., when $z_i \varphi < 0$, the argument of the exponential in eq. 104 is negative and $A_i \leq 1$.²⁶ There follows from what was indicated above that the Frumkin correction should hold. Further correction of the Levich type may be necessary when there is repulsion of the discharged species as indicated below.

Comparison with the Treatment of Matsuda and Delahay.

—In a previous work from this Laboratory a general equation (see eq. 11 in ref. 9a) was derived for $(C_i)_{x=0}$ in the form of inverse Laplace transform by consideration of mass transfer in the boundary value problem for relaxation methods. Comparison of this result with eq. 103 reveals that these results are equivalent if one sets for A_i of eq. 104 the value (see eq. 25 of ref. 9a)

$$\begin{aligned} a_i &= \frac{\exp[(\pm |z_i| - |z|/2)F|\varphi_0|/RT] - 1}{\pm |z_i/z| - 1/2} \\ &+ \frac{\exp[(\mp |z_i| - |z|/2)F|\varphi_0|/RT] - 1}{\mp |z_i/z| - 1/2} \quad (106) \end{aligned}$$

where the upper and lower signs correspond to $z_i \varphi_0 > 0$ and $z_i \varphi_0 < 0$, respectively. It was emphasized in the previous work^{9a} that this result is only a first approximation because it corresponds to retaining the first two terms in a series expansion. Correlation between a_i and A_i is immediate after the integration of eq. 104 is performed. Thus by setting

$$\xi = \exp \left(\frac{|z| F}{RT} |\varphi| \right) \quad (107)$$

in eq. 104 and noting that

$$(26) \text{ Thus } A_i = \kappa \int_0^{\delta_\kappa} \exp \left(- \frac{|z| F}{RT} |\varphi| \right) dx, \text{ i.e., } A_i \leq \kappa \int_0^{\delta_\kappa} dx \text{ or } A_i \leq 1 \text{ since } 1/\kappa \approx \delta_\kappa.$$

$$\frac{d\varphi}{dx} = \left(-\frac{\kappa}{2}\right) \frac{2RT}{|z|F} \left[\exp\left(\frac{|z|F}{2RT} |\varphi|\right) - \exp\left(-\frac{|z|F}{2RT} |\varphi|\right) \right] \left[\frac{1}{\kappa} \cdot \frac{1}{(D_i t)^{1/2}} \right]^2 \cdot (A_i)_{\text{repul.}} \ll 1 \quad (113)$$

one obtains

$$A_i = \int_{\xi_0}^{\xi_1} \frac{2\xi \pm 2|z_i/z|}{\xi^2 - 1} d\xi \quad (109)$$

where $\xi_0 = \exp\left[\frac{|z|F/2RT}{|\varphi_0|}\right]$. If φ_0 is sufficiently large, $\exp\left[-\frac{|z|F/2RT}{|\varphi_0|}\right]$ can be dropped in eq. 108 and one has

$$A_i = \int_{\xi_0}^{\xi_1} \frac{2\xi \pm 2|z_i/z|}{\xi^2} d\xi \quad (110)$$

The condition for application of eq. 110 is also $\xi^2 \gg 1$; cf. eq. 109. Since $\xi_\kappa = 1$ ($\varphi = 0$ for $x = \delta_\kappa$) integration of eq. 110 yields

$$A_i = \frac{\exp\left[\frac{\pm |z_i| - |z|/2}{|z_i/z|} \frac{F|\varphi_0|}{RT}\right] - 1}{\pm |z_i/z| - 1/2} \quad (111)$$

Equation 111 is approximate and holds provided that $\exp(-|z|F|\varphi_0|/2RT) \ll \exp(|z|F|\varphi_0|/2RT)$ for values of φ corresponding to the region near the plane of closest approach where electrostatic action is most pronounced, i. e., for $|\varphi|$ not too small in comparison with $|\varphi_0|$. The same approximation was made in the derivation of eq. 106.

It is seen from eq. 106 and 111 that for $|z_i| > |z|/2$ and repulsion of the discharged species ($z_i \varphi > 0$), A_i reduces for all practical purposes to A_i . There is thus identity between the correction of Matsuda and Delahay and the above treatment, i. e., the Levich correction. *The Levich correction thus can be applied to relaxation methods for repulsion of the discharged species when the Frumkin correction does not suffice as already pointed out by Matsuda and Delahay.*

It can be shown that, besides the condition

$$\frac{1}{\kappa} \cdot \frac{1}{(D_i t)^{1/2}} \ll 1 \quad (112)$$

the additional condition

should be fulfilled for application of eq. 106 to the case of repulsion, t being the time elapsed since the beginning of electrolysis for non-steady state electrolysis. Since $1/\kappa \approx \delta_\kappa$ and $(\pi D_i t)^{1/2}$ corresponds to δ_i , eq. 9 agrees with the starting condition, $\delta_\kappa \ll \delta_i$, of the above treatment.

It was shown above that the Frumkin correction suffices in all cases for attraction of the discharged species. However, this conclusion is not reached when the approximate value of a_i of eq. 107 is used, and conditions for application of this equation must be fulfilled for attraction of the discharged species. The condition for application of eq. 106 to the case of attraction can be written, in addition to eq. 112 as

$$\left[\frac{1}{\kappa} \cdot \frac{1}{(D_i t)^{1/2}} \right]^2 [(A_i)_{\text{repul.}}]^2 \ll 1 \quad (114)$$

This condition is not fulfilled except for extremely small values of δ_κ/δ_i . The limitation to the application of eq. 106 (cf. eq. 25 in ref. 9a) is much stricter for attraction than for repulsion of the discharged species, and the approximation made by Matsuda and Delahay^{9a} is practically equivalent to the Levich correction.

It is to be noted with respect to the boundary condition at $\kappa = \delta_\kappa$, that the boundary condition used by Matsuda and Delahay reduces to the boundary equation used in this paper when eq. 112 is fulfilled in the case of repulsion, while in the case of attraction the additional condition should

$$\frac{1}{\kappa} \frac{1}{(D_i t)^{1/2}} \cdot (A_i)_{\text{repul.}} \ll 1 \quad (115)$$

be fulfilled. Equation 115 implies that the Frumkin correction must be valid irrespective of other conditions.

Conclusion.—The Levich type of correction of kinetic parameters for electrode processes can be used as a first approximation in relaxation methods when there is repulsion of the discharged species and the duration of electrolysis is so short, or the frequency so high, that departure from the Frumkin correction can be expected. The Frumkin correction seems applicable in general for attraction of the discharged species.

EFFECTS OF QUANTIZATION AND OF ANHARMONICITY ON THE RATES OF DISSOCIATION AND ASSOCIATION OF COMPLEX MOLECULES¹

By O. K. RICE

Department of Chemistry, University of North Carolina, Chapel Hill, North Carolina

Received April 17, 1961

In a unimolecular decomposition the energy levels of the decomposing molecule are broadened. It is shown that under the assumptions of the Rice-Ramsperger-Kassel theory, as elaborated by Marcus and Rice, these levels are, as a minimum, broadened so that they just overlap. The inverse reaction, association, cannot therefore be affected, independently of other assumptions, by the necessity of matching energy levels. The broadening in a unimolecular decomposition appears to be fourfold greater, for a given reaction rate, than that found in predissociation or the tunnel effect. The reasons for this, and certain possible effects at low pressures, are discussed. Quantization has a quantitative effect on the rate of activation of a complex molecule. This depends upon whether the frequencies are low enough to be handled classically for both the average molecule and the activated molecule; of intermediate magnitude, requiring quantum considerations for the average molecule but not for the activated molecule; or high, requiring quantum considerations in both cases. Anharmonicity of the vibrations is responsible for transfer of energy from one quasi-normal mode of vibration to another. This phenomenon is probably more important than is usually supposed, because a molecule visits regions in its configuration space where anharmonicity is great on the average many times before it reacts. This tends to invalidate the Slater picture of unimolecular reactions, in which it is supposed that anharmonicity is of minor importance. Anharmonicity has a tendency to increase the number of activated molecules (and hence the rate of activation) by increasing the number of energy levels. The "loosening" of vibrations into rotations or their equivalent is another effect involving quantization and anharmonicity. Some rather peculiar properties of a "loose" activated complex can be demonstrated on general principles, and some speculations concerning the nature of the complexes are offered. The importance of zero-point energy in a "rigid" complex is noted.

The theory of unimolecular reactions has been developed principally upon the basis of a number of

(1) Work supported by the National Science Foundation. Presented at the Symposium on Experimental and Theoretical Advances in Elementary Gas Reactions, 139th meeting of the American Chemical Society, St. Louis, March, 1961.

models, and any approach more fundamental than this will admittedly be rather difficult to come by. It seems, however, that it might be possible to examine some of these models critically, in the light of what we do know about fundamental principles.

In this way we may, perhaps, hope to see to what extent they are self-consistent, to effect some choice between models, and to consider how results may be affected by certain aspects of the true physical situation which are generally neglected.

In this paper we wish to examine the effects of quantization and of anharmonicity. In each case two aspects of the problem appear. We may ask how these factors, when viewed critically, affect our fundamental concepts of the mechanisms involved, or at least we may inquire how they fit in with the ideas that we already have. We may also look at what may be called secondary effects, which do, however, need to be considered in any actual attempt to calculate reaction rates.

In formulating these problems we shall often find it helpful to consider the unimolecular decomposition and the inverse reaction, the bimolecular association, simultaneously. These are, of course, closely related, and if we knew all about the one we would presumably know all about the other, also. It is often, however, easier to think about one rather than the other.

1. Role of the Uncertainty Principle in Unimolecular Decompositions.—In a bimolecular association we have two molecular systems, which have a relative kinetic energy, uniting to form a single system in which the continuum associated with the relative translation is replaced by quantized levels. The quantized levels, on the other hand, are broadened, because the associated molecule can again dissociate; the broadening depends upon the lifetime of the associated molecule in the level involved. The question arises as to whether the broadening is sufficient to assure the possibility of association of all pairs which could associate classically. This problem was considered a long time ago by Kassel,² and he concluded that, from a practical point of view, they were sufficiently broadened, a conclusion we do not wish to dispute though it apparently has not always been accepted.³ In any case, something is to be learned by the attempt to tie this question to the model used in a somewhat more basic way.

Marcus and Rice,⁴ in their formulation of unimolecular reaction rates, considered the rate at which activated molecules having total energy in a range E (called by them E') to $E + dE$ would react. It was assumed that this was to be found by considering that what was essentially an equilibrium distribution was established between the $N_E dE$ energy levels of the activated molecules in this range, and the energy levels of the activated complex. The activated complex was defined in the usual way; it was a molecule in which a reaction coordinate was passing over a potential-energy maximum, of energy E_m , in one of several continua, P_{E-E_m} in number.⁵ The usual assumption that

the separating pairs in the several continua are streaming outward in equilibrium numbers simply means that in the reverse reaction all the pairs streaming inward will stick together.

If k_E (called k_a by Marcus and Rice) is the rate constant for dissociation from the energy range E to $E + dE$ then the total rate of dissociation from this range will, according to these assumptions, be given by

$$k_E N_E dE = (P_{E-E_m}/h) dE \quad (1.1)$$

where h is Planck's constant h^{-1} having been shown to be the rate of dissociation per unit energy range from any continuum.

Let us now choose dE equal to the average energy δE between discrete states. Then we will have $N_E \delta E = 1$ and

$$k_E = (P_{E-E_m}/h) \delta E \quad (1.2)$$

Let us set $\tau_E = 1/k_E$, the average lifetime of molecules in the energy level, and suppose that we are in a range of energies where there is only one continuum, $P_{E-E_m} = 1$; this will give the longest possible lifetime. Then we see from eq. 1.2 that

$$\tau_E \delta E = h \quad (1.3)$$

The assumption of equilibrium rate of dissociation means, then, that, at least under the conditions under which eq. 1.3 holds, each discrete level furnishes decompositions over a range δE . In the reverse reaction, associating fragments having relative energies over a range δE stream over the potential-energy hump and immediately suffer a transition to the discrete state. Thus the discrete level is broadened to this extent. The interesting point is that the mechanism described by Marcus and Rice is equivalent to the assumption that the discrete states are broadened at a minimum by an amount just equal to the energy between them. If $P_{E-E_m} > 1$, then, of course, the lifetime is shortened, presumably the states are broadened still more, and overlap appreciably; but they do at least overlap slightly. If they were not broadened as much as indicated by eq. 1.3, then τ_E would have to be greater and k_E smaller. This would correspond to a lack of efficiency in the transfer to the discrete state of systems which had passed over the potential-energy hump; some of them would go back over the hump again. There would be a corresponding inefficiency in the transfer of systems which were in a position to go from the discrete state to the continuum. In view of the violence of the vibrations, the degree of anharmonicity necessarily involved, the "perturbation" for this transition should be large, and its efficiency would be expected to be of the order of magnitude of 1. In any case P_{E-E_m} will be greater than 1 except when E is quite close to E_m ,

complex in which some of the vibrations have changed to rotations; but P_{E-E_m} may simply be defined to include any such rotational states. Over-all rotations of the molecule which give rise, in the rate expression, to a ratio of the corresponding partition function in the complex to that in the decomposing molecule (see Section C of ref. 4) need not be considered here, since this factor comes from averaging over all rotational states, taking into account the effect of the rotational potential on the activation energy [O. K. Rice and H. Gershinowitz, *J. Chem. Phys.*, **2**, 853 (1934)]. Here we are interested in the rate of decomposition from a definite rotational state, which, of course, remains fixed in the process of dissociation, since over-all angular momentum is conserved.

(2) L. S. Kassel, *J. Am. Chem. Soc.*, **53**, 2143 (1931).

(3) See for example, J. C. Giddings and H. Eyring, *J. Chem. Phys.*, **22**, 538 (1954).

(4) R. A. Marcus and O. K. Rice, *J. Phys. Colloid Chem.*, **55**, 894 (1951).

(5) P_{E-E_m} is the number of ways the excess energy $E - E_m$ (or less) can be distributed among the various internal degrees of freedom, the difference between $E - E_m$ and the energy so distributed going to the reaction coordinate. It is essentially what Marcus and Rice called ΣP_E , separate treatment being given by them for an activated

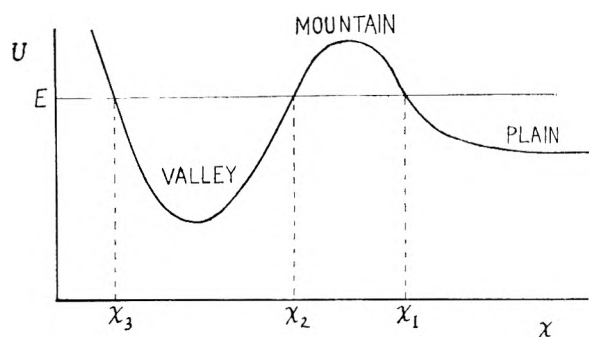


Fig. 1.

and especially in the case of a loose activated complex. So the quantization, in itself, will not present a barrier to recombination, contrary to what apparently has been believed.³

Equation 1.3 is essentially an uncertainty relation. The value of the uncertainty is, however, somewhat unexpected. There are some processes which resemble unimolecular decompositions to some degree, namely predissociation, and leakage through a potential-energy barrier from a discrete state into a continuum, as in radioactive decomposition (the tunnel effect), and in these cases the relation between lifetime and broadening has been given as

$$\tau \delta E = h/2\pi \quad (1.4)$$

Although the uncertainty principle is guaranteed to give only the order of magnitude of the product of the uncertainties in the time and the energy, the difference between eq. 1.3 and 1.4 appears at first sight rather puzzling and will bear some further analysis, which will be given in the next section.

2. Predissociation and Leakage through a Barrier.—These processes were discussed by a number of investigators around 1930. I find it convenient to use my own formulation; references to earlier work may be found in the papers I shall cite. I have already considered the relation of these processes to unimolecular decomposition⁶; a resurvey of the situation indicates, however, that there are some points yet to be made. I showed⁷ that predissociation and leakage from a discrete state through a barrier parallel each other in great detail. It would seem that we could consider either case, as might be most convenient, and we will confine ourselves here to leakage through a barrier.

We shall consider a one-dimensional case, coordinate x giving the distance between a pair of particles having a mutual potential-energy, U , as shown in Fig. 1, which will serve to fix the notation. (A three-dimensional case can be reduced to one dimension by a proper transformation of variables and use of a rotational potential, so there is no loss of generality from this cause.) This situation was discussed⁸ with the aid of the WKB approximation. In this discussion integrals of the form

$$\kappa \int_{x'}^{x''} (E - U)^{1/2} dx$$

(where $\kappa^2 = 8\pi^2\mu/h^2$, with μ the reduced mass of the separating particles, and where E is the total, constant energy) between certain limits here indicated in general form as x' and x'' , constantly recur. We shall write

$$I(x', x''; E) = \kappa \int_{x'}^{x''} (E - U)^{1/2} dx - \pi/4 \quad (2.1)$$

We shall also have occasion to make use of the quantities

$$\theta = 2 \exp \left[\kappa \int_{x_2}^{x_1} (U - E)^{1/2} dx \right] \quad (2.2)$$

and

$$b = \tan [I(x_3, x_2; E) - I(x_3, x_2; E_1)] \quad (2.3)$$

where E_1 is the energy of the unperturbed discrete state (the center of the broadened discrete level). If broadening is not too great we may write

$$\begin{aligned} b &\cong I(x_3, x_2; E) - I(x_3, x_2; E_1) \\ &\cong (E - E_1) \partial I(x_3, x_2; E) / \partial E \\ &= b'(E - E_1) \end{aligned} \quad (2.4)$$

defining b' . Kramers⁹ showed that the energy E_1 of a discrete state in a valley such as shown in Fig. 1 is given by the condition

$$\kappa \int_{x_3}^{x_2} (E_1 - U)^{1/2} dx = n\pi \quad (2.5)$$

where n is a quantum number, equal to $1/2, 3/2, 5/2, \dots$. If, however, n is considered to be a continuous function of E , we may write

$$b' = \pi dn/dE \quad (2.6)$$

It is possible, by double application of the WKB approximation^{8,9} to find how a certain solution of the wave equation in the valley goes over to the corresponding solution in the plain. If the wave function in the asymptotic part of the plain is normalized to give an average probability density of $1/2 (E - U_a)^{-1/2}$ (where U_a is the asymptotic value of U), the correlation is

$$\begin{aligned} \theta(1 + b^2\theta^4)^{-1/2} (E - U)^{-1/4} \{ \cos[I(x, x_2; E)] + \\ b[\sin I(x, x_2; E)] \} \\ \xrightarrow[\text{valley}]{\text{plain}} - (1 + b^2\theta^4)^{-1/2} (E - U)^{-1/4} \\ \{ \sin [I(x_1, x; E)] + b\theta^2 \cos [I(x_1, x; E)] \} \end{aligned} \quad (2.7)$$

$I(x, x_2; E)$ and $I(x_1, x; E)$ are, of course, functions of the variable x , while x_1, x_2 and E play the roles of parameters. As indicated by the direction of the arrow the solution for the valley is the first of these expressions.

It was possible to set up a wave packet, such that the part in the valley represented a solution for the stationary state E_1 , but with a decrement with time, while that in the plain represented an outgoing wave which broke off, becoming suddenly zero, at a point x equal to the distance a particle could move in time t , i.e., at a cut-off point, where $(\kappa/2E_a^{1/2})x - 2\pi t/h = 0$, where $E_a = E_1 - U_a$. This wave packet, normalized to have a probability density equal to 1 at the cut-off point in the asymptotic part of the plain, has the form

(6) O. K. Rice, *Phys. Rev.*, **34**, 1451 (1929).

(7) O. K. Rice, *ibid.*, **35**, 1551 (1930).

(8) O. K. Rice, *ibid.*, **35**, 1538 (1930).

(9) H. A. Kramers, *Z. Physik*, **39**, 828 (1926); E. C. Kemble, "Fundamental Principles of Quantum Mechanics," McGraw-Hill Book Co., New York, N. Y., 1937, Sec. 21.

$$E_a^{1/2}(E_1 - U)^{-1/2} \theta \cos [I(x, x_2; E_1)] \exp(-2\pi i E_1 t / h) \exp(-2\pi t / hb'\theta^2)$$

plain (asympt.)
 \longleftrightarrow valley
 $\{ \sin [I(x_1, x; E_1)] - i \cos [I(x_1, x; E_1)] \}$

$$\times \exp(-2\pi i E_1 t / h) \exp\{[(\kappa/2E_a^{1/2})x - 2\pi t/h]/b'\theta^2\}$$

(2.8)

It is seen that this is a wave with an exponential decrement equal to $2\pi t/hb'\theta^2$; the rate constant for the decrease of probability density in the valley is $4\pi/hb'\theta^2$ and the loss of material in the valley may be shown, with the use of eq. 2.5, to be equal to the material flowing outward in the plain at $x \cong 0$; furthermore, there is complete conservation of probability density in time out to the cut-off point where $(\kappa/2E_a^{1/2})x - 2\pi t/h = 0$.

In order to set up the wave packet which we have described, it was necessary to multiply the normalized stationary wave function for energy E , including the time factor $\exp(-2\pi i Et/h)$, by a weighting factor proportional to $(1 + b^2\theta^4)^{-1/2} = [1 + b'^2(E - E_1)^2\theta^4]^{-1/2}$, and sum over all energy levels (the continuum was changed into a closely spaced set of discrete levels by assigning an upper limit, x_∞ , to the values which x can take, but the sum was converted into an integral with respect to E by dividing by ϵ , the energy between adjacent levels). It will be noted from (2.7) that the probability density of the wave function in the valley which is correctly connected with the normalized wave function in the plain is approximately proportional to the square of this quantity [from (2.7) the ratio of the densities in valley and plain is proportional to $(1 + b^2)/(1 + b^2\theta^4)$ which is approximately $(1 + b^2\theta^4)^{-1}$ since b is small and θ is large]. So the width, w , of the broadened discrete state was taken as the width at half the maximum of $[1 + b'^2(E - E_1)^2\theta^4]^{-1}$, found by setting

$$w = 2/b'\theta^2 \tag{2.9}$$

From the preceding paragraph we have for the lifetime of the discrete state

$$\tau = hb'\theta^2/4\pi \tag{2.10}$$

hence

$$w\tau = h/2\pi \tag{2.11}$$

which is seen to be like eq. 1.4 and which is to be contrasted with eq. 1.3. It might be more logical to define the width of the discrete state by the integral

$$w = \int_{-\infty}^{\infty} [1 + b'^2(E - E_1)^2\theta^4]^{-1} d(E - E_1) = \pi/b'\theta^2 \tag{2.12}$$

which is equal to the width which would be required to give the same total weight to the discrete part of the eigenfunctions (*i.e.*, the same integrated "intensity" of the discrete energy level) if the intensity were a step-function constant over the width w and zero outside this. This would give

$$w\tau = h/4 \tag{2.13}$$

but the discrepancy with eq. 1.3 still exists.

We can gain a better understanding of the significance of this discrepancy by a further consider-

ation of the stationary wave functions as represented in the relation (2.7). It will be noted that when $b = 0$, *i.e.*, $E = E_1$, there is left a cosine term in the valley and a sine term in the plain, and $\cos[I(x, x_2; E)]$ is, indeed, the approximate wave function for a discrete state as furnished by the WKB approximation. If the mountain is high and wide, θ is large, and the discrete part of the wave function (2.7) has a large amplitude, as compared to the part in the plain, if $E = E_1$. There being thus a direct connection between $\sin[I(x_1, x; E_1)]$ and $\cos[I(x, x_2; E_1)]$, the latter having much the greater amplitude, it seems natural to interpret this wave function in the following way. There is a stream of particles coming from the plain toward the mountain, *all* these particles tunnel through the mountain, they are trapped for a time in the valley, they eventually pass through the mountain again, forming a stream in the other direction. This is too detailed a description to be drawn with certainty from the wave function, but it obviously represents a maximum rate for passage of particles into the valley. The WKB connection for $\cos[I(x_1, x; E)]$ is with $\sin[I(x, x_2; E)]$, and the coefficients of these terms increase as E departs from E_1 and b increases, but the cosine term in the plain obviously increases much faster than the sine term in the valley if θ is large. Indeed, the sine term in the valley never becomes appreciable if the discrete level is not much broadened, as may be seen from eq. 2.4 and 2.6. There will therefore be no effective penetration of the barrier from the cosine term in the plain. Indeed this is to be expected since the cosine term is of the correct form for an eigenfunction in the plain if the valley did not exist. As one approaches the energy E_1 there is a gradual change of phase¹⁰ until just at E_1 the eigenfunction in the plain is just 90° out of phase with what it would be if it did not interact with the valley at all, or if there were no valley.

The rate of association or dissociation will be equal to half (since half of the particles are moving in each direction at equilibrium) the average square of the coefficient of the $\sin[I(x_1, x; E)]$ in eq. 2.7, times the average value of the square of the sine (equal to $1/2$), times the asymptotic velocity of the particles, or $[2(E - U_a)/\mu]^{1/2}$. This is equal to

$$1/2(2\mu)^{-1/2} (1 + b^2\theta^4)^{-1} \tag{2.13}$$

The total square of the amplitude of the wave function inside the valley, with the same normalization, is equal to

$$(1 + b^2\theta^4)^{-1}\theta^2 \int_{x_1}^{x_2} (E - U)^{-1/2} \cos^2[I(x, x_2; E)] dx \tag{2.14}$$

This neglects the sine term in the valley, which, as noted, is legitimate if the discrete state is not broadened too much. The average value of $\cos^2[I(x, x_2; E)]$ may be safely taken as $1/2$, so eq. 2.14 becomes

(10) It is of interest that just the same change of phase occurs in the case of predissociation, since the perturbed energy levels lie between the levels of the continuum (made discrete by assuming a largest possible value of x) in just the right positions to cause the phase changes to occur in the same way.

$$\frac{1}{2}(1 + b^2\theta^4)^{-1}\theta^2 \int_{x_1}^{x_2} (E - U)^{-1/2} dx = (\theta^2/\kappa)b'(1 + b^2\theta^4)^{-1} \quad (2.15)$$

Dividing (2.13) by (2.15) we see that the fraction of material in the valley flowing in or out per unit time is given by

$$k_{\text{eq}} = \kappa/2(2\mu)^{1/2}b'\theta^2 = \pi/hb'\theta^2 \quad (2.16)$$

essentially independently of the energy of the state considered, so long as it is not far beyond the broadened discrete line. So for the equilibrium "lifetime" we have

$$\tau_{\text{eq}} = hb'\theta^2/\pi \quad (2.17)$$

and, combining eq. 2.12 and 2.17

$$w \tau_{\text{eq}} = h \quad (2.18)$$

which now has the same form as eq. 1.3.

These considerations are confined to the case where θ is large and the penetration of the barrier is small. The result, therefore, depends sensitively upon the details of the connection between the valley and the plain through the barrier. The rate given by (2.16) is certainly, as we have noted, the maximum possible for the equilibrium case; but a greater rate is obtained by setting up the wave packet of (2.8). It appears that the difference between the rates based on equilibrium considerations and on the wave packet arises largely from the fact that in the former we treat the wave function of each energy level separately assuming no correlation of phases, while in the case of the wave packet the phase relations are predetermined and coherence effects appear. In earlier work^{6,8} we have considered in some detail the way in which a wave packet can be set up. If it is to be done by absorption of radiation it must be done by a short burst so as to contain a sufficient range of energies to excite the broadened discrete level coherently.

We have seen that the relation (2.18), obtained for the equilibrium case in barrier leakage or predissociation, also holds for the equilibrium theory of chemical reaction. However, since we are accustomed to considering reaction rates very far removed from equilibrium (or under such circumstances as to be unaffected by the attainment of equilibrium), the question very naturally arises as to whether we are underestimating the reaction rate by a factor of the order of four by using an equilibrium theory. If we suppose that the collisions (which are processes of short duration compared to the lifetime of an activated molecule and hence not well-defined in energy) set up an average situation which is well described by wave functions representing broadened discrete states, which are connected with continua, in much the same way⁶ that a short burst of radiation can set up a broadened discrete state in predissociation or tunnel effect, as represented by (2.8) at zero time, then we might suppose by analogy that this would be the case. In order to assess this possibility we need to consider differences as well as similarities in the two processes. In the case of barrier leakage or predissociation, the system generally has plenty of time after its excitation to complete many cycles in its discrete state before it dissociates through a quantum-mechanical process. This would seem

to be the most important difference. In an activated molecule, on the other hand, the dissociation takes place, with essentially 100% efficiency, as soon as a certain phase in the motion is reached, *i.e.*, as soon as the energy accumulates in a particular bond. In the case of the unimolecular decomposition the exciting collision is localized, and the averaging over the various phases of the motions is effected at least in part, and especially when the pressure is high, by the randomness of the collisions as regards position and orientation, rather than by retracing of the phase path. In some respects it might be better to represent the motion of the activated molecule more or less as a localized and moving wave packet. This is not the case in the predissociation or barrier leakage, where the discrete state may be said to be excited "as a whole." The relative slowness of dissociation in the barrier leakage is due to the improbability of the quantum penetration process; in the unimolecular reaction it is due to the difficulty of localizing energy in a bond. In the latter case, one might expect the semi-classical picture of flow of energy to give the correct result, taking account only of the density of energy levels, without considering more subtle quantum effects. This is an argument in favor of the Marcus-Rice result, but it may be less cogent at low pressures where the time between collisions becomes of the order of magnitude of, or greater than, the lifetime of the active molecule. In such a case the bond will on the average almost break at least several times before it receives the requisite energy actually to break, as noted in Section 4. Thus the phases of the vibrational motion of the molecule could be approximately retraced a number of times before the dissociation occurs, and the situation would more closely resemble that in the barrier leakage, and could perhaps be roughly represented by a wave packet analogous to (2.8). If this results in an increase in the rate of decomposition it would cause the apparent unimolecular rate constant to fall off at a higher pressure than would otherwise be expected. The effect would probably not be great enough to be distinguished experimentally from other factors.

3. Effect of Quantization on the Rate of Activation.—As a practical matter, quantization can affect the rate of activation, and thereby the pressure at which the falling-off in the unimolecular rate constant occurs, simply by changing the distribution of energy in the molecule. Although this was the first quantum effect to be considered in the development of the theory of unimolecular reactions, it seems worth while to point out that several distinct cases occur, associated with vibrational frequencies of different magnitude in comparison with the characteristic energies involved. Low frequencies can, of course, be handled by means of the classical approximation. Intermediate frequencies may be defined as those which are high enough so as not to be appreciably excited at the temperature of the experiment, but low enough so that they would be excited at a temperature such that the average energy would coincide roughly with that of the activated mole-

cules. High frequencies would not be excited under either of these conditions.

The cases of intermediate and high frequencies may be compared with the classical case. The rate of activation is generally assumed to be proportional to the equilibrium fraction, W_a , of molecules in the particular range of energies which constitute the activated state under consideration. We wish to find $W_a/W_{a,cl}$, where $W_{a,cl}$ is the fraction which would exist were the molecule classical.

In the intermediate case $W_a/W_{a,cl}$ is easily evaluated.¹¹ The fact that the activated molecule is "classical" means that its energy levels are fairly closely spaced. Both the unactivated and the activated molecules would behave classically, if all the frequencies had some low value, say ν_c . The ratio of the true density of levels arising from, let us say, n vibrations, in the activated range, to the density if they all had frequency ν_c

would be $\nu_c^n / \prod_{i=1}^n \nu_i$. The ratio of the effective densities of levels in the unactivated molecules will be given by a ratio of corresponding vibrational partition functions Q , or $\left(\prod_{i=1}^n Q_i \right) / Q_c^n = (h\nu_c/kT)^n$

$\prod_{i=1}^n Q_i$ since a classical partition function $Q_c = kT/h\nu_c$. Thus

$$\begin{aligned} W_a/W_{a,cl} &= \left(\nu_c^n / \prod_{i=1}^n \nu_i \right) \left[(h\nu_c/kT)^n \prod_{i=1}^n Q_i \right] \\ &= \prod_{i=1}^n [(kT/h\nu_i)/Q_i] = \prod_{i=1}^n (Q_{i,cl}/Q_i) \end{aligned}$$

since $kT/h\nu_i$ is the high temperature or classical limit for Q_i . $W_a/W_{a,cl}$ is, in this case, always greater than 1; however, it must be noted that it has a temperature coefficient, and this must be taken into account when determining the parameters which enter into the theoretical estimate of the activation energy from the experimental temperature coefficient. This was considered¹¹ in the case of the decomposition of F_2O , which is a good example of a unimolecular reaction in its low-pressure stage, and it was found that the net effect was a reduction in the rate of activation. This, however, is strictly a secondary effect.

This contrasts with the situation with high frequencies. In this case the higher levels corresponding to these frequencies are not excited at all, and the extra energy levels at high energy which increase $W_{a,cl}$ are not available in W_a . In other words, a high frequency is not one to which the energy can be distributed, and so the number of distributions in the high energy range is cut down. This is a direct effect of quantization. It was taken into account by Rice and Ramsperger¹² by assuming that the energy of only a limited number of classical oscillators was available for accumulation in the reaction coordinate, and by Kassel,¹³ by

using a larger number of oscillators with an "average" frequency.

4. Near-dissociation and Effect of Anharmonicity.—There will be times when the reactive bond in a molecule gets almost, but not quite, enough energy to dissociate it. Since the energy levels are close together near the dissociation limit, this will have somewhat the same effect as dissociation on the rest of the molecule.

Let us consider the case where a molecule has barely enough energy to dissociate. After dissociation the fragments are in their ground states. There is no choice, then, for the distribution of energy; the state of the activated molecule will connect to a single continuum. If we are dealing with a relatively complex molecule, we may expect there to be several vibrational modes with low frequencies, the corresponding $h\nu$ being only a few times kT . If any one of these frequencies retains one quantum of excitation, the reactive bond can receive an excitation to a point only slightly lower than its dissociation limit. This process would certainly not occur less rapidly than the dissociation. The levels in the activated molecule are already broadened by the dissociation so that they merge together, but this process might broaden them still further in a certain sense. If the vibrational levels of the reactive degree of freedom^{13a} (before considering the perturbation due to the rest of the molecule) are sufficiently closely spaced, the energy levels of the whole molecule may well be "broadened" enough (considering only the interaction with discrete levels of the reactive bond) to cover several of them. On the other hand, if the energy localized in the reactive degree of freedom is sufficiently low to cause it to be far enough below its dissociation limit so that its levels are spaced farther apart than the levels of the molecule as a whole, the levels of the reactive vibration may be expected to be "broadened" so as to overlap, and thus cover several of the levels of the whole molecule. For one of these vibrations of the reactive degree of freedom is strongly perturbed by the rest of the molecule at least once during a single vibration, when the bond is at its minimum distance. Indeed, the lifetime of such a vibration would scarcely be expected to exceed its period. Thus the broadening, δE , would be related to the period, τ , by the usual relation, as indicated in the preceding section of this paper

$$\tau \delta E \sim h$$

But then, by the correspondence principle, δE is just equal to the distance between levels. Thus we may expect free interaction between the levels of the reactive vibration with the various levels of the molecule as a whole. Perhaps we should say that the expectation of such a strong interaction, due to the strong perturbations which must exist, cannot be inhibited by quantum effects. Since there would be various ways that the energy could come into the reactive bond in such a way as to nearly break it, contrasted to the one way it can actually break it, the bond will be nearly broken a number of times before it is actually broken.

(11) O. K. Rice, *Monatsh. Chem.*, **90**, 330 (1959).

(12) O. K. Rice and H. C. Ramsperger, *J. Am. Chem. Soc.*, **49**, 1617 (1927).

(13) L. S. Kassel, *J. Phys. Chem.*, **32**, 1065 (1928).

(13a) Synonymous with "bond which breaks."

The preponderance of near misses will presumably be greater when the molecule has excess energy so that there are more ways in which the energy can be distributed.

According to the theory which has been advanced and discussed in recent years by Slater,¹⁴ the process of dissociation is assumed to occur when the phase relations between various excited normal vibrations become such that the displacement of a certain bond from its equilibrium position becomes greater than a certain value. One result of this hypothesis is that excitation in certain degrees of freedom is very much more effective than in others in producing dissociation. Thus, in a quasi-unimolecular reaction, the pressure at which the rate constant began to fall off from its high-pressure value would be that which might be expected for a molecule with a smaller number of degrees of freedom—that is, the molecule would act as though it were smaller than it really is. The effect of anharmonicity was assumed to be that of a minor perturbation, which might cause slow exchange of energy between nearly normal modes of vibration. However, we have seen that the bond which is to break visits a region in which the anharmonicity is extreme at least several times on the average before it will break. Further, in the course of the motion before the dissociation occurs, other bonds will be stretched to the point where anharmonicity is at least quite appreciable. To be sure, we can hardly conceive of transfer of energy from a bond at the moment when it is stretched to the end of its swing, but it will encounter appreciable anharmonicity on the way. It hardly seems, therefore, that the effects of anharmonicity can be regarded as those of a minor perturbation; one may expect the exchange of energy between degrees of freedom to be rapid compared to the rate of dissociation. It is, perhaps, conceivable that in certain cases the symmetry of the molecule would be such that completely free transfer of energy between all the degrees of freedom would not be possible, but it seems likely that such a situation would occur only rarely. These ideas are supported by recent experimental results¹⁵ in which certain excited radicals are formed in different ways. Subsequent decomposition of the excited radicals gives a new set of products, but always the same set, and occurs at rates whose differences can be accounted for by differences in the energy of the decomposing radical. As indicated by the authors of these papers, the results would seem to indicate efficient redistribution of energy.

The Slater hypothesis that the criterion for dissociation is stretching of a bond to a certain point seems somewhat unrealistic in physical detail when we consider the known nature of potential-energy curves in the neighborhood of the dissociation energy. As Slater pointed out, it puts additional restrictions on the criterion for dissociation beyond that of merely having sufficient energy to break a certain bond. Effectively

this results from the presumption that there are other constants of the motion than merely the total energy. Our argument of the preceding paragraph indicates that in almost all cases the total energy is the only important constant of the motion. There is much redistribution of energy before the reaction finally occurs, so that it seems reasonable to suppose that before the final event, the initial state of the excited molecule is "forgotten." Especially should this be true where quantum mechanics is taken into account. Therefore, it seems most reasonable to treat the problem of dissociation as a statistical problem in the redistribution of energy, as is done in the Rice-Ramsperger-Kassel-Marcus theory. Our discussion applies specifically to the case of a rigid activated complex, but it would apply *a fortiori* to the case of a so-called loose activated complex.⁴

It is true that if the time between collisions is very small there will not be time for the transfer of energy from one degree of freedom to another to occur, but when the pressure is such that the time between collisions is of the order of magnitude of the average life time of a molecule at any given energy range (which is the important pressure in the determination of the effect of pressure on the unimolecular rate constant) the anharmonicity should already be effective. Thus, it seems unlikely that the falling off of the rate constant with decreasing pressure will be slowed by a gradual increase in the number of effective degrees of freedom, as has often been suggested. It will be noted that such an effect would, in a certain sense, be opposite to that tentatively predicted at the end of Section 2.

5. Quantitative Effects of Anharmonicity on the Rate of Dissociation at Low Pressures.—Anharmonicity can increase the equilibrium fraction of activated molecules, because at higher energies the bonds are more stretched, even with the average distribution of energy within the molecule, and the levels are closer together than if the anharmonicity did not occur. We have discussed this¹¹ in considerable detail for the case of F_2O . In this case there are only three degrees of freedom of vibration, and we assumed that they all had, at least approximately, the same dissociation energy. An activated molecule contains enough energy to break one of them, so on the average each bond is about one-third dissociated, the energy levels are about $\frac{2}{3}$ as far apart as if the molecule were in its ground state, and the probability of the activated state is therefore increased by a factor of about $(\frac{3}{2})^3$. The rate of activation, and hence the rate of reaction at the low pressure limit, is increased by this same factor.

In the general case, if the bonds in a molecule with n vibrations all had the same dissociation energy, the factor would be $[n/(n-1)]^n$, and would approach e for large n . However, since most of the bonds would have a higher dissociation energy, the true ratio would be less than this, and the effect would be unimportant except for small molecules. It was important in the F_2O case as a partial explanation for an apparently very high preexponential rate factor. The other factors

(14) N. B. Slater, "Theory of Unimolecular Reactions," Cornell University Press, Ithaca, N. Y., 1959.

(15) R. E. Harrington, B. S. Rabinovitch and H. M. Frey, *J. Chem. Phys.*, **33**, 1271 (1960); J. N. Butler and G. B. Kistiakowsky, *J. Am. Chem. Soc.*, **82**, 759 (1960).

involved in the high rate were the effect of energy of rotation on the rate of reaction, and a chain of two steps in the decomposition.

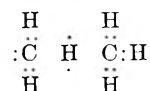
6. The Problem of Loose Activated Complexes.—When there is a "loose" activated complex⁴ certain vibrations, usually bending vibrations, become "loosened" into the equivalent of rotations; this is the same as saying that in the reverse association reaction no mutual orientation of the combining parts is required. How such a state of affairs can come about is a problem involving both quantization and anharmonicity, the former because the vibrations and rotations (or their equivalent) are quantized very differently, the latter because, if the vibrations were truly harmonic, no such change in their character would be possible. It is rather difficult to understand why some activated complexes are loose, while others which seem rather similar are rigid. However, in cases in which they are known to be loose some conclusions concerning their character and behavior can be drawn from general principles.

One must suppose that when the reactive bond is not stretched the bending vibrations will not have changed to rotations or to a looser configuration. On the other hand, when the bond is stretched nearly to its breaking point, this change has taken place if the activated complex is loose. Since there are many more available energy levels when the bond is stretched than when it is at its normal length (accounting for the increased rate of reaction of a loose complex), there must be many more molecules, among those having the requisite energy, in which the bond is stretched than in which it is not stretched. In order for this to be true we must suppose that, once the bond is stretched, it does not readily return to its equilibrium position. However, if this were true only for those molecules in which sufficient energy is localized in the reactive bond to break it, this could not result in the high value for the pre-exponential factor characteristic of the loose activated complex. For the reaction then could not proceed without going through a situation in which the reactive bond had sufficient energy and was unstretched. Since the loosening of the bending vibrations would occur only after the bond was stretched the rate at which the above described situation could arise would be that characteristic of a rigid complex. We will have to suppose that the loosening occurs when the reactive bond is stretched, even though it does not have sufficient energy to break, and that the reaction generally occurs through the attainment of further energy by this bond when the molecule is in this condition. In other words, the molecule is loosened first, breaks up afterward. In the association reaction we must imagine ways by which the associating parts can be held together with the bond stretched, a condition from which the system relaxes only after a lapse of time, but in general before it can dissociate again.

When the reactive bond is stretched the bending vibrations of the attached groups must become much freer. Such a vibration could change into a wagging motion which is almost as free as rota-

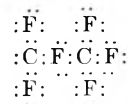
tion. If this were the mechanism in the dissociation of ethane into two methyls, for example, the almost separated methyls could turn their hydrogens toward the bond, in which case the bond could not shorten readily to its normal length. Furthermore, assuming equilibrium is established (as we must, if the full increase in rate of reaction is to be attained), the wagging motion would be slower than the vibration in just the ratio that the distance between energy levels would be decreased. The time during which the bond would remain stretched would thus be expected to be increased in about the same ratio, whether we look at the situation from a mechanical or statistical point of view.

The very high rate of recombination of methyl radicals, which occurs at nearly every collision,¹⁶ indicating that the bending vibrations are fully loosened to rotations in the activated complex, suggests the possibility that the mechanism described in the preceding paragraph needs to be modified or supplemented. It suggests itself that the unpaired electrons are able to interact at relatively great distances, almost without regard to the orientation of the radicals to which they are attached. Thus three-center bonds might be formed on any hydrogen, giving a structure such as



which would have some stability though of course less than the usual form. Such a structure would be expected to have considerably loosened bending vibrations, and this would be necessary, for it is not possible to account for the high rate of dissociation of methyl radicals and the correspondingly high frequency factor for the dissociation of ethane simply by the number of such bonds which could be formed, though this would be a factor.

The recombination of ethyl radicals also proceeds rapidly,¹⁶ with a steric factor of about 0.1; the decomposition of azomethane is a case where the frequency factor is large,¹⁷ about $10^{17.3}$ which could just about be accounted for by free rotation of *both* methyls in the activated complex, with some contribution from rotation of N_2 . In these cases, also, three-center bonds would be a possibility. In the case of the recombination of fluoromethyl radicals,¹⁶ which also has a steric factor of about 0.1, structures such as



might be intermediates.

If intermediates such as these were only sufficiently stable so that they would revert to the most stable structure more rapidly than they would decompose again, they could serve to stabilize the molecule temporarily, thus giving

(16) S. W. Benson, "The Foundations of Chemical Kinetics," McGraw-Hill Book Co., New York, N. Y., 1960, p. 302.

(17) W. Forst and O. K. Rice, 139th meeting of the American Chemical Society, St. Louis, March, 1961. Paper No. 118, Division of Physical Chemistry.

time for the bond to be formed without the immediate necessity for the orientation of the radicals, which is characteristic of the rigid activated complex.

Van der Waals forces could, of course, hold the radicals together, and this has been suggested several times. However, in this case the dissociation energy would be so small and the interaction of the radicals so weak that they would probably dissociate again before a normal bond could be formed. Especially would this be expected to be true in the case of methyl radicals. Van der Waals forces between two methyl radicals might be expected to be somewhat greater than those between two methane molecules, since the methyl radicals might be more polarizable. However, the difference between methyl and methane would have to be considerable in order for a van der Waals complex of two methyl radicals to be sufficiently stable, in the light of the low boiling point of methane.

When the bending vibrations which are to be changed to rotations or looser oscillations involve C-H bonds, they will in general be in the category of high frequencies discussed in Section 3. This means that, in order for the rotations to come into something resembling an equilibrium state, the zero-point energy of the bending vibrations must be dissipated. This implies transfer of energy between these degrees of freedom and other degrees of freedom in the molecule. Conversely, if the complex is rigid, the vibrational levels are not broadened,¹⁸ and the reverse association requires matching of energy levels. This means that zero-point energy must be furnished for the vibrations formed. The importance of this concept has already been pointed out.¹⁹

(18) These are vibrational levels of the *activated complex*, and the broadening which is significant is that due to interaction with the rotations of the dissociated fragments.

(19) O. K. Rice, *J. Chem. Phys.*, **4**, 53 (1936).

THE VARIATION OF LATTICE PARAMETER WITH CARBON CONTENT OF TANTALUM CARBIDE¹

BY ALLEN L. BOWMAN

Los Alamos Scientific Laboratory of the University of California, Los Alamos, New Mexico

Received April 21, 1961

A lattice constant of $a_0 = 4.4555 \pm 0.0003$ Å. has been determined for $\text{TaC}_{0.994 \pm 0.005}$ at 25°. The equation $a_0 = 4.3007 + 0.1563$ (C/Ta) has been calculated relating composition to lattice parameter of TaC. Solution of this equation for $\text{TaC}_{1.00}$ gives a lattice parameter of 4.4570 ± 0.0010 Å.

Introduction

TaC forms a face-centered cubic crystal lattice for which the lattice constant, c_0 , decreases as the crystal becomes deficient in carbon. An exact knowledge of the relationship between a_0 and the TaC composition provides a possible analytical tool, and, by extrapolation, gives a value of a_0 for the stoichiometric composition $\text{TaC}_{1.00}$.

Lesser and Brauer,² Smirnova and Ormont,³ Robins⁴ and Kempter and Nadler⁵ have determined the variation of lattice parameter with composition for the TaC phase, but with a notable lack of agreement. Kovalskii and Umanskii⁶ have measured the lattice parameter of an analyzed sample of tantalum carbide. In addition, van Arkel,⁷ Becker and Ebert,⁸ von Schwarz and Summa,⁹ Burgers and Basart,¹⁰ McKenna,¹¹ Norton

and Mowry,¹² and Brownlee¹³ have measured lattice constants of TaC. The lack of analytical data on the material studied leaves most of the reported values in question. It should be noted that in most cases the reported lattice parameters are about 4.455 Å.; thus the compositions are probably close to $\text{TaC}_{1.00}$.

Experimental

TaC samples were prepared by two different methods.

(1) Kennametal high-purity tantalum powder and AUC graphite powder, outgassed at 2000°, were used as starting materials. Spectroscopic analysis of the tantalum showed major impurities, in p.p.m., to be Nb 300, Fe 200, W 150, Zn 100, Mo 50. The graphite was analyzed and found to be 99.4% C. After thorough mixing the tantalum-carbon powder was loaded into a graphite crucible and heated inductively for 10 min. at 2400° under vacuum of 10^{-4} mm. or better. In some cases the sample was removed from the crucible, ground to a powder, and then returned for similar additional heatings. In every sample a large evolution of gas was noted at 1000° and again at 1500° as the sample was brought slowly to heating temperature. No evolution of gas was noted when a sample was heated for a second time. The sample size was about 5 g. The TaC was removed from the crucible as a firm plug with a gold or light-brown color. This color was uniform throughout when the sample had a C/Ta ratio greater than about 0.90, but with lower carbon content the gold color was observed only on the surface, with the interior

(1) This work supported in part by the U. S. Atomic Energy Commission.

(2) R. Lesser and G. Brauer, *Z. Metallk.*, **49**, 622 (1958).

(3) V. I. Smirnova and B. F. Ormont, *Zhur. Fiz. Khim.*, **30**, 1327 (1956).

(4) D. A. Robins, "The Physical Chemistry of Metallic Solutions and Intermetallic Compounds," Paper 7B, Her Majesty's Stationery Office, London, 1959.

(5) C. P. Kempter and M. R. Nadler, *J. Chem. Phys.*, **32**, 1477 (1960).

(6) A. E. Kovalskii and Ya. S. Umanskii, *Zhur. Fiz. Khim.*, **20**, 769 (1946).

(7) A. E. van Arkel, *Physica*, **4**, 286 (1924).

(8) K. Becker and F. Ebert, *Z. Physik*, **51**, 268 (1925).

(9) M. von Schwarz and O. Summa, *Metallwirtschaft*, **12**, 298 (1933).

(10) W. G. Burgers and J. C. M. Basart, *Z. anorg. allgem. Chem.*, **216**, 209 (1934).

(11) P. M. McKenna, *Ind. Eng. Chem.*, **28**, 767 (1936).

(12) J. T. Norton and A. L. Mowry, *Trans. AIME*, **185**, 133 (1949).

(13) L. D. Brownlee, *J. Inst. Metals*, **87**, 58 (1958).

of the sample gray in color. The surface was scraped off, and the remainder of the sample was pulverized in a mullite mortar.

(2) Fansteel high-purity tantalum powder and spectroscopic grade Madagascar flake graphite were used as starting materials. Analysis of the tantalum showed Ta 99.8%, and, in p.p.m., C 900, H 45, N 325, O 940, Nb 400, W 100, Fe 500. The melting point was 2990°. The lattice parameter was 3.307 Å. before melting and 3.304 Å. after melting. The thoroughly mixed powders were heated inductively in 25-g. batches in graphite crucibles at 1850°, under vacuum of 10^{-4} mm., for six 1.5 hour periods, with material ground to a powder after each heating. As the preparation progressed, the light-brown surface coat gradually decreased on the samples with C/Ta less than 0.85, leaving a sample uniformly gray in color. The finished samples of C/Ta greater than 0.85 were brown in color throughout the sample.

All of the samples were analyzed for tantalum and total carbon by combustion, and for free carbon by a chemical method.¹⁴ The samples prepared by method (2) were also analyzed for nitrogen by a modified Winkler technique. The sample is dissolved in hot $H_2SO_4-K_2SO_4$, then made strongly alkaline with KOH, and the ammonia is steam-distilled into boric acid, which is titrated with HCl. The samples prepared by method (2) were also analyzed for hydrogen by burning at 1000° in a stream of oxygen and weighing the water absorbed in $Mg(ClO_4)_2$, and for oxygen by vacuum extraction.¹⁵ The nitrogen content ranged from 50 to 200 p.p.m., the hydrogen content from 0 to 100 p.p.m., and the oxygen content from 30 to 159 p.p.m. It should be noted that the lattice parameters of the two samples with high hydrogen analysis, $TaC_{0.990}$ and $TaC_{0.801}$, exhibited the maximum negative deviations from the lattice parameter vs. composition curve. Spectroscopic analysis of the samples (2) indicated Nb 400 p.p.m. and W 100 p.p.m. There was no iron present in the carbide samples. The absence of major impurities and the fact that in all cases the sums of the analyses of tantalum and total carbon were within 0.15% of 100% give assurance as to the high purity of the TaC samples. Repeated analyses on several samples indicated a standard deviation in the C/Ta ratio of ± 0.005 .

The X-ray powder patterns were made in a 11.46 cm. Debye-Scherrer camera using copper radiation with a nickel filter. The a_0 values were obtained from the back-reflection lines by applying the least-squares extrapolation of Cohen¹⁶ as modified by Hess¹⁷ using an IBM-704 computer. A standard deviation was calculated from each film. In addition, three films were prepared for several samples. The separate films agreed within the standard deviation in all cases.

Results

The experimental data are summarized in Fig. 1 as a plot of lattice parameter, a_0 at $25 \pm 2^\circ$, vs. the mole ratio, C/Ta, of combined carbon in the total sample. The data are also listed in Table I.

The data were fitted to a least-squares line.¹⁸ Since both x and y values were subject to error, a specialized weighting scheme was used.¹⁹ The function

$$Q = \sum_{i=1}^N w_i [y_i - (A + Bx_i)]^2$$

was minimized. Here w_i is the weight of the i th data point, y_i and x_i are the coordinates of the i th

(14) O. H. Kriege. Los Alamos Scientific Laboratory Report LA-2306, March, 1959.

(15) W. R. Hansen and W. M. Mallett, *Anal. Chem.*, **29**, 1868 (1957).

(16) M. U. Cohen. *Rev. Sci. Instr.*, **6**, 68 (1935); **7**, 1955 (1936); *Z. Kristallogr.*, **94A**, 288 (1936); **94A**, 306 (1936).

(17) J. B. Hess, *Acta Cryst.*, **4**, 209 (1951).

(18) R. H. Moore and R. K. Zeigler, Los Alamos Scientific Laboratory Report LA-2367, Oct. 1959.

(19) W. Edwards Deming, "Statistical Adjustment of Data," John Wiley and Sons, Inc., New York, N. Y., 1943, Chap. 8.

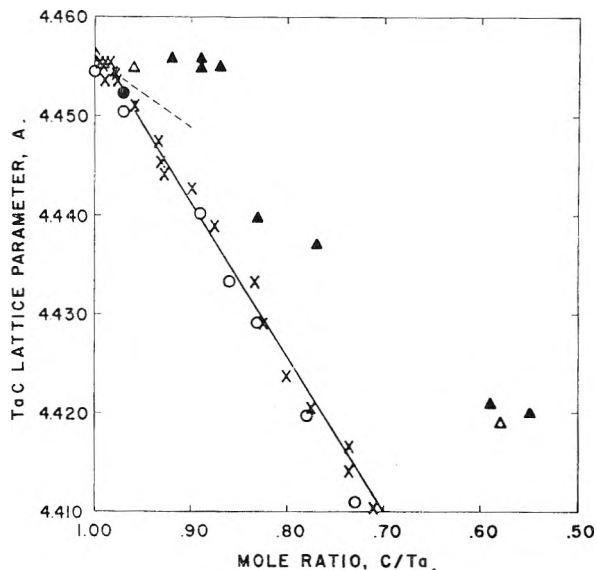


Fig. 1.—Variation of TaC lattice parameter with composition: X, this work; O, Lesser and Brauer; ▲, Smirnova and Ormont; △, Robins; ---, Kempter and Nadler; ●, Kovalskii and Umanskii.

TABLE I
SUMMARY OF THE DATA

Com- position, C/Ta	Error	a_0	Error	Method of prep.
0.994 ^a	0.005	4.4555	0.0003	1
.990	.005	4.4536	.0005	2
.989 ^a	.005	4.4552	.0005	1
.987 ^a	.010	4.4554	.0005	1
.985 ^a	.010	4.4554	.0005	1
.978	.010	4.4543	.0003	1
.978	.010	4.4545	.0005	1
.976	.005	4.4537	.0004	2
.958	.005	4.4511	.0010	1
.934	.005	4.4475	.0003	2
.932 ^a	.008	4.4453	.0003	1
.927 ^a	.010	4.4440	.0010	1
.898	.005	4.4429	.0004	2
.877	.008	4.4389	.0003	1
.833	.005	4.4333	.0005	2
.826	.005	4.4291	.0004	1
.801	.005	4.4237	.0004	2
.776	.008	4.4204	.0009	1
.737 ^a	.005	4.4167	.0003	2
.736	.008	4.4142	.0008	1
.710	.010	4.4104	.0010	1

^a Indicates free carbon present by analysis, but less than 0.7% by weight.

data point (a_0 and C/Ta), A is the intercept, and B the slope of the fitted equation. The weights were taken as a function of the variance of x and y . The solutions for A and B were $A = 4.3007 \pm 0.0032$, $B = 0.1563 \pm 0.0035$. The standard deviation of the fit was 3.4×10^{-5} . The quadratic form does not yield a better fit. Thus the data are fitted to the equation

$$a_0 = 4.3007 + 0.1563X \quad X = C/Ta \quad (1)$$

Solving this equation for X

$$X = 6.398a_0 - 27.516 \quad (2)$$

A solution of equation 1 for $X = 1.00$ gives an

a_0 value of $a_0 = 4.4570 \pm 0.0010$ Å. for the composition $\text{TaC}_{1.000}$. The closest experimental approach to this composition was $\text{TaC}_{0.994} \pm 0.005$, with $a_0 = 4.4555 \pm 0.0003$ Å.

Solution of equation 1 for the X-ray density yields, as a good approximation

$$\rho = 15.11 - 0.64X \quad (3)$$

This gives an X-ray density of 14.47 g./cm.³ for the composition $\text{TaC}_{1.000}$.

Discussion

The values reported by Lesser and Brauer (open circles on Fig. 1), Smirnova and Ormont (closed triangles) and Robins (open triangles), the curve obtained by Kempter and Nadler (dashed line), and the value of Kowalskii and Umanskii (closed circle) are shown for comparison. It is evident that, within experimental error, the values of Lesser and Brauer are in agreement with the present work. The samples prepared by Lesser and Brauer were heated repeatedly until they appeared to be homogeneous and did not contain any free carbon by analysis. The one value reported by Kowalskii and Umanskii is also in agreement with the present work after conversion from kX. to ångström units.

It is believed that the deviation from the present work of the data of Smirnova and Ormont, Robins and Kempter and Nadler is due to inhomogeneity of the samples. The analyses reported by Smirnova and Ormont indicate the presence of free carbon in almost every preparation. Such samples cannot be at equilibrium, and thus will probably not be homogeneous. In addition, the very small size of their samples (200–400 mg.) would make precise analyses very difficult to obtain. The primary method of preparation used by Robins, carbiding a heated tantalum filament in an atmosphere of methane, could be expected to yield an inhomogeneous specimen, since the diffusion of carbon from the surface through the TaC to the center of the filament would be very slow. The

data of Kempter and Nadler were obtained by distilling carbon from pressed compacts of initial composition $\text{TaC}_{0.955}$, and by heating pressed mixtures of $\text{TaC}_{0.955}$ plus excess graphite at about 2500°. The results from the latter preparations agree well with the present work, whereas the data from the distillation residues do not agree at all. This is most probably due to the inhomogeneity of the samples.

The limits of homogeneity of the TaC phase vary with temperature.²⁰ The lower limit is about $\text{TaC}_{0.74}$ at 1850° and $\text{TaC}_{0.71}$ at 2400°. The upper limit is about $\text{TaC}_{0.99}$ at 2400°, with a variation toward lower carbon content at higher temperatures. The upper limit may reach $\text{TaC}_{1.000}$ at lower temperatures.

It is interesting to note the differences between the lattice parameters of TaC and NbC. Although the atomic radii of the metals are essentially the same (Nb, $a_0 = 3.300$ Å.²¹; Ta, $a_0 = 3.304$ Å.), the lattice parameters of the stoichiometric carbides are significantly different (NbC, $a_0 = 4.470$ Å.; TaC, $a_0 = 4.457$ Å.). In addition Storms and Krikorian²² have demonstrated a distinct curvature in the plot of lattice parameter *vs.* composition for NbC, as compared with the linear fit for TaC.

Acknowledgment.—The author gratefully acknowledges the advice of Dr. Melvin G. Bowman, Dr. E. K. Storms, Mr. W. G. Witteman and Mr. N. H. Krikorian during the course of this work. Acknowledgment is also due to Dr. R. L. Petty for computing the lattice parameter data, and to Dr. R. K. Zeigler and Mr. P. T. McWilliams for computing the least-squares fit of the data. Thanks are due to Dr. E. H. Van Kooten, Mr. G. C. Heasley and Mr. M. H. Peek for the analyses, and to Mrs. M. J. Jorgensen and Mr. B. G. Lee for reading the X-ray diffraction patterns.

(20) A. L. Bowman, unpublished research.

(21) A. U. Seybolt, *Trans. AIME*, **200**, 774 (1954).

(22) E. K. Storms and N. H. Krikorian, *J. Phys. Chem.*, **63**, 1747 (1959).

THE EFFECT OF TEMPERATURE ON ION-EXCHANGE EQUILIBRIA. IV. THE COMPARISON OF ENTHALPY CHANGES CALCULATED FROM EQUILIBRIUM MEASUREMENTS AND CALORIMETRICALLY MEASURED VALUES^{1,2}

BY O. D. BONNER AND J. R. OVERTON

Department of Chemistry, University of South Carolina, Columbia, South Carolina

Received April 24, 1961

Ion-exchange equilibria between hydrogen and lithium ion on Dowex 50 resins of 4, 8 and 16% DVB content have been studied over the temperature range 0 to 98° while maintaining a constant solution ionic strength of 0.1 *M*. Calorimetric measurements of the heat of exchange of hydrogen for lithium and sodium for hydrogen ion have been made on these same resins at 25°. The calorimetric measurements confirm the effect of resin composition on the heat of exchange as calculated from the equilibrium measurements at the various temperatures. The data for the hydrogen-lithium exchange indicate that the ion-exchange process may be considered enthalpy-wise as primarily a concentration of one ionic species with the simultaneous dilution of the other. In the exchange of sodium for hydrogen ion it appears that there is a considerable contribution to the heat effect caused by the ionization of the acid exchange sites when the resin is predominantly in the salt form.

The effect of temperature on ion-exchange equilibria has been reported for several systems investigated in these laboratories. In a report on two of these systems, the exchange of ammonium for hydrogen ion and of thallous for hydrogen ion,³ a "differential" process was considered in which one equivalent of ions was exchanged between quantities of solution and resin which were so great that there was no resultant change in the composition of either phase. Differential free energy, enthalpy or entropy changes calculated for this process are related to the corresponding standard changes by equations of the type

$$\Delta F^0 = \int_0^1 \Delta F^* dX$$

where ΔF^0 is the standard free energy change, ΔF^* is the differential free energy change for an exchange of one equivalent of ions at constant resin composition and X is the mole fraction of the preferred ion. It was possible, from the treatment of these data, to show the effect of resin composition on the free energy, enthalpy and entropy changes accompanying the exchange reaction. The enthalpy changes calculated from the van't Hoff equation were so great that the probable percentage error appeared to be small and therefore no calorimetric measurements were made for comparison. The free energies and enthalpies of exchange were found to be of the order of magnitude to be expected if one considers the exchange process to be primarily a dilution of the ion initially held by the exchanger and simultaneously a concentration of the ion initially in the aqueous phase. The values of these functions were found to be extremely dependent on resin composition.

Experimental

Equilibrium Measurements.—The methods of equilibration, temperature control and separation of the resin and aqueous phases have been described previously. The concentrations of the ions in each phase were determined

experimentally for each exchange reaction. Solutions of sodium chloride, lithium chloride and hydrochloric acid were used in the hydrogen-lithium and sodium-hydrogen exchange studies. The concentrations of hydrogen and chloride ion in the aqueous solutions were determined volumetrically. The concentration of sodium or lithium ion in the solution was calculated to be the difference between the concentrations of chloride and hydrogen ion. The number of equivalents of hydrogen ion in the resin phase was determined volumetrically after exhaustive elution of the resin with 2 *M* KCl solution. The total capacity of this resin sample was then determined by conversion to the hydrogen form and a second elution and titration. The lithium or sodium ion on the resin was calculated to be the difference between the total capacity and the hydrogen ion found to be present at equilibrium.

Calorimetric Measurements.—The calorimeter used for these experiments is a 500-ml. Dewar flask placed in an air-bath which is in turn immersed in a constant temperature maintained at $25 \pm 0.01^\circ$. Temperature fluctuations in the water-bath are effectively damped before reaching the calorimeter. Temperature changes in the calorimeter are measured by two Western Electric type 14A thermistors having a resistance of about 100,000 ohms and a sensitivity of about 5,000 ohms/° at 25°. By correctly placing these thermistors as two arms of a Wheatstone Bridge so that their resistance changes are additive a temperature change of 10^{-4} degree, equivalent to a change of about one ohm in the point of balance of the bridge circuit, is easily detectable. The detector is a Hewlett Packard Model 425A microvoltmeter with a detection limit of 0.1 microvolt. All leads to the thermistor and resistors in the bridge are shielded monoconductor cable, with all shields as well as the chassis of the instrument connected to a common ground.

The temperature-resistance relationship was determined by measuring resistance changes corresponding to the temperature change from 24.5 to 25.5°, which were measured with a Beckmann thermometer. The heat capacity of the calorimeter was determined by measuring the temperature change in the system resulting from the dissolution of solid chloride.⁴

Heats of exchange were measured in the following manner: approximately 0.02 equivalent of fully wet resin of known composition was sealed in a glass cylinder and immersed in the calorimeter until thermal equilibrium was reached. This required about 24 hours. The calorimeter also contained during this period of equilibration an aqueous solution of 0.1 *M* ionic strength adjusted so that at equilibrium the desired amount of exchange would have occurred. After a steady state was reached the aqueous and resin phases were brought in contact and the resistance change as function of time was noted. Thermal equilibrium was in all instances re-established within one minute. The resin and solution samples

(1) These results were developed under a project supported by the United States Atomic Energy Commission.

(2) The authors are indebted to Mr. Rex Collins and Mrs. Mary W. Purdy, Summer Research Participants supported by a grant from the National Science Foundation, for assistance with some of the results reported herein.

(3) O. D. Bonner and Robert R. Pruett, *J. Phys. Chem.*, **63**, 1417 (1959).

(4) Integral heats of dilution of sodium chloride were calculated from data in F. R. Bichowsky and F. D. Rossini, "The Thermochemistry of Chemical Substances," Reinhold Publishing Corp., New York, N. Y., 1936.

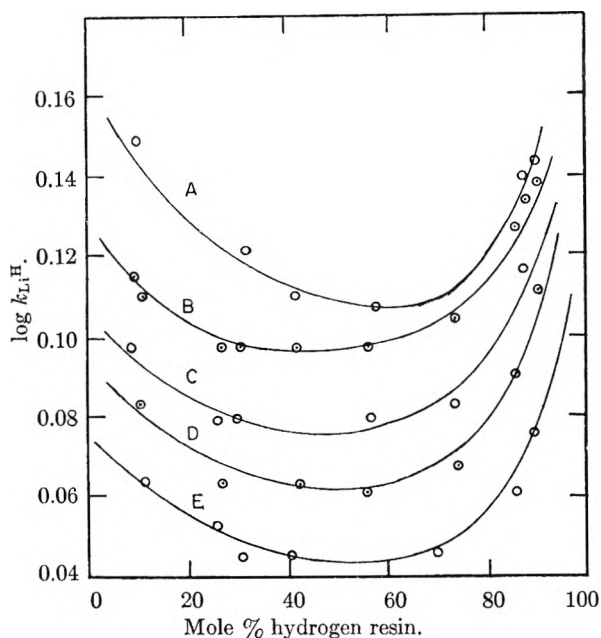


Fig. 1.—Hydrogen-lithium exchange equilibrium data on 4% DVB resin: A, 0°; B, 25°; C, 50°; D, 75°; E, 98°.

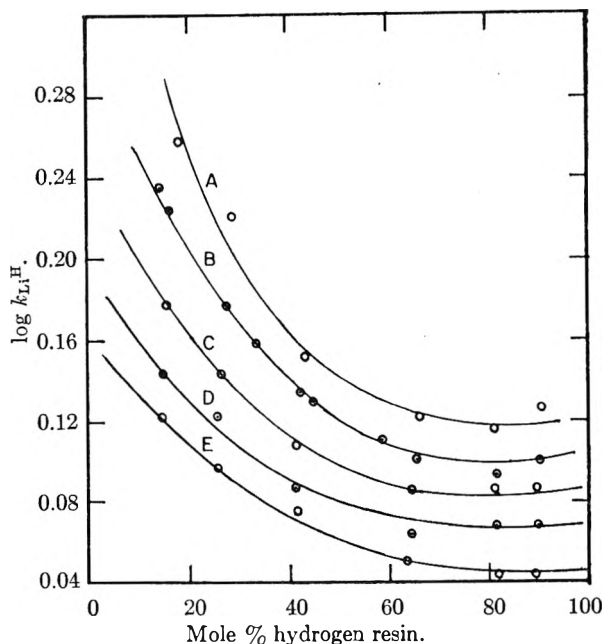


Fig. 3.—Hydrogen-lithium exchange equilibrium data on 16% DVB resin: A, 0°; B, 25°; C, 50°; D, 75°; E, 98°.

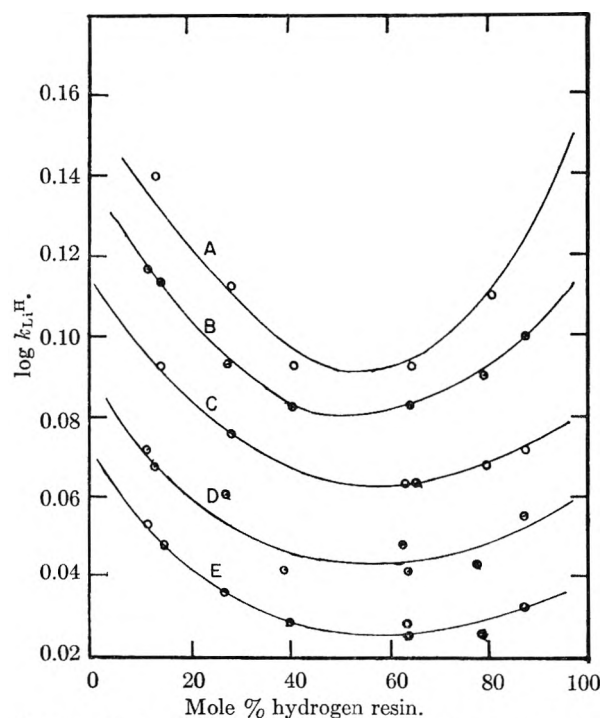


Fig. 2.—Hydrogen-lithium exchange equilibrium data on 8% DVB resin: A, 0°; B, 25°; C, 50°; D, 75°; E, 98°.

were then removed and analyzed and the heat effect per equivalent of exchange was calculated.

Discussion and Results

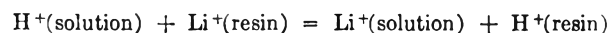
Hydrogen-Lithium Exchange.—Equilibrium studies involving hydrogen and lithium ion have been made over the temperature range 0–98°. The results of these investigations using Dowex 50 resins of 4, 8, and 16% divinylbenzene content are shown graphically in Figs. 1–3. The data for 25° are from a previous publication.⁶ Hydrogen ion is

preferred over lithium ion by all of the resins studied, with the selectivity quotient

$$k_{Li^+H^+} = \left(\frac{m_{Li^+}}{m_{H^+}} \right)_{\text{soln}} \left(\frac{\text{mole fr. } H^+}{\text{mole fr. } Li^+} \right)_{\text{resin}}$$

decreasing as the temperature is raised. This decrease of selectivity with increasing temperature has been observed for all exchanges between univalent ions. Since the resin has the greater affinity for the smaller ion (which is likewise the lesser hydrated ion), the decrease in resin selectivity indicates that at higher temperatures the univalent ions are more nearly the same size than at room temperature.

The shapes of the curves representing the dependence of the selectivity coefficient upon resin composition are similar for exchanges using all three resin samples. The hydrogen-lithium exchange is one of the few exchanges in which the selectivity-resin composition curve exhibits a maximum or a minimum. The variation in the separation of the curves with loading indicates that the effect of temperature upon the selectivity coefficient is greater for 4 and 16% DVB resins with high lithium ion loadings while for the 8% DVB resin the effect is greater when the resin is predominantly in the hydrogen form. One should then expect larger "differential" heats of exchange to accompany exchanges on the 4 and 16% DVB resins when they are predominantly in the lithium form and on 8% DVB resin when the hydrogen loading is high. This is experimentally verified by the chord plots of calorimetric data in Fig. 4. These data also indicate that the heat of exchange is greater for the 8% DVB resin than for either the 4% or 16% DVB resins. The variations of the differential heat of exchange with resin loading for the various resins may be interpreted qualitatively in the light of some previous observations.³ For the exchange reaction



(5) O. D. Bonner, *J. Phys. Chem.*, **58**, 318 (1954).

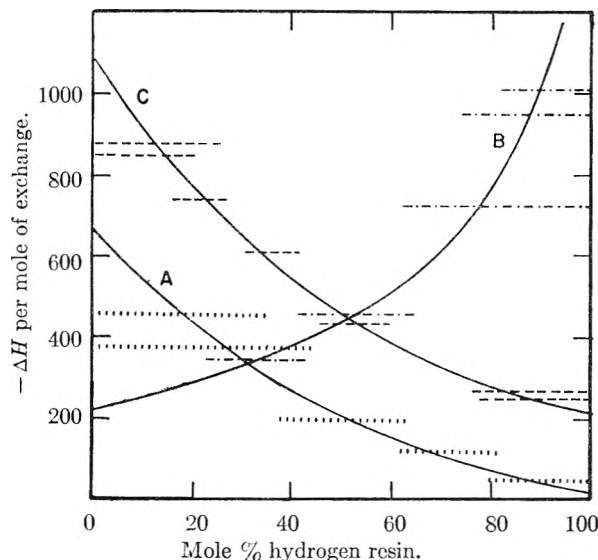


Fig. 4.—Heats of exchange data for the hydrogen-lithium exchange: A, 4% DVB resin; B, 8% DVB resin; C, 16% DVB resin.

lithium ion is being diluted while hydrogen ion is being concentrated. In all exchanges the aqueous solution is maintained at a concentration of 0.1 *M*. The concentration of the ion in the resin phase depends, however, on the water uptake of the resin. Previously published data⁶ indicate that the hydrogen forms of the 4 and 16% DVB resins have greater maximum water uptakes than the lithium form of the same resin while the reverse is true for the 8% DVB resin. This would result in the largest concentration changes for the ions, upon exchange, when the exchange takes place on 4 and 16% DVB resins high in lithium loading or on 8% DVB resins high in hydrogen loading.

Standard free energy, enthalpy and entropy changes for the hydrogen-lithium exchange on the three resin samples are given in Table I. The en-

TABLE I

HYDROGEN-LITHIUM EXCHANGE DATA AT 25°^a

% DVB	K _{LiH}	ΔF° (cal.)	ΔH° (cal.)	ΔS° (e.u.)
4	1.30	-155	-244	-0.30
8	1.26	-137	-528	-1.31
16	1.45	-220	-516	-0.96

^a Cruickshank and Meares⁶ report a value of ΔH° = -387 cal. for a sample of 10% DVB resin.

thalpy change is seen to be greatest for the exchange on the 8% DVB resin. It has been previously observed^{3,7} that sulfonate type ion exchangers were similar in certain respects to nitrate salts. For example, the selectivity scale for both univalent and divalent ions is in exactly the same sequence as the activity coefficient values for the corresponding nitrates. It is thus of interest to note the heats of dilution of the nitrates. Heats of dilution to infinite dilution⁸ for nitric acid and sodium and lithium nitrate solutions are shown in Fig. 5. The

(6) E. H. Cruickshank and P. Meares, *Trans. Faraday Soc.*, **53**, 1289 (1957).

(7) O. D. Bonner and Linda Lou Smith, *J. Phys. Chem.*, **61**, 326 (1957).

(8) Values are calculated from data given in Bichowsky and Rossini, ref. 4, pp. 33, 34, 134, 142, 143.

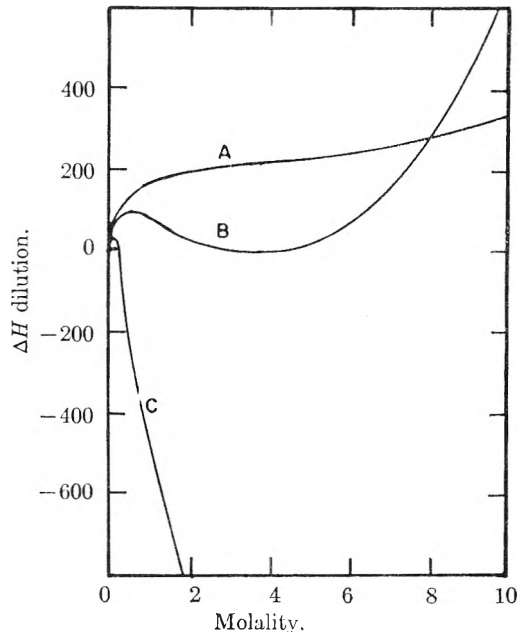


Fig. 5.—Heats of dilution of some nitrates to infinite dilution: A, LiNO₃; B, HNO₃; C, NaNO₃.

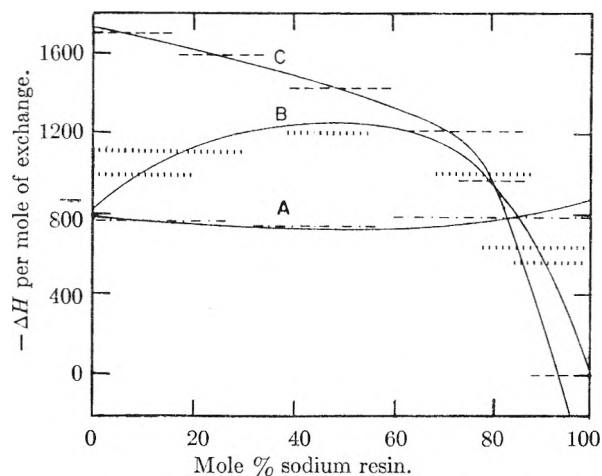


Fig. 6.—Heats of exchange for the sodium-hydrogen exchange: A, 4% DVB resin; B, 8% DVB resin; C, 16% DVB resin.

differences in heats of dilution of nitric acid and lithium nitrate increase until a concentration of about 5 *M* is reached and then they decrease. If the heats of dilution of the sulfonates vary in a similar fashion with concentration, one would expect higher enthalpy changes for the hydrogen-lithium exchange on 8% DVB resin than on resins of higher or lower DVB content. It is of interest that these data also indicate that there is a possibility of a reversal in sign for the enthalpy of exchange on resins of very high DVB content.

Sodium-Hydrogen Exchange.—The effect of temperature on equilibria in the sodium-hydrogen exchange system on a 16% DVB resin has been reported.⁹ A few data for 4 and 8% DVB resins also were given. The value of ΔH° for this exchange on 16% DVB resin at 26° was given as -787 cal./mole. There was considerable uncertainty in this

(9) O. D. Bonner and Linda Lou Smith, *J. Phys. Chem.*, **61**, 1614 (1957).

room temperature value, however, because of the uncertainty of the slope of the $\log K$ vs. $1/T$ curve between 0 and about 35°. Since reporting these data, additional equilibrium experiments have been conducted at 9° which indicate that the heat effect is probably greater than that reported. Since the 9° curve for $\log k$ as a function of resin composition fits smoothly into the figure published previously,⁹ these data are not presented. The effect of resin composition is of greater interest than the effect of temperature upon the selectivity and upon the heat of exchange for this system. The heat of exchange, as calculated from the equilibrium measurements, is large for resins of high hydrogen loading and is very small for resins of high sodium loading. Extrapolation of the equilibrium data to 100% sodium loadings on the 16% DVB resin indicates a reversal of the heat effect, *i.e.*, an exothermic rather than an endothermic process for the exchange reaction



Similar calculations have been made by Duncan¹⁰ on an unidentified sample of "Dowex 50." Heats of exchange calculated for the sodium-hydrogen system were reported as ranging from about 800 cal. per mole for resins of 10% sodium loading to 500 cal. per mole for resins of 90% sodium loading. The effect of resin loading on the heat of exchange appeared thus to be relatively unimportant.

The calorimetric data, as presented in Fig. 6, confirm the heats of exchange as calculated from

(10) J. F. Duncan, *Australian J. Chem.*, **8**, 1 (1955).

equilibrium measurements for the 16% DVB resin. The heat of exchange is observed to become quite small also for high sodium loadings on the 8% DVB resin, but is essentially independent of resin loading on the 4% DVB resin. From these data it would appear that the resin used by Duncan contained about 5% crosslinking. If the heat effect observed in these calorimetric experiments were due only to the effect of the concentration or dilution of the ions as mentioned previously it would be expected that a larger heat effect would be expected for exchanges on resins of high sodium loading where the water uptake is smaller. The deviation from the anticipated behavior on the 8 and 16% DVB resins possibly is due to an opposing heat effect which results from the ionization of sulfonic acid exchange sites. A larger fraction of un-ionized sites should be used in exchanges on resins high in sodium loading than on those exchanges in which the resin is predominantly in the hydrogen form. The calorimetric data for the sodium-hydrogen exchange thus indicate that there are many more un-ionized exchange sites on the 16% DVB resin in the acid form than on the 8% DVB resin and that the 4% DVB resin is essentially free of un-ionized sites. This is in conformity with the previously reported relationship between the exchange capacity of a resin and the nominal crosslinking¹¹ and also the influence of structure upon the strengths of sulfonic acids.^{11,12}

(11) O. D. Bonner and R. R. Pruett, *Z. physik. Chem.*, **25**, 75 (1963).

(12) O. D. Bonner and O. C. Rogers, *J. Phys. Chem.*, **64**, 1499 (1960).

THE ACTIVITY AND OSMOTIC COEFFICIENTS OF SOME *p*-TOLUENESULFONATES AT 40, 60 AND 80°¹

BY O. D. BONNER AND WILLIAM C. RAMPEY

Department of Chemistry, University of South Carolina, Columbia, South Carolina

Received April 24, 1961

Osmotic and activity coefficients have been determined for lithium, sodium and potassium *p*-toluenesulfonates and *p*-toluenesulfonic acid at 40, 60 and 80° by isopiestic comparisons with solutions of sodium chloride. In concentrated solutions the coefficients of the lithium and hydrogen sulfonates decrease while those of potassium sulfonate increase with increasing temperature. The behavior of the sodium sulfonate as the temperature changes approximates that of sodium chloride. These variations are explained as resulting from an increase of kinetic energy and a decrease of ionic hydration at elevated temperatures. The behavior of the activity coefficients of these sulfonates is related to the decrease of resin selectivity with increasing temperature in ion-exchange equilibria.

Investigations of ion-exchange equilibria have been pursued in these laboratories for the past several years. Summaries of the results of these investigations at 25° on Dowex 50 resins of 4, 8 and 16% DVB content have been published.²⁻⁴ The thermodynamic interpretation of these results has been somewhat difficult since the determination of activity coefficients in crosslinked resins is impossible because of the inability of the resin to swell

sufficiently, when immersed in water, to form infinitely dilute solutions. It has been possible, however, to study the properties of monomeric and dimeric sulfonates, similar in structure to the monomer units making up the ion-exchange resin and to relate the properties of solutions of these electrolytes to the behavior of the exchanger.⁵⁻⁷

Recently, these investigations⁸⁻¹¹ of ion exchange

(1) These results were developed under a project supported by the United States Atomic Energy Commission.

(2) O. D. Bonner, *J. Phys. Chem.*, **59**, 719 (1955).

(3) O. D. Bonner and Linda Lou Smith, *ibid.*, **61**, 326 (1957).

(4) O. D. Bonner, C. F. Jumper and O. C. Rogers, *ibid.*, **62**, 250 (1958).

(5) O. D. Bonner, G. D. Esterling, D. L. West and V. F. Holland, *J. Am. Chem. Soc.*, **77**, 242 (1955).

(6) O. D. Bonner, V. F. Holland and Linda Lou Smith, *J. Phys. Chem.*, **60**, 1102 (1956).

(7) O. D. Bonner and O. C. Rogers, *ibid.*, **64**, 1499 (1960).

(8) O. D. Bonner and L. L. Smith, *ibid.*, **61**, 1614 (1957).

(9) O. D. Bonner and Robert R. Pruett, *ibid.*, **63**, 1417 (1959).

equilibria have been extended over the temperature range 0 to 98°. It was noted that the selectivity of the resin for the alkali metal and hydrogen ions relative to one another decreased as the temperature increased, indicating that the values of the activity coefficients of these resins were approaching one another. It was thought desirable to investigate these trends using "model" compounds and the *p*-toluenesulfonates were chosen for these studies because (1) the activity coefficients of these sulfonates are in the same order as the selectivity of the resin for these ions^{5,12} at 25° and (2) *p*-toluenesulfonates are reasonably soluble in water and are easily purified.

Experimental

All determinations of osmotic and activity coefficients of *p*-toluenesulfonates at 25° have been made by the isopiestic method.^{5,12} The measurements at room temperature offer no great difficulty since covers may be quickly placed on the dishes containing the solutions after removal from the constant temperature bath without excessive loss of solvent. At temperatures above 25°, however, this procedure is not possible because of the rapid evaporation of the solvent. Soldano^{13,14} and co-workers have overcome this difficulty by construction of a magnetic balance within the isopiestic apparatus so that the dishes might be weighed without removing them. This type of elaborate apparatus was not available in these laboratories and so it was necessary to devise a means of placing covers securely on the isopiestic dishes while the apparatus remained immersed in the bath. Difficulties were encountered in obtaining a satisfactory seal between cover and dish for the gold plated silver dishes which are used at 25°. Glass dishes 2³/₈" in diameter and 3¹/₄" in height with 24/40 standard taper lids eventually proved to be quite satisfactory. It was possible to remove and replace the lids inside the evacuated isopiestic apparatus by means of a hook which could be manipulated from outside the apparatus. Although glass dishes are not entirely satisfactory for isopiestic work at 25° because of the slow transfer of heat through the walls of the vessels this limitation is not so severe at elevated temperatures where the vapor pressure of the solvent is higher and solvent transfer is more rapid. Satisfactory thermal equilibrium in the system was obtained by suspending the dishes in a solution of sodium chloride which also served to regulate the final equilibrium concentration of sulfonates.

Sodium chloride was used as the reference electrolyte for these isopiestic comparisons. Osmotic and activity coefficients were calculated from the equations

$$\phi = \frac{\nu_r m_r}{\nu_m} \phi_r = R \phi_r$$

and

$$\ln \gamma = \ln \gamma_r + \ln R + 2 \int_0^{\sqrt{m_r \gamma_r}} \frac{(R-1)}{\sqrt{m_r \gamma_r}} d\sqrt{m_r \gamma_r}$$

where the subscript r refers to the reference electrolyte.

Results and Discussion

Osmotic and activity coefficients of lithium, hydrogen, sodium and potassium *p*-toluenesulfonates are given at 40, 60 and 80° in Tables I-III. These data form smooth families of curves when incorporated with the previously published data at 25°.^{5,13,14} The maximum error in these results occurs in the dilute solution range where isopiestic

results are more uncertain. Within the accuracy of the experiments, however, it appears that these data for the sulfonates in dilute solutions parallel those of sodium and potassium chlorides and hydrochloric acid¹⁵ in that the activity coefficients decrease as the temperature is increased. In this concentration range the Debye-Hückel forces should be most important and the slight decrease in the dielectric constant-temperature product would account qualitatively for this behavior.

TABLE I

OSMOTIC AND ACTIVITY COEFFICIENTS OF *p*-TOLUENESULFONATES AT 40°

<i>m</i>	Osmotic coefficients				Activity coefficients			
	Li ⁺	H ⁺	Na ⁺	K ⁺	Li ⁺	H ⁺	Na ⁺	K ⁺
0.1	0.926	0.917	0.921	0.916	0.766	0.755	0.764	0.760
.2	.914	.897	.904	.901	.717	.693	.706	.695
.3	.907	.882	.893	.887	.687	.653	.671	.658
.4	.902	.871	.883	.874	.667	.623	.643	.628
.5	.899	.861	.875	.862	.649	.599	.621	.602
.6	.896	.852	.868	.849	.635	.578	.602	.579
.7	.894	.844	.861	.836	.625	.560	.587	.558
.8	.892	.837	.855	.824	.616	.545	.573	.539
.9	.891	.830	.848	.812	.607	.532	.560	.522
1.0	.889	.825	.842	.800	.600	.520	.548	.506
1.2	.887	.817	.830	.777	.586	.499	.526	.477
1.4	.885	.811	.818	.756	.575	.482	.506	.450
1.6	.884	.806	.807	.738	.566	.467	.488	.427
1.8	.884	.802	.797	.721	.558	.455	.472	.407
2.0	.885	.799	.788	.707	.551	.445	.458	.389
2.5	.890	.800	.767	.679	.541	.426	.427	.352
3.0	.900	.812	.754	.657	.536	.416	.404	.325
3.5	.915	.833	.744	.637	.537	.413	.385	.302
4.0	.934	.861	.741	.622	.541	.416	.370	.283
4.5	.953	.894	.744	.611	.548	.425	.359	.269
5.0	.973	.930			.558	.437		

TABLE II

OSMOTIC AND ACTIVITY COEFFICIENTS OF *p*-TOLUENESULFONATES AT 60°

<i>m</i>	Osmotic coefficients				Activity coefficients			
	Li ⁺	H ⁺	Na ⁺	K ⁺	Li ⁺	H ⁺	Na ⁺	K ⁺
0.1	0.924	0.914	0.919	0.917	0.758	0.742	0.754	0.751
.2	.911	.891	.902	.901	.705	.678	.697	.693
.3	.902	.876	.891	.887	.674	.640	.662	.655
.4	.897	.864	.882	.873	.651	.609	.635	.624
.5	.892	.854	.875	.862	.633	.584	.615	.600
.6	.888	.845	.869	.850	.619	.563	.594	.578
.7	.884	.837	.863	.838	.605	.545	.580	.558
.8	.882	.830	.858	.827	.594	.529	.567	.540
.9	.880	.823	.853	.817	.585	.515	.554	.523
1.0	.879	.819	.847	.807	.577	.504	.542	.508
1.2	.875	.812	.835	.789	.563	.484	.522	.481
1.4	.873	.807	.824	.771	.552	.468	.504	.457
1.6	.871	.803	.814	.754	.542	.454	.487	.435
1.8	.870	.800	.803	.738	.535	.443	.473	.415
2.0	.871	.798	.795	.726	.529	.434	.460	.400
2.5	.878	.800	.780	.702	.520	.417	.434	.367
3.0	.890	.812	.769	.684	.513	.407	.413	.341
3.5	.906	.831	.763	.670	.513	.403	.394	.320
4.0	.926	.855	.762	.657	.516	.405	.381	.303
4.5	.946	.888	.765	.647	.523	.413	.372	.287
5.0	.968	.925	.771		.532	.424	.366	

In the more concentrated solutions the activity coefficients of lithium sulfonate decrease markedly with an increase in temperature while those of *p*-toluenesulfonic acid decrease to a lesser extent, those of sodium sulfonate exhibit a maximum between 40 and 60° and those of potassium sulfonate increase over the entire temperature range studied. Although data are not available for the correspond-

(10) O. D. Bonner and Robert R. Pruett, *J. Phys. Chem.*, **63**, 1420 (1959).

(11) O. D. Bonner and J. R. Overton, *ibid.*, **65**, 1599 (1961).

(12) R. A. Robinson and R. H. Stokes, *Trans. Faraday Soc.*, **45**, 612 (1949).

(13) B. A. Soldano and coworkers, *A High Temperature Isopiestic Unit*, in "The Structure of Electrolytic Solutions," Walter J. Hamer, Ed., John Wiley and Sons, Inc., New York, N. Y., 1959.

(14) C. Stuart Patterson, L. O. Gilpatrick and B. A. Soldano, *J. Chem. Soc.*, 2730 (1960).

(15) H. S. Harned and B. B. Owen, "The Physical Chemistry of Electrolytic Solutions," Reinhold Publ. Corp., New York, N. Y., pp. 717, 726, 727.

TABLE III
OSMOTIC AND ACTIVITY COEFFICIENTS OF
p-TOLUENESULFONATES AT 80°

<i>m</i>	Osmotic coefficients				Activity coefficients			
	Li ⁺	H ⁺	Na ⁺	K ⁺	Li ⁺	H ⁺	Na ⁺	K ⁺
0.1	0.920	0.910	0.917	0.915	0.749	0.729	0.742	0.742
.2	.904	.886	.901	.900	.695	.669	.685	.684
.3	.894	.869	.890	.887	.659	.626	.649	.647
.4	.887	.857	.881	.874	.634	.595	.623	.619
.5	.881	.846	.875	.863	.616	.570	.602	.594
.6	.876	.837	.868	.852	.599	.549	.584	.572
.7	.871	.829	.863	.841	.585	.531	.569	.552
.8	.868	.822	.858	.831	.573	.514	.557	.535
.9	.865	.816	.853	.821	.563	.500	.543	.519
1.0	.863	.812	.847	.811	.554	.488	.523	.505
1.2	.862	.804	.837	.793	.539	.468	.512	.478
1.4	.861	.798	.827	.775	.527	.452	.494	.454
1.6	.861	.794	.817	.761	.518	.439	.478	.434
1.8	.862	.791	.808	.748	.510	.427	.464	.417
2.0	.863	.789	.800	.737	.503	.417	.451	.402
2.5	.871	.790	.785	.717	.493	.399	.425	.371
3.0	.883	.800	.775	.703	.488	.387	.405	.347
3.5	.899	.818	.772	.689	.487	.382	.389	.326
4.0	.918	.842	.774	.778	.490	.381	.379	.308
4.5	.938	.874	.779	.667	.496	.386	.370	.294
5.0	.959	.912	.785		.504	.399	.362	

ing chlorides over this temperature range it is known¹⁵ that the activity coefficients of hydrochloric acid in concentrated solutions decrease in the temperature range 0–60°, while those of potassium chloride increase in the range 0 to 40°, and those of sodium chloride increase to a maximum value at about 60° and then decrease up to 100°. In concentrated solutions of electrolytes the macroscopic dielectric constant of the solvent ceases to be as meaningful as in dilute solutions and it appears that the change of activity coefficient with temperature might depend primarily on two opposing effects: an increase in the kinetic energy and a decrease in the solvation of the ions as the temperature increases. The potassium ion is the least solvated of the cations considered and the increase in activity coefficient with increased temperature probably results from a decrease in ion pair formation as the kinetic energy of the ions increases. The lithium ion, on the other hand, is substantially solvated at 25° and the primary effect of an increase in temperature is to decrease the solvation, reducing the size of the ion and thus increasing the ion pairing. In the case of the hydrogen and sodium sulfonates these two effects are more nearly matched with the solvation being slightly more important in the case of the acid and the kinetic energy in-

crease influencing the activity coefficient of the sodium salt to a great extent, at least in the range 25 to 40°. It is of interest to note that at a sufficiently high temperature the values of the activity coefficients of all of these sulfonates would approach one another and at still higher temperatures, where the ions would be essentially unhydrated, the values of these coefficients should be in the reverse order of those at 25°.

Activity coefficients of these sulfonates are useful in the interpretation of ion-exchange equilibria. Myers and Boyd¹⁶ have recognized that the partition of ions between an ion-exchange resin and an aqueous solution may be treated as a Donnan membrane equilibrium and have related the equilibrium constant, *K*, for the exchange to the swelling pressure, *P*, and the activity coefficients of the resin sulfonates and of the ions in the aqueous solution by the equation

$$\log k = P(\bar{V}_{B^+} - \bar{V}_{A^+})/2.3RT + \log \left(\frac{\gamma_{B^+}}{\gamma_{A^+}} \right)_i - \log \left(\frac{\gamma_{B^+}}{\gamma_{A^+}} \right)_0$$

The term making the most important contribution to the equilibrium constant is the activity coefficient ratio of the resinates. Recent equilibrium studies^{8,11} involving lithium, hydrogen and sodium ion indicate a decrease in selectivity of the resin for sodium over hydrogen and lithium ions as the temperature is increased. This parallels the behavior of the activity coefficients of the *p*-toluenesulfonates. The activity coefficients of sodium *p*-toluenesulfonate and *p*-toluenesulfonic acid illustrate this trend in an interesting manner. In dilute solutions, the activity coefficients of the salt are larger than those of the acid while in concentrated solutions the reverse is true. A plot of activity coefficients of the acid and salt as a function of concentration shows a crossover which occurs at about 2.1 *M* at 25°, 2.6 *M* at 40°, 3.2 *M* at 60° and 3.8 *M* at 80°. At still higher temperatures this crossover would not be expected to occur until extremely high concentrations were reached. This would correspond in ion-exchange equilibria to a preference of the resin phase for hydrogen over sodium ion at very high temperatures. This phenomenon has not been observed experimentally for fully sulfonated resins and it is probable that hydrolysis of the sulfonic acid exchange sites would occur before sufficiently high temperatures were reached.

(16) G. E. Myers and G. E. Boyd, *J. Phys. Chem.*, **60**, 521 (1956).

HYDROGEN FORMATION IN THE RADIOLYSIS OF TOLUENE¹

By R. B. INGALLS

*Research Department of Atomic International, A Division of North American Aviation, Inc., Canoga Park, Calif.**Received May 2, 1961*

The evolution of hydrogen² from the radiolysis of liquid toluene, toluene- α,α,α - d_3 , toluene- d_8 , and equimolar solutions of pairs of these toluene analogs was studied. Results indicate that a disproportionately large fraction of the hydrogen gas evolved during radiolysis is from the hydrogen atoms of the methyl group, that a fraction of the gas is formed by an intramolecular process, and that some of the gas is formed by a bimolecular process other than abstraction from the methyl group. An interpretation based on free radical reactions is presented which accounts qualitatively for the data presented in this paper.

Introduction

Hydrogen atoms are often considered important intermediates in the degradation of organic material by ionizing radiation.³ Reactions of these atoms contribute to the formation of high molecular weight products as well as to the formation of hydrogen gas in aromatic and vinyl hydrocarbon systems.⁴ Therefore, a knowledge of their reactions is necessary for an understanding of the radiation chemistry of unsaturated hydrocarbons. A knowledge of hydrogen atom reactions would also contribute indirectly to our knowledge of energy transfer and other important processes in radiation chemistry by allowing the separation⁴ of these reactions from other effects.

There have been a number of studies of the action of hydrogen or deuterium atoms with aromatic or double bond systems in the gas and solid phases reported,^{5a} but to the author's knowledge, only one direct experimental study of the reactions of thermal hydrogen atoms in liquid aromatic systems^{5b} has been made.

A study of the radiolysis of toluene provides an opportunity to examine the radiation-induced reactions of hydrogen atoms⁶ with an organic liquid under favorable conditions. The toluene molecule contains both an aromatic ring, which is probably somewhat less reactive to addition than benzene or biphenyl,^{7a} and hydrogen atoms of the methyl group, which are abstracted^{7b} more easily than the hydrogen atoms of a purely aromatic hydrocarbon. Thus, hydrogen atom reactions with the aromatic ring are not expected to overwhelm abstraction reactions with the methyl group at

room temperature.⁸ One might therefore expect observable competition between the two types of reactions of hydrogen atoms with toluene. Thus, it may be possible to compare these competing reactions of hydrogen atoms with a single chemical species, unperturbed by the difficulties inherent in the interpretation of work done on solutions.

In this work, the hydrogen evolved during irradiation from toluene, toluene- α,α,α - d_3 , toluene- d_8 , equimolar binary solutions of these, and a sample of 1.0% toluene- d_8 in toluene was examined. Evidence has been found that hydrogen is evolved preferentially from the methyl group, that some of the hydrogen molecules contain two atoms from the same toluene molecule, and that some of the hydrogen is formed by a bimolecular process other than abstraction.

Experimental

Reagents.—Toluene (Mallinckrodt reagent grade) was distilled in a 70-cm. glass-helices-packed column and a center cut was taken. Gas chromatographic analysis showed no impurities. The deuterated toluenes were obtained from Merck and Company, Limited, of Canada. Analysis by gas chromatography showed that the toluene- α,α,α - d_3 had slightly over 1% of higher-boiling chemical impurities and the toluene- d_8 had a similar percentage of lower-boiling impurities. The isotopic purities of the labeled toluenes were determined by low-voltage mass spectroscopy.⁹ The isotopic purities were 94.5 and 95.7 mole % or better for the toluene- α,α,α - d_3 and toluene- d_8 , respectively.

Irradiations.—About 1 ml. of previously degassed toluene was vacuum-transferred into a weighed ampoule. The toluene was then frozen with liquid nitrogen and the ampoule sealed off and reweighed. Where equimolar mixtures were required, a 0.5-ml. pipet (sealed off at the small end and sealed into the vacuum system at the other) was used to measure equal volumes at room temperature of the differently labeled toluenes. Each isomer was flashed (successively) from the same pipet into the same ampoule. Two pipets of appropriate volume were used to fill ampoules with a solution of 1.0% toluene- d_8 in toluene. The ampoules were sealed off under vacuum, weighed, and shaken vigorously for several minutes to mix the components. The ampoules were irradiated in a nearly homogeneous field of about 1.5×10^{18} electron volts absorbed per gram minute inside a Co⁶⁰ hollow cylinder source described elsewhere.¹⁰ The temperature of irradiation was the ambient temperature of the source, about 40°.

Product Handling and Analysis.—After irradiation, the ampoules were broken in an evacuated ampoule breaker. All the volatile material was vacuum transferred into liquid nitrogen cooled traps where it was degassed carefully by repeated warming, vacuum transfer to another trap, and pumping. The hydrogen and methane, which are volatile at -196°, were pumped into a calibrated volume with a

(1) Work performed under AEC Contract AT(11-1)-GEN-8.

(2) The word hydrogen is used in this paper to refer to H₂ + HD + D₂.

(3) A. J. Swallow, "Radiation Chemistry of Organic Compounds," Pergamon Press, London, 1960.

(4) M. Burton and W. N. Patrick, *J. Phys. Chem.*, **58**, 421 (1954); W. N. Patrick and M. Burton, *ibid.*, **58**, 424 (1954).(5) (a) B. de B. Darwent and R. Roberts, *Disc. Faraday Soc.*, **14**, 55 (1953); H. W. Melville and J. C. Robb, *Proc. Roy. Soc. (London)*, **A218**, 311 (1953); R. Klein and M. D. Scheer, *J. Phys. Chem.*, **62**, 1011 (1958); (b) R. B. Ingalls and J. R. Hardy, *Can. J. Chem.*, **38**, 1734 (1960).

(6) The hypothesis that hydrogen atoms are chemically important intermediates in the radiation induced formation of hydrogen from toluene has not been unequivocally established. It is the purpose of this paper to demonstrate that this hypothesis is not inconsistent with the experimental data presented here if all of the reactions of hydrogen atoms are taken into account. See equations 7, 8, 9 and 10.

(7) (a) M. Szwarc and J. H. Binks, "Theoretical Organic Chemistry," Butterworth Publications, Ltd., London, 1959, pp. 262-298. (b) M. Szwarc, *J. Chem. Phys.*, **16**, 128 (1948); H. Blades, A. I. Blades and E. R. W. Steacie, *Can. J. Chem.*, **32**, 298 (1954); C. H. Leigh and M. Szwarc, *J. Chem. Phys.*, **20**, 403 (1952).

(8) See page 1606-1607 of this report.

(9) D. P. Stevenson and C. D. Wagner, *J. Am. Chem. Soc.*, **72**, 5612 (1950).(10) J. G. Burr and J. M. Scarborough, *J. Phys. Chem.*, **64**, 1367 (1960).

Toepler pump and the pressure measured. This pressure-volume measurement was used to calculate the $G(\text{non-condensable gas})$ values tabulated in Table I. The gas then was forced into an evacuated sample bulb for analysis on a modified Consolidated Electrodynamics Corporation Model 21-620 mass spectrometer.

TABLE I
 $G(\text{NON-CONDENSABLE GAS})$

Toluene	0.13 ± 0.005
Toluene- α, α, α - d_3	.075 ± .002
Toluene- d_8	.055 ± .003
Toluene and toluene- d_3 (equimolar soln.)	.10 ± .004
Toluene and toluene- d_8 (equimolar soln.)	.095 ± .003
Toluene- d_3 and toluene- d_8 (equimolar soln.)	.06 ± .007
One mole % toluene- d_8 in toluene ^a	.14

^a Based on one determination.

Results and Discussion

Experimental Evidence for Selectivity.—Values for $G(\text{non-condensable gas})$ ¹¹ are summarized in Table I. These values include about 6% methane and traces of higher boiling materials with hydrogen as the principal constituent. These values for toluene were found to be independent of total dose from 2×10^{21} to 6×10^{21} e.v./g. Packing with glass capillary had no effect on $G(\text{non-condensable gas})$, implying that wall effects are not important.

The disproportionately large effect of substituting deuterium for the three hydrogens of the methyl group on the yield of non-condensables is evident from the table. Substituting deuterium for the methyl hydrogen atoms reduces $G(\text{non-condensable gas})$ by a factor 1/1.73. Replacing all eight hydrogen atoms in the molecule with deuterium reduces $G(\text{non-condensable gas})$ by a factor 1/2.36 of the yield from protonated toluene. The ratio of the reduction factors 1.73/2.36 is approximately equal to 3/4. This is about twice the ratio of fractions of protons replaced in the molecule, *i.e.*, $3/8 \div 8/8 = 3/8$, indicating selectivity. Also, the yields from mixtures of toluene with toluene- α, α, α - d_3 and toluene- d_8 are very close to the same, indicating that substituting deuterium for hydrogen on the aromatic ring of the molecules has little effect on the yield. Thus, it is evident that substituting deuterium on the methyl group of toluene is much more effective in reducing the yield of hydrogen gas than replacing the ring hydrogen atoms with deuterium.

In Table II, the isotopic composition of the hydrogen gas evolved during radiolysis as determined by mass spectroscopy is presented. From these data the value of the $\%H = (H_2 + \frac{1}{2}HD) \times 100 / H_2 + HD + D_2$ and $\%D = (D_2 + \frac{1}{2}HD) \times 100 / H_2 + HD + D_2$ in the product hydrogen can be calculated. In Table III $\%H$ and $\%D$ are compared with the per cent. of the hydrogen atoms in the original substrate which are H^1 atoms ($\%h$) and the per cent. which are H^2 atoms ($\%d$). The selective evolution of hydrogen from the methyl group is evident upon inspection of this table. Note that pure toluene- α, α, α - d_3 is the only sample

irradiated that evolved gas richer in deuterium than the original material. This is evidence that the substitution of deuterium for hydrogen atoms of the methyl group of the toluene has a disproportionately large effect on the isotopic composition of the hydrogen gas evolved during irradiation.

It is important to note that isotopic equilibration of the hydrogen gas evolved during radiolysis occurs to only a very limited extent, if at all. The values for the reaction quotient $J = (HD)^2 / (H_2 \cdot D_2)$ range from $J = 4.3$ for the gas evolved from toluene- α, α, α - d_3 (which is, probably fortuitously, very close to the value to be expected for complete equilibration¹²) to $J = 1.6, 1.9$ and 2.5 for the gas evolved from the equimolar solutions of toluene and toluene- d_8 , toluene and toluene- α, α, α - d_3 and toluene- α, α, α - d_3 and toluene- d_8 , respectively. The low values for J are interpreted to indicate that the extent of equilibration in the gas phase is slight.¹³ This indicates that the values of J and the isotopic composition of the evolved hydrogen are determined by the processes of hydrogen formation.

TABLE II
ISOTOPIC COMPOSITION OF THE HYDROGEN GAS EVOLVED DURING IRRADIATION

Sample	% H ₂	% HD	% D ₂
Toluene	100		
Toluene- α, α, α - d_3	32.1	49.8	18.1
Toluene- d_8	3.2	4.6	91.9
Toluene and toluene- d_8 (equimolar mixture)	51.1	34.5	14.4
Toluene- α, α, α - d_3 and toluene- d_8 (equimolar mixture)	13.8	39.8	46.4
Toluene and toluene- α, α, α - d_3 (equimolar mixture)	71.6	24.2	4.2
1.0% Toluene- d_8 and toluene ^a	99.3	0.63	0.09

^a Based on one determination.

TABLE III
HYDROGEN ISOTOPIC COMPOSITION OF SUBSTRATE AND EVOLVED HYDROGEN

Substrate	% H Obsd. in hydrogen evolved	% D	% h in original substrate	% d
Toluene	100	0	100	0
Toluene- d_3 (D3)	57	43	63	37
Toluene- d_8 (D8)	5.5	94.2	0.5	99.5
Equimolar soln. of H8 and D8	68	32	51	49
Equimolar soln. of H8 and D3	83.7	16.3	82	18
Equimolar soln. of D3 and D8	33.7	66.3	32	68
1.0 mole % D8 in H8 ^a	99.7	0.4	99	1

^a Based on one determination.

Evidence for the "Intramolecular" Formation of Hydrogen.—The values of J for the gas evolved from the equimolar solutions of the differently labeled toluenes are distinctly lower than the value expected for hydrogen which has been equilibrated or formed in a random fashion. This fact suggests that a significant fraction¹⁴ of the hydrogen is

(11) The notation $G(X)$ refers to the number of molecules of X formed for every 100 e.v. of energy absorbed during irradiation.

(12) L. M. Dorfman, *J. Phys. Chem.*, **60**, 826 (1956).

(13) J. G. Burr, *J. Chem. Phys.*, **25**, 587 (1956).

formed intramolecularly.¹² It is not clear whether (1) this intramolecular formation of hydrogen represents the simultaneous loss of two hydrogen atoms as a hydrogen molecule, or (2) the liquid "cage" increases the probability that an atom lost from a toluene molecule will abstract from the remaining molecular fragment, or (3) still other processes are involved. In any case, these low values of J are evidence that some of the hydrogen molecules evolved are made up of two atoms from the same molecule.

Additional evidence for the intramolecular formation of hydrogen from toluene during radiolysis is obtained from the yields of D_2 from a solution of 1.0% toluene- d_8 in toluene. Since the toluene- d_8 is in dilute solution, the results of bimolecular reactions of toluene- d_8 are largely suppressed. Thus, the yield of D_2 from this solution is a measure of the intramolecular yield.¹⁵ If this yield $G(D_2) = 0.00013$ is divided by the mole fraction of toluene- d_8 in the solution an approximate value for the intramolecular yield of D_2 from pure toluene- d_8 ($G(D_2) = 0.013$) is obtained.¹⁶ This value is 24% of the yield of D_2 from pure toluene- d_8 ($G(D_2) = 0.055$) for perdeuteriotoluene (see Table I), indicating that about one-fourth of the hydrogen evolved from toluene is formed intramolecularly.

Evidence that the Hydrogen Gas Evolved is Formed in Part by a Bimolecular Process.—The relative yields of H_2 from toluene- $\alpha, \alpha, \alpha-d_3$ and from the equimolar solution of toluene- $\alpha, \alpha, \alpha-d_3$ and toluene- d_8 is

$$\frac{G(H_2)_{-d_3}}{G(H_2)_{-c_2, -d_8}} = \frac{0.075 \times 32.1/100}{0.06 \times 13.8/100} = 2.91 \quad (1)$$

Thus, a twofold increase in the concentration of protonated rings resulted in almost three times the yield of H_2 . If it is assumed that H_2 is formed from toluene- $\alpha, \alpha, \alpha-d_3$ by processes which are either first or second order with respect to the concentration of protonated rings, the relative importance of these two types of processes in the formation of hydrogen gas can be determined.

From expression 1, we can write

$$\frac{k_1(2R) + k_2(2R)^2}{k_1(R) + k_2(R)^2} = 2.9 \quad (2)$$

where k_1 and k_2 are the sums of the specific reaction rate constants for the unimolecular and bimolecular process producing H_2 from toluene- $\alpha, \alpha, \alpha-d_3$ and $2R$ is the concentration of phenyl rings or methyl groups in pure toluene in moles/liter.

Solving for k_1/k_2 we obtain $k_1/k_2 = 1.22R = 5.72$ moles/l., where R is the concentration of protonated rings in an equimolar mixture of toluene-

(14) If the expression $M \geq 1 - (J/4)^{1/2}$ used by Dorfman to calculate the fraction of hydrogen formed intramolecularly is evaluated for the toluene-toluene- d_8 solution, this fraction $M \geq 36\%$. It is difficult to justify the use of this expression in a system such as this one, however, because of the possibility of complicating reactions involving the aromatic ring.

(15) A discussion of the principles involved in this type of data analysis can be found in a recent paper by Dyne and Jenkinson.¹⁷

(16) Although this value is based on one experiment it is supported by two determinations in which the 1% solution was irradiated at 11°. These values are about 60% of the value reported here.

(17) P. J. Dyne and W. M. Jenkinson, *Can. J. Chem.*, **38**, 539 (1960).

$\alpha, \alpha, \alpha-d_3$ and toluene- d_8 . The relative rates of production of H_2 from toluene- $\alpha, \alpha, \alpha-d_3$ by unimolecular processes is

$$\frac{k_1(2R)}{k_2(2R)^2} = \frac{k_1}{k_2} \frac{1}{(2R)} = 5.75 \text{ mole/l.} \frac{1}{9.4 \text{ mole/l.}} = 0.61$$

Thus about 38% of the hydrogen formed from atoms which were attached to the aromatic ring of toluene are produced by intramolecular processes, and 62% by intermolecular processes, respectively.

Similarly, the relative yields of D_2 from toluene- $\alpha, \alpha, \alpha-d_3$ and from the equimolar solution of toluene- $\alpha, \alpha, \alpha-d_3$ and toluene is

$$\frac{G(D_2)_{-d_3}}{G(D_2)_{-d_8, -d_3}} = \frac{0.075 \times 18.1/100}{0.010 \times 4.2/100} = 3.4 \quad (3)$$

By a similar treatment, the quotient k_1'/k_2' of the sum of specific rate constants for unimolecular processes producing D_2 from toluene- $\alpha, \alpha, \alpha-d_3$ divided by the sum of competing second-order rate constants is $k_1'/k_2' = 0.43R = 2.02$ moles/l. Thus the ratio of intramolecular to intermolecular production of D_2 from toluene- $\alpha, \alpha, \alpha-d_3$ is

$$\frac{k_1'(2R)}{k_2'(2R)^2} = \frac{k_1'}{k_2'} \times \frac{1}{(2R)} = 2.02 \text{ mole/l.} \times \frac{1}{9.4 \text{ mole/l.}} = 0.215 \quad (4)$$

Therefore, about 18% of the hydrogen evolved from the methyl group of toluene is produced by intramolecular processes and 82% by intermolecular processes.

These values suggest that a significant fraction of the hydrogen gas evolved during radiolysis is produced by bimolecular processes. It is also interesting to note that the fraction of D_2 evolved from the methyl group which is formed by a bimolecular process (82%) appears to be greater than the fraction of H_2 which is produced bimolecularly from the ring (62%). This is consistent with the view that part of the hydrogen is formed by abstraction which is bimolecular and will occur much more rapidly at the rather labile methyl hydrogen atoms than from the ring hydrogen atoms.

Evidence for a Bimolecular Process Other than Abstraction.—It has been shown by several workers that, in a series of related elementary reactions, the energy of activation E of the reaction can be related empirically to the heat of reaction in a simple manner.¹⁸ For abstraction reactions, there is some evidence¹⁹ for the relationship

$$E = 11.4 - 0.25Q$$

where Q is the exothermic heat of reaction in kcal. per mole.

Taking the value 77.5 kcal. for the heat of dissociation of the C-H bonds of the methyl group of toluene, the heat of reaction, Q_1 for reaction 5 is 24.9 kcal.²⁰

(18) M. G. Evans and M. Polanyi, *Trans. Faraday Soc.*, **32**, 1933 (1936); **34**, 11 (1938); E. T. Butler and M. Polanyi, *ibid.*, **39**, 19 (1943); H. Steiner and A. R. Watson, *Disc. Faraday Soc.*, **2**, 88 (1947); N. N. Tikhomirova and V. V. Voevodskii, *Doklady Akad. Nauk S.S.S.R.*, **79**, 993 (1951) (English translation, Can. Nat. Res. Coun. TT-260 (1951)).

(19) A. N. N. Semenov, "Some Problems of Chemical Kinetics and Reactivity," Pergamon Press, London, 1958.

(20) If 89.9 kcal. per mole is taken to be the value for the heat of dissociation of the methyl C-H bonds, $Q_1 = 13.5$ kcal.



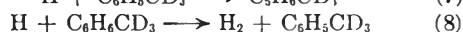
Similarly, if 104 kcal. per mole is assumed for the dissociation energy of the C-H bonds of the ring, the heat of reaction Q_2 for reaction 6 is 0.6 kcal.



It can be shown from the above relationship that the difference in the activation energy for the two reactions is $E_1 - E_2 = 6.1$ kcal. per mole. At 40° this activation energy difference will practically prevent abstraction from the ring if the pre-exponential terms are within a factor of 200.²¹

Thus, the H_2 formed by a bimolecular mechanism from toluene- α, α, α - d_3 is probably not a result of hydrogen atom abstraction since this would require that an H atom be abstracted from the ring. Some other bimolecular process must be invoked to explain this result.

The following mechanism is proposed to explain the formation of H_2 from toluene- α, α, α - d_3



The first reaction involves the addition of a hydrogen atom to the aromatic ring of toluene to produce a free radical. The second reaction may be considered an abstraction reaction in which a hydrogen atom abstracts one of the two hydrogen atoms on a ring carbon, or it may be thought of as the disproportionation of a hydrogen atom and the free radical produced in (7).

There is the possibility that a deuterium atom might also participate in the reaction. In this case



then



where the production of H_2 is favored by an isotope effect.

Other types of mechanisms have been proposed to explain the bimolecular formation of hydrogen in systems where abstraction is not expected to compete with the addition of hydrogen atoms to an aromatic ring.¹⁰ However, it has since been found that HD is produced during the bombardment of liquid *o*-terphenyl with thermal deuterium atoms.^{5b} These observations support the mechanism proposed here.²² The temperature dependence

(21) Even if the value of 89.9 kcal. is used for the methyl C-H bond dissociation energy only 0.3% of the hydrogen atoms would be expected to abstract from the ring if the pre-exponential terms are equal.

(22) In order to obtain a meaningful comparison of the results of the radiolysis of toluene reported in this paper and the results of the deuterium bombardment of *o*-terphenyl reported in reference 5b, two differences in the experimental conditions must be taken into account. First, hydrogen atoms probably add to *o*-terphenyl about 10 times faster than they add to the aromatic ring of toluene by analogy with the relative reaction rates of methyl radical addition.²⁰ Second, the differences in the concentrations of the free radical inter-

of hydrogen and bibenzyl yields from irradiated toluene is being studied in order to obtain more evidence concerning the mechanism of hydrogen formation.

Conclusion

It is possible, then, to account for both the yield and the isotopic composition of the hydrogen gas from the irradiated toluene samples by two general types of mechanisms. One is purely free radical in nature and accounts for about 60% of the hydrogen produced.²⁴ The second is some intramolecular process.

This second type of process may also be free radical in nature. A hydrogen atom evolved from a toluene molecule or ion in liquid toluene may be confined near the parent ion or molecular fragment by the "cage effect" to make abstraction of hydrogen from this relatively labile species an important process. Although such a reaction would occur in two separate steps it would be intramolecular and its rate would show a first-order dependence on toluene concentration. Therefore, the data presented in this paper are consistent with the view that substantially all the hydrogen evolved from liquid toluene during irradiation is produced by free radical processes.

Acknowledgment.—The author is grateful to R. A. Meyer for the mass spectrometric analyses. Special thanks are due to J. G. Burr for suggesting the problem and to him and D. E. McKenzie for many helpful and provocative discussions.

mediates in the two experiments must be taken into account. To calculate the steady state free radical concentrations during the radiolysis of toluene we must estimate the rate of initiation of hydrogen atoms into the system. For simplicity it is assumed that the atoms are formed homogeneously with a yield of $G(\text{H}) = 1$. (The actual free radical distribution is inhomogeneous and will tend to favor radical reactions.) The rate of initiation of hydrogen atoms into toluene during the radiolysis experiments reported here is approximately

$$I \approx \frac{\text{dose rate}}{100} \times G(\text{H}) = 3.6 \times 10^{-7} \text{ mole sec.}^{-1} \text{ l.}^{-1}$$

If all the specific rate constants of the mechanism proposed for the reaction of deuterium atoms with *o*-terphenyl²³ are assumed to be applicable to the reaction of hydrogen atoms with toluene except that k_1 is taken to be 10^6 moles liter⁻¹ sec.⁻¹, the steady-state concentrations of hydrogen atoms during toluene radiolysis can be calculated and is found to be 3.8×10^{-14} mole/liter. Similarly, the $\text{C}_6\text{H}_5\text{CH}_2$ radical concentration is 6.0×10^{-7} mole/liter. Therefore, the rate of addition of hydrogen atoms to the aromatic ring of toluene is approximately 3.6×10^{-7} mole liter⁻¹ and the rate of exchange by reaction 8 is 6.7×10^{-10} . This corresponds to a yield of hydrogen by reaction 8 $G_8(\text{H}_2) = 1.9 \times 10^{-3}$ which is about a factor of 20 below the observed value of 3.7×10^{-2} . In view of the nature of the approximations used in reference 23 as well as those made here, this agreement is remarkably good.

(23) R. B. Ingalls and J. R. Hardy, ref. 5b.

(24) It should be noticed that lack of knowledge of the elementary reactions of hydrogen atoms in liquid aromatic systems made necessary a direct experimental investigation of these reactions before it was possible to account for the observed hydrogen yields reported in this paper in a simple manner. It is likely that a better understanding of free radical reactions in condensed phases would be of help in improving our understanding of organic radiation chemistry in liquid and solid phases.

THERMODYNAMIC PROPERTIES OF POTASSIUM AND AMMONIUM TARANAKITES

BY EDWARD P. EGAN, JR., ZACHARY T. WAKEFIELD AND BASIL B. LUFF

Division of Chemical Development, Tennessee Valley Authority, Wilson Dam, Alabama

Received May 6, 1961

The low temperature heat capacities of potassium and ammonium taranakites, $H_6K_3Al_5(PO_4)_8 \cdot 18H_2O(c)$ and $H_6(NH_4)_3Al_5(PO_4)_8 \cdot 18H_2O(c)$, were measured at 10 to 310°K. The respective entropies at 298.16°K. are 335.6 ± 0.6 and 339.9 ± 0.6 e.u.—the enthalpies, 54,780 and 57,180 cal. mole⁻¹. The heats of formation from the elements at 298.16°K., as determined in a solution calorimeter, and calculated solubility product constants are -4523 ± 5 kcal. mole⁻¹ and $pK = 187.1$ for the potassium salt, -4432 ± 5 kcal. mole⁻¹ and $pK = 183.7$ for the ammonium salt.

Potassium taranakite, $H_6K_3Al_5(PO_4)_8 \cdot 18H_2O$, and its ammonium analog, $H_6(NH_4)_3Al_5(PO_4)_8 \cdot 18H_2O$, have been found among the products of reaction of soils with the concentrated acidic solutions resulting from the dissolution of some phosphate fertilizers.¹ Properties of the taranakite minerals thus are of interest in relation to the phosphorus status of soils. Measurements of their solubilities are reported in a companion paper.²

298.16°K. derived therefrom, and the heats of formation at 25° as determined in a solution calorimeter. The entropies and heats of formation are combined with other values from the literature in calculations of solubility product constants, which are compared with values derived from the direct measurements of solubilities.²

Apparatus and Materials.—The low temperature calorimeter³ and the solution calorimeter⁴ have been described.

TABLE I

OBSERVED HEAT CAPACITY OF POTASSIUM TARANAKITE, $H_6K_3Al_5(PO_4)_8 \cdot 18H_2O(c)$, CAL. DEG.⁻¹ MOLE⁻¹

Point ^a	T, °K.	C _p	Point ^a	T, °K.	C _p	Point ^a	T, °K.	C _p
80	9.77	0.985	20	97.66	126.6	9	213.90	268.5
91	11.30	1.277	45	101.44	132.0	61	217.61	272.2
81	12.43	1.625	21	104.95	136.6	10	221.43	276.3
92	15.00	2.890	46	108.80	141.8	62	225.24	280.1
82	16.42	3.761	22	112.40	146.7	11	229.20	284.4
93	18.92	5.782	47	116.02	151.5	63	232.71	287.9
83	20.46	7.236	23	119.75	156.5	12	236.81	292.4
94	23.67	10.85	48	123.42	161.4	64	240.89	296.9
84	25.19	12.77	24	126.99	166.1	13	244.27	300.2
95	28.38	17.16	49	130.76	170.9	65	248.04	304.2
85	30.86	20.89	25	134.43	175.7	14	251.59	307.6
96	33.58	25.15	50	138.03	180.3	66	255.23	311.3
86	36.14	29.34	26	141.82	185.1	15	258.96	314.9
97	39.56	34.93	51	145.50	189.6	67	262.65	318.6
87	41.99	38.95	27	149.16	194.2	16	266.39	322.3
98	45.34	44.58	52	152.94	198.7	68	270.11	326.0
88	48.50	49.97	28	156.71	203.3	17	272.83	328.8
99	51.58	55.09	53	160.35	207.6	1	276.55	332.3
89	54.67	60.19	29	164.23	212.3	69	279.83	335.8
34	56.42	63.09	54	167.97	216.8	2	283.19	339.0
39	58.86	67.11	30	171.74	221.1	70	286.69	342.7
35	61.65	71.84	55	175.58	225.6	3	290.14	346.0
40	64.85	77.23	31	179.98	230.7	74	291.95	347.8
36	67.31	81.17	56	183.39	234.4	71	293.82	350.0
41	70.67	86.33	32	187.27	238.8	75	295.69	351.6
37	73.71	91.08	57	190.79	242.6	76	299.02	355.2
42	76.75	95.94	33	193.99	246.2	72	301.04	357.4
38	80.35	101.8	58	197.05	249.4	77	302.41	358.7
18	83.58	106.7	7	199.76	252.7	5	304.12	360.3
43	86.92	111.7	59	203.08	256.3	78	306.15	362.7
19	90.54	116.8	8	206.60	260.5	73	308.32	365.1
94	93.93	121.4	60	210.02	264.1	6	310.40	366.8

^a Numbered in chronological order.

Presented here are measurements of the heat capacities of potassium and ammonium taranakites at 10 to 310°K., entropies and enthalpies at

One defined calorie was taken as 4.1840 abs. j.—the ice point as 273.16°K. The heat capacities were corrected for curvature.³ Temperatures were read to four decimal places, as small temperature differences were important; they were rounded to two decimal places in the final tabulation.

(1) W. L. Lindsay and A. W. Taylor, *Proc. 7th International Congress Soil Sci.* (1960) (in press).

(2) A. W. Taylor and E. L. Gurney, *J. Phys. Chem.*, **65**, 1613 (1961).

(3) E. P. Egan, Jr., and Z. T. Wakefield, *ibid.*, **64**, 1953 (1960).

(4) E. P. Egan Jr., and B. B. Luff, *ibid.*, **65**, 523 (1961).

The potassium and ammonium taranakites were the crystalline preparations used in solubility measurements.² As the taranakites lost weight under vacuum, air in the low temperature calorimeter was replaced with helium by a flushing procedure. The calorimeter was evacuated as rapidly as was feasible to < 0.1 mm. and refilled with helium immediately. This procedure was repeated twice. On the third filling, the helium pressure was limited to 0.33 atm., and the calorimeter was sealed.

Aluminum sulfate hexahydrate was prepared by the method of Young.⁵ Its ignition loss in 1 hr. at 1200° was 77.32%, which corresponded to a residue of 22.68% Al₂O₃ (stoichiometric, 22.645%).

Potassium sulfate (Mallinckrodt reagent-grade salt) was dried at 120° for 2 hr. An assay gave 99.70% K₂SO₄.

Ammonium sulfate (Fisher "primary standard") was dried at 105°.

Potassium dihydrogen phosphate (reagent-grade salt) was dried at 105°. Reagent from the same source had been found repeatedly (by TVA) to have essentially stoichiometric composition.

Low Temperature Heat Capacity. Potassium Taranakite.—The calorimeter charge was 80.032 g. (vacuum) or 0.05962 mole of potassium taranakite (formula wt., 1342.336).

Observed molal heat capacities are shown in Table I—smoothed heat capacities and the corresponding entropy and enthalpy increments in Table II. The average deviation of the observed from the smoothed heat capacities was less than 0.1% except at temperatures below 30°K., where the small magnitudes impaired the accuracy. The low end

TABLE II

MOLAL THERMODYNAMIC PROPERTIES OF POTASSIUM TARANAKITE, H₆K₃Al₃(PO₄)₃·18H₂O(c), CAL. DEG. ⁻¹

T, °K.	C _p	S ^o	H ^o - H ^o ₀
10	0.841	0.282	2.108
15	2.845	0.947	10.63
20	6.801	2.260	33.92
25	12.55	4.366	81.64
30	19.60	7.262	161.6
35	27.41	10.86	278.9
40	35.66	15.06	436.4
45	44.02	19.74	635.6
50	52.42	24.81	876.7
60	69.08	35.84	1484
70	85.36	47.73	2277
80	101.2	60.16	3190
90	116.0	72.94	4277
100	129.9	85.39	5507
110	143.5	98.31	6874
120	156.8	112.0	8376
130	170.0	125.0	10010
140	182.8	138.1	11770
150	195.2	151.2	13660
160	207.2	164.1	15680
170	219.1	177.1	17810
180	230.6	189.9	20060
190	241.7	202.7	22420
200	252.9	215.4	24890
210	264.1	228.0	27480
220	274.8	240.5	30170
230	285.2	252.9	32970
240	295.8	265.3	35880
250	306.1	277.6	38890
260	316.0	290.0	42000
270	325.9	301.9	45210
280	335.9	313.9	48520
290	345.9	325.9	51920
300	356.2	337.8	55430
273.16	329.0	305.7	46240
298.16	354.3	335.6	54780

(5) T. F. Young, *J. Am. Chem. Soc.*, **67**, 257 (1945).

of the heat capacity curve was located by plotting C_p/T against T² and extrapolating smoothly to 0°K.

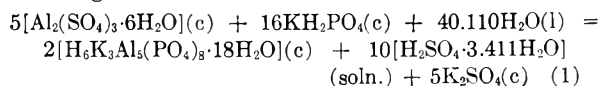
The entropy of H₆K₃Al₃(PO₄)₃·18H₂O(c) at 298.16°K. is 335.6 ± 0.6 e.u. On the assumption that the measured solid represents the ideal state, the enthalpy, H^o - H^o₀, at 298.16°K. is 54,780 cal. mole⁻¹. The calculations were made on an IBM 704 computer.³

Ammonium Taranakite.—The calorimeter charge was 80.612 g. (vacuum) or 0.06302 mole of ammonium taranakite (formula wt., 1279.156).

Observed molal heat capacities are shown in Table III—smoothed heat capacities and the corresponding entropy and enthalpy increments in Table IV. The average deviation of the heat capacities was the same as for the potassium salt.

The entropy of H₆(NH₄)₃Al₃(PO₄)₃·18H₂O(c) at 298.16°K. is 339.9 ± 0.6 e.u. The enthalpy, H^o - H^o₀, at 298.16°K. is 57,180 cal. mole⁻¹.

Heat of Formation. Potassium Taranakite.—The heat of formation of potassium taranakite was determined from heats of solution as measured in a solution calorimeter according to the over-all reaction



Combination of the measured heats of solution in the proper sequence yielded the heat of reaction for equation 1. Heats of formation were known for the reactants and for all the products except potassium taranakite.

A weighed volume of 850 ml. of 4 m HCl solution was used as solvent in all measurements of heat of solution. The calorimeter system was calibrated electrically immediately before and after each measurement, and over the same temperature increment.

The dissolution characteristics of the taranakites at 25° did not lead to a satisfactory temperature rise in a reasonable time (1 hr. or less). All heats of solution therefore were measured at 40°. The water-bath around the calorimeter was operated at 41° so that all temperature drifts were in one direction.

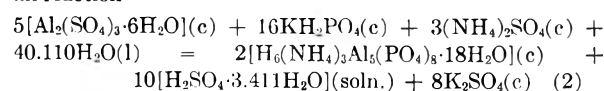
Substitution of the measured heats of solution (Table V) in equation 1 yielded -69,837 cal. as the ΔH of reaction at 40°.

To compute the enthalpy increment ΔH]₂₅⁴⁰ for each heat of formation, cubic equations were fitted to the heat capacities and integrated to obtain enthalpy or were fitted directly to the values of enthalpy that were available. The six or eight points of heat capacity or enthalpy nearest the increment 25 to 40° were chosen. The calculated enthalpy increment for each compound and for the required elements are shown in Table VI.

The heat of formation of H₂SO₄·3.411H₂O at 25° was calculated by analytical interpolation of heats of formation for H₂SO₄ solutions.⁶ Shown in Table VII are the heats of formation from the elements at 25° (from the literature) and the heats of formation at 40° as calculated from the combination with the enthalpy increments.

Combination of the heats of formation at 40° with the heat of reaction for equation 1 (-69,837 cal.) yielded -4,523,990 cal. mole⁻¹ for the heat of formation at 40° of potassium taranakite. Subtraction of the enthalpy increment for formation of potassium taranakite, ΔH]₂₅⁴⁰ = -824 cal. mole⁻¹, yielded -4,523,170 cal. or -4523 kcal. mole⁻¹ for the heat of formation of potassium taranakite from the elements at 25°. The estimated uncertainty is ±5 kcal. mole⁻¹.

Ammonium Taranakite.—The heat of formation of ammonium taranakite was determined similarly from the over-all reaction



Again, the heats of solution was measured at 40° with 4 m HCl as solvent.

Substitution of the measured heats of solution (Table V) in equation 2 yielded -73,496 cal. as the heat of reaction at 40°. Combination of this value with the pertinent heats of

(6) National Bureau of Standards Circular 500, U. S. Govt. Printing Office, Washington, D. C., 1952.

TABLE III

OBSERVED HEAT CAPACITY OF AMMONIUM TARANAKITE, $H_6(NH_4)_3Al_5(PO_4)_8 \cdot 18H_2O(c)$, CAL. DEG.⁻¹ MOLE⁻¹

Point ^a	T, °K.	C _p	Point ^a	T, °K.	C _p	Point ^a	T, °K.	C _p
87	9.81	0.822	45	92.53	116.3	61	203.98	273.0
77	10.80	0.856	20	96.20	122.0	8	206.36	276.3
88	12.20	1.081	46	99.96	127.7	62	210.15	281.3
78	13.75	1.523	21	103.36	133.0	9	213.35	285.5
89	16.28	2.604	47	106.86	138.3	63	216.99	290.0
79	18.46	3.910	22	110.65	144.1	10	221.00	294.7
90	20.78	5.578	48	114.18	149.4	64	224.89	299.4
80	23.66	8.174	23	118.05	155.3	11	228.69	303.9
91	25.22	9.774	49	121.89	161.0	65	232.63	308.6
81	28.79	13.96	24	125.57	166.5	12	236.20	312.8
92	30.75	16.48	50	129.68	172.5	66	239.99	317.3
82	34.16	21.25	25	133.48	178.0	13	243.56	321.5
93	37.26	25.83	51	137.11	183.1	67	247.40	326.0
83	39.87	29.80	26	140.75	188.4	14	250.94	329.9
94	43.34	35.19	52	144.85	194.2	68	254.66	334.1
84	45.88	39.32	27	148.18	198.9	15	258.37	338.2
95	48.98	44.44	53	152.11	204.4	69	261.98	342.2
85	52.08	49.58	28	155.53	209.1	16	265.66	346.2
96	55.04	54.39	54	159.08	214.0	70	269.52	350.5
86	58.10	59.49	29	162.83	219.1	17	272.84	354.0
39	59.67	62.00	55	166.64	224.3	1	275.15	356.3
35	60.32	63.18	30	170.08	228.9	71	276.90	358.4
40	63.05	67.85	56	173.57	233.5	2	280.09	361.6
36	66.23	73.29	31	177.12	238.1	72	283.38	365.3
41	68.07	76.30	57	180.48	242.6	3	286.48	368.4
37	72.82	83.97	32	184.15	247.5	73	289.75	371.9
42	74.89	87.39	58	187.58	251.8	4	293.14	375.2
38	79.56	95.31	33	191.16	256.5	74	296.40	378.7
43	81.53	98.50	59	194.48	260.8	5	299.69	382.1
18	81.80	99.06	34	198.00	265.3	75	302.77	385.4
44	85.60	105.3	60	198.37	266.0	6	306.16	388.8
19	89.15	111.1	7	201.20	269.4	76	309.57	392.5

^a Numbered in chronological order.

TABLE IV

MOLAL THERMODYNAMIC PROPERTIES OF AMMONIUM TARANAKITE, $H_6(NH_4)_3Al_5(PO_4)_8 \cdot 18H_2O(c)$, CAL. DEG.⁻¹

T, °K.	C _p	S ⁰	H ⁰ - H ₂₅ ⁰
10	0.673	0.323	2.169
15	1.977	0.796	8.213
20	4.997	1.737	24.93
25	9.618	3.321	60.86
30	15.53	5.580	123.2
35	22.41	8.480	217.7
40	29.98	11.96	348.5
45	37.91	15.95	518.1
50	46.09	20.36	728.0
60	62.67	30.23	1272
70	79.42	41.15	1982
80	96.02	52.83	2859
90	112.3	65.09	3902
100	127.9	77.74	5103
110	143.1	90.64	6458
120	158.2	103.7	7964
130	172.8	117.0	9620
140	187.4	130.3	11420
150	201.4	143.7	13370
160	215.3	157.2	15450
170	228.8	170.6	17670
180	242.0	184.1	20020
190	255.0	197.5	22510
200	268.0	210.9	25120
210	281.1	224.3	27870

220	293.6	237.7	30740
230	305.5	251.0	33740
240	317.3	264.2	36850
250	328.8	277.4	40080
260	340.0	290.6	43430
270	350.9	303.6	46880
280	361.6	316.6	50450
290	372.1	329.4	54110
300	382.4	342.2	57890
273.16	354.3	307.7	48000
298.16	380.5	339.9	57185

formation at 40° (Table VII) in equation 2 yielded -4,434,-750 cal. mole⁻¹ as the heat of formation of ammonium taranakite at 40°. Subtraction of the enthalpy increment for formation of ammonium taranakite, $\Delta H_{125}^{40} = -2,304$ cal. mole⁻¹, yielded -4,432,450 cal. or -4432 kcal. mole⁻¹ as the heat of formation of ammonium taranakite from the elements at 25°. The estimated uncertainty is ± 5 kcal. mole⁻¹.

Measurement of the heats of solution on the right-hand sides of equations 1 and 2 in reverse order was tried as a means of conserving the supply of taranakite crystals. This procedure would not require additions of the taranakites in stoichiometric quantities to keep the ion concentrations in order. When ammonium taranakite was added to a solution containing K⁺ and SO₄²⁻ ions, however, dissolution was negligible; it was necessary to measure the heat of solution of ammonium taranakite first and then to add the sulfuric acid solution and K₂SO₄. Potassium taranakite, to less extent, exhibited the same behavior. The phenomenon is attributable perhaps to precipitation of amorphous aluminum phosphate on the surface of taranakite particles

TABLE V
 HEATS OF SOLUTION IN HYDROCHLORIC ACID SOLUTION (4 m, 850 ML.)

Solute	No. of detns.	Wt., g.	Preliminary addn. to solvent (in stoichiometric amt.)	Heat of solution, cal. mole ⁻¹
H ₂ O(l)	6	4.9 to 8.8	None	-67.98 ± 1.12
KH ₂ PO ₄ (c)	6	15 to 25	H ₂ O	6746 ± 18
Al ₂ (SO ₄) ₃ ·6H ₂ O(c)	5	16 to 21	H ₂ O, KH ₂ PO ₄	-27,332 ± 94
H ₂ SO ₄ ·3.411H ₂ O	4	8.6 to 8.8	K-taranakite	-3252 ± 11
	6	9.3 to 9.7	NH ₄ -taranakite	-3242 ± 7
K ₂ SO ₄ (c)	4	4.8 to 5.0	K-taranakite, H ₂ SO ₄ ·3.411H ₂ O	9799 ± 19
	5	8.4 to 8.8	NH ₄ -taranakite, H ₂ SO ₄ ·3.411H ₂ O	9752 ± 5
(NH ₄) ₂ SO ₄ (c)	5	3.0 to 6.0	H ₂ O, KH ₂ PO ₄ , Al ₂ (SO ₄) ₃ ·6H ₂ O	6343 ± 34
K-taranakite(c)	5	14 to 15	None	12,115 ± 35
NH ₄ -taranakite(c)	5	15.2 to 16.6	None	8898 ± 44

TABLE VI

ENTHALPY INCREMENTS, ΔH]₂₅⁴⁰, CAL. MOLE⁻¹

Substance	ΔH] ₂₅ ⁴⁰	Substance	ΔH] ₂₅ ⁴⁰
P(white)	86.04 ^a	H ₂ O(l)	89.55 ^f
Al	87.77 ^b	K ₂ SO ₄ (c)	469.4 ^g
K	105.77 ^c	H ₂ SO ₄ ·3.411H ₂ O(soln.)	1066.3 ^h
S(Rh)	81.71 ^d	Al ₂ (SO ₄) ₃ ·6H ₂ O(c)	1806.7 ⁱ
N ₂ (g)	104.44 ^e	KH ₂ PO ₄ (c)	429.28 ^j
		(NH ₄) ₂ SO ₄ (c)	679.75 ^k
O ₂ (g)	105.47 ^e	H ₂ K ₃ Al ₅ (PO ₄) ₈ ·18H ₂ O(c)	5432.8
H ₂ (g)	103.60 ^e	H ₆ (NH ₄) ₃ Al ₅ (PO ₄) ₈ ·18H ₂ O(c)	5824.0

^a T. G. Maple and C. C. Stephenson, Thesis, Mass. Inst. Tech., 1949. ^b W. F. Giauque and P. F. Meads, *J. Am. Chem. Soc.*, **63**, 1897 (1941). ^c F. Simon and W. Zeidler, *Z. physik. Chem.*, **123**, 383 (1926). ^d E. D. Eastman and W. C. McGavock, *J. Am. Chem. Soc.*, **59**, 145 (1937). ^e National Bureau of Standards, "Selected Values of Chemical Thermodynamic Properties," Vol. I, Series III (Loose Leaf), U. S. Govt. Printing Office, Washington, D. C., March 31, 1947. ^f N. S. Osborne, H. F. Stimson and D. C. Ginnings, *J. Research Natl. Bur. Standards*, **23**, 197 (1939). ^g G. E. Moore and K. K. Kelley, *J. Am. Chem. Soc.*, **64**, 2949 (1942). ^h Landolt-Börnstein, "Physikalisch-chemische Tabellen," Supplement 3, 5th ed., Julius Springer, Berlin, 1936, p. 2283. ⁱ C. H. Shomate, *J. Am. Chem. Soc.*, **67**, 765 (1945). ^j C. C. Stephenson and J. G. Hooley, *ibid.*, **66**, 1397 (1944). ^k C. H. Shomate, *ibid.*, **67**, 1096 (1945).

TABLE VII

HEATS OF FORMATION, KCAL. MOLE⁻¹

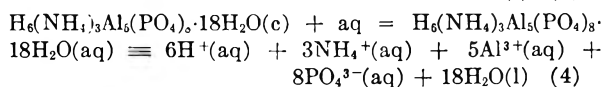
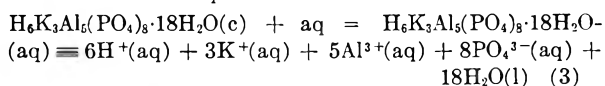
Substance	ΔH] _f ^o , 25°	ΔH] _f ^o , 40°
K ₂ SO ₄ (c)	-342.67 ^a	-342.70
KH ₂ PO ₄ (c)	-374.9 ^a	-374.98
H ₂ O(l)	-68.317 ^a	-68.384
Al ₂ (SO ₄) ₃ ·6H ₂ O(c)	-1268.15 ^b	-1268.33
H ₂ SO ₄ ·3.411H ₂ O(soln.)	-206.13 ^a	-205.99
(NH ₄) ₂ SO ₄ (c)	-281.86 ^a	-281.99

^a Ref. 6. ^b Ref. 5.

when added to a solution already containing K⁺ and SO₄⁻ ions.

Solubility Product Constant.—The heats of formation and entropies at 25° required in the calculation of solubility

product constants are listed in Table VIII. Substitution of these values in the equations



yielded, for potassium taranakite, ΔH(aq - c) = 31,140 cal. mole⁻¹ and ΔS(aq - c) = -751.65 e.u.—for ammonium taranakite, ΔH(aq - c) = 27,321 cal. mole⁻¹ and ΔS(aq - c) = -748.49 e.u. Substitution of these values in the relations

$$\Delta F(\text{aq} - c) = \Delta H(\text{aq} - c) - T\Delta S(\text{aq} - c)$$

$$\Delta F(\text{aq} - c) = -RT \ln K_{sp}$$

$$pK = -\log K_{sp}$$

gave pK = 187.1 for potassium taranakite and pK = 183.7 for ammonium taranakite at 25°.

TABLE VIII

HEATS OF FORMATION AND ENTROPIES AT 25° FOR CALCULATION OF SOLUBILITY PRODUCT CONSTANTS^a

Substance	ΔH] _f ^o	S ^o
H ₆ (NH ₄) ₃ Al ₅ (PO ₄) ₈ ·18H ₂ O(c)	-4432.5	339.9
H ₆ K ₃ Al ₅ (PO ₄) ₈ ·18H ₂ O(c)	-4523.2	335.6
H ⁺ (aq)	0	0
K ⁺ (aq)	-60.04	24.5
NH ₄ ⁺ (aq)	-31.74	26.97
Al ³⁺ (aq)	-125.4	-74.9
PO ₄ ³⁻ (aq)	-306.9	-52
H ₂ O(l)	-68.317	16.72

^a All values except those for taranakites from ref. 6.

These values may be compared with pK = 178.7 for potassium taranakite and pK = 175.4 for ammonium taranakite as calculated from direct solubility measurements.² The differences are not great for complex compounds of low solubility and may be accounted for, in part, by uncertainties in some of the heats of formation and entropies used here or in some of the ion activities used in the direct solubility calculations. The difference between the constants for the two salts is the same by both methods of calculation.

SOLUBILITIES OF POTASSIUM AND AMMONIUM TARANAKITES

BY A. W. TAYLOR AND E. L. GURNEY

*Division of Chemical Development, Tennessee Valley Authority, Wilson Dam, Alabama**Received May 6, 1961*

The solubility products of potassium taranakite, $H_6K_2Al_5(PO_4)_8 \cdot 18H_2O$, and ammonium taranakite, $H_6(NH_4)_3Al_5(PO_4)_8 \cdot 18H_2O$, were calculated from the compositions of solutions in equilibrium with synthetic preparations of the minerals. Owing to the presence of complex ions, the respective pK_{sp} values, 178.7 and 175.5, must be regarded as apparent rather than true thermodynamic values. In solutions where the aluminum phosphate ion activity product, $a_{Al}a_{PO_4}$, exceeded 1×10^{-20} , both compounds dissolved incongruently to form amorphous aluminum phosphate which prevented the solutions from reaching equilibrium with the taranakites in less than 200 days.

Occurrences of the taranakites as natural aluminum phosphate minerals were discussed by Bannister and Hutchinson.¹ Laboratory preparations of the potassium form were described by Haseman, Lehr and Smith²; its X-ray properties were reported by Smith and Brown,³ who assigned it the formula $H_6K_3Al_5(PO_4)_8 \cdot 18H_2O$ on the basis of density, unit-cell content and chemical analysis.

The potassium mineral and its ammonium analog, $H_6(NH_4)_3Al_5(PO_4)_8 \cdot 18H_2O$, have been found among the compounds formed when soils are acted upon by the concentrated acidic phosphate solutions resulting from the dissolution of some phosphate fertilizers.⁴ Information on the solubility of the taranakites thus is important in relation to the efficiency of such fertilizers.

Measurements of apparent solubility products of the potassium and ammonium taranakites by equilibrium methods are presented here, together with information about the range of solution composition over which the taranakites dissolve congruently. Cryogenic measurements are reported in a companion paper.⁵

Measurements. Methods.—To prepare potassium taranakite, a solution of 21.6 g. of aluminum in 870 ml. of 53.5% phosphoric acid was filtered and diluted to 2 l. The pH was adjusted to 3.4 with 10% potassium hydroxide solution. The resulting slurry, diluted to 3.5 l., was digested at 50° for 24 hours in a polyethylene bottle to yield crystals of taranakite. The product was filtered, washed 10 times, and vacuum-dried over calcium chloride at room temperature. It consisted of 40 μ lamellar aggregates of hexagonal platelets with the optical properties reported for potassium taranakite.^{1,2} It contained 8.6% K, 9.6% Al and 56.6% PO_4 .

Ammonium taranakite was made the same way, except that the partial neutralization was made with 28% ammonium hydroxide to pH 4.0. The product consisted of 50 μ hexagonal aggregates of well-formed uniaxial (-) crystals with $N_w = 1.520$ and $N_c = 1.513$. It contained 4.1% NH_4 , 10.5% Al and 59.6% PO_4 .

Two-gram portions of the taranakites were equilibrated in 16-oz. polyethylene bottles with 500-ml. charges of dilute solutions of aluminum chloride and potassium phosphate or potassium chloride. The initial pH of the solutions was adjusted with HCl. The bottles were rotated end over end in a water-bath at $25 \pm 0.05^\circ$. Aliquots of clear solution were withdrawn for analysis at irregular intervals and (about twice as often) pH's were measured with a Beckman Model G meter, which was standardized against 0.05 N potassium acid phthalate buffer at pH 4.00. Potassium ion

concentrations were measured by flame photometry, ammonium by a micro-Kjeldahl procedure, and phosphate by spectrophotometry based upon molybdenum blue. Aluminum was determined either by a fluorimetric estimation of the 8-quinolinolate complex in a chloroform extract or by a direct spectrophotometric estimation of the same complex. The compositions of most of the solutions became constant after about 60 days. The solid phases were examined petrographically at regular intervals.

Results.—Final compositions of the solutions equilibrated with potassium taranakite, each based on the mean value of at least three analyses, are given in Table I.

When the activity of water is assumed to be unity, the solubility product of potassium taranakite, $H_6K_3Al_5(PO_4)_8 \cdot 18H_2O$, may be defined by the expression

$$pK_{sp} = 6pH + 3pK + 5pAl + 8pPO_4 \quad (1)$$

where pK , pAl and pPO_4 represent the negative logarithms of the activities of the respective ionic species. In acid solutions, where the PO_4^{3-} concentration is very low, pK_{sp} is conveniently expressed in terms of the $H_2PO_4^-$ ion activity

$$pK_{sp} = 3pK + 5pAl + 8pH_2PO_4 - 10pH + C \quad (2)$$

where $C = 8p(K_2K_3)$, K_2 and K_3 being the second and third dissociation constants of phosphoric acid. At 25°, $C = 156.2$.

Equation 2 may be rearranged in the form

$$pK_{sp} = 3pKH_2PO_4 + 5pAlPO_4 + C \quad (3)$$

where $pKH_2PO_4 = pK + pH_2PO_4$ (representing the activity of potassium dihydrogen phosphate) and $pAlPO_4 = pAl + pH_2PO_4 - 2pH$ (a simple function of the activity of aluminum phosphate, $AlPO_4$).

To calculate the ion product for taranakite in any solution, the true concentrations of $H_2PO_4^-$ and Al^{3+} must be derived. When the activity coefficient for an ionic species of valency z in a solution of ionic strength I less than 0.1 is represented by the Güntelberg approximation to the Debye-Hückel expression

$$-\log f_i = 0.5z^2\sqrt{I}/(1 + \sqrt{I}) \quad (4)$$

which is equivalent to assuming a common value of 3.04 Å. for "the distance of closest approach" of all the ions,⁶ the ratio of the concentrations of H_3PO_4 and $H_2PO_4^-$ may be calculated from the equation

$$\log [(H_3PO_4)/(H_2PO_4^-)] = pH - pK_1 + 0.5\sqrt{I}/(1 + \sqrt{I}) \quad (5)$$

where pK_1 is the first dissociation constant of phosphoric acid, 7.52×10^{-3} at 25°.

The concentration of Al^{3+} may be calculated from the equation

(6) R. A. Robinson and R. I. Stokes, "Electrolytic Solutions," Academic Press, New York, N. Y., 1955, p. 229.

(1) F. A. Bannister and G. E. Hutchinson, *Mineral Mag.*, **28**, 31 (1947).

(2) J. F. Haseman, J. R. Lehr and J. P. Smith, *Soil Sci. Soc. Am. Proc.* (1950), **15**, 76 (1951).

(3) J. P. Smith and W. E. Brown, *Am. Mineralogist*, **44**, 138 (1959).

(4) W. L. Lindsay and A. W. Taylor, *Proc. 7th International Congress Soil Sci.*, 1960 (in press).

(5) E. P. Egan, Jr., Z. T. Wakefield and B. B. Luff, *J. Phys. Chem.*, **65**, 1609 (1961).

TABLE I
 SOLUTIONS EQUILIBRATED WITH POTASSIUM TARANAKITE AT 25°

No.	pH	K	Concn., mmoles/l.		Cl	Ionic strength	$p\text{KH}_2\text{PO}_4$	$p\text{AlPO}_4^a$	pK_{sp}
			Al	P					
1	1.88	10.4	3.3	10.7	23.0	0.039	4.51	1.91	179.26
2	2.16	5.5	1.6	6.2	11.0	.020	4.85	1.56	178.54
3	2.22	3.8	1.9	4.8	8.0	.018	5.08	1.43	178.61
4	2.17	3.9	2.9	4.8	1.5	.027	5.12	1.47	178.88
5	2.97	1.2	1.0	1.0	4.0	.008	6.06	0.53	177.00
6	1.93	6.1	4.5	11.0	20.0	.040	4.70	1.64	178.52
7	2.04	22.0	3.2	5.1	50.0	.055	4.44	1.96	179.29
8	3.82	20.1	0.06	0.15	20.0	.020	5.65	1.05	178.42
9	2.14	2.7	3.8	6.6	30.0	.038	5.16	1.39	178.68
10	2.02	3.1	5.6	8.3	33.0	.049	5.08	1.51	178.98
11	2.02	3.5	4.3	8.0	30.0	.042	5.03	1.58	179.22
12	2.06	3.7	4.1	8.0	30.0	.041	4.98	1.50	178.65
13	2.82	1.4	0.36	1.6	3.0	.005	5.79	1.01	178.63
14	2.73	1.5	0.37	1.9	3.0	.006	5.70	1.13	178.94
15	2.73	1.5	0.43	1.85	3.0	.006	5.71	1.08	178.77
16	2.69	1.6	3.3	1.93	12.0	.023	5.74	0.58	176.31 ^b
17	1.97	28.8	0.6	26.0	20.0	.037	3.63	2.02	177.17
18	2.17	8.6	1.8	5.5	20.0	.027	4.71	1.61	178.42 ^b
19	2.80	3.0	2.3	2.1	5.0	.016	5.39	0.35	174.12 ^b

^a $p\text{AlPO}_4 = p\text{Al} + p\text{H}_2\text{PO}_4 - 2p\text{H}$. ^b Initially supersaturated.

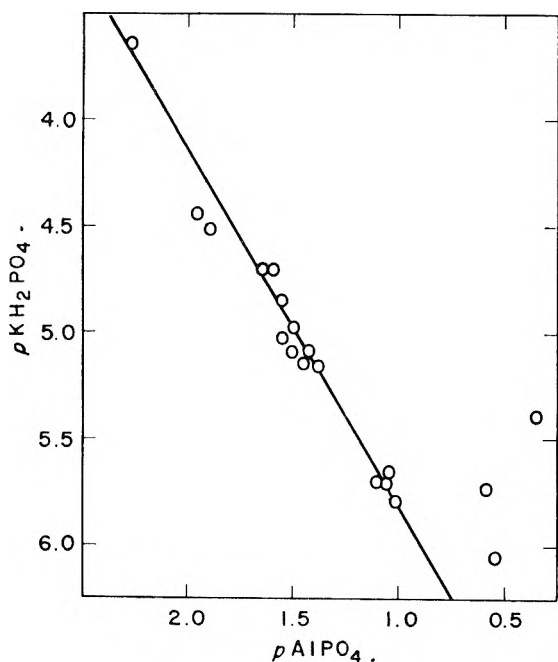


Fig. 1.—Solubility isotherm for potassium taranakite, $\text{H}_6\text{K}_3\text{Al}_3(\text{PO}_4)_9 \cdot 18\text{H}_2\text{O}$: line corresponds to $pK_{sp} = 178.7$.

$$\log \left[\frac{(\text{Al}^{3+})}{(\text{AlOH}^{2+})} \right] = pK_h - p\text{H} + \frac{2.5 \sqrt{I}}{1 + \sqrt{I}} \quad (6)$$

where K_h is the hydrolysis constant of the aluminum ion, 1×10^{-5} at 25°. Because the ionic strength of the solution depends upon the amounts of aluminum and phosphate ions, the correct values for these concentrations must be found by successive approximations before the activities of the ions are calculated on the basis of activity coefficients given by equation 4. Values of pK_{sp} , $p\text{KH}_2\text{PO}_4$ and $p\text{AlPO}_4$ (equation 3), as calculated on an IBM 610 computer, are given in Table I.

In a plot of the compositions of the solutions (Fig. 1), the scales of $p\text{KH}_2\text{PO}_4$ (ordinate) and $p\text{AlPO}_4$ (abscissa) are so arranged that the activi-

ties of the salts increase in directions away from the origin. On this diagram, the taranakite solubility product is represented by a straight line of slope $-5/3$.

With due allowance for experimental error (discussed below), most of the experimental points lie close to the line corresponding to $pK_{sp} = 178.7 \pm 0.5$. The exceptions lie in the region where $p\text{AlPO}_4$ is less than 0.5, which corresponds to an aluminum phosphate ion product, $a_{\text{Al}}a_{\text{PO}_4}$, greater than 1×10^{-20} . The rate of change of composition of these solutions was also significantly different from the rest. All the solutions whose final compositions fell close to the isotherm were equilibrated within 40 to 60 days, whereas the approach to equilibrium was slow and irregular in the solutions with the higher aluminum phosphate activities. The difference between solutions 18 and 19 (Table I), both of which were initially supersaturated with respect to taranakite, is particularly noticeable. Aluminum and phosphate were lost from solution 19 without loss of potassium, whereas the concentrations of all three ions decreased in solution 18 and the final composition was close to the isotherm. Solutions 5 and 6, initially undersaturated, showed slight increases in pH and potassium concentration, but the release of aluminum and phosphate was less than would be expected from congruent dissolution of the taranakite. These observations suggest that an aluminum phosphate phase other than taranakite was precipitated from the solutions, although no other phase was found in petrographic examination of the solids.

All the solutions were supersaturated with respect to the mineral variscite, $\text{AlPO}_4 \cdot 2\text{H}_2\text{O}$, as indicated by its solubility product of 1×10^{-22} (corresponding to $p\text{Al} + p\text{H}_2\text{PO}_4 - 2p\text{H} = 2.48$) as measured by Lindsay, Peech and Clark.⁷ Three solutions that had been equilibrated with potassium taranakite for 80 days were seeded with 10

(7) W. L. Lindsay, M. Peech and J. S. Clark, *Soil Sci. Soc. Am. Proc.*, **23**, 357 (1959).

TABLE II
SOLUTIONS EQUILIBRATED WITH AMMONIUM TARANAKITE AT 25°

No.	pH	NH ₄	Concn., mmoles/l.		Cl	Ionic strength	pNH ₄ H ₂ PO ₄	pAlPO ₄ ^a	pK _{sp}
			Al	P					
1	2.00	12.0	5.8	14.6	25.0	0.052	4.26	1.32	175.57
2	2.22	6.5	3.0	8.3	13.0	.028	4.64	1.11	175.66
3	2.30	4.7	3.1	6.8	12.5	.027	4.83	0.98	175.57
4	2.41	4.2	2.4	5.3	10.0	.021	4.94	.87	175.40
5	2.88	1.6	0.8	2.6	3.2	.008	5.53	.39	174.74
6	2.65	2.3	2.4	3.4	8.4	.018	5.33	.49	174.62
7	2.04	7.2	6.8	14.4	32.0	.057	4.47	1.19	175.57
8	2.76	2.3	4.4	3.5	13.5	.030	5.32	0.11	172.70
9	2.42	10.3	4.8	9.7	20.0	.042	4.32	.49	170.60 ^b
10	2.80	3.3	1.5	1.9	11.0	.015	5.39	.57	175.22

^a $p\text{AlPO}_4 = p\text{Al} + p\text{H}_2\text{PO}_4 - 2p\text{H}$. ^b Initially supersaturated.

mg. of crystalline variscite, but no significant change in composition was observed within a further 200 days. The effect of formation of variscite in any of the solutions listed in Table I is therefore unlikely to be significant.

Other less well defined forms of aluminum phosphate, however, may have been present. An amorphous form of aluminum phosphate readily is formed as a colloidal precipitate on rapid dilution of a solution of aluminum in concentrated phosphoric acid.⁸ It apparently can be formed in any solution in which the value of $p\text{Al} + p\text{H}_2\text{PO}_4 - 2p\text{H}$ is less than 0.5. Although it is metastable with respect to variscite, it does not crystallize readily. Samples stored in the laboratory for several months showed no evidence of change.

Owing to the small difference between the refractive index of the amorphous phosphate (1.460 ± 0.01) and that of taranakite, petrographic analysis may fail to detect the formation of small amounts of the amorphous material, particularly as a thin coating on the surface of the taranakite crystals which could impede their approach to equilibrium with the solution.

Final compositions of the solutions equilibrated with ammonium taranakite are given in Table II, together with the values of $p\text{NH}_4\text{H}_2\text{PO}_4$, $p\text{AlPO}_4$ and pK_{sp} calculated as in Table I. Values of $p\text{NH}_4\text{H}_2\text{PO}_4$ are plotted as a function of $p\text{AlPO}_4$ in Fig. 2. Most of the points are close to the isotherm corresponding to $pK_{sp} = 175.5 \pm 0.5$, but again those for which $p\text{AlPO}_4$ is less than 0.5 show supersaturation with respect to the isotherm. In two of the suspensions (9 and 10, Table II), a white colloidal precipitate was formed during a 220-day period. This material could be separated only by centrifuging; it could not be identified petrographically but appeared to be similar to the colloidal aluminum phosphate described above.

Evaluation.—The greatest sources of experimental errors are the measurements of pH and aluminum ion concentration. An error of ± 0.02 pH unit introduces an uncertainty of ± 0.2 unit in the final pK_{sp} values. Experimental errors in determinations of the other ions are such that uncertainties of ± 0.15 unit are contributed to the final result by the aluminum and ± 0.06 each by the potassium and phosphate. The total uncertainty in the final result due to experimental errors is thus about ± 0.5 unit.

(8) A. W. Taylor and E. L. Gurney, unpublished TVA data.

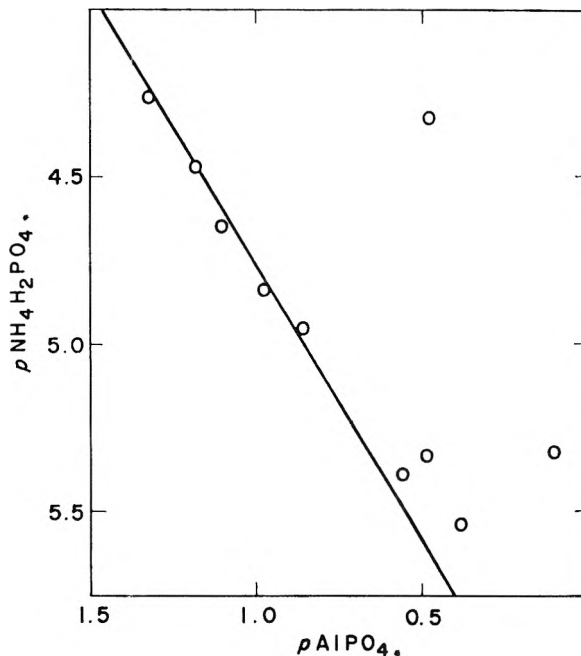


Fig. 2.—Solubility isotherm for ammonium taranakite, $\text{H}_6(\text{NH}_4)_3\text{Al}_5(\text{PO}_4)_8 \cdot 18\text{H}_2\text{O}$: line corresponds to $pK_{sp} = 175.5$.

The variations in the results shown in Tables I and II (excluding those not representing equilibrium) lie within this range. The assumptions made in equations 4 to 6 thus seem to be valid within the experimental range of ionic strengths. A plot of the derived pK_{sp} values against the ionic strength shows that no simple relationship exists between the two and that the variations are random.

These assumptions are of doubtful applicability to solutions with higher ion concentrations. Salmon and co-workers⁹⁻¹¹ demonstrated an extensive complex ion formation in acid solutions containing aluminum and phosphate ions at concentrations above 0.05 M. Several ionic species may be present, depending on the solution composition. Mononuclear ionic species such as $[\text{Al}(\text{HPO}_4)_3]^{3-}$ are present in concentrated solutions with a pH of 1.0 to 1.5 and a P:Al mole ratio of 3.0, whereas less acid systems with lower P:Al ratios may contain cationic species such as $[\text{AlHPO}_4]^+$, $[\text{AlH}_2\text{PO}_4]^{++}$

(9) R. F. Jameson and J. E. Salmon, *J. Chem. Soc.*, 4013 (1954).

(10) J. E. Salmon and J. G. L. Wall, *ibid.*, 1128 (1958).

(11) J. A. R. Genge and J. E. Salmon, *ibid.*, 1459 (1959).

and $[\text{Al}(\text{H}_2\text{PO}_4)_2]^+$. The radius of the aluminum ion is such that these complex ions, which have a chelate structure, may polymerize¹¹ with the precipitation of large cross-linked structures. The amorphous aluminum phosphate formed in some of the taranakite solutions may be of this nature.

According to Bjerrum and Dahm,¹² 60 to 90% of the aluminum in solutions similar to those listed in Tables I and II may be present in the form of

(12) N. Bjerrum and C. R. Dahm, *Z. physik. Chem., Bodenstein Festband*, 627 (1931).

complex ions. Their calculations do not appear, however, to be accurate enough to allow any trustworthy corrections to be applied in the calculation of the ionic activities.

Under these circumstances, the results reported here for the solubilities of the taranakites are regarded as apparent values of the solubility products, which may differ appreciably from the true thermodynamic values. Similar qualifications may be applied to data obtained by similar methods for any other iron or aluminum phosphate compounds.

INTRAMOLECULAR REARRANGEMENTS.¹ II. PHOTOLYSIS AND RADIOLYSIS OF 4-METHYL-2-HEXANONE

By P. AUSLOOS

Division of Physical Chemistry, National Bureau of Standards, Washington, D. C.

Received May 22, 1961

In the photolysis and radiolysis of 4-methyl-2-hexanone, three butene isomers are formed by an intramolecular rearrangement process in which a secondary or primary γ -hydrogen is transferred to the carbonyl group. In the vapor-phase photochemical decomposition, the ratios 1-butene/2-butene and *cis*-2-butene/*trans*-2-butene increase with decrease in wave length and increase in temperature. In the liquid-phase photolysis, however, no dependence on wave length was observed, although the effect of temperature on the butene distribution was very pronounced. Similar results were obtained in the photochemical decomposition of *sec*-butyl acetate. In the transition of the liquid to the solid phase there was a drastic change in the butene distribution. The butene distribution obtained in the photosensitized decomposition at 2537 Å. agrees closely with the one obtained in the non-sensitized decomposition at the same wave length. A comparison of the results obtained in the photolysis with those obtained in the radiolysis in the vapor and liquid phase indicates that in the latter case the butenes may be formed by way of a highly electronically excited molecule.

Introduction

Earlier photochemical investigations² have shown that ketones and aldehydes containing one or more hydrogens in the γ -position decompose photochemically into olefins and the corresponding lower ketones or aldehydes. Indirect evidence has been obtained recently for the formation of the enol form of acetone in the photolysis of 2-hexanone.³ This substantiates the suggestion made earlier² that this rearrangement involves an intermediate having a six-membered ring.

It has been pointed out before^{4,5} that a correlation exists between the photochemical primary act and the mass spectrometric cracking pattern, as well as between the photochemical decomposition and the radiolysis.⁶ The study of the photodecomposition of compounds that yield more than one type of olefin may be expected to provide a better understanding of these primary events.

In the case of 4-methyl-2-hexanone, *cis*- and *trans*-2-butene will be formed if a secondary γ -hydrogen is transferred, and 1-butene will be produced if a primary γ -hydrogen is transferred. Comparison of the butene distributions produced in the radiolysis with the ones produced in the photolysis under comparable conditions was ex-

pected to provide information about the importance of neutral-molecule decompositions in radiolysis.

Experimental

A flat, spiral, low-pressure mercury arc and a Corning filter 7-54 was used in the photo-sensitized experiments. The experiments at short wave length (1900 Å.) were done with a Hanovia hydrogen-discharge lamp with the front window in contact with the quartz window of the reaction cell. An experiment in which a Corning filter 7-54 was placed between the lamp and the cell, indicated that at low partial pressures of ketone (0.7 cm. mercury) absorption at wave lengths greater than 2100 Å. was negligible. All other photochemical experiments were performed with a medium-pressure Hanovia S 100 lamp in conjunction with a grating monochromator.

The quartz cell for gases was 10 cm. in length and 5 cm. in diameter. The latter was provided with two outlets, one of which was sealed after filling, while the other was closed with a break seal. The cell was immersed in a Pyrex Dewar having double quartz windows. A water-bath was used for experiments at constant temperatures above 0°, and one having isopentane as the refrigerant was used for temperatures below 0°.

The NBS 2000 Curie Cobalt 60 source was used in the radiolysis experiments. The vapor phase was irradiated in a Pyrex vessel (14.5 cm. in length, 4.7 cm. in diameter). The liquid-phase cells were made of Pyrex tubing (10 cm. in length, 0.3 cm. i.d.) provided with a break seal. No attempt has been made to determine *G*-values.

The butenes were analyzed with a gas chromatograph. A Perkin-Elmer column "L" was used at 0°.

4-Methyl-2-hexanone was prepared by Merck and Company and had a purity better than 99.5 mole %. Conversions were kept below 2% in the vapor-phase experiments and below 0.05% in the liquid-phase runs.

Results

Vapor Phase.—Besides the butenes given in Table I, the volatile products include CO, CH₄ and C₂H₆. At 3130 Å. and 44° the CO yield is less

(1) This research was supported in part by a grant from the U. S. Public Health Service, Department of Health, Education, and Welfare, and in part by a grant from the U. S. Atomic Energy Commission.

(2) For a review see: J. N. Pitts, Jr., *J. Chem. Educ.*, **34**, 112 (1957).

(3) R. Srinivasan, *J. Am. Chem. Soc.*, **81**, 5061 (1959).

(4) A. J. C. Nicholson, *Trans. Faraday Soc.*, **60**, 1067 (1954).

(5) P. P. Manning, *J. Am. Chem. Soc.*, **79**, 5151 (1957).

(6) P. Ausloos and J. Paulson, *ibid.*, **80**, 5117 (1958).

than 2% of the total butene yield and at 150° it increases to 10%. The yields of CO were considerably higher in the short wave length (*ca.* 1900 Å.) photolysis and in the radiolysis. Under these conditions additional products, such as H₂, C₂H₄, C₃H₆ and C₃H₈ are also produced. The C₂H₄ and C₃H₆ yields in the radiolysis experiment were 5 and 15%, respectively, of the butene yield. Addition of oxygen reduced the H₂, C₂H₆ and C₃H₈ yields to negligible amounts in both the short wave length photolysis and in the radiolysis, whereas those of the olefins were unaffected. Similar observations have been made in the photolysis of 2-pentanone⁷ at short wave lengths.

The acetone yield was measured occasionally and was always equal to the total butene yield, to within 10%, in both photolysis and radiolysis experiments.

The experimental results given in Table I can be summarized as follows.

TABLE I
VAPOR PHASE

Wave length, Å.	Temp., °C.	Pressure, cm.	Butene distribution			
			1-Butene, %	<i>trans</i> -2-Butene, %	<i>cis</i> -2-Butene, %	<i>cis/trans</i> , %
3130	44	0.7	9.7	68.5	21.8	0.318
3130 ^a	44	0.7	9.6	68.8	21.8	.318
3130	84	5.0	11	67.1	21.9	.327
3130	150	0.7	13.0	64.3	22.7	.353
3130	150	.6	13.0	64.0	23.0	.359
3130	258	.7	14.7	61.9	23.4	.379
2537	44	.7	21.3	55.2	23.5	.404
2537 ^b	44	.7	18.0	57.7	24.3	.420
2537 ^b	150	.7	19.0	55.3	25.7	.464
<i>ca.</i> 1900 ^a	44	.7	25.3	50.0	24.7	.493
<i>ca.</i> 1900	44	.7	28.5	48.0	23.5	.492
Radiolysis ^a	44	.7	35.9	39.6	24.5	.620
Radiolysis	44	.7	31.2	44.0	24.8	.564

^a 0.25 cm. oxygen added. ^b Hg photosensitized.

(1) At 3130 Å. oxygen has no effect on the butene distribution, while minor changes occur in the short wave length photolysis and radiolysis.⁸

(2) An increase in temperature and decrease in wave length leads to an increase in the ratios 1-butene/2-butene and *cis*-2-butene/*trans*-2-butene.

(3) The butene distribution obtained in the mercury sensitized decomposition is in good agreement with the one obtained in the non-sensitized photolysis at the same wave length.

(4) The butene distribution obtained in the radiolysis is comparable to the one obtained in the photochemical decomposition at *ca.* 1900 Å.

Liquid Phase.—Because of the experimental problems involved, no photolysis experiments were performed at wave lengths shorter than 2300 Å.

In the liquid-phase photolysis, butenes and acetone accounted for more than 95% of the products.

The total butene quantum yield was independent of temperature in the range -140 to +73°. Solvents had no effects on the quantum yield.

(7) P. Ausloos and E. Murad, *J. Am. Chem. Soc.*, **80**, 5929 (1958).

(8) The fact that oxygen inhibits the addition of H atoms to butene may explain the variations in the butene distribution caused by oxygen. Positioning of the hydrogen discharge lamp with respect to the cell has also some effect on the butene distribution.

The results given in Table II can be summarized as follows.

TABLE II
LIQUID PHASE

Wave length, Å.	Temp., °C.	Solvent 80 mole %	Distribution of butenes			
			1-Butene, %	<i>trans</i> -2-Butene, %	<i>cis</i> -2-Butene, %	<i>cis/trans</i> , %
3130	73	Ethanol	8.6	66.9	24.5	0.366
3130	28	Ethanol	5.8	70.8	23.4	.330
3130	0	Ethanol	4.6	73.2	22.2	.303
3130	-77	Ethanol	2.3	79.2	18.5	.233
3130	-100	Ethanol	2.1	81.2	16.7	.206
3130	-140	Ethanol	4.3	78.1	17.6	.225
3130	-195	Ethanol	67.7	17.6	14.7	.835
3130	28	Octane	7.0	69.2	23.8	.342
3130	28	None	7.0	70.0	23.0	.330
3130	44	None	7.6	69.0	23.4	.34
2650	28	None	6.8	69.6	23.6	.339
2537	28	None	7.0	70.0	23.0	.325
2360	28	None	7.7	69.0	23.3	.337
Radiolysis	28	None	11.9	65.7	22.4	.342
Radiolysis	-80	None	8.0	74.2	17.8	.240

(1) Within experimental error there is no wave length effect on the butene distribution in the region 2360 to 3130 Å.

(2) In agreement with the data for the vapor phase the ratios 1-butene/2-butene and *cis*-2-butene/*trans*-2-butene increase with temperature from -100 to +73°. This trend is, however, reversed at temperatures below -100°.

(3) Solvents have no effect on the butene distribution.

(4) The distribution of the butenes in the liquid-phase radiolysis is similar to the one obtained in the photolysis at the same temperature.

Discussion

Photolysis—Vapor Phase.—The observed increase of the ratio 1-butene/2-butene with the energy absorbed by the molecule is consistent with the difference in bond strength between the primary and secondary hydrogen. The variations of the ratios *cis*-2-butene/*trans*-2-butene are more difficult to visualize. It may, however, be expected that the higher the energy content of the dissociating molecule, the more this ratio will approach the value of unity corresponding to a selection of structures based on chance. Very similar trends have been observed recently in the photolysis of *sec*-butyl acetate.⁹

In accordance with the rule for conversion of the spin angular momentum, it may be expected that in the Hg(³P₁)-sensitized decomposition, a triplet rather than a singlet excited molecule undergoes dissociation. Although it cannot be decided from the results presented in Table I whether a singlet or triplet state is involved, the close similarity between the distribution of the butenes in the photosensitized and the non-sensitized decomposition indicates that the dissociating molecule is in the same excited state in both cases. Recently Brunet and Noyes¹⁰ reported that oxygen does not inhibit

(9) R. Borkowski and P. Ausloos, *J. Am. Chem. Soc.*, **83**, 1053 (1961).

(10) V. Brunet and W. A. Noyes, Jr., *Bull. soc. chim. France*, 121 (1958).

the intramolecular rearrangement in the case of 2-hexanone, and that consequently the dissociating excited molecule is in a singlet state. This conclusion was based on the assumption that a molecule in the triplet state undergoes a fast reaction with oxygen. Recent experiments¹¹ carried out in this Laboratory on the photolysis of 2-pentanone at 3130 Å. did, however, reveal that at sufficiently high oxygen concentration the yields of ethylene and acetone are reduced. The latter observation indicates that a triplet state may very well be responsible for the intramolecular decomposition of 4-methyl-2-hexanone.

Photolysis—Liquid Phase.—The fact that in the liquid-phase photolysis the butene distribution does not depend on the wave length indicates that collisional deactivation is important and that the energy level from which the molecule decomposes is always the same regardless of the initially excited state of the ketone.

The energy level from which decomposition occurs does, however, depend on the equilibrium temperature. There is, indeed, in analogy with the results for the vapor phase a definite increase in the ratios 1-butene/2-butene and *cis*-2-butene/*trans*-2-butene with increase in temperature from -100 to $+73^{\circ}$.

The drastic change of the butene distribution in the temperature range associated with the formation of a glassy state has also been observed in the photolysis of *sec*-butyl acetate⁹ and can be ascribed to a hindered rotation about the C—C bonds.

Radiolysis.—The results indicate that there is some degree of similarity between the products formed in the vapor-phase radiolysis and the short-wave length photolysis. The fact that in the radiolysis the ratios 1-butene/2-butene and *cis*-2-butene/

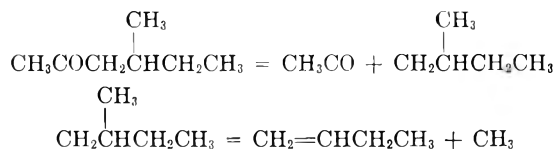
(11) P. Ausloos and R. Rebert (to be published).

trans-2-butene are both greater than the ones obtained in the photolysis does not preclude the formation of a highly excited molecule. It may be pointed out that the formation of products such as H₂, C₂H₄ and C₃H₆, with somewhat larger yields in the radiolysis than in the short wave length photolysis is in agreement with this view.

However, regardless of the excitation of the ketone molecule in the liquid-phase radiolysis, one should expect a butene distribution which does not differ from the one found in the liquid-phase photolysis. The results of Table II indicates that the ratios *cis*-2-butene/*trans*-2-butene and 1-butene/2-butene are very closely the same¹² in the radiolysis and photolysis at 28 and at about -80° .

The quantitative agreement between the distributions obtained in the liquid phase radiolysis and photolysis indicates that the butenes formed in the radiolysis may originate from electronically excited molecules, identical to the ones producing butene in the photochemical process. It is conceivable that direct excitation by secondary electrons as well as neutralization of the positive parent ion¹³ may lead to the formation of highly excited molecules, of which some may undergo collisional deactivation prior to decomposition.

(12) The somewhat larger yield of 1-butene found in radiolysis as compared to the photolysis, may be due to the formation of 1-butene by a sequence of steps such as



Except for the rearrangement process no reasonable mechanism can be written for the formation of 2-butene.

(13) A. H. Samuel and J. L. Magee, *J. Chem. Phys.*, **21**, 1080 (1953).

LIGHT SCATTERING OF COPOLYMERS. I. THE COMPOSITION DISTRIBUTION OF A STYRENE-METHYL METHACRYLATE BLOCK COPOLYMER¹

By SONJA KRAUSE

Research Division, Rohm and Haas Company, Bristol, Pa.

Received May 31, 1961

The validity of an equation which relates the light scattering of copolymers in solution to the composition distributions in the samples, first derived by Stockmayer, *et al.*,² has been investigated experimentally. This equation indicates that the intensity of light scattered by a copolymer in solution, after extrapolation to infinite dilution and to zero scattering angle, depends not only on the weight average molecular weight of the copolymer sample but also on two molecular parameters connected with the composition distribution of the sample, and that these three parameters can be determined from light scattering measurements on the copolymer in three solvents of different refractive index. The qualitative validity of the equation was checked by obtaining the three parameters for a block copolymer of styrene and methyl methacrylate from light scattering measurements in six different solvents. The parameters calculated from any three of these six measurements are consistent. To show that these parameters are also quantitatively correct, the copolymer was fractionated and the three parameters calculated from the measured molecular weights and compositions of the fractions. Within experimental error, the three parameters are the same when determined by either method.

(1) Presented at the meeting of the Am. Chem. Soc., New York, N. Y., Sept., 1960.

(2) W. H. Stockmayer, L. D. Moore, Jr., M. Fixman and B. N. Epstein, *J. Polymer Sci.*, **16**, 517 (1955).

Introduction

It has been known for some time that the weight average molecular weight of a copolymer cannot, in

general, be obtained from light scattering measurements using the analysis and equations applicable to homopolymer solutions. In 1952, Tremblay, Rinfret and Rivest,³ in a discussion of some light scattering data of a butadiene-styrene copolymer, noted that the intensity of light scattered by a copolymer in dilute solution depends not only on the weight average molecular weight of the copolymer, but also on the variations in composition between its constituent polymer chains. Soon thereafter, Stockmayer and co-workers² derived an equation which showed how the intensity of light scattered by a copolymer solution, after extrapolation to infinite dilution and zero scattering angle, should vary with the composition⁴ distribution of the copolymer sample. They assumed, for the purpose of their calculation, that the refractive index increment of a copolymer in a solvent varied linearly with the composition of the copolymer. In the present work, the validity both of this assumption and of the final equation, eq. 2, has been investigated. It has been demonstrated that these simple equations, which will be discussed below, quantitatively describe the refractive index increments and light scattering behavior of a block copolymer of styrene and methyl methacrylate in solution in six different solvents.

Since this work was started, Bushuk and Benoit^{5,6} have shown that the light scattering behavior of several copolymers of styrene and methyl methacrylate in a number of solvents is in qualitative agreement with the equation of Stockmayer, *et al.*

When used for copolymer solutions, the equation that gives the weight average molecular weight of a homopolymer from the light scattering data gives only an apparent molecular weight, M_{app}

$$\left(\frac{I_{\theta}}{K'c}\right)_{c \rightarrow 0, \theta \rightarrow 0} = \left(\frac{dn}{dc}\right)_0^2 M_{app} \quad (1)$$

where I_{θ} is the ratio of the intensity of scattered light measured at angle θ and at a fixed distance from the scattering volume to the intensity of light incident on the solution, c is the concentration of the polymer in the solution, $(dn/dc)_0$ is the measured refractive index increment of the copolymer-solvent system, and $K' = 2\pi^2 n_0^2 K / (\lambda_0^4 N)$, where n_0 is the refractive index of the solvent for light of wave length λ_0 *in vacuo*, N is Avogadro's number, and K is a function of θ which includes the instrument calibration constant.

For binary copolymers, Stockmayer, *et al.*,² have derived the following relationship, assuming only that the refractive index increment of a copolymer chain was proportional to its composition

$$\left(\frac{I_{\theta}}{K'c}\right)_{c \rightarrow 0, \theta \rightarrow 0} = \left(\frac{dn}{dc}\right)_0^2 \bar{M}_w + 2b \left(\frac{dn}{dc}\right)_0 \langle M \Delta x \rangle + b^2 \langle M (\Delta x)^2 \rangle \quad (2)$$

where

(3) R. Tremblay, M. Rinfret and R. Rivest, *J. Chem. Phys.*, **20**, 523 (1952).

(4) The word "composition," for the purpose of this paper, will refer to the average composition of a copolymer molecule. That is, a block copolymer and a random copolymer molecule of the same average composition are assumed indistinguishable in this discussion.

(5) W. Bushuk and H. Benoit, *Compt. rend.*, **246**, 3167 (1958).

(6) W. Bushuk and H. Benoit, *Can. J. Chem.*, **36**, 1616 (1958).

$$b = \left(\frac{dn}{dc}\right)_A - \left(\frac{dn}{dc}\right)_B \quad (3)$$

where subscripts A and B refer to the two homopolymers corresponding to the copolymer in question.

$$\langle M \Delta x \rangle = \sum w_i M_i (\Delta x)_i \quad (4)$$

$$\langle M (\Delta x)^2 \rangle = \sum w_i M_i (\Delta x)_i^2 \quad (5)$$

where w_i is the weight fraction of molecules in the copolymer sample having molecular weight M_i and composition x_i (composition being given as volume fraction of monomer A), with $(\Delta x)_i = (x_i - x_0)$. x_0 is the average composition of the copolymer sample. Bushuk and Benoit⁶ have derived eq. 2 in another entirely equivalent form.

Since eq. 2 contains three unknowns, \bar{M}_w , $\langle M \Delta x \rangle$, and $\langle M (\Delta x)^2 \rangle$, it should be possible to determine these quantities for any binary copolymer from light scattering and $(dn/dc)_0$ measurements in three different solvents. These measurements provide three different statements of eq. 2 which constitute three linear equations in three unknowns which are easily solved. One purpose of the present paper is to demonstrate that, within experimental error, the same values of the three unknowns are obtained using any of the possible combinations of light scattering and $(dn/dc)_0$ data of a copolymer in more than three different solvents. Another purpose of this paper is to show that these values of \bar{M}_w , $\langle M \Delta x \rangle$, and $\langle M (\Delta x)^2 \rangle$ are quantitatively correct. For this purpose, the copolymer sample was fractionated and these parameters calculated from the molecular weights and compositions of the fractions.

Experimental

The styrene-methyl methacrylate block copolymer studied in this work was the one prepared by Graham and co-workers⁷ by addition of methyl methacrylate monomer to sodium-naphthalene initiated unimerated polystyrene. This copolymer was chosen specifically because of its method of preparation. Since the polystyrene portion of the block should have a fairly narrow molecular weight distribution, the block copolymer molecules of different final molecular weight should have different compositions. Therefore, a fractionation by molecular weight was expected to be a fractionation by composition also, thus making a double fractionation, by composition and by molecular weight, unnecessary for this sample.

A 30-g. portion of the copolymer was fractionated from 0.5% solution in butanone using diisopropyl ether as non-solvent at 30°. Stockmayer, *et al.*,² have shown that this solvent system leads to fractionation of styrene-methyl methacrylate copolymers primarily by molecular weight with very little influence by variable composition of the copolymer molecules. Since it is well known that diisopropyl ether forms peroxides very easily in the presence of oxygen, a number of special precautions were taken during the fractionation. The solvent was stored in a refrigerator and tested for peroxides before each use. The fractionation flasks were filled with nitrogen while each precipitate was settling, and the fractions were never heated when they were dry or almost dry.

Reagent grade butanone was used for the viscosity and osmotic pressure measurements without further purification. For light scattering, reagent grade butanone, 1,2-dichloroethane, toluene and *o*-dichlorobenzene were distilled through a packed column and center cuts of constant boiling point were collected. Bromoform and α -chloronaphthalene were distilled at about 20 mm.; center cuts of constant boiling point were collected. Refractive indices of the solvents just before use, at 25° using the sodium-D line, were: butanone,

(7) R. K. Graham, D. L. Dunkelberger and E. S. Cohn, *J. Polymer Sci.*, **42**, 501 (1960).

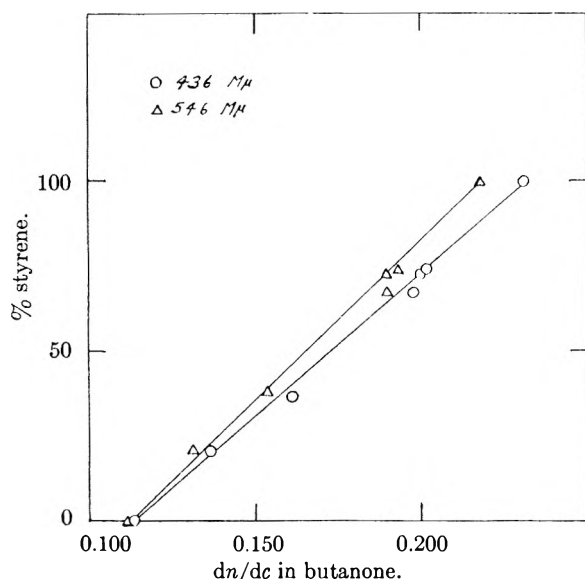


Fig. 1.—Per cent. styrene from infrared measurements vs. refractive index increment of the block copolymer fractions.

1.37612 \pm 0.02; 1,2-dichloroethane, 1.44206; toluene, 1.49352; *o*-dichlorobenzene, 1.54908 \pm 0.02; bromoform, 1.59424; α -chloronaphthalene, 1.62987 (the limits of error refer to variations between batches). The refractive indices of the solvents at 436 and 546 $m\mu$ were calculated from the above n_D^{25} and the known dispersion of each solvent.

Intrinsic viscosities were obtained at 30° using Cannon-Ubbelohde semimicro viscometers with solvent flow times above 100 sec. so that no kinetic energy corrections were necessary. No shear corrections were necessary because of the low values of all the intrinsic viscosities obtained.

The osmotic pressure measurements were obtained in the modified Schulz-Wagner osmometer, and by the method of analysis discussed by Fox, Kinsinger and Schuele.⁸

The refractive index increments for light of 436 and 546 $m\mu$ were measured with a Brice-Phoenix differential refractometer. This instrument could not be used for α -chloronaphthalene, whose refractive index exceeded the range of the instrument. The refractive index increments of the unfractionated copolymer in α -chloronaphthalene were obtained as follows. A plot of measured $(dn/dc)_0$ vs. n_0 was made for each wave length; a straight line could be drawn through each set of points and could be extrapolated to the refractive index of α -chloronaphthalene to give the $(dn/dc)_0$ at 436 and at 546 $m\mu$.

Light scattering data were obtained at 436 and 546 $m\mu$ on a Brice-Phoenix light scattering photometer at scattering angles from 30 to 135°. All solvents and polymer stock solutions were clarified by pressure filtration through sintered glass ultrafine filters. Runs were always made by adding polymer stock solution to solvent in the light scattering cell; five concentrations were run for each M_{app} determination. Light scattering data were extrapolated first to zero angle and then to infinite dilution. Instrument calibration factors for the different solvents were obtained as follows: for butanone and toluene from the 90° scattering of a 0.5% solution of the Cornell polystyrene light scattering standard⁹ in the manner discussed by Cohn-Ginsberg, Fox and Mason,¹⁰ and for the other solvents from the zero angle-infinite dilution extrapolated scattering of a polymethyl methacrylate sample whose \bar{M}_w was obtained in butanone and assumed constant in the other solvents.

The average composition of each fraction was determined from its $(dn/dc)_0$ in butanone, after the $(dn/dc)_0$ vs. composition curve had been calibrated using compositions determined from the infrared spectra of selected fractions (Fig. 1). The monomer ratios in these fractions were obtained from

(8) T. G. Fox, J. B. Kinsinger and E. M. Schuele, in preparation for publication.

(9) P. Doty and R. F. Steiner, *J. Chem. Phys.*, **18**, 1211 (1950).

(10) E. Cohn-Ginsberg, T. G. Fox and H. F. Mason, in preparation for publication.

the relative intensities of the two absorption peaks at 5.75 and 14.2 μ , using a calibration curve which was established using samples with known monomer ratios.

Results

The number average molecular weight of the unfractionated polymer was 3.16×10^5 , and its intrinsic viscosity in butanone 0.85 dl./g. The results of the light scattering runs are shown in Table I.

TABLE I

LIGHT SCATTERING RESULTS FOR THE UNFRACTIONATED BLOCK COPOLYMER

Solvent	$(dn/dc)_0$		$M_{app} \times 10^{-6}$	
	436 $m\mu$	546 $m\mu$	436 $m\mu$	546 $m\mu$
1 Butanone	0.184	0.178	1.05	1.16
2 1,2-Dichloroethane	.135	.126	0.97	1.12
3 Toluene	.075	.075	1.11	1.08
4 <i>o</i> -Dichlorobenzene	.018	.019	4.28	4.73
5 Bromoform	-.025	-.023	6.78	7.90
6 α -Chloronaphthalene	-.075	-.053	2.20	2.21

The constant, b , as defined in eq. 3, which is necessary for the use of eq. 2, was calculated from the refractive index increments of the corresponding homopolymers in butanone and in 1,2-dichloroethane as shown in Table II. It can be seen that b is the same, within experimental error, in these two solvents; the same value for b was assumed in the other four solvents.

TABLE II

REFRACTIVE INDEX INCREMENTS OF POLYSTYRENE AND POLYMETHYL METHACRYLATE

Solvent	dn/dc				b	
	Polystyrene		Polymethyl methacrylate		436 $m\mu$	546 $m\mu$
	436 $m\mu$	546 $m\mu$	436 $m\mu$	546 $m\mu$		
Butanone	0.231	0.218	0.114	0.113	0.117	0.105
1,2-Dichloroethane	0.168	0.155	0.050	0.051	0.118	0.104

The compositions, intrinsic viscosities and light scattering data for the fractions in butanone are shown in Table III.

TABLE III

DATA FOR THE FRACTIONS OF THE BLOCK COPOLYMER IN BUTANONE

Fraction no.	% of total	$[\eta]_{30}$ (dl./g.)	$(dn/dc)_0$		$M_{app} \times 10^{-6}$		Vol. % styrene
			436 $m\mu$	546 $m\mu$	436 $m\mu$	546 $m\mu$	
1	3.4	1.79	0.123	0.119	7.9	8.5	7
2	2.5	1.33	.137	.132	3.57	4.09	19
3	5.0	1.19	.144	.139	2.24	2.10	25
4	4.2	1.22	.153	.148	1.36	1.56	33
5	7.5	1.17	.161	.154	1.41	1.75	40
6	4.7	1.06	.166	.158	1.21	1.33	44
7	8.6	1.05	.184	.176	1.11	1.19	60
8	10.3	1.02	.202	.190	1.02	1.12	74
9	7.3	0.94	.202	.193	0.79	0.83	75
10	7.9	.85	.205	.194	.68	.72	77
11	5.8	.70	.211	.200	.57	.58	83
12	5.5	.68	.203	.193	.53	.53	76
13	3.9	.56	.204	.194	.420	.430	77
14	3.8	.47	.200	.190	.380	.403	73
15	3.4	.456	.208	.198	.311	.325	80
16	7.4	.395	.198	.190	.272	.294	72
17	3.0

94.2% recovered

TABLE IV
MOLECULAR PARAMETERS OF THE BLOCK COPOLYMER CALCULATED FROM DIFFERENT DATA

Data used for calculation	\bar{M}_n $\times 10^{-4}$	\bar{M}_w $\times 10^{-4}$	$\langle M\Delta x \rangle$ $\times 10^{-6}$	$\langle M(\Delta x)^2 \rangle$ $\times 10^{-4}$
UFP, ^a solvents 1-5, 436 m μ		1.28 \pm 0.15	-2.34 \pm 1.08	1.89 \pm 0.86
UFP, solvents 1-5, 546 m μ		1.37 \pm .03	-2.28 \pm 0.24	1.87 \pm .17
UFP, solvents 1-6, 436 m μ		1.24 \pm .12	-2.16 \pm .70	1.72 \pm .56
UFP, solvents 1-6, 546 m μ		1.20 \pm .20	-1.68 \pm .72	1.90 \pm .49
Unfractionated polymer	3.16			
Fractions, M_{app} at 436 m μ	3.14	1.23	-2.4	1.4
Fractions, M_{app} at 546 m μ	3.23	1.34	-2.6	1.5

^a Unfractionated polymer.

No light scattering data are reported on fraction 17 since this fraction was colored yellow and no good light scattering data could be obtained. It was possible, however, to obtain a number average molecular weight.

The data in Table III indicate that the fractionation of the copolymer was, as expected, a fractionation mainly by molecular weight; both the intrinsic viscosities and the apparent molecular weights of the fractions in butanone decrease monotonically, within experimental error, from fraction 1 to fraction 16. The fractionation was also by composition for fractions 1 through 8. Beyond this fraction, the per cent. styrene in the fractions fluctuates; this indicates that the styrene portion of the block copolymer was not as monodisperse as expected. If the styrene had been completely monodisperse, the per cent. styrene in the fractions would have increased monotonically as the molecular weight decreased. The polydispersity of the styrene portion of the block copolymer leads to the suspicion, confirmed by the data in Table V below, that the fractions had appreciable composition distributions. In spite of this, the average value of M_{app} in butanone for each of fractions 1 through 16 was used as the true molecular weight of the fraction in calculations.

Table IV shows the values of the number average molecular weight, the weight average molecular weight, $\langle M\Delta x \rangle$, and $\langle M(\Delta x)^2 \rangle$ as obtained, first, from the data on the unfractionated block copolymer in Table I, and second, from the data on the fractions in Table III. The weight average molecular weight, the $\langle M\Delta x \rangle$ and the $\langle M(\Delta x)^2 \rangle$ values given for the unfractionated polymer are those obtained as an average of all possible groups of three of the light scattering solvents. Values for the data at 436 and at 546 m μ were calculated separately because the precision of the actual light scattering measurement is different at these two wave lengths and because different values of the constant b enter into eq. 2. The values calculated with and without the data in α -chloronaphthalene are shown separately because, as mentioned above, the $(dn/dc)_0$ values for this solvent were extrapolated, not measured quantities. Since the values obtained with and without the data in this solvent are the same within the limits of error given (the mean deviation), it appears probable that the extrapolated values for $(dn/dc)_0$ in α -chloronaphthalene are correct. It is also pleasant to note that the calculations from the data on the fractions were not sensitive to the incompleteness of the frac-

tionation by composition of the lower molecular weight fractions.

The calculation of the number average molecular weight of the sample from data on the fractions included the number average molecular weight data on fraction 17. Other calculations from data on the fractions were made from data on fractions 1 through 16 only. This includes a calculation of the expected intrinsic viscosity of the unfractionated copolymer in butanone

$$[\eta]_{\text{calcd}} = \sum w_i [\eta]_i = 0.92; [\eta]_{\text{measd}} = 0.85$$

Table V shows light scattering data on four of the fractions of the block copolymer in two additional solvents each. Each of fractions 3, 7, 12 and 16 had the same M_{app} , within experimental error, in another solvent in which its $(dn/dc)_0$ was high, as it did in butanone. This can be used as an indication that \bar{M}_w lies near these apparent molecular weights. The fact that M_{app} in a third solvent is quite different from its value in the first two indicates that the fractions have appreciable composition distribution. This already was surmised above from the fractionation data.

TABLE V
DATA FOR SOME FRACTIONS IN SOLVENTS OTHER THAN BUTANONE

Fraction no.	Solvent	$(dn/dc)_0$		$M_{app} \times 10^{-4}$	
		436 m μ	546 m μ	436 m μ	546 m μ
3	1,2-Dichloroethane	0.076	0.075	2.24	1.88
3	Toluene	.028	.032	7.3	8.9
7	Toluene	.070	.071	1.30	1.20
7	<i>o</i> -Dichlorobenzene	.0135	.017	11.2	11.6
12	Toluene	.092	.091	0.480	0.494
12	<i>o</i> -Dichlorobenzene	.021	.024	3.85	3.36
16	Toluene	.090	.087	0.297	0.276
16	<i>o</i> -Dichlorobenzene	.030	.031	1.68	2.23

The molecular parameters calculated for these four fractions from the light scattering data as observed in three different solvents each are given in Table VI. For some of the fractions, the weight average molecular weight calculated from data in the three solvents is not very close to the apparent molecular weight in butanone, which was used in the calculations for Table IV. This is probably because of experimental error; the error in three different $(dn/dc)_0$ measurements and in three different M_{app} measurements enters into the calculations. In order to minimize this error, samples should probably be run in at least four different solvents, and the calculations from each set of three solvents averaged out.

TABLE VI
MOLECULAR PARAMETERS OF FOUR FRACTIONS CALCULATED
FROM LIGHT SCATTERING DATA

Frac- tion no.	$\bar{M}_w \times 10^{-6}$		$\langle M\Delta x \rangle \times 10^{-6}$		$\langle M(\Delta x)^2 \rangle \times 10^{-6}$	
	436 $m\mu$	546 $m\mu$	436 $m\mu$	546 $m\mu$	436 $m\mu$	546 $m\mu$
3	2.96	4.15	-0.43	-20	Negative	17
7	1.15	1.53	-0.79	-4.7	1.53	4.6
12	0.69	0.72	-1.92	-2.40	1.68	2.45
16	0.368	0.53	-1.26	-3.05	1.50	3.35

Discussion

The first thing to be noted is the excellent agreement between the molecular parameters of the block copolymer as calculated from measurements on the unfractionated copolymer with those calculated from data on the fractions. It has therefore been shown that eq. 2 is adequate to explain the light scattering behavior in dilute solution (after extrapolation to zero scattering angle and to infinite dilution) of a block copolymer of styrene and methyl methacrylate. It is expected that the same equation will also explain the light scattering of block, graft and random binary copolymers containing a variety of monomers. Thus light scattering data in three or, better, in four or five different solvents can be used to obtain the weight average molecular weights, and some parameters related to the composition distribution of such binary copolymers. The parameters $\langle M\Delta x \rangle$ and $\langle M(\Delta x)^2 \rangle$ ¹¹ should turn out to be very useful quantities for discussing the composition distribution of copolymer samples. The parameter, $\langle M\Delta x \rangle$, is a measure of the drift in the composition of the copolymer molecules comprising the sample with molecular weight. This quantity can be either positive or negative; the sign calculated for this parameter indicates which monomer pre-

(11) These parameters will probably be more useful in their normalized forms, $\langle M\Delta x \rangle / \bar{M}_w$ and $\langle M(\Delta x)^2 \rangle / \bar{M}_w$.

dominates in the higher molecular weight molecules in the sample. In the case of the block copolymer of styrene and methyl methacrylate discussed here, the negative sign of $\langle M\Delta x \rangle$ indicates, correctly, that the highest molecular weight molecules in the sample contain a larger proportion of methyl methacrylate than the lower molecular weight molecules. As expected, this quantity was also negative for the four fractions in Table VI. The quantity $\langle M(\Delta x)^2 \rangle$ is a measure of the width of the composition distribution of the sample, somewhat weighted toward high molecular weights. This quantity, which must be positive, came out negative in the calculations for fraction 3 using the data at 436 $m\mu$. As stated above, this probably was caused by the accumulation of experimental error in the calculation. Some of the combinations of light scattering data of the unfractionated copolymer, before they were averaged for Table IV, also gave some rather unbelievable results. For example a combination of the light scattering data of the unfractionated copolymer in *o*-dichlorobenzene, bromoform and α -chloronaphthalene at 546 $m\mu$ also gives a negative value for $\langle M(\Delta x)^2 \rangle$. It therefore appears essential to combine data in more than three solvents for an unambiguous determination of the molecular parameters of copolymers.

Acknowledgments.—Thanks are given to Mr. Joseph Bonafiglia who fractionated the block copolymer and obtained the $(dn/dc)_0$ and light scattering data, also to Mr. Harry F. Mason and Mrs. Elizabeth Cohn-Ginsberg under whose supervision the intrinsic viscosities were obtained, to Dr. Aldenlee Spell and Mr. Warren Myers for the infrared measurements, to Dr. Roger Graham and Mr. David Dunkelberger for providing the copolymer sample, and to Mr. Lester DeFonso for programming our Bendix G-15 computer for all the light scattering calculations.

NOTES

INVESTIGATION OF THE PHOTOOXIDATION OF ACETONE AT 3130 Å USING INFRARED ANALYSIS

BY A. D. OSBORNE, J. N. PITTS, JR., AND
SANDRA L. FOWLER

Dept. of Chemistry, University of California, Riverside, California
Received April 29, 1961

The photolysis of acetone in the presence of oxygen has been studied by a number of workers.¹⁻⁶ Acetyl and methyl radicals produced when acetone

absorbs light in the near ultraviolet react quickly and completely with oxygen. The reaction of oxygen with acetyl radicals occurs before these radicals can decompose thermally into methyl radicals and carbon monoxide, even at pressures of oxygen below 1 mm.

The fate of the resulting peroxyacetyl radicals is less certain. In the acetaldehyde-oxygen system large amounts of peracetic acid are formed by abstraction of hydrogen from the aldehyde.⁷ In the acetone-oxygen system this does not occur to any appreciable extent because acetone has no readily abstractable hydrogen. Other proposed reactions have been inter-reaction to give diacetyl peroxide⁶ or acetic acid radicals,² disproportionation with other radicals to give acetic acid radicals²

(1) F. B. Marcotte and W. A. Noyes, Jr., *Disc. Faraday Soc.*, **10**, 236 (1951).

(2) R. R. Hentz, *J. Am. Chem. Soc.*, **75**, 5810 (1953).

(3) Margaret I. Christie, *ibid.*, **76**, 1979 (1954).

(4) J. R. Dunn and K. O. Kutschke, *Can. J. Chem.*, **36**, 421 (1958).

(5) J. Brown, N. T. Mitchell and G. R. Martin, *Proc. Chem. Soc.*, 115, March, 1960.

(6) W. A. Noyes, Jr.; *Festschrift Arthur Stoll* (Birkhäuser AG., Basel) 1957, p. 64.

(7) C. A. McDowell and L. K. Sharples; *Can. J. Chem.*, **36**, 251 (1958).

and decomposition to give a methoxy radical and carbon dioxide.^{2,8}

Calvert and Hanst⁸ reinvestigated the photooxidation of acetaldehyde at room temperature using infrared spectrophotometry to determine products. They found that amounts of acetyl peroxide formed were below the limits of detection of their method (less than 0.003 mm./min.). Acetic acid was produced as well as large amounts of peracetic acid.

Hentz² and Christie³ both reported acetic acid in the photooxidation products of acetone. Christie using acetone labelled with C¹⁴ estimated its quantum yield to be at least unity. Her method involved treatment of the reaction products, in the presence of a large excess of unreacted acetone, with aqueous barium hydroxide, evaporating to dryness and igniting the residue at 400°. Quantum yield of acetic acid was based upon measurement of the radioactivity of the resulting gas. However, recently Brown, *et al.*,⁵ have shown that this method is subject to doubt. They were able to produce similar results with the original labelled but unphotolyzed acetone. Using a titration method involving spectrophotometric observation of an acid-base indicator, they estimated the quantum yield to be less than 0.01. The present investigation was undertaken in an attempt to resolve some of these anomalies by using infrared techniques to identify and determine the more reactive products.

Experimental

Chemicals.—Acetone was Matheson Co. A.C.S. analyzed reagent and was degassed and used without further purification. No impurities were detected by gas chromatography. Oxygen was taken from a cylinder and passed through a column of magnesium perchlorate, then a column of potassium hydroxide pellets.

The reaction vessel was made of borosilicate glass in the form of a cross having fused silica windows cemented at the ends of one arm and rocksalt at the ends of the other. The volume of the reaction cell was 235 ml. Photolysis experiments were carried out in the beam of a Perkin-Elmer Model-221 spectrophotometer. For experiments at room temperature no attempt was made to control the temperature. For experiments at 120° a small brass furnace was designed which could be mounted in the beam of the infrared instrument. The furnace had fused silica and rocksalt windows. In this preliminary design, temperature control was not very good, being $\pm 8^\circ$ over the whole reaction vessel.

Light Source.—An Osram HBO-200 high pressure mercury arc was used. For experiments at room temperature the light was collimated and filtered through 1 mm. of Pyrex and 10 mm. of 0.9 M nickel chloride solution. This limited the wave length of the radiation to 3130 Å. and some green light. The latter was removed from the radiation emerging from the reaction vessel with a Corning 9863 Red-Purple Corex filter. Transmittancy measurements for purposes of actinometry were made with a phototube. Diethyl ketone was used as an actinometer; Φ_{CO} was taken at 0.86 at 30°. For experiments at 120° the light was filtered only through 1 mm. of Pyrex. Acetone was used for actinometry making filters and transmittancy measurements unnecessary. Φ_{CO} was taken as unity.

Procedures.—The reaction vessel was evacuated on a high vacuum system and acetone and oxygen admitted to the required pressures. The cell was transferred to the infrared instrument and the spectrum recorded. The mixture was photolysed for the required time and a second spectrum was obtained. Scale expansion was used to look for trace amounts of reaction products. It was possible to observe and measure methanol and formic acid

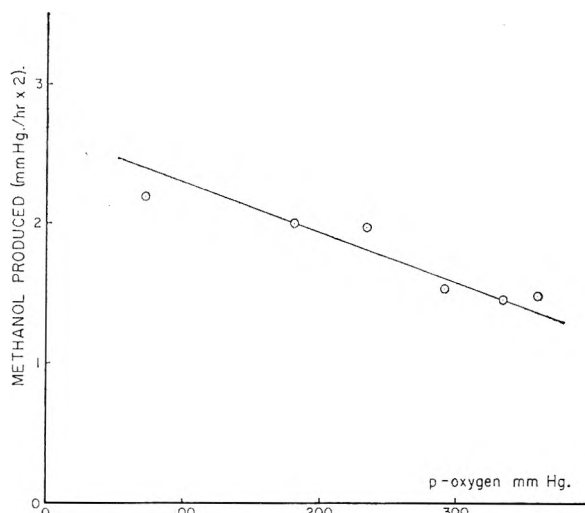


Fig. 1.—Rate of formation of methanol plotted against initial oxygen pressure.

without scale expansion. The measurement of carbon dioxide was not attempted because it was not possible to remove all the atmospheric carbon dioxide from the instrument by flushing with dry nitrogen. In a few check runs carbon dioxide was separated from the reaction products by conventional high vacuum techniques and measured. Φ_{CO_2} at 25° and 3130 Å. was 0.55 compared with the value 0.5 obtained by Hentz under somewhat different conditions (full arc, 48°).²

Calibration.—Calibration curves of optical density against pressure (at the wave lengths used for analysis) were obtained for methanol, formic acid and acetic acid. Pure compounds were monitored as vapors into the cell from the high vacuum apparatus or alternatively introduced quantitatively to the cell through a rubber septum. Because of the small amounts involved they were introduced as a solution in acetone. The results from the two methods agreed. Beer's law was essentially obeyed.

Results

Effect of Oxygen Pressure.—A slight dependence of the rate of formation of methanol on oxygen pressure was observed. Figure 1 shows a plot of the rate of formation of this substance with oxygen pressure. The rate decreased with increasing pressure of oxygen.

Figure 2 shows a typical infrared spectrum before and after photolysis. Methanol, formic acid and acetic acid bands are clearly shown and were in wave length regions where acetone does not absorb. No diacetyl peroxide or methyl hydroperoxide were observed. This is the same result as found by Calvert and Hanst⁸ for the acetaldehyde-oxygen system. Acetone is a more fortunate system than acetaldehyde for the detection of diacetyl peroxide, because peracetic acid is not formed. Peracetic acid has strong bands at 8.6 and 11.75 μ , which are the regions used for detecting diacetyl peroxide. No build up in optical density was observed in either region. In the acetaldehyde-oxygen system peracetic acid had to be "blanked out" by placing this substance in the reference beam.

From infrared optical density measurements the following quantum yields were obtained at 30° for the less volatile products, using a mixture of 42 mm. of acetone and 200 mm. of oxygen: $\Phi_{HCOOH} = 0.27$, $\Phi_{CH_3COOH} = 0.02$, $\Phi_{CH_3OH} = 0.21$. Using the same reactant concentrations the following

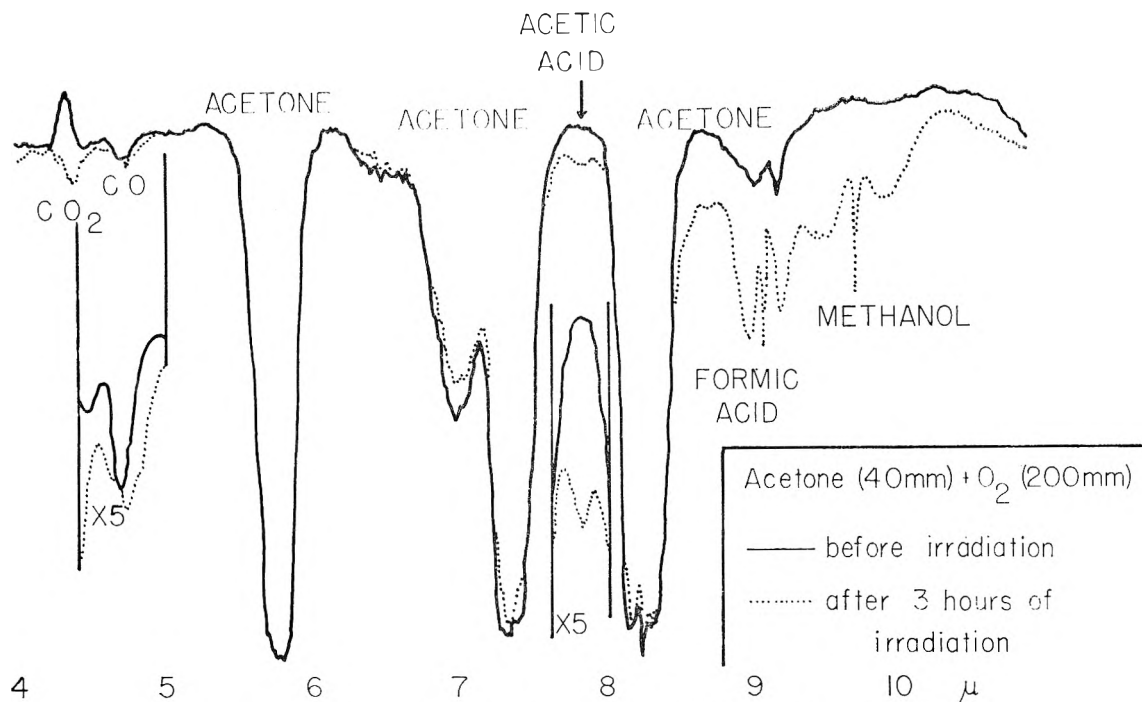


Fig. 2.—Infrared spectrum of acetone-oxygen mixture before and after photolysis.

quantum yields were obtained by conventional high vacuum experiments: $\Phi_{\text{CO}} = 0.10$; $\Phi_{\text{CO}_2} = 0.55$; $\Phi_{\text{CH}_4} = 0.03$. The latter may be compared with the quantum yields obtained by Hentz under somewhat comparable conditions: $\Phi_{\text{CO}} = 0.1$; $\Phi_{\text{CO}_2} = 0.5$.

At 120° no acetic acid was detected (*i.e.*, $\Phi < 0.01$) and the yield of formic acid was very low, dropping from 0.27 at 30° to 0.04 at 120° . $\Phi_{\text{CH}_3\text{OH}}$ at 120° increased from 0.21 at 30° to 0.32.

Formaldehyde has been mentioned as an important product by Hentz² and also by Christie.³ The latter obtained quantum yields greater than unity for this substance. Formaldehyde was not observed in the present investigation, since the infrared absorption bands of acetone preclude detection of small quantities of this substance, whose absorption bands occur in the same regions of the spectrum.

Water was a product and was detected by gas chromatography, trapped at the column exit and characterized by mass spectrometry. This procedure also was carried out to confirm that methanol and acetic acid were in fact responsible for the infrared absorption bands observed. An unsuccessful attempt was made to detect formic acid chromatographically. However, this substance has a very sharp and characteristic Q-branch absorption at 9.05μ which makes further characterization unnecessary.

Discussion

The results indicate that peroxyacetyl radicals under the conditions of our experiments do not inter-react to form diacetyl peroxide. This is a finding similar to that of Calvert and Hanst⁸ for the acetaldehyde-oxygen system. The limits of detection of the method were such that acetyl peroxide would have been detected if its quantum

yield had exceeded 0.01. It should be pointed out that this finding does not preclude the possibility that acetyl peroxide is formed but is removed quickly from the system—*e.g.*, by decomposition or reaction with radicals—in which case acetyl peroxide might be present only in a low steady state concentration corresponding to a quantum yield less than 0.01.

Shahin and Kutschke⁹ found that methyl hydroperoxide decomposed heterogeneously on metal surfaces to give formaldehyde and water. On the other hand, Subbaratnam and Calvert^{8,10} found that methyl hydroperoxide and diacetyl peroxide were both relatively stable in their infrared cell, in which the only metal was the gold forming the mirrors. Since our reaction cell was of glass it is reasonable to assume that these peroxides would build up above the limits of detection were they formed to any appreciable extent. No methyl hydroperoxide nor diacetyl peroxide was available to us so it was not possible to ascertain how stable these compounds were under our conditions.

The quantum yield of acetic acid was 0.02 at 30° and essentially zero at 120° . Brown, *et al.*,⁶ using pressures of acetone from 30 to 130 mm. and pressures of oxygen from 0.5 to 5 mm., conducted experiments at 3130 \AA . and 120° , and estimated that the quantum yield of total acid was less than 0.01. This is in reasonably good agreement with the results of our experiments, which showed no acetic acid and a yield of formic acid of 0.04. It is evident in any case that the yield of acid is small at 120° .

In the case of acetic acid this is probably because most of the $\text{CH}_3\text{COO}\cdot$ radicals produced de-

(9) M. Shahin and K. O. Kutschke, *J. Phys. Chem.*, **65**, 189 (1961).

(10) N. R. Subbaratnam and J. G. Calvert, *Advanced Papers of the Symposium, "Chemical Reactions in the Lower and Upper Atmosphere,"* San Francisco, April, 1961, Pub. Stanford Research Institute.

compose quickly, particularly at elevated temperatures, to give carbon dioxide and a methyl radical, only a small fraction abstracting hydrogen to form acetic acid.

Formic acid is clearly a major product at 30°. This substance presumably is formed by oxidation of formaldehyde in a secondary process, probably on the walls. The low yield of formic acid at 120° can be explained in three ways: (1) formic acid disappears from the system in some way at 120°, (2) formaldehyde is not produced in the photooxidation of acetone at 120° and (3) formaldehyde is produced but does not oxidize to formic acid at 120°.

Formic acid is a comparatively stable substance under the experimental conditions which makes (1) unlikely; (2) can be discounted on the basis of the findings of previous workers¹⁻⁴; (3) is a more likely explanation. Recent work gives supporting evidence for this.⁹ Formic acid, while a major product in the photooxidation of formaldehyde below 110°, gives rapidly decreasing yields above this temperature.¹¹

Hentz² found that the over-all yield of oxygen uptake was approximately 1.2 and invariant over the temperature range from 48–150°. In order to account for the former he proposed that oxygen must have been regenerated in some way, e.g.



The quantum yield for carbon dioxide was 0.5 and invariant with temperature below 150°. This he explained by assuming that 50% of the $\text{CH}_3\text{CO}(\text{OO})\cdot$ and $\text{CH}_3\text{COO}\cdot$ radicals decomposed to give CO_2 . This also involves the implicit assumption that the quantum yield of the primary process



is unity, and that the rate of decomposition of $\text{CH}_3\text{CO}(\text{OO})\cdot$ and $\text{CH}_3\text{COO}\cdot$ radicals into CO_2 does not change with temperature.

This argument gives a quantum yield for oxygen uptake of 1.25, in agreement with experiment. The remainder of the $\text{CH}_3\text{CO}(\text{OO})\cdot$ and $\text{CH}_3\text{COO}\cdot$ radicals were assumed to end up as acetic acid and diacetyl peroxide.

Our failure to find these in significant quantities in the reaction products at either 25 or 120° implies either that diacetyl peroxide or $\text{CH}_3\text{CO}(\text{OO})\cdot$ radicals or both are reacting to form some other compound not observed or that the quantum yield of acetyl radicals formed in the primary photochemical step is less than unity.

The photochemical reactions of acetone with oxygen have been discussed by Noyes,⁶ who concluded on the basis of quantum yields of products at 25° that the primary quantum yield in acetone in the presence of oxygen at this temperature was less than unity. He also indicated that oxygen might have a noticeable effect on the primary quantum yield at 120°. Our results may be taken as supporting evidence that this is the case at both temperatures.

It is interesting that Calvert and Hanst⁸ found with the acetaldehyde-oxygen system at 25° that

(11) J. H. Sharp, private communication.

the product yields varied inversely with oxygen pressure. This effect was tentatively put down to deactivation of excited acetaldehyde molecules by oxygen.

Acknowledgment.—We are grateful to the United States Public Health Service for financial support through Grant RG-7005. We also wish to acknowledge a contribution from the Air Pollution Foundation, San Marino, California, to defray part of the cost of the infrared spectrophotometer.

A PREPARATION OF HIGHLY CONCENTRATED NITROGEN-15 BY EXCHANGE OF NO AND N_2O_3 ¹

BY E. U. MONSE, T. I. TAYLOR AND W. SPINDEL

Chemistry Department, Columbia University, New York, N. Y.

Received May 8, 1961

Recent experiments in short exchange columns² indicated that the concentration of nitrogen-15 by the exchange reaction might have certain advantages over a previous method which used the exchange between NO and a solution of nitric acid.³

The rate of isotopic exchange of NO with N_2O_3 is significantly faster than that for the NO– HNO_3 system. This is evidenced by a threefold decrease in the height of column equivalent to a theoretical plate (H.E.T.P.) at a comparable flow, measured in moles of nitrogen per unit time. From this it was estimated that high enrichments of nitrogen-15 could be expected from considerably shorter columns using liquid nitrogen oxides even though the enrichment factor, α , of 1.031 for the NO– N_2O_3 exchange is appreciably smaller than 1.055 observed for the NO– HNO_3 exchange. The sizes of the columns and the method of operating them were predicted from the above data for a tapered cascade to produce ~ 99% nitrogen-15.²

Although data on the separation factor and the H.E.T.P. obtained in short columns normally provide a reasonable basis for estimating cascade characteristics, the actual operation of a cascade occasionally discloses unforeseen additional problems. Often the H.E.T.P. is considerably increased in long columns because of channeling of the liquid through the packing. In a system composed of low boiling liquids such as nitrogen oxides, where the chemical composition of the phases is markedly temperature dependent, the possibility remained that the temperature gradient in a long column might produce pressure and composition gradients which would adversely affect the over-all separation. Further, the calculated separation in a cascade may not be realized if small losses of enriched material occur at the product end of the system as a result of incomplete chemical reflux. For example, the maximum rate at which product

(1) This research was supported in part by a grant from the U.S. Atomic Energy Commission.

(2) E. U. Monse, W. Spindel and T. I. Taylor, *J. Chem. Phys.*, **32**, 1557 (1960).

(3) W. Spindel and T. I. Taylor, *ibid.*, **24**, 626 (1956); W. Spindel and T. I. Taylor, *Trans. N. Y. Acad. Sci.*, **19**, 3 (1956); T. I. Taylor and W. Spindel, "Proceedings International Symposium on Isotope Separation," North-Holland Publishing Co., Amsterdam, 1958, p. 158.

containing 99 atom % nitrogen-15 may be withdrawn from the NO-N₂O₃ system is about 0.01% of the interstage flow in the first exchange column. While a loss of this magnitude in the product reflux reaction will have a negligible effect in a short column, it could considerably decrease the over-all separation in a cascade. Therefore, in order to evaluate the feasibility of the NO-N₂O₃ system for producing highly concentrated nitrogen-15, it was necessary to construct and operate a cascade. The present paper describes our experiments with a cascade of two columns which successfully yielded 99.7% nitrogen-15.

Experimental Method

The total length of column required for 99% nitrogen-15 was calculated using the following experimental values²: $\alpha = 1.031$ at -9° and H.E.T.P. = 1.2 cm. for an interstage flow of 20 to 30 mg. atoms of nitrogen per cm.² per min. The diameters of the two columns were proportioned so as to minimize the time required to approach steady-state separation and thus reduce the consumption of chemicals. Since one of the aims of the experiment was to determine the minimum requirements for a laboratory unit to prepare useful amounts of a highly enriched nitrogen isotope, a minimum diameter of 0.6 cm. was chosen for the final enriching column.

The first column (I) was 250 cm. long, 2.5 cm. i.d., packed with stainless steel helices (Helipak No. 3013, Podbielniak, Inc., Chicago, Ill.), and the second column (II) was 300 cm. long by 0.6 cm. i.d., packed with smaller helices (Helipak No. 3012). Both columns were jacketed and maintained at a temperature of -10 to -12° by circulating a refrigerated coolant. The columns and all the remaining cooled portions of the system were covered with a layer of glass-fiber insulation, a layer of aluminum foil, and finally a layer of polyethylene film which served as a vapor barrier to prevent the formation of ice on the cooled portions of the glass apparatus. Gaseous NO₂ from a tank of liquid N₂O₄ (Allied Chemical and Dye Corp., Hopewell, Va.) was fed through a rotameter flowmeter to the upper end of the column (I) where it was liquefied in a condenser. There it reacted with an ascending stream of NO to form an equilibrium amount of N₂O₃. The liquid N₂O₃-N₂O₄ mixture passed down column (I) at an interstage flow of about 220 mg. atoms of nitrogen per min. It then entered a product refluxer (90 cm. long, 4.5 cm. i.d., packed with glass helices), where it was first vaporized and treated with dilute sulfuric acid to form HNO₃, which then reacted with an ascending stream of SO₂ to form NO and H₂SO₄, as described previously.²

Column (I) was operated for several days until the concentration of nitrogen-15 at the lower end was 13.9%. Then, a portion of the enriched oxides of nitrogen was transferred to a condenser at the top of column (II) using a pump with Teflon bellows. The pumping rate was adjusted to give an interstage flow of about 6.5 mg. atoms of nitrogen per minute in column (II), or approximately 3% of the interstage flow in column (I). At the lower end of column (II) a product refluxer, similar but smaller than the one used for column (I), reduced the nitrogen oxides to NO which then passed up through the column and back to the lower end of column (I).

Since the equilibrated gas phase at 1 atm. and -10° contains only about 20 mole per cent. +4 nitrogen as compared to about 60 mole per cent. +4 nitrogen in the liquid phase,⁴ it was necessary to pump material having the chemical composition of the liquid phase in column (I) to the upper end of column (II). This was accomplished by vaporizing the liquid completely at the bottom of column (I) in a flash evaporator, and feeding this vaporized liquid to the interstage pump. The complete cascade was operated continuously until the concentration of nitrogen-15 at the lower end of column (II) was at an approximate steady state, and then product was withdrawn.

Results and Discussion

At intervals of about 12 hours, samples of the

oxides of nitrogen were withdrawn from the lower end of each column. These were decomposed to N₂ and O₂ in an electrical discharge for analysis with a mass spectrometer. Throughout the run, the concentration of nitrogen-15 at the lower end of column (I) was relatively constant at about 10%. After column (II) was started, the concentration of nitrogen-15 reached 50% in 2.25 days, 90% in 5 days, and 99.7% in 12.5 days. Product was then withdrawn for one day at a rate of 0.3 g./day, and at a rate of 0.5 g./day for an additional 3.5 days. During this time, the concentration remained between 99.4 and 99.7% nitrogen-15. Product was then withdrawn rapidly until the concentration was 95% nitrogen-15.

The over-all separation

$$S = (N^{15}/N^{14})_{\text{product}} / (N^{15}/N^{14})_{\text{feed}}$$

where the notation (N¹⁵/N¹⁴) refers to the ratio of the mole fraction of nitrogen-15 to the mole fraction of nitrogen-14, was 2780 for column (II), and 90,700 for the entire cascade. From the relation, $S = \alpha^n$, the number of stages, n , calculated for column (II), was 260, corresponding to an H.E.T.P. of 1.15 cm. The system was not operated sufficiently long before product was withdrawn from column (I) to achieve its steady-state concentration, and the maximum separation for the whole system was probably not achieved.

The value of the H.E.T.P. for column (II) is in good agreement with previous determinations of H.E.T.P. in shorter columns of larger diameter. Thus, it is evident that, although the diameter of the column was rather small, "wall effects" or other disturbances such as channeling did not appreciably affect the H.E.T.P. The total pressure drop in the cascade was about 0.1 atm., and this had no major influence on the over-all separation. The reflux reaction for the product end of the column, though slightly different from the one used earlier on the NO-HNO₃ system,³ has proven to be equally satisfactory.

Finally, the present experiments demonstrate the feasibility of using NO-N₂O₃ exchange for preparing highly concentrated nitrogen-15 on a laboratory scale and verify previous estimates of the sizes of columns required. It is interesting to note that the need to refrigerate the column to a temperature of approximately -10° , which is a disadvantage of this system relative to the NO-HNO₃ system for producing large quantities of nitrogen-15, is not a significant factor for operation on a laboratory scale. A refrigerator rated at one horse power provided more than sufficient cooling capacity to maintain the entire system at the required low temperature during the summer months when the temperature in the laboratory ranged from 27-35°.

Acknowledgments.—Special thanks are due Mr. Martin Friedlander for his construction and maintenance of the mechanical and control devices for the columns. The authors wish to acknowledge with thanks the important assistance of Dr. Alfred Narten and Mr. Harry Taylor in the construction of the equipment; Mr. Peter Lieberman, Mr. Ephraim Fischbach, Mr. David Goldman and Mr.

(4) R. H. Purcell and G. H. Chocoman, *J. Chem. Soc.*, 826 (1932).

Burhan Hakioglu in the operation of the cascade; Mr. Vincent Saltamach for operation of the mass spectrometer; Mrs. Julia Barton for chemical analyses; and Mr. Karl Schumann for construction of the glass columns and the reflux systems.

COMPLEX IONS IN FUSED SALTS. CADMIUM AND LEAD BROMIDES¹

By F. R. DUKE AND H. M. GARFINKEL

Institute for Atomic Research and Department of Chemistry, Iowa State University, Ames, Iowa

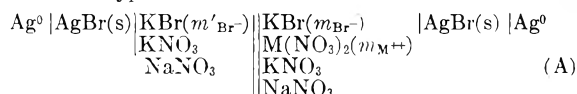
Received November 14, 1960

Van Artsdalen² has used freezing point depression measurements in molten NaNO_3 to determine the stability constants of lead chloride, cadmium chloride and cadmium bromide complexes. Christie and Osteryoung³ have made a polarographic determination of the formation constants for lead and cadmium chlorides in fused LiNO_3 - KNO_3 solvent. Moreover, the complex formation constants for lead chloride, lead bromide, cadmium chloride and cadmium bromide complexes in fused NaNO_3 - KNO_3 eutectic have been determined by measuring the increase in solubility of the slightly soluble metal chromate as halide was added.⁴ The same technique has been used to determine complex formation constants involving lead and cadmium ions with chloride ion in fused lithium perchlorate solvent.⁵ In addition the bromo-complexes of zinc have been studied by determining the effect of complex ion formation on the kinetics of the zinc bromide-bromate reaction in molten NaNO_3 - KNO_3 .⁶ In this study the bromo-complexes of lead and cadmium were studied by following the e.m.f. of a concentration cell as a function of the concentration of the metal ion employed. This was done at various initial bromide ion concentrations and several temperatures.

Experimental

ACS reagent grade chemicals were used. The cadmium and lead nitrates were dried under vacuum at 100° and stored in a vacuum desiccator.

The e.m.f. measurements were made on a concentration cell of the type



where m is the molality of the ions indicated by the subscript and M is either lead or cadmium. The cell used for the measurements has been described in a previous publication.⁷ The reference half-cell was a sealing tube with a fine Pyrex fritted disc, 10 mm. in diameter, partially fused to reduce diffusion. The silver-silver bromide electrodes were prepared by dipping equal lengths of #22 gauge silver wire (99.9% pure) into molten AgBr ; the electrodes were sealed into 3 mm. Pyrex tubing to position them.

(1) Contribution No. 968. Work was performed in the Ames Laboratory of the U. S. Atomic Energy Commission.

(2) E. R. Van Artsdalen, *J. Phys. Chem.*, **60**, 172 (1956).

(3) J. Christie and R. A. Osteryoung, *J. Am. Chem. Soc.*, **82**, 1841 (1960).

(4) F. R. Duke and M. L. Iverson, *J. Phys. Chem.*, **62**, 417 (1958).

(5) F. R. Duke and W. W. Lawrence, *ibid.*, **63**, 2087 (1959).

(6) F. R. Duke and W. W. Lawrence, *J. Am. Chem. Soc.*, **83**, 1271 (1961).

(7) F. R. Duke and H. M. Garfinkel, *J. Phys. Chem.*, **65**, 461 (1961).

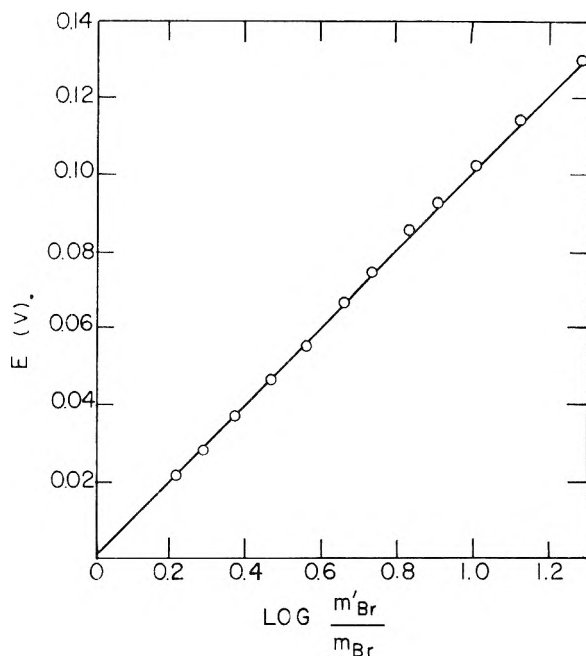


Fig. 1.—Test of the validity of the Nernst limiting law for cells of type (B) at 261° .

A fused alkali nitrate melt was used as constant temperature bath. Temperatures were measured with a calibrated Chromel-Alumel thermocouple with an ice-bath as cold junction; the temperature was maintained to at least $\pm 1^\circ$ during a series of measurements. All e.m.f. measurements were made with a Type K Leeds and Northrup potentiometer.

Results

The applicability of the Nernst equation to the silver-silver bromide electrode in the nitrate melt was investigated first. Consider the cell (B)



where the left-hand half-cell is the reference electrode. Previously dried KBr was added to the right-hand compartment and the potential against the reference electrode was measured. The results of these measurements at 261° are shown in Fig. 1, where the e.m.f. of the cell is plotted as a logarithmic function of the ratio of the bromide concentrations. The concentration of KBr in the reference half-cell was 9.32×10^{-2} molal. From Fig. 1 it is readily seen that the relationship is linear with a slope of 0.102. That calculated from the Nernst equation

$$E_n = \frac{2.30RT}{F} \log \frac{m'_{\text{Br}^-}}{m_{\text{Br}^-}} \quad (1)$$

was 0.106. This also was tried at 299° where the calculated slope was 0.113 and the experimental slope was 0.110 and at 325° where the calculated slope was 0.118 and the experimental slope was 0.117. This good agreement between the theoretical and experimental values indicates that the solution of potassium bromide in the nitrate melt, for the concentration range 2×10^{-3} to 9×10^{-2} molal, is ideal and justifies neglect of the liquid junction potential.

Now as lead or cadmium nitrate was added to the right-hand compartment of cell (A) deviations

from Nernst behavior were noted and these were ascribed to complex ion formation. The procedure used was to determine the formation constant for the species MBr^+ and then with this value, determine the succeeding constants. Consider the reaction



The total bromide ion concentration can be expressed as a sum

$$T_{Br^-} = Br^- + MBr^+ \quad (3)$$

If $T_{M^{++}} \gg T_{Br^-}$, then

$$K_1 = \frac{[MBr^+]}{[Br^-] \cdot T_{M^{++}}} \quad (4)$$

where $T_{M^{++}}$ is total heavy metal ion concentration. If ΔE is defined as

$$\Delta E = E_{obs.} - E_n \quad (5)$$

where E_n is the calculated potential in the absence of M^{++} then

$$\frac{\Delta EF}{10^{2.30RT}} = \beta = 1 + K_1 T_{M^{++}} \quad (6)$$

A plot of β vs. $T_{M^{++}}$ should give a straight line with intercept of unity and slope of K_1 . Some typical data are given in Table I for the lead and cadmium systems. The correction due to dilution, although small, was applied and the value of K_1 for the monobromo-cadmium complex was corrected since K_1 was so large. This correction amounted to about 5%.

TABLE I

VARIATION OF THE E.M.F. OF CELL (A) IN THE DETERMINATION OF K_1 FOR THE LEAD AND CADMIUM SYSTEMS

A. Lead					
$t = 255^\circ$			$t = 303^\circ$		
$T_{Pb^{++}} \times 10^2$	$E(v.)$	β	$T_{Pb^{++}} \times 10^2$	$E(v.)$	β
0.372	0.0028	1.06	0.139	0.0009	1.02
0.643	.0048	1.11	0.538	.0033	1.07
1.27	.0093	1.22	1.27	.0078	1.17
2.00	.0141	1.35	1.92	.0119	1.27
2.64	.0179	1.47	2.74	.0165	1.38
3.46	.0223	1.61	3.65	.0211	1.51
4.22	.0262	1.75	4.51	.0251	1.64
5.04	.0301	1.91	5.52	.0295	1.79
5.86	.0339	2.07	6.64	.0337	1.95
6.86	.0381	2.26	7.54	.0371	2.07
7.79	.0417	2.44			

B. Cadmium					
$t = 256^\circ$			$t = 298^\circ$		
$T_{Cd^{++}} \times 10^2$	$E(v.)$	β	$T_{Cd^{++}} \times 10^2$	$E(v.)$	β
0.177	0.0071	1.17	0.308	0.0102	1.23
.519	.0191	1.52	0.808	.0227	1.58
.795	.0270	1.80	1.14	.0297	1.83
1.07	.0338	2.09	1.64	.0380	2.16
1.55	.0435	2.58	2.04	.0438	2.43
2.02	.0509	3.04	2.41	.0484	2.66
2.41	.0564	3.42			
2.86	.0621	3.87			
3.40	.0682	4.42			
3.95	.0734	4.94			
4.34	.0768	5.32			
4.93	.0814	5.87			

In order to determine the higher constants,

the metal and bromide ion concentrations were of the same order. Then one may write

$$T_{Br^-} = Br^- + \sum_{n=1}^r n MX_n^{2-n} \quad (7)$$

and

$$T_{M^{++}} = M^{++} + \sum_{n=1}^r MX_n^{2-n} \quad (8)$$

It is now advantageous to define

$$K_n = \frac{[MX_n^{2-n}]}{[MX_{n-1}^{3-n}][Br^-]} \quad (9)$$

Using eq. 7, 8 and 9 and making some simple algebraic substitutions one derives the equation

$$A + BK_1 + CK_1K_2 + DK_1K_2K_3 + \dots = 0 \quad (10)$$

where

$$A = \frac{T_{Br^-} - (Br^-)}{T_{M^{++}}} \quad C = (A - 2)(Br^-)^2$$

$$B = (A - 1)(Br^-) \quad D = (A - 3)(Br^-)^3$$

The constants K_1 and K_2 were determined for the lead system. In the cadmium system K_3 was also included in solving simultaneously for the constants. Some typical data are given in Table II and the results at various temperatures are listed in Table III.

TABLE II

DATA FOR THE DETERMINATION OF THE HIGHER COMPLEXING CONSTANTS OF LEAD AND CADMIUM

$t = 306^\circ$		$t = 274^\circ$	
$T_{Pb^{++}} \times 10^2$	$E(v.)$	$T_{Cd^{++}} \times 10^2$	$E(v.)$
0.581	0.0032	0.126	0.0033
0.986	.0053	.328	.0087
1.51	.0081	.584	.0152
2.12	.0113	.837	.0213
2.64	.0140	1.20	.0295
3.27	.0170	1.61	.0377
4.04	.0210	2.05	.0454
4.62	.0227	2.54	.0532
5.29	.0256	3.04	.0599
6.12	.0291	3.71	.0679
7.58	.0356	4.40	.0751
8.61	.0397	5.23	.0823
9.46	.0427	5.90	.0875

TABLE III

FORMATION CONSTANTS, K_n , IN $NaNO_3$ - KNO_3 EUTECTIC SOLVENT

Complex	K_n, molal^{-1}	$t, ^\circ C.$	K_n^a	$t, ^\circ C.$
PbBr	18.4 ± 0.5	255	18 ± 3	250
	$14.2 \pm .4$	303	13 ± 3	275
	$11.3 \pm .3$	319	11 ± 2	300
PbBr ₂	$6.2 \pm .6$	306	2 ± 1	300
	108 ± 4	256	20 ± 4	250
CdBr	95.0 ± 6.0	274
	75.0 ± 3.7	298	24 ± 3	300
	51.2 ± 4.0	256	5 ± 3	250
CdBr ₂	47.6 ± 9.0	274	5 ± 3	300
	10.5 ± 3.0	256
CdBr ₃ ⁻	2.6 ± 1.0	274

^a Values determined by Duke and Iverson.⁴

Discussion

These results show that the mono- and tri-bromo species in the cadmium system are thermo-

dynamically important as proposed by Duke and Iverson⁴ although the values for the complex formation constants are somewhat higher and exhibit a definite temperature dependence. In this respect these values agree rather well with the results of Christie and Osteryoung,³ although in a different solvent, as to order of magnitude.

It has been shown that deviations from ideal behavior in reciprocal molten salt solutions can be ascribed to complex ion formation. Moreover it seems that when applied to the experimental data the "chemical" and lattice-model⁸ approaches are hardly distinguishable and any choice between the two must be a matter of personal preference.

(8) M. Blander, *J. Phys. Chem.*, **63**, 1262 (1959).

COMPLEX IONS IN FUSED SALTS. EFFECT OF SOLVENT CATION¹

By H. M. GARFINKEL AND F. R. DUKE

Institute for Atomic Research and Department of Chemistry, Iowa State University, Ames, Iowa

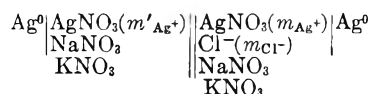
Received November 21, 1960

Lantratov and Alabyshev² in determining the activities of MCl_2 in solutions containing chlorides of alkali metals found that the negative deviations from ideality decreased as the size of the solvent cation decreased. Blander and Braunstein³ noted this same trend on comparing the results of the quasi-lattice theory for ion pair formation in molten sodium nitrate and potassium nitrate. Gruen and McBeth⁴ found that Ni(II) behaved more ideally in molten LiCl than in molten CsCl; Dahl and Duke⁵ observed the same trend with Pb(II). In the present study the formation constants for Ag^+Cl^- and $AgCl_2^-$ were determined as a function of the solvent cation concentration by following the change in e.m.f. on the addition of Cl^- , for different mole fractions of $KNO_3(N_{K^+})$, mixed with $NaNO_3$.

Experimental

ACS reagent grade chemicals were used in all the determinations. Before use the salts were dried in the oven at 110° and then stored in a vacuum desiccator.

The e.m.f. measurements were made on a cell of the type



where m is the molality of the ion indicated by the subscript. The composition of the solvent was varied for each series of measurements, and complexing constants were determined at various mole fractions of $KNO_3(N_{K^+})$. The cell used for the measurements has been described in a previous publication.⁶ The electrodes were silver electrodes spot-welded to long lengths of platinum wire and sealed into 3 mm. Pyrex tubing to position the electrodes. A fused alkali nitrate melt was used as constant tempera-

ture bath and the temperature, which was measured with a calibrated Chromel-Alumel thermocouple, was maintained to $\pm 1^\circ$.

Results

The applicability of the silver-silver nitrate electrode to solutions of silver nitrate in molten potassium nitrate,⁷ sodium nitrate,⁸ and mixtures of the two^{6,9} has been demonstrated previously. On the addition of chloride to cell (A) any deviations from ideality were ascribed to complex ion formation. The concentrations of $AgNO_3$ and MCl were such that no silver chloride precipitated. It has been shown⁶ that the complex formation constants can be determined using the equation

$$10^{-\Delta E F / 2.30RT} = 1 + K_1 T_{Cl^-} + K_1 K_2 T_{Cl^-}^2 \quad (1)$$

where $-\Delta E$ is the difference between the Nernst value and the observed value of the e.m.f. after the addition of chloride; T_{Cl^-} is the total chloride concentration (the experiment is run such that $T_{Cl^-} \gg T_{Ag^+}$); and K_1 and K_2 are given by

$$K_1 = \frac{[Ag^+Cl^-]}{[Ag^+][Cl^-]}, \quad K_2 = \frac{[AgCl_2^-]}{[Ag^+Cl^-][Cl^-]} \quad (2)$$

Equation 1 can be rewritten in more suitable form, *viz.*

$$(10^{-\Delta E F / 2.30RT} - 1) / T_{Cl^-} = \theta = K_1 + K_1 K_2 T_{Cl^-} \quad (3)$$

For each solvent composition a plot of θ vs. T_{Cl^-} should give a straight line with an intercept of K_1 and slope of $K_1 K_2$. Some typical data

TABLE I

TYPICAL DATA FOR THE DETERMINATION OF THE FORMATION CONSTANTS FOR Ag^+Cl^- AND $AgCl_2^-$ AS A FUNCTION OF N_{K^+} AT 374°

$N_{K^+} = 0.17$			$N_{K^+} = 0.36$		
$T_{Cl^-} \times 10^2$	$-E(v.)$	θ	$T_{Cl^-} \times 10^2$	$-E(v.)$	θ
0.476	0.0052	20.6	0.487	0.0064	25.1
1.02	.0113	22.2	1.12	.0145	26.6
1.62	.0176	23.0	1.69	.0215	27.9
2.13	.0227	23.7	2.15	.0269	29.0
2.70	.028±	24.7	2.64	.0323	29.8
3.27	.0340	25.8	3.20	.0386	31.3
3.91	.0397	26.7	3.82	.0449	32.5
4.52	.0450	27.6	4.38	.0504	33.7
5.04	.049±	28.4	4.92	.0555	34.8
5.50	.0532	29.2	5.44	.0603	36.0
$N_{K^+} = 0.77$			$N_{K^+} = 1.00$		
$T_{Cl^-} \times 10^2$	$-E(v.)$	θ	$T_{Cl^-} \times 10^2$	$-E(v.)$	θ
0.525	0.0105	39.6	0.488	0.0120	49.4
0.824	.0159	40.2	1.02	.0240	52.9
1.27	.0239	42.3	1.57	.0359	57.8
1.66	.0305	44.0	2.08	.0459	61.7
2.03	.036±	45.6	2.59	.0554	66.0
2.44	.042±	46.9	3.11	.0642	69.9
3.02	.0508	49.5	3.69	.0734	74.4
3.54	.0580	51.9	4.29	.0824	79.3
3.96	.0638	54.3	4.93	.0911	84.3
4.48	.0705	57.0	5.44	.0981	89.0

(1) Contribution No. 969. Work was performed in the Ames Laboratory of the U. S. Atomic Energy Commission.

(2) M. F. Lantratov and A. F. Alabyshev, *Zhur. Priklad. Khim.*, **26**, 235, 321 (1953); **27**, 685 (1954).

(3) M. Blander and J. Braunstein, *Ann. N. Y. Acad. Sci.*, **79**, 838 (1961).

(4) D. M. Gruen and R. L. McBeth, *J. Phys. Chem.*, **63**, 393 (1959).

(5) J. L. Dahl and F. R. Duke, *ibid.*, **62**, 1498 (1953).

(6) F. R. Duke and H. M. Garfinkel, *J. Phys. Chem.*, **65**, 461 (1961).

(7) M. Blander, F. F. Blankenship and R. F. Newton, *ibid.*, **63**, 1259 (1959).

(8) D. G. Hill, J. Braunstein and M. Blander, *ibid.*, **64**, 1038 (1960).

(9) S. N. Flengas and E. Rideal, *Proc. Roy. Soc. (London)*, **233A**, 443 (1956).

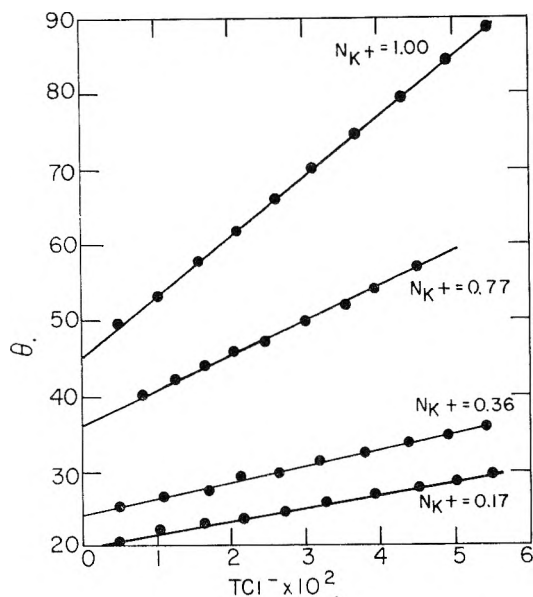


Fig. 1.—Plot to show linearity of equation 3 at 374°.

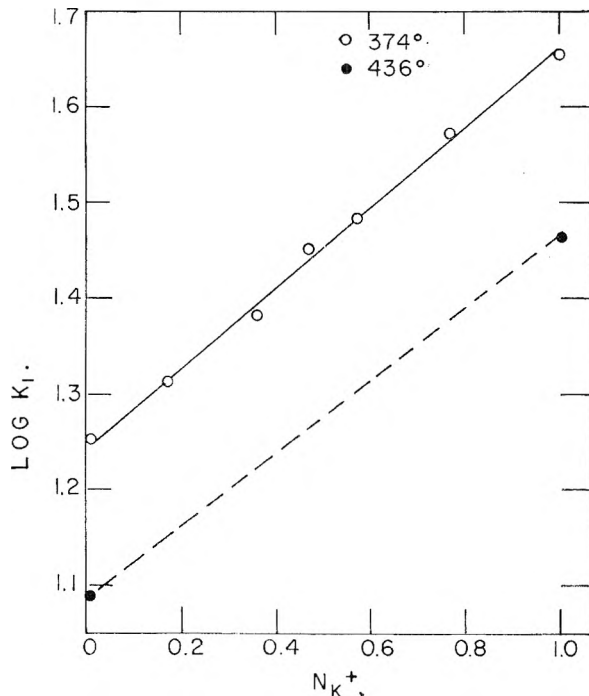


Fig. 2.—Logarithmic dependence of K_1 in the silver-chloride system on the concentration of the solvent cation.

are shown in Table I, and Fig. 1 shows the linearity of the above plots. Table II shows the variation of K_1 and K_2 as a function of N_{K^+} and these data are used to show the logarithmic dependence of K_1 on N_{K^+} in Fig. 2.

Discussion

The variation in the equilibrium constants for the formation of Ag^+Cl^- and AgCl_2^- as a function of cation type and concentration may very likely be ascribed to coulombic effects. Forland¹⁰

(10) T. Forland, "On the Properties of Some Mixtures of Fused Salts," ONR, Technical Report No. 69, Penna. State U., University Park, Penna., June, 1956.

TABLE II

VARIATION OF K_1 AND K_2 WITH N_{K^+} AT 374°		
N_{K^+}	K_1	K_2
0.00	17.7	6.78
.17	20.3	7.98
.36	24.2	8.97
.47	28.0	8.93
.57	30.3	8.91
.77	36.9	11.6
1.00	44.9	18.0

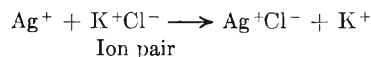
has used a simple one-dimensional model based upon the coulombic stability of ion pairs, and the manner in which this affects the availability of either ion in the pair in its possible reactions. For example in a dilute solution of Ag^+ and Cl^- in a mixture of NaNO_3 and KNO_3 , the tendency will be for the chloride ions to be adjacent to and under the coulombic influence of the sodium and potassium ions. When the silver ion closely approaches the chloride ion of such an ion pair the potential energy, U , is given by the equation

$$U = -\frac{Ne^2}{D} \left[\left(\frac{1}{r_0 - \Delta r} \right) - \left(\frac{1}{r_0 + \Delta r} \right) \right] \quad (4)$$

where r_0 is the distance between the approaching Ag^+ and the center of the dipole of the ion pair; Δr is one-half the distance between the centers of the ions in the ion pair; N is Avogadro's number; e , the electronic charge; and D the dielectric constant of the medium. It is then assumed that

$$\Delta F_a^0 - \Delta F_b^0 = U_a - U_b \quad (5)$$

where ΔF_a^0 is the standard free energy change accompanying the reaction



in KNO_3 solvent, and ΔF_b^0 is the corresponding change in which Ag^+ reacts with Na^+Cl^- in pure NaNO_3 ; U_a and U_b are the potential energies calculated according to eq. 4 in pure KNO_3 and pure NaNO_3 respectively. Since

$$\Delta F^0 = RT \ln K \quad (6)$$

one finds that

$$\ln \frac{K_{1a}}{K_{1b}} = \frac{2e^2}{kT} \left[\frac{1}{D_a} \left(\frac{\Delta r_a}{r_{0a}^2 - (\Delta r_a)^2} \right) - \frac{1}{D_b} \left(\frac{\Delta r_b}{r_{0b}^2 - (\Delta r_b)^2} \right) \right] \quad (7)$$

where k is the Boltzmann constant. Unfortunately the dielectric constants of these molten nitrates have not been measured. However D may be estimated by means of the equation first derived by Born¹¹ for aqueous solutions. Flengas and

$$-\Delta F_{\text{solv.}} = \frac{N(Ze)^2}{2r_i} \left(1 - \frac{1}{D} \right) \quad (8)$$

Rideal⁷ have shown that eq. 8 should be more applicable to a melt than an aqueous solution since the radii of the ions, r_i , are more accurately known for the melt than the aqueous solution. By means of the equation

$$-U_{\text{AgCl}} = (\Delta F_{\text{sol.}})_{\text{AgCl}} - (\Delta F_{\text{solv.}})_{\text{AgCl}} \quad (9)$$

$\Delta F_{\text{solv.}}$ can be determined, and using the crystal radii of Ag^+ and Cl^- one can show that $D_a \cong$

(11) M. Born, *Z. Physik*, 1, 4 (1920).

$D_b \cong 6$. It was found by means of eq. 7 that K_{1a}/K_{1b} was approximately 1.6 and the ratio determined experimentally was 2.5. A more elegant treatment than the above is not warranted at this time, particularly because of the unknown values of the dielectric constants of the salts. However, this simplified treatment gives strong indication that nothing other than coulombic effects need be considered in explaining the noted differences between the two pure alkali nitrates as solvents.

AN APPROACH TO GAS MEMBRANE OSMOMETRY

BY KAROL J. MYSELS AND EMANUEL GONICK

Departments of Chemistry, University of Southern California, Los Angeles 7, California, and Phoenix College, Phoenix, Arizona

Received December 22, 1960

It is well recognized that osmometry, that is, the direct determination of the hydrostatic pressure difference required to equalize the activity of a solvent in a solution and in the pure state, is in principle the most sensitive method of measuring colligative properties. There are, however, many factors which render osmotic measurements either difficult or impossible in many cases. The most important, perhaps, is the difficulty of finding membranes which are truly semipermeable. The availability of membranes which are impervious to large particles accounts for the popularity of the osmotic method in the field of macromolecules. For small molecules, however, the best membrane seems to be the old and cumbersome copper ferrocyanide supported by a porous ceramic. This has been used extensively in the study of sugar solutions, but is not semipermeable for smaller particles, especially the common electrolytes.

A membrane which is theoretically the simplest and is sometimes discussed in elementary texts is formed by an inert gas held in non-wetted capillaries between the solvent and the solution. This gas-phase gap is permeable to water vapor but is completely impervious to any non-volatile solute. The present paper reports experiments showing that such membranes can be prepared easily and that they can be used in osmotic measurements. Auxiliary aspects of osmometry required for high precision have not yet been perfected, however. Some theoretical aspects of the method also are discussed briefly.

The membranes are prepared simply by siliconizing a commercially available membrane filter of high porosity and pores of 1μ or less. It should be noted that a circular pore 1μ in radius can prevent the passage of water under a pressure of one atmosphere provided the advancing contact angle be 110° or more.

Our method should be compared with the so-called porous disc method¹ in which the solvent is supported by *wetted* capillaries of a porous disc and subjected to a negative pressure, the solution being generally placed in an annulus around the porous disc and separated therefrom by a glass partition. The vapors of the two communicate in an evacuated chamber. Thus, the physical

distance between the two surfaces is relatively large; while there is little resistance to the transport of vapor from one surface to the other, the transport of heat between the two surfaces is quite slow. In our method, on the other hand, the two surfaces are separated only by the thickness of the *non-wetted* membrane which is 0.15 mm. and could in principle be further reduced substantially. Thus thermal contact between the two surfaces is relatively good. On the other hand, the gas filling the pores of the membrane reduces the rate at which molecules of water can pass from one surface to the other.

The practical criterion of the sensitivity of an osmometric method is the rate at which solvent is transported when the pressure differential departs slightly from the equilibrium one. In both methods the driving force for the transport is the difference in vapor pressure between the two surfaces. This in turn is determined not only by the imbalance between the equilibrium osmotic pressure and the pressure actually exerted but also by the temperature difference between the two surfaces. This difference in temperature is intrinsic and not due to imperfect thermostating. It stems from the fact that whenever water distills from one surface onto another, the first one cools and the second warms up. Thus, under steady state conditions a flow of water must be accompanied by a flow of heat in the opposite direction. The driving force for the flow of heat is of course the temperature difference between the two surfaces. Resistances either to the mass flow of water vapor or to the flow of heat between the two surfaces slow down the whole process. The calculation given below shows the effect of both types of resistances should be of the same order in our method. The experimentally found rate of transport is, however, considerably higher than the calculated one.

Theoretical

Let us consider a steady state of an isolated system in which a flux J_w ($\text{g. cm.}^{-2} \text{sec.}^{-1}$) of water occurs from the solvent to the solution. This must be accompanied by a flux J_q ($\text{erg cm.}^{-2} \text{sec.}^{-1}$) of heat in the opposite direction. The two are related by the heat of vaporization λ (erg g.^{-1})

$$J_q = -\lambda J_w \quad (1)$$

The flux of water is proportional to the difference of vapor density $\Delta\rho$ (g. cm.^{-3}) at the two surfaces since this difference is small.

$$J_w = -K_w \Delta\rho \quad (2)$$

Similarly the flux of heat is proportional to the temperature difference between the two surfaces. Equations 2 and 3

$$J_q = -K_q \Delta T \quad (3)$$

neglect the contribution of thermal diffusion of water vapor in the mixture of water vapor and inert gas (air) in the pores and the reciprocal phenomenon of diffusional thermoeffect. This may be justified by a cursory calculation which shows that, for a given temperature difference, the partial pressure difference generated by thermal diffusion is much less than 1% of the corresponding vapor

(1) A. T. Williamson, *Proc. Roy. Soc. (London)*, **A195**, 97 (1948).

pressure difference and that it must be similarly negligible for other vapor-gas combinations.

If we assume that equilibrium between liquid and vapor at its surface is established rapidly, the density difference of vapor at the two surfaces is due to the difference $P - \pi$ between the applied pressure and the (equilibrium) osmotic pressure, and to the temperature difference ΔT . The equality of the Gibbs free energies of liquid and its ideal vapor gives

$$\bar{V}_l dP - S_l dT = RT dp/p - S_v dT \quad (4)$$

and since $S_v - S_l = \lambda/T$ and $dp/p = d\rho/\rho$

$$\bar{V}_l dP + (\lambda/T)dT = RT d\rho/\rho \quad (5)$$

For the very small changes in T and ρ involved, this can be integrated to

$$\bar{V}_l(P - \pi) + (\lambda/T)\Delta T = RT\Delta\rho/\rho \quad (6)$$

Combining these equations we obtain

$$J_w \left[\frac{1}{K_w} + \frac{\rho\lambda^2}{RT^2} \frac{1}{K_q} \right] = - \frac{\rho \bar{V}_l(P - \pi)}{RT} \quad (7)$$

which shows that the flux of water is impeded by both the material resistance $1/K_w$ and the thermal resistance $1/K_q$ while the right-hand term represents the driving force.

The two resistance terms depend on the nature of the membrane, and ours consists of a cellulose ester with 80% open space. If we neglect other heat paths compared to the thermal conductivity of the membrane, we can estimate K_q to be at most that of a parallel arrangement of 80% air: $K = 2.4 \times 10^3$ erg cm.⁻¹ deg.⁻¹ sec.⁻¹; and 20% having the conductivity of most plastics: $K = 6.5 \times 10^5$. Since the membrane is 1.5×10^{-2} cm. thick, $K_q = 1.5 \times 10^{-2} [0.8 \times 2.4 \times 10^3 + 0.2 \times 6.5 \times 10^5] = 2.2 \times 10^2$ erg deg.⁻¹ sec.⁻¹.

If we assume that the vapor is transported only by diffusion in the pores and neglect any tortuosity of these pores, then $K_w = 0.8D/1.5 \times 10^{-2}$. The diffusion coefficient of water in air, D , is about 0.27 cm.² sec.⁻¹ so that $K_w = 14$ cm. sec.⁻¹.

Introducing the constants $\lambda = 2.5 \times 10^{10}$ erg g.⁻¹, $\rho = 2.5 \times 10^{-5}$ g. cm.⁻³, $R = 4.6 \times 10^6$ erg g.⁻¹ deg.⁻¹, and $T = 300^\circ\text{K}$., the first term in the brackets of eq. 7 becomes 7×10^{-2} and the second 4×10^{-2} sec. cm.⁻¹. Thus the two resistance terms are of similar magnitude and neither can be neglected.

If the pressures are expressed in millibars (\approx cm. H₂O), the flux of water becomes (according to eq. 7)

$$J_w = 5.5 \times 10^{-4} (P - \pi) \text{ g./hr.}$$

This can be translated into the rate of motion of a meniscus in a capillary of 0.3 mm. i.d. for a membrane of 3.4 cm. in diameter (which corresponds to our apparatus) and yields 0.078 mm./hr. per millibar difference between the applied and the osmotic pressure.

In the porous disc osmometer the vapor diffuses *in vacuo* so that $1/K_w$ is negligible and as pointed out by Williamson,¹ it is the thermal resistance which determines the rate of distillation. Since the thermal conductivity of water (6.3×10^4 erg cm.⁻¹ deg.⁻¹ sec.⁻¹) is only a few times that assumed for our membrane, but the average distance

between the two surfaces is of the order of centimeters, it is apparent that the flux should in principle be higher in our method. On the other hand, it should be possible to greatly reduce this distance by judicious physical arrangement and thus obtain comparable rates of transport by the porous disc method.

Experimental

Preparation of the Membranes.—The membranes were prepared from a commercial, hydrophilic membrane filter "Millipore"² which is a cellulose ester material having an 80% porosity and pores of very uniform size. Its surface is very smooth and its thickness is 0.15 mm. Type "HA" whose pores average 0.45μ was generally used, but other types gave substantially the same results. It was rendered hydrophobic by contact with the vapor of a commercial mixture of methylchlorosilanes "Dry Film SC-77."³ Good contact was obtained either by depositing the membrane filter in a desiccator containing some Dry Film for a period of 3–4 minutes, or by drawing air charged with vapor of the Dry Film through the membrane placed on a sintered glass support for a few seconds. The membranes were then placed under water or in a desiccator over dilute NaOH to remove traces of HCl.

A preliminary test for the presence of leaks was made using a filtering assembly designed for the membrane filters which is essentially a sintered glass filter with a removable but tightly fitting top. The membrane was placed on top of a filter paper impregnated with ferric chloride and secured by the removable top. A solution of potassium thiocyanate then was placed on top of the membrane and full suction of an aspirator applied for half a minute. Red spots on the filter paper indicated leaks. Leaky membranes also gave, of course, zero or very low osmotic pressure readings in the osmometer.

Membranes generally were treated in groups of 3 to 6 and the proportion of leaky ones varied rather unpredictably from 20–80%. A large fraction of failure generally was associated with an old and frequently used sample of Dry Film. Prolonged treatment tended to make the membranes excessively brittle.

Membranes which were leak-free in the preliminary test almost always proved satisfactory in the osmometer. In a few instances membranes which were originally leak-free would develop leaks in the osmometer after a few days. Most of them, however, remained leak-free until accidentally damaged or removed from the osmometer after periods ranging from a couple of days to two or three weeks. Because of the design of the osmometer, it was not practical to reuse the same membrane once it had been removed from the osmometer.

The Osmometer.—We used a slight modification of the apparatus described by Scatchard, Gee and Weeks.⁴ The principal modifications were replacement of the Lucite collar by one made of Teflon, replacement of the Lucite plate by a glass plate bearing a short integral glass capillary which terminated in a ball joint connecting to the remainder of the system, and the use of a horizontal capillary for observing the movement of the meniscus. Dodecane was used as the indicating liquid because of its very low solubility in water and still reasonable fluidity.

Results and Difficulties.—Our experiments were conducted mainly with $3 \times 10^{-4} M$ KCl on the solution side. The equilibrium osmotic pressure was therefore 14.8 millibars. In practice it was very difficult to obtain steady values, and when these were observed, they differed from the predicted one by anywhere from insignificantly to 30%. This may be ascribed in part to trivial problems which are nevertheless difficult to recognize and control, such as those of maintaining a small but constant pressure over long periods of

(2) Millipore Filter Corp., Bedford, Mass.

(3) General Electric Co., Silicone Products Dept., Waterford, New York.

(4) G. Scatchard, A. Gee and J. Weeks, *J. Phys. Chem.*, **58**, 783 (1954).

times, of leaks at the joints and stopcocks of an order of magnitude less than the rate of transport, of consistent avoidance of contaminations of the order of 10^{-5} molar in small volumes of solution where even the usual CO_2 content of distilled water is fatal, or of adiabatic heating and cooling during pressure change. Other difficulties could be traced to two more basic problems: One is the flexibility and hysteresis of the membrane and its somewhat flexible support by the filter paper. Hence any change of pressure produces a bulk flow as the membrane stretches or contracts and this is followed by further slow motion until a mechanical equilibrium is reached. The other major difficulty lies in temperature control. It should be remembered that a 10^{-4}° temperature difference between the two surfaces corresponds to an error of 8.2 mbar in the osmotic pressure, *i.e.*, over 50% of our equilibrium value as indicated by eq. 6. It was hoped that the close proximity and good thermal contact between the two surfaces would prevent minor temperature fluctuations or drifts from influencing our results. We used finally either an air-bath, whose short range fluctuations were not visible on a tapped Beckmann thermometer, and long-time drift amounted to a few thousandths degree or a water-bath whose variations could not be observed on a tapped Beckmann thermometer. While these gave better results than less elaborate thermostating, they still seemed insufficient.

The Rate of Transport.—When steady values were obtained, it was often possible to compute the rate of transport as a function of the difference between the applied pressure and the equilibrium pressure. This was reasonably reproducible and of the order of $0.8 \text{ mm. hr.}^{-1} \text{ mbar}^{-1}$, *i.e.*, about ten times higher than the rate of transport computed above. This difference cannot be accounted for by a heat conductivity greater than assumed. Even if thermal resistance were zero, the rate determined by diffusion alone becomes only $0.12 \text{ mm. hr.}^{-1} \text{ mbar.}^{-1}$. It cannot be due to a reduction of the apparent thickness of the membrane due to the curvature of the menisci since this can amount only to one diameter, which is only $1/300$ of the thickness. It would also be unlikely that the liquid should penetrate the membrane for even 50% of its thickness over most of its area without causing a leak at some point. Finally, the high rate cannot be due to a leak because a leak causing a tenfold acceleration also would reduce the measured osmotic pressure to one-tenth of the calculated one and this was emphatically not the case in our experiments. Hence an additional vapor phase transport mechanism, such as convection, which appears unlikely, or perhaps surface diffusion, seems to be operating in our membranes.

Acknowledgment.—This work was made possible for E. G. by collaboration in two National Science Foundation Summer Research Participation Programs at the University of Southern California and by a grant from Research Corporation to Phoenix College. It is also a pleasure to acknowledge the help of early exploratory experiments by Mr. B. D. Sharma.

ABSORPTION SPECTRA OF OXYGEN AND NITRIC OXIDE IN SOLUTION

BY JOSHUA JORTNER AND URIEL SOKOLOV

Department of Physical Chemistry, The Hebrew University, Jerusalem, Israel

Received February 9, 1961

It has become evident recently that some oxygen containing liquids in the ultraviolet region are not inert spectroscopic solvents as was formerly believed. Spectrophotometric investigations of oxygen solutions in aromatic¹ and aliphatic hydrocarbons^{1,2} as well as in water³ recently were reported. Oxygen dissolved in aromatic solvents leads to the enhancement of singlet-triplet transitions⁴⁻⁷ superimposed on a continuous absorption, which was assigned to a charge transfer transition.¹

After the present work was completed the intensive study of the interaction of oxygen with organic solvents was published.⁸

Our results are in complete agreement with the conclusions of Tsubomura and Mulliken.

Experimental

Materials and Gases.—Benzene, methanol and ethanol of Analar grade and acetonitrile of Eastman "spectro" grade were used. The alcohols were purified by refluxing with diphenylhydrazine and magnesium metal and finally distilled from calcium oxide. The water was triply distilled. Nitric oxide gas was purified of all traces of nitrogen dioxide by bubbling through sodium hydroxide solution and dried by passing over calcium oxide. Nitrogen was freed from traces of oxygen by passing through a copper-asbestos column at 400° . Oxygen, nitrogen and hydrogen were freed from soluble impurities by bubbling the gases through a trap containing the solvent.

Spectrophotometric measurements were carried out using a Beckman DU Spectrophotometer equipped with an IP 21 photomultiplier, and with a Hilger Uvispek Spectrophotometer. One and 10 cm. absorption cells were used. The absorption cells were equipped with attachments for gas bubbling and for evacuation on a vacuum line. Optical densities were measured against air as a reference.

Procedure.—Solutions were prepared by saturating the liquids for two hours with the appropriate gas at 25° . The absorption spectra of these solutions were measured in the following order: (a) air saturated; (b) nitrogen saturated; (c) oxygen saturated; (d) nitrogen or hydrogen saturated. Nitric oxide solutions were prepared by evacuation of the solvent on a vacuum line through a liquid air trap, followed by saturation of the solution with the gas. During the evacuation and the saturation process the solution was stirred continuously with a magnetic stirrer. Oxygen solutions containing varying gas concentrations were prepared by the same method.

Results and Discussion

Absorption Spectra of Oxygen Solutions.—Oxygen solutions in methanol and ethanol in the ultraviolet region gave rise to a continuous absorption. Similar results were obtained for benzene and water in agreement with previous work.¹⁻⁴ A weak absorption of oxygen in acetonitrile could be detected only in a 10 cm. cell. The optical absorp-

- (1) D. F. Evans, *J. Chem. Soc.*, 345 (1953).
- (2) A. U. Munck and J. F. Scott, *Nature*, **177**, 587 (1956).
- (3) (a) L. J. Heidt and L. E. Ekstrom, *J. Am. Chem. Soc.*, **79**, 1260 (1957); (b) L. J. Heidt and A. M. Johnson, *ibid.*, **79**, 5587 (1957).
- (4) D. F. Evans, *J. Chem. Soc.*, 1351 (1957).
- (5) D. F. Evans, *ibid.*, 3885 (1957).
- (6) G. J. Hoijtink, *Mol. Phys.*, **3**, 67 (1960).
- (7) J. N. Murrell, *ibid.*, **3**, 319 (1960).
- (8) H. Tsubomura and R. S. Mulliken, *J. Am. Chem. Soc.*, **82**, 5966 (1960).

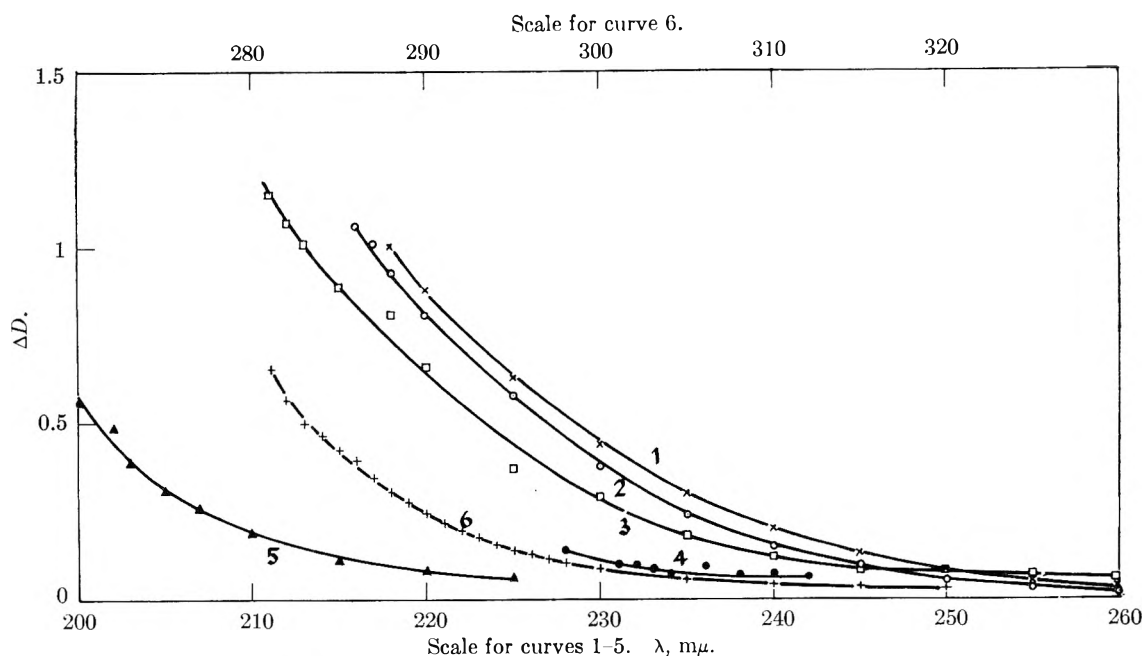


Fig. 1.—Absorption spectra of oxygen and nitric oxide solutions at 25°.

		<i>P</i> , mm.	10°C, <i>M</i>	$\lambda(\epsilon = 10)$, m μ	Optical cell length, cm.
1	O ₂ in methanol	540	7.2	248	1
2	O ₂ in ethanol	630	8.1	251	1
3	NO in methanol	214	3.3		1
4	O ₂ in acetonitrile	600		<228	10
5	O ₂ in water	670	1.12	215	10
6	O ₂ in benzene	630	7.7	301	1

tion disappeared on removing the dissolved oxygen by saturation with nitrogen or hydrogen or by evacuation.

The contribution of the dissolved oxygen to the optical absorption was obtained from: $\Delta D = D - D_0$, where D_0 is the optical density of the oxygen-free solution. The apparent molar absorption coefficient of oxygen at 25° was obtained from $\epsilon = \Delta D/C$, where C is the concentration of oxygen calculated from the solubility data.⁹ These absorption spectra are presented in Fig. 1. The band maxima could not be determined in the region under investigation. This difficulty is due to the overlap of the continuous band with the absorption of the solvent.

The dependence of ΔD on oxygen concentration was investigated in methanol and ethanol solutions saturated with oxygen. The partial pressure of oxygen was varied in the region 50–500 mm. ΔD was found to vary linearly with the oxygen pressure.

Absorption Spectrum of NO in Methanol.—An absorption band of nitric oxide in methanol was obtained below 260 m μ (Fig. 1). No optical absorption of gaseous nitric oxide at a pressure of 1 atm. in a 1 cm. cell in the region 300–220 m μ was observed. The continuous absorption band of nitric oxide in methanol was found to be shifted toward longer wave lengths compared to the oxygen absorption band. A linear dependence of ΔD on NO concentration was observed.

Nature of the Optical Absorption.—The absorption spectra observed under these conditions are

diffusive and no fine structure could be detected. The molar absorption coefficients for oxygen and nitric oxide solutions are about 10^2 higher than the singlet-triplet transitions of liquid benzene enhanced by O₂⁵ and by NO.⁶ Thus it appears that these bands are not due to singlet-triplet transitions of the solvent molecules. The marked dependence of the absorption band on the solvent clearly indicates that the absorption is not due to the forbidden $^3\Sigma^- \rightarrow ^3\Sigma^+$ transition of the dissolved oxygen.

Following previous suggestions^{1,8,10,11} these continuous bands are assigned to charge transfer spectra of oxygen and nitric oxide. The electron affinity of O₂ based on thermochemical data is of the order of 0.7–1 e.v.,^{12,13} while the electron affinity of NO is positive.¹² Thus these molecules may act as electron acceptors in an electron transfer process.¹⁴ A support for this conclusion in the case of oxygen is obtained by considering the relation between the energy associated with the optical process and the ionization potential of the solvent molecule. As the maxima of these absorption bands could not be determined, the band onset energies $h\nu_0$ were chosen. For the solvents experimentally investigated we chose arbitrarily $\epsilon = 10$ as the band onset. It is thus assumed that the vibrational broadening is independent of the nature of the electron donor. For the iodine charge transfer complexes the energy difference

(10) D. F. Evans, *J. Chem. Phys.*, **23**, 1424 (1955).

(11) R. S. Mulliken, quoted in ref. 3b.

(12) H. O. Pritchard, *Chem. Revs.*, **62**, 529 (1953).

(13) M. G. Evans and N. Uri, *Trans. Faraday Soc.*, **45**, 217 (1949).

(14) R. S. Mulliken, *J. Am. Chem. Soc.*, **74**, 811 (1952).

(9) A. Seidel, "Solubilities of Inorganic and Organic Compounds," D. Van Nostrand Co., New York, N. Y., 1940.

U between band maximum and band onset energies remains constant within 0.2 e.v. In Fig. 2 the linear plot of $h\nu_0$ against the ionization potential for oxygen solutions is presented over a somewhat more extended region than was recently given.⁸ The band onset of acetonitrile is located at $\lambda < 228 \text{ m}\mu$, $h\nu_0 > 126 \text{ kcal.}$, which is consistent with the high ionization potential 12.2 e.v.¹⁵ of this molecule. This linear plot is a straightforward result of Mulliken's^{14,16} theory.

Considering the quantitative relation between the charge transfer absorption and ionization potential, Mulliken's theory leads to the result¹⁶: $h\nu_0 = I - E + W + 2\beta^2/(I - E + W) - U$ where I is the vertical ionization potential of the electron donor, E is the vertical electron affinity of oxygen, W the stabilization energy of the excited state in the nuclear configuration corresponding to the ground state and β the resonance integral.

For extremely weak complexes $\beta^2 \ll I - E + W$ and no deviation from linearity¹⁶ should be expected. The slope obtained from Fig. 2 is 0.65. This deviation of the slope from unity may be due to the dependence of W on I ¹⁷; however, the data are not accurate enough to establish these points.

Analysis of Solubility Data of O_2 .—The pronounced temperature effect on ΔH for the solubility of oxygen in water was explained³ as being caused by the formation of two distinct species involving hydrated oxygen. However, a similar temperature dependence of ΔH was observed for the rare gases, nitrogen and hydrogen dissolved in water.¹⁸ As was shown by Eley¹⁸ this behavior is due to the temperature effect on the energy and entropy changes associated with the breaking of the water structure and the formation of cavities in this liquid.

From the solubility data of oxygen in methanol,⁹ ethanol⁹ and benzene¹⁹ linear plots of $\log \beta$ (β -Ostwald solubility coefficient) against $1/T$ were obtained over a wide temperature region. For these solvents, in variance with the properties of aqueous solutions ΔH for the solubility of oxygen is temperature independent. In the case of organic solvents the temperature effects on the heats and entropies of solubilities should be much smaller.²⁰

These results indicate the lack of thermochemical evidence for consecutive complex formation in oxygen solutions. The temperature effect on the absorption bands of oxygen in water⁴ may be due to the effect of the increase of the amplitude of thermal vibrations leading to temperature broadening of the band threshold.

The numerical values for heats of solution of oxygen in water and in benzene are of the same

(15) K. Watanabe and T. Nakayama, "Technical Report No. 1," University of Hawaii, 1958.

(16) S. H. Hastings, J. L. Franklin, J. C. Schiller and F. A. Matsen, *J. Am. Chem. Soc.*, **75**, 2900 (1953).

(17) H. McConnell, J. S. Ham and J. R. Platt, *J. Chem. Phys.*, **21**, 66 (1953).

(18) D. D. Eley, *Trans. Faraday Soc.*, **35**, 1281 (1939).

(19) J. Horinti, *Sci. Papers Inst. Phys. Chem. Res. Tokyo*, **17**, 125 (1931).

(20) D. D. Eley, *Trans. Faraday Soc.*, **35**, 1421 (1939).

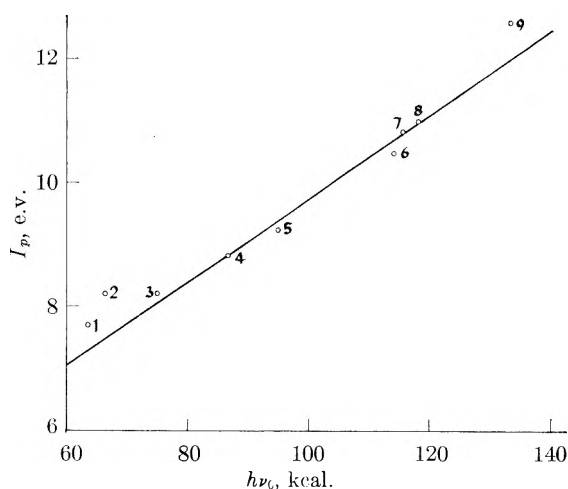


Fig. 2.—The dependence of the equivalent energy of the charge transfer band onset on the ionization energy of the solvent molecule; ionization potentials from K. Watanabe, *J. Chem. Phys.*, **26**, 542 (1952) and ref. 16: (1) aniline¹; (2) pyrrole¹; (3) anisole¹; (4) toluene¹; (5) benzene; (6) ethanol; (7) methanol; (8) cyclohexane²; (9) water.

order of magnitude within 0.5 kcal. as for other gases of comparable size and polarizability.

The solubility data of oxygen, nitrogen and argon were compared.

For water at 4°

$$\Delta H(O_2) = 3.9 \text{ kcal. mole}^{-1} \text{ }^4$$

$$\Delta H(A) = 3.73 \text{ kcal. mole}^{-1} \text{ }^{18}$$

For benzene at 20°

$$\Delta H(O_2) = 0.36 \text{ kcal. mole}^{-1}$$

$$\Delta H(N_2) = 0.86 \text{ kcal. mole}^{-1}$$

and

$$\Delta H(A) = 0.82 \text{ kcal. mole}^{-1} \text{ }^{21}$$

It thus appears that there is no thermochemical evidence for complex formation in these solutions. As was suggested recently³ these continuous absorption bands of oxygen and nitric oxide probably are the result of a contact charge transfer²² process.

(21) R. P. Bell, *ibid.*, **33**, 496 (1937).

(22) L. E. Orgel and R. S. Mulliken, *J. Am. Chem. Soc.*, **79**, 4389 (1957).

POTENTIAL DETERMINING IONS AND THE COAGULATION VALUE

By MIRKO MIRNIK

Institute "Rudjer Bošković," Zagreb, and Department of Physical Chemistry, Faculty of Science, University of Zagreb, Zagreb, Yugoslavia

Received February 27, 1961

In a paper by Kratochvil, Orhanović and Matijević¹ the problem of dependence of the coagulation concentration of the potential determining, constituent and stabilizing ions was brought forward and the role of Bjerrum's distance in the coagulation discussed.

The dependence of the coagulation value of the potential determining ion was in the majority of papers of this school (ref. 1 and the cited literature) represented by plots "logarithm coagulation concentration (value) against logarithm total concen-

(1) J. P. Kratochvil, M. Orhanović and E. Matijević, *J. Phys. Chem.*, **64**, 1216 (1960).

tration of the stabilizing ion." This description is formally correct but it is thermodynamically justified to use only the excess concentration (activity) of this ion.

As the first approximation for the activity of the excess constituent ion the difference of the total concentration of the ion in excess and of the concentration of the second precipitating ion (*i.e.*, $C_{Br^-} - C_{Ag^+}$) can be taken. Then in the plots "logarithm coagulation value - logarithm activity of the potential determining ion." the slope of these lines becomes much smaller in the region of low activities.

In the AgI system the effects of supersaturation, crystallization and recrystallization are the smallest and the coagulation processes can be studied practically free from accompanying crystallizations or recrystallizations. The influence of the activity of the stabilizing I⁻ ion, determined potentiometrically, upon the coagulation value was found to be practically negligible.²

The addition of 10 mole % ethanol, 1.8 mole % glycine and 10 mole % acetone³ changes the coagulation values of Na⁺, Ba⁺⁺ and La⁺⁺⁺ insignificantly compared with the shift of the negative stability limit from *pI* 9.8 in pure water to 11.5, 12.9 and 13 in the respective mixed solvents.

The slope, *i.e.*, the change of the logarithm coagulation value for one *pI* unit is for Ba⁺⁺ ($10^{-3} N$) and La⁺⁺⁺ ($10^{-4} N$) in all four cases smaller than 0.03 and for Na⁺ ($0.1 N$) it amounts to 0.1. Thus the coagulation value can be considered as practically constant over 8.8, 10.5, 11.9, resp., 12 *pI* units. For an ideal coagulating system the conclusion has to be made that the coagulation value is independent of the activity of the potential determining and stabilizing ion from *pI* equal to log concentrations of the ion of lowest valency to the negative stability limit.

The influence of the concentration of Br⁻ and Cl⁻ ion upon the coagulation value is greater and complex and can be connected with greater differences in solubility in different concentrations, which cause faster crystallizations and recrystallizations. These processes take place with rates similar to those of coagulations, especially in the AgCl system. Therefore the (*i.e.*, tyndallometrically) observed processes are pure coagulations only in narrow regions of the activity of the potential determining ion. Generally, coagulations mixed with crystallizations or recrystallizations are taking place causing apparent changes of the observed coagulation values with *pBr* or *pCl*.

According to Bjerrum the distance δ between two associated ions is proportional to the valency z of the second ion if the valency z^- of the first ion is constant

$$\delta = z \frac{Ne^2 z^-}{nRTD}$$

This may also apply for the ion pair "adsorbed potential determining ion-adsorbed coagulating counter ion." Therefore the relation $\log c_{coag} - \delta$

for D and z constant must be linear for the same reason as the relation $\log c_{coag} - z$ is linear, while the slopes of the lines $\log c_{coag} - \delta$ for different z should be proportional to $1/D$. Considering the great influence of D upon the solubility, crystallization and recrystallization, and that concentrations were used instead of activities, the results of Figs. 5 and 6 in ref. 1 confirm the correctness of the z/D term in Bjerrum's formula as well as the correctness of any theory postulating a linear $\log c_{coag} - z$ relation. A thermodynamic deduction of this linear relation based on the adsorption, respectively, ion exchange theory of coagulation is given elsewhere.⁴

(4) M. Mirnik, *Nature*, **190**, 689 (1961); *J. Colloid Sci.*, in course of publication.

E.P.R. OBSERVATION OF NH₃⁺ FORMED BY X-RAY IRRADIATION OF AMMONIUM PERCHLORATE CRYSTALS

BY JAMES S. HYDE AND

Instrument Division, Varian Associates, Palo Alto, California

ELI S. FREEMAN

Pyrotechnics Chemical Research Laboratory, Picatinny Arsenal, Dover, N. J.

Received March 3, 1961

Freeman and Anderson,¹ and Freeman, Anderson and Campisi² have reported profound changes in the decomposition characteristics or chemical reactivity of ammonium perchlorate crystals following X-ray and γ -ray irradiation. In an effort to understand the nature of the radiation damage in these crystals, we have undertaken an investigation using electron paramagnetic resonance (e.p.r.) techniques. One would expect, with these techniques, to observe those damage sites in the crystal which happen to contain unpaired electron spins.

Sample Preparation.—The ammonium perchlorate crystals used in this work were doubly recrystallized from triply distilled water. The original material was certified reagent grade salt obtained from the Fisher Scientific Company. Both crystalline powders and larger crystals of several cubic millimeters were prepared. The samples were irradiated with an exposure dose of 10^6 roentgens at a rate of 2×10^5 roentgens per hour by means of an OEG-50 X-ray tube with a molybdenum target.

Electron Paramagnetic Resonance Apparatus.—The electron paramagnetic resonance experiments were performed using the Varian V4501 EPR Spectrometer. This instrument employs 100 kc. field modulation, and a microwave frequency of 9.5 mc. A Varian V4547 Variable Temperature Accessory permitted studies over a continuous range of temperature.

Results and Discussion

Figure 1 shows the e.p.r. spectrum at room temperature obtained from a single crystal of irradiated ammonium perchlorate. The spectrum is that expected from hyperfine interaction with one nucleus of spin 1 and three equivalent nuclei of spin $1/2$, and almost certainly arises from an unpaired electron spin strongly localized on an NH₃ molecule. Contact with the nitrogen nucleus splits the spectrum into three lines of equal spacing and

(1) E. S. Freeman and D. A. Anderson, *J. Phys. Chem.*, **63**, 1344 (1959).

(2) E. S. Freeman, D. A. Anderson and J. J. Campisi, *ibid.*, **64**, 1727 (1960).

(2) M. Mirnik, F. Flajšman, K. F. Schulz and B. Težak, *J. Phys. Chem.*, **60**, 1473 (1956).

(3) M. Mirnik, F. Flajšman and B. Težak, *ibid.*, in course of publication.

intensity, and contact with the three equivalent protons splits each of these three lines into a quartet of equally spaced lines with intensity ratios of 1:3:3:1. This analysis is illustrated in Fig. 1. Presumably the radical is a positive ion, although the e.p.r. technique would not distinguish from a negative ion. No resonances other than that associated with the NH_3^+ radical were found in these crystals.

Several interesting observations can be made concerning the anisotropy and temperature dependence. Figure 2 shows spectra obtained with a powder sample at $+100$, $+25$, -100 and -180° . At $+25^\circ$, the spectra from the powder and the single crystal differ markedly, but at $+100^\circ$ the spectra are nearly the same. We conclude that at the high temperature the NH_3^+ molecules are rotating rapidly and the anisotropy which causes the difference in spectra found at lower temperatures is being averaged out. The critical rotation frequency is $\gamma \overline{\Delta H}$, where γ is the gyromagnetic ratio of the electron dipole and $\overline{\Delta H}$ is an average shift in the position of the hyperfine lines because of the anisotropy. The separation of the lines at $+100^\circ$ is therefore a measure of the isotropic hyperfine splitting, and we find that contact with the nitrogen nucleus splits the lines by 18.1 oersteds and contact with the hydrogen nuclei splits the lines by 25.0 oersteds. The splittings were measured to an accuracy of 1% by comparison with the resonance of nitrosodisulfonate (peroxylamine disulfonate) ion $(\text{ON})(\text{SO}_3)_2^-$, which is split into three lines 13.0 oersteds apart.

At -100° (Fig. 2) the central quartet corresponding to $M = 0$ for the nitrogen nucleus is well defined and of much greater intensity than the quartets corresponding to $M = \pm 1$. It is quite possible that the observed anisotropy arises from interaction with the quadrupole moment of the nitrogen nucleus, since the nitrogen splittings are so much more drastically affected than are the hydrogen splittings. Hydrogen, of course, has no quadrupole moment. It is also possible that the electron dipole has stronger anisotropic interaction with the dipole moment of the nitrogen nucleus than with the proton dipoles. In any event, the molecule is rotating slowly compared with $(\gamma \overline{\Delta H}_N)$, where $\overline{\Delta H}_N$ refers to the average anisotropic shift arising from interaction with the nitrogen nucleus. At still lower temperatures (-180°) the spectrum from the powder becomes asymmetric with respect to the center of the spectrum (Fig. 2), although the single crystal spectrum remains symmetric. Anisotropy arising from interaction between the electron dipole and the proton dipoles is entering the picture, and the molecule is rotating slowly compared with $(\gamma \overline{\Delta H}_P)$ where the subscript "P" refers to the protons. Rogers and Pake³ have reported similar anisotropic effects when the vanadyl ion, VO^{++} , is in aqueous solution. The behavior of the anisotropy of the NH_3^+ resonance as a function of temperature suggests that freedom of the ion to rotate is frozen out in several fairly well-defined steps.

(3) R. N. Rogers and G. E. Pake, *J. Chem. Phys.*, **33**, 1107 (1960).

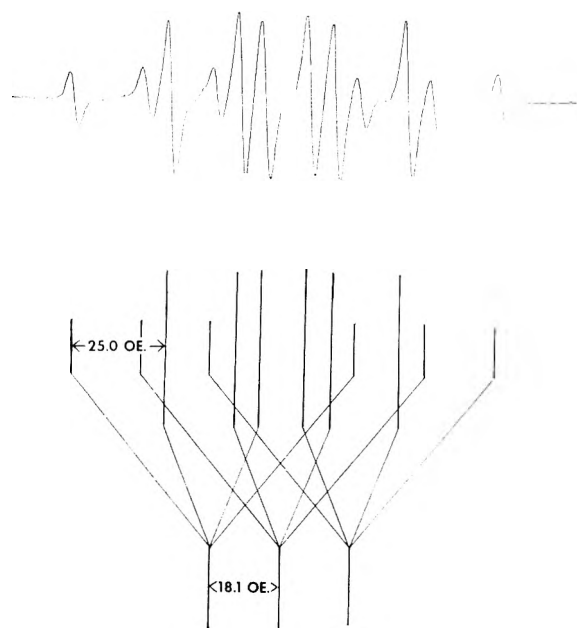


Fig. 1.—Room temperature e.p.r. spectrum from a single crystal of irradiated ammonium perchlorate, and the reconstructed spectrum from NH_3^+ assuming isotropic hyperfine interaction.

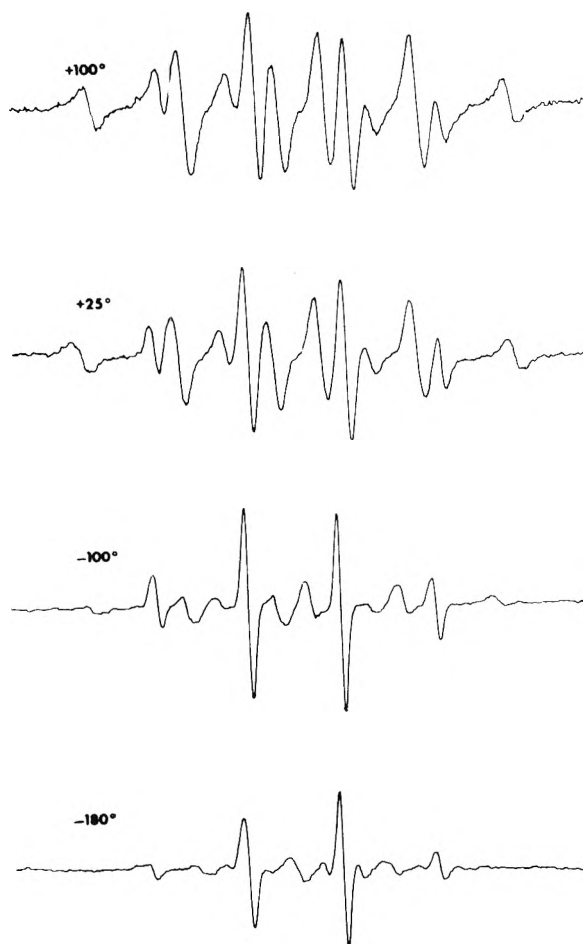


Fig. 2.—E.p.r. spectra at $+100$, $+25$, -100 and -180° from a crystalline powder of irradiated ammonium perchlorate.

The ammonia ion is quite stable with respect to time and temperature. No decay of the resonance intensity was noted on heating to +125° or upon storing for several months at room temperature.

The resonance cannot be saturated with the available microwave power (200 mw. at the sample cavity) at room temperature, but at lower temperatures it is necessary to reduce the power level to avoid saturation. The *g*-value of the center of gravity of the spectrum was measured by comparison with crystalline α, α -diphenyl- β -picrylhydrazyl ($g = 2.0036$) and found to be 2.0034 ± 0.0001 .

KINETICS OF THE 2,4-TOLYLENE DIISOCYANATE-ALCOHOL REACTION

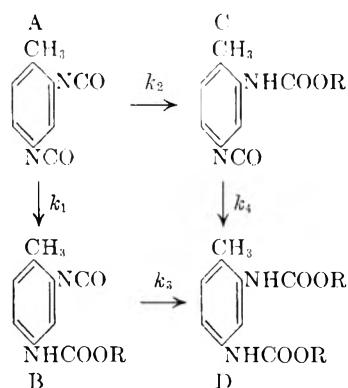
BY FRED H. BROCK

Contribution No. 210 from the Chemical Division of Aerojet-General Corp., Azusa, Calif.

Received March 8, 1961

The kinetics of the 2,4-tolylene diisocyanate-alcohol reaction have been analyzed in terms of a parallel and series reaction scheme consisting of two simultaneous reaction paths instead of the usual method of considering essentially one reaction path only.¹⁻⁴ The results show that the final rate plot obtained from this theoretical treatment is similar to the one obtained from experimental data but that, contrary to current assumptions, the rate constant values obtained from the two linear portions of this rate plot are not those of the *para* and *ortho*-isocyanato groups.

Derivation of Equations.—The reaction of 2,4-tolylene diisocyanate with an alcohol ROH involves the reaction scheme



For simplicity, letters will be used to represent the compounds as above. Also, the alcohol concentration will be considered to be in large excess, so that pseudo-first order reactions only need to be considered. The alcohol concentration is hence included in the values of the rate constants, *i.e.*, $[\text{alcohol}] k_{\text{true}} = k_{\text{pseudo-first order}}$.

For this reaction scheme, these equations hold

(1) J. Burkus and C. F. Eckert, *J. Am. Chem. Soc.*, **80**, 5948 (1958).

(2) L. L. Ferstandig and R. A. Scherrer, *ibid.*, **81**, 4838 (1959).

(3) J. C. Kogan, *J. Org. Chem.*, **24**, 438 (1959).

(4) J. J. Tazuma and H. K. Latourette, presented before the Division of Paints and Plastics at the 130th national meeting of the American Chemical Society, Atlantic City, N. J., September, 1956.

$$\frac{dA}{dt} = -(k_1 + k_2)A$$

$$\frac{dB}{dt} = k_1A - k_3B$$

$$\frac{dC}{dt} = k_2A - k_4C$$

These equations are integrated readily to yield the concentrations of each species at any time, *i.e.*

$$A = A_0 e^{-(k_1+k_2)t}$$

$$B = \frac{k_1 A_0}{k_3 - k_1 - k_2} [e^{-(k_1+k_2)t} - e^{-k_3 t}]$$

$$C = \frac{k_2 A_0}{k_4 - k_1 - k_2} [e^{-(k_1+k_2)t} - e^{-k_4 t}]$$

where A_0 is the initial concentration of A.

The measured isocyanate concentration at any time is given by

$$[\text{NCO}] = 2A + B + C$$

which in view of the above relationships becomes

$$[\text{NCO}] = A_0 \left\{ 2e^{-(k_1+k_2)t} + \frac{k_1}{k_3 - k_1 - k_2} \times [e^{-(k_1+k_2)t} - e^{-k_3 t}] + \frac{k_2}{k_4 - k_1 - k_2} [e^{-(k_1+k_2)t} - e^{-k_4 t}] \right\}$$

In order to show the time-dependence of the concentrations of these isocyanates, k_2 , k_3 and k_4 will be expressed in terms of k_1 by use of an equation that has been shown to hold for the isocyanate-alcohol reactions,⁵ *i.e.*

$$\log \frac{k}{k_0} = \rho \Sigma \sigma + n \log 0.34$$

where

k is the reaction rate constant of an isocyanate

k_0 is the reaction rate constant of a reference isocyanate, *e.g.*, phenyl isocyanate

ρ is the reaction series constant

σ is a substituent constant

n has the value of 1 when a methyl group is *ortho* to the reacting isocyanato group, and 0 in the absence of the *ortho*-methyl group.

The expressions for the rate constants thus become

$$\log \frac{k_1}{k_0} = \rho [\sigma_{m-\text{NCO}} + \sigma_{p-\text{CH}_3}]$$

$$\log \frac{k_2}{k_0} = \rho [\sigma_{m-\text{NCO}} + \sigma_{o-\text{CH}_3}] + \log 0.34$$

$$\log \frac{k_3}{k_0} = \rho [\sigma_{m-\text{NHCOOR}} + \sigma_{o-\text{CH}_3}] + \log 0.34$$

$$\log \frac{k_4}{k_0} = \rho [\sigma_{m-\text{NHCOOR}} + \sigma_{p-\text{CH}_3}]$$

The values of $\sigma_{o-\text{CH}_3}$ and $\sigma_{p-\text{CH}_3}$ are equal. These relationships help to show clearly, without assumptions as to the σ values of the isocyanato groups, that only 3 rate constants instead of 4 need to be considered, since one dependent relationship exists between the 4 constants, *i.e.*

$$\frac{k_2}{k_3} = \frac{k_1}{k_4}$$

Rearrangement of the above equations shows that

(5) F. H. Brock, *J. Org. Chem.*, **24**, 1802 (1959).

$$\log \frac{k_2}{k_1} = \log 0.34$$

$$\log \frac{k_3}{k_1} = \rho[\sigma_{m\text{-NHCOOR}} - \sigma_{m\text{-NCO}}] + \log 0.34$$

$$\log \frac{k_4}{k_1} = \rho[\sigma_{m\text{-NHCOOR}} - \sigma_{m\text{-NCO}}]$$

The required values, obtained from the reference cited, are: $\rho = 1.69$, $\sigma_{m\text{-NHCOOR}} = 0.04$ and $\sigma_{m\text{-NCO}} = 0.43$. Substitution of these values in the above equations yields $k_2 = 0.34k_1$, $k_3 = 0.0745k_1$ and $k_4 = 0.219k_1$.

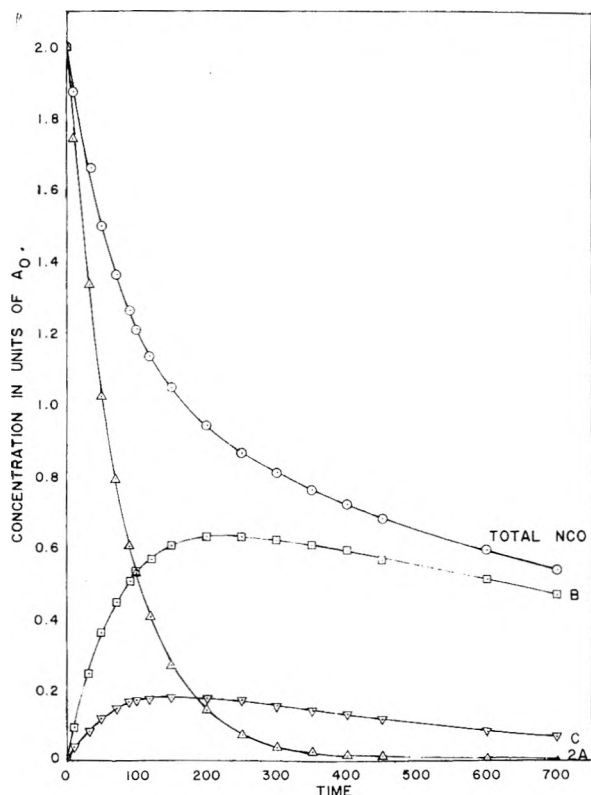


Fig. 1.—Plots of concentrations of isocyanates vs. time.

Hence, the time-dependence of the isocyanate concentration becomes

$$[\text{NCO}] = A_0 [2e^{-1.34 k_1 t} + 0.790 (e^{-0.0745 k_1 t} - e^{-1.34 k_1 t}) + 0.303 (e^{-0.219 k_1 t} - e^{-1.34 k_1 t})]$$

In this expression the first, second and third terms refer to twice the concentration of A and the concentrations of B and C, respectively.

A reasonable value of k_1 of 0.01 was assumed. The calculated values of twice the concentration of A and the concentrations of B, C and total isocyanate as a function of time (in the same units as those used for k_1) are graphed in Fig. 1.

Data Analysis.—The method of data analyses that is currently being used to calculate the rate constants is to plot $\log [\text{NCO}]/2$ against time, resulting in a graph considered to consist of two linear portions. The rate constant calculated from the first and steeper slopes is assumed to be equal to k_1 ,^{3,4} or to $k_1 + k_2$,^{1,2} whereas the rate constant derived from the second slope is equated to k_3 ,^{2,4} or to $k_3 + k_4$.¹

In order to determine the type of plot obtained from the data of the analysis presented in the fore-

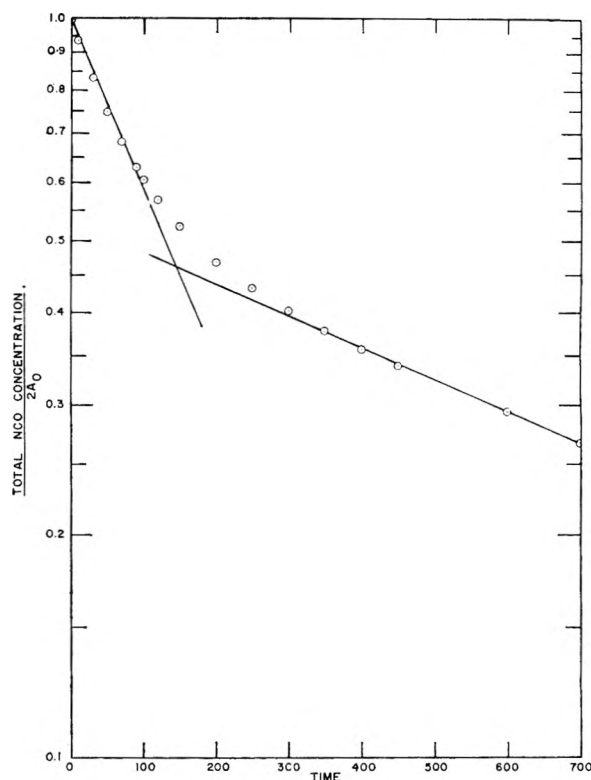


Fig. 2.—First-order rate plot.

going sections, the data of the total isocyanate concentration were plotted in this usual first-order manner as shown in Fig. 2. This plot also consists of two linear portions similar to the plots of experimental data. The rate constants that would be calculated from the two slopes are 0.00528 and 0.00100 for the *para* and *ortho* group reactions, respectively, compared to the assumed values of 0.01 and 0.000745, respectively.

Inspection of Fig. 2 shows that the slopes of the straight lines and hence the values of the two calculated rate constants are highly dependent on the location of the lines, e.g., the theoretical maximum value of the first rate constant, obtained from the tangent to the curve at zero time, is $1.34k_1$, or 0.0134, as compared to the above value 0.00528. Reasonable changes in the values of the ratios of the rate constants and steric factor of an *ortho*-methyl group would not affect the findings, but only the absolute values of the concentrations.

THE EFFECT OF FLUORINATION ON THE SURFACE ACIDITY OF CATALYTIC ALUMINA AND THE LOSS IN ACIDITY DUE TO WATER VAPOR ADSORPTION

By E. V. BALLOU, R. T. BARTH AND R. A. FLINN

Gulf Research and Development Company, Pittsburgh, Pennsylvania

Received March 8, 1961

Halide treated alumina catalysts have been commonly used in isomerization reactions.¹ The commercial importance of fluorinated alumina

(1) H. Pines and J. M. Mavity, "The Chemistry of Petroleum Hydrocarbons," Vol. III, Reinhold Publ. Co., New York, N. Y., 1955, Chapter 39, p. 40.

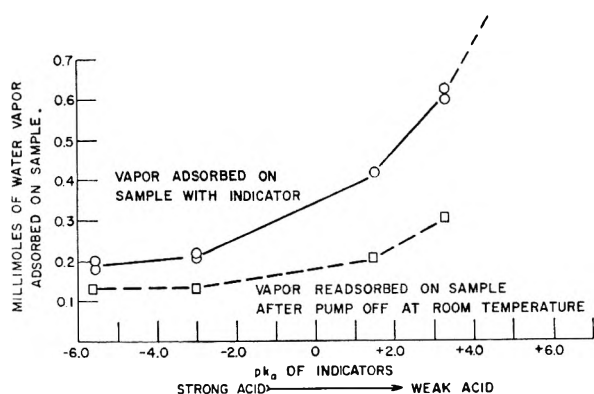


Fig. 1.—Water vapor adsorption on 1% fluorinated F-10 alumina—amount of water necessary to change color of various strength indicators.

has led to investigations of the surface characteristics of the substrate and its comparison with the non-fluorinated alumina surface. Webb,² for example, applied gaseous ammonia adsorption to this material. An alternate approach to the surface characteristics of a catalyst is the liquid phase adsorption of *n*-butylamine, combined with the use of Hammett acid-base indicators. Such an indicator test for acidity was described by Benesi,³ who reported no acid colors on alumina with any of the Hammett indicators. No results were given for fluorinated alumina.

In the work described here, water vapor adsorption was found to markedly affect the results of the Hammett indicator tests. These data also suggested that one difference in the fluorinated and non-fluorinated alumina was the enhanced retention of water by the latter.

Experimental

Materials.—Tests were carried out on commercial grade F-10 alumina, obtained from the Aluminum Company of America, Pittsburgh, Pa. Impurities, determined in this Laboratory by chemical analysis, were 0.04% Si, 0.05% Fe, 0.1% Na, 0.5% Cl and 0.15% S. The BET surface area from nitrogen adsorption was 128 m.²/g.

Samples were fluorinated by puddling the solid with aqueous hydrofluoric acid solution, followed by drying at temperatures slowly increasing to 540°. Chemical analyses of calcined samples for fluorine showed 0.9 to 1.1% F. Fluorination reduced the chlorine content of the samples to 0.1%. The BET surface area of a fluorinated sample was 119 m.²/g.

The benzene solvent was reagent grade from J. T. Baker Co., which was refluxed and distilled, and the first 10% of the distillate discarded. This method of dehydration of benzene has been described by W. E. Hanson.⁴ The water content of the residue was determined by a Karl Fischer method and found to be less than 10 p.p.m. *n*-Butylamine was "certified" reagent grade from Fisher Scientific Company and was used without further purification. The five indicators used in the tests were benzalacetophenone, dicinnamalacetone, benzeneazodiphenylamine, butter yellow, and neutral red, with reported pK_a values of -5.6, -3.0, +1.5, +3.3 and +6.8, respectively. Indicators were chemical and stain grades from Eastman and National Aniline Companies. Flushing nitrogen was prepurified grade from the Air Reduction Company, the water content from the tank being 250 to 400 p.p.m. The tank nitrogen was passed through a column 2.5 cm. in diameter and 39 cm. in length containing predried

Linde Type 5A Molecular Sieves, which lowered the water content of the nitrogen gas to about six p.p.m.

The Measurement of Surface Acidity.—Prior to the acidity measurements the catalysts were treated in the following steps: first, one-gram samples were calcined in 25-ml. erlenmeyer flasks at 540° for three hours; then the flasks were closed with ground glass stoppers before removal from the furnace, and cooled in an aluminum desiccator which was flushed with dry nitrogen. When cool, the samples were quickly covered with benzene by pipetting a sufficient amount of solvent just as the stopper was removed from the flask. After this step, the required amount of butylamine in benzene solution was added, and each flask gently agitated for three hours.

The indicator tests were performed either on porous spot plates, in enclosed glass tubes, or in benzene slurries. In the first two methods, the equilibrated slurry from each butylamine titer was apportioned to five wells in either the white porcelain spot plates or in enclosed glass tubes. The material was dried under heat lamps while being flushed with liquid nitrogen. When each powdered sample was just dry, the heat lamps were turned off and the indicators were added. Colors were then observed. In the third method, the indicator was added directly to the catalyst in benzene slurry for each butylamine titer. This was similar to the technique described by Benesi.⁵

Water Vapor Adsorption Studies.—The possibility of interference of adsorbed water on indicator measurements of alumina and fluorinated alumina led to more quantitative determinations of this effect. In one series of experiments indicators were added to the calcined, fluorinated and non-fluorinated alumina samples prior to water adsorption tests. In another series, samples already exposed to 30% relative humidity for 24 hours were evacuated at various temperatures until the return of the acidic color of benzalacetophenone indicator (pK_a value -5.6).

Results

The Measurement of Surface Acidity.—The surface acidity values (Table I) obtained for 1% fluorinated alumina and non-fluorinated alumina, by the three techniques described above, show a marked difference between the two samples observed on spot plates, as well as differences for each sample by the various methods. This was in contrast to tests of silica-alumina catalysts, in which all three techniques had appeared equivalent. Observations on spot plates had previously been found suitable to confirm Benesi's data⁵ on silica-alumina, silica-magnesia and mounted acids.

In the case of non-fluorinated alumina, the exposure of the catalyst to small amounts of water vapor appeared critical. For example, the introduction of water vapor into the nitrogen stream at a concentration of 400 p.p.m. was sufficient to completely suppress the action of the alumina toward three of the indicators. The fluorinated alumina still showed 0.08 to 0.10 meq./g. of acid over the strength range. Using an enclosed system, it was possible to keep the water vapor concentration of a slowly flowing stream of nitrogen to six p.p.m., and the maximum cumulative amount of water vapor during the test to about 0.002 millimole (Table IB). In dried benzene solvent the apparent acidities of the samples were still higher (Table IC), even though the benzene had a greater water content per flask than the cumulative water content of the nitrogen stream.

The 0.5% chlorine impurity present in the non-fluorinated alumina, as commercially available, does not appear to be critical with regard to the surface acidity. This is shown by the very low acidity of the non-fluorinated alumina in spot plate

(2) A. N. Webb, *Ind. Eng. Chem.*, **49**, 261 (1957).

(3) H. A. Benesi, *J. Am. Chem. Soc.*, **78**, 5490 (1956).

(4) W. E. Hanson, "Directions for the Use of the Modified Menzies-Wright Molecular Weight Apparatus," Report of the Mellon Institute of Industrial Research, Pittsburgh, Pa., June, 1943.

(5) H. A. Benesi, *J. Phys. Chem.*, **61**, 970 (1957).

TABLE I

COMPARISON OF SURFACE ACIDITY VALUES OBTAINED ON FLUORINATED F-10 ALUMINA AND NON-FLUORINATED F-10 ALUMINA BY DIFFERENT INDICATOR TECHNIQUES

Catalyst	H_0 Range					Meq./g. total acidity
	6.8 to 3.3	3.3 to 1.5	1.5 to -3.0	-3.0 to -5.6	< -5.6	
A. Acidity determinations with dried catalysts in spot plates						
1% Fluorinated F-10	0.0	0.0	0.02	0.0	0.08	0.10
Non-fluorinated F-10	.005	.02	.0	.0	.0	.025
B. Acidity determinations with dried catalysts in enclosed tubes						
1% Fluorinated F-10	0.0	0.0	0.0	0.0	0.10	0.10
Non-fluorinated F-10	.0	.0	.0	.0	.10	.10
C. Acidity determinations in benzene slurry						
1% Fluorinated F-10	0.02	0.0	0.0	0.0	0.28	0.30
Non-fluorinated F-10	.0	.0	.0	.0	.30	.30

tests (Table IA), as well as by increased acidity noted upon chlorination of alumina, when carried out in a manner similar to fluorination. Presumably, the halogen impurity is present in the bulk of the catalyst structure, probably as a salt, while halogenation treatment affects the exposed acid sites of the alumina.

Water Vapor Adsorption Studies.—Figure 1 shows the amounts of water vapor necessary to destroy the acid color of four selected indicators on 1% fluorinated alumina. The reproducibility of this experiment is shown by the pairs of points on the top curve. To ensure that the observed color change was complete, samples were momentarily exposed to saturated water vapor. Then they were evacuated at room temperature until the acidic indicator color returned—a procedure which took several minutes for the indicators denoting weak acid, but hours for the indicators denoting strong acid. Readsorption of water vapor on the evacuated samples until the indicators again lost their characteristic acid color took place according to the lower curve. In similar experiments with non-fluorinated alumina, 0.3 to 0.4 mmole/g. more water vapor was needed to change the color of each indicator, than was required for the fluorinated material.

Discussion and Conclusions

The attribution of surface acidity to fluorinated alumina comes primarily from the effectiveness of such catalysts, when metal promoted, in isomerization reactions,¹ since an acid surface is necessary for the reaction step involving carbonium ion formation. The results of the study presented here show that the acid surface of both the fluorinated and non-fluorinated alumina can be poisoned by trace amounts of water vapor. These data indicate a competition between water vapor, butylamine and indicator dye for the acidic centers on each surface.

When the adsorbed water vapor is eliminated, the number of acid sites on alumina and fluorinated alumina appear to be the same, and both are very strong as judged by the effect on indicators. The difference between the fluorinated and non-fluorinated types of F-10 alumina surfaces was in their sensitivity to, and retention of, water vapor. The non-fluorination, and water poisoned, alumina may

not exhibit acidity until some Al-OH sites are dehydrated to Al-O-Al, whereas the fluorinated alumina may exhibit sufficient acidity upon the removal of physically adsorbed HOH.

HOLE INJECTION DURING REDUCTION OF FERRICYANIDE AT A GERMANIUM ELECTRODE

BY WALTER W. HARVEY

Lincoln Laboratory¹ Massachusetts Institute of Technology, Lexington 73, Massachusetts

Received March 22, 1961

The present note reports results of a limited investigation of carrier injection in germanium by electrochemical reaction. The experiments undertaken extend the work of Pleskov² and complement previous results of the author.³ Injection of holes as the result of a cathodic reaction at a germanium surface was discussed for the first time by Brattain and Garrett (see pp. 159, 160 of ref. 4). Subsequently, Gerischer and Beck⁵⁻⁸ and others⁹⁻¹¹ observed hole injection during corrosion of *n*-type germanium in solutions of oxidizing agents.

The phenomenon of carrier injection relates to the peculiar circumstance that both valence-band electrons and conduction-band electrons can participate in electrochemical processes at the interface. Electrons produced by an anodic reaction can enter the valence band of the crystal only if electron vacancies are present, positive "holes" being consumed thereby. Conversely, holes are produced by consumption of valence electrons in a cathodic reaction. A net production of holes and conduction electrons in *n*-type germanium, in which holes are the minority carrier, is referred to as "hole injection." The measurement of hole injection is significant for the information it affords with regard to the detailed mechanism of the electrode process.

Pleskov's observation² of hole injection during cathodic reduction of ferricyanide is subject to interpretation since the role of thermal generation of carriers at the surface was not fully considered. The manner in which thermal generation of holes and electrons at the back surface of a thin germanium electrode can contribute to the limiting anodic current at the front surface has proven difficult to understand. Figure 1 shows in a

(1) Operated with support from the U. S. Army, Navy and Air Force.

(2) Yu. V. Pleskov, *Doklady Akad. Nauk SSSR*, **126**, 111 (1959).

(3) W. W. Harvey, *Phys. and Chem. Solids*, **14**, 82 (1960).

(4) W. H. Brattain and C. G. B. Garrett, *Bell System Tech. J.*, **34**, 129 (1955).

(5) H. Gerischer and F. Beck, *Z. physik. Chem. (Frankfurt)*, **13**, 389 (1957).

(6) F. Beck and H. Gerischer, *Z. Elektrochem.*, **63**, 943 (1959).

(7) H. Gerischer and F. Beck, *Z. physik. Chem. (Frankfurt)*, **23**, 113 (1960).

(8) H. Gerischer and F. Beck, *ibid.*, **24**, 378 (1960).

(9) Yu. V. Pleskov, *Doklady Akad. Nauk SSSR*, **130**, 362 (1960).

(10) D. R. Turner, *J. Electrochem. Soc.*, **107**, 810 (1960).

(11) Experimental results of D. R. Turner, quoted by J. F. Dewald in "The Surface Chemistry of Metals and Semiconductors," John Wiley and Sons, Inc., New York, N. Y., 1960, edited by H. C. Gatos, pp. 216-218.

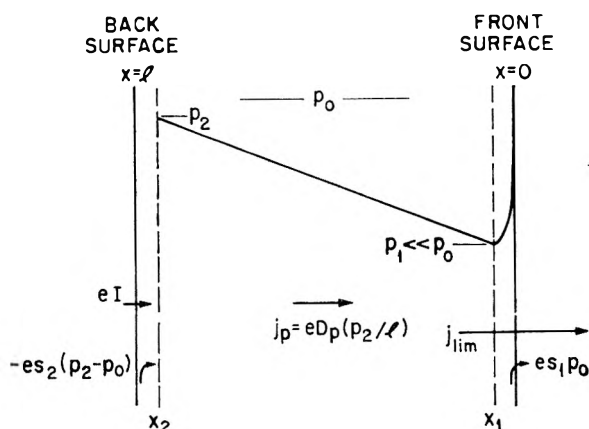


Fig. 1.—Distribution of holes and contributions to the hole current density for one-dimensional current flow across a thin, *n*-type germanium anode. The extents of the regions of space charge, designated by broken lines, are shown greatly exaggerated.

schematic way the contributions of optical and thermal generation to the supply of holes. Electrochemical hole injection is equivalent in effect to absorption of radiation capable of producing electron-hole pairs.

For hole flow entirely by diffusion, the hole current density for the one-dimensional case is

$$j_p = -eD_p \text{grad } p = -eD_p \left(\frac{dp}{dx} \right) \quad (1)$$

where $+e$ is the charge of a hole, D_p is its diffusion constant, and $\delta p = p - p_0$ is the deviation of the hole concentration p from its equilibrium value p_0 . Combining eq. 1 with the continuity equation for holes and using the boundary conditions indicated in Fig. 1, it can be shown that the limiting hole diffusion current to the front surface ($x = 0$) is realized when the concentration gradient at x_1 attains the value

$$\left(\frac{dp}{dx} \right)_{x_1} = \frac{p_0(1 - \cosh \lambda) - p_2}{L_p \sinh \lambda}, \quad \lambda = l/L_p \quad (2)$$

where l is the electrode thickness and L_p is the diffusion length¹² for holes. For $\lambda \ll 1$, the gradient at x_1 becomes equal to $-p_2/l$, so that the limiting anodic current density to the front surface is

$$j_{lim} = \alpha e D_p (p_2/l) \quad (3)$$

where α is the ratio of total current to hole current.⁴

In terms of the operationally defined surface recombination velocities¹² s_2 and s_1 , the net rates of thermal generation (*i.e.*, excess of generation over recombination) at the back and front surfaces are $-s_2(\delta p)_{x_2} = -s_2(p_2 - p_0)$ and $-s_1(\delta p)_{x_1} = s_1 p_0$, respectively. Including carrier generation by light absorption and electrochemical reaction at the back surface, and eliminating p_2 from (3), the limiting anodic current density⁹ for the thin anode is³

$$j_{lim} = \alpha e l [1 + (l/D_p)s_2]^{-1} (I + J) + \alpha e p_0 \{s_2 [1 + (l/D_p)s_2]^{-1} + s_1\} \quad (4)$$

where $I + J$ is the sum of the absorbed light intensity and the electrochemical hole injection rate. According to (4), the limiting anodic cur-

rent in the dark and in the absence of injection is determined by the recombination velocities at the two surfaces. Therefore, since s for germanium electrodes is known to depend upon the composition of the electrolyte,^{3,13} the hole injection rate will be greater or less than an observed increase in j_{lim} , depending upon the change in s_2 for the solutions compared.

The foregoing considerations have been tested experimentally using the thin-anode technique. Essential features of the apparatus are described elsewhere.³ Figure 2 shows anodic limiting currents for various compositions of solution in contact with the back surface. In the absence of oxidizing agents, germanium is inert to water and aqueous solutions, so that the observed increase in j_{lim} on removing dissolved oxygen and on adding KOH can only be the result of an increase in s_2 . Thus, if the electrochemical reduction of ferricyanide is accompanied by injection of holes into the germanium, the rate of hole injection is almost certainly not given by the increase in anodic limiting current shown in Fig. 2 (compare corresponding figure of ref. 2).

The contributions of injection and changes in s_2 can be separated by measuring the limiting anodic current as a function of absorbed light intensity at the back surface. For constant α and s_1 , properties of the anodically polarized front surface and solution, and for $J = 0$, eq. 4 predicts that changes in s_2 will result in a family of straight lines with a common intersection at $I = D_p(p_0/l)$ when the limiting current is plotted against light intensity. The calculated absorbed light intensity at the intersection in Fig. 3, which shows j_{lim} as a function of relative light intensity for the solutions of Fig. 2, is $4.8 \times 10^{15} \text{ cm.}^{-2} \text{ sec.}^{-1}$.

From the upward displacement of the j_{lim} vs. I characteristic for the alkaline ferricyanide solution, it is readily apparent that reduction of ferricyanide is indeed accompanied by hole injection. At the same time, however, the surface recombination velocity is decreased considerably, as evidenced by the greater slope of the line. It turns out, in fact, that if the ferricyanide characteristic is shifted downward, it can be made to coincide very nearly with the characteristic of the water containing some dissolved oxygen, indicating approximate equality of s_2 for the two solutions. For equal s_2 , the increase in j_{lim} due to electrochemical hole injection is

$$\Delta j_{lim} = \frac{\alpha e J}{1 + \frac{l}{D_p} s_2} \quad (5)$$

With the ferricyanide solution of Figs. 2 and 3, the injection current density e_j is estimated as 0.9 ma. cm.^{-2} .

If the reasonable assumption is made that s_1 is small during steady-state anodic polarization at the limiting current density,¹⁴ then s_2 may be estimated from the intercepts by equation 4. (Actually, it is probably more reliable to extrapolate to $I = 0$ as shown in Fig. 3, since the current flow is

(12) W. Shockley, "Electrons and Holes in Semiconductors," D. Van Nostrand Co., Inc., Princeton, N. J., 1950.

(13) W. W. Harvey and H. C. Gatos, *J. Appl. Phys.*, **29**, 1267 (1958).

(14) J. B. Flynn, *J. Electrochem. Soc.*, **105**, 715 (1958).

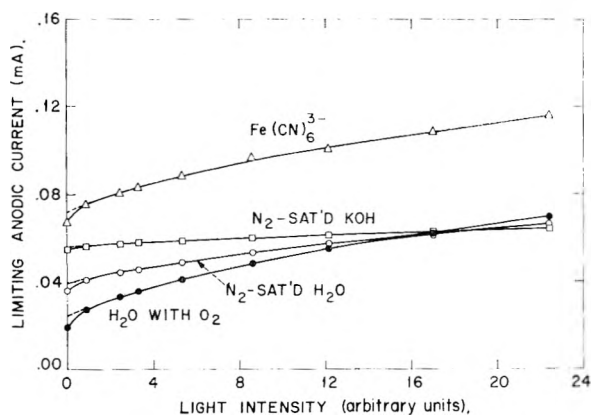


Fig. 2.—Current-voltage characteristics of a thin, *n*-type germanium anode, {100} orientation, for various compositions of solution in contact with the back surface. Anode area = 0.043 cm.², thickness *l* = 0.0150 cm., *L_p* = 0.24 cm., *ρ* = 4.6 ohm cm.

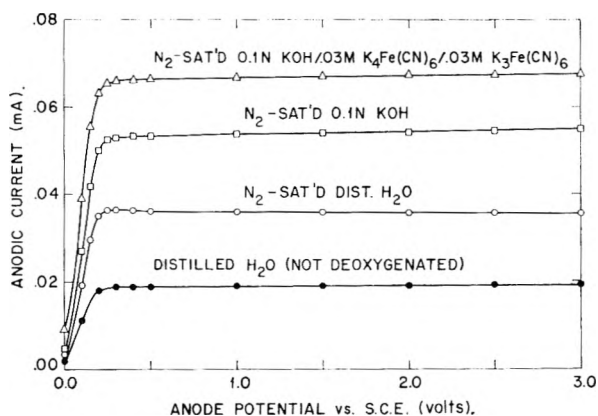


Fig. 3.—Dependence of limiting anodic current on incident light intensity at the back surface. Same electrode and solutions as for Fig. 2.

far from one-dimensional initially.) For α equal to 2.0, the calculated recombination velocities are, reading from the bottom, 1700, 4200 and 19,000 cm. sec.⁻¹, respectively. These values are at best semiquantitative, but the trend is unmistakable. Clearly, the assumption that *s* is small for non-polarized germanium electrodes is not generally valid. The experimental results reported herein emphasize the importance of taking into account thermal generation and recombination of carriers when considering electrochemical reactions at semiconductor surfaces.

THE STRUCTURE OF TARTAR EMETIC AND EVIDENCE OF THE EXISTENCE OF PENTAVALENT ANTIMONY AS [Sb(OH)]⁺

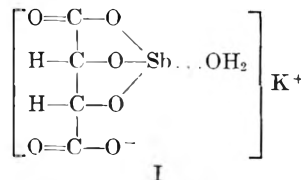
BY EFTHIMIOS CHINOPOROS AND NICHOLAS PAPATHANASOPOULOS¹

Suffolk University, Boston, Mass.

Received March 22, 1961

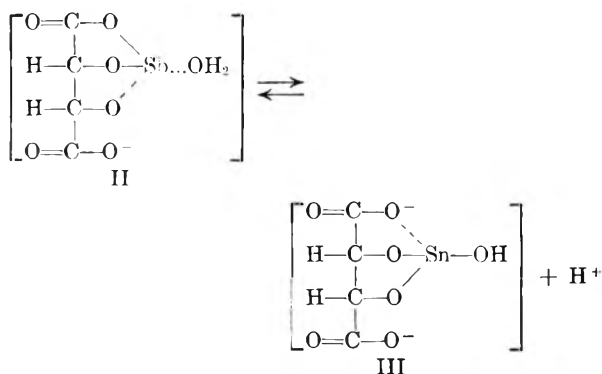
The structural formula of tartar emetic has been a much debated subject, and two types of formulas have been propounded. The advocates of the first type² maintain that the antimonyl

group is bound to the organic residue by replacing a hydrogen atom either of the hydroxyl group or the carboxyl group of tartaric acid, whereas those believing in the second type³ insist that the antimonyl group is bound to the oxygen of both carboxyl groups. Finally a formula (I) was proposed⁴ in which the antimony is bound to the oxygens of both hydroxyl groups and one in the carboxyl group.



The reaction of tartar emetic with mercuric ions was reported in a recent paper.⁵ A further study of this reaction led us to believe that formula (I) truly represents the structure of tartar emetic.

According to Reihlen⁴ tartar emetic in water dissociates as



This equilibrium explains the acidity of the solution. The addition of mercuric ions to a solution of tartar emetic precipitated a compound with the formula C₄H₃HgO₇Sb, which suggests a mercury salt with an organic residue of the structure III.

Since solutions of tartar emetic do not form a complex with cupric ions, it is indicated that the alcoholic hydroxyls of the tartrate are bound with the antimony, as in structures II and III. When the above-mentioned salt of mercury reacted with potassium hydroxide, mercury was precipitated as the metal and pentavalent antimony was isolated as sodium antimonate [NaSb(OH)₆]. This reaction suggests that the antimony in the group >Sb-OH of structure III was oxidized to pentavalent antimony in the form [Sb(OH)]⁺ which hydrolyzed to antimonate ions. The same salt precipitated from anhydrous solvents, when reacting with pyridine, gave also metallic mercury and pentavalent antimony ions which were not isolated as such.

Solutions of tartar emetic have a greater molecular rotation than those found for potassium tartrate.⁶ This shows that the antimony does not exist as antimonyl ions (SbO⁺), but rather is firmly bound with the tartar residue. Also the

(3) E. Jordis, *Z. angew. Chem.*, **15**, 909 (1902).

(4) H. Reihlen and E. Hegel, *Ann.*, **487**, 213 (1931).

(5) E. Chinoporos, *Anal. Chem.*, **32**, 1364 (1960).

(6) L. Kahlenberg, *Z. physik. Chem.*, **17**, 605 (1895).

(1) 7 Anderson Street, Boston 14, Mass.

(2) E. Jungfleisch, *Bull. soc. chim.*, [2] **40**, 98 (1883).

reaction of antimony trioxide with α -hydroxy acids^{7,8} and its failure to react with β -hydroxy acids^{7,8} and α -chloro acids⁹ confirms that the antimony in tartar emetic is bound to both hydroxyls and to the carboxyl group.

(7) B. Moritz and C. Schneider, *ibid.*, **41**, 129 (1902).

(8) G. G. Henderson and D. Prentice, *J. Chem. Soc.*, **67**, 1030 (1895).

(9) E. Jordis and W. Meyer, *Z. angew. Chem.*, **17**, 169 (1904).

THE IONIZATION CONSTANTS OF 2-THIOPHENE-*trans*-ALDOXIME AND 2-FURAN-*trans*-ALDOXIME

BY S. G. TANDON¹

Contribution Number 466 from the National Chemical Laboratory,
Poona, India

Received March 22, 1961

2-Thiophene-*trans*-aldoxime² and 2-furan-*trans*-aldoxime³ are useful reagents for the gravimetric determination of palladium. The present investigation deals with the determination of their thermodynamic ionization constants, pK . These data are of importance in various analytical procedures and in the elucidation of the structure of their metal complexes.

A survey of literature revealed that absorption spectrophotometry provides elegant and accurate means of determining the pK values.^{4,5} The method is suited particularly to these reagents which are weak organic acids and are sparingly soluble in water.

Experimental

Apparatus.—Measurements were made on Beckman Model DU and automatic ratio recording Model DK-2 quartz spectrophotometers, the same matched pair of 10 mm. quartz cells being used throughout. The instruments were calibrated according to the procedure recommended by Ewing and Parsons.⁶ The pH measurements were made at $25.0 \pm 0.01^\circ$ with a glass electrode in an atmosphere of nitrogen gas on a specially fabricated unit employing a Leeds and Northrup vernier potentiometer in conjunction with an Osram ET-3 valve. The accuracy of pH measurements was 0.01 of pH unit. All measurements were made in an air-conditioned room maintained at 25° . Graduated apparatus of standard calibration was used for measurements.

Reagents.—2-Thiophene-*trans*-aldoxime and 2-furan-*trans*-aldoxime were prepared by the methods of Tandon and Bhattacharya² and Brady and Goldstein,⁷ respectively. These were recrystallized twice from 30% ethyl alcohol as white needle shaped crystals and were vacuum dried; m.p. for the former 132.0 to 132.5 and for the latter, 92.0 to 92.5° . The solubility of 2-thiophene-*trans*-aldoxime and 2-furan-*trans*-aldoxime in water is 2.26 ± 0.02 and 17.0 ± 0.1 grams per liter, respectively, at 30° . Stock solutions of these acids for spectroscopic measurements were prepared in carbon dioxide-free distilled water. Other reagents used were of analytical grade.

Experimental Procedure.—The samples for absorption measurements were prepared by diluting an aliquot volume of a stock solution of the organic acid in water with a suitable

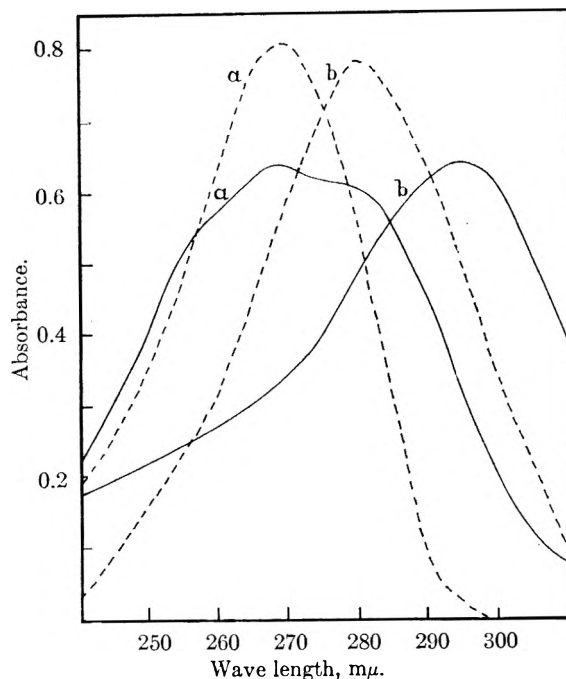


Fig. 1.—Absorption spectra of $5.02 \times 10^{-5} M$ 2-thiophene-*trans*-aldoxime (—) and $4.25 \times 10^{-5} M$ 2-furan-*trans*-aldoxime (-----) in (a) 0.1 N HCl solution and (b) 0.1 N NaOH solution.

volume of acid, alkali or buffer solution as required. The ionic strength was adjusted at 0.1 mole per liter by adding potassium chloride solution. The spectrum of each sample was measured from 220 to 320 $m\mu$ against a reference having the same composition except for the organic acid. The same supply of the distilled water was used to make up all other volumetric solutions of the series. Conformity to Beer's law in solutions of different pH at selected wave lengths was established for the relevant concentration range. At least three series of measurements were made for each acid. pH was measured immediately after absorbance measurements.

Results

The absorption spectra of the two acids in aqueous acid and alkali are presented in Fig. 1. 2-Thiophene-*trans*-aldoxime is characterized by maxima at 268 $m\mu$ (molar absorbance index, ϵ 12,750 l./mole cm.) and 294 $m\mu$ (ϵ 12,750) in acid and alkaline solutions, respectively, with isosbestic point at 284.5 $m\mu$ (ϵ 11,100). 2-Furan-*trans*-aldoxime has maxima at 269 $m\mu$ (ϵ 18,900) in acid solution and at 280 $m\mu$ (ϵ 18,500) in alkaline solution with isosbestic point at 275 $m\mu$ (ϵ 16,750).

Thermodynamic ionization constants were calculated at selected wave lengths from the equation

$$pK = pH + \log \frac{A_{NaOH} - A_B}{[A_B] - A_{HCl}} - \log \gamma_{A^-}$$

where A_{NaOH} , A_{HCl} and A_B are the observed absorbances in 0.1 N NaOH, 0.1 N HCl and buffered solutions, respectively. Here pK is the negative logarithm of the thermodynamic ionization constant for the equilibrium $HA \rightleftharpoons H^+ + A^-$, and γ_{A^-} is the activity coefficient of the acid anion. The value of $\log \gamma_{A^-}$ at 25° was calculated from the modified form of Davies' equation⁸ $-\log \gamma_{A^-} = AZ^2\sqrt{I}/[1] + \sqrt{I} - 0.2I$, where Z is the valency of

(8) R. A. Robinson, M. M. Davis, M. Paabo and V. E. Bower, *J. Research Natl. Bur. Standards*, **64A**, 347 (1960).

(1) Department of Chemistry, Mahakoshal Mahavidyalaya, Jabalpur.

(2) S. G. Tandon and S. C. Bhattacharya, *Anal. Chem.*, **32**, 194 (1960).

(3) J. R. Hayes and G. C. Chandlee, *ibid.*, **14**, 491 (1942).

(4) R. A. Robinson and A. I. Biggs, *Trans. Faraday Soc.*, **51**, 901 (1955).

(5) H. S. Harned and B. B. Owen, "The Physical Chemistry of Electrolytic Solutions," Reinhold Publ. Corp., New York, N. Y., 1950, p. 502.

(6) G. W. Ewing and T. Parsons, Jr., *Anal. Chem.*, **20**, 423 (1948).

(7) O. L. Brady and R. F. Goldstein, *J. Chem. Soc.*, **130**, 1961 (1927).

acid anion (equal to unity in the present study), I is the ionic strength of the medium and A is a constant whose value is 0.5115.⁹

The experimental results are given in Tables I and II. The average pK values of 2-thiophene-*trans*-aldoxime and 2-furan-*trans*-aldoxime are 10.76 ± 0.02 and 11.16 ± 0.02 , respectively. Thermodynamic ionization constants of these oximes do not seem to have been reported in the literature. Brady and Chokshi,¹⁰ however, measured the apparent ionization constant of 2-furan-*trans*-al-

doxime by a distribution method and reported pK (apparent) to be 10.82 at 25°.

Acknowledgments.—The author is indebted to the Director, National Chemical Laboratory, Poona, for permitting him to work as guest chemist. He wishes to thank Dr. S. C. Bhattacharya for his interest and assistance with this work.

RADIATION INDUCED IONIC POLYMERIZATION OF BUTADIENE

BY YONEHO TABATA, HIROSHI SOBUE AND EISUKE ODA

Department of Applied Chemistry, Faculty of Engineering, University of Tokyo, Tokyo, Japan

Received March 23, 1961

Although most radiation-induced vinyl polymerizations are known to proceed by a free radical mechanism there is evidence¹ that irradiation of some monomers at low temperatures leads to polymerization by an ionic mechanism.

Chapiro² found that butadiene is slowly polymerized by ionizing radiation. Recently, Anderson³ reported that electron irradiation of butadiene leads to polymerization by an ionic mechanism; his work was done largely with the monomer in the liquid phase. We have investigated the radiation-induced polymerization of both liquid and solid butadiene; the temperatures ranged from -20 to -196°.

The butadiene monomer was distilled into 15-ml. ampoules cooled to -78°, and the ampoules were evacuated to 10^{-2} - 10^{-3} mm. The polymerization, which was initiated by irradiation with Co^{60} γ -rays, was carried out at a dose rate of 6×10^4 to 3.2×10^5 r./hr. To determine the yields of polymer, the irradiated samples were opened at -78°, benzene was added, the monomer and benzene were evaporated and the polymer residue weighed. Viscosities in benzene at 25° and infrared spectra were measured.

For the liquid state polymerization, the relation between the yield of polymer and the irradiation dose is shown in Fig. 1. It is obvious from the figure that the polymerization is not preceded by an induction period. The yield of polymer increased with decreasing temperature in the liquid state polymerization. From an Arrhenius plot of the logarithmic rate against the reciprocal absolute temperature we obtained a value for the over-all energy of activation of about -0.4 kcal./mole. An activation energy of -0.3 kcal./mole can be calculated from Anderson's experimental results. Magat^{4c} has reported that a negative activation energy was obtained in the polymerization by Grosmanigin.

The yield of polymer decreased very slightly with decreasing temperature in the solid state polymerization and the over-all energy activation is a

- (1) (a) W. N. T. Davison, S. H. Pinner and R. Worrall, *Chemistry and Industry*, 1274 (1957); (b) W. J. Burlant and D. H. Green, *J. Polymer Sci.*, **31**, 227 (1957); (c) M. Magat, *Makromol. Chem.*, **35**, 159 (1960); (d) E. J. Lawton, W. T. Grubb and J. S. Balwit, *J. Polymer Sci.*, **19**, 445 (1956); (e) H. Sobue and Y. Tabata, *ibid.*, **43**, 459 (1960); (f) Y. Tabata, E. Oda and H. Sobue, *ibid.*, **45**, 469 (1960)
 (2) A. Chapiro, *J. chim. phys.*, **47**, 764 (1950).
 (3) W. S. Anderson, *J. Phys. Chem.*, **63**, 765 (1959).

TABLE I

IONIZATION CONSTANT OF 2-THIOPHENE-*trans*-ALDOXIME^a AT 25°

Buffer	pH	A_B	$\log \frac{A_{NaOH} - A_B}{A_B - A_{HCl}}$	pK
Series I: 291 m μ , $A_{NaOH} = 0.636$, $A_{HCl} = 0.410$				
a	10.60	0.517	0.046	10.75
b	10.77	.536	-.100	10.77
c	10.88	.548	-.195	10.79
d	10.97	.559	-.287	10.79
Series II: 293 m μ , $A_{NaOH} = 0.640$, $A_{HCl} = 0.355$				
a	10.60	0.493	0.027	10.73
b	10.77	.517	-.120	10.75
c	10.88	.530	-.202	10.78
d	10.97	.549	-.329	10.74
Series III: 296 m μ , $A_{NaOH} = 0.636$, $A_{HCl} = 0.288$				
a	10.60	0.452	0.050	10.75
b	10.77	.485	-.116	10.76
c	10.88	.506	-.225	10.76
d	10.97	.523	-.318	10.76
Series IV: 300 m μ , $A_{NaOH} = 0.587$, $A_{HCl} = 0.201$				
a	10.60	0.378	0.072	10.78
b	10.77	.417	-.104	10.77
c	10.88	.439	-.206	10.78
d	10.97	.460	-.310	10.76

Av. pK 10.76, $K = 1.74 \times 10^{-11}$

^a The molarity of 2-thiophene-*trans*-aldoxime was $5.02 \times 10^{-3} M$ throughout; $-\log \gamma_{A^-} = 0.103$.

TABLE II

IONIZATION CONSTANT OF 2-FURAN-*trans*-ALDOXIME^a AT 25°

Buffer	pH	A_B	$\log \frac{A_{NaOH} - A_B}{A_B - A_{HCl}}$	pK
Series I: 281 m μ , $A_{NaOH} = 0.780$, $A_{HCl} = 0.458$				
a	10.62	0.540	0.466	11.19
b	10.91	.590	.158	11.17
c	10.98	.605	.076	11.16
Series II: 284 m μ , $A_{NaOH} = 0.747$, $A_{HCl} = 0.300$				
a	10.62	0.413	0.471	11.19
b	10.91	.490	.131	11.14
c	10.98	.504	.076	11.16
Series III: 287 m μ , $A_{NaOH} = 0.690$, $A_{HCl} = 0.165$				
a	10.62	0.307	0.431	11.15
b	10.91	.390	.125	11.14
c	10.98	.407	.068	11.15

Av. pK 11.16, $K = 6.92 \times 10^{-12}$

^a The molarity of 2-furan-*trans*-aldoxime was $4.25 \times 10^{-3} M$ throughout; $-\log \gamma_{A^-} = 0.103$.

(9) R. A. Robinson and R. H. Stokes, "Electrolyte Solutions," Academic Press, Inc., New York, N. Y., 2nd ed., 1959, app. 7.1, p. 468.
 (10) O. L. Brady and N. M. Chokshi, *J. Chem. Soc.*, 946 (1929).

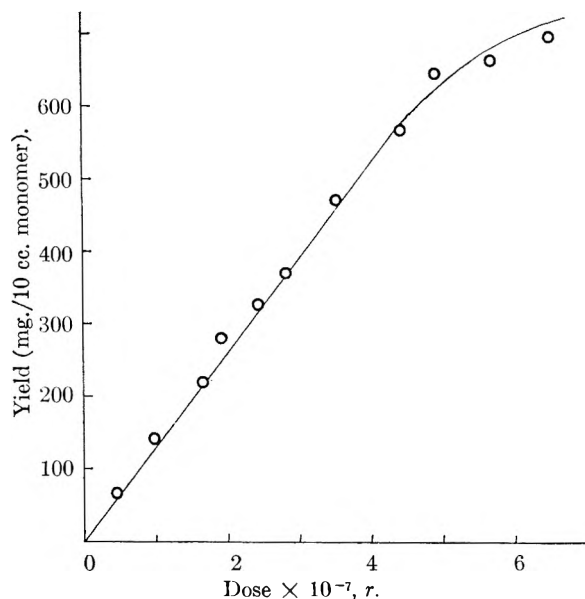


Fig. 1.—The relation between the yield of polymer and the radiation dose in the liquid phase polymerization at a dose rate of 3.2×10^5 r./hr. and temperature of -78° .

very small positive value (about 0.1 kcal./mole).⁴

The effect of the polymerization temperature on the viscosity of the polymer is shown in Table I.

TABLE I

THE RELATION BETWEEN VISCOSITY AND POLYMERIZATION TEMPERATURE (dose rate = 3.2×10^5 r./hr.).

Polymerization temp., $^\circ\text{C}$.	Dose $\times 10^{-7}$, r.	Intrinsic viscosity in benzene, dl./g.
-20	2.4	0.11
-45	1.9	.12
-78	2.8	.18
-196	1.8	.46
-196	1.4	.39 ^a

^a This sample was prepared by γ -irradiation of the monomer in a metal tube at atmospheric pressure.

The table shows that the molecular weight of the polymer increases gradually with decreasing temperature in the liquid state polymerization. The molecular weight of the polymer obtained in the solid state polymerization is much greater than that of the polymers prepared by liquid state polymerization.

Polymer samples, prepared at polymerization temperatures ranging from -20 to -196° , gave almost identical infrared absorption spectra. It was estimated from the spectrum that 67% of the double bonds are due to *trans*-1,4-monomer units and 32% to vinyl groups, a result similar to that reported by Anderson.³ The absorption band at 750 cm^{-1} , which is associated with *cis*-1,4 units, was not observed.

Cationic polymerizations are generally characterized by negative temperature coefficients⁵ which can be accounted for on the basis of a zero energy of activation of the initiation process and an activation energy of the termination process greater than that of the propagation step. The radical propagation of butadiene requires a large positive

activation energy,⁶ as do radical polymerizations in general which have activation energies for the propagation step ranging from about 6 to 10 kcal./mole, values larger than those of the termination process. Our finding that the radiation-induced polymerization rate of the liquid monomer at relatively low temperatures increases with decreasing temperatures (activation energy = -0.4 kcal./mole), indicates, therefore, that the reaction proceeds by an ionic mechanism as reported by Anderson.³

On the other hand, the polymerization rate of the solid monomer decreases slightly with decreasing temperature, a finding which might suggest that the liquid and solid state polymerizations have different propagation and termination mechanisms, even if the polymerizations proceed by the same ionic mechanism. For a cationic mechanism, the activation energy of the propagation step is thought to be zero in a liquid phase polymerization; the approach of a carbonium ion to a system of closed electronic shells of a molecule involves no energy barrier in the case of a liquid state polymerization. Although the solid monomer would polymerize in an extremely rigid state, the monomer molecule must move or rotate somewhat in order to polymerize in the propagation step. Mobility of the monomer in the solid state would be increased by the heat produced in the exothermic propagation step and also by an increase in the polymerization temperature. Thus, the small positive activation energy of the solid state polymerization is not inconsistent with an ionic reaction mechanism. Apparently the over-all propagation step has a small positive activation energy which can be explained by the temperature dependency of the mobility of the monomer molecule.

In previous papers,^{1e,f} we reported activation energies of about 0.4 and 0.3 kcal./mole, respectively, for the radiation-induced, solid state polymerizations of acrylonitrile and methacrylonitrile. These activation energies, which are small in comparison with the values estimated for the liquid state polymerizations (5 kcal./mole for acrylonitrile and 6.3 kcal./mole for methacrylonitrile), led us to conclude that these solid state polymerizations proceed by an ionic mechanism. In the case of butadiene also, the solid state polymerization has a small positive activation energy, much smaller than the values typical for free radical polymerizations. We conclude, therefore, that the solid state polymerization proceeds by an ionic mechanism.

To obtain a high molecular weight polymer at a fast rate by the homogeneous radical polymerization of butadiene, a very high temperature must be used.⁷ However in radiation-induced polymerization, the viscosity of the polymer increases with decreasing temperature in the liquid state polymerization, and the highest molecular weights were obtained at -196° in the solid state polymerization. This is further evidence that a non-radical mechanism is operating in the solid state poly-

(4) Polymerization rate were measured at $-130 \pm 3^\circ$ and at -196° .

(5) C. S. Marvel, et al., *J. Polymer Sci.*, **6**, 483 (1951).

(6) M. Morton, P. P. Salatiello and H. Landfield, *ibid.*, **8**, 279 (1952).

(7) C. E. Schildknecht, "Vinyl and Related Polymers," John Wiley and Sons, Inc., New York, N. Y., 1957, p. 208.

merization. The fact that the highest molecular weight products were obtained in the solid state polymerization probably is due to the longer lifetime of ions in the solid phase.

Oxygen, DPPH and pyrogallol are known to inhibit or retard free radical polymerizations but do not effect ordinary ionic polymerizations. The radiation-induced polymerization of butadiene was not inhibited by oxygen or DPPH.

Acknowledgment.—The authors are greatly indebted to the Ministry of Education of Japan for financing this research. The authors wish to express their thanks to Dr. Weissberger for the preparation of the manuscript.

EXTRACTION OF TRACER QUANTITIES OF URANIUM(VI) FROM NITRIC ACID BY TRI-*n*-BUTYL PHOSPHATE¹

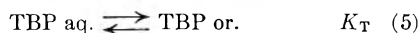
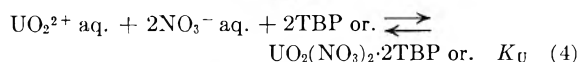
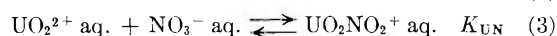
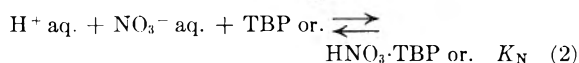
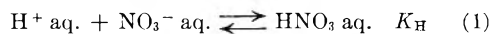
BY Y. MARCUS

Israel Atomic Energy Commission Laboratories, Rehovoth, Israel

Received March 24, 1961

The thermodynamic equation relating D_U , the distribution coefficient of uranium(VI) tracer between tri-*n*-butyl phosphate (TBP) in an inert diluent and nitric acid, to the concentrations of nitric acid and TBP, C_H and C_T , may be evaluated quantitatively as shown below.

The calculations are an extension of the ideas put forward by Hesford and McKay² to describe the extraction of nitrates at tracer concentrations by TBP. The following chemical reactions describe the system adequately in the range of 0–7 *M* nitric acid and 0–1 *M* TBP.



The symbols are the thermodynamic equilibrium constants. The distribution coefficient will be given by the equation

$$D_U = [UO_2(NO_3)_2 \cdot 2TBP] \text{ or.} / ([UO_2^{2+}] \text{ aq.} + [UO_2NO_3^+] \text{ aq.})^{-1} = K_U [NO_3^-]_{\text{aq.}}^2 y_{\pm U}^3 [TBP]^2 \text{ or.} y_T^2 y_{UT}^{-1} (1 + K_{UN} [NO_3^-]_{\text{aq.}} y_{\pm U}^3 y_{\pm UN}^{-2})^{-1} \quad (6)$$

Ordinary brackets denote molar concentrations, y denotes the various activity coefficients on the molar scale, $y_{\pm U}$ for uranyl nitrate and $y_{\pm UN}$ for $UO_2NO_3^+NO_3^-$, both as tracers in nitric acid, y_T for TBP and y_{UT} for $UO_2(NO_3)_2 \cdot 2TBP$ or. Values of $[NO_3^-]_{\text{aq.}} = f(C_H)$ at 25° are obtainable from the work of Krawetz.³

Values of $y_{\pm U}$ are available directly only for high

(1) Cf. Y. Marcus, Israel AEC Report IA/582, 1960.

(2) E. Hesford and H. A. C. McKay, *Trans. Faraday Soc.*, **54**, 573 (1958).

(3) A. A. Krawetz, quoted by T. F. Yound, *et al.*, in "The Structure of Electrolytic Solutions," W. J. Hamer, Editor, John Wiley and Sons, Inc., New York, N. Y., 1959, p. 42.

nitric acid concentrations.⁴ Jenkins and McKay⁴ applied the Harned rule expression

$$\log y_{\pm U} = \log y_{\pm U}^0 - 2\alpha_U I \quad (7)$$

where $y_{\pm U}^0$ is the activity coefficient of pure uranyl nitrate solutions at the same ionic strength I as those of the other nitrate, to various electrolytes. They presented data of $\alpha_U = f(I)$ for lithium, sodium, ammonium and potassium nitrates, and within a short concentration range also for nitric acid. In the regions of overlapping I the curves are reasonably parallel. The curve for nitric acid may therefore be extrapolated and values of $y_{\pm U}^0$ obtained for low nitric acid concentrations. As $|\alpha_U| < 0.01$ in the range of extrapolation, $y_{\pm U}^0$ is not sensitive to errors in α_U . This is important since $y_{\pm U}^0$ appears to the third power in eq. 6.

The concentration of free TBP, $[TBP]_{\text{or.}}$, changes with nitric acid concentration

$$[TBP]_{\text{or.}} = C_T (1 + K_N [NO_3^-]_{\text{aq.}}^2 y_{\pm H}^2 y_{HT}^{-1})^{-1} = C_T F_T^{-1} \quad (8)$$

where $y_{\pm H}$ is the mean ionic activity coefficient for nitric acid and y_{HT} the activity coefficient of $HNO_3 \cdot TBP$ or. Data for $F_T = f(C_H)$ are given by Hesford and McKay² at 25°. Although they allow y_T and y_{HT} to vary individually with C_H and C_T , their ratio is assumed constant and $K_N y_T y_{HT}^{-1} \approx 0.16 \text{ l.}^2 \text{ mole}^{-2}$. It may be assumed similarly that the ratio $y_T y_{UT}$ does not vary with C_H and C_T . These assumptions amount to ascribing the same salting coefficient to all three species in the organic phase TBP, $HNO_3 \cdot TBP$ and $UO_2(NO_3)_2 \cdot 2TBP$.

To evaluate the function $F_N = (1 + K_{UN} [NO_3^-]_{\text{aq.}} y_{\pm UN}^3 y_{\pm UN}^{-2}) = f(C_H)$, K_{UN} and $y_{\pm UN}$ must be known. A value of $K_{UN} = 0.2 \text{ l. mole}^{-1}$ was selected, as implicitly suggested by Hesford and McKay,² and since $UO_2NO_3^+NO_3^-$ is a trace 1:1 electrolyte in nitric acid, its activity coefficient was taken to be equal to that of nitric acid, $y_{\pm H}$. The values of F_N are not strongly affected by this assumption concerning $y_{\pm UN}$ up to 7 *M* nitric acid.

Finally y_T was calculated from measurements of the distribution coefficient, D_T , of labelled TBP between the inert diluent and aqueous nitric acid.

$$y_T = K_T F_T D_T^{-1} \quad (9)$$

assuming the aqueous solutions of TBP to be ideal. Published values were used for kerosene diluent,⁵ while some values for dodecane, measured in a similar way in this Laboratory, are reported below.

When all these data are introduced into eqn. (6), it becomes

$$D_U = K_U' C_T^2 [NO_3^-]_{\text{aq.}}^2 y_{\pm U}^3 (F_N F_T D_T)^{-1} \quad (10)$$

where $K_U' = K_U K_T y_T y_{UT}^{-1}$. K_U' is assumed constant, but depends on the diluent. F_T , F_N and $y_{\pm U}^0$ depend only on C_H , while D_T depends on both C_H and C_T . These functions, calculated as described above, are shown in Figs. 1 and 2. Curves $D_U = f(C_H)_{C_T}$, calculated according to eq. 10 using these data, $K_U' = 5.6 \times 10^4 \text{ l.}^4 \text{ mole}^{-4}$ for kerosene and $K_U' = 2.5 \times 10^4 \text{ l.}^4 \text{ mole}^{-4}$ for dodecane dil-

(4) I. L. Jenkins and H. A. C. McKay, *Trans. Faraday Soc.*, **50**, 107 (1954).

(5) K. J. Alcock, S. S. Grimley, T. V. Healy, J. Kennedy and H. A. C. McKay, *Trans. Faraday Soc.*, **52**, 39 (1956).

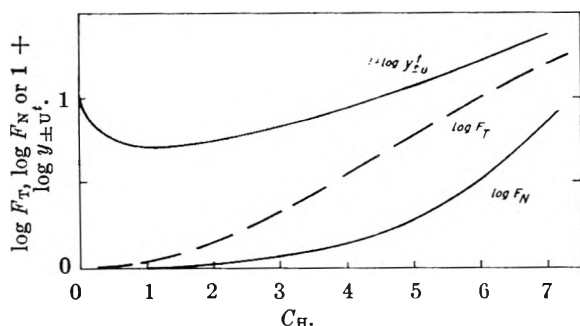


Fig. 1.—The dependence of the auxiliary data F_T , F_N and $y_{\pm v}^t$, on the nitric acid concentration in the aqueous phase, C_H .

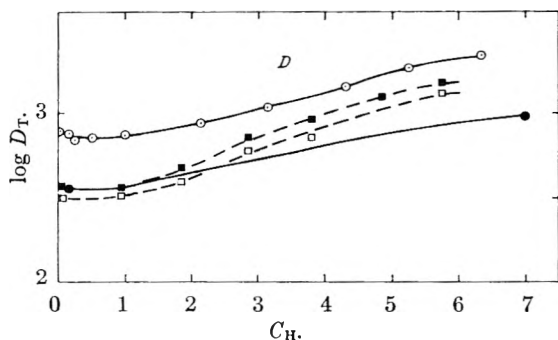


Fig. 2.—The distribution coefficient of TBP, $\log D_T$, as function of the nitric acid concentration in the aqueous phase, C_H : \circ , 20% TBP in kerosene⁵; \bullet , 5% TBP in kerosene⁵; \square , 12% TBP in dodecane; \blacksquare , 18% TBP in dodecane (this work).

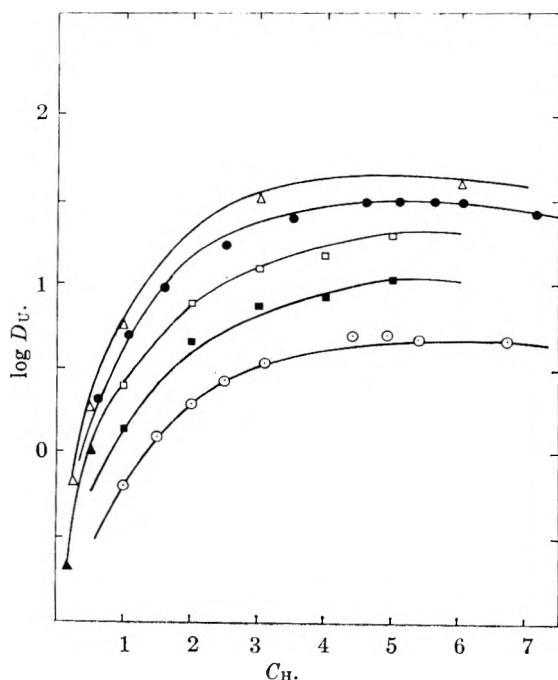


Fig. 3.—The distribution coefficients of uranium(VI) tracer between nitric acid and TBP in inert diluents: \bullet , 19% TBP in kerosene⁵; \circ , 4.8% TBP in kerosene⁵; Δ , 25% TBP in kerosene⁷; \blacktriangle , 15% TBP in kerosene⁷; \square , 18% TBP in dodecane⁸; \blacksquare , 12% TBP in dodecane⁸. Solid lines are calculated from eq. 10.

uents, are shown in Fig. 3, where they are compared with experimental data from the literature.⁶⁻⁸ The agreement is seen to be satisfactory.

(6) K. J. Alcock, G. F. Best, E. Hesford and H. A. C. McKay, *J. Inorg. & Nuclear Chem.*, **6**, 331 (1958).

(7) C. J. Rodden, U.S.A.E.C. Report TID 10153 (1951).

(8) D. P. Ames and D. G. Karraker, U.S.A.E.C. Report DP 275 (1958).

THE KINETIC ORDER OF THE REACTION BETWEEN SODIUM NITRITE AND OXYGEN

BY DAVID A. ANDERSON AND ELI S. FREEMAN

Pyrotechnics Chemical Research Laboratory, Picatinny Arsenal, Dover New Jersey

Received March 25, 1961

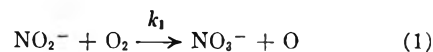
In a previous investigation Freeman¹ found that in the reaction between sodium nitrite and oxygen the order was unity with respect to the nitrite. The order of reaction with respect to oxygen was assumed to be unity; however, no experimental determination of the order was made. Since there is some question as to whether the rate-controlling reaction involves atomic oxygen resulting from dissociation on the surface of the molten salt or reaction between molecular oxygen and nitrite, experiments were carried out to clarify this point.

Experimental

The sodium nitrite and nitrate used were Fisher Scientific Company C.P. Grade materials. Approximately 430-mg. samples were heated in a Chevenard thermobalance at 450 and 480°. During the experimental runs mixtures of oxygen and nitrogen at a total pressure of one atmosphere were passed over the samples. The minimum purity of the gases is 99.6%. The concentration of oxygen was varied by pre-mixing with nitrogen. Both gases were passed through concentrated sulfuric acid prior to mixing. The flow rate of each was measured by a Matheson Company flowmeter as they passed to a mixing vessel and then through a flowmeter used to measure the rate of flow of the gases over the sample. The flow rate was maintained at a rate equivalent to 3×10^2 cc./min. of air. The partial pressure of oxygen varied from 0.25 to 1.0 atmosphere. A 28 gage Chromel-Alumel thermocouple located directly above the sample was used to measure temperature. A two-pen Leeds and Northrup Speedomax strip chart recorder recorded both changes in sample weight and temperature as a function of time.

Results and Discussions

Assuming that the reaction of nitrite and oxygen to form nitrate involves reactions (1), (2) and (3)



then the rate of nitrate formation may be given by the expression

$$\frac{\partial[\text{NO}_3^-]}{\partial t} = k_1[\text{NO}_2^-][\text{O}_2] + k_2[\text{O}][\text{NO}_2^-] \quad (4)$$

and

$$\frac{\partial[\text{O}]}{\partial t} = k_1[\text{NO}_2^-][\text{O}_2] - k_2[\text{O}][\text{NO}_2^-] - k_3[\text{O}]^2 \quad (5)$$

where k_1 , k_2 and k_3 are rate constants; $[\text{NO}_2^-] =$

(1) E. S. Freeman, *J. Phys. Chem.*, **60**, 1487 (1956).

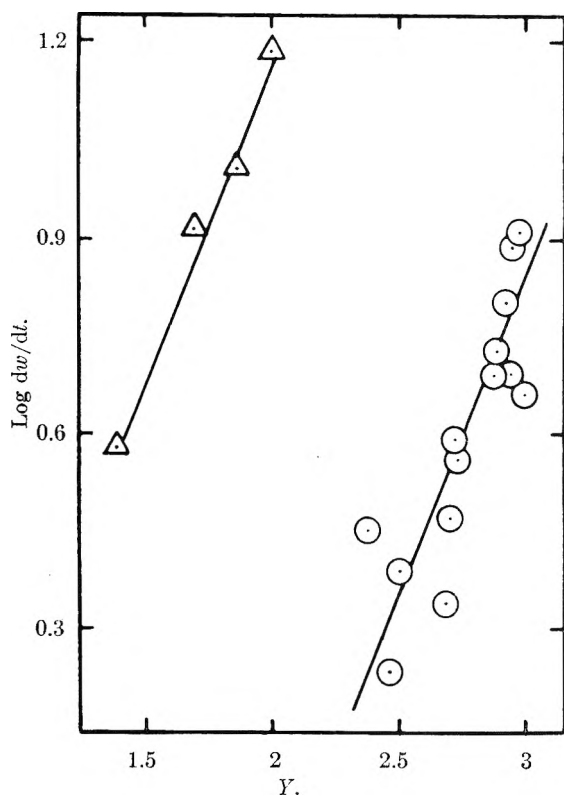


Fig. 1.—Plot of the logarithm of reaction rate as a function of $Y:Y$ (\circ), logarithm of nitrite mole fraction $\times 10^3$ at 0.50 atm. partial pressure of oxygen and 480° ; Y (Δ), logarithm of partial pressure of oxygen at 450° at 10% reaction.

mole fraction of nitrite; $[O_2]$ = concentration of O_2 on surface of melt; and $[O]$ = concentration of atomic oxygen.

Assuming a steady-state approximation for the rate of change of atomic oxygen then from equation 5.

$$[O] = \frac{k_1[NO_2^-][O_2]}{k_3[O] + k_2[NO_2^-]} \quad (6)$$

Substituting for $[O]$ in equation 4

$$\frac{\partial[NO_3^-]}{\partial t} = k_1[NO_2^-][O_2] \left(1 + \frac{k_2[NO_2^-]}{k_3[O] + k_2[NO_2^-]} \right) \quad (7)$$

If it is assumed that $k_3[O]$ is small compared to $k_2[NO_2^-]$ then

$$\frac{\partial[NO_3^-]}{\partial t} = k_1'[NO_2^-][O_2] \quad (8)$$

where

$$k_1' = 2k_1$$

The decomposition of sodium nitrate is neglected. It was determined experimentally that the rate of decomposition of the nitrate under the conditions of temperature and pressure used in these experiments was negligible compared to the rate of oxidation. If equation 8 is valid, plots of the log of the rate of reaction as a function of the log of the concentration of oxygen and of nitrite should give straight lines with slopes of unity.

Figure 1 shows the plot of the logarithm of the rate of reaction, as a function of the logarithm of the mole fraction of nitrite. Ideal behavior of these

salts is assumed. The partial pressure of oxygen was maintained at 0.5 atm. at a total pressure of one atmosphere. Reaction temperature is $480 \pm 1^\circ$. The slope of the line representing the order of reaction with respect to nitrite was found to be essentially unity in agreement with the previously reported results of Freeman¹ obtained by a different method.

Figure 1 also shows a graph of the logarithm of the rate of reaction as a function of the log of oxygen concentration at 450° . The points are taken from experiments conducted under partial pressures of oxygen ranging from 0.25 to 1.00 atmosphere, and at a given weight gain corresponding to a constant concentration of nitrite. The only variable is the partial pressure of oxygen. A linear plot is obtained. The order of reaction was calculated to be unity, indicating that the rate-controlling reaction is between nitrite ion and molecular oxygen presumably at the surface of the melt. It has been shown that varying the interface area¹ between the gaseous environment and the molten salt affects the reaction rate. This is evidence in support of the previously published hypothesis concerning the reaction mechanism.

ELECTROLYSIS WITH CONSTANT POTENTIAL: EFFECT OF DIFFUSION COEFFICIENTS ON REVERSIBLE REACTIONS AT A SPHERICAL ELECTRODE

BY IRVING SHAIN AND DANIEL S. POLCYN

Department of Chemistry, University of Wisconsin, Madison, Wis.

Received March 27, 1961

The use of stationary spherical electrodes in electrolysis experiments at constant potential has been suggested recently¹ as an unambiguous method of determining diffusion coefficients of electroactive materials. The equation describing the current-time curves obtained at potentials relatively far from the formal E^0 contains two terms: one time-dependent term containing $D_0^{1/2}$ and a time-independent term containing D_0 . Thus, values of the diffusion coefficient can be obtained from both the slope and the intercept of the i vs. $1/\sqrt{t}$ plot, and the effect of various other experimental parameters can be evaluated unambiguously.² The same approach can be extended to potentials closer to the formal E^0 , and, with somewhat decreased accuracy, the method can be used to determine the diffusion coefficients of the product of the electrode reaction.

For the case of a reversible reaction (in which both the reactant and product are soluble in the solution) taking place at potentials near the formal E^0 , the equation for the current-time curve has been reported as

$$i = \frac{nFAD_0C_0^*}{(1 + \gamma\theta)} \left[\frac{1}{(\pi D_0 t)^{1/2}} + \frac{1}{r_0} \right] \quad (1)$$

where the notation is that used previously.¹ This equation holds only when the diffusion coef-

(1) I. Shain and K. J. Martin, *J. Phys. Chem.*, **65**, 254 (1961).

(2) See D. J. Macero and C. L. Rulf, *J. Am. Chem. Soc.*, **81**, 2942 (1959), for a discussion of the interaction of these effects, particularly electrode area, on a plane electrode.

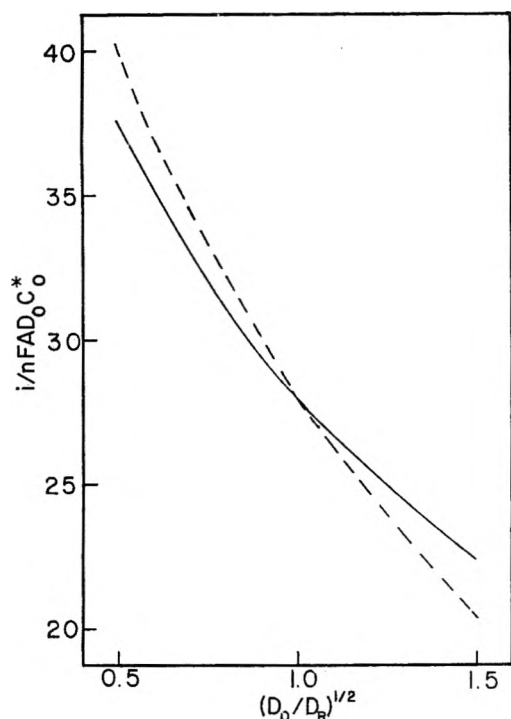


Fig. 1.—Effect of diffusion coefficients on current flowing 25 seconds after the start of electrolysis: ———, calculated from equation 1; - - - -, calculated from equation 3.

ficients of the reactant and product are equal, that is, when $\gamma = 1$. It is possible, however, to obtain a more general solution for this boundary value problem without making any assumption regarding the ratio of the diffusion coefficients. Conventional application of the Laplace transform³ leads to

$$i = nFAD_0C_0^* \left[\frac{1}{(1 + \gamma\theta)(\pi D_0 t)^{1/2}} + \frac{1}{(1 + \gamma^2\theta)r_0} + \frac{\theta(1 - \gamma)^2}{r_0(1 + \gamma\theta)^2(1 + \gamma^2\theta)} e^{\alpha^2 t} \operatorname{erfc} \alpha\sqrt{t} \right] \quad (2)$$

where

$$\alpha = \frac{1}{r_0} \left(\frac{D_R + \theta D_0}{\sqrt{D_R} + \theta \sqrt{D_0}} \right)$$

and all other terms are defined as in equation 1.

Substitution of typical numerical values for the various parameters into equation 2 indicates that for the times which are of interest in this method, the last term never amounts to more than a few tenths of a per cent. of the total current flowing. Thus, equation 2 reduces to

$$i = nFAD_0C_0^* \left[\frac{1}{(1 + \gamma\theta)(\pi D_0 t)^{1/2}} + \frac{1}{(1 + \gamma^2\theta)r_0} \right] \quad (3)$$

Equation 3 differs from equation 1 only in the spherical correction term, *i.e.*, the term in r_0 which corrects for the convergent nature of the electrode process. This term is not negligible, and can amount to as much as 10% of the total current flowing at times as short as 10 seconds. At longer times, this term becomes relatively more important. As a result of the linear dependence

of this term on D_0/D_R the measured currents can deviate significantly from those calculated from equation 1. This can be seen in Fig. 1, where the current flowing at 25 seconds after the start of the electrolysis as calculated from equation 1 is compared with that calculated from equation 3.

The normal analysis of current-time curves by equation 1, in which the current is plotted against $1/(t)^{1/2}$, results in lumping all uncertainties regarding the diffusion coefficients with the "formal" E^0 . If equation 3 is used, however, the slope of the i vs. $1/(t)^{1/2}$ plot is a function of $\gamma\theta$, while the intercept is a function of $\gamma^2\theta$. This permits a separation of these two parameters. Since an unambiguous value of D_0 for the same solution can be calculated by analyzing diffusion limited current-time curves obtained at very cathodic potentials, it is possible to calculate a reasonably accurate estimate of D_R .

Using the data of Martin,⁴ current-time curves for the reduction of titanium(IV) oxalato complex (0.2 M oxalic acid, 1% sulfuric acid) were analyzed using a least squares technique, and γ was calculated at several potentials near the formal E^0 (Table I).

TABLE I
ANALYSIS OF CURRENT-TIME CURVES FOR THE REDUCTION OF TITANIUM(IV) OXALATO COMPLEX

Potential (vs. S.C.E.)	$\gamma\theta$ (from slope)	$\gamma^2\theta$ (from intercept)	γ
-0.310	0.42	0.53	1.2 ₆
-0.290	0.89	1.2 ₆	1.4 ₂
-0.270	1.93	2.5 ₈	1.3 ₃
-0.250	4.30	5.8 ₀	1.3 ₅
		Av.	1.3 ₄

Combining this value of γ with the previously measured value of D_0 (0.61×10^{-5} cm.²/sec.), the value of D_R was calculated to be 0.34×10^{-5} cm.²/sec. The results indicate that the diffusion coefficient of the Ti(III) complex is less than that of the Ti(IV) complex, as was reported by Pecsok.⁵ However, the value of D_0 calculated previously¹ and the value of D_R calculated here are both lower than the values calculated from the diffusion current constants reported by Pecsok. It is felt that within the specified error limits, the values reported here are more reliable than those calculated from the Ilkovic equation. If the Lingane-Loveridge equation⁶ is used to calculate diffusion coefficients from Pecsok's data, the values are lower, but still somewhat higher than the values reported here.

The value of γ , which was obtained as indicated in Table I, then was used to calculate the formal E^0 from values of $\gamma\theta$ at several potentials. This value was calculated to be -0.280 v. vs. S.C.E.

This method of calculating D_R is not as accurate as the more direct measurement based on diffusion limited current-time curves obtained at potentials relatively far from E^0 . Nevertheless, this approach offers some important advantages when, as in this case, known solutions of the product of

(4) K. J. Martin, Ph.D. Thesis, University of Wisconsin, 1960.

(5) R. L. Pecsok, *J. Am. Chem. Soc.*, **73**, 1304 (1951).

(6) J. J. Lingane and B. A. Loveridge, *ibid.*, **72**, 438 (1950).

(3) R. V. Churchill, "Operational Mathematics," 2nd Ed., McGraw-Hill Book Co., New York, N. Y., 1958.

the electrode reaction cannot be prepared conveniently.

This work was supported in part by funds received from the United States Atomic Energy Commission, under Contract No. AT (11-1)-64, Project No. 17.

KINETIC STUDIES ON THE DECARBOXYLATION OF OXAMIC ACID IN DIMETHYL SULFOXIDE AND IN TRIETHYL PHOSPHATE

BY LOUIS WATTS CLARK

Department of Chemistry, Western Carolina College, Cullowhee, North Carolina

Received March 27, 1961

The results of kinetic studies on the decarboxylation of oxalic acid in various polar solvents have indicated that, in weakly basic solvents, unionized oxalic acid decomposes by a transition-complex mechanism.¹ In more strongly basic solvents primary ionization of the oxalic acid must occur, the acid oxalate anion then undergoing decarboxylation.² In the case of the unionized di-acid, a "supermolecule" cluster composed of several molecules of oxalic acid apparently takes part in the rate-determining step,³ whereas, in the reaction in ionizing solvents, the acid oxalate ion appears to be involved singly.⁴

Kinetic studies have been reported also on the decarboxylation of oxamic acid in several non-aqueous solvents.^{3,4} Since oxamic acid is a weaker acid than oxalic acid it does not ionize as readily. Also, having but one carboxyl group, it apparently does not form an association cluster, single molecules only participating in the rate-determining step. The reaction has been found to be reversible in the presence of aromatic amines.

In order to gain more information on this reaction, and especially in order to ascertain whether or not non-nitrogenous solvents are able to catalyze the reverse reaction, kinetic studies have been carried out in this Laboratory on the decarboxylation of oxamic acid in the solvents triethyl phosphate and dimethyl sulfoxide. Results of this investigation are reported herein.

Experimental

Reagents.—(1) The oxamic acid used in this investigation was analytical reagent grade, 100.0% assay. (2) Reagent grade triethyl phosphate was used. Further purification was effected by distillation of each sample at atmospheric pressure directly into the reaction flask immediately before the beginning of each experiment. (3) The dimethyl sulfoxide used in this research was 99.9% pure, the remainder being water. Distillation of this solvent was not feasible due to its instability at the boiling point.

Apparatus and Technique.—The kinetic experiments were conducted in a constant-temperature oil-bath by measuring the volume of CO₂ evolved at constant pressure, as described in a previous paper.⁵ In each experiment a 0.1585-g. sample of oxamic acid (the amount required to produce

40.0 ml. of CO₂ at STP on complete reaction) was introduced in the usual manner into the dried reaction flask containing a weighed sample of solvent saturated with dry CO₂ gas.

Results

The rate of decarboxylation of oxamic acid was measured in triethyl phosphate and in dimethyl sulfoxide over a temperature range of about 20°. At a fixed temperature no appreciable difference in the specific reaction velocity constant could be detected when the quantity of solvent was varied from 50 to 140 g. Generally about 130 g. of solvent was used in each experiment. Duplicate experiments were performed at each temperature. In every experiment 95% or more of the theoretical volume of CO₂ was collected. There was very little tendency for the reverse reaction to take place in either of these solvents as shown by the fact that, on allowing the system to remain intact overnight after decarboxylation was complete, a very few milliliters, if any, of the evolved CO₂ was resorbed. This was a marked contrast with the behavior of the system using aromatic amines as solvents. The amines acted as very strong catalysts for the reverse reaction.^{3,4}

The plot of $\log(V_{\infty} - V_t)$ vs. t was linear over nearly the entire experiment, indicating that the reaction is first order. The average rate constants calculated in the usual manner from the slopes of the logarithmic plots are shown in Table I. The parameters of the Eyring equation, based upon the data in Table I, are shown in Table II, along with those for the reaction in several other solvents previously investigated. Shown also for comparison are corresponding data for oxalic acid.

TABLE I
APPARENT FIRST-ORDER RATE CONSTANTS FOR THE DECARBOXYLATION OF OXAMIC ACID IN DIMETHYL SULFOXIDE AND IN TRIETHYL PHOSPHATE

Solvent	Temp. (°C. cor.)	$k \times 10^1$ (sec. ⁻¹)	Av. dev.
Dimethyl sulfoxide	140.14	1.87	±0.01
	150.72	6.10	± .01
	160.69	17.12	± .02
Triethyl phosphate	131.23	1.65	± .01
	138.20	4.01	± .02
	149.61	15.79	± .02

TABLE II
KINETIC DATA FOR THE DECARBOXYLATION OF OXAMIC ACID AND OXALIC ACID IN SEVERAL POLAR SOLVENTS^a

Solvent	—Oxamic acid—		—Oxalic acid—	
	ΔH^* (kcal./mole)	ΔS^* (e.u./mole)	ΔH^* (kcal./mole)	ΔS^* (e.u./mole)
Aniline ^{3,1}	59.7	+68.0	40.3	+16.2
Quinoline ^{4,1}	47.0	+37.5	38.9	+15.8
Triethyl phosphate ¹	40.9	+24.7	28.9	- 5.8
Dimethyl sulfoxide ¹	37.7	+14.9	40.6	+20.7
8-Methylquinoline ^{4,3}	36.0	+12.2	37.7	+13.7

^a The first superscript after the name of the solvent refers to the source of the oxamic acid data, the second to that of the oxalic acid data. For the solvents triethyl phosphate and dimethyl sulfoxide the single superscript refers to the source of the oxalic acid data.

Discussion of Results

The solvents listed in Table II are arranged in the order of decreasing activation energy for the

(1) L. W. Clark, *J. Phys. Chem.*, **61**, 699 (1957).

(2) L. W. Clark, *ibid.*, **62**, 633 (1958).

(3) L. W. Clark, *ibid.*, **65**, 180 (1961).

(4) L. W. Clark, *ibid.*, **65**, 659 (1961).

(5) L. W. Clark, *ibid.*, **60**, 1150 (1956).

oxamic acid reaction, and this corresponds also to the order of increasing nucleophilicity. This coincidence is good verification for the hypothesis that the rate-determining step of the reaction is the formation of a transition complex between solute and solvent.

The ΔH^* values for the oxalic acid reaction likewise decrease progressively on going from aniline to quinoline and from quinoline to triethyl phosphate—thus far in accord with theoretical predictions assuming a mechanism similar to that of the oxamic acid reaction. In each of these solvents, furthermore, the ΔH^* is higher for the oxamic acid reaction than it is for that of oxalic acid, a result which is consistent with the fact that the polarized carbonyl carbon atom of oxamic acid has a lower effective positive charge than does that of oxalic acid.² In each of these three solvents it will be observed, also, that the ΔS^* values for the oxamic acid reaction are higher than they are for that of oxalic acid in spite of the nearly equal sizes of the two acids. This circumstance has been attributed, previously, to the greater tendency of the dicarboxylic acid to associate through hydrogen-bonding to form a "supermolecule" cluster.²

In the solvents dimethyl sulfoxide and 8-methylquinoline the ΔH^* as well as the ΔS^* values for the oxalic acid reaction deviate abruptly from the regular order observed for the oxamic acid reaction (lines 4 and 5 of Table II). Evidence has been presented previously that in these two solvents primary ionization of the oxalic acid takes place, the acid oxalate ion, rather than the un-ionized di-acid, then undergoing decarboxylation.² The fact that, in these two solvents, the H^* values for the acid oxalate ion reaction are slightly higher than they are for that of oxamic acid is consistent with the difference in the relative acidities of these two species.⁴ It will be noted, also, that the S^* values of the acid oxalate ion reaction in these two solvents are slightly larger than those of oxamic acid—a result which is consistent with the difference in the relative sizes of the two species.

In quinoline, the enthalpy of activation for the decarboxylation of oxalic acid is about 8 kcal./mole higher than that of oxamic acid, whereas, in aniline, it is more than 19 kcal./mole higher (see Table II, lines 1 and 2). In view of the fact that these two amines do not differ appreciably in basicity (pK for aniline is 9.42, for quinoline 9.2),⁶ this abnormally high value of ΔH^* in the case of oxamic acid in aniline poses a problem. Inductive and steric effects noted in studies on the decarboxylation of oxamic acid in the two primary amines aniline and *o*-toluidine,³ as well as in the tertiary amines quinoline and 8-methylquinoline,⁴ were indicative of the formation of a transition complex involving coordination between acid and solvent. Apparently, however, in the case of primary amines, the orientation of solute molecules with respect to solvent must differ from that in the case of other nucleophilic sol-

vents. This circumstance may be connected with the structural relationship of oxamic acid to α -keto acids, for it has been observed that the decarboxylation of such acids is specifically catalyzed by primary amines.⁷ The fact that oxalic acid, itself a type of α -keto acid, does not show this same behavior may be attributed to its tendency to associate through hydrogen-bonding to form a "supermolecule" cluster.

Further work on this problem is contemplated.

Acknowledgment.—The support of this research by the National Science Foundation, Washington, D. C., is gratefully acknowledged.

(7) J. Hine, "Physical Organic Chemistry," McGraw-Hill Book Co., Inc., New York, N. Y., 1956, p. 288.

THERMOCHEMISTRY OF ZIRCONIUM HALIDES

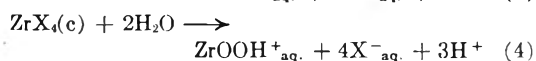
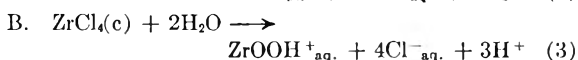
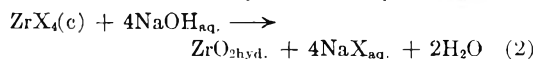
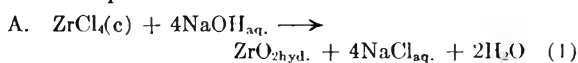
BY A. G. TURNBULL

*Division of Mineral Chemistry, Chemical Research Laboratories,
C.S.I.R.O. Australia*

Received April 1, 1961

Thermodynamic data for zirconium compounds are accurately known for the oxide and tetrachloride only.^{1,2} Development of a consistent set of heat of formation and free energy data would assist in understanding the reactions of ore extraction, metal reduction and Zr-Hf separation, and also promises to reinforce the still sketchy ideas on zirconium solution chemistry.

For the measurement of ΔH°_{298} of $ZrBr_4$ and ZrI_4 , the direct union of elements in a bomb calorimeter is difficult to initiate and complete. However values relative to those of ZrO_2 and $ZrCl_4$ may be obtained by suitable solution reactions. These two independent schemes were used



Such reactions went to completion in a few minutes at 25°, giving reproducible final states, and their validity was based on the recent systematic zirconium chemistry proposed by Blumenthal.³

Experimental

Heats of reaction were measured in a suitably thermostated Dewar vessel containing the glass sample bulb in 100 ml. of solution, glass stirrer, glass covered constantan heater and copper-constantan thermocouple. Temperature rise was amplified and recorded on a Leeds and Northrup Speedomax recorder at 4 in./hr.

The maximum sensitivity was 0.1 cal., while heats of reaction were 100–150 cal. Electrical calibrations before and after each reaction and for different fillings agreed within 0.5%, with power measured to 0.2%. To verify the absence of systematic errors, the heat of solution of

(1) F. D. Rossini, *et al.*, National Bureau of Standards Circular 500, 1952.

(2) P. Kubachewski and E. Evans, "Metallurgical Thermochemistry," 3rd Ed. Pergamon Press, New York, N. Y., 1958.

(3) W. B. Blumenthal, "The Chemical Behavior of Zirconium," D. Van Nostrand Co., New York, N. Y., 1959.

(6) N. A. Lange, "Handbook of Chemistry," 9th ed., Handbook Publishers, Inc., Sandusky, Ohio, 1956, p. 1204.

$\text{KNO}_3(\text{c})$ in 500 moles of water was measured to be 8.55 ± 0.1 kcal./mole in agreement with the best literature value of 8.56 kcal./mole.¹ The heat of breaking the evacuated sample bulbs was measured to be 0.3 cal., representing only 0.2% of the total heat evolution.

Samples of ZrBr_4 , ZrI_4 and HfCl_4 were made by halogenation of the pure metals in a silica tube at 500–700°. The ZrCl_4 was made by chlorination of zirconium carbide from zircon with a Hf/Zr weight ratio of 0.017. All halides were vacuum sublimed into thin Pyrex bulbs and the sample weight found by difference. The chlorides and bromides were pure white, crystalline solids and it has been amply shown that such a preparation leads to the formula MX_4 .³ The iodide was pale orange-brown of formula ZrI_4 within analytical accuracy (calcd. Zr 15.23%, found 15.18%). Spectrographic analysis of the Hf metal showed only 0.06% total impurity (apart from 2.4% Zr) and the "reactor grade" Zr metal had the same order of purity, so that no correction of reaction heats for impurities was warranted.

Results

A. Reaction with NaOH.—The solid halides were treated with a small excess of aqueous NaOH, using a halide to water molar ratio of 1:1500. No dependence on sample weight was observed, as expected at such high dilution. The product was pulpy white hydrated ZrO_2 in all cases. It was verified by separate measurements that the effect of the small excess of NaOH on ΔH_{298} of the NaX product was negligible. Also the solubility of ZrO_2 in the excess NaOH was extremely small.⁴

Since the Zr contained 1.7% Hf and the Hf contained 2.4% Zr, it was possible to solve simultaneous equations and find the heats of reaction of the pure tetrachlorides. The correction was negligible for ZrCl_4 and only 0.3 kcal./mole for HfCl_4 . The elements are so similar that any heat of mixing should be quite negligible. Values of ΔH for reactions 1 and 2 are given in Table I. Beck⁵ treated ZrCl_4 with $\text{NH}_4\text{OH}(\text{aq})$, but his single value of -54.3 kcal./mole apparently is in error. Combination of reaction heats with values of ΔH_{298}^0 for $\text{NaOH}(\text{aq})$, $\text{NaCl}(\text{aq})$, $\text{NaBr}(\text{aq})$ and $\text{NaI}(\text{aq})$ ¹ and the latest value for $\text{ZrCl}_4(\text{c})$ of 234.7 \pm 0.4 kcal./mole⁶ led to values of ΔH_{298}^0 for $\text{ZrBr}_4(\text{c})$, -182.2 ± 0.7 kcal./mole and $\text{ZrI}_4(\text{c})$ -115.6 ± 0.8 kcal./mole.

TABLE I

Material	HEATS OF REACTION	
	NaOH aq. $-\Delta H$ (kcal./mole)	H_2O $-\Delta H$ (kcal./mole)
$\text{Zr}(1.7\% \text{ Hf})\text{Cl}_4(\text{c})$	103.2, 102.1, 102.8	59.1, 59.3, 58.5
$\text{ZrCl}_4(\text{c})$	102.7	59.0
$\text{ZrBr}_4(\text{c})$	110.4, 110.7, 111.3	68.6, 69.0, 68.6
$\text{ZrI}_4(\text{c})$	114.6, 115.2, 115.8	70.5, 71.3, 70.9, 71.1
$\text{Hf}(2.4\% \text{ Zr})\text{Cl}_4(\text{c})$	108.7	65.7
$\text{HfCl}_4(\text{c})$	109.0	66.0

B. Reaction with Water.—The solid halides were treated with water to give clear, colorless solutions. As above, the molar ratio was about 1:1500 and no dependence on sample weight was observed. The correction for the Hf content of the ZrCl_4 was again negligible. Values of ΔH for reactions 3 and 4 are given in Table I, and combined with values of ΔH_{298}^0 for H_2O , $\text{HCl}(\text{aq})$, $\text{HBr}(\text{aq})$

(4) F. K. McTaggart, *Rev. Pure Appl. Chem.*, **1**, 152 (1951).

(5) G. Beck, *Z. anorg. allgem. Chem.*, **174**, 31 (1928).

(6) P. Gross, C. Hayman and D. L. Levi, *Trans. Faraday Soc.*, **53**, 1285, 1601 (1957).

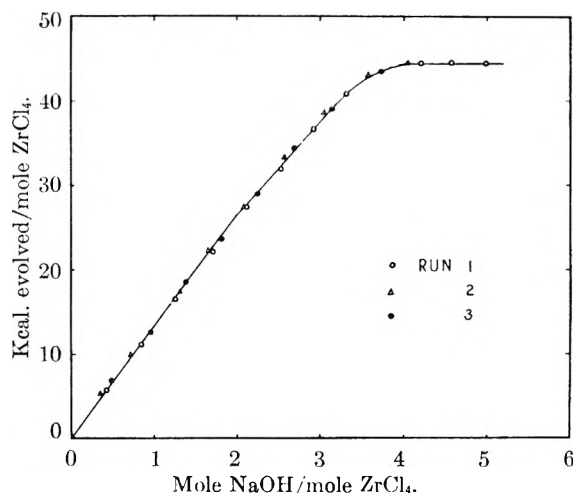


Fig. 1.—Thermometric titration of 0.01 M ZrCl_4 with 4 M NaOH.

and $\text{HI}(\text{aq})$,¹ and $\text{ZrCl}_4(\text{c})$ ⁶ led to values of $\Delta^0 H_{298}$ for $\text{ZrBr}_4(\text{c})$, -181.0 ± 0.5 kcal./mole and $\text{ZrI}_4(\text{c})$, -116.3 ± 0.8 kcal./mole.

For the thermometric titration of $N/40$ ZrCl_4 with $N/40$ NaOH, Chauvenet⁷ found -46 kcal./mole, which compares well with -43.7 kcal./mole found here from the difference of reactions 1 and 3 for a similar order of concentration. This titration was repeated to provide an independent check on the above results. A ZrCl_4 solution was titrated with 1 cc. of 4 M NaOH using a syringe-type microburet inside the calorimeter. As shown in Fig. 1 the total heat evolved up to the equivalence point was -44.5 kcal./mole, in good agreement with the above value. The initial slope of the titration curve, -13.6 kcal./mole, corresponded within experimental error to the heat of the reaction



After two moles of NaOH per mole of ZrCl_4 had been added, neutralization of the zirconium cation evidently commenced as the rate of heat evolution fell.

Discussion

There appears to be no significant difference in values of ΔH_{298}^0 for $\text{ZrBr}_4(\text{c})$ and $\text{ZrI}_4(\text{c})$ obtained by the two methods. The final average values are -181.6 ± 0.6 kcal./mole and -115.9 ± 0.8 kcal./mole⁸, respectively, which are considerably lower than previous estimated values, -192 ± 10 kcal./mole and -130 ± 5 kcal./mole,² respectively. Entropies S_{298} of $\text{ZrBr}_4(\text{c})$ and $\text{ZrI}_4(\text{c})$ have been estimated by the method of Latimer⁹ to be 52.1 ± 5 and 67.5 ± 5 cal./°mole, respectively, leading to values of ΔF_{298}^0 of -172.5 ± 2 and -116.6 ± 2 kcal./mole, respectively. For $\text{ZrCl}_4(\text{c})$ the value of ΔF_{298}^0 is -213.4 ± 0.6 kcal./mole, calculated from the best reported values of ΔH_{298}^0 and S_{298}^0 . When values of ΔH_{298}^0 for the tetrahalides of Ti, Zr and Th are plotted against values for the corresponding oxides, the regular shape of the curves confirms the new values for ZrBr_4 and ZrI_4 and

(7) E. Chauvenet *Compt. rend.*, **164**, 630 (1917).

(8) Standard states assumed to be $\text{Zr}(\text{c})$, $\text{Cl}_2(\text{g})$, $\text{Br}_2(\text{l})$, $\text{I}_2(\text{c})$.

(9) W. M. Latimer, "Oxidation Potentials," 2nd Ed., Prentice-Hall Inc., New York, N. Y., 1952.

enables prediction of -160 ± 5 kcal./mole for ΔH_{298}^0 of $\text{ThI}_4(\text{c})$.

The value of ΔH_{298}^0 for hydrous ZrO_2 , -260.3 ± 0.6 kcal./mole, found from reaction 1, is not significantly different from that reported for monoclinic ZrO_2 , -261.5 ± 0.2 kcal./mole. This would indicate that the water in ZrO_2 hyd. must be only loosely held by physical trapping in the micelles of the solid. There is slight X-ray evidence reported of a tetragonal arrangement of ZrO_2 in the hydrous form on heating to below 600° ,³ but the difference in ΔH between monoclinic and tetragonal is only about 1 kcal./mole.² Latimer⁹ already has cast doubt on the heat of hydration of ZrO_2 of -25.3 kcal./mole previously reported.¹

From reaction 3 the value of ΔH_{298}^0 for the $\text{ZrO}-\text{OH}^+(\text{aq})$ ion is -270.7 ± 0.5 kcal./mole.

Acknowledgments.—The author wishes to thank Mr. N. Gye for chemical analyses and Mr. I. J. Newnham for continued support and advice.

THE INFLUENCE OF PRESSURE ON THE CATIONIC POLYMERIZATION OF ISOAMYL VINYL ETHER

By S. D. HAMANN AND D. R. TEPLITZKY¹

Division of Physical Chemistry, Australian Commonwealth Scientific and Industrial Research Organization, Fishermen's Bend, Melbourne, Australia

Received April 13, 1961

Although it is now well established that high pressures have a profound influence on the rates and products of free-radical polymerizations in the liquid phase,^{2,3} it appears that very little work has been done on ionic polymerizations under pressure. Kilroe and Weale⁴ have examined the cationic polymerization of α -methylstyrene catalyzed by trichloroacetic acid, and found it to be accelerated by an increase in pressure in much the same way as the free-radical polymerization of the same monomer. But the kinetic form of this reaction is unknown, even at atmospheric pressure,⁵ and it is difficult to draw any useful conclusions from the results.

Here we report some measurements of the effect of pressure on the rate of polymerization of isoamyl vinyl ether, catalyzed by iodine. Eley and Richards⁷ and Eley and Saunders⁸ have made a detailed study of this type of polymerization at atmospheric pressure and concluded that it occurs by a carbonium ion mechanism, initiated by I^+ ions. This supposition is supported by more re-

cent evidence⁹ that although vinyl ethers are resistant to attack by free radicals, they are readily attacked by the stable tropylium carbonium ion.

In the present work we have examined the polymerization both in diethyl ether solution and in the undiluted monomer, at pressures up to 10,000 atm.

Experimental

The reactions were carried out in glass hypodermic tubes, sealed with sliding glass plugs, and immersed in petroleum ether in a pressure vessel similar to the one described by David and Hamann.¹⁰ The progress of each polymerization was followed by extracting samples of the reaction mixture, quenching the reaction with an aqueous solution of sodium thiosulfate, and estimating the amount of polymer by removing the unchanged monomer and solvent by prolonged evaporation at 75° and 0.04 mm. The average molecular weight of the polymer was measured cryoscopically in benzene solution.

The sample of isoamyl vinyl ether was kindly given to us by the Distillers Co., England, and was purified by fractionation under vacuum. The diethyl ether was dried over sodium.

The reaction mixtures in diethyl ether were prepared by first dissolving iodine in the solvent and then adding the monomer. In the absence of solvent, the addition of solid iodine to the pure monomer caused a violent polymerization before the iodine could fully dissolve.¹¹ For the reactions in the "undiluted" monomer we were therefore forced to add the iodine in the form of a concentrated solution in diethyl ether. It is unlikely that the small amount of diethyl ether introduced in this way (1% of volume) would have affected the kinetics.

Results and Discussion

Reactions in Diethyl Ether Solution.—In the ether solutions we confirmed Eley's^{7,8} kinetics

$$-\frac{1}{[\text{M}]} \cdot \frac{d[\text{M}]}{dt} = k[\text{I}_2]^2 \quad (1)$$

(where $[\text{M}]$ = concentration of monomer, $[\text{I}_2]$ = concentration of iodine) at atmospheric pressure, but we found discrepancies at higher pressures. It was obvious that iodine was consumed during the high pressure reactions and in some instances no free iodine was left after 40 minutes (starting from a concentration $[\text{I}_2]_{t=0} = 0.001$ mole l.⁻¹). It appeared that the iodine had formed a strong complex or an addition compound with the vinyl ether. This could be hydrolyzed, with the liberation of iodine, by adding a little water to the mixture.

To avoid this complication we were compelled to work at pressures below 1500 atm. and to estimate the rate constants from the initial slopes of the reaction curves over fairly short times. Our results are given in Table I.

Although the rate constants may not be very accurate, there is no doubt that the reaction was accelerated at high pressures. On the other hand there was no significant change in the degree of polymerization between 1 and 1000 atm. This is not surprising since the degree of polymerization is determined by the ratio of the rate constants (k_3 and k_5 in the notation of Eley and Saunders⁸) for two closely analogous reactions between growing polymer and monomer. It is understandable

(1) Now at the School of Biological Sciences, University of New South Wales, Sydney, Australia.

(2) S. D. Hamann, "Physico-Chemical Effects of Pressure," Butterworths, London, 1957, pp. 189-192.

(3) M. G. Gonikberg, "The Rates and Equilibria of Chemical Reactions at High Pressures," Acad. Sci. U.S.S.R., Moscow, 1953, pp. 156-167.

(4) J. G. Kilroe and K. E. Weale, *J. Chem. Soc.*, 3849 (1960).

(5) The kinetics may be the same as those for the cationic polymerization of 1:1 diphenylethylene (i.e., α -phenylstyrene) under the same conditions,⁶ but this has not been proved.

(6) A. G. Evans, N. Jones and J. H. Thomas, *J. Chem. Soc.*, 1824 (1955).

(7) D. D. Eley and A. W. Richards, *Trans. Faraday Soc.*, **45**, 425 (1949).

(8) D. D. Eley and J. Saunders, *J. Chem. Soc.*, 4167 (1952).

(9) D. N. Kursanov, M. E. Volpin and I. S. Akhrem, *Doklady Akad. Nauk S.S.S.R.*, **120**, 531 (1958).

(10) H. G. David and S. D. Hamann, *Trans. Faraday Soc.*, **50**, 1188 (1954).

(11) W. Chalmers, *Can. J. Res.*, **B7**, 464 (1932).

TABLE I

POLYMERIZATION OF ISOAMYL VINYL ETHER IN DIETHYL ETHER SOLUTION AT 0°

Pressure, atm.	k sec. ⁻¹ mole ⁻² l. ⁻²	Mol. wt. of polymer
1	5.0	2300 ± 200
500	6.6	
750	9.6	
1000	13.2	2500 ± 200

that these two reactions should be influenced similarly by a change of pressure.¹²

Unfortunately we are unable to decide definitely which step in the polymerization was primarily responsible for the acceleration at high pressures. But it certainly appears that the effect of pressure on the initiating steps

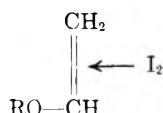


could be sufficient to account for the whole acceleration. Taken together, reactions 2 and 3 are identical with the rate-determining step in the addition of iodine to olefins in solvents of low dielectric constant.^{13,14}



We have found previously¹⁴ that this reaction is accelerated by a factor of 3.1 at 1000 atm., which is close to the change shown in Table I. The reaction is favored by an increase in pressure because it involves the appearance of electrical charges and a consequent electrostriction of the surrounding solvent.^{15,16}

Reactions in Undiluted Monomer.—In these experiments the iodine reacted completely and almost instantaneously with the monomer to form a colorless complex, or addition compound, having an absorption band at 280 m μ . This was presumably the "inactive complex"



discussed by Eley and Saunders.⁸ However we found that the complex was active as a catalyst, and that the vinyl ether proceeded to polymerize slowly according to the rate equation

$$-\frac{1}{[M]} \frac{d[M]}{dt} = k [MI_2], ([M] \gg [MI_2]) \quad (5)$$

where $[MI_2]$ denotes the concentration of the iodine complex. In contrast to the polymerization in diethyl ether solution, this reaction was well behaved under pressure and we were able to make measurements to 10,000 atm. without complications. Our results are given in Table II.

(12) It is significant that Eley and Saunders⁸ have found that although a change in the structure of the vinyl ether may have a large effect on the rate of polymerization, it has only a small effect on the degree of polymerization.

(13) C. K. Ingold, "Structure and Mechanism in Organic Chemistry," G. Bell and Sons Ltd., London, 1953, p. 666.

(14) S. D. Hamann and D. R. Teplitzky, *Disc. Faraday Soc.*, **22**, 114 (1956).

(15) J. Buchanan and S. D. Hamann, *Trans. Faraday Soc.*, **49**, 1425 (1953).

(16) Reference 2, p. 164, *et seq.*

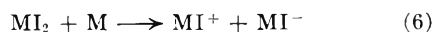
TABLE II

POLYMERIZATION OF PURE ISOAMYL VINYL ETHER AT 0°^a

Pressure, atm.	$10^3 k$ sec. ⁻¹ mole ⁻¹ l.
1	1.5
1,000	4.5
2,000	7.8
3,000	11.0
10,000	40

^a The molecular weight of the polymer was not determined.

We can explain the change of reaction order with respect to the total amount of iodine (equations 1 and 5) in the following way. In diethyl ether solution the initiating step (2) requires the presence of two I_2 molecules and for this reason the rate of polymerization is of the second order in $[I_2]$. But, in the undiluted monomer, the absence of any free iodine rules out the possibility of reaction 2 and we suggest that instead the initiation occurs through breakdown of the addition complex as



This mechanism implies that, in the presence of a large excess of monomer, iodide ions can form complexes with the monomer in the same way as they do with iodine. This is a reasonable supposition since it is known that iodide ions form strong complexes with other olefinic compounds such as maleic anhydride.¹⁷ Initiation by reaction 6 would lead to over-all kinetics of the first order in $[MI_2]$.

It is likely that reaction 6 proceeds through a transition state in which the initial I-I bond is partially ionized. It is closely analogous to reaction 2 and it should be similarly accelerated by pressure. We can therefore conclude, again, that the increase in rate of the initiating step *could* account for the whole of the influence of pressure on the polymerization. But on the present evidence we are unable to be sure that it is the only factor involved.

(17) E. M. Kosower, R. L. Martin and V. W. Meloche, *J. Chem. Phys.*, **26**, 1353 (1957).

CRYSTALLIZATION ON A SEED FROM FUSED SALT SOLUTIONS BY THE TEMPERATURE DIFFERENCE METHOD

By G. F. REYNOLDS AND H. J. GUGGENHEIM

Bell Telephone Laboratories, Inc., Murray Hill, New Jersey

Received April 14, 1961

Recently considerable success has been obtained in the growth of single crystals of refractory oxides and other water-insoluble materials from fused salt solutions. With a little perseverance, one can usually find a salt or combination of salts which will dissolve, reversibly, in the molten state, considerable quantities of the material to be crystallized. The main criterion for success is that the crystal desired exists as the stable solid phase at the temperatures and compositions of molten solution employed.

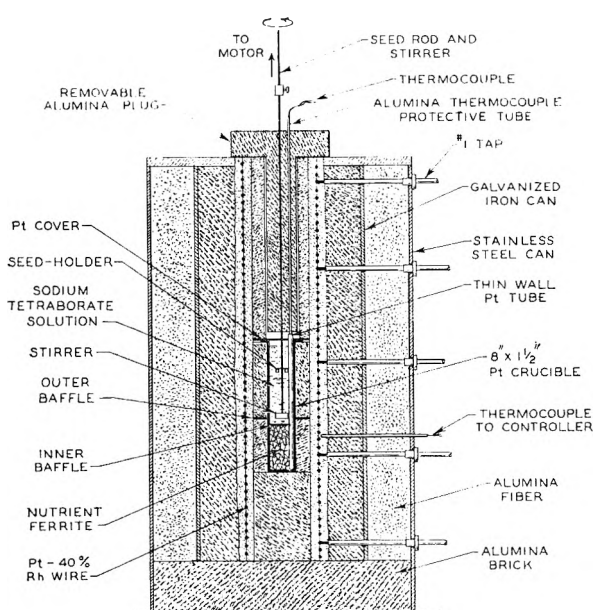


Fig. 1.

Analogous to crystal growth from aqueous solutions, there are three major methods by which single crystals can be grown from fused salt solutions. These are: (1) growth by the slow cooling of a saturated solution; (2) growth by the evaporation of the solvent phase and (3) growth by the temperature difference method, sometimes known as the Krüger-Fincke principle.¹

Examples of the application of the first method to fused salt solutions are the growth of single crystals of barium titanate from molten potassium fluoride² and magnetic garnets from molten lead oxide.³ The second method occasionally has been employed,⁴ but it is handicapped by the difficulty in obtaining controlled evaporation and the high temperatures required. The third method, growth by a temperature difference between a nutrient zone and a crystallization zone, has not previously been exploited for growth from fused salt solutions; and it is the purpose of this note to present the results of a preliminary investigation of the extension of this method to fused salt systems.

The procedure as outlined in the experimental section describes the growth of cobalt ferrite from molten sodium tetraborate as an example of the application of the temperature difference method to fused salt solutions. This method also has been used with some success for growing calcium fluoride from a lithium chloride-potassium chloride eutectic mixture.

Experimental

Figure 1 shows the details of the apparatus used in these experiments. Since the control of temperature differential and fluctuation were believed to be most important to the controlled growth of crystalline material on a seed from a fused salt solution, care was taken in the design and con-

struction of the furnace equipment. Some features of the furnace are as follows: (1) High temperature alumina brick and alumina fiber were used as insulation, and all the space around the crucible inside the furnace was filled with insulation to give a larger thermal mass. (2) Many taps leading from the furnace winding were made available in order to vary the voltage distribution over the length of the furnace to give flexibility in adjusting the temperature differential. (3) Platinum baffles were fixed inside and outside of the crucible to effect a sharp thermal gradient between the nutrient chamber and the crystallization chamber. (4) A thin wall platinum tube attached to the inside wall of the crucible made it possible to telescope a thermocouple, up or down, to record temperatures at different levels in the molten solution. (5) The platinum rod used for holding the seed was extended out of the furnace and attached to a motor for stirring the solution and rotating the seed. (6) A tightly fitting platinum cover on the crucible made the loss of material by vaporization negligible. (7) A saturable core reactor temperature controller was employed to give a stepless temperature control.

The procedure followed in obtaining growth on a cobalt ferrite (CoFe_2O_4) seed by the temperature difference method was as follows.

The CoFe_2O_4 which was used for nutrient and seed material was prepared by crystallizing sintered CoFe_2O_4 from a slowly cooled PbO solution.⁵ These crystals were unusually large, but badly flawed by cracks and solvent inclusions. The sodium tetraborate (borax) which was used as the solvent in most of the experiments was prepared by heating sodium metaborate with boric anhydride. The solution was prepared by mixing CoFe_2O_4 sintered powder with borax and heating to 1100° for 48 hours. The molten liquid was then decanted into an iron dish leaving behind the undissolved CoFe_2O_4 . This procedure ensured a solution very near the saturation point.

The bottom two inches of the platinum crucible were filled with crystalline CoFe_2O_4 . The baffle and thermocouple protection tube were put in place and the crucible was filled with chunks of the saturated solid solution of ferrite in borax. The crucible was lowered into the furnace and the temperature slowly raised until all the solid solution was molten. Additional chunks were added until the charge was full. When all of the material above the baffle was liquid, the stirring apparatus without the seed was lowered into the solution and the furnace plug put into place in order to make accurate temperature measurements. The temperature above the baffle was raised to 1120° . After 24 hours under these conditions, the temperature was lowered 30° in order to supersaturate the solution. The stirring apparatus then was withdrawn and a small seed attached. After preheating, the seed was lowered into the solution and stirring begun. From time to time the seed was withdrawn for inspection, and the amount of growth noted.

Results and Discussion

Employing growth times of 2 to 20 hours, temperature differences of 10 to 50° , and crystallization temperatures of 1100 to 1200° , one obtains growth rates averaging 5 weight % increase per hour. These crystals were grown to twice the original seed size and measured 1 to 1.5 cm. in the largest dimension. The growth occurred by means of terraces parallel to the 111 octahedron faces. In several runs it was noted that when spontaneous nucleation produced crystals on the stirring rod above the seed, these crystals developed into regular octahedra with smooth 111 faces. This would lead one to infer that the imperfections (both stoichiometric and crystallographic) in the crystal seed caused the irregular growth features.

Although the temperature difference method has several intrinsic advantages, and has worked admirably for growth from aqueous solutions⁶ and for hydrothermal crystal growth,⁷ its application

(1) F. Krüger and W. Fincke, German Patent 228,246, Kl. 120, Gr. 2, Nov. 5, 1910.

(2) J. P. Remeika, *J. Am. Chem. Soc.*, **76**, 940 (1954).

(3) J. W. Nielsen and E. F. Dearborn, *Phys. Chem. Solids*, **6**, 202 (1958).

(4) V. A. Timofeeva and A. V. Zaleskii, *Rost Kristallov*, **2**, 88 (1958).

(5) J. P. Remeika, *J. Am. Chem. Soc.*, **78**, 4259 (1956).

to fused salt solutions presents a number of difficulties.

It was found that even though the "average" temperature of the growing chamber could be held almost constant, still hot currents existed which would cause a crystal seed to dissolve at one position in the crystallization zone while at the same time to grow in another. For this reason, an apparatus was designed for the rotating of the seed concurrently with the stirring of the solution in order to dissipate these hot currents.

Further, it is difficult to obtain a sharp temperature gradient between the nutrient and crystallization chambers in the vertical furnace employed in this work with but a single inner baffle because of the efficient heat conduction of the platinum crucible containing the fused salt solutions. However, it was found that by employing an outer baffle of platinum around the cylindrical crucible to reflect the furnace heat downward, together with a properly positioned inner baffle, a fairly sharp temperature gradient of up to 80° could be obtained.

Once these difficulties are overcome the temperature difference method should be capable of yielding crystals of high perfection. This is because the crystal is grown under isothermal conditions and, hence, should have a minimum of thermal strains, and also because by controlling the magnitude of the temperature difference, the crystals can be grown at any desired constant supersaturation. If the stoichiometry of the crystals can be used as a measure of their perfection, then the CoFe_2O_4 crystals grown as described above are superior to the CoFe_2O_4 crystals previously grown by the slow cooling of molten solutions of PbO_2 . They have a Co to Fe ratio of 0.50, whereas the aforementioned crystals gave a Co to Fe ratio of anywhere from 0.56 to 0.67,³ as determined by direct analysis.

Work is now in progress to grow larger crystals using longer growth times, and to increase crystal perfection and minimize spontaneous nucleation by finding optimum conditions of supersaturation and temperature. Also, this investigation is being extended to other crystals and other fused salt solvent systems.

(6) A. C. Walker and G. T. Kohman, Bell Telephone System, Tech. Pub., Monograph B-1562; also, *Trans. Am. Inst. Elec. Engrs.*, **67**, 565 (1948).

(7) R. A. Laudise and J. W. Nielsen, "Hydrothermal Crystallization, Solid State Physics," Academic Press, New York, N. Y., in press.

(8) J. W. Nielsen, private communication.

SPIN-SPIN COUPLING CONSTANTS BETWEEN NON-BONDED C^{13} AND PROTON.

II.1 DEPENDENCE OF $J_{\text{C}^{13}\text{-C-H}}$ ON HYBRIDIZATION OF C^{13}

BY GERASIMOS J. KARABATSOS, JOHN D. GRAHAM AND FLOIE VANE

Kedzie Chemical Laboratory, Michigan State University, East Lansing, Michigan

Received April 14, 1961

Theoretical and experimental studies on n.m.r. interactions between non-bonded H-H, H-F and

(1) Part I, G. J. Karabatsos, *J. Am. Chem. Soc.*, **83**, 1230 (1961).

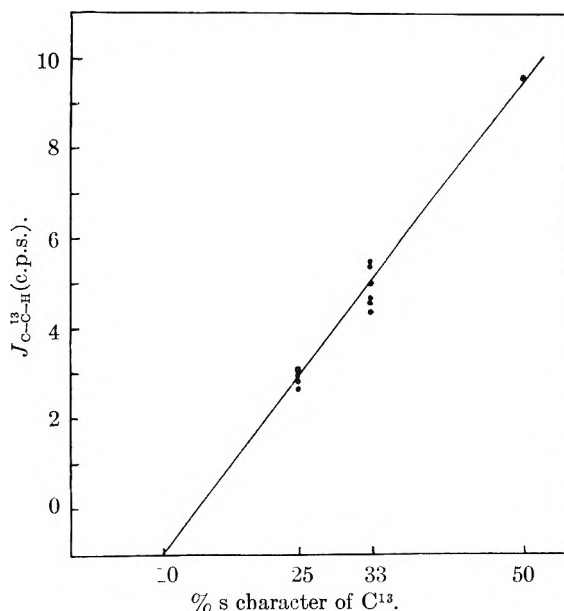


Fig. 1.

F-F have been carried out and published, while analogous studies involving non-bonded C^{13} and protons have not been made.¹ We wish to report here some of our findings involving C^{13} and protons separated by one carbon atom.

The spin-spin coupling constants ($J_{\text{C}^{13}\text{-C-H}}$) for eleven compounds were measured and the results are summarized in Table I. The enrichment in the samples varied from 30 to 60% excess C^{13} . All spectra were taken with a model V-4300D Varian Associates Spectrometer, at 60 Mc.; spin-spin coupling constants were measured by the standard side band technique.²

The data fall into three categories: (1) When the C^{13} is sp^3 hybridized $J_{\text{C}^{13}\text{-C-H}}$ has an average value of about 4.0 c.p.s. (2) When the C^{13} is sp^2 hybridized the average value of $J_{\text{C}^{13}\text{-C-H}}$ is about 5.9 c.p.s. (3) When the hybridization of C^{13} is sp the value of $J_{\text{C}^{13}\text{-C-H}}$ is about 10.6 c.p.s. (only one value available).

It has been shown³ that for protons directly bonded to C^{13} a linear correlation exists between the magnitude of $J_{\text{C}^{13}\text{-H}}$ and the extent of sp hybridization of the carbon atomic orbitals. The data presented in Table I show that this correlation is a general one and can be applied to interactions between C^{13} and protons separated by two bonds. If a plot of $J_{\text{C}^{13}\text{-C-H}}$ vs. % s character of C^{13} atomic orbitals is made, a linear relationship is obtained (Fig. 1). However, while no appreciable intercept is found^{3a} in the case of $J_{\text{C}^{13}\text{-H}}$, an intercept in the case of $J_{\text{C}^{13}\text{-C-H}}$ is evident. In order to assess the importance of the Fermi contact term theoretical calculations were performed, using the procedure of Gutowsky and Karplus.⁴ The following assumptions were

(2) J. T. Arnold and M. E. Packard, *J. Chem. Phys.*, **19**, 1608 (1951).

(3) (a) J. N. Shoolery, *ibid.*, **31**, 1427 (1959); (b) N. Muller and D. E. Pritchard, *ibid.*, **31**, 768, 1471 (1959).

(4) H. S. Gutowsky, M. Karplus and D. M. Grant, *J. Chem. Phys.*, **31**, 1278 (1959).

made: (1) The Fermi contact term is the important one, and (2) replacing a proton by C^{13} does not change the coefficients in the ground state wave function.⁵ The electron density at the C^{13} nucleus was estimated from the appropriate terms in the square of the hybrid carbon bonding orbital (normalized), which is $a^2\psi_{2s}$. A 2s hydro-

COMPLEXES OF IRON WITH *d*-TARTARIC AND *meso*-TARTARIC ACIDS

By R. W. GREEN AND GWENDA M. PARKINS

School of Chemistry, Sydney University, Sydney, Australia

Received May 1, 1960

The only reported quantitative measurement of complexing of iron(III) by tartrate appears to be a dissociation constant of 0.9×10^{-18} , determined polarographically for the tris-(tartrato) complex by Toropova,¹ who states this to be the only complex in solution between pH 3.4 and 7.0. On the other hand, Bobtelsky and Jordan² found a variety of evidence for a complex $Fe_2(H_2T)_3$ and two different complexes $Fe_3(H_2T)_2^{5+}$, where tartaric acid is written H_4T . We describe here the effect of *d*-tartrate and *meso*-tartrate on the oxidation-reduction potentials of solutions of iron(II) and iron(III) below pH 4.

Experimental

Iron(II) and iron(III) perchlorates were prepared and analyzed by standard methods. *d*-Tartaric acid (Analar) and *meso*-tartaric acid (Laboratory Reagent grade), both from British Drug Houses, Ltd., were estimated in solution by potentiometric titration with standard alkali.

All measurements were made in a closed cell at $25 \pm 0.02^\circ$. Solutions were stirred by a stream of nitrogen previously freed from traces of oxygen and carbon dioxide and equilibrated with boiled water at 25° before entering the titration vessel. Oxidation-reduction potentials were measured with a Leeds and Northrup Model K potentiometer connected to a bright platinum electrode and a saturated calomel half cell, the two being joined by an ammonium nitrate-sodium nitrate agar bridge.³ pH measurements were made with a Cambridge portable pH meter, using the same calomel half cell and salt bridge, and glass electrodes standardized against 0.05 *M* potassium hydrogen phthalate and 0.05 *M* potassium tetroxalate.⁴ Dissociation constants of the two acids were determined from pH titrations of 0.02 *M* solutions, and stability constants of the iron(II) complexes were similarly obtained by titration of 0.02 *M* iron(II) perchlorate containing one or two moles ligand. The stability of the iron(III) complexes was investigated by simultaneous oxidation-reduction and pH measurements on solutions of one mole iron(II), one mole iron(III) and six moles ligand, together with sufficient sodium hydroxide (0-10 moles) to produce pH values between 1.5 and 4.0.

Results

Dissociation constants of the two acids at ionic strength approximately 0.05, calculated from the pH titration data, are shown in Table I, together with values corrected for activity by the simple Guntelberg⁵ formula for a *z*-valent ion

$$-\log \gamma_z = 0.5z^2\sqrt{I}/(1 + \sqrt{I})$$

The corrected values for *d*-tartaric acid are in reasonable agreement with the results obtained by Bates and Canham⁶ with a hydrogen electrode in a cell without liquid junction; and the values for *meso*-tartaric acid, which is noticeably weaker, agree fairly well with those reported by Feldman, North and Hunter⁷ for ionic strength 0.133.

(1) V. F. Toropova, *J. Gen. Chem. (U.S.S.R.)*, **15**, 603 (1945).

(2) M. Bobtelsky and J. Jordan, *J. Am. Chem. Soc.*, **69**, 2286 (1947).

(3) D. D. Perrin, *J. Chem. Soc.*, 3120 (1958).

(4) V. E. Bower and R. G. Bates, *J. Research Natl. Bur. Standards*, **69**, 261 (1957).

(5) E. Guntelberg, *Z. physik. Chem.*, **123**, 199 (1926).

(6) R. G. Bates and R. G. Canham, *J. Research Natl. Bur. Standards*, **47**, 343 (1951).

TABLE I

Compound	$J_{C^{13}-C-H}$ (c.p.s.)	
$CH_3-CO_2-CH_2CH_3$ ¹³	6.0	± 0.1
$(CH_3-CH_2)_2C=O$ ¹³	5.7	$\pm .1$
$CH_3-CH_2-CO_2H$ ¹³	6.4	$\pm .2$
$CH_3-CH_2-CO_2CH_3$ ¹³	6.5	$\pm .3$
$(CH_3)_2CH-CO_2CH_3$ ¹³	5.6	$\pm .1$
$(CH_3)_2CH-CO_2H$ ¹³	5.2	$\pm .1$
$(CH_3)_2C(OH)CH_2-CH_3$ (α) ¹³	4.1	$\pm .1$ (β) 4.0 ± 0.1
$(CH_3)_2C(Cl)CH_2-CH_3$ (α) ¹³	3.9	$\pm .1$ (β) 3.7 $\pm .2$
$CH_3-CH_2-CD_2OH$ ¹³	$\bar{< 4}$	
$(CH_3-CH_2)_2C(D)OH$ ¹³	4.0	$\pm .2$
$(CH_3-CH_2)_3COH$ ¹³	3.8	$\pm .2$
$CH_3-C\equiv C-H^c$	(α) 10.6	(β) 50.8

^c Values taken from J. N. Shoolery, *J. Mol. Spec.*, **63**, 110 (1960).

gen-like wave function was used with $Z = 3.25$ and evaluated at $r = 0$. The difference in magnetic moments of C^{13} and proton was taken into

$$\Psi = a\psi_{2s} + b\psi_{2p}$$

account, and a mean excitation energy of 8.0 e.v. was used. The $C^{13}-C-H$ angle was taken as tetrahedral.

The results are as follows: (1) For sp^3 hybridization $J_{C^{13}-C-H} = 3.8$ c.p.s. (2) For sp^2 , $J_{C^{13}-C-H} = 5.1$ c.p.s.; (3) For sp , $J_{C^{13}-C-H} = 7.6$ c.p.s. Surprising agreement between experiment and theory is found, indicating that the Fermi contact term is the dominant term, even when the proton is not directly bonded to C^{13} (two bond separation).

The small variations in $J_{C^{13}-C-H}$ when the C^{13} is sp^2 hybridized could arise from the fact that sp^2 is an approximation; it is widely accepted that non-integral values of n in sp^n are not unreasonable. The question of the magnitude of $J_{C^{13}-C-H}$ with variations in the $C^{13}-C-H$ angle is an interesting one, and we hope to elucidate it by studying compounds where the carbon separating the interacting nuclei is part of various ring systems.

The synthesis of the labeled compounds will appear elsewhere.

Acknowledgment.—Acknowledgment is made to the donors of the Petroleum Research Fund, administered by the American Chemical Society.

(5) A similar approximation has been used in the case of F^{19} ; M. Karpus, *J. Chem. Phys.*, **30**, 11 (1959).

TABLE I

DISSOCIATION CONSTANTS OF TARTARIC ACIDS AND STABILITY CONSTANTS OF COMPLEXES WITH IRON(II)			
	Ionic strength	<i>d</i> -Tartaric acid	<i>meso</i> -Tartaric acid
pK_1	0.05	2.93	3.11
	Corr. to zero	3.11	3.29
pK_2	0.05	3.90	4.40
	Corr. to zero	4.26	4.76
$\log K^{II}$	0.05	2.61	2.45

Complex formation between iron(II) and the tartaric acids is quite weak and, under the conditions of our experiments, only one stage was detectable. The stability constants, K^{II} , calculated in the conventional manner on the assumption that the ligand is the normal anion, $C_4H_4O_6^{2-}$, are also shown in Table I.

In the case of iron(III), the experimental results, in the form of E vs. pH curves, are plotted in Fig. 1. Treatment of the data is based on the equations

$$E_0' - E = 0.05915 \log [Fe^{3+}]/[Fe^{2+}] \quad (1)$$

$$[Fe(II)] = [Fe^{2+}] (1 + K^{II} [H_2T^{2-}]) \quad (2)$$

$$[Fe(III)] = [Fe^{3+}] + [Tartrato\ complexes] \quad (3)$$

where E_0' is the standard electrode potential, E_0 , modified by any approximately constant terms, such as liquid junction potential, inherent in the experimental arrangement. Measurements in the absence of tartrate gave the value -0.756 v. for E_0' . Equation 2 is based on the absence of higher iron(II) complexes at this concentration, and equation 3 assumes negligible hydrolysis and perchlorate ion pair formation, as indicated by reported values of the relevant equilibrium constants.^{8,9}

Determination of the probable nature of the complexes and evaluation of their stability constants is now a matter of successive approximation and curve fitting. This presents a formidable problem in computing which, however, is somewhat moderated by two experimental conditions, namely, the presence of free ligand in some excess, and the fact, which can be deduced from the oxidation-reduction potentials of Fig. 1, that even at pH 1.5 only about 1% of the total iron(III) remains uncomplexed. Moreover, the course of the E vs. pH curve proves to be remarkably sensitive to small changes in stability constants.

Consideration of molecular models and of the high polarizing power of the Fe^{3+} ion suggests that the first complex probably involves a six-membered ring with one carboxylate group and one hydroxyl oxygen coordinated to the metal, resulting in the equilibrium



governed by the expression $\beta_1 = [FeHT][H^+]/[Fe^{3+}][H_2T^{2-}]$.

Calculation by successive approximations showed that this assumption could account for the observed oxidation-reduction potentials below pH 3 for *d*-tartaric acid and below pH 2.4 for *meso*-tartaric acid, but that a higher complex began to appear

(7) I. Feldman, C. A. North and H. B. Hunter, *J. Phys. Chem.*, **64**, 1224 (1960).

(8) L. G. Sillén, *Quart. Rev.*, **13**, 146 (1959).

(9) K. W. Sykes, *J. Chem. Soc.*, 2473 (1959).

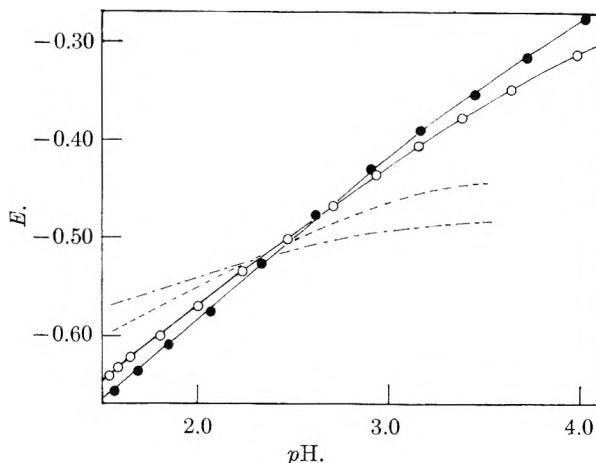
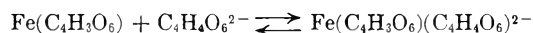


Fig. 1.—Oxidation-reduction potentials of solutions containing equimolar proportions of iron(II) and iron(III) together with an excess of *d*-tartaric acid, O, or *meso*-tartaric acid, ●, at ionic strength 0.1. Unbroken curves are calculated from stability constants of Tables I and II. ---, calculated on the assumption that only one complex, FeH_2T^+ , with $\log \beta = 8.2$, is formed; --, calculated on the assumption that only one complex, $Fe_3(H_2T)_3^{3+}$, (ref. 2) with $\log \beta = 24.0$, is formed.

at higher pH . Extension of the calculations showed that the second tartrate ion was bound without liberation of another proton, so that binding must now be at the carboxylate groups, and the equilibrium is



governed by

$$\beta_2 = [Fe(HT)(H_2T)^{-}]/[FeHT][H_2T^{2-}]$$

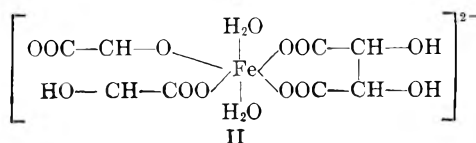
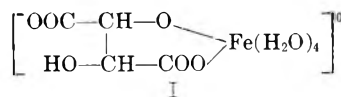
The numerical values of $\log \beta_1$ and $\log \beta_2$ are shown in Table II.

TABLE II

Ionic strength	STABILITY CONSTANTS OF IRON(III) COMPLEXES			
	<i>d</i> -Tartaric acid		<i>meso</i> -Tartaric acid	
	0.05	0.10	0.05	0.10
$\log \beta_1$	5.45	5.89	5.45	5.85
$\log \beta_2$..	8.1	..	9.0

A number of other possible formulations of the complexes were tested by the same computational technique. The assumption of three successive complexes, $Fe(H_2T)^+$, $Fe(H_2T)_2^-$ and $Fe(H_2T)_3^{3-}$ with carboxylate coordination only, fitted the experimental data moderately well for about 80% of the range, but diverged at the extremes and, moreover, required three parameters. Other formulas, suggested by other authors, gave curves of quite the wrong slope. Examples are shown in Fig. 1.

We conclude that solutions of iron(III) and tartrate below pH 4 contain two complexes, I and II, in equilibrium.



THE RACEMIZATION OF THE DIMETHYL
ESTER OF *L*-BROMOSUCCINIC ACID BY
LITHIUM BROMIDE IN ACETONE

By J. O. KONECNY

Shell Development Company, Emeryville, California

Received May 8, 1961

The racemization of the dimethyl ester of *L*-bromosuccinic acid by lithium bromide in acetone, investigated by Olson, Frashier and Spieth,¹ has been interpreted as a reaction with the rate law

$$-d \ln C/dt = r = k_1(\text{Br}^-) + k_2(\text{LiBr}) \quad (1)$$

The pseudo-unimolecular rate r is an increasing function of the lithium bromide concentration and a very slowly decreasing function of the initial (*i.e.*, total) ester concentration. A good fit of the data, representing a wide range of experimental conditions, has been obtained with properly selected values of k_1 and k_2 and of K , the apparent ionization constant of lithium bromide. The value of K was taken to be independent of the ionic strength in the experimental range of lithium bromide concentrations.

Professor Olson himself, however, deemed a test of this interpretation desirable and therefore suggested a determination of the ionization constant of lithium bromide in acetone. The results² do not agree completely with those derived by Olson and his co-workers from the kinetic data. The rate data therefore were re-examined on the basis of the new ionization constants. The new interpretation leads to a simpler representation. There is no indication of a lithium bromide catalyzed path; the rates are proportional to the concentration of bromide ions.

Results

The results for anhydrous acetone at 24.9° are shown in Table I. The bromide ion concentrations, given in the third column, were calculated by successive approximations from the equation

$$K = K^0/\gamma^2 = (\text{Li}^+)(\text{Br}^-)/(\text{LiBr}) \quad (2)$$

where γ , the mean activity coefficient of the ions, is given by the equation

$$\ln \gamma = -e^2\kappa/2DkT(1 + \kappa a) \quad (3)$$

of Debye and Hückel. The value of K^0 used in the calculation was 2.0×10^{-4} and was obtained by the extrapolation of the ionization constant² from the slightly wet acetone (about 0.4 wt. % H₂O) to the anhydrous medium. The extrapolated value of the sum of ionic radii a was 2.20 Å. The dielectric constant D , 19.0, was taken from Åkerlöf.³ As shown by the results in Table I the values of r are directly proportional to the concentration of the bromide ions.

At 35.0°, the ratios $r/(\text{Br}^-)$, calculated with the extrapolated values of K^0 (1.76×10^{-4}) and of a (2.45 Å.), and with D equal to 18.1,³ are also satisfactorily constant and have the average value of 15.7 ± 0.4 .

(1) A. R. Olson, L. D. Frashier, and Frances J. Spieth, *J. Phys. Chem.*, **55**, 860 (1951).

(2) A. R. Olson and J. O. Konecny, *J. Am. Chem. Soc.*, **75**, 5801 (1953).

(3) G. Åkerlöf, *ibid.*, **54**, 4125 (1932).

TABLE I
REACTION RATES IN DRY ACETONE AT 24.9°

$(r = d \ln C/dt); 0.1348 M \text{ ester}$			
$10^3(\text{LiBr})$, moles/l.	10^3r , min. ⁻¹	$10^3(\text{Br}^-)$, moles/l.	$r/(\text{Br}^-)$, l./mole min.
0.05179	0.2746	0.0423	6.50
.2590	.1021	.160	6.38
.5179	.1703	.263	6.46
1.295	3.14	.493	6.37
2.590	5.08	.780	6.51
2.590	4.96	.780	6.36
5.179	8.03	1.24	6.48
7.768	10.36	1.62	6.42
12.95	14.59	2.26	6.46

In the slightly wet acetone (approx. 0.15 M H₂O) at 25°, the value of $r/(\text{Br}^-)$ calculated with the experimental² K^0 (2.56×10^{-4}) and a (2.28 Å.) and with D equal to 19.3,³ is 4.08 ± 0.10 in the concentration range of lithium bromide from 0.001 to 0.02 M . At lower concentrations the values of $r/(\text{Br}^-)$ decrease slowly to 3.16 in $6.02 \times 10^{-5} M$ lithium bromide. However, the validity of the low r values appears to be open to question. This series of runs was carried out with an impure sample of the ester.¹ The last two values reported by Olson, Frashier and Spieth¹ in their Table 8 for a pure ester sample, as well as later results⁴ at low lithium bromide concentrations, give a satisfactorily constant ratio $r/(\text{Br}^-)$ with the average value of 4.43 ± 0.09 .

Lithium perchlorate, which is a much stronger electrolyte in acetone than lithium bromide (its ionization constant K^0 is 1.0×10^{-2} at 25°⁴) strongly represses the racemization rate of the ester. Under these conditions the rate increases proportionally to the stoichiometric concentration of lithium bromide,¹ provided that the lithium perchlorate concentration is sufficiently high and constant. This result, which has been attributed to the catalysis by LiBr, is also consistent with Br⁻ catalysis because with an excess of lithium perchlorate in the solution the concentration of bromide ions is proportional to the stoichiometric concentration of lithium bromide. As a matter of fact, the assumption of Br⁻ catalysis is in accord with the observation that the rates, at a constant concentration of lithium bromide, do not approach a limiting value at high lithium perchlorate concentrations but decrease with the increasing perchlorate in a slow but steady fashion. This decrease may plausibly be attributed to the slowly increasing concentration of lithium ions. The rates in lithium perchlorate solutions are of course related to the rates at low ionic strengths through the ionization constants of the two salts. The ionic strength, however, is too high for the approximations of Debye and Hückel. A sufficient agreement has been obtained for the most dilute solutions.⁴

An examination of the results reported¹ for the lithium perchlorate inhibited reaction at 25 and 35° shows that the ratio of the rates at the two temperatures in 0.00259 M lithium bromide is independent of lithium perchlorate from 0 to 1.133

(4) J. O. Konecny, Ph.D. Dissertation, University of California, Berkeley, 1954.

M and has a constant value of 2.35 ± 0.01 . There is, therefore, no indication of a reaction catalyzed by undissociated lithium bromide.

The activation energy of the reaction, calculated from the average values of $r/(\text{Br}^-)$ at 24.9 and 35.0° in anhydrous acetone is 16100 cal. The collision frequency has a "normal" value of 7.5×10^{10} l. mole⁻¹ sec.⁻¹. The combination of all the results then leads to the approximate rate law

$$-d(l\text{-ester})/dt = 7.5 \times 10^{10}(\text{Br}^-)(l\text{-ester}) \exp(16100/RT) \quad (4)$$

Strictly speaking, this equation applies only to solutions containing 0.135 M ester. The rates r extrapolated to the zero ester concentration, are about 10% higher. Since this solvent effect is small, no attempt has been made to incorporate it into the rate law.

Acknowledgments.—The author gratefully acknowledges the advice and assistance of the late Professor A. R. Olson, to whom he owes many hours of discussion on the subject. He has lost a stimulating teacher and sincere friend.

FOREIGN CATION EFFECTS ON MEASURED STABILITY CONSTANTS

BY JACK F. TATE AND MARK M. JONES¹

Department of Chemistry, Vanderbilt University, Nashville, Tennessee
Received June 12, 1961

The general methods for the study of complex formation in solution are based upon some measurement of the changes that occur upon addition of a coordinating anion X , in the form of a simple salt such as NaX or KX , to a solution of a metal perchlorate, $\text{M}(\text{ClO}_4)_x$. The equilibrium constants then can be obtained from measurements of the concentration of free M^{+z} , X^- , or some other quantity related to these. It is usually assumed that, within rather wide limits, it is a matter of complete indifference what cation is added along with the coordinating anion. There is some scattered evidence in the literature which indicates that this assumption is not strictly true, even under circumstances where a swamping electrolyte is present in very high concentration. This phenomenon is to be distinguished from the variations which arise when metal perchlorates are not used as the source of the coordination center. In this latter case there is very definitely an effect of the anion in MZ_x upon the equilibria² which is related to the stabilities of the complexes between M^{+z} and Z^- .

The effect of the cation may be seen in at least three cases.³⁻⁵ Fialkov and Spivakowski³ reported that in the case of the $\text{Cd}^{+2}\text{-Cl}^-$ system even the coordination number of the cadmium changed as various chlorides of the alkali metal (and ammonium) ions were used. They also reported a

(1) To whom correspondence concerning this paper should be addressed.

(2) L. G. Van Uitert, W. C. Fernelius and B. E. Douglas, *J. Am. Chem. Soc.*, **75**, 2739 (1953).

(3) Ya. A. Fialkov and V. B. Spivakowski, *Zhur. Neorg. Khim.*, **4**, 1501 (1959); *C. A.*, **54**, 8407 (1960).

(4) R. W. Ramette, *J. Chem. Educ.*, **36**, 191 (1959).

(5) Yu. A. Katov and B. N. Lebedev, *Trudy Inst. Met. i Obogashcheniya, Akad. Nauk Kazakh S. S. R.*, **2**, 92 (1960); *C. A.*, **54**, 23617i (1960).

decrease in the stability constants of the chloro complexes of cadmium on passing from rubidium chloride to lithium chloride as the source of chloride. A similar difference in the solubility equilibria involved in acidic solutions of cupric iodate containing added sodium perchlorate and lithium perchlorate was reported without comment by Ramette.⁴ The variation in the solubility of lead chloride in solutions of various metal chlorides⁵ shows a similar trend. Here the ability of solutions of a metal chloride to dissolve lead chloride decreases with increasing cation charge, other factors being equal. A more systematic study of one aspect of the problem may be seen in some studies by Sillén and co-workers.^{6,7} These, and an earlier study by Leden,⁸ showed how variations in activity coefficients may be the ultimate basis of variations in complexity constants when the ionic medium undergoes considerable variation in composition.

The purpose of the present study was to obtain specific information of the effect of varying the cation on the measured stability of the CdNO_3^+ complex. The experiments were planned so that the composition of the ionic medium varied as little as possible. This system was selected for several reasons: (a) it can be examined by a highly precise differential potentiometric method in which the first stability constant is obtained by extrapolation to a condition of zero liquid junction potential as the cell is initially one with no liquid junction, (b) the nitrates required for the titrant solution can be obtained readily in a state of high purity, and (c) preliminary studies by Leden⁹ indicate that this system has an equilibrium constant of a suitable magnitude (*i.e.*, close to unity) for precision measurement to within $\pm 1\%$. Included in the present study is an examination of two systems to determine the effect of such foreign cation variations on the enthalpy of complexation.

Experimental

The potential measurements and titrations were carried out as previously described.¹⁰ The titrating solutions used were prepared from reagent grade chemicals and all had an ionic strength of 3, the same as that of the solution into which they were titrated. The water circulating through the jacket of the titration cell was obtained from a constant temperature bath which was controlled to $\pm 0.01^\circ$ for the runs at 25, 35, and 45°.

Results and Discussion

The experimental results (Table I) show that the cation used in the titrant solution does have an effect on the measured equilibrium constant for the CdNO_3^+ complex. The equilibrium constants vary within a range of about an order of magnitude for the nitrates used. The difference shows up in a plot of

$$F(A) = (x - [\text{Cd}^{+2}])/[\text{Cd}^{+2}][\text{A}^-] \text{ vs. } [\text{A}^-]$$

where x is the total concentration of cadmium(II), $[\text{Cd}^{+2}]$ is the concentration of free cadmium(II) and $[\text{A}^-]$ is the concentration of free complexing anion, and in this case uncomplexed nitrate anion. It should be recalled that $F(A)$ is also equal to

(6) L. G. Sillén, *J. Inorg. Nuclear Chem.*, **8**, 176 (1958).

(7) G. Biederman and L. G. Sillén, *Arkiv Kemi*, **5**, 425 (1953).

(8) I. Leden, *Acta Chem. Scand.*, **6**, 971 (1952).

(9) I. Leden, *Z. physik. Chem.*, **A188**, 165 (1941).

(10) C. E. Vanderzee and H. J. Dawson, Jr., *J. Am. Chem. Soc.*, **75**, 5659 (1953); J. F. Tate and M. M. Jones, *ibid.*, **83**, 3024 (1961).

$\sum_i^n K_i [A]^{i-1}$ so this plot extrapolates to $F(A) = K_1$ (the stability constant of the first complex) when $[A^-]$ goes to zero. The stability constant for the CdNO_3^+ ranges from 0.142 for lithium nitrate as titrant to 1.06 for strontium nitrate as titrant. An approximate value for this constant was determined previously by Leden⁹ who reported a value of 1.29 at 25° using sodium nitrate in the titrating solution. Our values under these same conditions were 0.748 and 0.746 in duplicate determinations. A more recent polarographic study resulted in a value of 0.62.¹¹ This was available only in abstract and the titrant was not specified.

TABLE I

SUMMARY OF RESULTS OF POTENTIOMETRIC TITRATION OF

CERTAIN NITRATE SALTS WITH CADMIUM(II)

Salt	Temp., °C.	$K_1(\text{CdNO}_3^+)$
$\text{Sr}(\text{NO}_3)_2$	25	1.063
$\text{Ca}(\text{NO}_3)_2$	25	0.904
$\text{Mg}(\text{NO}_3)_2$	25	.817
	35	.794
	45	.813
NaNO_3	25	.747
	35	.618
	45	.616
$\text{Nd}(\text{NO}_3)_3$	25	.550
$\text{Al}(\text{NO}_3)_3$	25	.539
$\text{La}(\text{NO}_3)_3$	25	.533
LiNO_3	25	.142

The number of nitrate salts which could be used in the titrant solutions was restricted by several factors. Any metal ion which is able to oxidize the cadmium in the amalgam will lead to erratic results (such were obtained with lead nitrate solutions). Furthermore, only those nitrates were used in which it is customarily assumed that the cation complexes the nitrate to a "negligible" degree. Finally, the problem of insolubility limited the selection. Barium nitrate has a sufficiently small solubility in water that it is impossible to prepare a titrating solution of anywhere near the required concentration. Potassium nitrate may not be used because of the insolubility of potassium perchlorate. However, even with these limitations a reasonably representative series of nitrates was studied.

The fact that the stability constant for CdNO_3^+ is affected by the presence of foreign cations is not unexpected if the charges on these are different. That such differences should also be found with very closely related ions of identical charge is also understandable and recalls Brønsted's concept of the specific interaction.¹² In the present case the specific interactions of the various cations with the nitrate ion seem to be the most obvious cause of the small, but definite and reproducible, variations found for the stability constant.

In addition to thermodynamic factors (*i.e.*, activity coefficient variations), the change in the measured (apparent) stability constant of the CdNO_3^+ ion may be considered to arise in part from a competition between Cd^{+2} and the foreign cation of the titrating solution for the available

nitrate anions. The formation of nitrate complexes, or relatively stable ion pairs, with the foreign cation obviously will have an effect on the amount of CdNO_3^+ formed from a given total amount of nitrate.

If comparisons are confined to systems of the same charge types it is possible to test the reasonableness of this conjecture. It is easily seen that the stability constant decreases as the complexing power of the foreign cation increases for Groups Ia and IIa cations. This is also supported by the general tendency of the dissociation constants of the nitrate salts to fall into groups according to the valency type of the salts considered.¹³ The order found for Groups Ia and IIa cations is the same as that reported by Fialkov and Spivakowski.³

The equilibrium constant for CdNO_3^+ was determined at 25, 35 and 45° for titrating solutions of sodium nitrate and of magnesium nitrate. From the slope of a plot of $\log K_1$ vs. $1/T$ (°K.), ΔH^0 for the reaction was determined. The data of Table I show that there is a very small temperature dependence and therefore a very low ΔH^0 . The ΔH^0 values are -7.7 cal./mole and -160 cal./mole for magnesium nitrate and sodium nitrate, respectively. Since K_1 is very close to unity the free energy changes are also rather small in most of these cases. Thus for the sodium nitrate titration, $\Delta F^0 = +176$ cal./mole, $\Delta H^0 = -160$ cal./mole and $\Delta S^0 = -1.1$ e.u. The ΔF^0 values range from -36 cal./mole for strontium nitrate to $+1160$ cal./mole for lithium nitrate.

In conclusion, this study shows that the measured stability constant of the CdNO_3^+ ion is dependent upon the specific nitrate used as the source of the added nitrate ion. This shows the limitation of the common assumption that, within rather broad limits, the cation added in the titrant solution has no effect on the measured stability constant. It proves that even in the presence of very high concentrations of a swamping electrolyte, such an effect *is present* and may affect the measured stability constant by as much as an order of magnitude. The previous reports³⁻⁵ of such phenomena seem to be most reasonably reinterpreted in terms of a constancy of behavior of the principal coordination center and a variation arising from changes in the species present in the added solutions. These include changes in activity coefficients due to specific interactions.

We wish to acknowledge, with thanks, the assistance furnished in preliminary studies by the late Mr. J. Davis Sibley, Jr. This work was supported by a grant from the U. S. Atomic Energy Commission, At-(40-1)-2676, for which we wish to express our gratitude.

(13) C. W. Davies, *Endavour*, **4**, 114 (1945).

OBSERVATIONS ON THE DECOMPOSITION OF X-RAY IRRADIATED AMMONIUM PERCHLORATE

BY ELI S. FREEMAN AND DAVID A. ANDERSON

Pyrotechnics Chemical Research Laboratory, Picatinny Arsenal, Dover, New Jersey

Received April 27, 1961

Photomicrographs by Bircumshaw and Newman¹

(11) Hung-Chi Chiang and Kuang-Hsien Hsu, *K'o Hsueh Tung Pao*, 397 (1959); *C. A.*, **55**, 3241 (1961).

(12) J. N. Brønsted, *J. Am. Chem. Soc.*, **44**, 877 (1922).

of undecomposed and partially decomposed ammonium perchlorate crystals showed that a general clouding of the surface occurs as the crystals are heated. Initially formed hemispherical opaque areas on the surface coalesce as the reaction progresses. These observations apparently were made under reflected light. Additional details of the surface decomposition, obscure under reflected light, may be observed readily under transmitted light. This was found for undecomposed and partially decomposed ammonium perchlorate crystals heated at 200°. The clouding described previously is observed in photomicrographs taken under reflected light. Under transmitted light, however, additional surface structure is evident. The disruption pattern on the surface of partially decomposed crystals indicates preferential regions of reaction along intermosaic boundaries and dislocations. In previous papers^{2,3} it was shown that exposure to X-ray and γ -ray radiation profoundly affects the thermal decomposition of ammonium perchlorate. This effect was determined by measuring loss in weight and by differential thermal analysis. The appearance of the decomposing irradiated crystal is significantly different from the decomposing unirradiated sample. This was observed microscopically under reflected light. The crystal was irradiated with an OEG X-ray tube containing a molybdenum target for $\frac{1}{2}$ hr. at a dose rate of 1.3×10^5 roentgen per hr. On heating, the striking contrast between the behavior of the unirradiated and irradiated samples is that, whereas in the former initial reaction occurs primarily at the surface, the irradiated sample undergoes reaction throughout the entire crystal. The surface of the irradiated crystal does not appear to be disrupted or to reveal preferential sites of reaction as in the case of the unirradiated solid. The apparent homogeneous clouding of the entire crystal indicates that nuclei for reaction were produced by radiation throughout the entire crystal.

By differential thermal analysis it was found that ammonium perchlorate sublimate exhibits decomposition characteristics similar to the irradiated sample. Recently Hyde and Freeman⁴ have identified the presence of NH_3^+ radical in irradiated ammonium perchlorate by electron spin resonance. Neither the sublimate nor partially decomposed ammonium perchlorate exhibited resonance spectra. The sublimate did not contain NH_3^+ radical, although its chemical reactivity is similar to that of the irradiated crystals.³ These results imply that radicals or positive holes may not entirely account for the changes in the decomposition details of irradiated ammonium perchlorate, a possibility previously suggested.³

It was recently shown that ClO_3^- ion may give rise to a sharp exothermic reaction following the crystalline transition of ammonium perchlorate.⁵ It was reported in the same paper that exothermic

(1) L. L. Birumslaw and B. H. Newman, *Proc. Roy. Soc. (London)*, **227**, 228 (1955).

(2) E. S. Freeman and D. A. Anderson, *J. Phys. Chem.*, **63**, 1344 (1959).

(3) E. S. Freeman and D. A. Anderson, *ibid.*, **64**, 1727 (1960).

(4) J. S. Hyde and E. S. Freeman, *ibid.*, **65**, 1636 (1961).

(5) J. C. Petricciani, S. E. Wiber, W. H. Bauer and T. W. Clapper, *ibid.*, **64**, 1309 (1960).

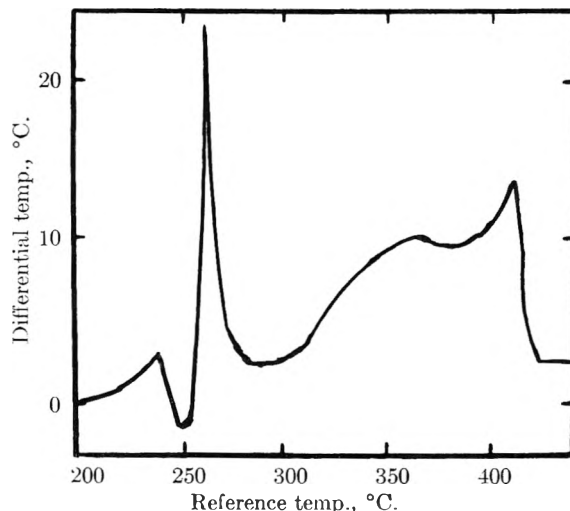


Fig. 1.—Differential thermal analysis at 4.4°/min. of 500 mg. of ammonium perchlorate containing 1 mole % KClO_3 . Sample prepared by evaporating solution to near dryness and by oven drying at 105°. The ammonium perchlorate was doubly recrystallized Fisher reagent grade material.

decomposition of ammonium perchlorate containing ClO_3^- ion impurity occurs only following crystalline transition. Our experiments show that significant exothermic reaction does occur prior to crystalline transition as is demonstrated in Fig. 1. The apparent discrepancy may be in part due to the higher rate of heating used in the differential thermal analysis (DTA) experiments of the referenced authors.⁵ In the referenced article it is also stated that complete decomposition occurs during the exothermic reaction following crystalline transition for samples containing more than 0.1 wt. % ClO_3^- ion impurity. Our DTA results shown in Fig. 1 demonstrate that reaction does not go to completion during this exotherm but at approximately 450°. Undoubtedly the referenced observation⁵ is due to a relatively large sample size (not specified in the referenced article) and is not a true chemical phenomenon. The fact that the exotherm following transition represents a stage of reaction which is a function of temperature seems to support the idea that ClO_3^- ion provides intermediate species which may act catalytically. Nevertheless the DTA decomposition pattern of irradiated ammonium perchlorate is strikingly similar in detail to that of the sublimate and of ammonium perchlorate containing ClO_3^- ion impurity.

Interestingly the presence of ClO_3^- ion in irradiated ammonium perchlorate was confirmed by the KI test for ClO_3^- ion but it was not found to be present in the sublimate. This is in agreement with previously reported data⁵ on the decomposition products formed during sublimation. Consequently, although the decomposition characteristics of the irradiated salt may be partially explained by the presence of the ClO_3^- ion, presumably in solid solution, this does not account for the details of the decomposition of ammonium perchlorate sublimate. If the mechanism of the decomposition

(6) H. M. Cassel and I. Liebman, *J. Chem. Phys.*, **34**, 343 (1961).

of irradiated ammonium perchlorate below 300° involves ClO_3 radical as an intermediate, then the role of ClO_3^- ion may principally be that of a source of radicals. The presence of ClO_3 may also, in part, account for the seemingly uniform reaction

throughout the irradiated crystal when heated at 200°.

Acknowledgment.—The authors wish to thank Dr. James Hyde of Varian Associates for conducting the electron spin resonance experiments.

COMMUNICATION TO THE EDITOR

EVIDENCE FOR ELECTRONIC INTERACTION BETWEEN IODINE AND A SOLID SURFACE

Sir:

The presence of an electric field at the surface of a solid has been inferred from certain phenomena associated with the solid-gas interface: namely, surface potentials¹ and a significant reduction in the intermolecular attraction within the adsorbed film,^{2,3} which has been traced to the effect of parallel-oriented induced dipoles. The surface fields for various solids have been estimated to lie in the range 10^7 to 10^8 volts cm.; a field of this order of magnitude would be expected to affect the electronic absorption spectrum of an adsorbed molecule in one or more of the following ways: shifts in the electronic states due to a highly polarized condition of the molecule; splitting of the electronic energy levels, *i.e.*, a molecular Stark effect; ionization of the adsorbate or partial charge transfer with the conduction bands of the substrate. Since iodine is known to enter into charge-transfer complex formation readily and since its major absorption band is in the visible range, its use as an adsorbate seemed likely to offer a method whereby perturbations of its electronic spectrum by the surface could be observed easily.

Preliminary experiments with adsorbed iodine have shown that the expected interaction does take place, with marked changes in the visible spectrum and in some systems with the production of strong absorption in the ultraviolet region. Spectral measurements from 300 to 700 $m\mu$ were made at room temperature by reflectance from powdered solids containing adsorbed iodine; in all cases the adsorption was reversible, the iodine being desorbed readily by evacuating the sample at 100°. The quantity of iodine adsorbed was known only approximately, but was always less than a complete monomolecular layer; nevertheless, the colored adsorbed film was clearly visible and its departure from the violet color of iodine vapor in many cases could be detected at once by the eye.

The material that displayed the least effect among those observed is silica (when freed of adsorbed water). The principal absorption band

of iodine vapor, centered about 520 $m\mu$, is shifted to about 480 $m\mu$. One specimen of silica in the form of a transparent, porous slab was suitable for transmission measurements down to 220 $m\mu$: adsorbed iodine on dry silica showed no ultraviolet absorption.

Silica-alumina cracking catalysts also show an absorption maximum in the visible region at around 450–480 $m\mu$, but have developed an increasing absorption below 350 $m\mu$. We could not investigate the absorption at shorter wave lengths with our present apparatus. The samples mentioned above were violet to pink in color.

Samples of pure alumina and boron nitride showed a gradual increase of absorption with decreasing wave length below 700 $m\mu$; they did not, however, display any absorption maximum in the visible region. The visible color of these systems is bright yellow to brownish. A slight difference between γ - and η -alumina is apparent to the eye: the slightly redder tint obtained with γ -alumina plus iodine can be traced to its greater absorption in the green portion of the spectrum.

On a third group of solids the adsorbed iodine film is characterized by having only a slight absorption in the visible spectrum, thus appearing white or faintly yellow in color. These substances include the alkali halides, calcium fluoride, and zirconium and titanium oxides. The reflectance spectra show sharply increasing absorption below 350 $m\mu$.

The colors formed by the interaction of iodine with various solid surfaces is reminiscent of the colors of iodine in various solvents. The greatest changes in the absorption spectra of iodine solutions are found with the more polar solvents, and presumably the same rough correlation exists with adsorbed iodine on surfaces of differing polarity. Furthermore, the charge-transfer complex mechanism postulated to account for the spectra of certain iodine solutions is also a reasonable explanation of the spectra of the adsorption complexes: if this is the case, the study of the spectra of adsorbed iodine should yield important information about the electronic nature of solid surfaces, which would be pertinent to their action in heterogeneous catalysis. A more detailed study of such systems is now in progress.

This work forms part of a program sponsored at Rensselaer Polytechnic Institute by Esso Research and Engineering Company.

RENSSELAER POLYTECHNIC INSTITUTE SYDNEY ROSS
TROY, N. Y. JAMES P. OLIVIER

RECEIVED JUNE 20, 1961

(1) J. C. P. Mignolet, "Chemisorption," ed. W. E. Garner, Butterworths, London, 1957, p. 118.

(2) J. H. de Boer, "The Dynamical Character of Adsorption," Clarendon Press, Oxford, 1953, pp. 168–169.

(3) H. Clark and S. Ross, *J. Am. Chem. Soc.*, **75**, 6081 (1953).

Announcing

5th Decennial Index to Chemical Abstracts

A **NINETEEN VOLUME** *index to
chemistry and chemical engineering for the
years 1947 TO 1956*

COVERING

543,064 Abstracts of Papers
104,249 Abstracts of Patents

KEYED BY

Authors • Formulas •
Subjects • Patent Numbers
Organic Rings

An expediter of progress in an age when nothing is as expensive as time.

Accurate • Comprehensive • Authoritative • Consistent

PRICES: *ACS Members \$ 600.00 per set
*Colleges & Universities \$ 750.00 per set
All Others \$1500.00 per set
(\$15.00 additional foreign postage)

*Sold under special lease agreement.



Special Issues Sales Department
AMERICAN CHEMICAL SOCIETY
1155 Sixteenth St., N.W., Washington 6, D.C.



TEMPERATURE MEASUREMENT IN ENGINEERING—Volume II

By H. DEAN BAKER, *Columbia University*; E. A. RYDER, *Pratt & Whitney Aircraft Division, United Aircraft Corporation*; and N. H. BAKER, *Columbia University*. It is quite possible that this work, with its companion volume, is the original treatise that will establish temperature measurement as an independent and integrated field in technology. The

purpose of the book is to present how-to-do-it directions for the measurement of temperatures in situations which actually arise in the laboratory, shop, and field; and the book itself is arranged in classes of circumstances where temperature measurements are desired. 1961. 510 pages. \$13.00.

QUANTUM MECHANICS

By EUGEN MERLBACHER, *University of North Carolina*. This book represents a new and valuable contribution to the subject of non-relativistic Quantum Mechanics, with emphasis on contemporary developments. By limiting the range of topics covered (i.e. omitting relativistic Quantum Mechanics and field quantization, and including only the elements of the many particle theory), the author has been able to present, in one volume, the

most thorough possible coverage of modern Quantum Mechanics and its application to simple physical systems. Throughout the book, priority is given to those physical ideas and mathematical techniques which the student will meet in practice and which will prepare him for further specialized study and the reading of current related literature. 1961. 544 pages. \$12.00.*

IODIDE METALS AND METAL IODIDES

By ROBERT F. ROLSTEN, *CONVAIR, A division of General Dynamics*. Presents the chemist, engineer, and metallurgist with the information necessary to design and operate an iodide cell, the details of the preparation, the properties of metal iodides (including boron, germanium and silicon iodides), and shows how these various compounds can be used

to prepare high purity elements or alloys. Sixty-one elements are discussed, and it is clearly shown how iodine—due to its reactivity with most metals—occupies a unique position in the periodic classification of the elements. 1961. Approx. 496 pages. Prob. \$17.50.

PHYSICAL CHEMISTRY OF MACROMOLECULES

By CHARLES TANFORD, *Duke University*. *Physical Chemistry of Macromolecules* treats, in turn, the major areas of physical chemistry: x-ray diffraction; molecular statistics; thermodynamics; light scattering transport processes and viscosity; electrostatics; and equilibria and kinetics of reactions.

A summary of the fundamental theory is included in each of the areas presented, and it is then shown how the theory may be modified or extended in order to become applicable to molecules of very high molecular weight. 1961. 710 pages. \$18.00.*

TRANSACTIONS OF THE SYMPOSIUM ON ELECTRODE PROCESSES

Edited by ERNEST YEAGER, *Western Reserve University*. This volume represents the papers presented at a symposium held in May, 1959, sponsored jointly by The Electrochemical Society, Inc., and the Office of Scientific Research of the United States Air Force. While it covers virtually all

phases of fundamental investigations of electrode processes, the general emphasis has been placed on new research developments and, more specifically, on hydrogen discharge kinetics, electrodeposition and dissolution of metals, and the kinetics of fast electrode processes. 1961. 374 pages. \$20.00.

THE RARE EARTHS

Edited by F. H. SPEDDING and A. H. DAANE, both of the *Ames Laboratory U.S.A.E.C.* A collection of individual papers presented at a "Symposium on Rare Earths and Related Metals" at the American Society of Metals meeting in November, 1959, this

book covers rare earths and the fields of rare-earth separation, preparation of the metals, and the properties of the metals and alloys. 1961. Approx. 640 pages. \$14.75.

AN INTRODUCTION TO INFRARED SPECTROSCOPY

By WERNER BRÜGEL, *Badische Anilin und Soda-Fabrik, Ludwigshafen, Germany*. Dr. Brügel's *Einführung in die Ultrarotspektroskopie*, published in 1954, was the first book to summarize in a single volume all of the essential topics of infrared spectroscopy.

This important translation incorporates extensive additions bringing the book up to the stage of the third German edition, ready this year. 1961. 406 pages. \$9.00.

*Textbook edition also available for college adoption.